UNDERSTANDING AND PREVENTING VISUAL LOSS IN COMMOTIO RETINAE

By

RICHARD JAMES BLANCH

A thesis submitted to the University of Birmingham for the degree of DOCTOR OF PHILOSOPHY

School of Clinical and Experimental Medicine

College of Medical and Dental Sciences

University of Birmingham

August 2013

Abstract

Commotio retinae describes retinal opacification following trauma and affected 16% of British soldiers suffering major trauma. The macula was affected in 55% of soldiers and 31% of civilian cases, permanently reducing vision to less than 6/9 in 26% of cases, associated with photoreceptor degeneration.

In an experimental rat model, commotio retinae was more readily induced by high velocity ballistic injury (20m/s) than low velocity weight drop (2-7m/s). In rats, after experimentally induced commotio retinae, photoreceptors died by a combination of necrosis (central to the impact site) and apoptosis (peripheral to it), demonstrated by morphological changes on electron micrographs and TUNEL staining. Photoreceptor death after commotio retinae was associated with reduced ERG a-wave amplitude. Apoptosis occurred through the intrinsic pathway, mediated by caspase 9 but not involving any of the classical executioner caspases (3, 6 and 7). Inhibition of caspase 9 reduced photoreceptor death and improved retinal function, assessed by a-wave amplitude.

Clinical studies suggested a protective effect of female gender after commotio retinae, but progesterone treatment increased photoreceptor death after ballistic injury in the experimental model.

Acknowledgements

A great many people have helped with the research and the preparation of this thesis.

Thanks go to my supervisor Prof Rob Scott for making me look at ocular blast injury in the first place and for encouraging, supporting and advising me at every stage of the project. Equal thanks go to Prof Ann Logan, my primary supervisor, for welcoming me into her research group, giving me the skills and support I needed to be able to make the laboratory side of the project work and supporting me throughout. I am also immensely indebted to Zubair Ahmed, without whose advice and teaching I couldn't have done research into apoptosis and to Prof Martin Berry for his research advice and for his endless patience in editing and redrafting manuscipts.

Thanks also go to Prof Attila Sik, Theresa Morris and Paul Stanley for teaching me to do electron microscopy and get publishable images. Thanks to David Snead for showing me how to look at electron micrographs and, along with Sean James, helping me do the first pilot study and giving me continued and invaluable support from their laboratories. Thanks to Peter Nightingale and Jon Bishop for statistical advice. Thanks to Peter Good and Antonio Calcagni for electrophysiology advice. Thanks to Ana Maria Gonzalez for help and advice in learning laboratory techniques.

Final thanks go to Andy Thewles, Lisa Hill, Hannah Botfield, Ben Mead, Sarina Kundi, Vasanthy Vigneswara, Jenna O'Neill and Peter Morgan-Warren for good company in the write-up room, advice and assistance with laboratory work and anaesthetic assistance in BMSU.

Funding

Ministry of Defence, UK

Drummond Foundation, UK

Sir Ian Fraser Foundation, Blind Veterans UK

Illustrations

Tables

Abbreviations

ADB	Antibody diluting buffer
Apaf-1	Apoptosis activating factor 1
BB	Ball bearing
BDNF	Brain derived neurotrophic factor
bVAD-fmk	Biotinylated valine-alanine-aspartate-fluoromethyl ketone
C6DN	Caspase 6 dominant negative protein
CF	Counting fingers
CNTF	Ciliary neurotrophic factor
d	Day/days
df	Degrees of freedom
ERG	Electroretinogram
HM	Hand movements
hr	Hour/hours
HtrA2	High temperature requirement protein 2
ILM	Inner limiting membrane
INL	Inner nuclear layer
IPL	Inner plexiform layer
IS	Inner segments
IUGR	Intra-uterine growth retardation
LE	Left eye
min	Minute/minutes
MOMP	Mitochondrial outer membrane permiabilisation
MPTP	Mitochondrial permeability transition pores
NPL	No perception of light
OLM	Outer limiting membrane
ONL	Outer nuclear layer
OPL	Outer plexiform layer

OS	Outer segments
OTS	Ocular trauma score
PB	Phosphate buffer
PBI	Primary blast injury
PBS	Phosphate-buffered saline
Pen1	Penetratin 1
PL	Perception of light
PTEN	Phosphatase and tensin homolog
RD	Retinal detachment
RE	Right eye
RGC	Retinal ganglion cell
RIP1	Receptor interacting protein kinase 1
RNFL	Retinal nerve fibre layer
RPE	Retinal pigment epithelium
SDS	Sodium dodecyl sulphate
sec	Second/seconds
smac	Second mitochondrial-derived activator of caspases
SOCS3	Suppressor of cytokine signalling
TBI	Traumatic Brain Injury
TBS	Tris-buffered saline
TBST	TBS with Tween
TSC1	Tuberous sclerosis complex 1
VA	Visual acuity
XBIR3	X-linked inhibitor of apoptosis (IAP)-baculoviral IAP repeat 3 domain
XIAP	X-linked inhibitor of apoptosis

Contents

1. Introduction

The eye is a complex and delicate organ on which we rely for vision. Our perceptions, our thoughts, our social and occupational interactions are all overwhelmingly visual in nature. Loss of vision is a tragedy that impairs all aspects of our lives, particularly traumatic loss of vision, which is usually sudden, unexpected and commonly affects the young.

1.1. Structure and Function of the Eye

A brief overview of ocular anatomy and physiology is provided, for a detailed description the reader is referred elsewhere (Snell, Lemp, and Grunther 1998), (Forrester, Dick, McMenamin, and Lee 2003), (Elkington, Frank, and Greaney 1999).

Figure 1.1.1. An illustrative cross-sectional diagram of a human eye.

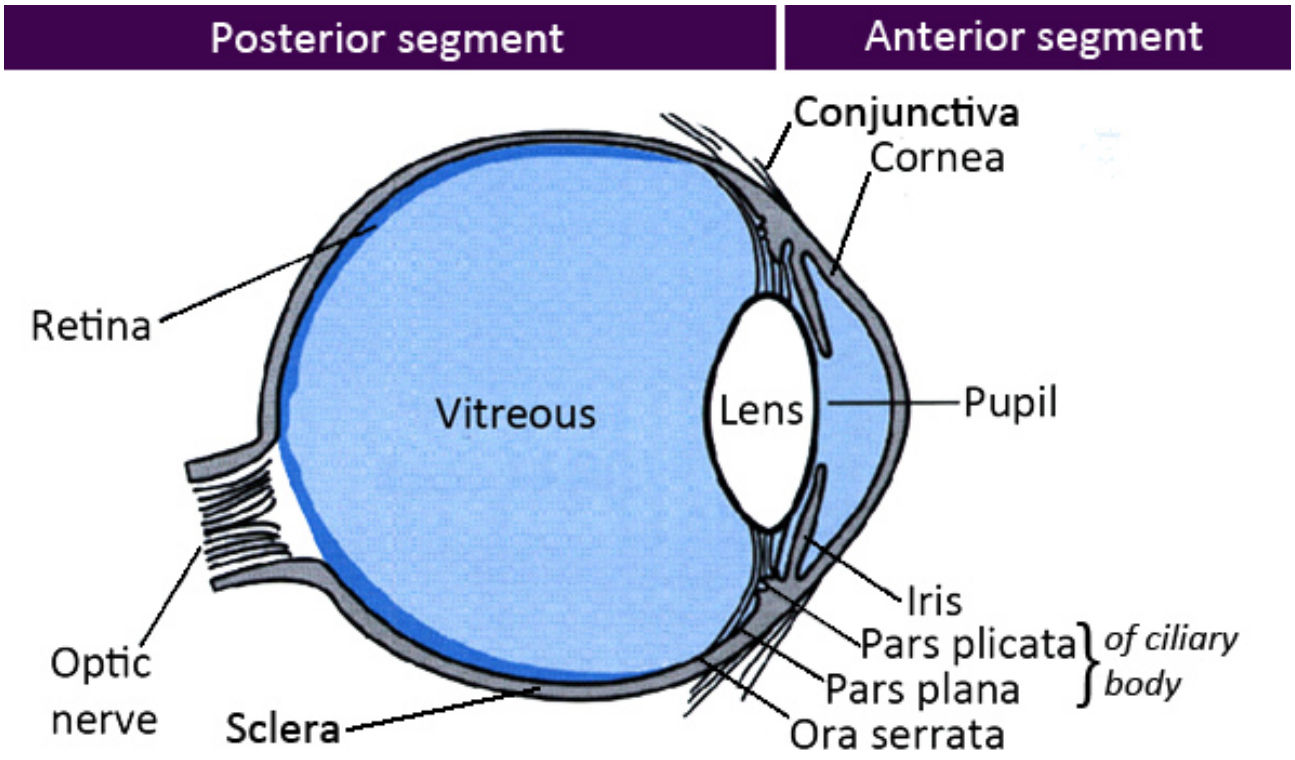

The eye (or globe) is suspended in the bony orbit by connective tissue and muscle attachments. In addition to the globe, extra-ocular muscles and connective tissue, the orbit contains nerves, blood vessels, orbital fat and the lacrimal gland. Anteriorly the orbit is covered by the eyelids, which

contain part of the lacrimal drainage apparatus. The anterior segment of the eye (anterior to the lens) is covered by cornea and contains aqueous. The posterior segment (posterior to the lens) is covered anteriorly by translucent conjunctiva. Beneath the conjunctiva is vascular episclera and Tenon's capsule. Tenon's capsule covers the globe from the optic nerve to the limbus (junction of cornea and sclera and is reflected back to envelop the extra-ocular muscles from their insertions onto sclera. The sclera is the tough collagenous outer coat of the globe. Inside the sclera is the choroid containing the choriocapillaris, which provides a rich blood supply, from which oxygen and nutrients diffuse to the outer retina (Figure 1.1.3).

Light enters the eye through the clear optical media (tear film, cornea, aqueous in the anterior segment, lens, vitreous) and is focussed on the retina. The tear film/cornea provide the main contribution to refractive power (approx 43 dioptres) and the lens provides a smaller, but modifiable component (approx 15 dioptres). The lens is suspended from the ciliary body by zonules. In younger people, contraction of the ciliary muscle changes lens shape allowing light emanating from objects at variable distances to be focussed on the retina. The 95% confidence interval for the axial length of the eye has been reported as 21.87 – 25.47 in a mixed white and Africian-Carrribean population and 20.78 - 24.42 in an Indian population (Oliveira et al. 2007), (Nangia et al. 2010). The average axial length of the human lens is 4mm (17% of the total) (Nangia et al. 2010).

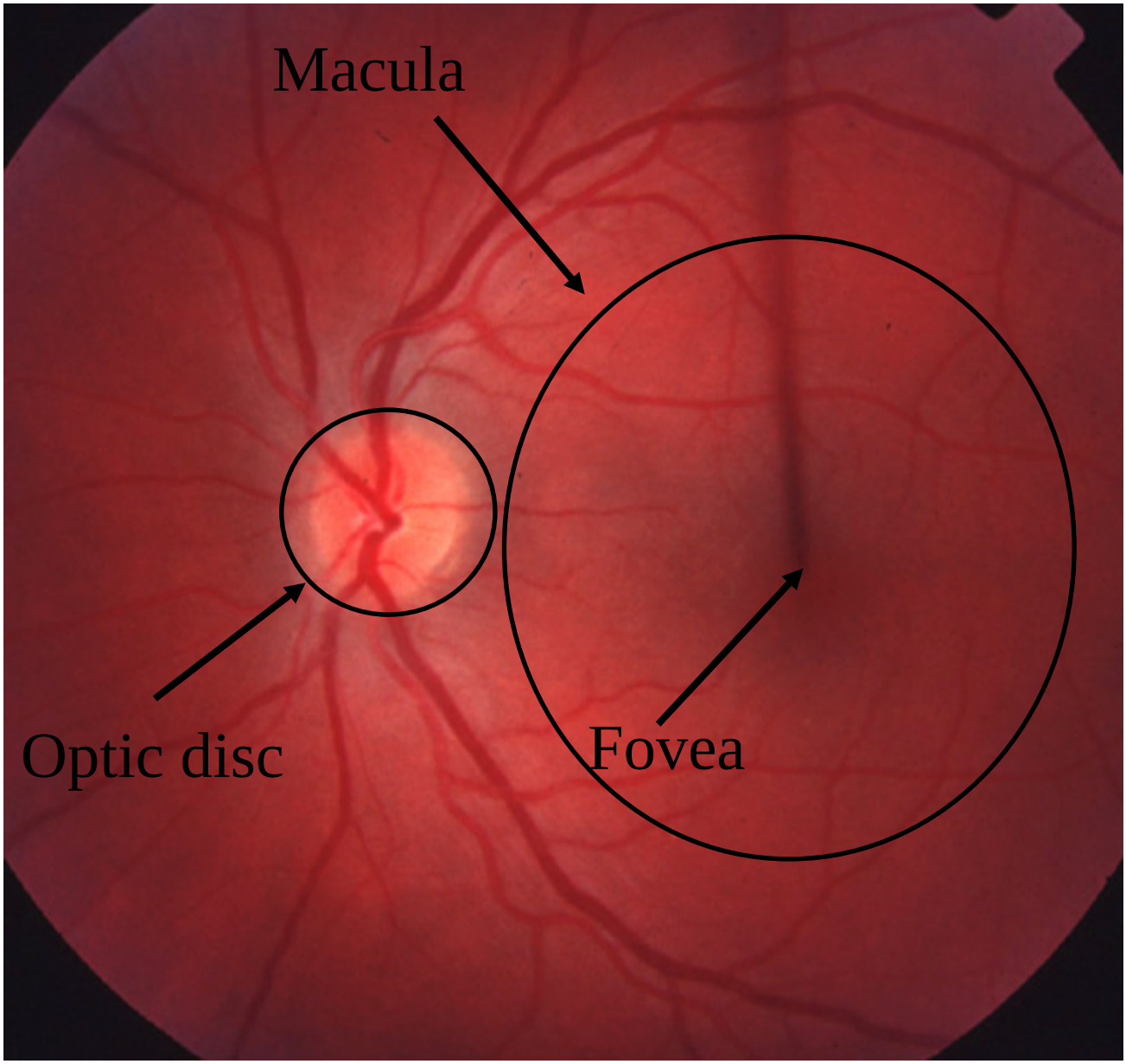

Figure 1.1.2. A fundus photograph showing the features most prominent on fundoscopy of a normal human eye. The optic disc is the point of exit from the eye for retinal ganglion cell axons. Posterior to the disc (after the lamina cribosa), axons are myelinated in the optic nerve. In their intra-ocular course they are usually unmyelinated. The fovea is the avascular central region of the macula responsible for detailed colour vision and contains only cone photoreceptors.

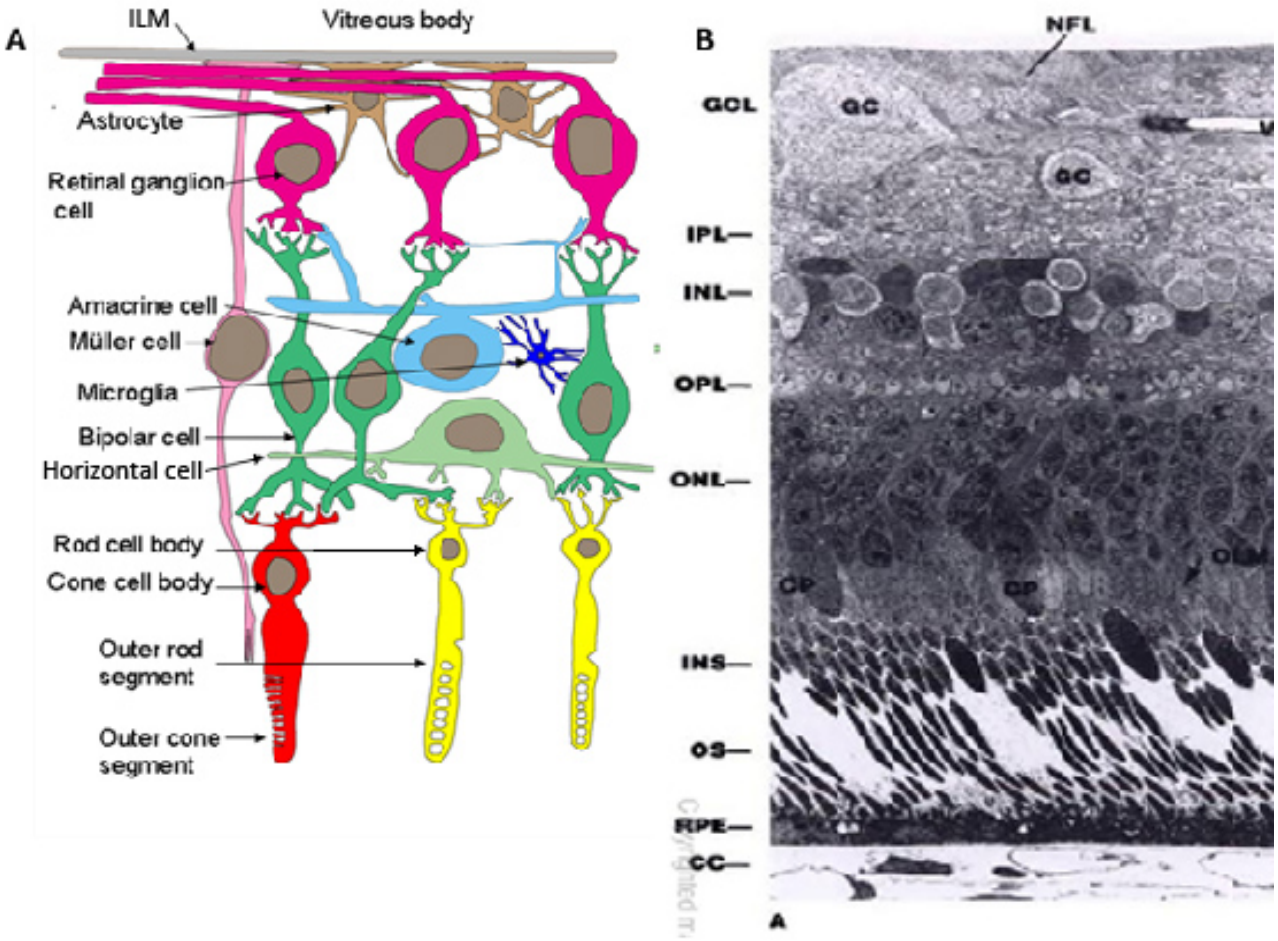

Figure 1.1.3. A. Diagram illustrating the retinal cell types (Berry et al. 2008). B. Low power electron micrograph of the primate retina demonstrating the layered arrangement: CC, choriocapillaris; RPE, retinal pigment epithelium; OS, outer segments; INS, inner segments; ONL, outer nuclear layer with rod and cone cell nuclei; OPL, outer plexiform layer; INL, inner nuclear layer with bipolar, Müller and amacrine cell nuclei; IPL, inner plexiform layer; GCL, ganglion cell layer with ganglion cell nuclei; NFL, nerve fibre layer; V, retinal vessel; OLM, outer limiting membrane; CP, cone pedicle/outer segment; ILM, internal limiting membrane. Original magnification x930" (Forrester, Dick, McMenamin, and Lee 2003).

Light passes through the retina from top to bottom as seen in Figure 1.1.3., and is detected by the photoreceptor outer segments (OS). In the OPL photoreceptors synapse with bipolar cells, whose nuclei are present in the INL. Bipolar cells synapse with the ganglion cell dendrites in the IPL and visual information is transmitted to the brain by the ganglion cell axons which run in the retinal nerve fibre layer (RNFL). Müller cells are radial glia that span the retina from the OLM, formed by their foot processes to the inner limiting membrane (ILM), their basement membrane.

Photoreceptors are sustained by the retinal pigment epithelium (RPE), which recycles and regenerates the light sensitive pigments. The two classes of photoreceptor are distinguished by the shape of their OS: rods contain the pigment rhodopsin, are most light sensitive and function under scotopic (dark) conditions; cones function under photopic (light) conditions and in different species contain a variety of cone opsins (light-sensitive pigments), which are maximally sensitive to different wavelengths of light, giving rise to colour vision.

In the human eye, there are three classes of cone sensitive to short (S), medium (M) and long (L) wavelengths, giving rise to trichromatic colour vision. The M and L cones are maximally concentrated at the fovea, whereas rods dominate the periphery; 95% of photoreceptors are rods. The photoreceptor OS containing the opsin pigments consist of membraneous discs that are constantly replenished. Discs are shed from the photoreceptor OS and are phagocytosed by the RPE. The human retina is described as holangiotic, i.e.the blood supply to the inner retina comes from a retinal circulation. The retinal blood vessels supply a capillary plexus in the GCL and another extending from the IPL to the OPL. The outer retina derives its blood supply from the choriocapillaris. In contrast, a merangiotic retina (e.g. in the rabbit) derives most of its blood supply from the choriocapillaris. The retinal blood vessels and the RPE (with its basement membrane, called Bruch's membrane) have tight junctions that prevent the passage of cells and larger molecules. This arrangement is referred to as the blood-retinal barrier (BRB).

Vitreous gel fills the posterior segment of the eye and is composed of water, collagen and glycosaminoglycans (mostly hyaluronic acid) with very few cells. The vitreous body is strongly attached to the retina posteriorly at the optic disc and anteriorly the vitreous base attaches to the ora serrata, where the most posterior of the zonular fibres, insert into the anterior hyaloid face (anterior face of the vitreous) instead of the lens (Bernal, Parel, and Manns 2006). Weaker attachments of the vitreous occur over retinal blood vessels and are responsible for retinal tears when the vitreous pulls off the retina in trauma or senile degeneration of the vitreous. The area of vitreous adjacent to the ILM is the lamina rara and is formed of collagen fibres running parallel to the retina and is 0.03 -0.06µm thick – this shows no species variations (Sebag 1992).

Visual function is usually assessed using a Snellen chart with different letter sizes from which visual acuity (VA) is measured as the smallest line of letters that the patient can read and specified as a fraction, the denominator of which is the distance at which the letters could be read by a patient with normal vision and the numerator the distance at which the chart is read, for example 6/6 represents normal vision and 6/120 is the level below which a patient can be registered as Severely Sight Impaired in the UK.

1.2. Ocular Trauma

Parts of the work in this section have been published in a review article in the Journal of the Royal Army Medical Corps (Blanch and Scott 2010); the paper is presented in Appendix 1.

Ocular trauma can affect people from all walks of life and the consequent visual loss can cause loss of career, major lifestyle changes and disfigurement. The Beaver Dam Eye Study reported a 19.8% lifetime prevalence of ocular trauma in a large civilian population in the USA (Wong, Klein, and Klein 2000). It is most common in young male manual workers, such as farmers and factory workers (Wong, Klein, and Klein 2000).

The military population are at particular risk of ocular trauma. British armed forces involved in combat operations in Iraq on operation TELIC from March 2003 to May 2011 and in Helmand

province, Afghanistan, on operation HERRICK since May 2006 have faced threats throughout the spectrum of conflict, from armoured manoeuvre warfare to counter-insurgency. British military ophthalmologists have not been routinely deployed in support of operations since the end of the first Operation TELIC in May 2003. Eye injuries requiring the input of an ophthalmologist in theatre are evacuated back to the UK and assessed and treated in the Royal Centre for Defence Medicine (RCDM) in Birmingham; a small number are sent locally to coalition partners' medical facilities in theatre and to US facilities in Germany for Ophthalmology input before Birmingham.

Historically the number of eye injuries as a proportion of those wounded in action varied from 0.5% in the American civil war to 13% in US forces in the first Gulf war with 70-80% of these due to blast (Blanch and Scott 2010), (Wong, Seet, and Ang 1997).

In modern warfare, most casualties are civilian. There are no widely accepted figures for civilian injuries in the current conflict in Iraq, however, the Congressional Research Service reviewed a variety of estimates ranging from 34,832 (Apr 2005 to Jun 2006 – the "Associated Press") to 601,027 individuals (May 2003 to Jun 2006) (Fischer 2008), (Burnham, Lafta, Doocy, and Roberts 2006). In terrorist bombings in civilian settings the proportion of eye injuries is reported to be up to 20.7% (Odhiambo, Guthua, Macigo, and Ahama 2002), though Arnold et al found it to vary from 1% to 6% depending on environment (Arnold, Halpern, Tsai, and Smithline 2004). The causes of injury are primary fragments from the ordnance casing and secondary fragments of glass, cement and mortar that may cause minimal damage to clothes or skin, but significant morbidity if they hit the eye (Carley and Mackway-Jones 1997) , (Mallonee et al. 1996) , (Thach et al. 2000).

Eye injuries are classified using the Birmingham Eye Trauma Terminology System (Pieramici et al. 1997) (Figure 1.2.):

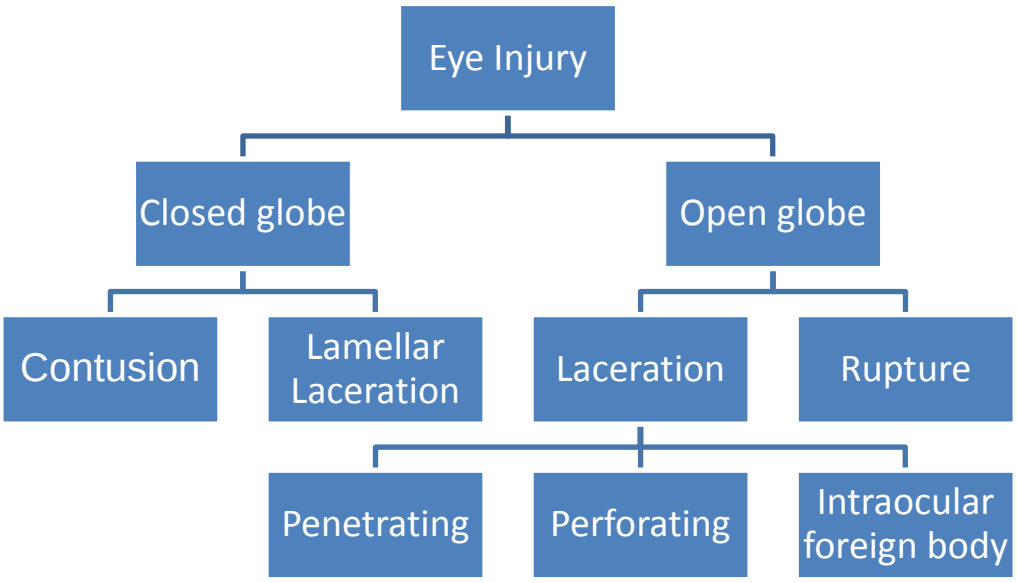

Figure 1.2. Birmingham Trauma Terminology System (Pieramici et al. 1997)

In the closed globe category, a blunt object striking the eye causes anteroposterior shortening and equatorial expansion – so that the lens-iris diaphragm is displaced posteriorly, while the peripheral structures are expanding outwards, which can tear ocular tissues such as those at the iridocorneal angle. Retinal stretching and shearing can cause retinal injuries such as dialyses, tears and commotio retinae.

1.2.1.Blast Injuries

In peacetime, unilateral eye injuries are typical, but ocular war injuries are bilateral in 15%-37% of cases (Weichel et al. 2008), (Belkin 1983). Though the eyes occupy just 0.1% of the total and 0.27% of the anterior surface of the body, soldiers' use of body armour makes explosions more survivable but leaves the face and eyes relatively exposed.

Blast injury is usually divided into 4 categories: Primary blast injury (PBI) is caused by the wave of blast overpressure ('blast wave'). Secondary blast injury is caused by fragments driven by the blast wind, which is movement of air due to the pressure differentials. Tertiary blast injury is caused by the effects of this blast wind, including displacement of the victim against other surfaces and structural collapse. Quaternary blast injury is due to mechanisms other than those above such as burns and toxic inhalation (DePalma, Burris, Champion, and Hodgson 2005).

The blast wave responsible for PBI is a shockwave caused by the sudden expansion of explosive products, which are greatly compressed and heated. The shockwave travels at the local speed of sound. The high pressure generated by the explosion means that the shockwave travels at hypersonic speeds with respect to undisturbed air. The impact of the blast wave on the body generates internal shockwaves and the different material speeds of sound mean that they propogate at different speeds through different tissues. This differing response causes shearing and tearing at tissue interfaces such as in the lung alveoli and the bowels (Cullis 2001). The eyes are less susceptible to a PBI than the air filled organs such as the lungs, bowel and ears (Sharpnack, Johnson, and Phillips 1991). However, the eye consists of tissues with differing densities and elastic properties, such as the photoreceptors-RPE interface, which is vulnerable to shearing injury as in commotio retinae and the vitreo-retinal interface, which is vulnerable to tearing.

In clinical practice it is difficult to separate the effects of primary, secondary and tertiary blast. The pattern of injury of 23 cases of suspected ocular PBI reported in the literature is summarised in Table 1.2.1. The most commonly reported injury is commotio retinae. The posterior segment is more affected than the anterior segment in 57% of cases, even though the blast wave traversed the anterior segment first, suggesting that it is more vulnerable to blast effects.

Injury	Number	Percentage
Chorioretinal lesions (commotio retinae, choroidal rupture, macular lesions, retinal detachment)	13	35%
Iris and papillary lesions (hyphaema, iridodialysis, iris rupture)	9	24%
Traumatic optic neuropathy	4	11%
Lens opacities	4	11%
Vitreous haemorrhage	3	8%
Extraocular muscle paralysis	2	5%
Conjunctival haemorrhage	1	3%
Orbital blow out fracture	1	3%

Table 1.2.1. Distribution of PBI reported in the literature (Beiran and Miller 1992), (Bellows 1947), (Blanch and Scott 2008), (Campbell 1941), (Chalioulias, Sim, and Scott 2007), (Zuckerman 1941).

1.3. Commotio Retinae

1.3.1.Clinical Picture

Commotio retinae describes grey-white opacification of the neuroretina and may affect the macula, reducing vision. It was first described by Berlin in 1873 and is also known as Berlin's oedema (Berlin 1873). The signs variably resolve over days to months. Visual loss may be transient or permanent (Eagling 1974), (Hart and Frank 1975), with recovery taking up to 6 months and leaving occasional RPE mottling (Eagling 1974), (Liem, Keunen, and van Norren 1995).

Large studies in UK Eye Casualty Departments have found that commotio retinae occurs in 0.4% of all eye injuries (Jones et al. 1986), (Vernon 1983). Such closed globe injuries are also a problem in the military. US sources report 21,965 soldiers wounded in action in the Iraq conflict from October 2001 – September 2006, of whom 13% had ocular and adnexal injuries requiring evacuation. In a US series of 432 globe injuries from this conflict, 54% were closed, 14.8% suffering commotio retinae of which 73% had macular involvement (Weichel et al. 2008).

There are few published data on the prognosis of commotio retinae. Hart and Frank. (1975) reported a series of 19 eyes with no abnormalities apparent on Fundus Fluorescein Angiography (FFA) and variable reduction in vision (Hart and Frank 1975). All recovered to a VA equal to that in the fellow eye by 3-4 months, bar one that remained at 6/12 with a paracentral scotoma at one month. Eagling (1974) followed a series of 108 posterior segment civilian closed globe injuries with hyphaema for 6 months. Of these, 30 had macular involvement including commotio retinae and choroidal rupture (Eagling 1974). The most common cause was assault. Anterior segment damage was reported in approximately 2/3 of cases and classified as "moderate" (lens opacity, multiple iris sphincter tears or 90-180° angle recession) or "severe" (cataract, lens malposition, iridodialysis or >180° angle recession). "Most" cases recovered within 2 weeks of injury, though, in some, improvement continued for up to 6 months. Twelve patients had permanent macular damage: 5 of whom had final VA in the affected eye of 6/6-6/12, 5 were of 6/18, 1 was 6/60 and 1 was left with no perception of light caused by a coincident optic nerve avulsion. Areas of absolute scotoma on central visual field testing did not recover, whereas areas of relative scotoma showed some recovery. An unspecified number of patients had peripheral commotio retinae only.

The optical coherence tomography (OCT) features of commotio retinae are disruption at the level of photoreceptor OS in all cases (Meyer, Rodrigues, and Mennel 2003), (Oh et al. 2011), (Sony, Venkatesh, Gadaginamath, and Garg 2006), (Souza-Santos et al. 2012). Souza-Santos et al. (2012) reported OCT findings on 11 patients, 5 of whom had disruption in the region of the photoreceptor inner segments (IS) and hyper-reflectivity of the ONL and other retinal layers; in these patients the ONL degenerated with associated visual loss (Souza-Santos et al. 2012). It is likely that the ONL hyper-reflectivity is predictive of ONL degeneration, as IS disruption has been reported to resolve without adverse long-term sequalae (Park et al. 2011).

There is one paper, in Portuguese, looking at the characteristics of commotio with full field electroretinography (ERG) and a case report in English (Knighton and Blankenship 1980), (Noia Lda et al. 2006) that both show a reduction in amplitude of the major components with full recovery within

2 weeks. Other reports of isolated cases with concomitant macular holes provide multi-focal ERG data on commotio retinae (Lai, Yip, Wong, and Lam 2005). The effects of commotio on pattern ERG have not been reported.

The BRB is assessed by FFA and indocyanine green angiography (ICG), which assess the retinal and choroidal circulations respectively. A series of 21 patients with FFA and ICG found fluorescein leakage in 9 eyes and a 'salt and pepper' fundus appearance in one, which the authors felt indicated a more severe injury (though they did not specify VA in these cases). In some cases early increases in choriocapillaris permeability developed into occlusion by day 4. All eyes with abnormal FFA had some abnormality of ICG (delayed filling/hypofluorescence). The authors speculated that in severe commotio retinae occlusion of the choriocapillaris leads to outer retinal ischaemia within days after injury and impaired recovery (Kohno, Miki, and Hayashi 1998).

1.3.2.Summary

In clinical studies of commotio retinae many patients recover completely, but an unknown proportion are left with reduced vision or paracentral scotomas. These patients have early ONL hyper-reflectivity on OCT and/or choroidal leakage with subsequent ONL degeneration and/or choroidal occlusion. There are no treatments available to improve the outcomes for those patients who suffer permanent loss of vision.

1.4. Retinal Injury in Experimental Models

Parts of the work in this section have been published as a "Perspectives" piece in Investigative Ophthalmology and Visual Science (Blanch et al. 2012b), the paper is presented in Appendix 2.

1.4.1.Comparative Anatomy of the Eye

The eyes of different mammals vary in size, refractive properties, retinal vasculature and visual photopigments. The cellular composition and thickness of the retina is conserved across mammals e.g. 0.24mm in the mouse eye compared to 0.249mm in the human eye (Glickstein and Millodot

1970), (Remtulla and Hallett 1985), (Alamouti and Funk 2003). The photoreceptors show particular variation in photopigments and in size. Rods all contain rhodopsin, which has 87% sequence homology between human, bovine, ovine, galline and murine DNA (Nathans 1992). Rod size varies with animal size and diurnal or nocturnal behaviours, whilst the proportion of cones and their function is highly variable between species. No mammals except primates have a macula.

The rabbit retina is merangiotic; humans, primates, pigs and murine rodents have holangiotic retinae. The arrangement of capillaries in mouse, pig and primate retinae is similar to humans, with capillary plexi in the ganglion cell/nerve fibre layer and bracketing the inner nuclear layer at its sclerad and vitread aspects (Simoens, De Schaepdrijver, and Lauwers 1992),(Snodderly and Weinhaus 1990),(Cuthbertson and Mandel 1986). The rat retina has been reported to have two only planes of capillary plexi – in the ganglion cell layer and the outer plexiform layer (Bhutto and Amemiya 1995), (Ninomiya and Kuno 2001); however, given the similarities in retinal vasculature between mouse, primate and porcine retinae, it is likely that more detailed studies would reveal a similar arrangement in rats.

1.4.1.1. Mice

The mouse eye has an average axial length of 3.4mm and 60% of this is taken up by the lens. The distance from the posterior lens surface to the retina is 0.56mm (Remtulla and Hallett 1985). There is some disagreement on the refractive status of the mouse eye, but existing evidence suggests that it is either emetropic (image focussed on the retina) or slightly myopic (image focussed in front of the retina) (Remtulla and Hallett 1985), (Glickstein and Millodot 1970). The average density of rods in mice is 437,000 /mm^2, with an outer segment diameter of 2µm, giving approximately 6.4 million rods per retina (Jeon, Strettoi, and Masland 1998). 3% of mouse photoreceptors are cones, which are distributed throughout the retina. The majority of cones co-express short (S - blue/UV) and medium (M - green) wavelength opsin pigments, with greater S opsin expression overall (Applebury et al. 2000). M opsin expression increases in a ventral to dorsal gradient and S opsin increases in a dorsal to ventral gradient (Applebury et al. 2000).

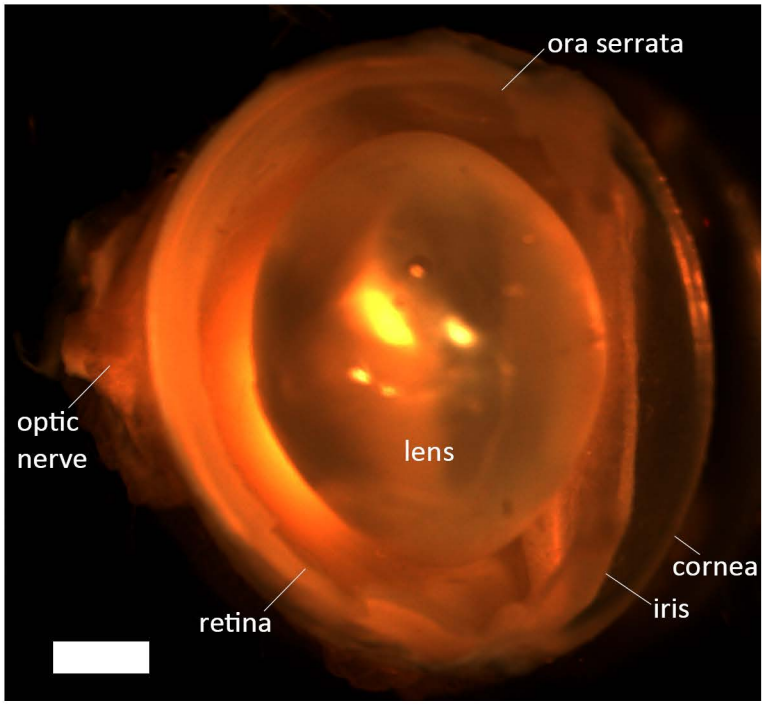

Figure 1.4.1.2
Labelled cross section of the eye of an adult Wistar rat. Scale bar = 1mm

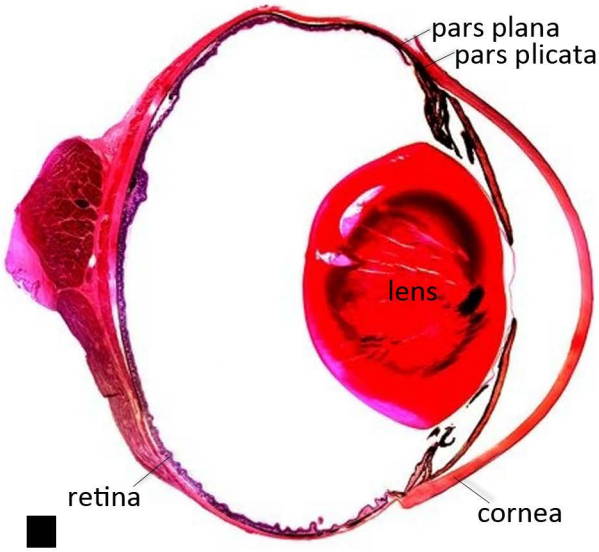

Figure 1.4.1.3.
Labelled cross section of an adult rabbit eye. Scale bar = 1mm

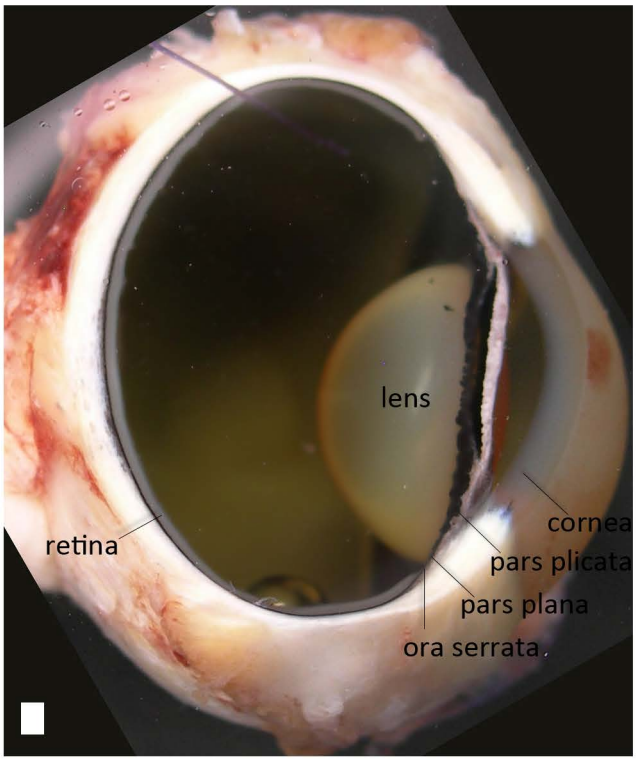

Figure 1.4.1.4.
Labelled cross section of the eye of an adult large white pig. Scale bar = 1mm

The vitreous body contains primarily type II collagen and hyaluronic acid. Collagen fibres of 15-20nm in diameter connect the vitreous cortex to the internal limiting membrane of the posterior retina and more strongly to the peripheral retina and lens zonules. The fibres are a similar size but are less frequent than in larger species, such as humans (Rhodes 1982), (Rhodes 1983), (Rhodes 1985).

1.4.1.2. Rats

The rat eye (Figure 1.4.1.2.) has an axial length of 6.29- 6.31mm, 8 times larger by volume than the mouse eye (Remtulla and Hallett 1985), (Hughes 1979). The lens accounts for 60% of axial length at 3.71mm (Hughes 1979). Existing evidence suggests that the rat eye is emmetropic, with a 0.3mm pupil giving a 30D depth of field (Hughes 1977). Rod densities are 400,000-500,000 /mm^2 and rod outer segment diameter is around 2µm (unpublished data – Blanch, RJ). Rats have two classes of cone, M and S, though M cones are most frequent (Szel and Rohlich 1992). They constitute only 1% of photoreceptors and are distributed throughout the retina, being denser dorsally (Szel and Rohlich 1992).

The vitreous base attachment spans the ora serrata, and has fewer collagen fibres than in larger species such as rabbits and humans (Rhodes 1983). It is hypothesised that smaller eyes require less glycoconjugate to maintain structural integrity.

Albino rats are commonly used for research purposes, but albinism is associated with multiple neuro-retinal abnormalities, including non-pigmented retinal pigment epithelium and abnormal decussation of retinal ganglion cell (RGC) axons at the optic chiasm (Prusky, Harker, Douglas, and Whishaw 2002). The visual function of albino rats is abnormal, the RPE is abnormal and exposure of albino rats to excessive ambient light results in photoreceptor apoptosis. Pigmented rats are therefore more suitable for visual system research.

1.4.1.3. Rabbits

The rabbit eye (Figure 1.4.1.3.) is large in relation to body size. It has an axial length of 16-19mm, slightly smaller than the human eye. The average lens thickness is 7.6mm, more similar to rat than

human dimensions. Different to the human eye, rabbit retina has: (1) RPE that is irregular in size and arrangement (human has a regular hexagonal configuration); (2) longer and thinner rods and cones; (3) myelinated nerve fibres in the retina, forming nasal and temporal crescents about the optic disc. The retinal arteries and veins supply only the retina below the myelinated fibres; the remainder of the retina is avascular (merangiotic) (Gwon 2008).

The peak density of rods is 300,000 /mm^2 (Famiglietti and Sharpe 1995). Rabbits do not have a macula but have cones concentrated in a "visual streak" (Famiglietti and Sharpe 1995). Approximately 5% of photoreceptors are cones in two classes – S and M (Famiglietti and Sharpe 1995), (De Monasterio 1978). The S cones are not collocated with medium wavelength cones (Famiglietti and Sharpe 1995), so dichromatic colour vision with colour opponency is limited (De Monasterio 1978).

Rabbit vitreous contains hyaluronic acid and collagen. The collagen fibres are thinner and less frequent than in humans (7nm *vs* 10-25nm), but attach the vitreous base to the ILM of the peripheral retina and the pars plana, spanning the ora serrata (similar to the arrangement in humans) (Sebag and Yee 2007), (Matsumoto, Blanks, and Ryan 1984).

1.4.1.4. Pigs

The porcine eye (Figure 1.4.1.4.) has an axial length of 22–23.9mm and a lens thickness of 6.75–7.4mm (Fatehee et al. 2011), (Sanchez, Martin, Ussa, and Fernandez-Bueno 2011), (Koopmans et al. 2004), (Wong, Koopmans, Terwee, and Kooijman 2007). The peak density of rods is 113,000 /mm^2 (Gerke, Hao, and Wong 1995). Pigs do not have a macula but, like rabbits, their cones are concentrated in a "visual streak," which contains capillaries but no arterioles or venules. Cones constitute approximately 20% of photoreceptors and have two visual pigments sensitive to short (blue) and medium (green) wavelength light (Simoens, De Schaepdrijver, and Lauwers 1992), (Hendrickson and Hicks 2002).

The vitreous base is most firmly attached to the pars plana. The attachment is widest temporally, where it is confined to the pars plana, which is also widest temporally, as in the human eye. Nasally, a thinner attachment spans the ora serrata to attach to pars plana and retina (Weidenthal and Schepens 1966). The concentrations of both hyaluronic acid and collagen are half that of the human vitreous (Sebag and Yee 2007).

1.4.1.5. Primates

Primate species have a great variation in eye size and structure. Diurnal rhesus monkeys have a peak rod density of 180,000 /mm^2 and a larger cell size, whilst smaller nocturnal primates have higher peak rod densities and correspondingly smaller rod photoreceptors. For example, peak rod density is 325,000 /mm^2 in the owl monkey and 450,000 /mm^2 in the bushbaby (Wikler and Rakic 1990). The majority of primates possess a macula and fovea and all have rod dominant retinae. Old World monkeys and great apes have three classes of cone with trichromatic colour vision and a fovea centralis (Jacobs 1998). New World monkeys are highly polymorphic, though all – except the owl monkey – have a fovea with a high cone concentration (Jacobs 2008), (Dyer et al. 2009). Inheritance of photopigment genes in New World monkeys (except the trichomatic Howler monkey (Jacobs 1998)) is by two genes on the X chromosome, so females may have variants of trichromatic vision, whereas males have only dichromatic vision (Jacobs 2008). The nocturnal owl monkey lacks a fovea centralis and has only one class of cone, giving monochromatic vision (Hamasaki 1967), (Dyer et al. 2009).

The rhesus monkey has vitreal constituents in the same concentrations as the human (though hyaluronic acid is half the molecular weight of human), whereas the owl monkey has a higher concentration of hyaluronic acid and no collagen (Sebag and Yee 2007). The cynomalous monkey has an internal limiting membrane whose thickness varies in the same way as in the human – being thinner at the fovea – and also shows vitreous syneresis (age related liquefaction) in a similar fashion to humans (Matsumoto, Blanks, and Ryan 1984). The vitreous body of the rhesus monkey has

collagenous attachments to the pars plana, though this circumferential band of attachment is only one sixth the antero-posterior thickness found in the human (Lutjen-Drecoll et al. 2010).

1.4.2.Neuroretinal Cell Death

Necrosis is uncontrolled and causes inflammation as inflammatory cells phagocytose the cellular remains. Cells undergo necrosis when an insult damages their structural integrity, as in trauma, gross ischaemia and excitoxicity. Apoptosis ensues after stress or injury and as part of normal development or tissue functions, e.g. T cell death in the adult thymus. Apoptosis can be precipitated by DNA damage causing activation of p53, withdrawal of growth factors, stimulation by neighbouring cells, activation of Fas receptor by T cells and traumatic damage of a lesser severity than induces necrosis. Different stimuli cause apoptosis through different routes and different cell types have different mechanisms (Pradelli, Beneteau, and Ricci 2010).

1.4.2.1. Morphological classifications of cell death

There is no binary distinction between apoptosis and necrosis though, rather both lie at opposite ends of a spectrum. Programmed cell death in development may not display features of apoptosis and necrosis may be regulated by cell death signalling pathways (Nicotera, Leist, and Manzo 1999), (Galluzzi et al. 2012). Cell death may be mediated by number of different overlapping molecular signalling pathways, giving rise to a variety of morphological features that may be termed apoptotic, necrotic or neither.

Apoptosis is characterised by cell and nuclear shrinkage, chromatin condensations (typically at the nuclear periphery), nuclear blebbing and cytoplasmic blebbing with the formation of apoptotic bodies in the presence of intact cellular organelles such as mitochondria and endoplasmic reticulum and enclosed by an intact plasma membrane (Elmore 2007). Necrotic cell death had a more diverse morphology, but is characterised by cellular swelling and swelling of organelles. The nucleus disintegrates late in the cell death process, but there may be chromatin condensation or karyolysis (chomatin dissolution). Due to leakage of cellular contents, local inflammation occurs with

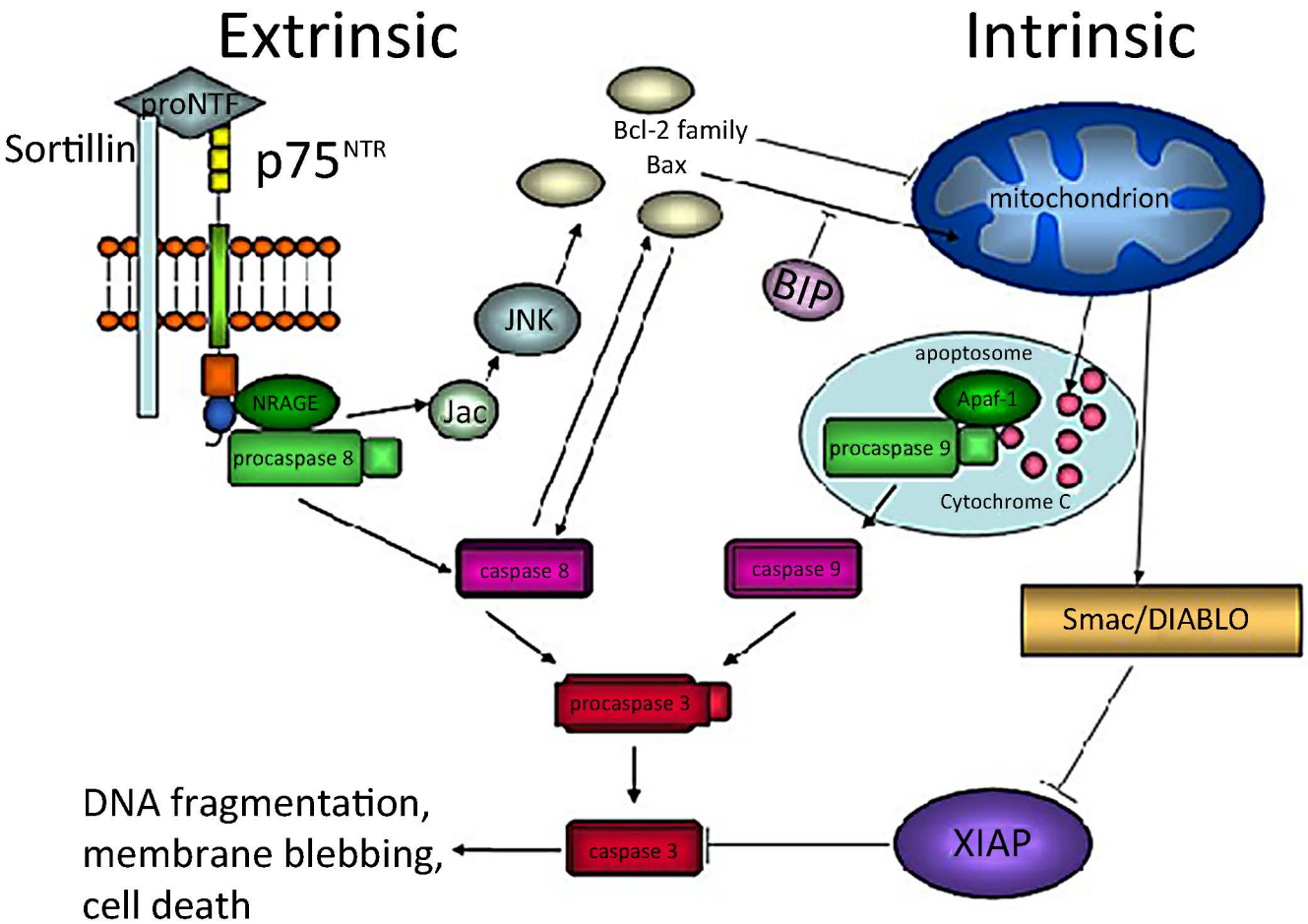

Figure 1.4.2. An outline of the main pathways of caspase dependent apoptosis (Berry et al. 2008). Sortillin complexes with the p75 neurotrophin receptor (NTR) to facilitate apoptosis in the extrinsic pathway. Neurotrophin receptor interacting melanoma-associated antigen homolog (NRAGE) is a p75 Intracellular binding partner that facilitates apoptosis through caspase 8 and c-Jun N-terminal kinase (JNK).

inflammatory cell infiltration. Necrosis may be autophagic, when cytoplasmic vacuoles filled with cellular contents are formed, or non-lysosomal, when there is no vacuolation (Ziegler and Groscurth 2004).

1.4.2.2. Molecular classifications of cell death

Factors that precipitate and prevent apoptosis are constitutively expressed and present in the cytosol. Most are present in inactive form and there is usually a balance between the pro- and anti-apoptotic factors. Stimulation of apoptosis often inhibits the function of inhibitors of apoptosis (IAPs) or upregulates or activates pro-apoptotic factors. The main route for apoptosis is through the caspase enzymes (Figure 1.4.3.2.1.), so called because they have cysteine in their active site and cleave target molecules at aspartate residues. Caspases can be activated by cleavage from pro-enzymes, oligomerisation and the formation of an apoptosome.

1.4.2.3. Mitochondria and the intrinsic pathway

Apoptosis may occur through either intrinsic or extrinsic pathways. Mitochondria are central to the cell death pathways:

1) They provide energy through oxidative phosphorylation, without which cells die.

2) They initiate apoptosis by releasing proapoptotic proteins.

3) They generate reactive oxygen species and nitric oxide.

4) They regulate the intrinsic pathway to apoptosis by controlling the redox state of cytochrome C.

5) They contribute to cellular calcium homeostasis.

Permeabilisation of mitochrondria leads to cell death through release of cytochrome C, apoptosis inducing factor (AIF) and endonuclease G among others as well as decreased ATP production, all of which may be terminal events. Permeabilisation is controlled by Bcl-2 family proteins, being dependent on the presence of either one of Bak and Bax. The other Bcl-2 family members are either anti-apoptotic (inhibiting Bak, Bax and other pro-apoptotic Bcl-2 proteins) or proapoptotic (activating Bak and Bax or inhibiting the anti-apoptotic Bcl-2 family members). Bak and Bax are normally present in inactive form in the cytosol, but during apoptosis they translocate to the mitochondria and undergo conformational changes and oligomerisation, inserting into the mitochondrial plasma membrane to increase permeability either by acting as channels themselves or destabilising the lipid bilayer (Borutaite 2010). Bcl-2 family members are additionally present in the endoplasmic reticulum, where they influence calcium homeostasis (Borutaite 2010).

The state of membrane lipids also influences mitochondrial outer membrane permiabilisation (MOMP). For example, reactive oxygen species peroxidate cardiolipin in the inner and to a lesser extent outer membranes affecting membrane interactions with Bax and Bak (Borutaite 2010). Mitochondrial membrane permeability is also increased (and mitochondrial ATP production

decreased) by the opening of non-specific channels in response to elevated intracellular calcium, called mitochondrial permeability transition pores (MPTP), which are permeable to small molecules and electrolytes. MPTP therefore allows water and electrolytes to move whilst trapping proteins, which causes swelling and ultimately rupture of mitochondria (Borutaite 2010).

MOMP releases cytochrome C, apoptosis activating factor 1 (Apaf-1), second mitochondrial-derived activator of caspases (smac/DIABLO) and serine protease high temperature requirement protein 2 (HtrA2/Omi) into the cytoplasm. In the cytosol, oxidised cytochrome C complexes with apaf-1 to form an apoptosome that binds and activates pro-caspase 9, which initiates the intrinsic pathway to apoptosis and activates downstream mediators and executioner caspases. The intrinsic pathway is activated by stimuli such as DNA damage, viral infection and growth factor deprivation and regulated by Bcl-2 proteins. Several IAP provide additional regulation and can even prevent apoptosis in the presence of activated executioner caspases.

smac/DIABLO and HtrA2 inhibit endogenous IAPs, promoting caspase activation (Borutaite 2010). Mitochondrial release of AIF and endonuclease G , which translocate to the nucleus causing caspase-independent cell death (Susin et al. 1999), is dependent on caspase activity (Arnoult et al. 2003). In addition to releasing cytochrome C, mitochondria also control its redox state – oxidisation being necessary for its pro-apoptotic activity (Borutaite 2010). Prevention of MOMP by knockout of Bcl-2 family proteins makes cells resistant to a wide variety of death stimuli (Pradelli, Beneteau, and Ricci 2010).

1.4.2.4. The extrinsic and other pathways

The extrinsic system is activated by cell surface receptors such as the Fas receptor, which activates Fas-associated death domain protein (FADD) which activates caspase 8. Caspase 8 and 9 are initiator caspases. Executioner caspases act downsteam of the initiator casapses and directly trigger cell death. The executioner caspases are 3, 6 and 7 and their targets include enzymes involved in cell cycle control, DNA repair, cytoskeletal assembly and other caspases, which creates feedback loops.

Caspase 2 has structural similarities to the initiator caspases, but substrate specificities similar to the executioner caspases. The exact role of caspase 2 is unclear though it may allow a mitochondria-independent intrinsic pathway (Troy and Ribe 2008).

In some cells during extrinsic apoptosis, caspase 8 directly activates caspase 3, whilst in others it mediates BH3-interacting domain death agonist (BID) cleavage to truncated-BID (tBID), which induces MOMP.

Troy et al. (1997) showed that caspase 2 is necessary for apoptosis caused by growth factor withdrawal but not oxidative stress in PC12 (rat pheochromocytoma) cells and Troy et al. (1996) showed IL-1β (activated by caspase 1) was necessary for apoptosis induced by copper/zinc superoxide dismutase downregulation but not by withdrawal of trophic factor support (though both were caspase-dependent). Thus, in the same cell line different stimuli result in apoptosis mediated by different caspases (Troy et al. 1996), (Troy, Stefanis, Greene, and Shelanski 1997).

Calpains are calcium-activated non-lysosomal (cytosolic) cysteine proteases that are implicated in apoptosis and necrosis. There a number of calpain-family proteins, of which μ- and m-calpain (calpain 1 and 2) are the best characterised. In apoptosis and necrosis, calpains cleave structural proteins including non-erythrocytic α2 spectrin into fragments of specific size distinct from those produced by caspase activity (Zhang et al. 2009b).

Receptor interacting protein kinase 1 (RIP1) is recruited by the death domain of the Fas receptor to form part of a death-inducing signaling complex (DISC) that regulates caspase-8, as part of the extrinsic apoptosic pathway (Galluzzi et al. 2012). In addition, RIP1 is ubiquitinated by cellular inhibitors of apoptosis to activate transcription factor (nuclear factor) NF-κβ and increase cell susceptibility to extrinsic apoptosis. However, RIP1 is also implicated in necroptic cell death precipitated by caspase inhibition, when its inhibition prevented necrosis (Trichonas et al. 2010).

1.4.3.Retinal Response to Closed Globe Injury

1.4.3.1. Commotio Retinae

Commotio retinae has been induced in pigs, rabbits, cats and rhesus and owl monkeys, by a projectile fired from either a modified air pistol or a catapult (Blight and Hart 1977), (Hart, Blight, Cooper, and Papakostopoulos 1975), (Blight and Hart 1978), (Gregor and Ryan 1982a), (Hui et al. 1993), (Bunt-Milam, Black, and Bensinger 1986), (Kohno et al. 1983), (Sipperley, Quigley, and Gass 1978). The energies and impact sites are summarised in Table 1.4.2.1. The report of Hui et al (1993; Table 1.4.2.1.) is unusual in reporting a very high impact energy. However, Scott et al. showed that a high velocity impact of a low weight projectile created more injury than a low velocity impact from a heavy projectile, despite similar kinetic energy (Scott, Lloyd, Benedict, and Meredith 2000).

The main finding in animal studies of commotio retinae is traumatic disruption of the photoreceptor OS (Hart, Blight, Cooper, and Papakostopoulos 1975), (Blight and Hart 1977), (Blight and Hart 1978), (Bunt-Milam, Black, and Bensinger 1986), (Kohno et al. 1983), (Sipperley, Quigley, and Gass 1978), consistent with optical coherence tomography findings in humans and reversible loss of cone pigment on fundus reflection densitometry (Meyer, Rodrigues, and Mennel 2003), (Liem, Keunen, and van Norren 1995), (Sony, Venkatesh, Gadaginamath, and Garg 2006). The RPE phagocytoses the OS and becomes a multilayered disorganised structure, that, in some cases, directly apposes the photoreceptor IS (Sipperley, Quigley, and Gass 1978). Outer retinal damage explains the clinical finding of reduced vision.

The evidence about BRB disruption in commotio retinae from porcine, feline and lapine studies conflicts with the human data. A normal fluorescein angiogram has been reported (Sipperley, Quigley, and Gass 1978), (Pulido and Blair 1987), (Hart and Frank 1975), but disruption of the BRB, at the level of the RPE has been shown with horseradish peroxidase and lanthanum (Gregor and Ryan 1982a), (Bunt-Milam, Black, and Bensinger 1986), (Hui et al. 1993). In a rabbit model, fluorescein angiography demonstrated an intact BRB but leakage from choroidal vessels using intrachoroidal

indocyanine green (Miki, Kitashoji, and Kohno 1992). This is consistent with some clinical findings in humans (Kohno, Miki, and Hayashi 1998), but the relevance may be limited because of the merangiotic rabbit retina. Intracellular oedema of Müller cell processes and axons in the RNFL and photoreceptors has been documented (Kohno et al. 1983), (Blight and Hart 1977), (Blight and Hart 1978), (Hart, Blight, Cooper, and Papakostopoulos 1975), (Dean Hart and Blight 1978), but no extracellular oedema, which would be expected with BRB disruption. The axonal oedema resolves within 4 hr and the glial oedema in 2-3 d (Hart and Blight 1979b). Axonal and glial oedema are probably responsible for the white retinal appearance seen on clinical examination.

Regeneration of photoreceptor OS begins at 1 week and continues for at least 2 months (Blight and Hart 1977), (Blight and Hart 1978), (Bunt-Milam, Black, and Bensinger 1986). This may explain the course of visual recovery. Photoreceptors die by necrosis and apoptosis detected by nuclear changes and TUNEL staining (Sipperley, Quigley, and Gass 1978), (An, Zhang, and Zhang 2004). Argyrophilia has been reported in unspecified retinal cells in a rabbit model (Antelava 1969). Argyrophillia is an early sign of compromised neurons that may later die by either apoptotic or necrotic routes (Gallyas, Zoltay, and Dames 1992), (Gallyas, Hsu, and Buzsaki 1993). The intrinsic and extrinsic mechanisms of cell death or regeneration have not been reported in these (Table 1.4.2.1.) models.

Group	Animal	Impact Site	Energy	Velocity	Weight	Injuries Reported
Blight and Hart (Blight and Hart 1977), (Hart, Blight, Cooper, and Papakostopoulos 1975), (Blight and Hart 1978), (Hart and Blight 1979a)	10-30kg store pigs	Nasal sclera over ora serrate	0.49-0.78J	50-64m/s	0.38g	Retinal breaks, choroidal rupture and RPE disruption at lower energy. Commotio retinae at >0.68J.
Gregor and Ryan (Gregor and Ryan 1982a)	11-27kg domestic pig	Lateral sclera over pars plana	0.32J	33m/s	0.57g	Commotio retinae, vitreous haemorrhage, no retinal breaks/dialyses.
Latanza et al (Latanza et al. 1988)	Rabbit	Lateral sclera over retina	0.57J	**46.8m/s**	*0.52g*	Retinal holes, commotio retinae, choroidal and vitreous haemorrhage.
Cox (Cox 1980)	Rabbit	Lateral sclera over retina	0.9-1.62J	58.8 – 79m/s	0.52g	Gross retinal damage with tears and necrosis and choroidal and vitreous haemorrhage with commotio retinae at lower energy. Globe rupture at higher energy.
Blight and Hart (Hart and Blight 1979a)	10-30kg store pigs	Nasal sclera over ora serrata	1.9J	100m/s	0.38g	Complete absence of neuroretina at impact site. Choroidal rupture, dispersed RPE, ciliary epithelial detachment.
Sipperley et al (Sipperley, Quigley, and Gass 1978)	Owl monkeys	Central cornea	**0.39-1.05J**	47m/s	**0.35-0.95g**	Commotio retinae only.
Bunt-Milam et al (Bunt-Milam, Black, and Bensinger 1986)	Cat	Central cornea	**0.44J**	50m/s	0.35g	Commotio retinae, variable hyphaema.
Blight and Hart (Hart and Blight 1979a)	10-30kg store pigs	Central cornea	0.49-1.9J	50-100m/s	0.38g	No injury at lower energy. Dialysis in 50% at higher energy.
Gregor and Ryan (Gregor and Ryan 1982a)	30kg domestic pig	Paracentral cornea	1.25J	52.3m/s	0.95g	Commotio retinae, RPE disruption, RPE and retinal detachment.
Hui et al (Hui et al. 1993)	Rabbit	Central cornea	2.87J	**18.9m/s**	16g	Commotio retinae only.

Table 1.4.2.1. Animal models of retinal injury induced by blunt ocular trauma. Bold figures are estimated or calculated from the material in the published paper; n/a = not available

Multiple mechanisms of injury are used in animal studies of commotio retinae. Some studies report central corneal trauma, whilst others report lateral scleral injury (Table 1.4.2.1.). Clinically, direct scleral injury is associated with chorioretinitis sclopetaria in which the retina is severely disrupted and retinal haemorrhages, holes and detachments are present that ultimately scar, but do not detach (Hart, Natsikos, Raistrick, and Doran 1980). The features of injury seen by electron microscopy are similar in both central corneal and scleral impact models and are consistent with those of commotio retinae. It is likely that chorioretinitis sclopetaria occurs with higher energy impacts only.

1.4.3.2. Retinal Tears and Dialyses

Deformation of the globe along the sagittal axis (long axis) during blunt trauma causes disinsertion of the retina at the ora serata (a retinal dialysis) and retinal tears. Delori et al. (1969) injured enucleated pig eyes embedded in gelatin with projectile impacts to the central cornea of 0.345g travelling at 62.3m/s and reduced axial length from 20.7 to 12.2 mm (41%) (Delori, Pomerantzeff, and Cox 1969). They did not report lens size, but speculated that during injury, the corneal endothelium would be in contact with the lens. Taking pig axial lens length as 6.75mm (Koopmans et al. 2004), there would be approximately 3.5mm between the retina and posterior surface of the lens at the point of greatest compression. This is less than the 3.9mm anterior chamber depth and corneolenticular contact is certain (Sanchez, Martin, Ussa, and Fernandez-Bueno 2011). With a lateral scleral impact in pigs, given that in coronal section the lens lies centrally instead of anteriorly in both axial and sagittal sections, the retina will impact the lens with a 40% deformation.

Weidenthal and Schepens (1966) supported the theory that retinal tears and dialyses are caused by deformation of the globe. They injured enucleated pig eyes with a central corneal ball bearing impact (0.76J) and supported the area between the ciliary body and equator by placing the eyes in a rigid plaster mould, which protected the nasal ora serrata from injury compared to the same injury within the orbit or using a flexible gelatin support (Weidenthal and Schepens 1966).

1.4.3.3. Blast injury

There is indirect evidence that ocular PBI is possible from the observed degeneration of RGC axons in the optic tracts following exposure of rats to a simulated blast in a “shock tube” and RGC apoptosis detected by terminal deoxynucleotidyl transferase-mediated dUTP nick end labelling (TUNEL) after exposure of rabbits’ eyes to firecrackers (Petras, Bauman, and Elsayed 1997), (Chen et al. 2003). However, neither experiment controlled for tertiary blast injury. In a model of air blast in dogs, orbital blow out fractures were demonstrated, almost certainly due to tertiary blast effects (Richmond, Pratt, and White 1962).

1.4.4.Retinal Response to Open Globe Injury

Injury	Animal	Cells affected	Response studied	Technical details
Incisonal retinal injury (Turner, Blair, and Chappell 1986)	Rat/mouse	Cells of all retinal layers near the wound	Cell death	Incision through sclera, choroid and retina, <1mm in length, closed with sutures.
Optic nerve crush (Berkelaar et al. 1994)	Rat/mouse	RGC	RGC apoptosis and axonal regeneration	Proximal injuries (0.5mm from globe) cause more aggressive cell death than distal (>8mm).
Optic nerve transection (Berkelaar et al. 1994)	Rat/mouse	RGC	RGC apoptosis	
Retinal detachment (Fisher, Lewis, Linberg, and Verardo 2005), (Fontainhas and Townes-Anderson 2011), (Lewis et al. 2010), (Zadro-Lamoureux et al. 2009), (Kayama et al. 2011), (Lewis et al. 2009)	Pig/cat/rat/mouse	Photoreceptors	Apoptosis, programmed necrosis, "deconstruction"	Detachment is created by subretinal injection of balanced salt solution (BSS) or hyaluronic acid (prevents reattachment) with/without vitrectomy and lensectomy. The cannula is introduced into the vitreous through a small pars plana/peripheral retinal sclerotomy and into the subretinal space.
		Bipolar, horizontal cells, RGC	Remodelling, neurite outgrowth	
		Müller cells, astrocytes	Gliosis	
	Rabbit	Photoreceptors, glia	Aggressive cell death, gliosis	
Intravenous sodium iodate (Burgi, Schaffner, and Seiler 2001)	Pig/rabbit/rat/mouse	RPE	Cell death and tissue regeneration	>10mg/kg is toxic in rats
Intraperitoneal N-methyl-N-nitrosourea (Wan et al. 2008), (Harada et al. 2011)		Photoreceptors		>15mg/kg is toxic in mice, 60mg/kg obliterates the outer nuclear layer
Intravitreal N methyl-D-asparate (Ohta, Ito, and Tanaka 2008)		RGC, amacrine cells		Dose dependent loss of RGC but wide variation in dosing
Phototoxicity (Organisciak and Vaughan 2010)	Rat/mouse	Photoreceptors, RPE	Apoptosis	Exposure to toxic light levels for minutes – days. Hours of exposure causes rod apoptosis; days causes RGC apoptosis.
Mechanical RPE debridement (Leonard et al. 1997), (Hayashi et al. 1999), (Valentino et al. 1995), (Kiilgaard et al. 2007)	Primate/pig/cat/rabbit	RPE	Tissue regeneration and scarring	A vitrectomy is performed through a pars plana incision and a retinal detachment created by subretinal BSS injection to expose RPE. Mechanical debridement is by abrasion with a silicone brush or tubing or tearing with forceps.
Hydraulic RPE debridement (Leonard et al. 1997)				

Table 1.4.3.2. Animal models used to study retinal injury responses.

1.4.4.1. Proliferative Vitreoretinopathy

In open globe injuries with vitreous loss that is managed conservatively, there is a high risk of developing intraocular fibrosis termed proliferative vitreoretinopathy (PVR). PVR is the endpoint of a number of disease processes and occurs most commonly after retinal detachment and surgical repair. A number of models of retinal injury have been designed to study PVR. *In vivo* models of PVR have been reviewed elsewhere (Agrawal et al. 2007).

Of the 27 existing models of PVR, four are primarily induced by posterior segment trauma and the rest by intravitreal injection of growth factors and/or cells including cultured fibroblasts and RPE cells (Agrawal et al. 2007), (Gregor and Ryan 1982b). In PVR after retinal injury, degeneration of photoreceptors and other retinal cells precedes scar formation (Topping, Abrams, and Machemer 1979), though inflammation and photoreceptor damage are associated with the retinal detachment (Gregor and Ryan 1982c). Most animal models of open globe retinal injury with time points longer than a few days are at high risk of PVR from posterior segment penetration with vitreous loss. In pigs, entering the posterior segment through the pars plana, abscising vitreous, injecting autologous blood and closing the wound with sutures causes PVR, with tractional retinal detachment by 2 weeks (Gregor and Ryan 1982b), (Gregor and Ryan 1983a). In the rhesus monkey, intracapsular lens extraction with reinjection of homogenised lens causes PVR, with fibrous ingrowth by 3 weeks (Cleary, Jarus, and Ryan 1980). PVR is avoided by vitrectomy at 1 or 14 d, though vitrectomy must be complete (Cleary and Ryan 1981), (Gregor and Ryan 1983b). In rabbits inhibiting matrix metalloproteinases 2, 3 and 9 and x-ray irradiation all prevent PVR (Chakravarthy, Maguire, and Archer 1986), (Chakravarthy et al. 1989), (Ozerdem et al. 2000), (Ozerdem et al. 2001).

In the rabbit, pars plana incision, intravitreal injection of autologous blood and vitreous lens admixture, and cryopexy, causes PVR (Westra et al. 1995), (Cleary and Ryan 1979). In the mouse, transcorneal excision of the lens and vitreous and peripheral retinal breaks causes PVR, with multilayered (RPE derived) fibroblasts expressing collagen VI as early as 1 week after injury (Saika et al. 2004). In the rat, serial limbal penetrations with a 27 guage needle has been documented to

create PVR (Bignami and Dahl 1979), though it is likely that there was undocumented intraocular injury, as in the rat an isolated limbal penetration would initially enter the anterior chamber.

1.4.4.2. Retinal Ganglion Cell Death and Axonal Regeneration

Optic nerve injury causes RGC axotomy, which is a closed globe injury. However, it is studied in the context of various surgical interventions – i.e. open globe injury – to manipulate retinal cell death and regeneration and many of the underlying molecular mechanisms are conserved throughout the CNS and retina.

Traumatic optic nerve injury is rarely recognised in civilians (Lee et al. 2010), but is damaged in up to 20% of military ocular trauma (Weichel et al. 2008), and traumatic optic neuropathy will often cause profound and intractable visual loss. The optic nerve represents a simple and readily accessible CNS tract to model the CNS response to injury. The response of RGC to axotomy caused by optic nerve injury has been extensively studied and reviewed (Cui, Yin, and Benowitz 2009), (Berry et al. 2008), (Benowitz and Yin 2010), (Chaum 2003). Intraorbital axotomy causes RGC to display transitory sprouting of proximal axon stumps, followed by apoptotic death in 90% by 14 d (Berkelaar et al. 1994). To restore or improve vision in patients with traumatic optic neuropathy, cell death must be prevented and RGC axonal regeneration promoted.

In murine models, optic nerve axotomy is caused without central retinal artery damage. In rats optic nerve transection causes a more aggressive pattern of RGC death than optic nerve crush, with differing transcriptional responses and susceptibility to the neuroprotective effects of neurotrophins (Agudo et al. 2008), (Parrilla-Reverter et al. 2009). Similarly, transection at greater distances from the eye result in more delayed and less extensive RGC death with a neuroprotective effect of brain derived neurotrophic factor (BDNF) demonstrable in distal injury only (Berkelaar et al. 1994), (Zhi et al. 2005). Therapeutic interventions to limit RGC loss and promote axonal regeneration such as neurotrophins, siRNA, shRNA and viral vectors encoding therapeutic molecules can be most easily

delivered by intravitreal injection, though viral transfection with retrograde axonal transport *via* the cut optic nerve stump has been reported (Kugler et al. 1999).

1.4.4.2.1. RGC Apoptosis

Apoptotic RGC death after axotomy is primarily caspase-dependent. Transient broad spectrum caspase inhibition by AAV-transduced p35 expression sustains RGC survival when p35 is no longer expressed (Kugler et al. 1999). In rats, z-DEVD-cmk inhibits activated executioner caspase 3 in the cytoplasm of apoptotic RGCs, rescuing up to 22% that would otherwise die (Kermer, Klocker, Labes, and Bahr 1998), (Kermer et al. 1999). The repulsive guidance molecule RGMa opposes caspase 3 dependent apoptotic cell death, by binding to its transmembrane receptor neogenin, and treatment with intravitreal RGMa rescues 26% of RGC (Koeberle et al. 2010). However, Kermer et al. (1999) did not use a cell marker for RGC, so activated caspase 3 in the RGC layer could be in glia and z-DEVD-cmk is not a completely specific caspase 3 inhibitor, so off-target effects are possible.

In contrast, after optic nerve crush and optic nerve transection in rats, Ahmed et al. (2011) found no activated caspase 3 in RGC or glia in the RGC layer, but specific localization of activated caspase 2 (both an initiator and an executioner) in RGC and cells of the inner nuclear layer (Ahmed et al. 2011), (Lamkanfi et al. 2002). In addition siRNA mediated knockdown of caspase 2 mRNA prevented cell death in almost 100% of RGC. Caspase 2 therefore seems to be necessary for axotomy-induced RGC death. Comparable efficacy of RGC rescue is achieved by AAV vector induced Bcl-X_L overexpression, emphasing the importance of mitochondrial permeabilisation in axotomy-induced RGC cell death (Malik, Shevtsova, Bahr, and Kugler 2005).

Upstream of the caspase pathways, a number of neurotrophic factors protect RGC from apoptosis after optic nerve injury in rats including BDNF, ciliary neurotrophic factor (CNTF), glial cell derived neurotrophic factor (GDNF), neurturin, neurotrophin-4 (NT-4), erythropoietin and inosine (Koeberle and Ball 1998), (Koeberle and Ball 2002), (Peinado-Ramon, Salvador, Villegas-Perez, and Vidal-Sanz 1996), (Hou et al. 2004). BDNF is temporarily neuroprotective for RGC after optic nerve transection

in rats (Mo et al. 2002), and acts through both the PI-3-kinase/Akt/mTOR (phosphatidylinositol 3-kinase/protein kinase B/mammalian Target Of Rapamycin) and the MEK/ERK (mitogen activated protein kinase/extracellular signal related kinase) tyrosine related kinase B (TrkB) receptor pathways (Klocker et al. 2000). The decrease in neuroprotective effect of BDκ is correlated with downregulation of its TrkB receptor and reversed by TrkB gene transfer by AAV vector (Cheng et al. 2002). CNTF is also RGC neuroprotective acting through the JAK/STAT (Janus kinase/signal tranducers and activators of transcription), MEK/ERK and the PI-3 kinase/Akt/mTOR pathways. Lentiviral CNTF gene transfer sustains RGC for up to 21 d (Park et al. 2004), (van Adel et al. 2003). Erythropoeitin is also RGC neuroprotective acting through the PI-3-kinase/pAkt/mTOR pathway (Weishaupt et al. 2004).

1.4.4.2.2. Axonal Regeneration

Many neurotrophic factors are axogenic as well as neuroprotective, however, the pro-regenerative mechanisms are distinct from the pro-survival (Ahmed et al. 2010). Glia have a prominent paradoxical role in either supporting or blocking axon regeneration. Activated glia in the retina and optic nerve produce multiple pro-regenerative neurotrophic factors (Ahmed et al. 2010), (Muller, Hauk, and Fischer 2007). However, reactive astrocytes in the optic nerve interact with invading fibroblasts to produce a glial scar, which contains proteoglycans that inhibit axon regeneration (Silver and Miller 2004). Nogo, a myelin-derived and Müller glial protein, and other myelin-derived inhibitors inhibit axon growth, acting through the Nogo-66 receptors to modulate GTPase Rho A and its downstream effector Rho-associated, coiled-coil containing protein kinase 1 (ROCK), and/or intracellular calcium levels (Sandvig et al. 2004), (Schwab 2010), (Wang, Chan, Taylor, and Chan 2008). Transfection with a dominant negative Nogo receptor enhances RGC axon regeneration, but only when combined with an activated growth state (Fischer, He, and Benowitz 2004).

PTEN (phosphatase and tensin homolog), SOCS3 (suppressor of cytokine signalling) and TSC1 (tuberous sclerosis complex 1) negatively regulate the mTOR pathway, and their deletion or

conditional knockout stimulates, while administration of the mTOR inhibitor rapamycin reduces RGC survival and axon regeneration (Park et al. 2008), (Smith et al. 2009).

1.4.4.2.3. Inflammation

RGC death is reduced and axonal regeneration induced after optic nerve injury by a number of inflammatory stimuli, including lens injury, intravitreal injection of zymosan (macrophage activating and chemoattractant) and intravitreal peripheral nerve grafting (Leon et al. 2000), (Cui, Yin, and Benowitz 2009), (Berry, Carlile, and Hunter 1996), (Berry et al. 1999), (Berry et al. 2008), though not by retinal injury alone (Fischer, Pavlidis, and Thanos 2000). Peripheral nerve grafts protect other retinal cells as well, preventing retinal die-back around the edge of transcleral incisions, whereas tendon and nerve sheath implants, which also cause inflammation, do not (Turner, Blair, and Chappell 1986). Peripheral nerve grafts secrete gp130 cytokines (such as CTNF and leukaemia inhibitory factor (LIF)), which may contribute to the neurotrophic effects (Turner, Blair, and Chappell 1986), (Jo, Wang, and Benowitz 1999), (Lorber, Berry, and Logan 2008). In rats, lens injury and intravitreal zymosan injection induce retinal astrocytes and Müller cells to release CNTF, which acts through the JAK/STAT3 pathway to promote axon regeneration (Muller, Hauk, and Fischer 2007), and Müller cell-derived factors may be essential for zymosan-induced axonal regeneration (Ahmed et al. 2010). The neurotrophic effects of intravitreally implanted peripheral nerve and lens tissue are enhanced by activated macrophages (Lorber, Berry, and Logan 2008).

Macrophages have multiple phenotypes with a variety of functions. “M2” type macrophages are pro-regenerative, whilst the “M1” type are neurotoxic in spinal cord organotypic cultures (Kigerl et al. 2009). Neurotoxic M1 macrophages may explain the apparently contradictory results of Thanos et al. (1993) who found increased RGC survival in rats after intravitreal macrophage inhibitory factor injections and decreased survival with macrophage stimulating factor in the optic nerve transection model (Thanos, Mey, and Wild 1993). Macrophages release the calcium binding protein oncomodulin, which acts through intracellular mammalian sterile 20-like kinase-3b (Mst3b), requiring high levels of cAMP to promote RGC survival and axon regeneration (Yin et al. 2006), (Lorber, Howe,

Benowitz, and Irwin 2009). The underlying mechanisms of RGC axonal regeneration in the peripheral nerve graft and lens injury models remain controversial.

The JAK/STAT, MEK/ERK and the PI3-kinase/Akt/mTOR intracellular signalling pathways are all important mediators of RGC neuroprotection. Though inhibition of these pathways abolishes the neuroprotective effects of different neurotrophins after optic nerve crush, their inhibition can also be neuroprotective and pro-regenerative (Park et al. 2004), an effect dependent on activated macrophages for the JAK/STAT and PI-3 kinase/Akt/mTOR pathways and independent of them for the MEK/ERK pathway (Luo et al. 2007).

1.4.4.3. Photoreceptor Cell Death and Retinal Remodelling

Animal models of open globe injury, used to study retinal cell death and tissue regeneration, damage the retina by incision, excision or abrasion and photoreceptor death also occurs in other – non-trauma – models (Table 1.4.3.2.).

Death of non-RGC retinal components has been little studied in models of trauma. Photoreceptor apoptosis occurs in closed globe injury and cells of all retinal layers die adjacent to penetrating wounds (Table 1.4.3.2.) (Sipperley, Quigley, and Gass 1978), (Turner, Blair, and Chappell 1986). In rats, fibroblast growth factor receptor (FGFR1) is upregulated in photoreceptors and fibroblast growth factor 2 (FGF-2), CNTF and pigment epithelium-derived factor (PEDF) are released within hours of penetrating injury and retinal detachment (Ozaki, Radeke, and Anderson 2000), (Penn et al. 2006), (Wen et al. 1995). FGF-2 and CNTF reduce photoreceptor apoptosis in other models of photoreceptor degeneration (Chaum 2003).

1.4.4.3.1. Retinal Detachment

Retinal detachment induced by subretinal hyaluronic acid infusion models the outer retinal damage and ischemia components of the injury response (Table 1.4.3.2.). Reattachment can be achieved by vitrectomy and fluid-gas exchange (Fisher, Lewis, Linberg, and Verardo 2005).

Photoreceptor OS are disrupted by detachment and in most models 20% die after 3 d, rising to 50% with longstanding detachment. In the rabbit retina, all photoreceptors die, as do cells of the inner retina (Fisher, Lewis, Linberg, and Verardo 2005). After retinal detachment in rats, 60% of photoreceptors die by apoptosis, the remainder by programmed necrosis dependent on RIP kinases (Trichonas et al. 2010). Caspase 3 and 9 activity are increased by retinal detachment and intrinsic pathway inhibition by AAV-transduced X-linked inhibitor of apoptosis (XIAP) over-expression or heat shock protein (HSP70) downregulation of the mTOR pathway partially protects photoreceptors after detachment. Extrinsic pathway inhibition by Fas receptor or TNF-α blockade or TNF-α knockout and caspase-independant pathway knockdown by apoptosis inducing factor-deficiency also protect photoreceptors from detachment-induced apoptosis (Zadro-Lamoureux et al. 2009), (Kayama et al. 2011), (Besirli, Chinskey, Zheng, and Zacks 2010), (Hisatomi et al. 2008), (Nakazawa et al. 2011), (Zacks et al. 2003). Thus all regulated cell death pathways are implicated, but complete photoreceptor protection has not yet been achieved in any study.

Retinal remodelling is a significant component of the response to detachment. Photoreceptor OS shorten within days (deconstruction) and mitochondria redistribute from the IS to the cell body (Fisher, Lewis, Linberg, and Verardo 2005). Rods show RhoA-dependent retraction of their axons from the outer plexiform layer (OPL) but maintain outer segment protein synthesis (Fontainhas and Townes-Anderson 2011). Cone synapses remain in the OPL but, by 7 d after detachment, cone-specific protein expression is undetectable by immunohistochemistry (Fisher, Lewis, Linberg, and Verardo 2005). Rod bipolar cells remodel leaving fewer dendrites, some innervating retracted rod synapses in the outer nuclear layer (Fisher, Lewis, Linberg, and Verardo 2005).

After retinal detachment, horizontal cells and RGC extend neurites throughout the retina and into the subretinal space (Fisher, Lewis, Linberg, and Verardo 2005). RPE cells proliferate and migrate in the subretinal space or onto the inner retinal surface (Fisher, Lewis, Linberg, and Verardo 2005). Müller cells proliferate, positively regulated by the mTOR pathway, and upregulate intermediate filament proteins, including GFAP, vimentin, nestin and synemin, extend thickened processes and

migrate through the retina, into the subretinal space, along the epiretinal surface and (after reattachment) into the vitreous to form gliotic scars (Lewis et al. 2010), (Lewis et al. 2009), (Luna et al. 2010). Astrocytes also proliferate and, along with Müller and RPE cells and RGC and horizontal cell neurites are found in epiretinal membranes after reattachment (Fisher, Lewis, Linberg, and Verardo 2005).

Retinal function after reattachment is reduced by altered synaptic connectivity, photoreceptor apoptosis and imperfect outer segment regeneration (especially cones), and is further impaired by subretinal scarring (Fisher, Lewis, Linberg, and Verardo 2005).

1.4.4.3.2. Phototoxicity

Light damage is commonly used to induce photoreceptor apoptosis and model retinal degenerative diseases and caspases 1, 3, 7, 8, and 9 and calpain have been implicated in light damage models. In some models, caspase 3 inhibition protects against light damage; in others activated caspase 3 is not found at all. DNA fragmentation occurs within hours of exposure and so may to be a direct effect of reactive oxygen species created by photopigment bleaching. Neuronal nitric oxide (NO) synthase inhibition reduces photoreceptor apoptosis after phototoxicity (NO has been reported to inhibit caspases by S-nitrosylation and to activate caspase 9), though without improving photoreceptor function, and NO increases neuronal necrosis in the rat brain (Organisciak and Vaughan 2010).

In an adult albino zebrafish model of light damage, prior application of CNTF prevents apoptosis of photoreceptors through a MAPK/ERK (mitogen activated protein kinase/extracellular signal regulated kinase) pathway and stimulates neuronal progenitor cell proliferation through a STAT3 dependent pathway (Kassen et al. 2009).

Faktorovich et al. (1992) studied the effects of intravitreal FGF-2 and PBS injections in albino rats subjected to either cyclic light or 1-2 weeks constant light exposure and then observed for up to 10 d, which is the turnover time of a rod outer segment in the rat (Faktorovich et al. 1992), (Lim, Umapathy, Baharuddin, and Zubaidah 2011). They found that intravitreal and subretinal FGF-2 and

subretinal (though not intravitreal) PBS injections protected photoreceptors from light induced cell death and resulted in greater regeneration of photoreceptor IS and OS, suggesting that either injury or inflammation induced neurotrophin release.

The intimate functional and structural relationship between photoreceptors and RPE links death and dysfunction of one to death and dysfunction of the other. The phototoxicity model highlights the relationship between the photoreceptors and RPE. The wavelength of maximal sensitivity to light damage in rods corresponds to the peak in the absorption spectrum of rhodopsin. Retinaldehyde (the light sensitive component) is present in both rod rhodopsin and in RPE cells in bis-retinaldehyde-phophatidylethanolamine (A2E), which is generated in the cycling and regeneration of visual pigments through the RPE. The absorption spectrum of A2E is slightly different from rhodopsin and preferentially absorbs higher energy blue light, increasing the likelihood of RPE damage, particularly after photoreceptor outer segment damage from a first light exposure with subsequent phagocytosis of damaged discs by the RPE and generation of A2E. In addition, there is a delayed effect with RPE damage and apoptosis occurring 5-10 hr after a broad spectrum light injury. RPE damage is more pronounced in rats reared in darkness than cyclic light (which induces greater concentrations of rhodopsin in rods). The mechanism of RPE damage is hypothesised to be oxidative stress on the RPE from light damaged rod outer segment discs (Organisciak and Vaughan 2010).

1.4.4.3.3. Chemotoxicity

Intraperitoneal N-methyl-N-nitrosourea induces photoreceptor apoptosis because 7-methyldeoxyguanosine DNA adducts form in the nuclei of photoreceptors (Ogino et al. 1993). Caspase 2, 3, 7, 8 and 9 are described as not active in some reports but active in others, with neuroprotective effects demonstrated by caspase 3 inhibitor Ac-DEVD-CHO (Doonan, Donovan, and Cotter 2003), (Yoshizawa et al. 1999), (Yoshizawa et al. 2000).

1.4.4.3.4. Retinitis Pigmentosa

Retinitis pigmentosa is an inherited retinal degeneration in which photoreceptors are progressively lost. The Royal College of Surgeons (RCS) rat is a well-known retinitis pigmentosa model, in which caspase 1 and 2 staining colocate in a small proportion of TUNEL +ve cells and in which apoptosis, (quantified by the proportion of TUNEL +ve cells), is reduced by caspase 1 inhibition (Katai et al. 1999).

Calpain inhibition by the highly specific calpastatin peptide (CAST) reduces photoreceptor apoptosis in retinal explants and rd1 mice (another model of retinitis pigmentosa) (Paquet-Durand et al. 2010). Conversely, the non-specific calpain inhibitor CX295 decreases cell death over the short term and increases cell death over the long term in retinal explants (Paquet-Durand et al. 2010). Calpain activates caspase 9 (intrinsic pathway) and caspase 3 may be the executioner (Sharma and Rohrer 2004). However, as caspase 3 inhibition is less effective than calpain inhibition in the 661W cone cell line, other pathways may be involved (Sharma and Rohrer 2004).

1.4.4.3.5. Photoreceptor Death In Vitro

In the cone photoreceptor cell line 661W, after growth factor deprivation caspase 3, 9 and 12 and m-calpain are activated and inhibition of caspase and calpain pathways in isolation reduces, but does not prevent, apoptosis (Gomez-Vicente, Donovan, and Cotter 2005).

After apoptosis induction by anti-human FAS ligand and UV irradiation, broad spectrum caspase inhibitors DEVD-CHO (inhibits caspase-3, -7, -1 and -4), zVAD-fmk (inhibits caspases-3, -6, -8, -1, -2 and -4) and BD-fmk (inhibits all caspases) do not reduce apoptosis as assessed by annexin-V-FITC binding to externalised phosphatidylserine, and western blotting shows an absence of activated caspase 3 (Carmody and Cotter 2000). These results have been confirmed *in vivo* in albino Balb-c mice after light injury and N-methyl-N-nitrosourea (MNU) injection and in C3H/HEN rd mice (Doonan, Donovan, and Cotter 2003), (Donovan, Carmody, and Cotter 2001), along with an absence of activated caspase 2, 7, 8, 9 and cytochrome C release.

1.4.4.4. Retinal Tissue Regeneration and Gliosis

The adult zebrafish (Danio rerio) regenerates axons and neural tissue. A peripheral retinal population of stem cells at the ciliary margin, known as the circumferential germinal zone, continually generates new cells of all retinal layers except rods, which are generated from a separate stem cell population in the outer nuclear layer (Otteson and Hitchcock 2003). The mechanisms of RGC and photoreceptor replacement after injury have been extensively studied at the genetic and cellular levels in models of trauma such as excision of retina as well as light injury, chemotoxicity, heat injury and transgenic models of degeneration (Stenkamp 2007), (Morris, Scholz, and Fadool 2008), (Becker and Becker 2008). The Müller cells dedifferentiate to form multi-potent progenitor cells that can migrate through the retina to replenish different cell populations including rod and cone photoreceptors and RGC (Stenkamp 2007), (Morris, Scholz, and Fadool 2008), (Becker and Becker 2008). In embryonic chick and rat, excised retina regenerates from the RPE and members of the FGF family and insulin are important in this process (Park and Hollenberg 1993), (Klassen, Sakaguchi, and Young 2004).

The adult mammalian retina has a low regenerative potential. After incisional injury to the rat inner retinal surface, there is limited RGC axon regeneration in the nerve fibre layer (McConnell and Berry 1982). Implanted hippocampus-derived stem cells incorporate into the host retina at the site of injury and show evidence of neural and glial differentiation and synapse formation (Nishida et al. 2000).

After chemical injury to the mouse and rat retina, a small number of Müller glia migrate through the retina and enter the cell cycle, expressing the progenitor cell markers nestin, proliferating cell nuclear antigen (PCNA), Pax6, glial fibrillary acidic protein (GFAP) and the glial marker, glutamine synthetase (Ooto et al. 2004), (Wan et al. 2008), (Karl et al. 2008). Pax6 is a transcription factor found in embryonic progenitors and is a phenotypic marker for Müller cell-derived progenitor cells in zebrafish (Fischer and Bongini 2010), (Bernardos, Barthel, Meyers, and Raymond 2007), (Thummel et al. 2008).

Dedifferentiation occurs through cyclin D1 and D3 related pathways and is positively regulated by the Notch and Wnt (wingless-type MMTV integration site family) 3a/β-catenin protein signalling pathways (Wan et al. 2008), (Karl et al. 2008), (Das et al. 2006), (Osakada et al. 2007). In mice, reelin is upregulated in the GCL, INL and ONL after incisional retinal injury and may attract and direct stem cells to the injury-site; a similar role is reported in embryonic development (Pulido, Sugaya, Comstock, and Sugaya 2007). *N*-Methyl-*N*-nitrosourea induced photoreceptor degeneration stimulates glial progenitors to generate photoreceptors. This effect is enhanced by exogenous BDNF acting through the TrkB receptor (Wan et al. 2008), (Harada et al. 2011).

After intravitreal N-methyl-D-aspartate-induced excitotoxicity of the inner retina, Müller cells show spontaneous photoreceptor and bipolar cell neogenesis, the latter being enhanced by intravitreal retinoic acid and, under the influence of epidermal growth factor (EGF) or FGF-1 combined with insulin, generate amacrine cells (Karl et al. 2008), (Ooto et al. 2004). The proliferation of retinal glial progenitor cells may be opposed by transforming growth factor β (TGFβ) (Close, Gumuscu, and Reh 2005). There is limited evidence for a similar pattern of proliferation in explants taken from cynomolous monkeys (Osakada et al. 2007).

In a rabbit model, incisional retinal injury without RPE injury stimulates retinal glia to express PCNA, send processes into the vitreous and along the inner limiting membrane and form a scar (Miller, Miller, Patterson, and Ryan 1986), (Cullinane et al. 2002). Incisional retinal injury in the rat upregulates cell cycle-related transcription factors c-fos and jun-B in the INL and to a lesser extent the GCL, within 30 min, probably associated with a reactive Müller gliosis (Ohki et al. 1995), (Yoshida et al. 1995). GFAP is upregulated within 3 d of retinal detachment caused by retinal tearing with a needle, associated with growth of glial processes into the subretinal space and expression of the apoptotic genes: Bax, Caspase 3, Ctsl, Litaf, Tnfrsf21, Mx3, Apobec1, Vdac1, A2m and Spinc2 (Vazquez-Chona, Song, and Geisert, Jr. 2004). This transcriptional response to injury is generic across the CNS (Vazquez-Chona et al. 2005).

Thus, after injury, mammalian glia form scars and block regenerating axons, whereas zebrafish glia regenerate lost retinal tissue by neurogenesis. When stimulated by the application of endogenous neurotrophins, mammalian glia have a limited potential to regenerate lost tissue in the same manner as zebrafish, though not yet to the same extent.

1.4.4.4.1. RPE Regeneration

RPE is injured with and without excising the overlying neuroretina (Hayashi et al. 1999), by hydraulic RPE debridement, abrasion with a silicone brush and tubing and grasping it with forceps (Table 1.4.3.2.) (Lopez et al. 1995), (Leonard et al. 1997), (Hayashi et al. 1999), (Del Priore et al. 1995), (Valentino et al. 1995). In primates, pigs, rabbits and cats, in order to induce a model of RPE damage, with an intact neuroretina, the RPE is injured beneath a retinal detachment that is first created by subretinal balanced salt solution injection (Del Priore et al. 1995), (Kiilgaard et al. 2007), (Lopez et al. 1995), (Leonard et al. 1997), (Valentino et al. 1995). Hydraulic RPE debridement leaves Bruch's membrane intact; however, grasping the RPE with forceps and mechanical debridement with silicone tubing results in areas of damage to Bruch's membrane with concomitant damage to the choriocapillaris (Leonard et al. 1997), (Valentino et al. 1995).

After denudement, RPE cells surrounding the area of bare Bruch's membrane lose their polygonal shape and apical basal polarity, become hypopigmented, flattened, enlarged and fusiform (Heriot and Machemer 1992), (Oganesian et al. 1997), migrate to cover the defect and remain hypopigmented, even after 9 months (Valentino et al. 1995). RPE multilayering, with or without neuroretinal retinal folds and tubuloacinus formation, has been reported and in some areas the RPE is replaced by fibroblast-like cells (Leonard et al. 1997), (Oganesian et al. 1997). RPE cells proliferate after intravitreal FGF-2 injection (Kimizuka, Yamada, and Tamai 1997).

Raising a retinal detachment shears photoreceptor OS. The presence of regenerated or autografted RPE permits photoreceptor outer segment regeneration (Zhang et al. 2009a), though there is still loss of photoreceptor nuclei (Lopez et al. 1995), particularly cones (Del Priore et al. 1995). Where Bruch's

membrane and choriocapillaris are damaged, the RPE does not resurface the defect and the outer retina degenerates (Leonard et al. 1997), (Valentino et al. 1995). However, the RPE resurfaces an intact Bruch's membrane, whether or not the neuroretina overlies the defect (Hayashi et al. 1999), (Ozaki et al. 1997), but only forms a pigmented monolayer when the neuroretina is present (Ozaki et al. 1997). When RPE resurfacing is prevented by subretinal mitomycin C, both the outer retina and choriocapillaris degenerate (Del Priore et al. 1996).

Excision of rabbit retina and RPE (leaving Bruch's membrane intact) and laser photocoagulation in primates stimulates local cellular proliferation, as identified by ^{3}H methylthymidine autoradiography, with complete resurfacing of Bruch's membrane by 4 d (Heriot and Machemer 1992), (Smiddy et al. 1986), (Ozaki et al. 1997). In pigs, after isolated RPE removal, there is peripheral RPE proliferation identified by 5-bromo-2'-deoxyuridine incorporation, but not proliferation at the lesion site (Kiilgaard et al. 2007). Peripheral RPE cells have a higher proliferative capacity *in vitro* than central cells and proliferation is enhanced by subretinal amniotic membrane grafting (Kiilgaard et al. 2007). Peripheral RPE cells also proliferate remote from a laser-induced RPE lesion (von Leithner, Ciurtin, and Jeffery 2010). A small (10-15 cells/eye) peripheral population of dividing RPE cells exists in mature pigmented and albino rats, which could function as a pool of peripheral progenitor cells (Al-Hussaini et al. 2008).

1.4.5.Comparison of Models

Experimental models of human diseases are usually best performed in animals whose anatomy most closely approaches that of humans for the area of interest. The choice of species is also based on availability and a body of previous work that allows comparison, although the use of cats, dogs, primates and equidæ require special justification due to public concern (National Centre for the Replacement Refinement and Reduction of Animals in Research). The optimal species and models for different ocular injuries are summarised in Table 1.4.4.

Rabbits have a merangiotic retina, which confounds any comparison with human injuries when blood supply and vascular responses of the inner retina may be relevant. In commotio retinae, the long thin rabbit photoreceptor OS may affect their vulnerability to shearing forces. The structure of the rabbit vitreous body is similar to humans and rabbits may be a good model for studies of vitreous.

Mice and rats have a similar retinal cellular and vascular structure to humans. Their small size, ease of husbandry and genetic manipulation and a ready availability of antibodies for molecular studies renders them very attractive for models of ocular trauma. However, the commonly used albino rats have marked neuroretinal and functional visual abnormalities, which renders them less suitable for studies of RPE, photoreceptors and *in vivo* functional/behavioural testing than pigmented rats. The rodent eye has a different gross structure to that of humans, with a very large lens, making them less suitable for biomechanical trauma studies. Larger animals such as pigs and primates have ocular anatomy comparable to humans and few experimental disadvantages. Their use is limited by capital costs, husbandry and political/ethical objections.

Closed globe injury is achieved by moderate (20-50m/s) velocity impact, most commonly to sclera rather than central cornea. For such injuries the rabbit is the smallest model reported. A mouse or rat model would be ideal, but has not been reported, thus at present, porcine and primate models have precedence.

Rats and mice are suitable for open globe injury modelling. A relative advantage of larger animals is the ease of surgical access to intraocular structures. In cases where macular and foveal architecture are studied, primate models are the only choice, though, as rodents possess cones distributed throughout the retina (rather than concentrated at a fovea), cone responses to injury may be more effectively studied in these smaller animals.

RGC death and axonal regeneration are most commonly studied in murine models. Optic nerve transection causes the most aggressive RGC death; however, optic nerve crush has a greater potential for RGC axonal regeneration. Axonal regeneration is stimulated by a number of surgical

manipulations including lens injury, intravitreal peripheral nerve grafting, recruitment of activated macrophages by intravitreal zymosan and intravitreal neurotrophic factors. However, the combination of activated macrophages with other stimulatory factors, such as in lens injury and intravitreal peripheral nerve grafting, results in the most marked RGC axon regeneration.

Surgical open globe injuries are most commonly trans-scleral, which causes neurotrophin release and has a significant risk of complications such as PVR. Smaller wounds and an approach through the pars plana or even the anterior chamber reduce these problems and allow more precise retinal injuries to be created, for example injuring the retina without damaging the RPE. In models where prolonged survival is required, it is important either to avoid vitreous loss, or manage it appropriately to reduce the risk of PVR.

Research area	Animal	Model	Pros	Cons
Cell death and regeneration in closed globe injury	Pig	High velocity (20-60m/s) contusion	Similar ocular dimensions to humans and same cellular structure and vasculature.	Capital costs and husbandry.
Axotomy-induced RGC death and axonal regeneration	Mouse/Rat	Optic nerve crush +/- lens injury or intravitreal peripheral nerve grafting	Availability of specific inhibitors, antibodies and transgenic mice. Low capital costs and ease of husbandry.	None.
Neuroretinal cell death and regeneration in open globe injury	Mouse/Rat	Retinal excision through a pars plana approach	Availability of specific inhibitors, antibodies and transgenic mice. Low capital costs and ease of husbandry.	Technically challenging surgery in mice.
RPE repair and regeneration	Rabbit	RPE excision through a pars plana approach, under an induced retinal detachment +/- preservation of the overlying neuroretina	Similar anatomy of the RPE and outer retina and ocular dimensions to humans.	None.

Table 1.4.4. – Choice of species and models for ocular trauma research

1.5. Assessment of Retinal Function

A detailed reference text on electrophysiological assessment of retinal function is “Principles and Practice of Clinical Electrophysiology of Vision” by Heckenlively and Arden (2nd Ed. MIT Press, Cambridge MA, USA. 2006).

Light hyperpolarises photoreceptors, reducing neurotransmitter release and thus changing the polarisation of second order neurons (ON-centre and OFF-centre bipolar cells), ultimately generating an action potential in RGC axons in the optic nerve - a process termed visual phototransduction. The electrical activity of the retina is measured as small changes in voltage – the electrical potential difference – between the ocular surface and surrounding skin. In electroretinography, a minimum of three electrodes are placed: (1), on the front of the eye; (2), behind the eye and; (3), away from the eye. Voltage is measured between electrodes 1 and 2 and the system grounded to electrode 3.

Electrode 1 can be placed anywhere from the central cornea to the inferior conjunctival fornix and in human studies is usually a thin, low impedance, silver/nylon wire termed a Dawson, Trick, and Litzkow (DTL) electrode; other electrodes include gold foils placed in the inferior fornix, gold rings held in contact with the cornea and electrodes embedded in contact lenses. Electrical connection with the eye relies on the presence of an ionic fluid to couple the electrode with the cornea. In humans the tear film is usually sufficient; in animal research, where the electrode is placed centrally on the exposed cornea, a dilute solution of methylcellulose is usually applied and a contact lens used to cover the cornea/DTL fibres, preventing evaporation. The volume of fluid present has a significant effect, in that too low a volume does not allow coupling, whereas too high a volume increases impedance by grossly increasing the electrode area (so the effective electrode becomes a large pool of fluid in contact with the whole ocular surface). Impedance is a measure of the opposition to variable current flow and incorporates both resistance (magnitude of the opposition to the passage of electric current) and the phase shift - the extent to which current and voltage differ in timing, due for instance to the storage of electrical charge in the system (capacitance).

Electrode 2 is usually a skin electrode placed close behind the lateral canthus and may be either skin surface, connected by coupling gel, or a needle electrode inserted subdermally. The relative position of electrodes 1 and 2 has a critical effect on the voltage recorded.

In humans, electrode 3 is usually placed on centre of the forehead and in rodents, at the base of the tail.

1.5.1.The Electroretinogram (ERG)

A typical rat ERG (shown in Figure 1.5.1) is recorded from three electrodes – as describe above – after a short duration flash of light. The corneal voltage so recorded is a summed response of positive and negative component potentials originating from all retinal layers. However, different specific components of the waveform primarily reflect the activity of specific retinal cells.

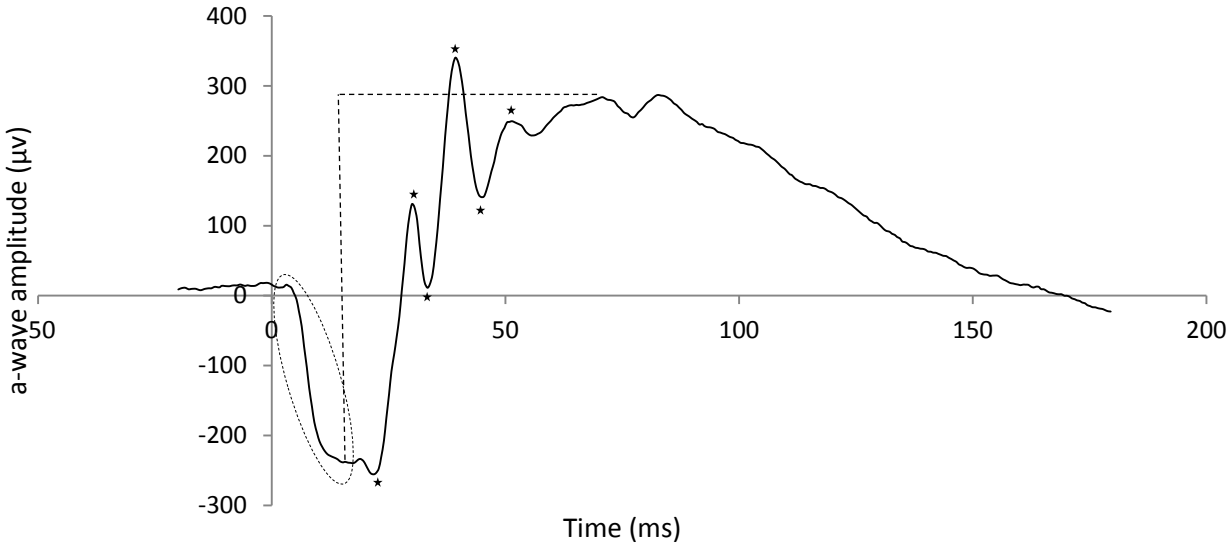

Figure 1.5.1. Typical rat ERG. The first negative deflection from baseline is the a-wave (circled). The b-wave amplitude is measured from the base of the a-wave (dotted lines). After the a-wave, on the rising edge of the b-wave, are high frequency, low amplitude, oscillatory potentials (stars), the precise cellular origins of which are unclear.

The first electrical response of the retina to incident light is photoreceptor hyperpolarisation, which is reflected as the negative (with respect to the cornea) a-wave. Approximately the first 70% of the

a-wave is generated by photoreceptors and the subsequent 30% by post-receptoral/downstream activation (e.g. OFF bipolar cells). However, the a-wave is usually curtailed by the onset of the positive b-wave. The b-wave is generated by the activity of second order neurons such as ON bipolar cells in the inner nuclear layer with a smaller contribution from Müller cells. The leading edge of the a-wave shows low voltage high frequency oscillations termed oscillatory potentials. These are more prominent in the rat (Figure 1.5.1.) than in humans. They are post-receptoral with the early components originating in the inner retina, though their exact retinal origins remain controversial.

The negative a-wave therefore reflects photoreceptor function and under scotopic (dark-adapted) conditions in humans and rats is dominated by rods, whilst under photopic (light-adapted) conditions, cones dominate. The other way in which cone function can be isolated is by a 30Hz flicker stimulus, which exceeds the temporal resolution of the rods. To ensure reproducible recordings, the extent of dark or light adaptation must be controlled – for scotopic ERG, rodents usually reach maximal dark adaptation in 40 min.

Photoreceptor function is assessed by measuring a-wave magnitude – baseline to trough – though such an assessment may be confounded by the b-wave, since conditions affecting b-wave latency may spuriously change a-wave magnitude. Alternatively, the leading edge of the a-wave may be modelled to predict the final amplitude that would be seen were the ERG “electronegative” (lacking a post-receptoral response) or, more simply, the gradient of the a-wave’s leading edge may be measured. Similarly, b-wave amplitude measured from the base of the a-wave to the peak of the b-wave measures mostly ON bipolar cell function, but is dependent on the magnitude of the photoreceptor response because: (1), being measured from the base of the a-wave, it incorporates this response and; (2), second order bipolar cells only generate electrical potentials in response to photoreceptor activity.

1.6. Aims and Hypotheses

1.6.1. Summary Rationale

Commotio retinae occurs after blast injury in the military or assaults in civilians. Ocular PBI may or may not exist; however, of those cases in which it is suspected clinically, commotio retinae is the most common manifestation.

Ocular trauma is common and retinal injury is the most common cause of post-traumatic loss of vision. Blunt ocular trauma causes commotio retinae, however the prognosis and outcomes are poorly defined. The cell death pathways activated in commotio retinae have not been previously studied. There are no pharmacological interventions currently available in the clinical setting that improve outcome after commotio retinae or retinal injury in general.

In commotio retinae there is damage to photoreceptor OS and some evidence of photoreceptor cell death. In other models of photoreceptor cell death caspase-dependent apoptosis (involving a variety of different caspases) and caspase-independent programmed necrosis have been demonstrated. In particular caspase 3 and 7 are the executioner caspases that have thus far been implicated in these models (though not consistently).

1.6.2. Hypotheses

I. Commotio retinae is common in deployed British military personnel.

II. After macular commotio retinae, one third of patients suffer permanent visual impairment.

III. Permanent visual impairment after commotio retinae is associated with loss of photoreceptors.

IV. Commotio retinae may be modelled experimentally by blunt ocular trauma or PBI to the eye.

V. Photoreceptor cell death in commotio retinae is by a combination of caspase-dependent apoptosis and caspase-independent necrosis.

VI. Photoreceptor cell death is prevented by interference with the caspase-dependent cell death signalling pathway.

VII. A reduction in photoreceptor cell death is associated with preservation of the ERG.

These hypotheses are stated as valid at commencement of the PhD; the work of Souza-Santos et al. (2012) has added evidence to support hypothesis III.

1.6.3. Aims

I. Identify the extent to which commotio retinae affects deployed British military personnel.

II. Characterise visual outcomes after commotio retinae in humans.

III. Identify patients with visual loss after commotio retinae and define the cause.

IV. Develop an experimental model of commotio retinae.

V. Characterise the ultrastructural features of the model.

VI. Characterise the electroretinographic features of the model.

VII. Characterise the cell death signalling pathways in the model.

VIII. Evaluate translational neuroprotective therapies in the model.

2. Materials and Methods

2.1. Development of a Rat Ocular Trauma Model

2.1.1. Animals

All animal studies were conducted in accordance with Home Office guidelines adhering to the UK Animals (Scientific Procedures) Act 1986 and were licensed by the Home Office. Rats strains used were Wistar, Sprague Dawley and Lister hooded (Charles River, Margate, UK). All rats were female and kept on a 12 hr light dark cycle with a day time luminance of 80 lux and fed and watered *ad libitum*. Unless otherwise stated, rats weighed 170-200g at commencement of each experiment. Rats were weighed, anaesthetised and placed in a head holder (Figure 6.4.1.) for surgery.

2.1.2. Anaesthesia

For terminal and some recovery ERG experiments, anaesthesia was induced by intraperitoneal injection of ketamine/medetomidine combination at a dose 0.06mg medetomidine + 14.4mg ketamine for a 200mg rat. Oxygen supplementation was given during ERG recording. Animals were killed by perfusion with fixative under terminal anaesthesia.

Unless otherwise stated, in recovery experiments, the anaesthetic was an inhalational isofluorane/oxygen combination titrated to achieve appropriate plane of anaesthesia. The default concentrations of isofluorane in oxygen were 5% into a sealed box for induction of anaesthesia, 2% for ERG recording, 2.5-3% for surgery at a flow rate of 1l delivered through a small tube over the nose and mouth with a separate scavenging tube to remove waste anaesthetic gases.

Schedule 1 killing by overdose of anaesthetic used intraperitoneal pentobarbital after gaseous induction with isofluorane.

2.1.3. Surgery

For improved access to the eye, a lateral canthotomy was performed. The skin and ocular surface were prepared with 5% povidone iodine in water, without shaving the incision site. The lateral canthus was divided using scissors to a depth of approximately 5mm. For access to the lateral sclera, a 6.0 vicryl suture was placed in a horizontally orientated subcuticular mattress configuration (Figure 2.1.3.) and used to retract the wound edges whilst the eye was injured and then tied at the end to close the wound. For access to the inferior sclera, a temporary traction suture was placed in the lower lid. A limbal traction suture was used to rotate the eye.

Figure 2.1.3. A representative diagram of a left lateral canthotomy. The suture is shown in blue with a dotted lining indicating that it is subcuticular. Black dotted lines indicate cut skin edges.

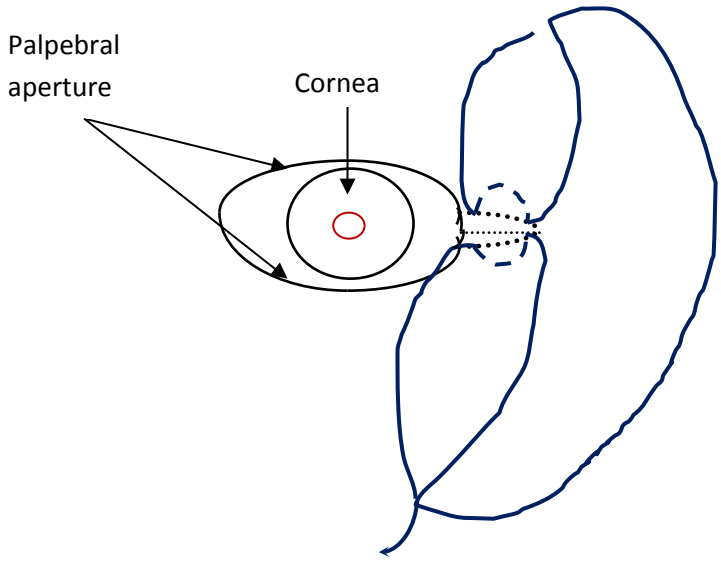

2.1.4.Electroretinography

2.1.4.1. Recording

ERG were recorded using a standard system specifically designed for small animals incorporating a mini-Ganzfeld stimultor (HMsERG – Ocuscience, Kansas City, MO USA) and interpreted using ERGView (Ocuscience). Animals were dark-adapted overnight and prepared for ERG under dim red light (>630nm) before recording scotopic flash ERG. Photopic flash ERG were recorded with background illumination of 30,000mcd/m2 during and for 10 min before recording. To dark-adapt,

the animals were placed in a cage covered with a combination of volatile organic compound-free black paint (Artifolk, Portsmouth, UK) and Rosco supergel medium red filter (blocks <630nm; Enlightened Lighting Ltd, Bath, UK). The electrodes used for recording were DTL fibre (Unimed Electrode Supplies, Farnham, UK) corneal electrodes connected to a DTL mini-grabber (Unimed) covered by pressure-moulded Aclar (Agar scientific, Stansted, UK) contact lenses and coupled by 0.3% hydroxypropylmethylcellulose eye drops (Tesco, Cheshunt, UK). The DTL grabber was positioned at the lateral canthus and the thread placed across the centre of the cornea before being trimmed to only that length in contact with the eye, and then the contact lens, moistened with hydroxypropylmethylcellulose was applied over the top. Subcutaneous needle electrodes (Unimed) were used for reference – inserted anteriorly at the base of the pinna towards the eye – and ground – inserted anteriorly at the midline dorsal aspect of the base of the tail.

2.1.4.2. Analysis

To assess retinal function, the major components of the ERG (a- and b-waves) were observed, quantified and compared between injured and control eyes. ERG interpretation and quantification used ERGView (Ocuscience) software.

2.2. Processing of Tissues

2.2.1.Protocols

2.2.1.1. Reagents

Unless otherwise stated, chemical and reagents came from Sigma (Poole, UK)

Reagent	Target/Purpose	Species	Supplier (location)	Catalogue No.	Batch No.	Dilution Used
Phosphate buffered saline (PBS)	Diluent	n/a	Scientific Laboratory Supplies (Nottingham, UK)	BR014G	Multiple	1 tab/100ml dH_2O
Mountant	Fluorescent mounting medium with DAPI	n/a	Vector Laboratories (Peterborough, UK)	H-1200	Multiple	n/a
	VectaMount permanent mounting medium	n/a	Vector	H-5000	Multiple	n/a
1^{y} Antibodies	Activated caspase 2 (P35)	Rabbit	Abcam (Cambridge, UK)	AB2251-100	10873	1/100 for IHC
	Activated caspase 3 (P17/P19)	Rabbit	Cell Signalling (New England Biolabs, Hitchin, UK)	9661S	18	1/100 for IHC 1/1000 for western blotting
	Activated caspase 6 (P18)	Rabbit	Cell Signalling	9761s	Lot 1	1/100 for IHC 1/1000 for western blotting
	Activated caspase 6 (P10)	Goat	Santa Cruz	sc-22177		1/50 for IHC
	Activated caspase 7 (p20)	Rabbit	Cell Signalling	9491S	Not known	1/100 for IHC 1/1000 for western blotting
	Caspase 8 (P20)	Rabbit	Santa Cruz (Santa Cruz, CA, USA)	sc-7890	B1203	1/100 for IHC 1/500 for western blotting
	Caspase 9 (P35)	Rabbit	Santa Cruz	Sc-8355	G2203	1/100 for IHC
	Caspase 9	Rabbit	Cell Signalling	9507S		1/1000 for western blotting
	ED1 (CD68)	Mouse	ABD Serotec (Kidlington, UK)	MCA341GA		1/200 for IHC
	OX42 (CD11b)	Mouse	ABD Serotec	MCA275B		1/200 for IHC
	RIP3	Rabbit	Abcam	Ab56164		1/200 for IHC
	Phospho-Akt	Rabbit	Cell Signalling	9271s	Lot 12	1/200 for IHC (in ADB made with TBS)

	Phospho-MToR	Rabbit	Cell Signalling	5536s	Lot 1	1/200 for IHC (in ABD made with TBS)
	Alexa fluor 488 (495/519nm) anti-rabbit IgG	Goat	Invitrogen (Paisley, UK)	A11034	461250	1/400 for IHC
2^{y} Antibodies	Texas red (595/615nm) anti-mouse IgG	Mouse	Invitrogen	T6390	Not known	1/400 for IHC
	FragEL™ DNA Fragmentation Detection Kit, Fluorescent - TdT Enzyme containing: *Proteinase K* *5X TdT equilibration buffer* *Fluorescein-FragEL™ labeling reaction mix* *TdT enzyme*	n/a	Merck (Feltham, UK)	QIA39	D000943 41	1/20 enzyme/ reaction mix
TUNEL	DNAase 1 (Vial 3 in the "Papain Dissociation System")	n/a	Worthington Biochemical (Lakewood, NJ, USA)	LK003150	Not known	Add 0.5ml to give 1µg/µl
	Gluteraldehyde – 25% EM grade	n/a	Taab (Aldermaston, UK)	G003	Multiple	4/25 to give 4% in 0.1M PB
Electron Microscopy	Osmium tetroxide – 4%	n/a	Electron Microscopy Sciences (Hatfield, PA, USA)	19150	0901522	1/4 in 0.1M PB
	Durcopan ACM Embedding Kit	n/a	Electron Microscopy Sciences	14040	1348248 3260713 3	10g of " A" 10g of "B" 0.3g of "C" 0.3g of "D"
	Uranyl Acetate	n/a	Unknown	Unknown	Unknow n	1% in 70% ethanol
	Polyvinyl formal	n/a	Unknown	Unknown	Unknow n	0.5% in chloroform
	Protease inhibitor cocktail	n/a	Sigma	P8340		5µl/ml
Western Blotting	2x Laemmli buffer	n/a	Sigma	S3401		Various
	Protogel	n/a	Geneflow (Lichfield, UK)	A2-0072		Various
	NNN´N´-Tetramethylethylenediamine (TEMED) Electran	n/a	VWR (Lutterworth, UK)	443083G		Various
	Sodium Dodecyl Sulphate (SDS) 20% Soln	n/a	Fisher Scientific (Loughborough, UK)	BP1311		Various
	Ammonium persulphate	n/a	Sigma	A3678		Various

	(APS)					
	Protein assay components A, B and S	n/a	Bio-Rad (Hemel Hempstead, UK)	A 500-0113 B 500-0114 S 500-0115		A* = 600µl of A + 12µl of S
	bVAD-fmk	n/a	MP Biomedicals (Solon, OH, USA)	FK-014	VM154	Dissolve 1mg in 149µl DMSO to give 10mM
	Streptavidin coated Dynabeads® - MyOne T1	n/a	Invitrogen	65601	1126902 60	
	ECL Western Blotting Detection Reagents	n/a	GE Life Sciences (Little Chalfont, UK)	RPN2109		1.5ml soln. 1 mixed with 1.5ml soln. 2
	Protease Inhibitor Cocktail	n/a	Sigma	P8340		1/200
ELISA	Progesterone Human ELISA Kit	Rabbit	Abcam	ab108670		

0.1M Phosphate buffer (PB)[1] was made by adding 7.84g Na_2HPO_4 and 5.38g NaH_2PO_4 to 1l dH_2O and titrating to pH 7.3 using HCl or NaOH. Reynolds lead citrate was made by boiling 100ml of dH_2O, letting it cool in an airtight container (to remove carbonate), then adding 1.33g lead nitrate and 1.76g sodium citrate to 30ml of this degased water. Tris buffered saline (TBS)[2] at a concentration of 20mM

[1] Phosphate buffer is subject to the following dissociation reactions:

1) $H_3PO_4 \leftrightarrows H^+ + H_2PO_4^-$ pKa 2.12
2) $H_2PO_4^- \leftrightarrows H^+ + HPO_4^{2-}$ pKa 6.8 to 7.2 dependant on ionic strength of solution – "true" pKa is 7.21
3) $HPO_2^{2-} \leftrightarrows H^+ + PO_4^{3-}$ pKa 12.32

Monobasic and disbasic sodium phosphate dissociate as follows: $Na_2HPO_4 \leftrightarrows 2Na^+ + HPO_4^{2-}$
$NaH_2PO_4 \leftrightarrows Na^+ + H_2PO_4^-$

At physiological pH $H_2PO_4^-$ and HPO_4^{2-} are the main ionic components (the first and third equations are pushed to the right and left respectively). $[HPO_4^{2-}]$ is determined by Na_2HPO_4 and $[H_2PO_4^-]$ by NaH_2PO_4.
According to the Henderson-Hasselbalch equation:
pH = pKa + log ([base]/[acid])
7.3 = 7.21 + log($[Na_2HPO_4]/[NaH_2PO_4]$)
$[Na_2HPO_4]/[NaH_2PO_4] = 1.23$
For 0.1M solution $0.1 = [Na_2HPO_4] + [NaH_2PO_4]$
This solves to give:
$[Na_2HPO_4] = 0.0552M$
$[NaH_2PO_4] = 0.0448M$
Molecular weight of Na_2HPO_4 is 141.958/M so 7.84g are required
Molecular weight of NaH_2PO_4 is 119.976g g/M so 5.38g are required

[2] Tris base - tris(hydroxymethyl)aminomethane,
Tris HCl - $(HOCH_2)_3CNH_2.HCl$
Molecular weight 121.14 g/mol without HCl, 157.6 with HCl, pKa of 8.06
For 20mM pH = 7.6
[tris acid] = 14.8mM or 2.33g
[tris base] = 5.2mM or 0.630g
NaCl molecular weight 58.44g

tris, 140mM NaCl, pH 7.6 was made by adding 0.63g tris base, 2.33g tris HCl and 8.18g NaCl to 1l dH_20 and titrating to pH 7.6. Tris-buffered saline with Tween (10mM tris, 150mM NaCl, 0.05% Tween; TBST) was made by adding 0.218g of tris base, 1.29g of tris HCl, 8.77g NaCl and 500µl Tween 20 to 1l of MilliQ water and adjusting to pH 7.4. Tris 1.5M pH 8.8 was made by adding 36.2g of tris HCl and 154g tris base to 1l of MilliQ water. Tris 0.5M pH 6.8 was made by adding 74.7g of tris HCl and 3.16g of tris base to 1l MilliQ water. Western blotting lysis buffer was made by adding 1.12g KCl, 1.19g HEPES and 0.1g CHAPS to 100ml MilliQ water and adjusting the pH to 7.4 (150mM KCl, 50mM HEPES, 0.1% CHAPS). $MgSO_4$ at 100mM in TBS (diluted at 1/100 to get 1mM) was made by adding 1.20g $MgSO_4$ to 100ml TBS. Antibody diluting buffer (ADB) was made by adding 0.2g bovine serum albumin (BSA) and 10µl Triton X-100 to 10ml 1x PBS. To make 1% osmium tetroxide, 2ml 4% OsO_4, 2ml 0.2M PB and 2ml dH_2O were mixed. Western blot running buffer was made by mixing 3.03g tris base, 14.4g glycine and 5ml 20% SDS with 1l of milliQ water. Western blotting transfer buffer was made by mixing 3.03g tris base, 14.4g glycine, 1ml 20% SDS and 200ml methanol with 1l milliQ water. Western blot stripping buffer was made by adding 7.5g of glycine to 1l of milliQ water and then adjusting to pH 2.9.

2.2.1.2. Electron Microscopy

2.2.1.2.1. Embedding

After perfusion with 4% gluteraldehyde, the eyes were removed and the cornea penetrated before leaving them in fixative for at least 24 hr. A section of lesioned retina and underlying sclera measuring less than 2x2mm was dissected out by first removing the cornea, iris and then lens under a dissecting microscope and then cutting the fixed retina with Vannas scissors. Equivalent sections were combined for processing to save time and reagents. The sections were washed in 0.1M PB for at least 30 min and then fixed in 1% osmium tetroxide buffered in 0.1M PB for 45 min. The osmium tetroxide was washed off with 3 x 10 min washes in 0.1M PB and the specimens were dehydrated in solutions with ascending concentrations of 50%, 70%, 90%, 100% and 100% ethanol with dH_2O for 10 min each. After 50% ethanol, the specimens were stained in 1% uranyl acetate in 70% ethanol for 45

min. After dehydration the absolute ethanol was replaced with propylene oxide by 2 x 10 min washes. The dehydrated specimens were transferred to resin (Durcopan) and left to infiltrate for 24 hr. The specimens were set in resin blocks with tissue orientated to give a section perpendicular to the retinal surface. The tissue was supported with fragments of pre-polymerised resin as necessary and then polymerised in a 56°C oven for >24 hr.

2.2.1.2.2. Sectioning

Glass knives were made using an LKB (Stockholm, Sweden) type 7801A knife-maker. A drop of distilled water placed on the scored glass extended the cutting edge (Slabe, Rasmussen, and Tandler 1990). Excess resin was trimmed from the block with a jeweller's saw and razor blades. Semithin sections were cut at 1µm using glass knives on a Reichert-Jung "ultracut" ultramicrotome (Reichert-Jung, Vienna, Austria), stained with toludine blue and used to locate the area to be cut for electron microscopy. The blocks were trimmed down with razor blades to square sections 0.5x0.5mm. Ultrathin gold sections (70-90nm) were cut with a glass or diamond knife, floated in distilled water and mounted on formvar-coated 50 mesh copper grids (Agar Scientfic, Stansted, UK).

2.2.1.2.3. Staining

After immersion in 30% uranyl acetate in ethanol for 7 min, sections were washed x3 in dH_2O and then stained in Reynold's lead citrate for 7 min and washed x1 in 50mM NaOH and x2 in dH_2O.

2.2.1.2.4. Microscopy

Ultrathin sections were examined on a Jeol 1200EX (JEOL [UK] Ltd., Welwyn Garden City, UK) transmission electron microscope fitted with a LaB6 filament at an operating voltage of 80 keV.

2.2.1.3. Cryosections

2.2.1.3.1. Embedding

After perfusion fixation, the eyes were enucleated, penetrated through the cornea, post-fixed in 4% paraformaldehyde for at least 24 hr and cryoprotected by immersion in 10%, 20% and 30% sucrose in

PBS for 24 hr each. The cornea, iris, lens and vitreous were removed and a strip cut from the remaining retinal/scleral cup spanning ciliary body to ciliary body through the optic disc and encompassing the lesion site (approximately 4mm wide), placed on its side in a block of OCT and frozen to -80°C for storage. This process ensured: (1) cutting of only sections that included lesioned retinal tissue and; (2), the retina was embedded in direct contact with OCT.

2.2.1.3.2. Sectioning

OCT blocks were fixed in a cryostat (Bright instruments, Huntingdon,UK) and sections cut at 15µm and mounted onto Superfrost™ (Fisher) coated glass microscope slides. The slides were dried overnight at 37°C and then frozen to -80°C for storage.

2.2.1.4. Retinal Whole Mounts

Animals were killed by overdose of anaesthetic. The eyes were enucleated and the cornea, iris and lens removed before 15-60 min immersion fixation in 4% paraformaldehyde. Retinae were separated from the sclera by cutting through the optic disc, placed onto Superfrost slides and cut into 4 leaves joined at the optic disc before 5 min drying and mounting with DAPI mountant.

2.2.1.5. Western Blotting

Animals were killed by overdose of anaesthetic. The eyes were enucleated and the cornea, iris, lens and vitreous removed. Retinae were separated from the sclera by cutting through the optic disc, placed in cryotubes and snap frozen in liquid nitrogen for later processing.

Retinae from each injury/treatment group were pooled and homogenised on ice at 1000rpm rising to 3000rpm over 2 min in 200µl western blotting lysis buffer supplemented with 5µl protease inhibitor cocktail per 1ml for every 6 retinae. The homogenate was stood on ice for 30 min and then centrifuged at 13,000g at 4°C for 10 min. The supernatant was collected, aliquoted and frozen at -80°C for later analysis.

For Western blotting, protein solution was mixed with an equal volume of 2x Laemmli buffer heated to 90°C for 5 min and loaded onto the gel.

To make an 8% resolving gel, a combination of 1.83ml Protogel, 1.65ml 1.5M Tris pH 8.8, 3.12ml MilliQ water, 66µl 10% SDS, 23.1µl 10% APS and 9.9µl TEMED (added last) was pipetted into a 1mm cassette, topped with ethanol to remove air bubbles and left to set for 15 min. To make a 12% resolving gel, a combination of 3.592ml Protogel and 1.358ml MilliQ water was mixed with the other ingredients. Stacking gel is a combination of 0.4ml Protogel, 1.85ml 0.5M Tris pH 6.8, 0.75ml MilliQ water, 30µl 10% SDS, 15µl 10% APS and 7.5µl TEMED (added last) pipetted on top of the resolving gel with a 10 or 12 well comb inserted and left to set for 15 min.

The gel was placed in a XCell SureLock® blot module (Invitrogen) with running buffer and samples were loaded in wells to give a total protein of 80µg/lane with 3 lanes per treatment group. Gels were run for 2 hr at the default settings on the PowerEase® 500 power supply (Invitrogen; 125V, 35mA) or until the blue marker in the buffer and/or the ladder neared the bottom.

To blot, the gel was removed, washed in transfer buffer for 15 min and placed under a Immobilon® polyvinylidene difluoride membrane that had been activated in pure methanol for 1 min, washed in transfer buffer and run at the default settings on the power pack (25V, 125mA) for 2 hr in the Western blot module in transfer buffer.

After blotting, the membrane was washed x3 in TBST for 10 min each and then blocked in 5% dried skimmed milk (Marvel) in TBST for 1 hr at room temperature (RT). Primary antibody in 5% Marvel/TBST was applied overnight at 4°C. The membrane was washed x3 in TBST, secondary antibody in 5% Marvel/TBST was applied for 1 hr at RT and then washed off as before. The membrane was immersed in ECL solution for 1 min and either exposed to photographic film or read on a digital imaging system (ChemiDoc™ MP System, Bio-Rad, Hemel Hempstead, UK). Membranes were stored in TBST at 4°C.

2.2.1.5.1. Protein Assay

To measure the concentration of protein in the lysate, stock solutions of 2mg/ml, 1.5mg/ml, 1mg/ml and 0.5mg/ml BSA were prepared along with serial dilutions (1 in 5, 1 in 8, 1 in 10, 1 in 20 and 1 in 100) of the lysate in western blotting lysis buffer in quantities of at least 6µl. A 5µl quantity of each sample was placed in a 96 well plate with 20µl of A* and 160µl of reagent B from the Bio-rad protein assay.

Plates were then kept in the dark for 20 min and read on a Victor™ X3 spectrophotometer (Perkin Elmer, Waltham, MA USA) at 750nm.

2.2.1.5.2. Caspase Pull-down Assay

To capture active caspases, 5µl of 1mM bVAD-fmk dissolved in 10% DMSO in PBS was injected intravitreally to both eyes of 3 animals. Retinae were removed as for Western blotting and homogenised on ice in CHAPS buffer (150mM KCl, 50mM HEPES, 0.1% CHAPS pH 8.5) supplemented with protease inhibitor cocktail. Samples were incubated on ice for 10 min, then centrifuged at 13,000g for 10 min and the supernatant collected. PBS/0.1% Tween-20 at pH 8.5 was used to wash 2mg of streptavidin-coated Dynabeads® x3, which were combined with 200µl of the PBS/Tween and the supernatant (except for 20µl, which was retained - *retain 1*). The beads and protein were gently rotated overnight at 4°C. The beads were washed x4 in PBS/Tween and the supernatant retained (*retain 2*). After washing, the beads were mixed with 60µl of 2x Laemmli buffer and incubated at 90°C for 5 min. The Laemmli buffer was removed and loaded onto a 12% gel (20µl per lane) and run as a Western blot.

A solution of 10% DMSO in PBS was used as a vehicle because 100% was found to be retinotoxic – causing visibly oedematous and friable retina 24 hr after injection. Streptavidin-coated Dynabeads® bind 400pM of peptide-bound biotin/mg of beads and 800pM (from the 2mg beads used) of biotin-bound bVAD is equivalent to 133pM/eye in the study (6 eyes of 3 animals contribute to the supernatant). A solution of 5µl of 1mM bVAD-fmk is 5000pM – i.e. 37.6x more biotin was injected

per eye than could be captured by the beads. PBS/Tween at pH 8.5 and 150mM KCL was used, as high pH and salt concentrations increase the specificity of the streptavidin-biotin interaction.

Although there is no published data on the speed at which bVAD-fmk penetrates to the ONL after intravitreal injection, it is likely to take several hours. The caspase-bVAD-fmk complexes are rapidly cleared and 5 hr after they are formed is the latest time point at which they can be easily detected (personal communication – Carol Troy, Columbia University, NY, USA). Therefore, for pull-down assay of initiator caspases, injection of bVAD-fmk was at 2 hr pre-injury and animals were killed at 5 hr post-injury.

2.2.1.6. Staining for Light Microscopy

2.2.1.6.1. Toludine Blue

Semithin resin-embedded sections were covered with Toludine blue stain and heated over a naked flame until vapour was seen to rise. The stain was washed off in dH_2O and the sections were left to dry.

2.2.1.6.2. H&E

Cryosections were rehydrated in dH_2O for 10-20 s, covered with Mayer's haematoxylin for 30 sec, washed in dH_2O, covered with eosin for 20 sec and washed in dH_2O before mounting using hard set mounting medium.

Semithin resin-embedded sections were either: (1), covered with Mayer's haematoxlin and heated on a 150°C surface until the stain boiled, washed in dH_2O and the process repeated with Eosin or; (2), de-plasticised in a saturated solution of NaOH in absolute ethanol for 5 min, washed x2 in absolute ethanol, rehydrated in 90%, 70% and 50% ethanol and then PBS for 5 min each and stained in the same way as cryosections.

2.2.1.6.3. Immunohistochemistry

The initial protocol was as follows: Frozen sections were left to thaw/dry for 30 min at RT and then fixed in absolute ethanol for 1 min, washed x2 in PBS for 5 min each, encircled with a hydrophobic marker, permiabilised in 0.1% Triton X-100 in PBS for 20 min at RT, washed x2 in PBS for 5 min each and then left to block in ADB, containing 0.5% BSA and 0.5% Tween-20 in PBS, for 30 min at RT. Blocking buffer was removed and primary antibody in ADB added and left overnight at 4°C in a humidified chamber. Slides were washed x3 in PBS for 5 min each and secondary antibody in ADB added and left to incubate for 1 hr at RT. Slides were washed x3 in PBS for 5 min each and then mounted in DAPI mounting medium and stored at 4°C in the dark.

The initial protocol was found to give unacceptably high levels of background staining and so was modified as follows: after drying for 30 min and encircling with a hydrophobic marker, sections were rehydrated in PBS for 5 min followed by 0.1% Triton-X in PBS for 15 min, blocking in the modified ADB described in Section 2.2.1.1. with the addition of 15% relevant normal serum (to match the secondary source animal, usually goat). Primary antibody in ADB was added and left overnight at 4°C in a humidified chamber. Slides were washed x2 in 0.1% Triton X-100 in PBS and x1 in PBS for 5 min each and incubated for 1 hr at RT with secondary antibody in ADB with the addition of 1.5% relevant normal serum. Slides were washed x2 in 0.1% Triton X-100 in PBS for 5 min each, then PBS for 5 min and then mounted as before.

2.2.1.6.4. TUNEL

The FragEL™ DNA Fragmentation Detection Kit, Fluorescent - TdT Enzyme was used. Reagents were kept on ice on the bench during use, except for the TdT enzyme, which was kept at -20°C. Specimens were encircled with a hydrophobic slide marker and then immersed in TBS for 5 min at RT. Specimens were permeabilised in 0.1% Triton X in PBS for 15 min and then washed x2 in TBS for 5 min each. The recommended permeabilisation step involving proteinase K was omitted because it was found to result in, (1), digestion of the specimen, which often fell off the slide, even when this

step was reduced to 2 min and, (2), a high rate of false TUNEL positive in control tissue. A 100µl solution of 1x equilibration buffer (5x TdT Equilibration Buffer diluted 1:5 with dH_2O) was added to the specimen and left for 10 min then replaced with 57µl Fluorescein-FragEL™ TdT Labeling Reaction Mix mixed with 3 µl of the TdT Enzyme before covering in Parafilm® and incubating for 1.5 hr at 37°C in a humidified chamber. The reaction was terminated by 3x 1 min washes in TBS and the sections were mounted on slides in DAPI mounting medium and stored at 4°C in the dark.

To generate a positive control, 1µg/µl of DNAase 1 in 1mM $MgSO_4$ in TBS was added and the slides incubated for 20 min at RT before the equilibration step.

2.3. Statistics

2.3.1.Theory

In general, data that are normally distributed can be analysed with parametric statistical tests, data that are not normally distributed or lack an underlying numeric structure (e.g. ordinal data) should be analysed with non-parametric tests. For relatively straightforward statistical analyses such as comparing means, this is a simple distinction; with 2 normal independent series of measurements, a Student's t-test can be used and with 2 ordinal or heavily skewed independent series, a Mann Whitney U test can be used.

Many of the analyses reported in this text are on repeated measures with multiple possible factors influencing the dependent variable and under these circumstances; more complex statistical modelling techniques are required. Analysis of variance (ANOVA) uses linear regression to predict one (dependent) variable on the basis of one or more predictor variables and tests the null hypothesis that there is no difference in the distribution of the dependent variable in groups clustered by the predictors. It assumes that the scores for each condition (one state of a predictor variable e.g. stimulus intensity = 300mcd/m^2 in an ERG data series) are normally distributed about the mean for that condition and (for standard ANOVA) that the variances are the same for each condition. The main weakness of ANOVA from the point of view of this text is that subjects with

missing data are excluded, so, in a repeated measures ANOVA used to analyse multiple ERG data points (with, e.g. 64 observations per rat – 2 eyes, 2 time points, 16 stimulus intensities), a single missing observation would mean exclusion of all of that subject's data. Generalised estimating equations are used to estimate the parameters of a generalised linear model, which is a more flexible version of ordinary linear regression and makes fewer assumptions about the variance and normality of the response variables. Generalised estimating equations incorporate datasets with missing data. The main choices to make when specifying the statistical model used are: (1), the choice of correlation matrix; (2), the choice of probability distribution; and, (3), the link function. The correlation matrix choice is between: (1), independent – assumes no correlation between clustered responses, e.g. if the a-wave at one stimulus intensity is of lower magnitude than the average, this does not affect the likelihood of other a-waves in the same subject being below average; (2), exchangeable – assumes any two responses within a cluster have the same correlation (ANOVA makes this assumption), e.g. a-waves at 300 and 3000mcd/m^2 have the same correlation as a-waves at 30 and 10,000mcd/m^2; (3), autoregressive (AR1) – assumes that the correlation between points is raised to a power corresponding to their separation (i.e. the correlation between adjacent measurements is R, measurements separated by 1 R^2, by 2 R^3 and so on), e.g. in a scotopic ERG series with stimulus intensity increasing in half log unit steps, if the correlation between a-waves at 300 and 1000mcd/m^2 is R, then the correlation between a-waves at 300 and 3000mcd/m^2 is R^2; (4), unstructured – makes no assumptions about the correlations; (5), M-dependant – which is a mixture of unstructured and independent with the cut-off between the two at a pre-specified degree of separation. The probability distribution that provides the best fit for the data may be specified as normal or gamma for numeric data. The link function may be linear or logistic depending on whether the factors directly predict the dependent variable or whether the response is logarithmic.

2.3.2.Analyses

All statistical analyses were performed in SPSS (v16-v21; IBM, Armonk, NY USA). The analyses used are specified in the relevant results sections. Where general (ANOVA) and generalised (generalised

estimating equations) linear models were used, model fit was assessed by plotting raw and standardised (Pearson) residuals and using the standard goodness of fit tests within SPSS. For generalised estimating equations, a model using an autoregressive correlation matrix and the gamma distribution with log link function provided the best fit for both ERG and cell count data. Models were initially specified to include all possible factors and factorial interactions and analysis was performed iteratively, removing non-significant interactions from the model one at a time, starting with the highest order.

Power calculations were performed in G*power (v. 3.1.4, Kiel University, Germany) and power calculations for ANOVA were taken to approximate the result that would be obtained were a simulation run to calculate the true power of the intended analysis with generalised estimating equations.

3. Retrospective Study of Ocular Trauma in Deployed British Forces

The work in this section has been published in Eye (Blanch, Bindra, Jacks, and Scott 2011), the full paper is presented in Appendix 3. The relevant sections are reproduced here.

3.1. Background

The patterns of ocular injury and visual outcomes have not previously been described for British military personnel deployed in Iraq and Afghanistan. This information is important for the planning of ophthalmic care to and ophthalmic research within the British Armed Forces.

3.2. Hypotheses

I. Visual outcomes from British military injuries conform to standard civilian ocular trauma score (OTS) predictions.

II. Blast is the major cause of injury in deployed British military personnel.

III. Retinal injury is the main cause of visual loss in deployed British military personnel.

IV. Commotio retinae is a major cause of morbidity in deployed British military personnel.

3.3. Aims

I. To present injury and outcome data on all ocular trauma occurring in British armed forces in Iraq and Afghanistan between 19 Jul ’04 and 2 May ’08.

II. To validate the dataset by relating OTS to visual outcomes and by comparing outcomes with previous reports.

III. To identify the main causes of visual loss in deployed British military personnel.

3.4. Materials and Methods

This study was registered as an audit with University Hospitals Birmingham NHS Trust and was a retrospective, non-comparative interventional case series.

The study included all cases of ocular trauma occurring in British military personnel who survived injuries (ocular or otherwise) severe enough to merit admission to hospital on return to the UK between 19 Jul 04 to 2 May 08. Cases were identified using the UK Joint Theatre Trauma Registry (JTTR) held in RCDM. In addition, cases that were not included in that database were identified by searching clinic letters for the keywords, “Iraq,” “Afghanistan,” “TELIC,” “HERRICK,” and, “Blast.” Patients who were treated in theatre by non-ophthalmologists and returned to duty were not included.

Data was extracted from the patients’ paper medical records and recorded on a Microsoft Excel spreadsheet for analysis. Where available, data were collected on: demography, time and place of injury, actions at time of injury, personal protective equipment, all ocular and other injuries sustained with initial examination findings, initial, best and final VA, all operative interventions, medical interventions relevant to ocular management (ocular medications and systemic antibiotics) and functional and occupational outcomes.

Injuries were categorised as open or closed, in line with the Birmingham Eye Trauma Terminology (Pieramici et al. 1997), as illustrated in Figure 1.2. To facilitate comparison with other studies that included only “severe” ocular injuries (Thach et al. 2008), (Mader et al. 2006), subconjunctival haemorrhage, corneal abrasion or superficial foreign bodies were not counted as significant injuries but placed in a minor injuries category. When describing open injuries, it was not possible to distinguish between rupture and perforating injuries, as in these cases the eye was severely disrupted and there were probable elements of both injury mechanisms present. Adnexal injuries occurring in conjunction with globe injury were counted as one injury. None occurred in isolation.

Initial VA may have been recorded in theatre by non-Ophthalmologists, on arrival in the UK on Ophthalmology assessment or may not have been recordable until after definitive treatment due to unconsciousness. Outcomes are reported by final VA either at 6-12 months post-surgery or at discharge from follow-up. Final VA is a useful measure in these patients because patients are followed up until full recovery and are rarely discharged or transferred to another centre before they are functionally stable and permanent occupational recommendations have been made.

For the purposes of analysis, Snellen VA measurements were converted to logMAR including those with acuity less than 1/60, as previously reported (Schulze-Bonsel et al. 2006). Severity was calculated retrospectively using the OTS (Kuhn et al. 2002), to grade eye injuries from 1 (most severe) to 5 (least severe).

The statistical analysis is descriptive, with average values given as either the median in those cases where the data are not numeric or do not appear to follow the normal distribution or the mean in other cases. Spearman's rank was used to calculate the correlation of final VA with Ocular Trauma Score.

3.5. Results

A total of 630 British soldiers survived major trauma from 19 Jul 04 to 2 May 08. Of these, 63 (10%) suffered ocular injuries affecting 82 eyes with 19 of these bilateral (30.2%). The ocular injuries were classed as significant in 58 eyes of 48 individuals, constituting 7.6% of major trauma. Over the same time period, 7447 UK soldiers were wounded in action (WIA) with 492 ocular injuries (6.6%). Because all major injuries were aeromedically evacuated from theatre, we calculated that 48 (0.64%) of those WIA suffered significant ocular injuries.

Only one soldier had a history of ambylopia in the affected eye. Two injuries occurred in women – one minor and one closed – and 54.5% were to the left eye and 44.5% to the right. The mean age at time of injury was 26.5 years (range 18-53) and 52% occurred in Iraq on operation TELIC and 48% in Afghanistan on operation HERRICK.

The aetiology was explosive blast in 54/63 patients (86%), closed globe contusion in 6/63 (9.5%) cases, disease non-battle injury (DNBI) in 3, a motor vehicle collision in 1, a non-combat related aircraft incident in 1 and an electrical burn in 1. Among the significant injuries, 40/48 (83%) were caused by explosive blast.

Mean follow up was 245 d for closed globe injuries and 220 d for open. The first recorded VA was at a mean of 7.8 d after closed globe injury for injuries and 3.6 d after open globe injury. Mean time to arrival in the UK was 2.63 d (median 1) after all injuries and 2.52 d after open globe injuries (median 1).

Figure 3.5. Injuries classified by the Birmingham Eye Trauma Terminology System. An additional 24 minor cases are not shown here (subconjunctival haemorrhage, corneal abrasion, superficial foreign body).

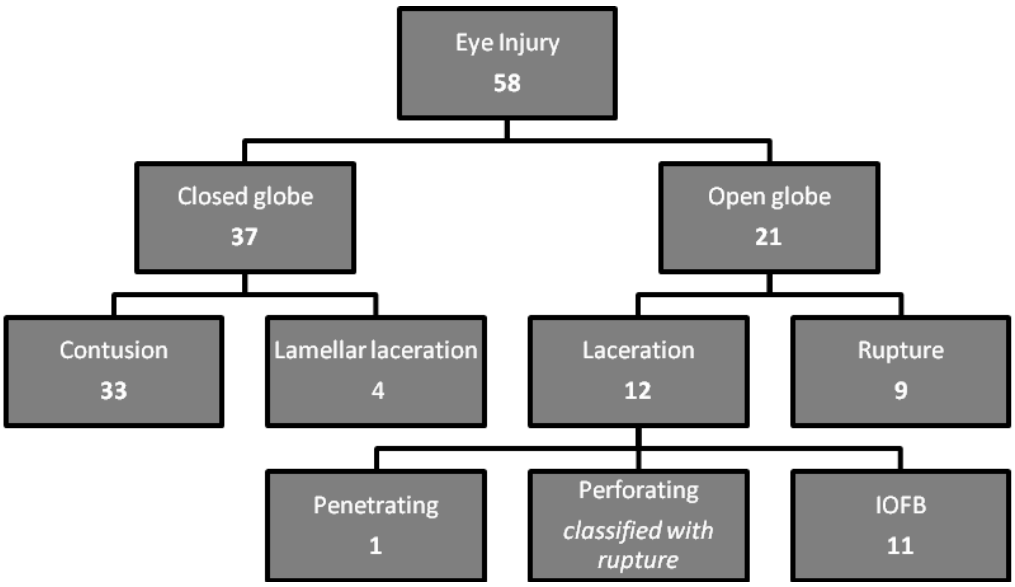

The distribution of cases in this cohort is shown in Figure 3.5. Of the 58 severely injured, 22 (38% of eyes) had associated adnexal damage e.g. lid lacerations, burns or orbital fractures. Facial or orbital fractures occurred in 17 of 48 patients (35%). Penetrating or closed brain injury with structural abnormality on imaging occurred in 9 patients (19%); known cases of mild traumatic brain injury/post-concussive syndrome were not included. Isolated ocular trauma occurred in 9 individuals

(19%), of which 1 was minor. A further 7 cases (2 minor) were associated with soft tissue fragmentation injuries, which required no treatment.

There were 21 open globe injuries (Figure 3.5.) of which 11 were associated with an intraocular foreign body (IOFB) – 1 of these penetrated the anterior segment only, 1 was intralenticular and 4 penetrated the eye posterior to the equator. Lens damage occurred in 6/11 (54.5%) of IOFB and 2 (18.2%) were recorded to have associated retinal detachments.

For open globe injuries, mean time to primary repair was 1.9 d (range 0-5) and there were an average of 1.57 operations per eye. Of the 9 ruptured globes, 7 (77.8%) were ultimately enucleated or eviscerated (5 as a primary procedure); the final VA in the two remaining eyes that ruptured were hand movements (HM) and no light perception (NLP).

Intravitreal antibiotics were given at the time of primary repair (with vitrectomy) in 5/13 eyes repaired. All open globe injuries received broad spectrum systemic antibiotics before evacuation. There were no cases of endophthalmitis and 2 cases (of 12 open globes repaired) of proliferative vitreoretinopathy (PVR), which caused the only two cases of retinal re-detachment.

The distribution of closed injuries is summarised in Table 3.5.1. Surgery was required in 10/37 cases with an average of 1.2 operations per eye. There were 9 cases of commotio retinae (16% of significant injuries), of which 5 (55% of commotio) affected the macula. In macular and extramacular cases, the median presenting VA were 3/60 and 6/21 and the median final VA were 6/9 and 6/7.5 respectively. However, both initial and final VA were affected by multiple other pathologies as detailed in Table 3.5.1.

Lids	Laceration	5
	Burn causing scarring	2
Cornea	Superficial foreign body	9
	Abrasion	6
	Partial thickness laceration	4
	Blunt trauma causing oedema	2
	All burns	6
	With limbal ischaemia	3
Subconjunctival haemorrhage		4
Iris	Iritis	4
	Sphincter damage/traumatic mydriasis	12
	Iridocorneal angle recession	2
	Hyphaema	9
Cataract		7
Posterior segment	Vitreous haemorrhage	8
	Commotio retinae/sclopetaria	11
	Retinal tear	1
	Choroidal rupture	4
Traumatic optic neuropathy		4
Orbit	Blow out/other fracture	11
	All foreign bodies	4
	Foreign body with intracranial penetration	1
	Muscle damage	1

Table 3.5.1. – Closed globe injuries. Eyes with minor injuries only excluded. A total of 37 eyes.

There were 34 eyes with initial VA≤6/60, 18 eyes had final VA<6/60 and 17 eyes had a final VA of 1/60 or worse, of which 6 (3 patients) were bilateral. The causes were rupture/extensive disruption (9 eyes), corneal scar (2 eyes), PVR (2 eyes), traumatic optic neuropathy (1 eye), subfoveal choroidal rupture (1 eye), IOFB impacted fovea (1 eye) and retinal burns from hot IOFB (1 eye).

The correlation of final VA with the OTS for all cases is shown in Table 3.5.2. The median OTS for closed-globe injuries was 4, with a median final VA of 0.2 (6/10). The median OTS for IOFB was 2.5, with a median final VA of 1.45 (6/169); this improved to a median final VA of 0.25 (6/11) when the two eviscerated eyes were excluded.

No. Points	OTS	NLP	LP/HM	CF -<6/60	6/60 -<6/12	≥6/12
0-44	1	83%	17%			
45-65	2	33%	17%	17%	17%	17%
66-80	3	7.1%	14%	14%	21%	43%
81-91	4				30%	70%
>92	5				6.9%	93%

Table 3.5.2. Correlation of final VA with OTS. Total number 65 eyes on which OTS could be calculated. Spearman's rank correlation coefficient = -0.730 (df=63, 2 tailed, tied rank corrected) $p<0.0001$. For 15 open globe injuries on which OTS could be calculated Spearman's rank correlation coefficient = -0.137, $p>0.05$ (df=13, 2 tailed, tied rank corrected). OTS = Ocular Trauma Score; NLP = No Light Perception; LP = Light Perception; HM = Hand Movements; CF = Counting Fingers

Eye protection was recorded as worn in only 7/63 patients. Of these, one had an IOFB injury with hot metal, ultimately requiring evisceration, and one had a closed globe injury with an orbital foreign body (vision recovered to 6/18), the remainder were minor injuries. Of those not recorded as wearing eye protection, 11/56 had a final VA of HM or worse (including enucleation/evisceration).

3.6. Discussion

This is a complete report of all United Kingdom military ocular injuries from Iraq and Afghanistan, as there is a single point of treatment delivery and follow-up that allows comprehensive data to be collected. This allows long-term outcomes to be recorded, unlike other reports of military trauma.

Military is much more severe than civilian ocular trauma, with an initial VA of 6/60 recorded in 71% compared with 27% among civilians (Kuhn et al. 2002) and is associated with severe polytrauma in 75% (source United Kingdom JTTR), which is rare in the civilian setting. Most military patients are male (98%) compared with 80% of civilians and high energy explosive blast causes 83% of injuries compared with 3% in civilians (Weichel et al. 2008). Despite these differences, the dataset recorded broadly conforms to OTS predictions, although, as in other reports of military trauma (Weichel et al. 2008), comorbidities often delayed or hampered assessment of initial VA, which may have made the scoring system less reliable particularly for the more severely injured open globe injury patients.

The total number of ocular casualties is much lower than that reported in the United States military (Colyer et al. 2008), (Mader et al. 2006), (Thach et al. 2008), (Weichel et al. 2008), reflecting differences in the overall number of casualties between the British and the United States Armed Forces. It is difficult to compare the proportion of eye trauma between different reports, as there are subtle differences in how the data are presented. In our series, 6.6% of WIA suffered ocular injuries, though only 0.64% suffered significant ocular injuries. This is in line with historical data (Wong, Seet, and Ang 1997), but much less than the 4.9% of WIA suffering 'severe' ocular injury reported by Thach et al. (Thach et al. 2008). Mader et al. reported 10% of surgical admissions with 'severe' eye injuries, similar to the 7.6% of major trauma in our series (Mader et al. 2006). Though both studies defined 'severe' differently, they were broadly similar to our definition of significant injury.

We report a high proportion of blast injuries (86%) compared to 70–80% in previous reports (Wong, Seet, and Ang 1997), but this is not representative of the United Kingdom JTTR as a whole, which in the same period recorded 57% blast injuries (source United Kingdom JTTR). It is possible that other causes of major trauma (gunshot wound, motor vehicle incidents, and DNBI) are less likely to involve the eyes compared with improvised explosive devices targeted at the face. The enforced use of safety devices in theatre, such as seatbelts and eye protection, may reduce the incidence of eye injuries from other causes and, when exposed to blast, the eye is vulnerable to small, low energy fragments that would cause only minor skin damage.

All soldiers were issued with polycarbonate spectacles and goggles for eye protection (Eye Safety Systems, Sun Valley, ID, USA), but a low proportion were documented as wearing them at the time of injury. We do not have data on the proportion of soldiers using eye protection in theatre and so cannot assess any protective benefits of eye protection. A recent study found a modest reduction in eye injury rates from 26% to 17% in those with and without eye protection respectively (Thomas et al. 2009).

Of the 17 eyes with final VA 1/60 or worse, 9 were grossly disrupted and so completely unsalvageable, 2 developed PVR and 3 had primary retinal damage. Retinal pathology therefore caused 5/8 potentially salvageable cases with a poor outcome. In general though, the outcome for non-ruptured/perforated open globe trauma was excellent.

Commotio retinae occurred in 16% of cases with significant injury. Of the closed globe injures, those with the potential to cause a permanent reduction in VA are commotio retinae, sclopetaria retinae, choroidal rupture, retinal tear and traumatic optic neuropathy, though the outcomes after closed globe injuries were excellent.

3.7. Conclusions

I. The visual outcomes after British military ocular trauma broadly conform to civilian OTS predictions and are in line with previous US military reports.

II. Blast is the most common cause of ocular trauma and injures the eye more than other body regions.

III. The main vision threatening injuries in British military trauma are open globe retinal injuries.

IV. Commotio retinae is more common in military than in civilian trauma, but did not cause significant visual loss in this series.

Blast causing retinal injury is the main cause of ocular morbidity in deployed British soldiers and there are no pharmacological interventions that are available to modulate the disease process, therefore identifying blast-related retinal injury as an important subject for further study.

4. Ocular Primary Blast Injury in a Porcine Model

4.1. Rationale

Blast is the most common cause of ocular trauma in deployed British military personnel (see Section 3). Secondary and tertiary blast injury cause penetrating and blunt ocular trauma, whereas PBI is an injury mechanism unique to blast. We have reported cases of commotio retinae after suspected PBI (Blanch and Scott 2008), (Chalioulias, Sim, and Scott 2007), and commotio retinae is the most common manifestation reported in the literature, though the existence of ocular PBI is disputed (Abbotts, Harrison, and Cooper 2007). The most commonly reported electron micrographic appearances of commotio retinae in animal studies are disruption of photoreceptor OS (Hart, Blight, Cooper, and Papakostopoulos 1975), (Blight and Hart 1977), (Blight and Hart 1978), (Bunt-Milam, Black, and Bensinger 1986), (Kohno et al. 1983), (Sipperley, Quigley, and Gass 1978), and swelling of Müller cell processes (Kohno et al. 1983), (Blight and Hart 1977), (Blight and Hart 1978), (Hart, Blight, Cooper, and Papakostopoulos 1975), (Dean Hart and Blight 1978). In this study, the retinal effects of primary blast exposure were evaluated in a porcine model of PBI at the Defence Science and Technology Laboratory (DSTL) Porton Down.

4.2. Hypotheses

I. Ocular PBI occurs with clinically relevant blast exposure

II. Ocular PBI causes causes commotio retinae.

4.3. Aim

To investigate whether ocular PBI occurred with clinically relevant blast doses in pigs by looking for evidence of commotio retinae and traumatic optic neuropathy.

4.4. Materials and Methods

4.4.1.Animal Model

A prospective, controlled animal study was conducted by the research team at DSTL on 3 large terminally anaesthetised white pigs (DSTL). Two animals were subjected to a standardised primary blast wave delivered to the right hand side, sufficient to cause reproducible, lethal blast lung as previously described (Garner et al. 2009). Secondary and tertiary blast were minimised by protecting the animals with a Kevlar™ blanket to stop fragments and mass movement of air and by strapping the animal to a trolley to prevent them being thrown against another surface.

Animals were anaesthetised and prepared as previously described (Garner et al. 2009), except that a liver snare was placed to cause uncontrolled haemorrhage. After blast a controlled haemorrhage was simulated by removal of 30% blood volume and then uncontrolled haemorrhage was created by pulling the liver snare to lacerate the liver. One animal became acidotic after surgery and was sacrificed without blast injury using an overdose of intravenous phenobarbitone and was used as the control. Of the two animals subjected to blast, case 1 survived for 55 min and case 2 for 3.5 hr. Due to the constraints of Home Office licensing and the primary use to which the model was put, pharmacological mydriasis was not possible and so fundoscopy was conducted with a direct ophthalmoscope through an undilated pupil.

4.4.2.Pathology

Post mortem globes were fixed by intravitreal injection of 4% gluteraldehyde in PBS within min of death followed by enucleation including the optic nerve up to the optic canal, *via* an inferior approach. Specimens were then immersed in 4% gluteraldehyde in PBS for >24 hr. Globes were cut into three segments: segment 1 was processed for light microscopy, segment 2 for electron microscopy and segment 3 was retained in the gluteraldehyde solution.

4.4.2.1. Light Microscopy

Sean James (Walsgrave Hospital, Coventry, UK) processed specimens for light microscopy. After automated processing though to paraffin wax, 3µm sections were cut and mounted onto Superfrost plus slides and incubated overnight in a 56°C oven. Sections were rehydrated in graded isopropyl alcohols to water and stained with haematoxylin and eosin (H&E) to examine nuclei and retinal structure using Harris's haematoxylin (Leica Microsystems, Milton Keynes, UK) and 1% aqueous eosin (Surgipath, UK). Vitreo-retinal attachments were defined by exposure to freshly prepared 1% periodic acid for 10 min, washing in distilled water, incubating at RT for 10 min in Schiff's reagent (PAS; VWR), immersing in cold running tap water for 10 min to develop the stain then counterstaining in Mayer's haematoxylin for 1 min and blued in Scott's tap water.

GFAP (Clone 6F2, Dako, Cambridge) immunohistochemistry using 3, 3'-diaminobenzidine (DAB) for light microscopy was carried out as previously described (Snead et al. 2004).

4.4.2.2. Electron Microscopy

Processing for electron microscopy was performed by technicians at Queens Medical Centre (Nottingham, UK). Specimens were embedded in agar, trimmed to a 2x2mm square, washed in PBS and excess agar removed. Samples were post-fixed in 1% aqueous osmium tetroxide for 2 hr, washed in water and dehydrated in ascending concentrations of ethanol (40%, 70%, 90%, X3 100%), then two changes of 100% acetone, all with gentle agitation. TAAB Embedding Resin of medium hardness was prepared and a 50% solution in acetone used for initial infiltration for 30 min followed by 100% resin mixture for 3 hr at 37°C and -400mbar vacuum using a TAAB embedding oven. Samples were embedded in fresh resin mixture using TAAB type G silicone flat embedding moulds before polymerisation overnight (15 hr) at 65°C and -400mbar vacuum using a TAAB embedding oven. Sections for light microscopy were cut at 0.5µm using glass knives on a Leica EM UC6 ultramicrotome and stained with 1% Toluidine Blue in 1% borax. Virtual microscopy images of the stained 0.5µm sections were recorded using a NanoZoomer scanner (Hamamatsu Photonics, Welwyn

Garden City, UK). Sections were cut at 80nm using a diamond knife on the EM UC6 before mounting onto copper 200HH grids (Guilder, UK) and staining with saturated uranyl acetate in 50% ethanol, followed by Reynold's lead citrate, both for 5 min, then washed in distilled water and viewed under a JEOL 1010 electron microscope at 100KV. Digital images were recorded using an integrated SIS Megaview III camera and iTEM software (Olympus-SIS, Münster, Germany)

4.5. Results

After blast injury and haemorrhage, the 2 injured animals became hypoxic and acidotic, demonstrated by blood gas analysis. It is unclear why the control animal became acidotic without blast or haemorrhage. Both animals subjected to blast had post-mortem blast-lung, visible as haemorrhage on post-mortem examination (case 1, 75% R caudal lobe, 10% L caudal lobe; case 2, 70% R caudal lobe, 5% L caudal lobe).

Direct ophthalmoscopy was normal.

There was no macroscopic evidence of commotio retinae and no structural changes in any eyes on light microscopy with H&E or PAS or GFAP labelling. On electron microscopy, there was artefactual separation of the retina and RPE with consequent damage to photoreceptor OS, but no changes consistent with commotio retinae. Photoreceptor OS were preserved (Figure 4.5.) in all eyes with no loose disc material. There was no swelling of Müller cell processes.

4.6. Discussion

The effects of isolated PBI on solid organs have not been reported elsewhere. A recent report of a mouse model did not control for tertiary blast injury (Hines-Beard et al. 2012). Ocular PBI is relevant to military ophthalmology, but also to wider considerations of the effects of blast exposure on the brain (Mac Donald et al. 2011).

Figure 4.5. Transmission electron micrographic images of pig retina. Right eyes are shown, as these were closest to the blast. Right - control (uninjured) tissue, preserved photoreceptor outer segments (arrowed). Left - case 2, preserved photoreceptor outer segments (arrowed).

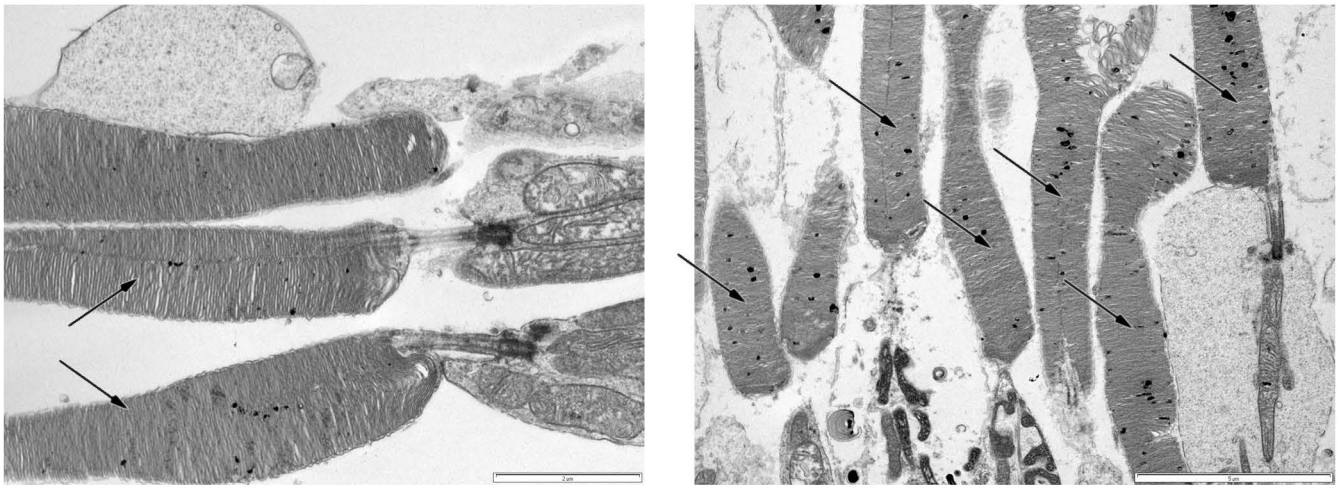

4.6.1.Study Findings

Commotio retinae, defined as macroscopic post-traumatic retinal whitening, did not occur in this study. Immediately after injury, the electron micrographic appearance of photoreceptor OS in commotio retinae is gross disruption with free disc material, neither of which were seen and, additionally, there was no Müller cell oedema, which is the next most frequently reported observation, so there were no ultrastructural features of commotio retinae either.

The optic nerve is often used to study CNS injury responses (Berry et al. 2008). There were no structural changes in the nerve fibre layer on electron microscopy or gross structural changes in the optic nerve on light microscopy. That GFAP was not upregulated is of limited significance as its gene is upregulated as a late response to injury and upregulation so quickly after injury has not been previously described (Vazquez-Chona, Song, and Geisert, Jr. 2004). Longer follow up would give a greater expectation of immunohistochemical changes, if injury occurs.

With only 2 cases (4 eyes) negative findings do not rule out ocular PBI. However, the blast dose administered caused reproducible lethal blast lung in pigs and we did not detect any evidence of ocular PBI in either the retina or optic nerve (Garner et al. 2009). Assuming that each eye was independently injured, the 95% confidence interval for the proportion of animals that could develop commotio retinae after exposure to blast is 0–55% (modified Wald method).

That the experimental animals developed severe blast lung demonstrates that they are susceptible to blast effects. We cannot exclude that porcine eyes have a particular resistance to blast effects, though their dimensions and structure are similar to human eyes so there is no anatomical reason to believe that this should be the case.

Both injured animals had severe blast lung. Therefore, if ocular PBI is possible, it requires a higher blast dose than pulmonary PBI. This is unsurprising, as PBI requires energy transfer at the interface between tissues of different densities and densities vary less in the eye than in the hollow organs. The blast wave decays rapidly with increasing distance from the explosion, so PBI requires closer

proximity than secondary and tertiary mechanisms. Secondary and tertiary blast effects cause commotio retinae by blunt trauma and it is therefore difficult clinically to separate commotio retinae caused by PBI from other mechanisms. To suffer ocular primary blast injury, a patient would usually have to be exposed to a blast dose at least sufficient to cause severe blast lung and would also therefore likely be close enough to the blast to suffer tertiary and secondary blast effects to the eyes. Thus ocular PBI is unlikely to be a major mechanism of wounding in surviving patients and it is likely that the 86% of military eye injuries caused by blast that were identified in Section 3 resulted from secondary and tertiary mechanisms.

4.6.2.Methodological Considerations

The artefactual separation of the neurosensory retina from the RPE was unfortunate given that the photoreceptor OS is the main area of interest. Better tissue preservation could be achieved through perfusion fixation.

Glutaraldehyde ($CH_2(CH_2CHO)_2$) cross links proteins much more effectively and rapidly than formaldehyde. Primarily the two terminal aldehyde groups cross link lysine ϵ-amino groups, but it reacts with other amino acids and with lipids, carbohydrates and nucleic acids. Because of this and because of its larger molecular size, it penetrates tissues more slowly than formaldehyde at approximately 500µm/3 hr (Bozzola and Russell 1999). The mammalian retina is approximately 240µm thick and thus after immersion of the eye cup or intravitreal injection of gluteraldehyde, photoreceptor-RPE junction fixation would take 1.5 hr (Hughes 1979). No part of the photoreceptors is more than 50µm from either the outer retinal capillary plexus or the choriocapillaris, so perfusion fixation would take 18 min. However, photoreceptor OS are largely membrane lipids, which are not strongly fixed by gluteraldehyde.

Osmium tetroxide (OsO_4) is a non-polar molecule that diffuses rapidly through lipid cell membranes and reacts with and stabilises membrane lipids, staining and providing contrast thus making photoreceptor OS visible under the electron microscope. Osmium preserves membrane structures

by oxidising unsaturated fatty acids and reacts with and stabilises proteins (Bozzola and Russell 1999). Glutaraldehyde followed by osmium tetroxide is the standard protocol for fixation of a wide range of tissues (Bozzola and Russell 1999).

Electron microscopy requires the selection of a very small piece of tissue for analysis and without clinical or macroscopic pathological abnormalities as a guide, it is possible that retina with occult pathology was not sampled. Pathological findings should be interpreted in the light of clinical findings and so for future studies, dilated fundoscopy is essential and electroretinography desirable.

Clinical examination, electroretinography, perfusion fixation and longer time points would be difficult within the context of the model at DSTL Porton Down because of the other uses to which the models are put, the large size of pigs used in the model and the fact that recovery experiments have not yet received ethical approval. In addition, the cost of these blast injury models is prohibitive (approx. £10,000 per animal). The initial negative findings were not encouraging with respect to overcoming these difficulties in order to obtain a useful animal model of ocular blast injury.

The study indicated that a blunt trauma model would be a more clinically relevant way to model commotio retinae and suggested refinements to the laboratory techniques relevant to Chapter 5 onwards, which are summarised in the conclusions below.

4.7. Conclusions

I. PBI is unlikely to be a major ocular wounding mechanism.

II. The porcine blast model at DSTL Porton Down is unsuitable for ocular research.

II. Retinal injury can be more reliably induced by blunt ocular trauma rather than blast.

III. Clinical examination is essential to guide selection of tissue for pathology and aid interpretation of results, so an animal model dedicated to ocular studies is required.

IV. Perfusion fixation is necessary for studies of photoreceptor morphology, so rodents are a more suitable species than pigs in which to model commotio retinae.

5. Characterising Commotio Retinae

The work in this chapter has been published in Ophthalmology, the paper is presented in Appendix 4.

5.1. Rationale

Commotio retinae is a common military and civilian retinal injury, that can affect the macula with consequent loss of vision. The proportion of patients in which the macula is affected, the probability and extent of recovery and the probability of complications are all unknown.

5.2. Hypotheses

I. After macular commotio retinae, one third of patients suffer permanent visual impairment.

II. Permanent visual impairment after commotio retinae is associated with loss of photoreceptors.

5.3. Aims

I. To describe the proportion of patients with commotio retinae in whom the macula is affected.

II. To describe the level of permanent visual loss in macular commotio retinae.

III. To describe the time course and extent of recovery of vision.

IV. To identify any factors which predict visual loss or recovery.

V. To describe complications and their frequency.

5.4. Materials and Methods

The study protocol was approved by the Birmingham East North and Solihull Research Ethics Committee. The NHS Research Ethics Committee application form is presented in Appendix 5.

This was a retrospective non-interventional case series.

We included all patients presenting to the Birmingham Midland Eye Centre Eye Casualty from 1st October 2007 to 23rd February 2011 who were given a diagnosis of either commotio retinae or sclopetaria retinae. There were no exclusion criteria. A total of 1262 cases with ocular trauma were identified by searching the Birmingham & Midland Eye Centre Eye Casualty clinical database for the Accident and Emergency diagnostic codes: 02104B/L/R – contusion bilateral/left/right eye; the 10th revision of the international statistical classification of diseases and related health problems (ICD-10) diagnostic codes: contusion – S001 or S051, other retinal disorders – H35, H358 or H359; the free text entries: assault, commotio, ecchymosis. Clinical records were examined to identify patients diagnosed with commotio retinae, defined as retinal whitening after ocular trauma or sclopetaria retinae defined as full thickness chorioretinal disruption associated with haemorrhages and retinal holes. Age, gender, VA, injury mechanism, clinical findings of extent of commotio retinae and associated features and the extent of recovery and complications on follow up were recorded. For the purposes of analysis, Snellen VA measurements were converted to the logarithm of the minimum angle of resolution (logMAR), including those with acuity of < 1/60 (Schulze-Bonsel et al. 2006).

Duration of follow-up was variable, with patients who completely recovered being discharged at that point. Follow-up for >3 months was considered adequate to determine final VA where it was reduced after injury. VA <6/9 was considered reduced and cases with follow-up <3 months and VA worse than 6/9 were excluded from analyses of visual outcomes.

Data were not normally distributed. Descriptive statistics used median values +/- interquartile range (IQR) and the range of extreme (highest and lowest) values; VA between groups were compared using Wilcoxon signed rank test and proportions were compared using Fisher's exact test. Linear regression was used to assess the effects of age, gender and initial VA in the injured eye on final VA, interaction between initial VA in the injured eye and gender was examined using analysis of variance (type III sum of squares) and model fit assessed with diagnostic plots.

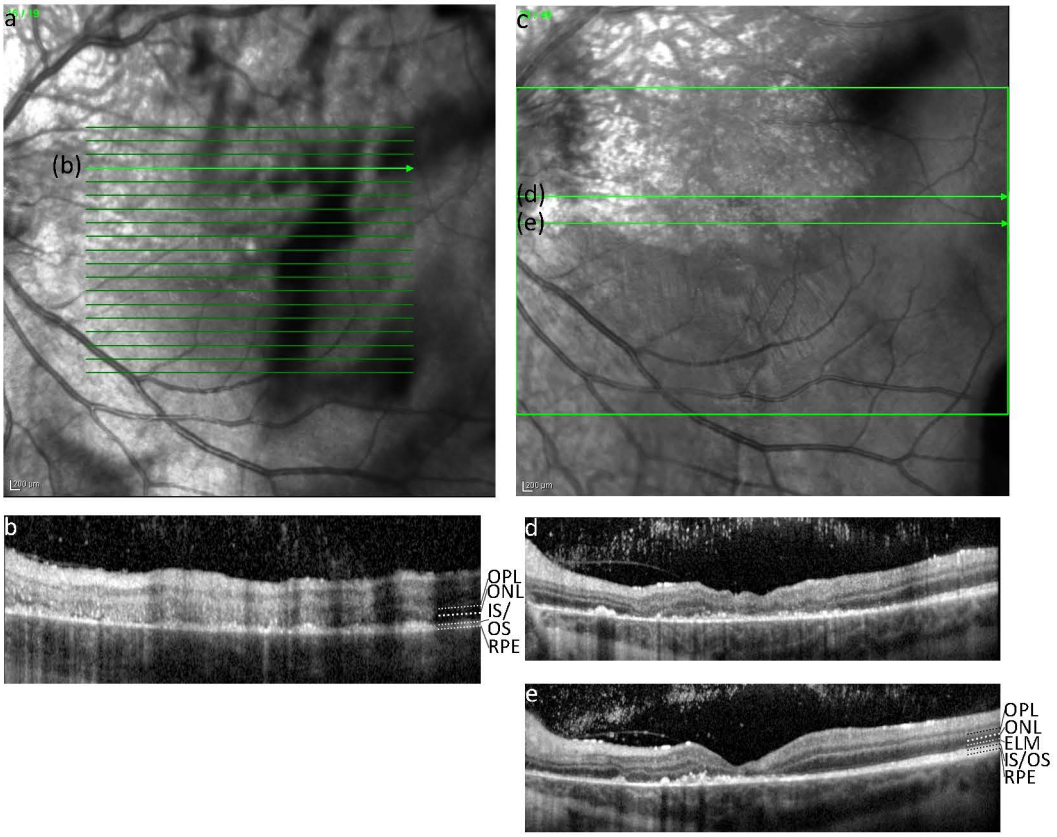

Figure 5.5.1. Fundus and OCTimages of the left eye of a 14 year old boy who was hit in the left eye by a soccer ball. At 3 days after injury his visual acuity was 20/80 right eye and he had an inferior altitudinal field defect corresponding to an area of commotio retinae; visual function was unchanged at 4 months follow up. (a and c), fundus images at 3 days (a) and 10 days (c) after injury. Vitreous hemorrhage obscures the view at 3 days; however, retinal pallor is still seen. By 10 days an area of retinal atrophy has developed superior to and involving the fovea, revealing the choroidal vasculature. (b), on OCT at 3 days, the inner retina is swollen and the outer retina disrupted, with thinning of the outer nuclear layer and photoreceptor outer segments. (c-d), on OCT at 10 days, the ONL and external limiting membrane are absent in the affected areas, leaving the outer plexiform layer (OPL) directly apposed to the retinal pigment epithelium, which is thinned.

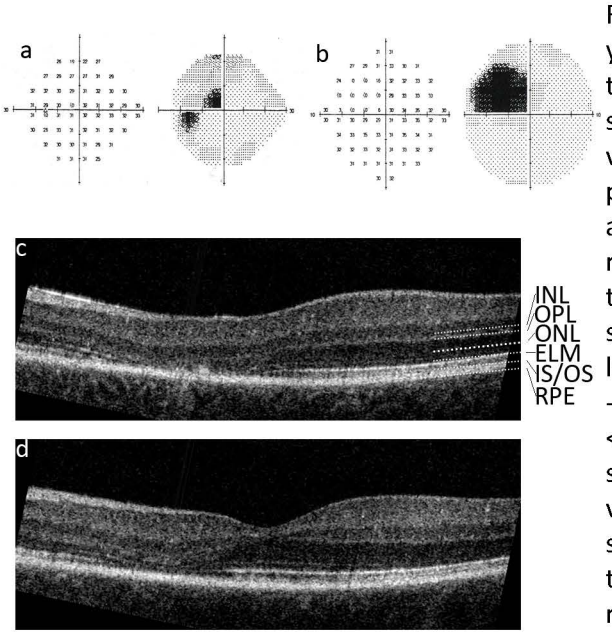

Figure 5.5.2. Humphrey visual field and OCT of a 34 year old competitive squash player who suffered blunt trauma to his left eye from the edge of his opponent's squash racquet 18 months previously. Presenting visual acuity was 20/20 right eye, 20/40 left eye with pinhole; examination showed a microscopic hyphaema and commotio retinae affecting the fovea, nasal macula and peripapillary area. Eighteen months after the injury he re-presented complaining that he lost the squash ball in upper left field. VA was 20/32 OS: (a), left eye Humphrey visual field 24:2, mean deviation -2.18 dB p < 5%, pattern standard deviation 6.05 dB, p <0.5%. An absolute scotoma is present superotemporal to fixation; (b), left eye Humphrey visual field 10:2 mean deviation -6.97, p<1%, pattern standard deviation 12.06, p<1%; (c), an OCT image of the left eye, showing the loss of the external limiting membrane and outer nuclear layer, leaving the outer plexiform layer (OPL) directly apposed to the retinal pigment epithelium; (d), an OCT image of the left eye, showing the same features as Figure 1c next to the fovea.

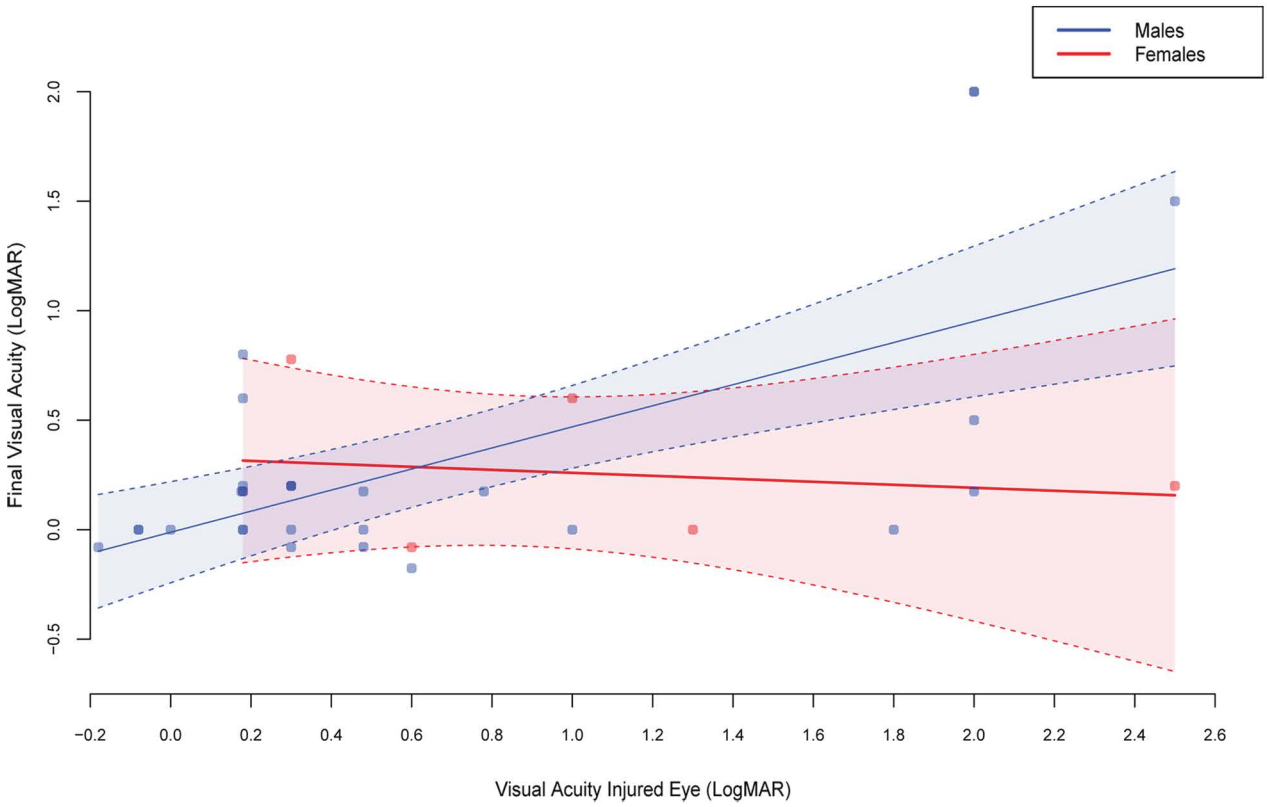

Figure 5.5.3. A scatter plot showing final VA (y axis) against initial VA in the injured eye (x axis) with males (blue dots) and females (red dots) shown separately. Lines denoting model predicted means obtained from fitting a linear regression with main effects of initial VA and gender and an interaction term between them to explain final visual acuity are overlaid with dashed lines indicating corresponding 95% confidence intervals. A positive correlation exists between initial and final VA in males (r = 0.53, 95% CI [0.24, 0.74]), but not in females (r = -0.18, 95% CI [-0.82, 0.66]). LogMAR = logarithm of the minimum angle of resolution.

5.5. Results

5.5.1.Macular Commotio Retinae

Macular commotio retinae was diagnosed in 53 patients (31% of all commotio retinae), of which 40 were injured by assaults, 4 by footballs, 2 by tennis balls, 1 by a squash racquet and the rest by accidents at home. There was adequate follow-up to determine final VA in 34 patients (19 were excluded). The median presenting VA was 6/12 (IQR 6/9-6/60) and the median time after injury to presentation was 12 hr (IQR 6-24). 25 (74%) of patients recovered to 6/9 or better, 9 (26%) patients remained worse than 6/9 (range 6/10-counting fingers); the overall median visual recovery was logMAR 0.18 (equivalent to approximately one Snellen line). The median VA in the uninjured eye was 6/6 (IQR 6/6-6/6) and was significantly better than the final VA (paired samples Wilcoxon signed rank test, median difference=0.18, p=0.002). Of those patients presenting with a VA <6/9, the median visual recovery was logMAR 0.52 (equivalent to approximately 3 Snellen lines). Of those patients with a final VA <6/9, one developed a macular hole, one had macular choroidal folds secondary to hypotony from a ciliary cleft; and the remainder had retinal atrophy (example shown in Figure 5.5.1.). Two patients developed symptomatic paracentral scotomas, despite VA of 6/6 and 6/9 (Figure 5.5.2.). The median age was 28 years (IQR 21-36) and 45 patients were male. Regression analysis suggested a model including main effects of initial VA in the injured eye, gender and a term to model their interaction provided a reasonable fit to the data, with little explanatory value to keeping age in the model as either a main effect or as an interaction term (model shown in Figure 5.5.3.; p=0.24 for gender, p=0.1 for initial VA, p=0.033 for gender*initial VA).

5.5.2.Extramacular Commotio Retinae

Extramacular commotio retinae was diagnosed in 117 patients (69% of all commotio). The median age was 23 years (IQR 17-33), 99 patients were male, 93 were injured during assaults, 10 playing football, 6 accidents in the home and 1 occupational injury, a military explosive blast injury. There was adequate follow up to determine final VA in 58 patients (59 were excluded); the median

presenting VA was 6/9 (IQR 6/6-6/12, range 6/4-3/60) and the median time after injury to presentation was 20 hr (IQR 8-24). Of 9 patients with presenting VA < 6/12, the median time post-injury of assessment was 15 hr (IQR 6-24) and the causes of reduced vision recorded in the notes were hyphaema (2), amblyopia (1) and corneal abrasion (1); no apparent cause was recorded in 5 patients. Three patients had final VA <6/9: 6/12, 6/12 and 6/18, with follow-up of 5, 24 and 31 months, respectively. Of these, the patient with a final VA 6/18 had a past history of amblyopia with no change from pre-injury VA and one had an extramacular choroidal rupture. Thus, a total of 2 patients (3%) had a significant VA reduction, of whom one had a significant additional injury. The median extent of visual recovery was logMAR 0.076. Median final VA was 6/6 (IQR 6/5-6/9). The median VA in the uninjured eye was 6/6 (IQR 6/6-6/9) and was not significantly different from the final VA (paired samples Wilcoxon signed rank test, median difference=0, p=0.124). There was one case of extramacular sclopetaria retinae. The 3 most common retinal locations of commotio, in order of frequency were; infero-temporal (37%), temporal (17%), supero-temporal (17%), <5% of cases were in a nasal location.

5.5.3.Associated Injuries

Anterior and posterior segment injuries occurred with similar frequencies in the two groups. Overall, hyphaema occurred in 24 patients and retinal tears in 3, 1 of whom also had a retinal dialysis. Orbital fractures were more likely to occur in patients with macular commotio, with 13 fractures (12 involving the floor, one the medial wall) in the macular group and 12 fractures (all involving the floor) in the extramacular group (p=0.02, Fisher's exact test, 2 tailed). Fractures of the inferior and lateral orbital rim occurred in two patients with extramacular commotio.

5.6. Discussion

This is the first report of the prognosis and retinal location of macular and extramacular commotio retinae. These data represent a complete capture of all ocular trauma presenting to Birmingham Midland Eye Centre from 1st October 2007 to 23rd February 2011.

In civilian practice macular commotio represents 31% of all cases , compared with 73% in the military (Weichel et al. 2008). After macular injury, 26% of patients were left visually impaired on the basis of VA ≤6/9. The true proportion with some visual impairment is higher because: (1), a deterioration from 6/4 to 6/9 will be significant to many patients and; (2), additional patients may be visually impaired by symptomatic paracentral visual field defects despite a normal VA.

The absence of an effect on prognosis of advancing age in our data is unsurprising, as most patients were under 30 and very few are over 40 years old. There is a positive correlation between initial and final VA – on average, the worse the presenting VA, the worse the final VA – and an interaction of gender with this correlation meaning that for poorer initial VA, females tend to have better final VA than males. However, with adequate follow-up data on only 7 females, this result requires confirmation. A protective effect of female gender in CNS trauma has been postulated and is thought to be mediated by progesterone (Roof and Hall 2000).

After extramacular injury, 2 patients (5%) suffered a long-term, but mildly, reduced VA, which may represent occult macular injury or previously undiagnosed visual impairment in the affected eye. Despite a highly variable presenting VA after extramacular commotio, the visual prognosis is generally excellent with visual recovery to the same level as the fellow eye in the vast majority of patients. In the acute setting after injury, reduced vision without other apparent causes may be due to occult macular injury or be non-organic or factitious

The association of macular commotio with orbital floor fractures is consistent with its presumed contrecoup mechanism of injury causing retropulsion and increased intraorbital pressure (Berlin 1873), as opposed to extramacular commotio, which occurs mostly in an infero-temporal to temporal location that is occasionally associated with orbital rim fractures, consistent with direct trauma to the sclera overlying the injured retina (Blight and Hart 1977).

5.7. Conclusions

I. Civilian commotio retinae affects the macula in 31% of cases.

II. At least 26% of patients with macular commotio retinae remain permanently visually impaired.

III. Patients with impaired vision have loss of the ONL, seen on OCT, indicating photoreceptor death.

IV. Extramacular commotio retinae is most often caused by direct scleral trauma.

6. Developing a Model of Blunt Ocular Trauma

Parts of the work in this section have been published in Investigative Ophthalmology and Visual Science (Blanch et al. 2012a), the paper is presented in Appendix 6.

6.1. Rationale

Our understanding of the mechanisms underlying retinal damage such as that seen after blast injury in soldiers or other blunt ocular trauma in civilians, is incomplete. There are no treatment options available to patients with visual loss from commotio retinae. These considerations identify a need for research into commotio retinae and the development of translational treatments using a suitable animal model. As previously described, rats are the most appropriate species to use, since:

- the anatomy of the rat and human retinae is similar
- antibodies for rat immunohistochemical studies are readily availabile
- alternative species have higher costs and maintenance
- the relatively large size of the rat eye facilitates *in vivo* manipulations and investigations

Ideally an animal model should demonstrate the same clinical and ultrastructural features of human commotio retinae, assessed by fundus examination and photography and electroretinography. Ultrastructural changes of photoreceptor outer segment disruption will be assessed with electron microscopy. Photoreceptor apoptosis will be assessed by ultrastructural features, TUNEL staining, and immunohistochemistry.

Previous animal studies have used modified airguns and catapults to deliver a high velocity (20-50m/s) weight to the eye, but control and calibration of the energy delivered using these methods is imprecise. For example, with a modified airgun measurement of the breach pressure before discharge is difficult and so assuring reproducibility is also problematic; with a catapult standardisation of the impact is also difficult.

The kinetic energy levels used to create commotio retinae in large animals vary from 0.49-2.87J, e.g. in the pig, 0.49J is sufficient, suggesting that a lower energy will be required in the rat.

6.2. Hypotheses

I. In the rat commotio retinae is induced by blunt ocular trauma.

II. The energy level required to create commotio retinae reproducibly is < 0.5J.

III. Photoreceptor apoptosis occurs after commotio retinae.

6.3. Aims

I. To create a rat model of commotio retinae

II. To assess the type of cell death (apoptotic *versus* necrotic) that occurs in commotio retinae.

6.4. Materials and Methods

The simplest and most reproducible way of delivering an impact of known energy is by weight drop. Therefore, a weight drop apparatus was manufactured to attach to a standard rat head holder (Figure 6.4.1.). To calculate the weight and height required to deliver a defined energy impact, the following formula was used:

$PE = m*g*h$

Where: PE = gravitation potential energy in Newton metres (Nm) or Joules (J); m = mass in kg; g = gravity in m/s^2; h = height in m. The maximum practical height was 0.5m and the expected maximum kinetic energy to be delivered was 0.5J. The weight that would be required to generate a potential energy of 0.5J was 100g, derived from:

$0.5 = m*9.8*0.5$

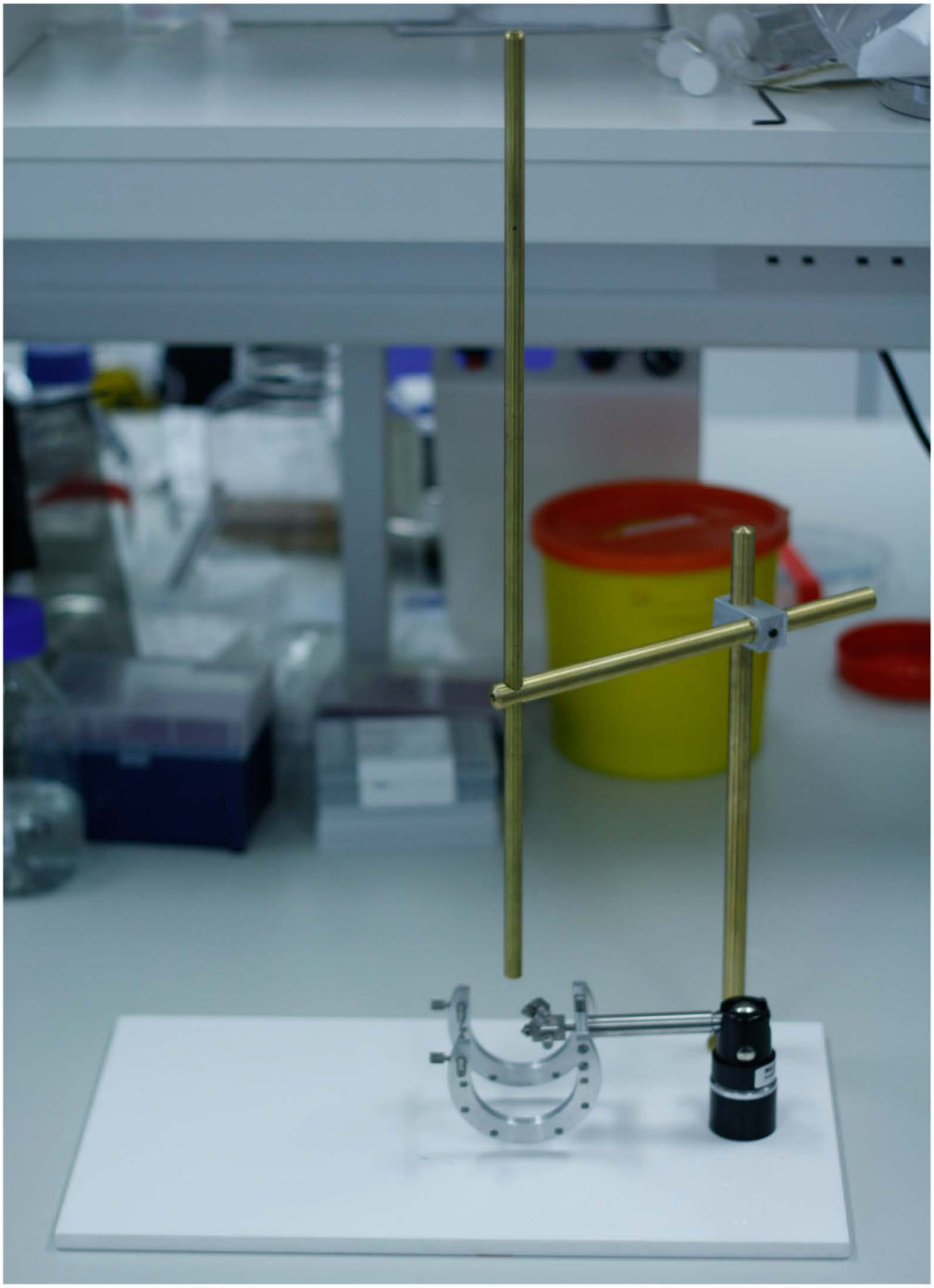

Figure 6.4.1.

The head holder and tubing used to deliver an impact to rat eyes by weight drop. The rat was held in place by the two ear bars and incisor clamp. The lower end of the tubing was aligned with the desired impact point on th eye and a weight dropped from the top of the tube. The tube was 50cm long. A small hole in the side released the weight from a height of 41cm. The internal diameter of the tube was 6mm.

Figure 6.4.2.

Three weights used with the apparatus shown in figure 6.4.1. (i) – 22.6g weight, 6mm impact tip, (ii) – 31.3g weight, 6mm impact tip, (iii) – adjustable weight with 3mm impact tip. 1 section weighs 5.85g, 2 11.3g, 3 17.6g and 4 23.0g.
Tip - *. Restraining cord attached to end to allow controlled excursion and ease of release and retrieval - **.

A weight of 100g intuitively seemed excessive for a rat eye, and 0.5J was taken as an upper limit, so smaller weights were chosen (Figure 6.4.2.). A 22.6g weight gives a kinetic energy of 0.111J and 31.3g a kinetic energy of 0.154J. To allow an increased energy to be investigated without increasing the weight, a catapult latex (Match System superpower catapult latex, Middy Tackle International, Heanor, UK) was placed over the tip of the tube (Figure 6.4.1) and used to propel the weight downwards – 7cm of catapult latex was tensioned by being stretched by an additional 7cm. The increased velocity was calculated as follows:

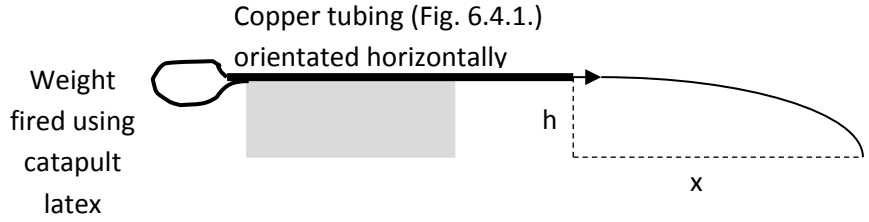

The drop-tube was held parallel to the ground and the weight fired. The height (h) was 19cm. The distance travelled (x) was measured. The results are shown below in Table 6.4.

	22.6g weight distance travelled (cm)	31.3g weight distance travelled (cm)
Mean	132.25	98.25
Standard deviation (n-1)	42.72	29.35
Mode	180 and 90	140 and 70
Mean velocity (m/s)	6.71	4.99
Mean KE (J)	0.51	0.39
PE of 50cm drop (J)	0.11	0.153
Mean total KE after 40cm drop + catapult latex (J)	0.62	0.543
Calculated velocity after 40cm drop + catapult latex (m/s)	7.41	5.89

Table 6.4. Horizontal distance travelled after the weight was released for 20 iterations with calculated velocity and kinetic energy (KE). PE = gravitational potential energy.[3]

[3] To calculate the KE and PE given in the table, the time taken to fall 19cm was 0.197s, calculated by the formula:
d = vi*t + 0.5*a*t2

The distribution of velocities in Table 6.4 was bimodal because the weight drop apparatus was not designed to be enhanced by the catapult band and so, if the weight was held slightly off-axis when fired, friction slowed it down. Logically the additional KE from the latex should have been the same whatever size of weight was used, so the lighter weight should have had a lower total KE than the heavier weight (lower PE). That it did not was attributable to the poor reproducibility achieved using the catapult latex. However, this apparatus allowed a higher velocity to be achieved easily. Had it become necessary to use such velocities of weight-drop in the final model, a higher weight drop tube would have been necessary.

6.5. Weight Drop Method

6.5.1. Cadaveric Study of Blunt Ocular Trauma

6.5.1.1. Hypothesis

Ocular injury in rats using the weight drop method rarely causes globe rupture.

6.5.1.2. Aim

To test the whether the weight drop can be used in rats without globe rupture.

Where vi = initial velocity (0m/s), d = distance in m (19 cm), a = acceleration (9.8m/s2), t = time in s
Velocity was then calculated by:
v = x/t
Where x = horizontal distance travelled.
PE = m*g*h
KE = 0.5*m*v2
Where m = mass in kg, g = gravity (9.8m/s2), h = height in m
KE was calculated for the experimental data in Table 6.4. PE was calculated for the weight drop (0.11J for 22.6g and 0.153J for 31.3g). The two were summed to get total KE for the weight drop + catapult band and then v was calculated from KE by working backwards through the equations.

6.5.1.3. Materials and Methods

Three male Wistar rats of weight 170-200g were used. One was killed by cervical dislocation. One was killed by overdose of anaesthetic and one was killed by exposure to progressively increasing concentrations of CO_2. One eye of each animal was exposed to a 31.3g weight drop from 50cm using the apparatus described in Figure 6.4.1. to deliver a KE of 0.153J. One eye of each animal was exposed to the same weight delivered using the catapult latex giving an approximate KE of 0.54J.

6.5.1.4. Results

Globe rupture did not occur in any injured eyes.

6.5.1.5. Conclusions

The apparatus delivered a weight drop injury without causing globe rupture and could therefore be used for future studies.

6.5.2.Terminal Study of Blunt Ocular Trauma

6.5.2.1. Hypotheses

I. Ocular injury in rats using the weight drop method induces commotio retinae without causing globe rupture.

II. Central corneal injury induces a contre-coup commotio retinae.

6.5.2.2. Aims

I. To test the potential of the weight drop system to induce commotio retinae in rats without causing globe rupture.

II. To demonstrate photoreceptor OS disruption in commotio retinae after central corneal weight drop injury.

6.5.2.3. Materials and Methods

Two female Wistar rats were used under terminal anaesthesia. In each animal, the right central cornea was impacted by a 31.3g weight (0.153J) and the left by a 22.6g (0.111J) weight – both with 6mm tips from 50cm – using the apparatus described in Figure 6.4.1.

Retinae were examined before and after injury by indirect fundoscopy, using tropicamide (Queen Elizabeth Hospital, Birmingham, UK) to dilate the pupils, and the sclera was marked at the sight of any identified abnormality with a permanent marker pen after dissecting off the conjunctiva and drying the scleral surface with a swab. Animals were killed 1 hr after death and retinae were processed for electron microscopy. Peripheral retinal areas that appeared macroscopically uninjured were used as control tissue.

Figure 6.5.2.
A, B and D: transmission electron micrographs of rat retina (gold sections) showing the ultrastructural effects of weight drop 1 hr after injury. C: Toludine blue stained 1µm semithin section of rat retina.

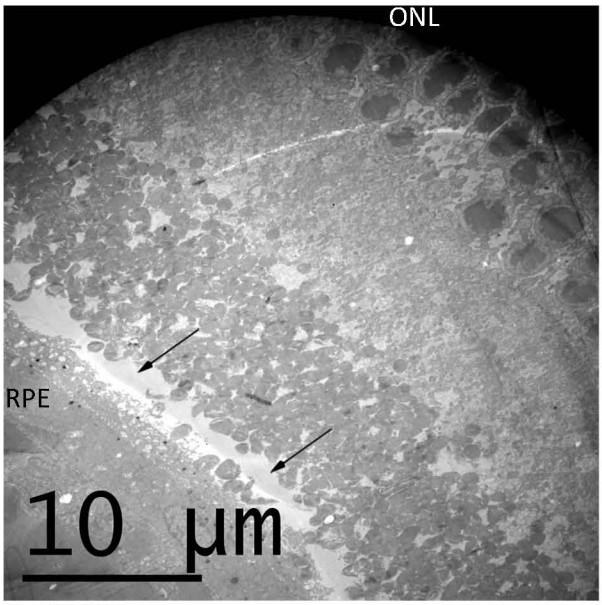

A - #2 LE
22.6g weight drop. Shows RPE to ONL. Preserved photoreceptor OS sectioned tangentially give an apparent ovoid shape. Artefactual retinal detachment (arrows).

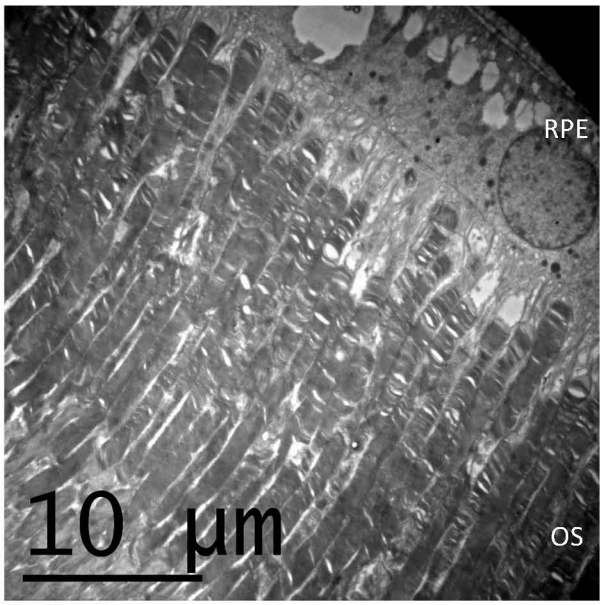

B - #3 LE
22.6g weight drop. Shows photoreceptor OS and RPE. Tissue architecture is normal

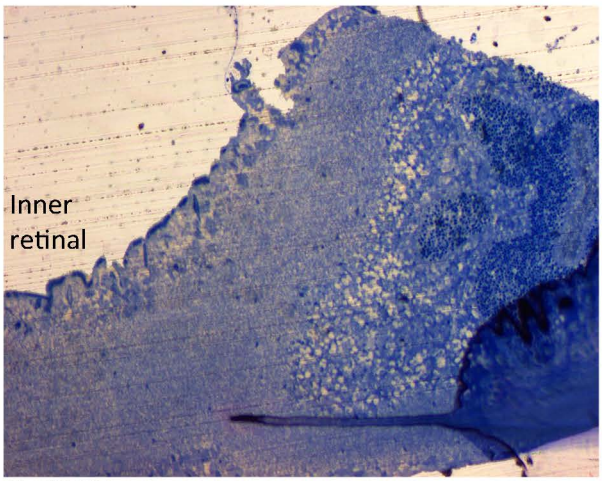

C - #2 RE
31.3g weight drop. Disorganised area of retina without recognisable retinal architecture. Magnification x10

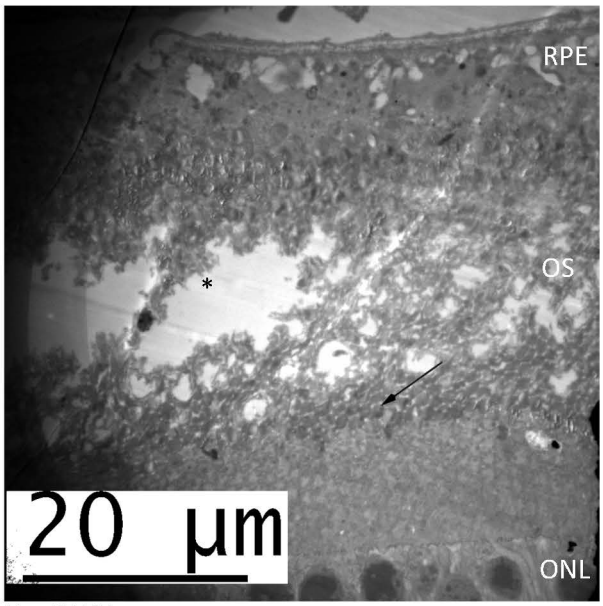

D - #3 RE
31.3g weight drop. Area of "control" retina from RPE to ONL. There is disruption of the photoreceptor OS with a tissue defect (*). Such a tissue defect is unlikely to have developed within 1 hr of injury, given the absence of any inflammatory cells. Partially formed ovoid OS are seen (arrow), which differs from previous reports of commotio retinae where the OS were completely disrupted. This is therefore likely to be artefactual damage occurring during tissue processing.

6.5.2.4. Results

Indirect fundoscopy revealed subtle retinal changes that may or may not have been consistent with the appearance of commotio retinae, but electron microscopic assessment did not show any injury consistent with commotio retinae in any eye (Table 6.5.2.4.).

Rat # - eye	Weight dropped (g)	Fundoscopy	Gross Pathology	Electron Microscopy (See Figure 6.5.2.)
2 – LE	22.6	Query retinal pallor inferotemporally – sclera marked at site; difficult to assess retinal pallor in an albino rat.	Poor fixation – *post-mortem* (artefactual) retinal detachments; marked area taken for EM.	Poor tissue architecture
3 – LE	22.6	Small vitreous haemorrhage at disc; query retinal pallor inferotemporally – sclera marked at site.	Well preserved retina looked normal. Retinal vasculature still visible in parts (inadequate PBS washout). Marked area taken for EM. Temporal retina taken as control.	Normal retinal structure
2 – RE	31.3	Vitreous haemorrhage; 2 large choroidal haemorrhages	Poor fixation – artefactual retinal detachments in addition to choroidal haemorrhages. Marked area taken for EM.	No recognisable retinal architecture
3 – RE	31.3	Larger vitreous haemorrhage than 2nd rat	Normal retina. Marked area taken for EM. Temporal retina taken as control.	Control area shows artefactual disruption of photoreceptor OS. Marked area shows normal retinal architecture (not shown).

Table 6.5.2.4.

6.5.2.5. Discussion/Conclusions

This was a terminal study and showed that the weight drop protocol can be used in recovery experiments with a low risk of globe rupture.

Commotio retinae was not induced by central corneal impact in this experimental model despite being seen clinically after both central corneal and direct scleral impact. Direct scleral impact is likely

to create a more reproducible injury to the underlying retina than the indirect contre-coup type injury generated by central corneal impact.

Since this protocol did not induce commotio and a previous studies used 6mm ball bearings on larger animals with bigger eyes such as the pig, it was concluded that the 6mm tip was inappropriately large in relation to the rat eye and so 3mm impact tips were developed for subsequent studies (Figure 6.4.2.).

6.5.3.Recovery Study Of Blunt Ocular Trauma

6.5.3.1. Hypotheses

I. Commotio retinae is reproducibly created by direct scleral impact.

II. A 3mm tip that gives a small impact area produces uniform and reproducible retinal injury.

6.5.3.2. Materials and Methods

Four female Wistar rats of weight 170-200g were used under recovery anaesthesia. Rats were killed 1 d after bilateral weight-drop injury and the eyes processed for electron microscopy. The 11.26g, 17.61g and 23.02g “iii” weights from Figure 6.4.2. were dropped from a height of 50cm using the apparatus described in Figure 6.4.1. to impact a 3mm tip onto the inferior sclera with KE of 0.055J, 0.086J and 0.113J respectively. The limbal traction suture was tied off to mark the clock hour of the injury site.

Rat #1 was injured by the 23.02g weight dropped onto the left eye and a 17.61g weight to the right eye, which ruptured. This animal was terminally anaesthetised and killed by perfusion with fixative for electron microscopy. The first and third rats were poorly perfused so fixation was by immersion.

6.5.3.3. Results

The results are presented in Table 6.5.3.3. In #1 LE (one eye of one animal only – Figure 6.5.3.3. and Table 6.5.3.3.) changes consistent with commotio retinae were seen by electron microscopy

Figure 6.5.3.1.
Scanned images of recorded findings on indirect fundoscopy after weight drop impacted the inferior retina. The abnormal areas in the inferior retinae were small and corresponded to the size and shape of

A -#2
Examination 1 day after injury. Left eye (L) 11.26g weight drop, right eye (R) 17.61g weight drop. Whitening (pallor) was difficult to assess in albino rats. The retinal appearance was subtly altered but suggestive of commotio retinae.

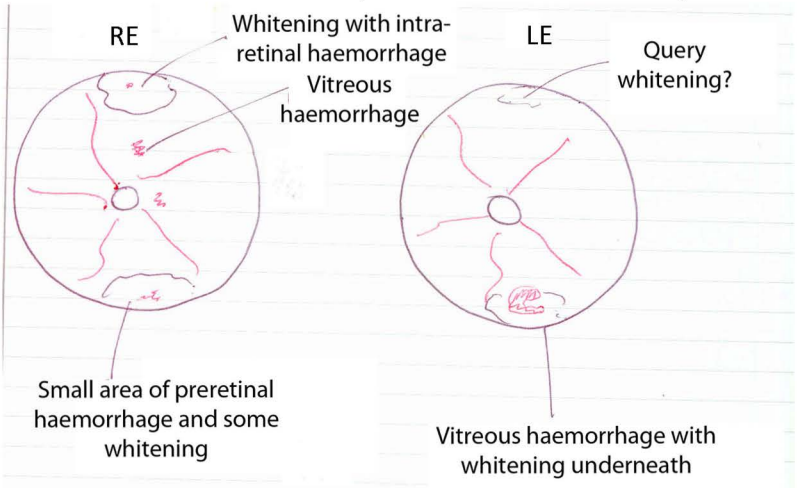

B - #3
Examination immediately after injury. LE 23.02g weight drop, RE 23.02g weight drop.

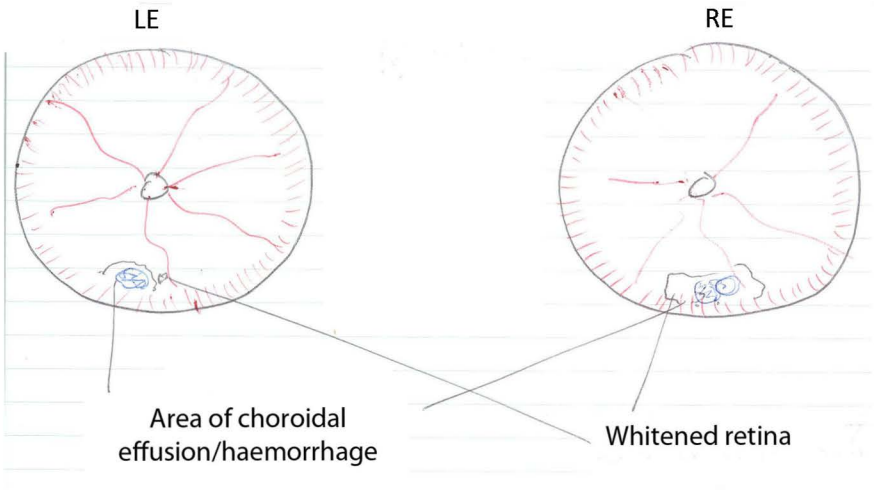

Figure 6.5.3.2.
Macroscopic pathology of fixed globes photographed down dissecting microscope.

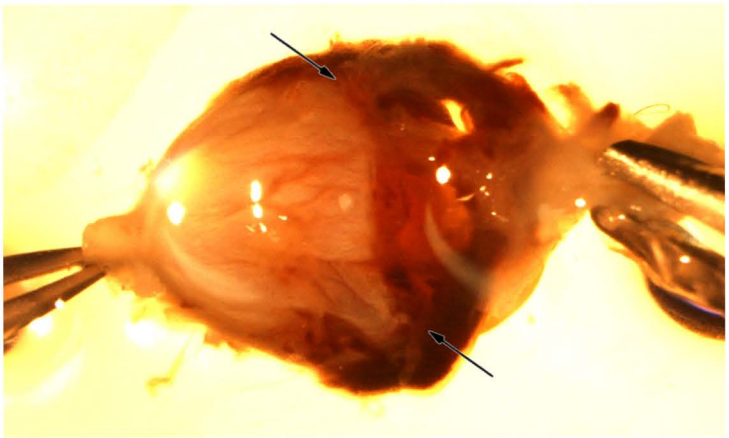

A - #1 RE
Whole eye showing limbal rupture running from 12 to 6 o'clock position (arrowed)

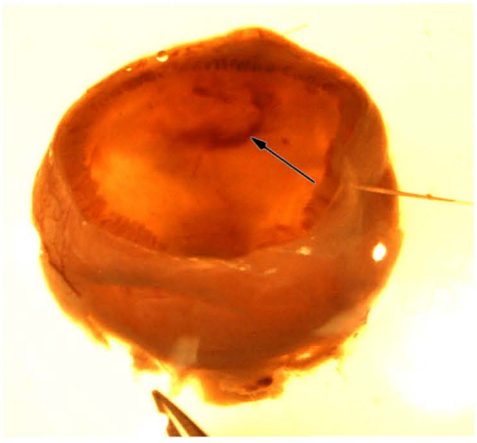

B - #2 RE
Eye cup after removal of cornea, lens and iris diaphragm. Vitreous haemorrhage overlying impact site on inferior retina (arrowed).

Figure 6.5.3.3.
Transmission electron micrographs of rat retina (gold sections) showing the effects of weight drop.

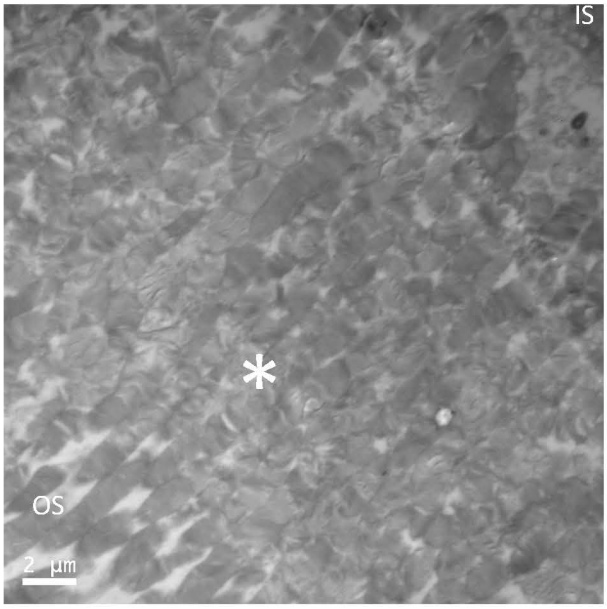

A - #1 LE
23.02g weight drop 1 hour before death. IS to OS. There is disruption of outer segments with some preservation of structure in the disrupted area (*). The rest of the retina (not shown) was normal.

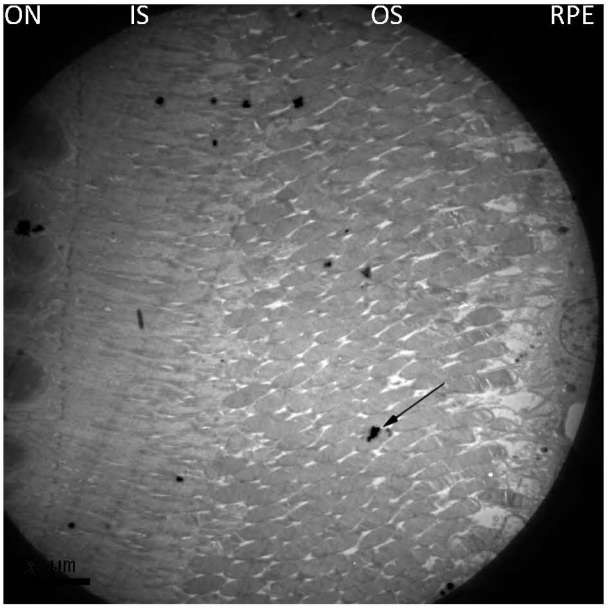

B #2 RE
17.61g weight drop 1 day before death. Normal retina. Black marks (e.g. arrow) are artefact from osmium tetroxide staining.

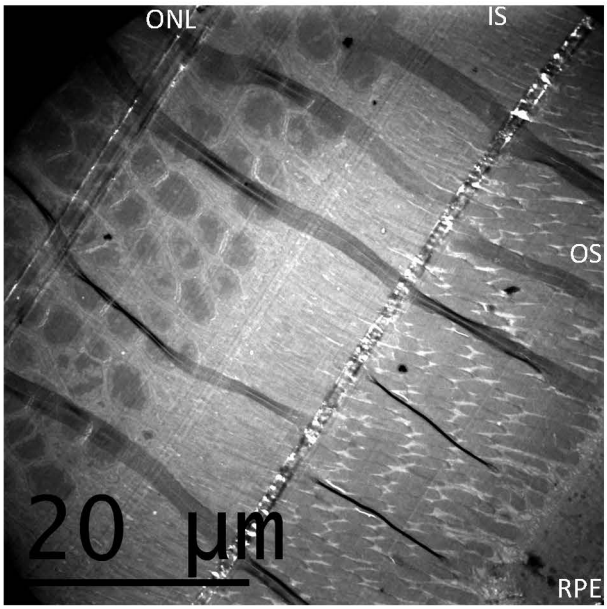

C - #3 LE
23.02g weight drop 1 day before death. Prominent linear striations running across the retina are folds in the section. Less prominent striations running parallel to the retinal layers are knife marks. Normal retina.

(photoreceptor outer segment disruption). Unfortunately this animal was killed immediately after injury, due to contralateral globe rupture, so any secondary changes that could have developed in response to OS disruption, such as inflammatory cell infiltration, did not occur. As a result, it was not possible to determine whether the changes seen were processing artefact or were present *in vivo*. The retina looked normal on fundoscopy, which suggested that the changes were artefactual, as commotio retinae should be seen clinically as retinal pallor.

Rat # - eye	Weight dropped (g)	Fundoscopy (see Figure 6.5.3.1.)	Gross Pathology (see Figure 6.5.3.2.)	Electron Microscopy (see Figure 6.5.3.3.)
1 - LE	23.02	No injury seen	Normal retina	OS disrupted
1 - RE	17.61	Rupture	Limbal globe rupture	Not processed
2 - LE	11.26	Day 1 – no injury seen Day 2 –inferior retinal pallor; overlying vitreous haemorrhage	Inferior vitreous haemorrhage – otherwise normal retina	Normal retina
2 - RE	17.61	Day 1 – preretinal haemorrhage inferiorly Day 2 – inferior pallor; superior whitening and intraretinal haemorrhage	Vitreous haemorrhage inferiorly and superiorly (contre-coup)	Normal retina
3 - LE	23.02	Day 1 – inferior choroidal effusion, haemorrhage and retinal pallor Day 2 – inferior vitreous haemorrhage	Inferior vitreous haemorrhage – otherwise normal retina	Normal retina (samples processed together)
3 - RE	23.02	Day 1 – inferior choroidal effusion, haemorrhage and retinal pallor Day 2 – inferior retinal haemorrhage	Artefactual retinal detachment away from injury site	
4 - LE	23.02	Day 1 - Inferior pallor and vitreous haemorrhage Day 2 – no change	Inferior vitreous haemorrhage; normal retina	
4 - RE	23.02	Day 1 - Inferior pallor Day 2 – no change	Normal retina	

Table 6.5.3.3.

6.5.3.4. Discussion

On fundoscopy, the abnormal areas (rats #2-4 - Figure 6.5.3.3. and Table 6.5.3.3.) were small (corresponding to the 3mm impact tip). With a limited injury, the area of abnormality may easily have been missed when selecting tissue for electron microscopy. In addition, the globe that ruptured was impacted by the light weight. With a small impact tip, a slightly off axis impact is likely

to have resulted in trauma by the sharp edge of the tip with an increased risk of globe rupture. A larger impact tip was therefore deemed less likely to cause globe rupture.

The abnormal retina (rats #2-4 – Figure 6.5.3.1. and Table 6.5.3.3.) seen on fundoscopy was very anterior and difficult to visualise by fundoscopy. A significant portion of the injured area may therefore have been ciliary body (anterior to the ora serrata) rather than retina. With an inferior approach, this was the most posterior that the impact could be delivered.

The naturally pale and translucent appearance of the albino fundus makes fundus examination and the detection of clinical signs difficult. In addition, albino rats display a variety of neuroretinal abnormalities that could affect their predisposition and response to the changes of commotio retinae (see Section 1.4.1.2.).

6.5.3.5. Conclusions

The clinical changes seen with this protocol were subtle. A relatively low energy impact was used in this experiment, so it was concluded that increasing the delivered energy may result in a more obvious injury.

6.5.4.Recovery Study of Higher Energy Blunt Ocular Trauma

6.5.4.1. Hypotheses

I. Higher (>0.113J) energy weight drop induces a more reproducible injury.

II. Lateral scleral impact injures more posterior retina than inferior scleral impact.

III. Commotio retinae is easier to visualise by fundoscopy in pigmented rats than albino rats and more similar to the clinical condition in humans.

6.5.4.2. Aim

To induce commotio retinae in pigmented rats by weight drop injury to the lateral sclera with KE >0.113J.

6.5.4.3. Materials and Methods

Four female Lister hooded rats of weight 170-200g were used under recovery anaesthesia. The "ii" weight from Figure 6.4.2. (6mm tip) was dropped from a height of 50cm onto the lateral sclera using the apparatus described in Figure 6.4.1., with (0.54J) or without (0.154J) a catapult latex to increase velocity (see Section 6.4.). Access to the lateral sclera was facilitated by a lateral cathotomy and the limbal traction suture was tied off to mark the clock hour of the impact site. Rats were killed 24 hr after bilateral weight-drop injury and tissues processed for electron microscopy.

When rat #4 RE was injured with the weight and catapult latex, the globe ruptured. This animal was killed by perfusion with 4% glutaraldehyde immediately after injury. Rat #3 RE sustained a posterior rupture that was unrecognised at the time and so this was killed with rats #1 and 2 after 24 hr.

6.5.4.4. Results

The results are presented in Table 6.5.4.3. Rat #2 RE (Figure 6.5.4.3. and Table 6.5.4.3.) had ultrastructural changes consistent with commotio retinae at the lesion site and opposite (contre-coup). The disrupted ILM of the contre-coup injury (Figure 6.5.4.3. D) suggests that this was caused by the lens impacting the retina. Unfortunately the KE required to cause these changes caused globe rupture in rats #3 and #4. No changes consistent with commotio retinae were seen with the lower energy level impacts.

Figure 6.5.4.1.
Fundoscopic images taken through the indirect ophthalmoscope 1 d after injury.

A - #1 RE
Normal appearance of peripheral retina at lesion site. Indented retina is seen at bottom of image.

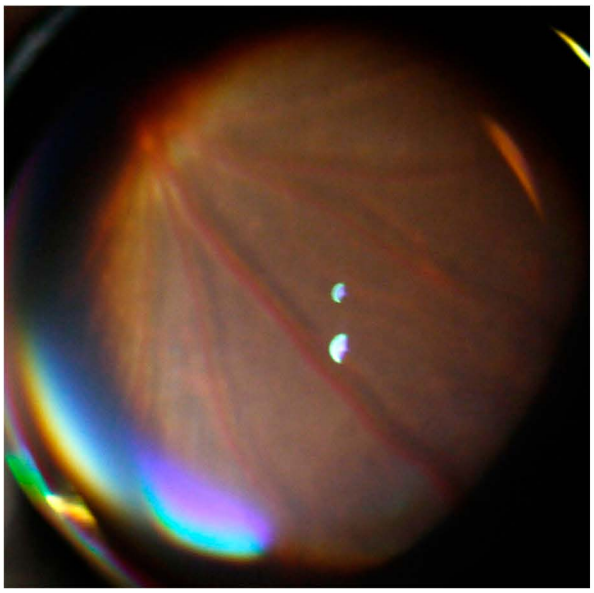

B - #2 LE
Normal appearance of retina temporal to optic disc (seen top left).

Figure 6.5.4.2.
Macroscopic retinal pathology photographed down dissecting microscope.

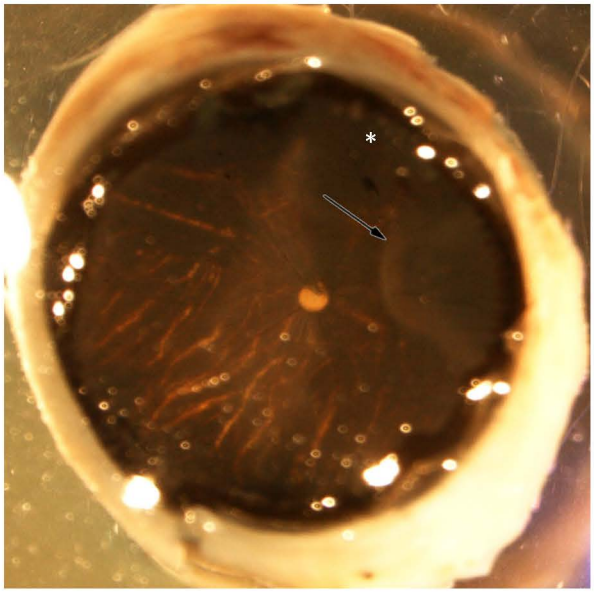

A #1 RE
Artefactual retinal detachment (arrowed) down right from lesion site (*). Note dark choroid and RPE in the Lister Hooded rats, which was not seen in albino rats.

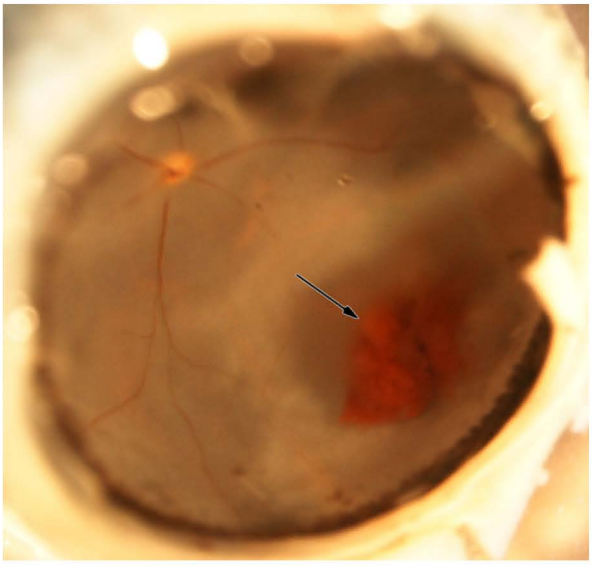

B - #4 LE
Vitreous haemorrhage (arrowed) overlying lesion site (surrounding area of retinal pallor).

Figure 6.5.4.3.
Histological appearance of rat retina 1 d after weight drop.

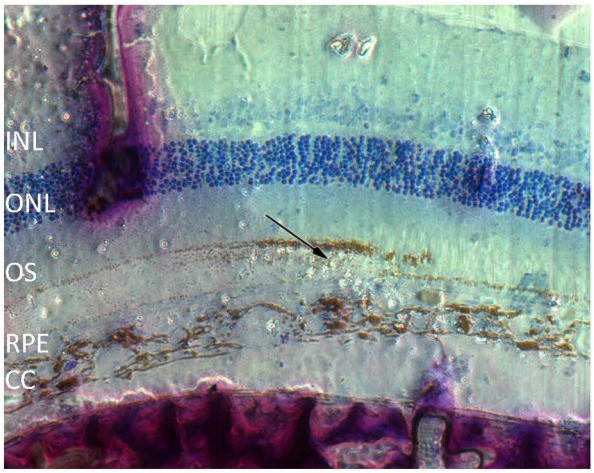

A - #1 LE
Toludine blue lightly stained section of a perilesional area in rat retina. Section thickness 1µm. Magnification x40. 31.3g weight drop. Retinal detachment may be due to processing artefact - there are pigmented cells collecting in subretinal space (arowed), but no inflammatory cells or proteinaceous material present.

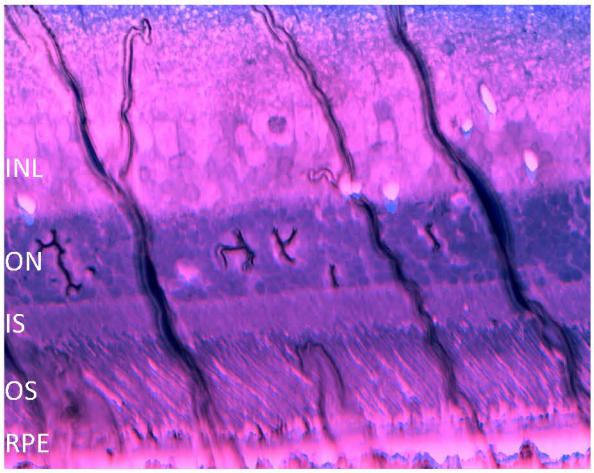

B - #2 LE
Toludine blue section of normal rat retina at lesion site. Section thickness 500nm. Magnification x40. 31.3g weight drop.

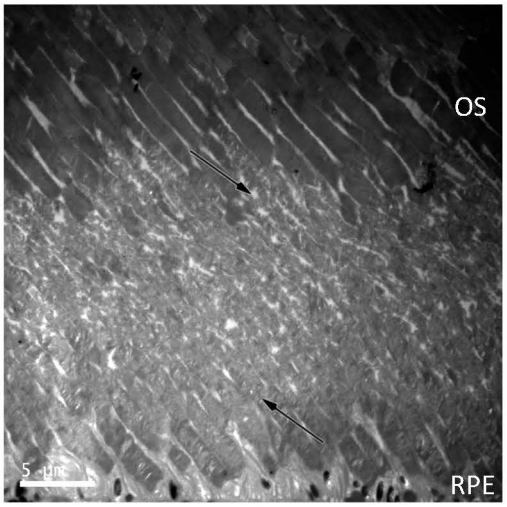

C #2 RE
Transmission electron micrograph of rat retina (gold section). RPE to OS. 31.3g + catapult latex. Disrupted photoreceptor OS at lesion site (arrows top and bottom of disrupted area). These changes are similar to those previously reported (Blight and Hart 1977).

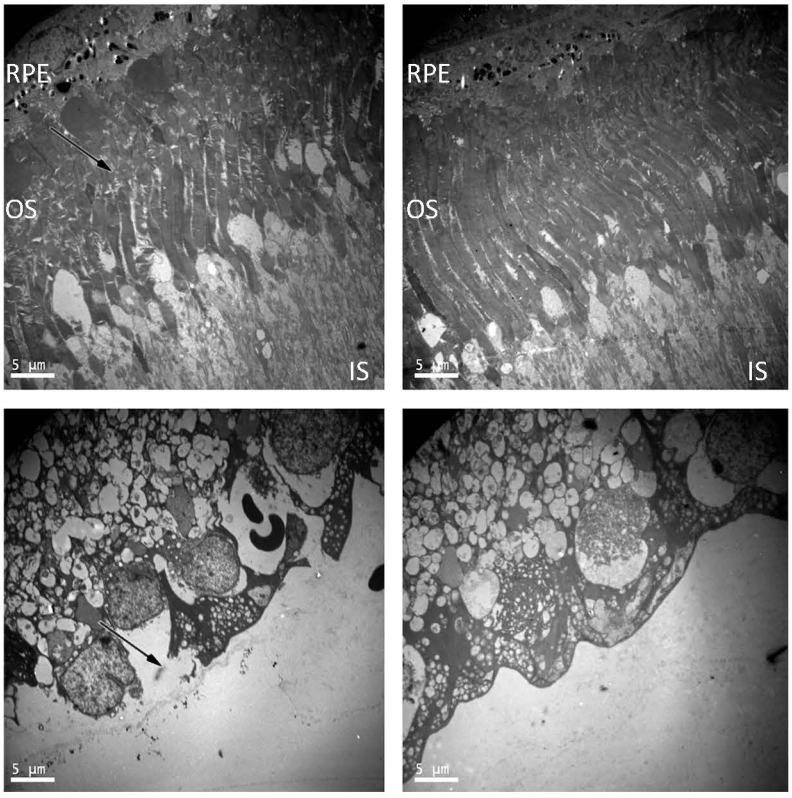

D - #2 RE
Transmission electron micrographs of rat retina opposite lesion site (gold sections). 31.3g + catapult latex. Disrupted photoreceptor outer segments (arrowed - top left) correspond to areas of disrupted ILM (bottom left - arrowed). Relatively intact outer segments (top right) correspond to intact ILM (bottom R).

Rat # - eye	Weight dropped (g)	Fundoscopy (see Figure 6.5.4.1)	Gross Pathology (see Figure 6.5.4.2.)	Electron Microscopy (see Figure 6.5.4.3.)
1 - RE	31.3	No injury seen	Perilesional RD	Area of perilesional RD shows pigment in subretinal space.
1 -LE	31.3	No injury seen	Some areas of RD	Normal retina – samples processed together.
2 - LE	31.3	No injury seen	Normal retina	
3 - LE	31.3	No injury seen	Normal retina	
4 - LE	31.3	No injury seen (killed on day 1)	Vitreous haemorrhage opposite lesion site. (processed separately). Perilesional RD.	Artefactual RD – stretched OS
2 - RE	31.3 + latex	No injury seen	Normal retina	Lesion site: - OS disrupted Opposite: areas of intact and disrupted ILM corresponding to intact and disrupted OS
3 - RE	31.3 + latex	Dense vitreous haemorrhage	Posterior rupture – lens outside of eye	Not processed
4 - RE	31.3 + latex	Rupture (killed on day 1)	Posterior rupture	ILM and OS disrupted

Table 6.5.4.3.

6.5.4.5. Discussion/Conclusions

Changes consistent with commotio retinae were only observed in eyes that had been impacted by the heaviest weight whose velocity had been increased using a catapult latex and that protocol ruptured 2/3 eyes so injured. Therefore to create commotio retinae reproducibly in future experiments, without causing globe rupture, it was concluded that a lower weight should be used with the catapult latex.

6.5.5.Recovery Study of Low Weight, High Energy Blunt Ocular Trauma

6.5.5.1. Hypothesis

Commotio retinae without globe rupture is induced by a 22.6g weight + catapult latex (estimated KE 0.62J, Section 6.4.).

6.5.5.2. Aim

To induce commotio retinae without globe rupture by weight drop with catapult latex using an impact energy of 0.62J.

6.5.5.3. Materials and Methods

Three male Sprague-Dawley rats of weights 289g, 265g and 269g were used. Rats were killed 3 d after bilateral weight-drop injury using the apparatus described in Figure 6.4.1. and the eyes processed for electron microscopy. The “i” weight shown in Figure 6.4.2. (6mm tip) was dropped from a height of 50cm onto the lateral sclera using a catapult latex to increase velocity (see Section 6.4.).

Figure 6.5.5.1.
Fundoscopic images taken through the indirect ophthalmoscope.

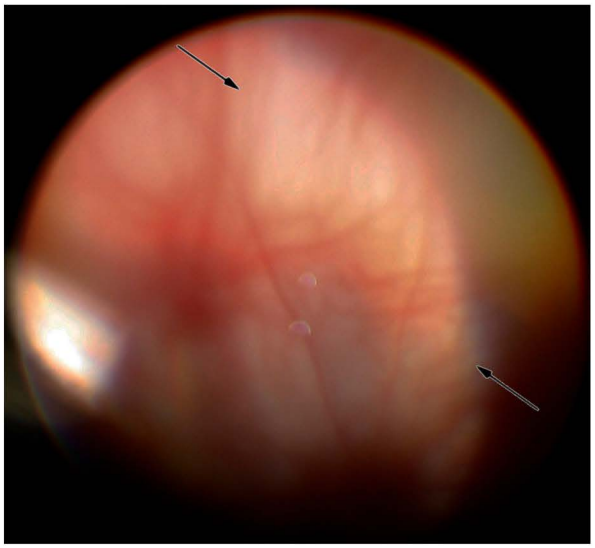

A - #2 RE
Day 1. Optic disc and temporal retina. The pale band from 11 o'clock to 3 o'clock (arrowed) is from the scleral indenter used to visualise the anterior retina.

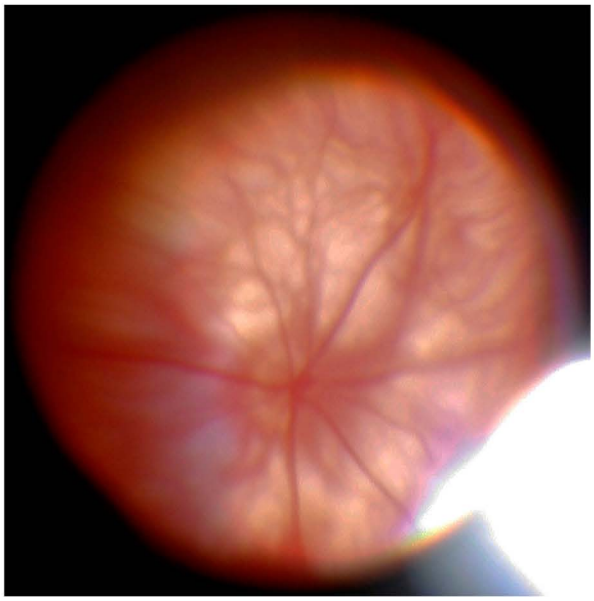

B - #2 RE
Day 4. Retina around the optic disc. Pale appearance is normal for albino rats.

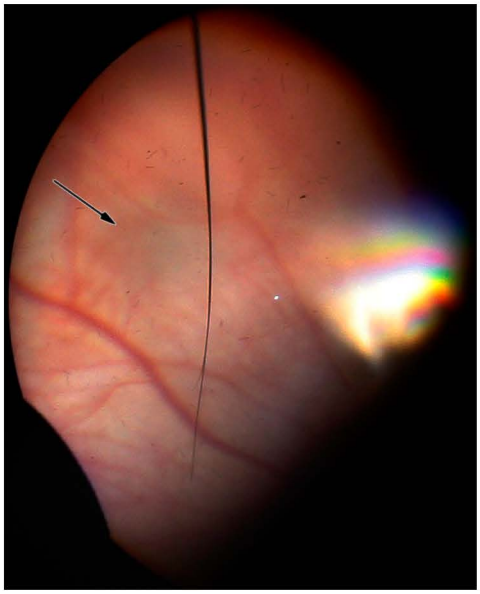

C - #2 RE
Day 4. Peripheral retina at lesion site.
A small patch of altered light reflex and subtle pallor was seen (arrowed).

Figure 6.5.5.2.
Light microscopic images of retina stained with toludine blue showing histological appearance after injury by weight drop + catapult latex. Section thickness 1µm. Magnification x40. Letters refer to specimens listed in Table 6.5.5.5.

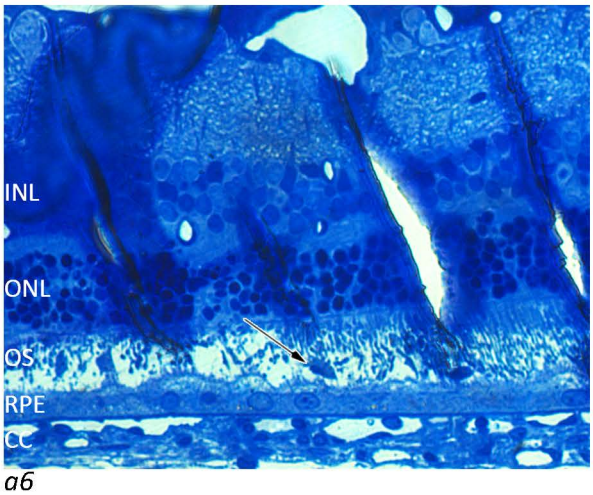

a6
Absent OS, RPE response and an inflammatory cell (arrowed) among the OS remnants.

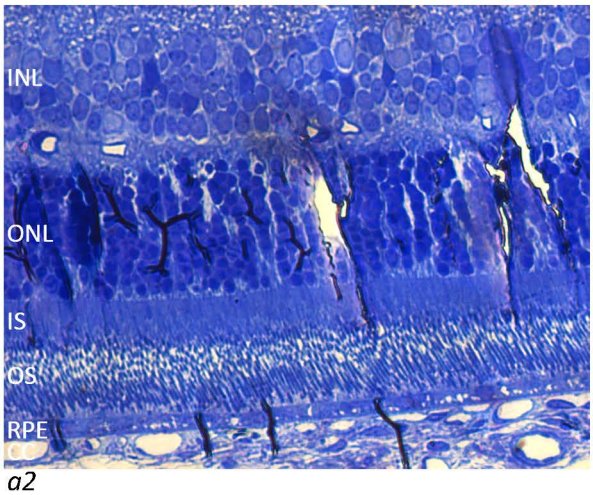

a2
Normal retina.

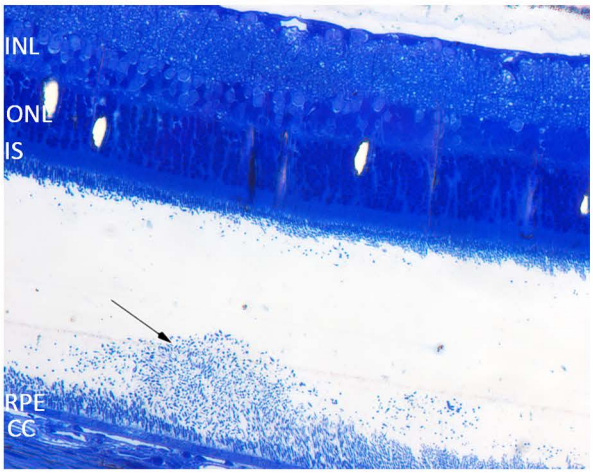

a1
Artefactual retinal detachment. This is processing artefact because there is no proteinaceous or cellular material in the subretinal space except for the fragmented photoreceptor outer segments (arrowed).

Figure 6.5.5.3.
Electron micrographic appearance of specimen *a6* (Table 6.5.5.5.) shown in Figure 6.5.5.2. Absent OS with an inflammatory cell (arrowed).

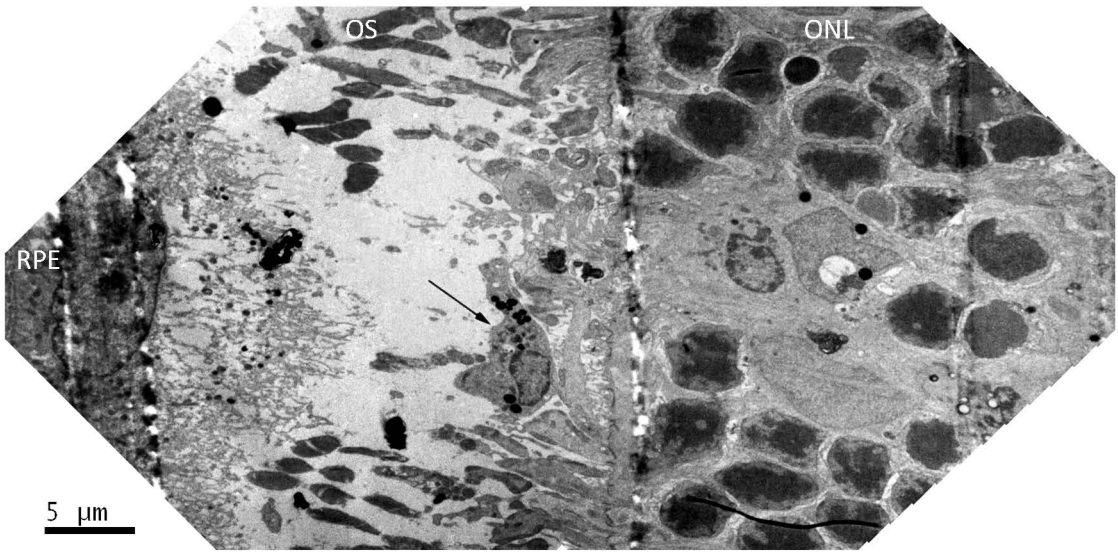

6.5.5.4. Results

The results are shown in Table 6.5.5.5. One area of one specimen (*a6* - Table 6.5.5.5. and Figures 6.5.5.2. and 6.5.5.3.) showed ultrastructural changes consistent with commotio retinae, in that absent OS and inflammatory cells in the subretinal space suggested previous OS damage.

Rat # - eye	Weight dropped (g)	Fundoscopy (see Figure 6.5.5.1.)	Toludine blue (see Figure 6.5.5.2.)	Electron Microscopy (see Figure 6.5.5.3.)
1 - LE	22.6 + latex	Vitreous haemorrhage and subtle underlying retinal pallor	Samples processed together. *a1* - shows artefactual RD. *a2-5* - specimens showed normal retina *a6* - specimen showed a section of abnormal OS associated with an RPE response	Samples processed together. *a6* - absent and disrupted OS with an RPE response
1 - RE	22.6 + latex	Subtle temporal retinal pallor		
2 - LE	22.6 + latex	Hyphaema with poor fundus view		
2 - RE	22.6 + latex	Query subtle temporal retinal pallor		
3 - LE	22.6 + latex	Dense vitreous haemorrhage		
3 - RE	22.6 + latex	Temporal retinal haemorrhage + pallor		

Table 6.5.5.5. Note: Specimens were labelled *a1-6* because eyes were pooled for processing.

6.5.5.5. Discussion/Conclusions

This weight drop apparatus with catapult latex delivered a variable energy impact with a moderately heavy weight moving slowly (up to 7 m/s – see Section 6.4.) that was difficult to standardise. Only with impact speeds >5m/s were any changes consistent with commotio retinae observed in the experiments so far. Published studies have used higher speed (20-50 m/s) impacts with lower weights (0.38 – 16g) than can be accommodated using the weight drop apparatus developed here. Reproducible injury is more likely to be created by replicating these higher velocity impact protocols.

6.6. Ballistic Injury

6.6.1.Hypothesis

Commotio retinae is more reproducibly created by a ballistic high speed (20-50m/s) low weight (≤1g) impact than by using the weight drop apparatus.

6.6.2.Aim

To cause commotio retinae in the retina underlying the site of impact of a 0.5-1g pellet delivered at 20-50m/s to the scleral surface of a rat eye.

6.6.3.Materials and Methods

A compressed air system was designed to deliver a high velocity projectile to the rat eye, using this ballistic injury to induce commotio retinae.

6.6.3.1. Device Components

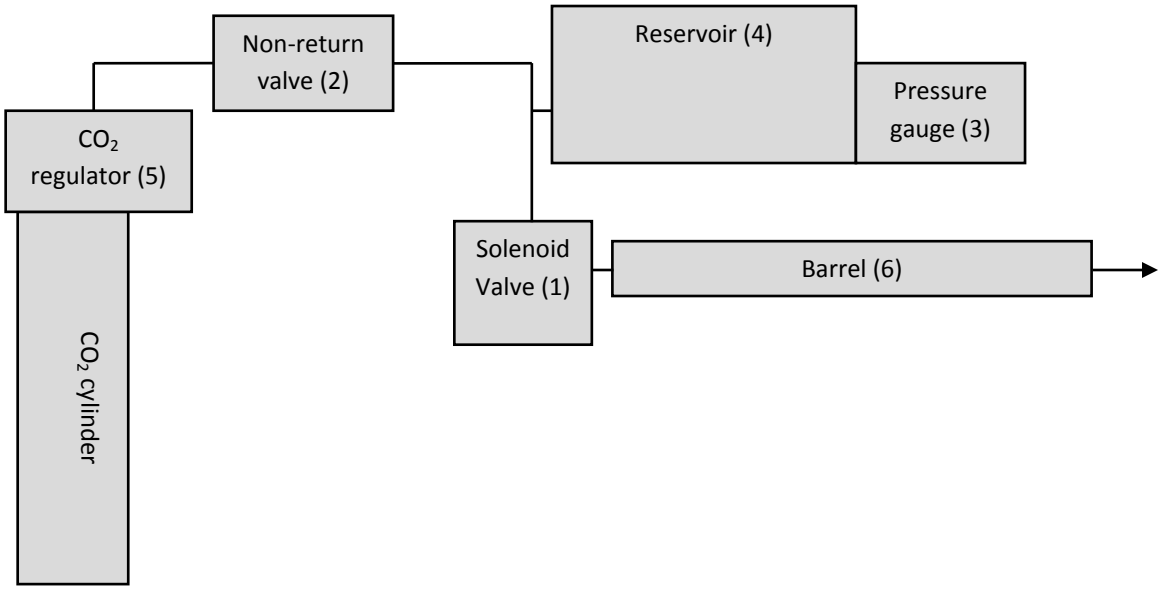

Figure 6.6.3.1. Diagram of the pneumatic components of the experimental apparatus shown in Figure 6.6.3.2. The numbered components are:

1. VQ20 2 port solenoid valve,24Vdc M5 8mm (RS components, Birmingham, UK)
2. Pneumatic in line non-return valve 8mm (RS components)
3. Pressure gauge,40mm dia 0-10bar R1/8 (RS components)
4. 1/8in BSP Norgren air reservoir,0.5l. M/163/50 (RS components)
5. Mini MIG CO2 regulator (Welding Equipment and Cutting Services, Sheffield, UK)
6. 0.22 inch barrel blank (cut to 300mm and machined to fit G1/4 female connector; Sandwell Field Sports, Sandwell, UK)

Black 8mm standard PU tubing,30m (RS components) is shown as black lines joining the components and was connected to the components using the hydraulic fittings: push-in branch tee adaptor,1/8inx8mm (RS components); male parallel straight adaptor,G1/4x8mm (RS components); female BSPP sleeve fitting,G1/4xG3/8 (RS components); female BSPP sleeve fitting,G1/4xG1/2 (RS components). A 24V/0.5A direct current power supply unit (RS components) and a Flex Switch (Maplin, UK VJ83E) were used to power and control the solenoid-actuated valve.

Figure 6.6.3.2
The head holder and ballistic injury apparatus used to deliver a low weight/high velocity projectile to rat eyes using compressed air. Opening the regulator on the CO_2 cylinder pressurises the system, monitored by the pressure guage. The barrel is loaded by unscrewing it from the push-fit adapter next to the valve. The electrical switch opens the solenoid actuated valve, propelling a projectile down the barrel.

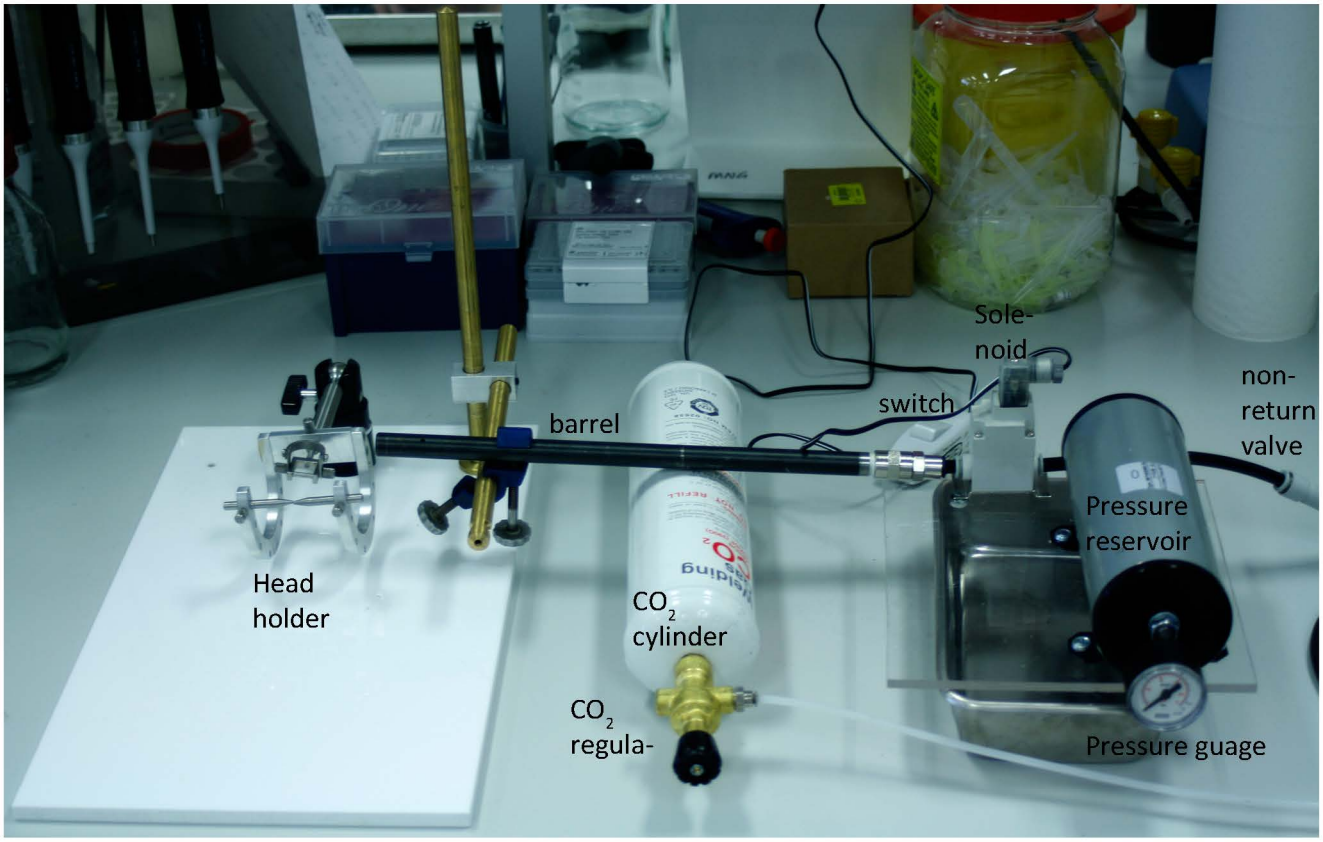

Figure 6.6.5.2.
Screenshot showing the sound waveform recorded when the ballistic injury apparatus above was used to fire a BB into a metal plate. The waveform was used to calculate velocity.

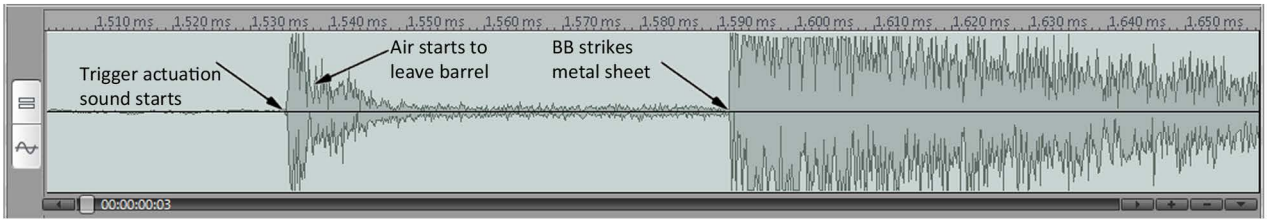

All parts are specified to withstand pressures of ≥6 bar. The VQ20 solenoid valve has a specified response time <5ms, an effective cross-sectional area of 9mm^2 and a flow rate of 491Nl/min. A muzzle velocity of 50m/s after linear acceleration would take the projectile 12ms to leave the barrel from valve opening (0.3m distance/25m/s average speed). Thus a response time of 5ms was deemed acceptable because the valve would go from fully closed to fully open in less than half the time it would take for the projectile to leave the barrel at 50m/s and a faster response time was unrealistic within the equipment budget. With a projectile travelling at 50m/s the flow rate of gas down the barrel would be 0.07l/min ($2.38x10^{-5}m^2$ cross sectional area x 50m/s x 60s) which is well below the maximum flow rate of the valve.

6.6.3.2. Energy calculations

A lower range estimate of projectile KE of 0.2J was derived from considering a 1g projectile (m=1g) travelling at 20m/s using the formula given in Section 6.4. To calculate the force required to generate a projectile KE of 0.2J:

Change in KE = Work Done = force * distance

Change in KE = 0.2J and distance = 0.3m (the length of the barrel), so force = 0.666N. The barrel has a diameter of 5.5mm (0.22 inches) giving a cross sectional area of $2.38*10^{-5}m^2$ (area = πr^2). To calculate the chamber pressure required:

Force = Pressure * Area

Thus pressure = 28011pa=0.28bar and internal chamber pressure before firing = 0.28bar above atmospheric pressure. Doing the same calculations for a 1J (1g, 45m/s) pellet yields an internal pressure difference of five times as much, thus a total chamber pressure of 2.4bar. Note that the energy of the projectile is related to chamber pressure and independent of the pellet weight. So a 0.5g pellet fired by 2.4bar has an energy of 1J and a velocity of 63m/s.

6.6.3.3. Methods

The head of an anaesthetised rat was fixed in a head-holder frame (as shown in Figure 6.6.3.2.), the inferior sclera exposed and the eye rotated superiorly with a limbal traction suture. The system was pressurised with CO_2 and a projectile fired against exposed sclera from a distance of 0.5 cm.

6.6.4.Cadaveric Study of Ballistic Ocular Injury

6.6.4.1. Aim

To determine the maximum chamber pressure that can be used to fire a projectile against a rat eye with minimal risk of globe rupture.

6.6.4.2. Materials and Methods

Thirteen female Wistar rat cadavers (140 – 420g) were used immediately after death to minimise any post-mortem drop in intraocular pressure. The ballistic injury apparatus described in Section 6.6.3. was used to deliver different weighted projectiles at high velocity to the lateral sclera. If rupture did not occur, the chamber pressure was increased and the eye injured again. Four weights of projectile were used: a commercially available 0.91g lead pellet (rsmsports, ebay.co.uk); a commercially available 0.5g alloy and plastic pellet (pointed tip reduced to a smooth dome; Keens Guns and Tackle, Bridgend, UK); a plastic 0.16g pellet custom-made in our laboratories; a 0.095g plastic BB (ball bearing; reduced in size from 6mm to fit the 0.22 inch barrel; Park Lane Gifts, amazon.co.uk). At the low pressures used, all stock ammunition tended to stick in the barrel and so needed to be trimmed down to a less tight fit.

6.6.4.3. Results

The results are presented in Table 6.6.4.3. Chamber pressures below 0.15 bar rarely caused globe rupture.

Animal	History	Projectile weight (g)	Eye	Chamber pressure (bar)	Expected velocity (m/s)	Globe injury
1	405g rat with IUGR anaethetised for 3 hr and killed by overdose of intravenous	0.91	RE	1	39.6	Rupture
			LE	0.5	28.0	Intact globe
				0.75	34.3	Rupture
2	300g rat anaesthetised for 3 hr, subjected to intermittent hypoxia/hypercapnia and killed by intravenous urethane overdose	0.91	RE	0.6	30.7	Rupture
			LE	0.5	28.0	Intact
				0.6	30.7	Intact
				0.8	35.4	Rupture
3	380g IUGR rat treated similarly to #1	0.91	RE	0.6	30.7	Rupture
			LE	0.5	28.0	Rupture
4	370g IUGR rat treated similarly to #1	0.91	RE	0.5	28.0	Rupture
			LE	0.4	25.1	Rupture
5	300g rat treated similarly to #2	0.91	RE	0.4	25.1	Rupture
			LE	0.3	21.7	Rupture
6	370g IUGR rat treated similarly to #1	0.91	RE	0.3	21.7	Rupture
			LE	0.25	19.8	Rupture
7	140g rat treated similarly to #1	0.5	RE	0.2	23.9	Rupture
			LE	0.1	16.9	Rupture
8	397g IUGR rat treated similarly to #1	0.095	RE	0.1	38.8	Intact
				0.2	54.8	Intact
				0.4	77.5	Intact
				0.8	109.7	Rupture
			LE	0.4	77.5	Rupture
9	375g IUGR rat treated similarly to #1	0.16	RE	0.3	51.7	Rupture
			LE	0.15	36.6	Rupture
10	150g rat treated similarly to #1	0.095	RE	0.2	54.8	Rupture
			LE	0.15	47.5	Rupture
11	305g rat treated similarly to #2	0.095	RE	0.1	38.8	Intact
				0.15	47.5	Rupture
			LE	0.1	38.8	Intact
				0.15	47.5	Intact
				0.2	54.8	Rupture
12	275g IUGR rat treated similarly to #1	0.095	RE	0.1	38.8	Intact
				0.15	47.5	Rupture
			LE	0.1	38.8	Intact
				0.15	47.5	Rupture
13	420g IUGR rat treated similarly to #1	0.095	RE	0.125	43.3	Intact
				0.15	47.5	Rupture
			LE	0.125	43.3	Intact
				0.15	47.5	Rupture

Table 6.6.4.3. Pressures causing rupture are shown in red. Expected velocity was calculated as described in Section 6.6.3.3. IUGR = intrauterine growth retardation

6.6.4.4. Discussion/Conclusions

The maximum chamber pressure tolerated for firing the projectile without causing globe rupture was 0.1-0.125 bar was. Because previous studies used projectile velocities of 20-50m/s to induce commotio retinae, the maximum velocity possible (achieved using the lowest weight) was preferred, so a 0.095g BB was used for future studies.

6.6.5. Measuring the Velocity of Projectiles Delivered by the Ballistic Injury Apparatus

6.6.5.1. Rationale

To assure reproducibility and ease of reporting of the injury protocol it is necessary to know the range of projectile velocities produced by the compressed air device.

6.6.5.2. Aim

To determine the mean muzzle velocity and its variation when a 0.095g BB is fired with a chamber pressure of 0.125 bar.

6.6.5.3. Materials and Methods

Bullet velocity was measured using a PC soundcard as has been previously reported (Courtney and Edwards 2006). Briefly, a Dell Studio XPS (Dell Corporation Ltd, Berkshire, UK) laptop was used to record the sound of the compressed air device being fired using MAGIX Music Editor 3 (MAGIX AG, Reno, NV USA) at a metal plate at known distance from the muzzle. The waveform was then viewed (see Figure 6.6.5.2.) and the time between air leaving the barrel and the BB impact with the metal plate recorded at ranges of 1cm, 10.5cm, 22cm, 31.5cm and 42cm from the muzzle for 10 iterations at each distance. Mean velocity at each range was calculated as distance/time.

6.6.5.4. Results

The results are shown in Table 6.6.5.3. and Figure 6.6.5. Velocity at 1cm from the muzzle was 20.2 ± 1.08m/s and velocity decays with time after injury. Assuming linear deceleration, the rate of decay is 0.19m/s for every cm travelled, thus 20.2m/s approximates muzzle velocity.

Distance (cm)	Time to impact (ms)	Mean velocity ± standard error (m/s)
1	30.7	20.2* ± 1.08
10.5	35.7	19.0 ± 2.24
22	44.8	14.9 ± 0.80
31	51.9	14.2 ± 0.66
42	61.9	13.1 ± 0.63

Table 6.6.5.3. Mean BB velocity at different distances from target. * Velocity at 1cm was taken as muzzle velocity and, assuming linear acceleration, was calculated as twice the mean velocity at which the BB travelled through the barrel.

Figure 6.6.5. Mean velocity at different distances from target ± SEM.

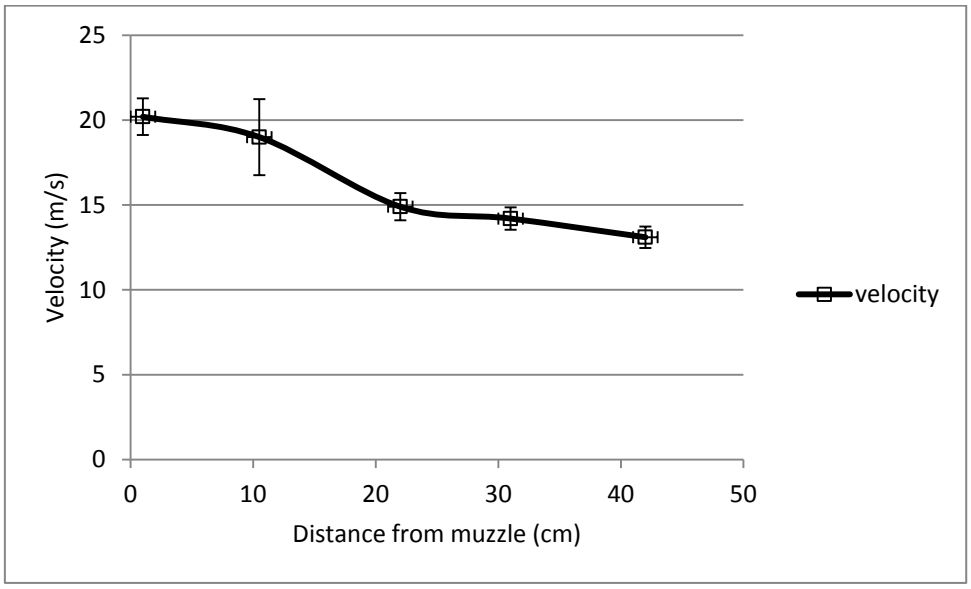

6.6.5.5. Discussion/Conclusions

The standard error of the mean velocity at each distance is small indicating that kinetic energy delivered to the eye by the compressed air delivery system is reproducible. The impact velocity with a 0.095g BB and a chamber pressure of 0.125 bar was 20m/s with a KE on impact of 0.019J.

6.6.6. Electron Microscopic Terminal Study of Ballistic Ocular Injury

6.6.6.1. Rationale

The experiments reported in Section 6.5. showed that, in rats, low velocity weight drop injury did not induce commotio retinae reproducibly and previous experimental studies of commotio retinae used high velocity (20-50m/s) projectiles. Further studies demonstrated that, in rats, ballistic injury with a 0.095g BB travelling at 20m/s did not cause globe rupture. This ballistic injury protocol was therefore used to induce commotio retinae.

6.6.6.2. Hypothesis

Ballistic injury from a 0.095g BB impacting the scleral surface at 20m/s reproducibly induces commotio retinae in the rat eye.

6.6.6.3. Aim

To cause commotio retinae by delivering a BB of 0.095g at 20m/s to the scleral surface of rat eyes without causing globe rupture.

6.6.6.4. Materials and Methods

Four female Lister Hooded rats of weight 170-200g were used under terminal anaesthesia. A 0.095g BB was fired at the lateral sclera of both eyes at 20m/s using the ballistic injury apparatus described in Section 6.6.3. The eye was rotated with a limbal traction suture, which was then tied off to mark the clock hour of the impact site. Indirect fundoscopy was performed to look for commotio retinae immediately after injury. Rats were killed 2 hr after injury and retinae were processed for electron microscopy. Uninjured inferior sclera was used as normal control tissue.

6.6.6.5. Results

Fundoscopy revealed retinal pallor underlying the impact site in all eyes and variable vitreous haemorrhage immediately after injury (Figure 6.6.6.1). Retinal pallor was also obvious under the dissecting microscope (Figure 6.6.6.2.). Electron microscopy of resin-embedded retinal sections

Figure 6.6.6.1.
Fundoscopic images taken through the indirect ophthalmoscope.

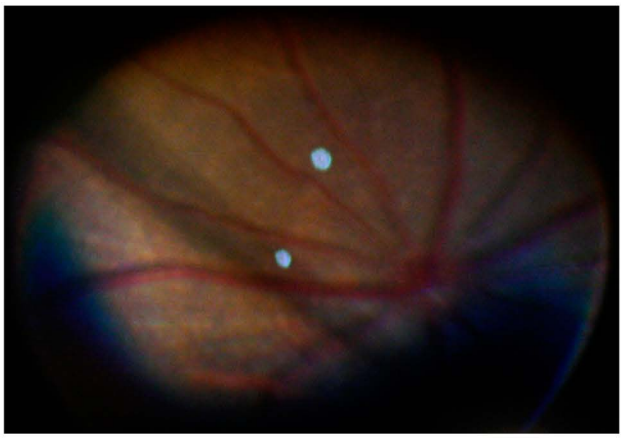

A
Normal appearance of retina before injury. Note the darker red/pink appearance and RPE texture visible through the retina.

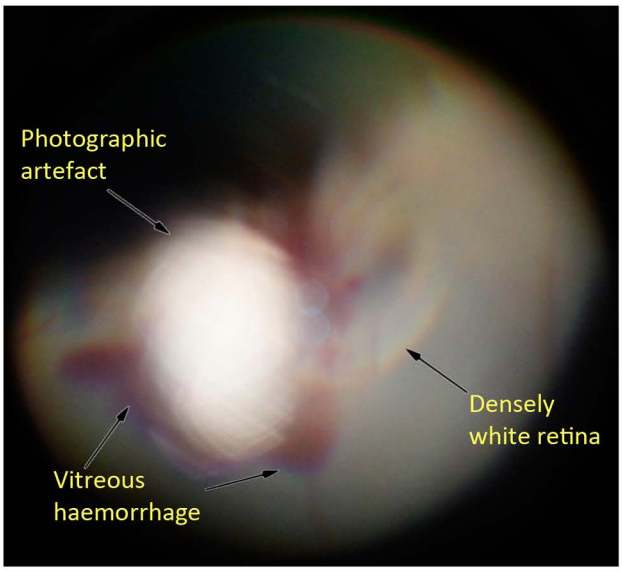

B
Vitreous haemorrhage with underlying white area of retina

Figure 6.6.6.2.
Macroscopic pathology of eyes photographed down dissecting microscope.

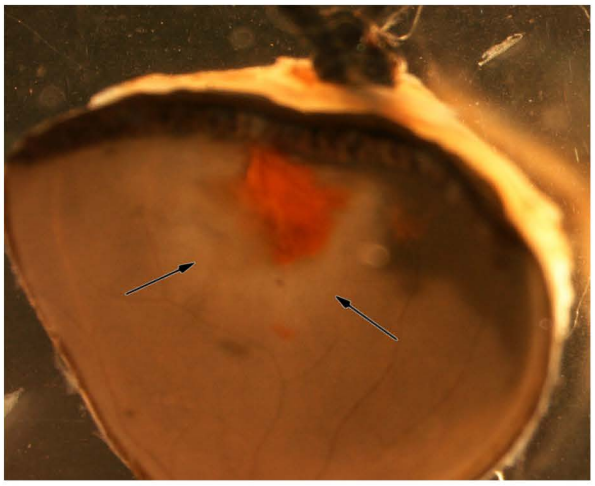

A
The eye shown in Figure 6.6.6.1.B. Vitreous/pre-retinal haemorrhage surrounded by an area of retinal pallor (commotio retinae - arrowed)

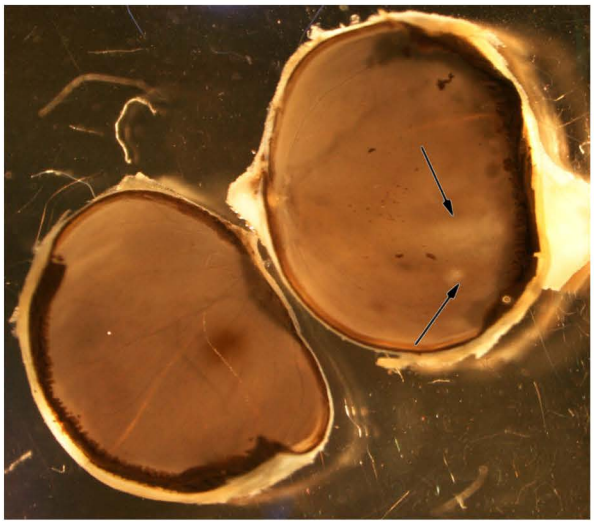

B
Eye cup has been cut in two. The left hand section shows a spot vitreous haemorhage overlying retina with a normal appearance. The right hand section shows areas of retinal pallor (commotio retinae - arrowed)

Figure 6.6.6.3.
Transmission electron micrographic appearance of rat outer retina (gold sections) 2 hrs after ballistic injury. (A) Normal control area of retina. (B) Disrupted photoreceptor inner and outer segments and external limiting membrane.

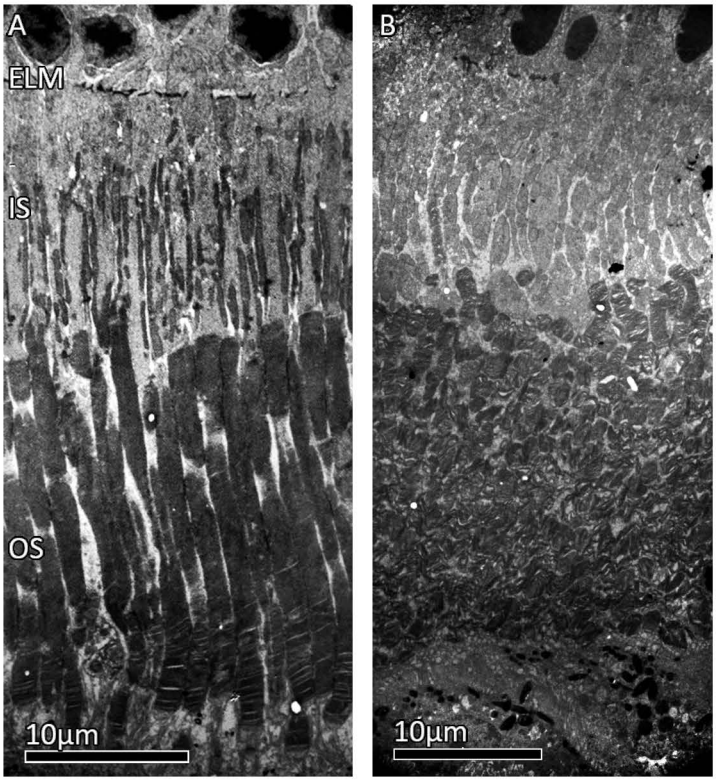

showed photoreceptor OS and IS disruption all 8 eyes and external limiting membrane (ELM) disruption in 3 eyes (Figure 6.6.6.3.). There were occasional apoptotic nuclei in the ONL (Figure 6.6.7.4.A)

6.6.6.6. Conclusions

The ballistic injury protocol induced a retinal injury with the clinical and ultrastructural features of commotio retinae, without globe rupture and was therefore used in subsequent recovery studies.

As 98% of rat photoreceptors are rods and the ONL contains exclusively photoreceptors, apoptotic ONL nuclei are those of photoreceptors and are likely to be of rods. The evidence for photoreceptor apoptosis is discussed in the next section.

6.6.7.Electron Microscopic Recovery Study of High Velocity Ocular Injury

6.6.7.1. Rationale

Ballistic trauma, as described in Section 6.6.6, caused an injury that looked clinically and ultrastructurally like commotio retinae. This study set out to demonstrate a cellular response of the photoreceptors to injury. If injury-induced photoreceptor death occurs, morphological features of cell death should be visible in these cells by 2 d.

Additionally, after macular commotio retinae in humans, 26% of cases stabilise with a visual acuity <6/9 and persistent, visually debilitating, paracentral scotomas are not uncommon, with visual impairment caused by photoreceptor degeneration(Blanch et al. 2013),(Souza-Santos et al. 2012). If photoreceptor apoptosis occurs, that would suggest that regulated apoptotic signalling mediates cell death in a proportion of photoreceptors, implying that antiapoptotic neuroprotective therapies have a potential role in the treatment of commotio retinae. It was therefore deemed important to look for evidence of apoptosis.

6.6.7.2. Hypotheses

I. Ballistic retinal injury causes commotio retinae characterised by damage to photoreceptor OS with associated infiltration of inflammatory cells.

II. Photoreceptor apoptosis occurs after ballistic retinal injury.

6.6.7.3. Aim

To cause commotio retinae and characterise the cellular response 2 d later.

6.6.7.4. Materials and Methods

Four anaesthetised female Lister-hooded rats received bilateral ballistic ocular injury (as described in Section 6.6.6.), except that injury was made to the inferior sclera, which, (1), afforded better surgical access than the lateral sclera and, (2), allowed comparison with the uninjured inferior retinal control tissue described in Section 6.6.6. Indirect fundoscopy was performed immediately and then 2 d after injury to look for commotio retinae. Animals were killed 2 d later and samples were processed for electron microscopy.

6.6.7.5. Results

Fundoscopy 2 d after injury revealed inferior retinal pallor in all eyes in which the inferior retina could be visualised (7/8) and vitreous haemorrhage in 5 eyes (Figure 6.6.7.1.). Retinal pallor was also visible under the dissecting microscope (Figure 6.6.7.2.). Light microscopy of semi-thin sections stained with toluidine blue and H&E revealed sub-retinal and intra-retinal haemorrhage in 2 eyes, gross disorganisation of retinal structure at the centre of the impact site in 3 eyes and abnormal or poorly staining nuclei at the centre of the impact site in all eyes (Figure 6.6.7.3.). Transmission electron micrographs demonstrated necrotic photoreceptor nuclei, oedema and histiocyte infiltration central to the impact site and apoptotic nuclei peripheral to it (Figure 6.6.7.4.).

Figure 6.6.7.1.
Fundoscopic images taken through the indirect ophthalmoscope.

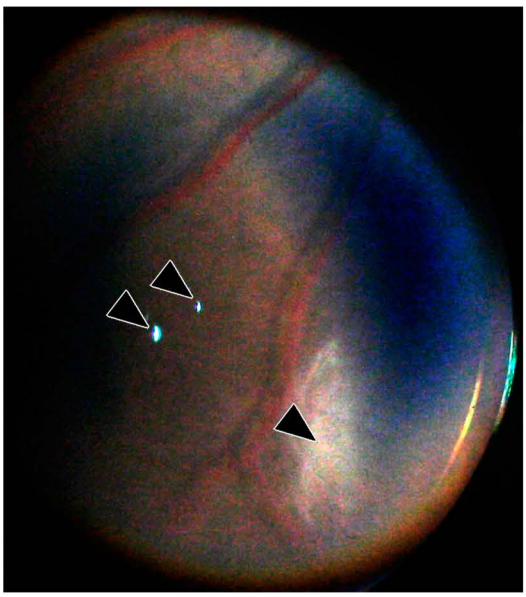

A
Normal appearance of retina before injury. Note the darker red/pink appearance and RPE texture visible through the retina.

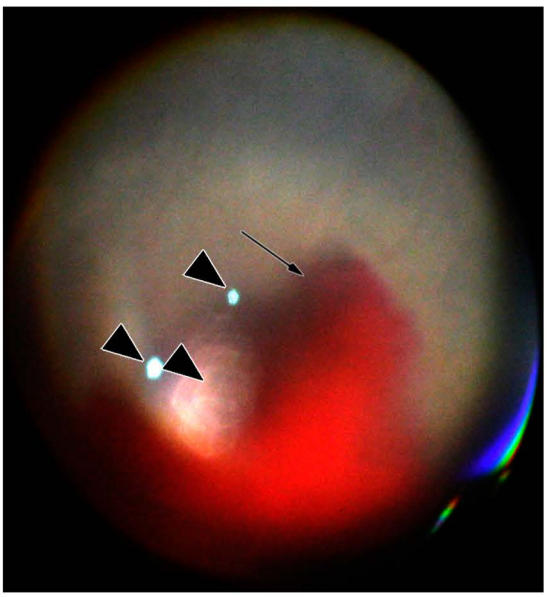

B
Vitreous haemorrhage (arrowed) and surrounding pale retina.

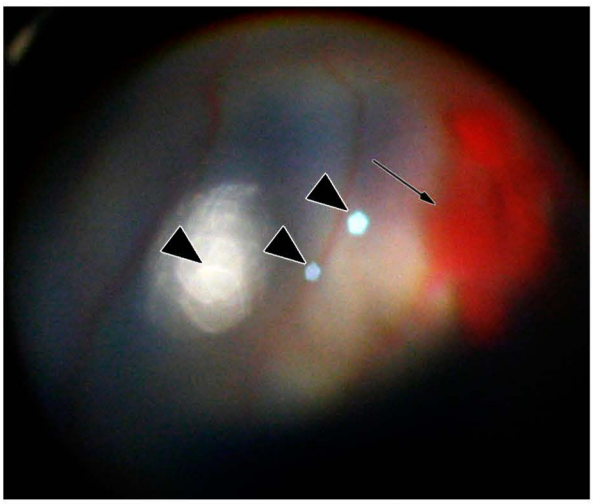

C
Vitreous haemorrhage (arrowed) and pale retina (yellow dotted circle).

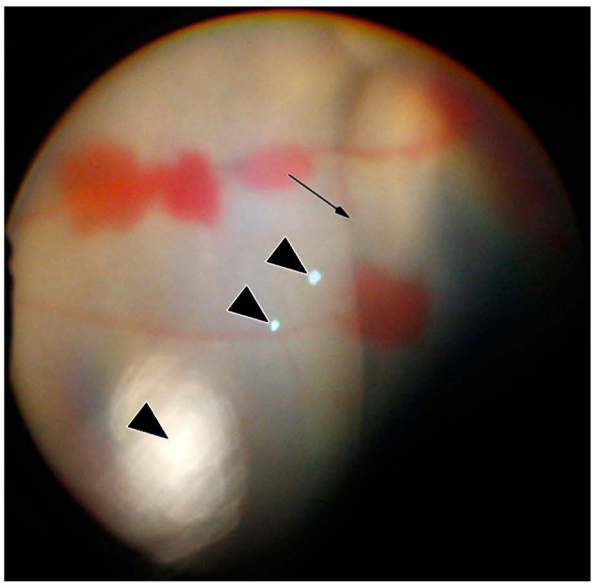

D
Vitreous haemorrhage originating along blood vessel, raised and pale area of retina (arrowed).

Figure 6.6.7.2.
Macroscopic pathology photographed down dissecting microscope.

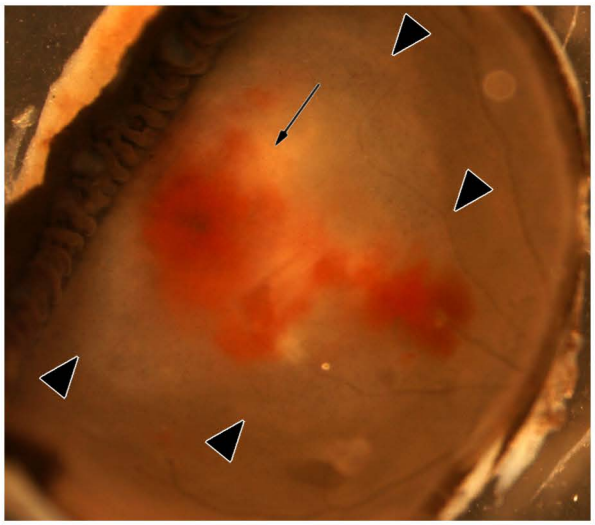

A
Vitreous haemorrhage overlying an area of raised and whitened retina (arrowed) wth surrounding subtle retinal pallor (arrowheads).

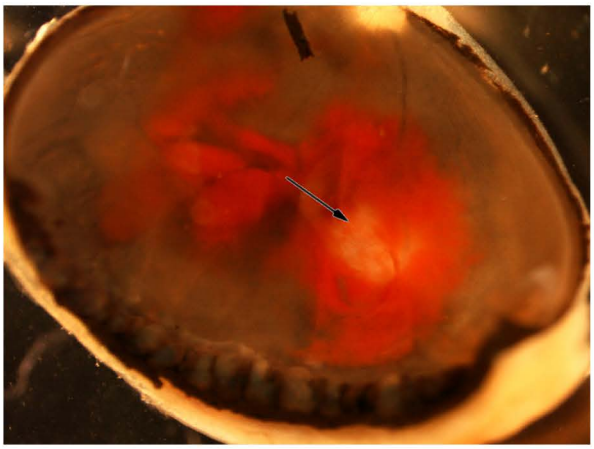

B
Vitreous haemorrhage overlying an area of raised and whitened retina (arrowed).

Figure 6.6.7.3.
1µm thick semi-thin resin embedded sections of rat retina 2 days after high velocity impact.

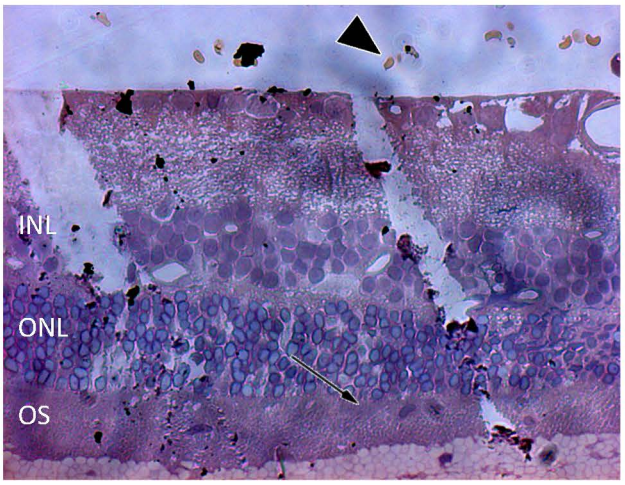

A

H&E stained section. Magnification x40. Inflammatory cells among OS remnants (arrow) - note variable thickness of OS. Few vitreal erythrocytes (arrowhead).

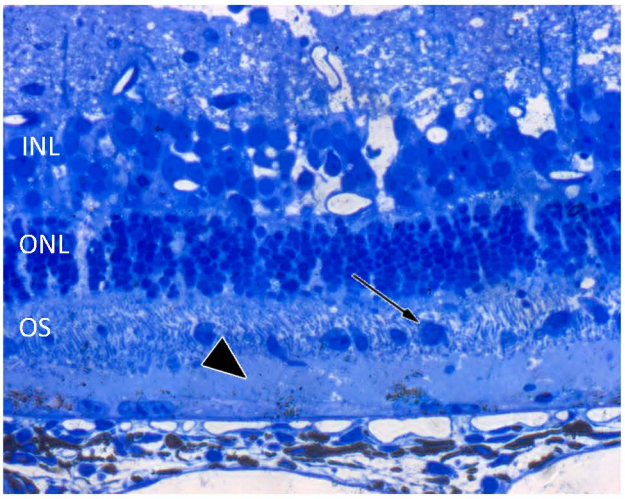

A2

Toludine blue stained section from same eye as A. Magnification x40. Inflammatory cells among OS remnants (arrow), shallow retinal detachment (arrowhead).

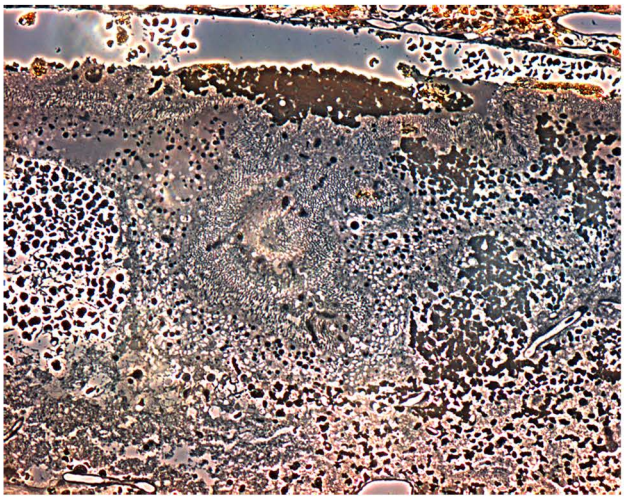

B

H&E stained section. Magnification x20. Disorganised /remodelled retina at lesion site with haemorrhage, oedema and inflammatory cells

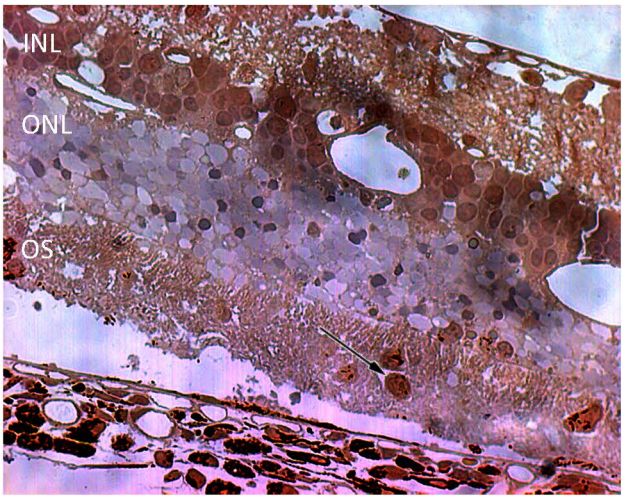

B2

Same H&E stained section from same eye as B. Magnification x40. Perilesional area with poorly stained nuclei in the ONL and inflammatory cells amongst the OS (arrow).

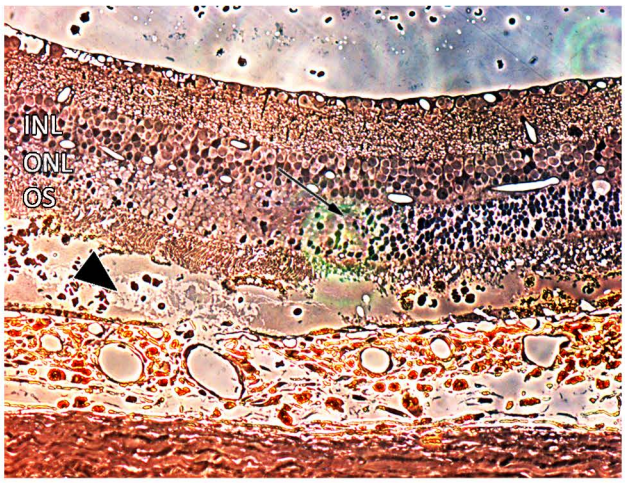

C

H&E stained section. Magnification x40. Perilesional area showing disrupted OS with a shallow retinal detachmnent arrowhead) and an abrupt demarkation with loss of nuclear staining in the ONL (arrow).

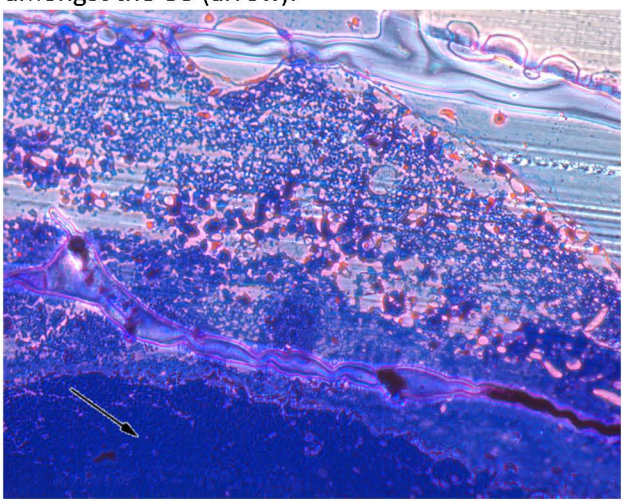

C2

Toludine blue stained section from the same eye as C. Magnification x20. Subretinal haemorrhage (arrow) with disrorganised/remodelled retina.

Figure 6.6.7.4. A-G. Transmission electron micrographs of rat outer retina. A. ONL 2 hrs after ballistic injury; blebbed, apoptotic, photoreceptor nucleus (arrowed). B-G. 2 days after ballistic injury. B. Close to the impact site, macrophage removing disrupted photoreceptor OS and IS (arrowed) and non-specific cell death with condensed and fragmented photoreceptor nuclei in the ONL – yelow boxed area shown at higher magnification in C. D. Close to the impact site, necrotic photoreceptor nucleus in an oedematous ONL with ruptured cell membranes (arrowed). E-H. Apoptotic photoreceptor nuclei further away from the impact site: E. Nuclear blebbing (arrowed); F. Nuclear blebbing (arrowed) with invasion of the photoreceptor cytoplasm by Müller cell processes (arrowhead); G. Condensed photoreceptor nucleus with chromatin aggregates at the periphery of the nucleus, typical of apoptosis; H. Chromatin aggregates (arrowhead) dispersed throughout the condensed photoreceptor nucleus (rather than peripherally), however the intact mitochodrion (arrowed) is suggestive of apoptosis. I. Apoptotic photoreceptor cell body with nuclear blebbing (arrowed) and a cytoplasmic apoptotic body (arrowhead). J. Apoptotic photoreceptor cell body with nuclear blebbing (arrowed) and a preserved mitochondrion (arrowhead). K. ONL at the edge of an area of necrosis towards the centre of the impact site with an abrupt demarcation between relatively normal nuclei on the left (arrowhead) and karyolytic nuclei (arrow) on the right.

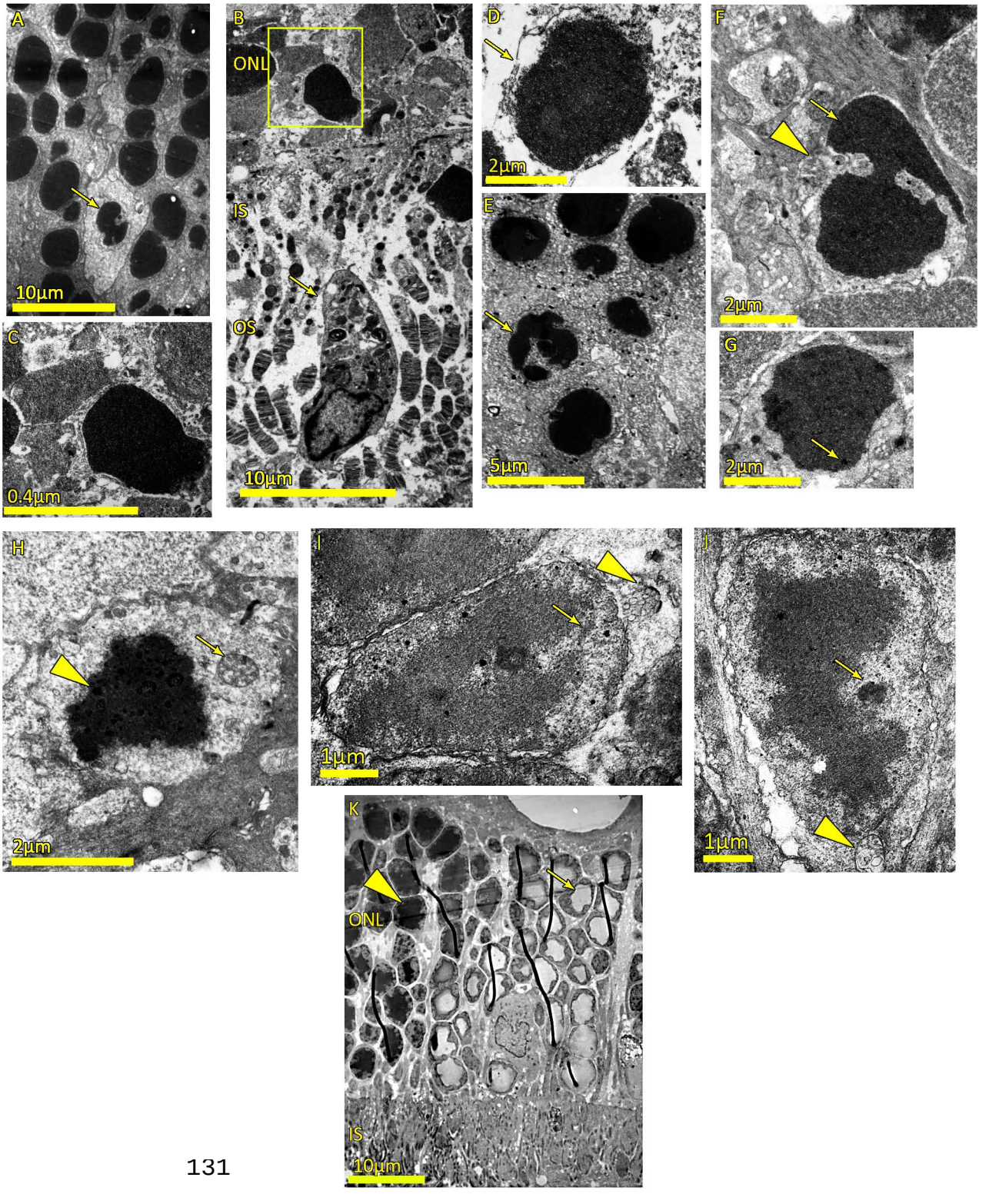

6.6.7.6. Discussion

The morphological features of apoptosis are cell and nuclear shrinkage, chromatin condensations (typically at the nuclear periphery) and nuclear blebbing and cytoplasmic blebbing with the formation of apoptotic bodies, all occurring in the presence of intact cellular organelles such as mitochondria and enclosed by an intact plasma membrane (Elmore 2007), all of which were been demonstrated peripheral to the impact site.

Necrotic cell death is characterised by cellular swelling and karyolysis which caused the loss of haematoxylin staining in the ONL demonstrated at the centre of the impact site in Figure 6.6.7.3.A, B2 and C and the loss of uranyl acetate nuclear staining demonstrated in Figure 6.6.7.4.K.

6.6.7.7. Conclusions

I. After commotio retinae, an inflammatory reaction with histiocyte infiltration occurred.

II. At the centre of the impact site, photoreceptors died by necrosis.

III. Peripheral to the impact site, photoreceptors died by apoptosis.

6.6.8.Assessing the Reduction in Photoreceptor Numbers After Ballistic Ocular Injury

6.6.8.1. Rationale

In humans, photoreceptors degenerate after commotio retinae, causing permanent visual loss (Chapter 5) and current studies in the rat ballistic injury model have shown photoreceptor apoptosis 2 d after injury. Both in humans and in the experimental model, injury-related changes are most prominent in the outer retinal layers. The proportion of cells that die in the different retinal layers and the variation in cell death with distance from the impact site is not known.

6.6.8.2. Hypothesis

I. Photoreceptors die after commotio retinae.

II. Cells in the inner retinal layers are relatively spared after commotio retinae.

6.6.8.3. Aim

To cause an outer retinal injury as in Section 6.6.6. and evaluate the extent and distribution of cell death 2 weeks later.

6.6.8.4. Materials and Methods

Four anaesthetised female Lister Hooded rats (200g) received a bilateral ballistic ocular injury (as described in Section 6.6.7.) and were killed 2 weeks later. Indirect fundoscopy was performed immediately and then 2 weeks after injury to look for commotio retinae. Retinae were processed as for electron microscopy. A strip of inferior retina including the optic disc and ciliary body and running radially through the centre of the lesion site was dissected out for embedding. Five control strips of retina including the optic disc and ciliary body were taken from the uninjured inferior retinal tissue from Section 6.6.6. Resin embedded sections were stained with Toludine blue and images captured at 40x magnification (0.25x0.3mm field of view) from the ONL of 5 different areas of each section as shown in Figure 6.6.8.1. ONL (photoreceptor) nuclei per 40x field were counted by an observer blind to the injury condition using the user-defined manual counting facility in ImagePro (Media Cybernetics, Bethesda, MD, USA).

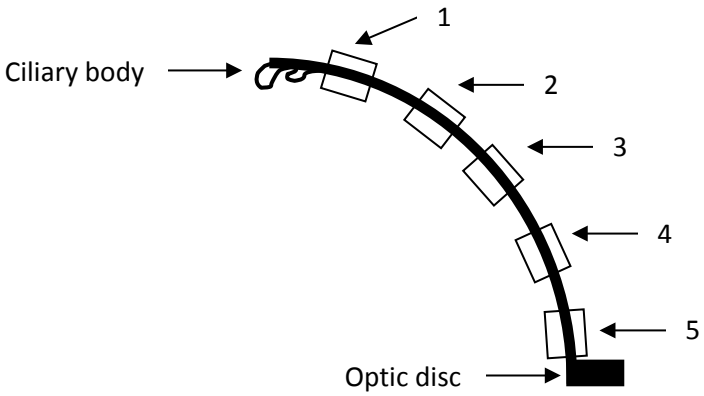

Figure 6.6.8.1. – A diagram (not to scale) showing the positioning of the 5 photographs on a radial cross section of retina running from optic disc to ciliary body through the lesion site.

6.6.8.5. Results

Fundoscopy immediately after injury confirmed the development of commotio retinae at the impact site. Six of 8 eyes injured had an area of central vitreous haemorrhage overlying the lesion site and one of the eyes (with vitreous haemorrhage) had a central area with the appearance of sclopetaria retinae. At 2 weeks after injury, fundoscopy of all eyes showed a large area of retinal and RPE atrophy of the same size (Figure 6.6.8.2.). There was variable resolution of the vitreous haemorrhages by 2 weeks. The appearances on dissection were the same as those on fundoscopy.

Toludine blue stained sections showed a reproducible injury with progressive loss of the ONL approaching the centre of the lesion site, but relative preservation of the INL and GCL and hypopigmentation and irregularity of the underlying RPE. At the centre of the impact site all neuroretinal layers were absent (Figure 6.6.8.3.-4.).

Figure 6.6.8.2.
Fundoscopy and gross pathologiy of rat retinae 2 weeks after ballistic injury.

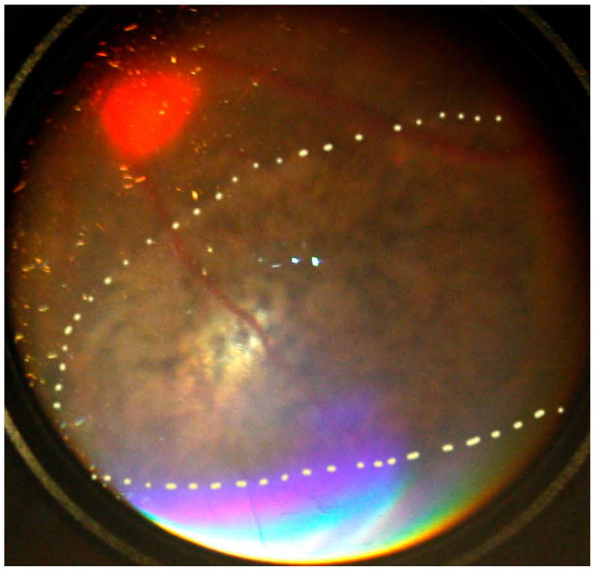

A
Fundoscopic image. Area of retinal atrophy with choroidal structure visible (circled with white dotted line).

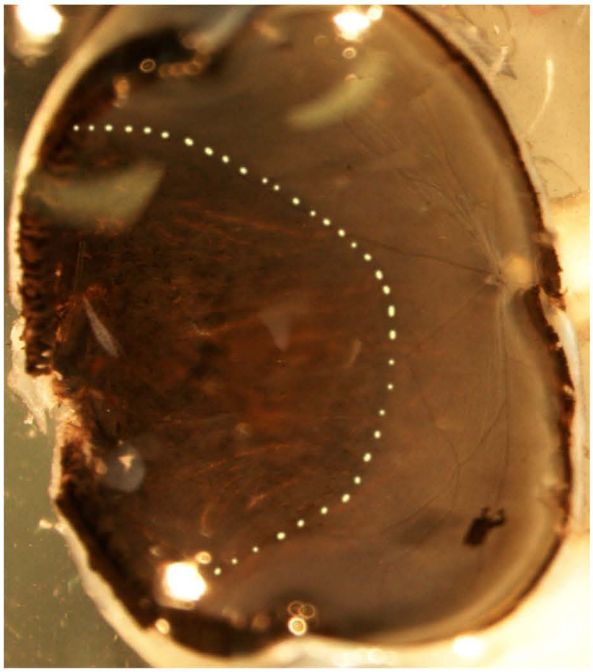

B
Gross pathology showing half of retinal cup including lesion site. Area of retinal atrophy (circled with white dotted line).

Figure 6.6.8.3.
A. Composite image of a toludine blue-stained resin section of rat retina 2 weeks after ballistic injury. The ONL is lost with relative preservation of the INL and GCL approaching the lesion site. Where some photoreceptor nuclei remain, the OS are shortened and, closer to the injury site, the ONL is directly opposed to the RPE. At the impact site there is loss of all retinal layers and obliteration of the underlying choriocapillaris. B. Higher magnification cut-out of A showing the point at which the ONL disappears.

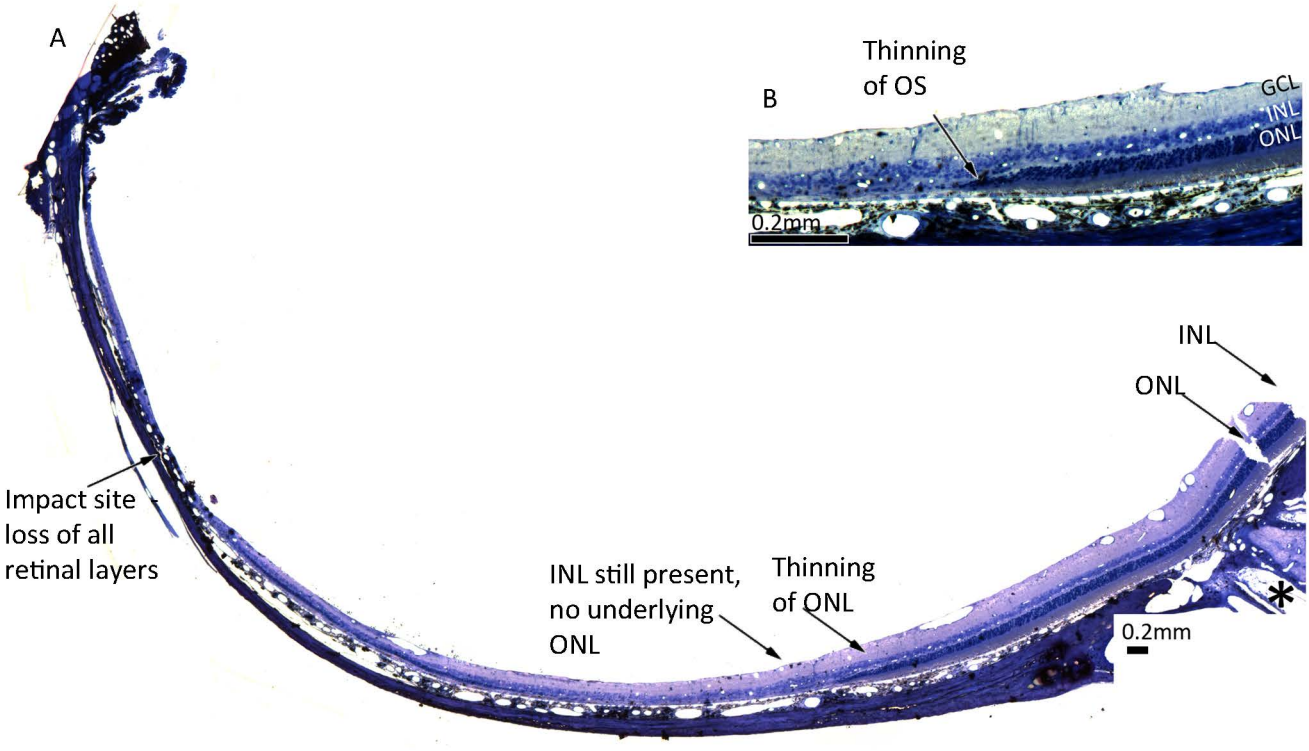

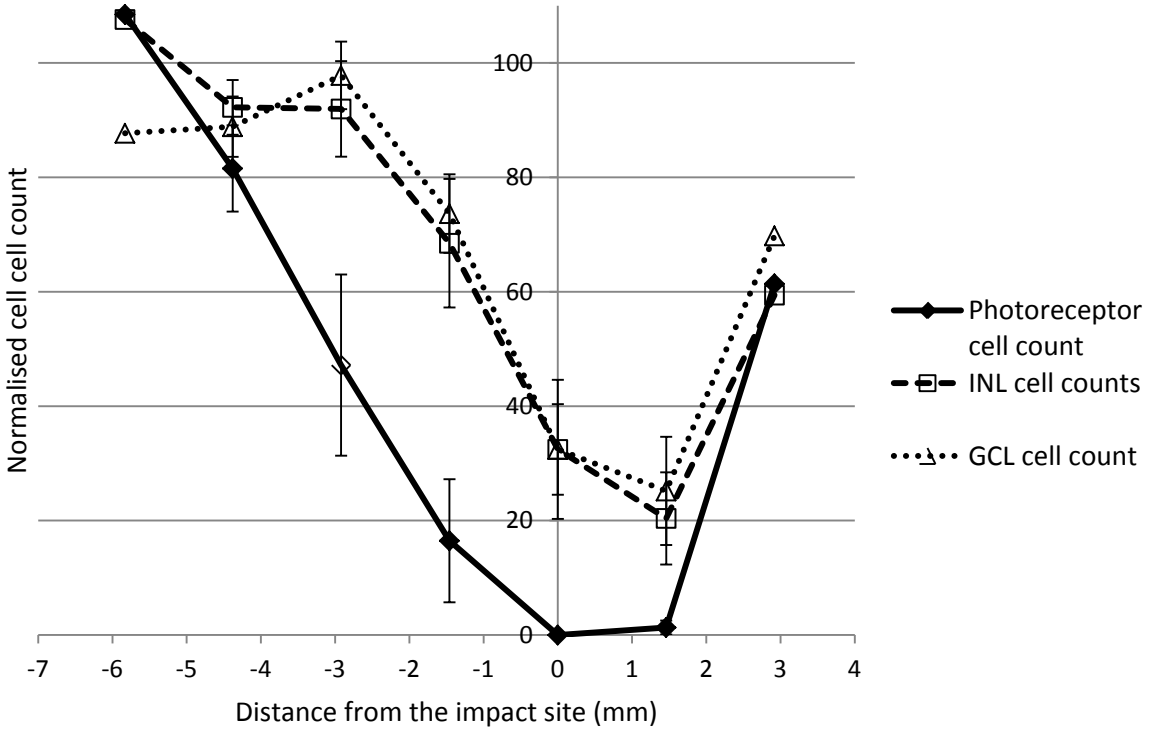

Figure 6.6.8.4. - Percentage of surviving nuclei in the different retinal layers plotted against distance from the lesion site. Cell counts are shown as percentages of the mean value for uninjured control tissue in the same retinal area (normalised). ONL survival is lowest, with the INL and GCL relatively spared. Standard error is shown at those distances where more than 2 measurements were taken.

6.6.8.6. Discussion

Central to the impact site, where photoreceptors die by necrosis (as demonstrated in Section 6.6.7.), there is complete loss of the ONL indicating complete loss of photoreceptors and extensive loss of the inner retinal layers. The reduction in cell counts compared to uninjured control tissue is similar in the INL and GCL, but much greater in the ONL, indicating that the injury predominantly caused photoreceptor death with relative sparing of the inner retinal layers.

Peripheral to the impact site, where photoreceptors die by apoptosis, the proportion of cells dying is lower and decreases with increasing distance from the impact site, but photoreceptors are still predominantly affected in comparison to cells of the INL and GCL. Therefore any attempt to improve visual outcomes by preventing apoptosis should focus on preventing photoreceptor death.

6.6.8.7. Conclusions

There is photoreceptor death around the lesion site and death of all retinal cells at the lesion site. The proportion of photoreceptors dying declines at increasing distance from the lesion site, with relative sparing of the inner retinal layers.

6.6.9. Assessing the Total Reduction in Photoreceptor Numbers After Ballistic Ocular Injury

6.6.9.1. Rationale

Cell death predominantly affects photoreceptors after ballistic ocular injury as demonstrated in Section 6.6.8. To give an indication of the severity of injury, the magnitude of potential functional impairment and potential benefits of neuroprotective treatment and to complete characterisation of the model, the total proportion of photoreceptor death needed to be determined.

6.6.9.2. Aim

To determine the total proportion of photoreceptor death after ballistic ocular injury.

6.6.9.3. Materials and Methods

Eight anaesthetised female Lister Hooded rats had unilateral ballistic ocular injury (as described in Section 6.6.7.) and were killed 2 weeks later and retinae processed for retinal whole mounts. Images of retinal whole mounts were captured at x40 magnification using a Zeiss epifluorescent microscope (Carl Zeiss, Hertfordshire, UK) equipped with a Axiocam HRc camera (Carl Zeiss) running the Axiovision software (Zeiss). Because of the poor axial resolution of the light microscope, which is greater than ONL thickness, cell counting was repeated using images captured at x63 magnification and ONL thickness measured as the axial distance between the farthest two points in which the ONL was visible, using a confocal laser scanning microscope (Carl Zeiss) running the LSM 510 software version 3.2 (Carl Zeiss). Images were captured from 3 different areas (at 1/6, 3/6 and 5/6 of the radius as shown in Figure 6.6.9.1.) of each quadrant (total = 12 counts per eye) in the middle of the ONL, to account for variation in photoreceptor numbers in the different areas and DAPI-stained

nuclei quantified using the built-in particle counting facilities in ImagePro and expressed as mean normalised photoreceptor density per high power field (0.143x0.143mm on confocal images).

Figure 6.6.9.1. Illustrative diagram showing location on retinal whole mounts of images for cell counts at 1/6, 3/6 and 5/6 of the radius of each quadrant (total = 12 counts per eye).

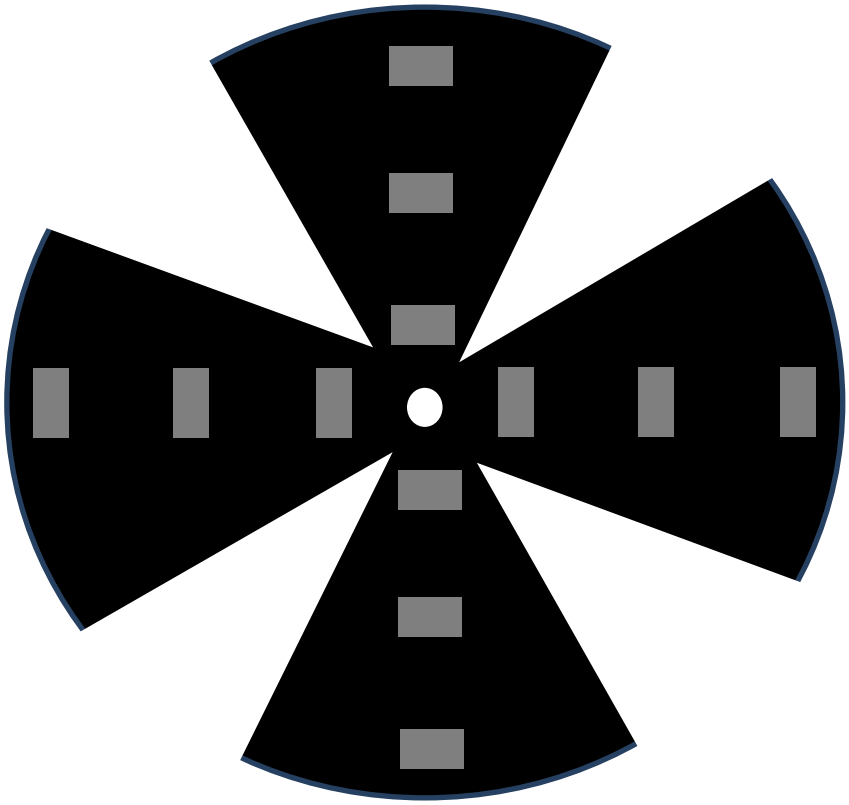

6.6.9.4. Results

ONL cell counting on epifluorescent images of retinal whole mounts showed that 18.4 ±4.6% photoreceptors had died. Similarly, ONL cell counting on confocal images showed that 18.3±4.1% photoreceptors had died. Adjusting confocal cell counts to take account of ONL thickness by multiplying cell count by ONL thickness, showed that 18.6±10.3% photoreceptors had died.

Figure 6.6.9.2. Mean number of surviving photoreceptors in injured and control eyes measured by cell counts on confocal images. p=0.004 for main effect of injury and p=0.005 for the 2-way interaction retinal position*injury (repeated measure ANOVA)

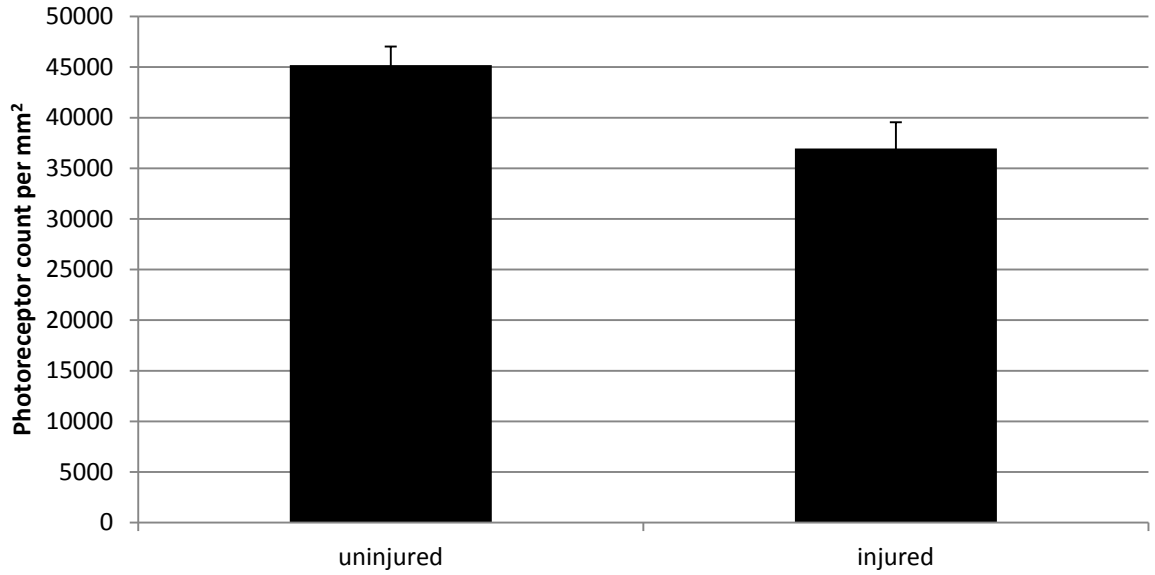

6.6.9.5. Discussion/Conclusions

After commotio retinae induced by ballistic ocular injury, 18% of photoreceptors die, indicating that visual function assessed by ERG should be reduced by at least this amount and setting 18% as the limit on the proportion of photoreceptors that could benefit from neuroprotective therapies.

6.6.10. Immunohistochemical Study of Ballistic Ocular Trauma

6.6.10.1. Rationale

After commotio retinae induced in rats by ballistic ocular injury, 18% of photoreceptors die by a combination of apoptosis and necrosis, with relative sparing of the inner retinal layers. Electron micrographs allowed assessment of cell death only in small, discrete areas of retina, which may not represent gross changes. TUNEL staining of retinal sections allows assessment of the mechanisms of cell death in a wider area of retina more easily.

It was noted on electron micrographs that histiocytic inflammatory cells infiltrated the retina after injury. Immunohistochemical staining would allow more precise identification of these cells to characterise the inflammatory response.

6.6.10.2. Hypotheses

I. Apoptosis is rare at the centre of the impact site, but more common in a penumbral zone at the periphery.

II. After ballistic ocular injury, macrophages infiltrate the retina.

6.6.10.3. Aim

I. To characterise the distribution of photoreceptor apoptosis in the whole retina after ballistic ocular trauma by TUNEL staining.

II. To identify infiltrating inflammatory cells in the retina after ballistic ocular trauma.

6.6.10.4. Materials and Methods

Four anaesthetised female Lister Hooded rats had unilateral, right ballistic ocular injury (as described in Section 6.6.7.) and were killed 2 d later. Eyes were processed for immunohistochemistry. The left eyes acted as controls. TUNEL staining and immunohistochemical staining for ED1 (CD68) and OX42 (CD11b) were performed.

6.6.10.5. Results

The results of immunohistochemistical analysis are presented in Figure 6.6.10. Examination of the necrotic central zone of the impact site revealed gross positive TUNEL staining in the ONL with very high levels of background fluorescence. Peripheral to the lesion site there were scattered TUNEL positive nuclei, decreasing in frequency with increasing distance from the impact site. Control tissue was TUNEL negative. There were many ED1 positive cells invading through the full thickness of the

Figure 6.6.10.
A-B. TUNEL -ve intact control retina. **A.** TUNEL staining in green. **B.** combined image with DAPI stained nuclei in blue. **C-F.** Injured rat retina 2 days after injury with DAPI-stained nuclei in blue. **C.** Whole injured area of retina; at the centre of the impact site (arrowhead), there is diffuse TUNEL positivity. The frequency of TUNEL positive nuclei reduces in frequency with increasing distance. **D-F**. Higher magnification cut-out from C at the periphery of the lesion site showing DAPI stained nuclei (D), TUNEL stained nuclei (arrowed; E), and combined image (F).

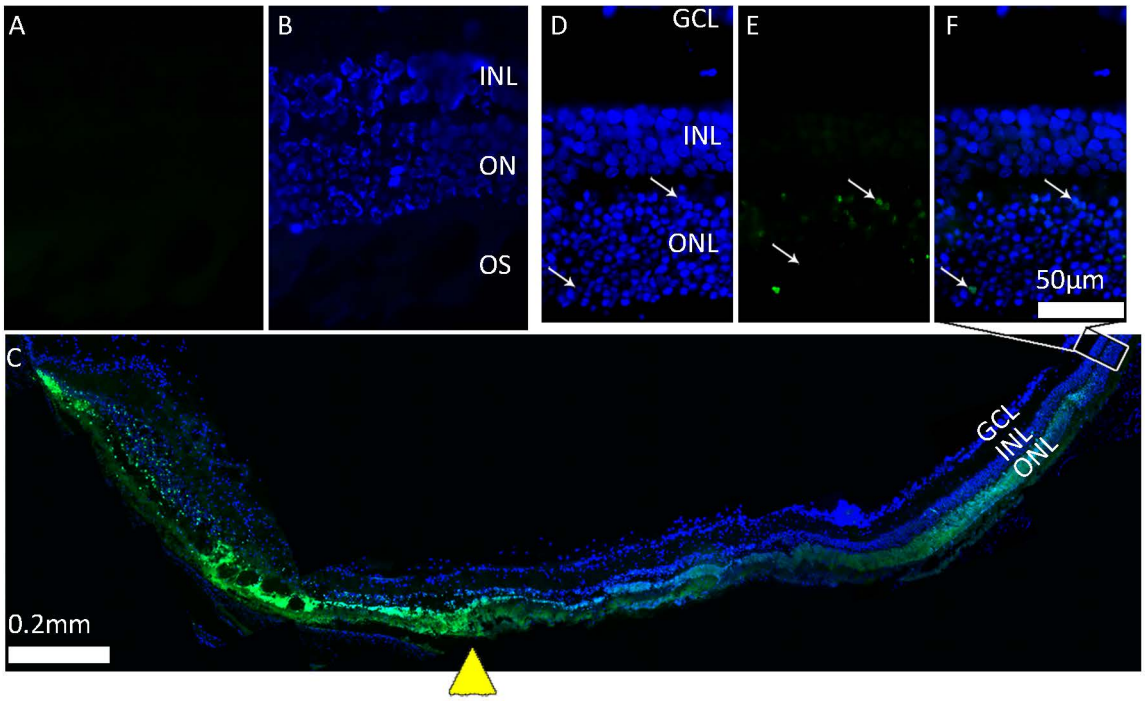

G-J. ED1 and OX42 staining showing negative OX42 (Santa Cruz, polyclonal) staining in red (G), green ED1 positive macrophages arrowed (H), blue DAPI stained nuclei (I) and combined image (J). **K-L**. Negative OX42 (Serotec monoclonal) staining in green (K) and combined image with DAPI stained nuclei in blue (L). Note that absent fluorescence on the red channel excludes autofluorescent inflammatory cells as a cause for positive staining on the green channel.

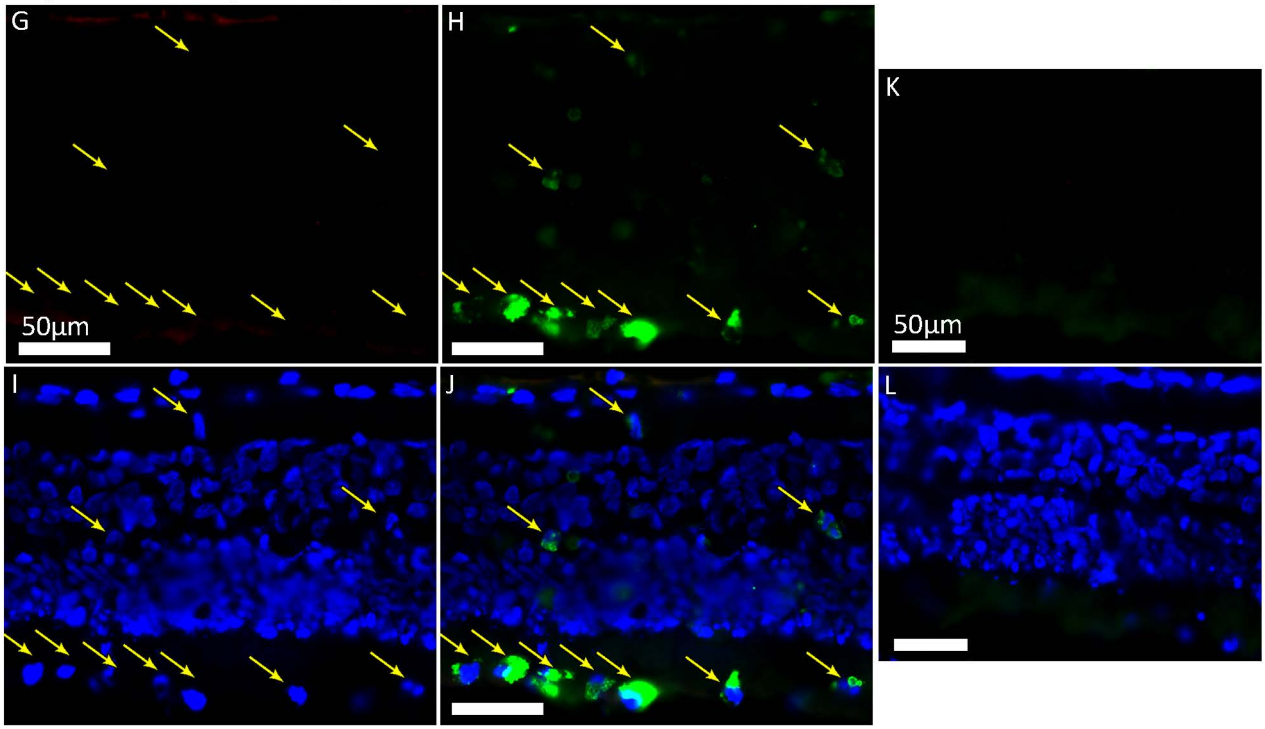

injured area of retina only, but present in greatest numbers in the region of the photoreceptor OS and outer nuclear layer. No OX42 positive cells were present in injured or control tissue.

6.6.10.6. Discussion

In the centre of the impact site, there was diffuse photoreceptor nuclear and cytoplasmic TUNEL staining, probably because direct cellular injury caused necrotic death (van Lookeren and Gill 1996). However, away from the impact site, the presence of specific TUNEL-positive photoreceptor cell nuclei in the ONL indicated apoptosis of these cells, confirming the electron micrographic findings.

ED1 (rat homologue of human CD68) is a transmembrane glycoprotein expressed by activated macrophages (though may also be expressed by activated microglia), whereas OX42 (rat homologue of human CD11b) is expressed on microglia (at any stage of activation) and neutrophils – and may be expressed on macrophages (Streit 2005), (Lloyd, Phillips, Cooper, and Dunbar 2008). In addition, all the inflammatory cells seen in electron micrographs were histiocytic (Section 6.6.7.). These three features – ED1 positive, OX42 negative with a histiocytic morphology suggest that these cells are macrophages.

The distribution of macrophages in the region of photoreceptor OS and throughout the retina suggests that they are both clearing damaged outer segments and debris from dying cells.

6.6.10.7. Conclusions

I. After ballistic ocular trauma, TUNEL positive photoreceptors are present in retinal areas peripheral to the impact site.

II. Macrophages infiltrate the retina after ballistic ocular trauma, being most frequent in the region of the photoreceptor outer segments.

6.7. General Discussion

The ocular injury induced in rats by weight drop was inconsistent. The energy threshold for induction of commotio retinae was close to that at which globe rupture occurred in 50% of animals (approx 0.62J). This was because low velocity injury did not cause commotio retinae, consistent with the body of literature in which commotio retinae has been created using high velocity impact (see Section 1.4.3.1.). In contrast, a lower energy injury with a 0.095g BB travelling at 20m/s (0.019J) reproducibly created central sclopetaria retinae at the impact site and surrounding commotio retinae, indicating that velocity rather than impact energy determined the development of commotio retinae, consistent with the work of Scott et al. (2000), who showed that a high velocity impact of a light projectile created more injury than a low velocity impact from a heavy projectile despite similar kinetic energy ((reference not available)).

After the closed globe ballistic injury there was a relative preservation of the inner retinal layers and most cell death occurred in the ONL so that approximately 18% of photoreceptors across the retina died by a combination of necrosis and apoptosis after ballistic retinal injury.

In the current studies photoreceptor apoptosis was assessed by TUNEL staining. During apoptosis, DNA is cleaved into fragments, which are detected by the TUNEL assay. The terminal deoxynucleotidyl transferase enzyme attaches fluorescein labelled deoxynucleotides to the cut ends of DNA fragments, thereby labelling the nuclei of apoptotic cells. False positive TUNEL can occur for a number of reasons including over-incubation with proteinase K and sectioning artefact. The frequency of false positive TUNEL staining is reported to be up to 30% with 15µm section widths, up to 69% with 5µm widths and 100% was observed with 1µm resin sections from the above experiments (Sloop et al. 1999). For this reason, TUNEL is an unreliable indicator of apoptosis and morphological nuclear changes assessed by transmission electron microscopy are the gold standard.

Central to the impact site there was gross retinal disruption and photoreceptor necrosis, demonstrated by grossly swollen cell bodies, ruptured cell and nuclear membranes and diffuse

TUNEL staining. Further away from the impact site, photoreceptors died by a combination of apoptosis and necrosis. Apoptosis was demonstrated by specific nuclear TUNEL staining, nuclear shrinkage with chomatin condensation and nuclear and cytoplasmic blebbing with invasion of the photoreceptor cytoplasm by adjacent cells, all in the presence of intact cellular organelles.

Cell death represents a spectrum between apoptosis and necrosis, with significant overlap. The present studies showed individual photoreceptors that had features of necrosis and others that showed features of apoptosis, though it is likely that many undergo a mixed form of cell death. Whilst necrosis is an unregulated form of cell death, apoptosis is controlled by specific cell death signalling pathways (see Section 1.4.2.), as is the mixed form of cell death (necroptosis) and these pathways can be experimentally suppressed to preserve cell viability (Ahmed et al. 2011), (Trichonas et al. 2010). Thus, these results imply that, after ballistic retinal injury, death of a proportion of photoreceptors is mediated by one or more regulated signalling pathways, suggesting a potential for successful neuroprotective therapies, for example by caspase inhibition.

In human studies, mild commotio retinae associated with photoreceptor recovery is characterised by outer segment disruption, whereas severe commotio retinae is associated with photoreceptor inner and outer segment disruption observed by OCT (Souza-Santos et al. 2012). Inner segment disruption was also present in our model, but has not been reported in other (mild, recovering) animal models of commotio retinae. The RPE and photoreceptor outer and inner segments appear as 3 bands on spectral domain OCT. The thinner line above them may represent the ELM or the myoid portion of the cone inner segments (Gloesmann et al. 2003). Loss of this line on OCT may be a marker of severe photoreceptor damage in commotio retinae and age related macular degeneration (Souza-Santos et al. 2012), (Oishi et al. 2010). If it represents cone inner segments, it may be that disruption of these mitochondria rich structures (seen in our model) is a lethal injury to photoreceptors, whilst outer segment disruption is less likely to cause photoreceptor death.

The rat lens accounts for 60% of axial length (Blanch et al. 2012b). With such a small vitreous cavity, it is likely that the lens impacted the retina during injury in our experiments with potential crushing

of the retina. This is also the case in larger animals in which ocular dimensions are close to humans, though with the larger lens this crushing may be more prominent in the rat (Blanch et al. 2012b). Importantly, the ballistic injury model developed reproducibly displayed the clinical and ultrastructural features of commotio retinae seen in previous human and animal studies and – similar to the human condition – results in photoreceptor death.

6.8. Conclusion

Current studies have developed an animal model of ballistic closed globe injury that induces a retinal response mirroring the outer retinal changes that occur after severe commotio retinae in humans, making it the first murine rodent model of blunt ocular trauma. The results suggest that outer retinal atrophy occurs as a result of photoreceptor apoptosis and necrosis due to a terminal injury to photoreceptor inner segments. The observed photoreceptor apoptosis is translationally relevant because it demonstrates that there is the potential to prevent photoreceptor death and improve visual outcomes by using anti-apoptotic neuroprotective therapies. This model provides an opportunity for both mechanistic and translational therapeutic studies, which are described in subsequent sections.

7. Electroretinographic Assessment of Blunt Ocular Trauma

Parts of the work in this section have been published in Investigative Ophthalmology and Visual Science (Blanch et al. 2012a), the paper is presented in Appendix 6.

7.1. Rationale

Photoreceptor death after ballistic retinal injury must affect retinal function. To be able to assess the efficacy of neuroprotective therapies, an objective measure of retinal function is required.

7.2. Hypothesis

Ballistic retinal injury reduces a-wave amplitude without affecting the b/a wave ratio.

7.3. Aims

I. To develop a method of recording reproducible ERG in rats, after ballistic retinal injury.

II. To assess the functional effects of ballistic retinal injury using ERG.

7.4. Developing ERG methodology

7.4.1.Aim

To develop a method of recording reproducible ERG in rats, after ballistic retinal injury.

7.4.2.Materials and Methods

One 570g male Sprague-Dawley rat was anaesthetised with intraperitoneal ketamine/medetomidine. Core temperature was maintained using a water heating system, to minimise electrical interference with the ERG signal that could occur using an electrical heating pad. The water heating system consisted of: an in-line thermostatically controlled heater, made from: a Protronic Nova water heater (Firstcall Photographic, Taunton, UK) sealed inside a 400x60mm cylindrical acrylic tank (Specialtech, Haverfordwest, UK); a second acrylic tank as a reservoir; a Phobya 12v watercooling pump

(Specialtech) to circulate water; a Phobya in-line G1/4” thermometer (Computers & Components (Central) Ltd, Redditch, UK) to monitor temperature; a Koolance HD-60 3.5" Hard Drive Wateblock (Specialtech) on which the rat was positioned during recording; with all parts connected by 8mm polyurethane tubing (RS Components). The apparatus was set to 38°C to maintain a constant body temperature in the physiological range.

Light flashes of standard intensity (3000mcd/m^2) were delivered and ERG recorded using a commercially available rodent ERG system (HMsERG).

7.4.3.Results/DIscussion

The traces recorded from both eyes had high amplitude noise, with no recognisable ERG waveform, examples of which are shown below in Figure 7.4.3.1.

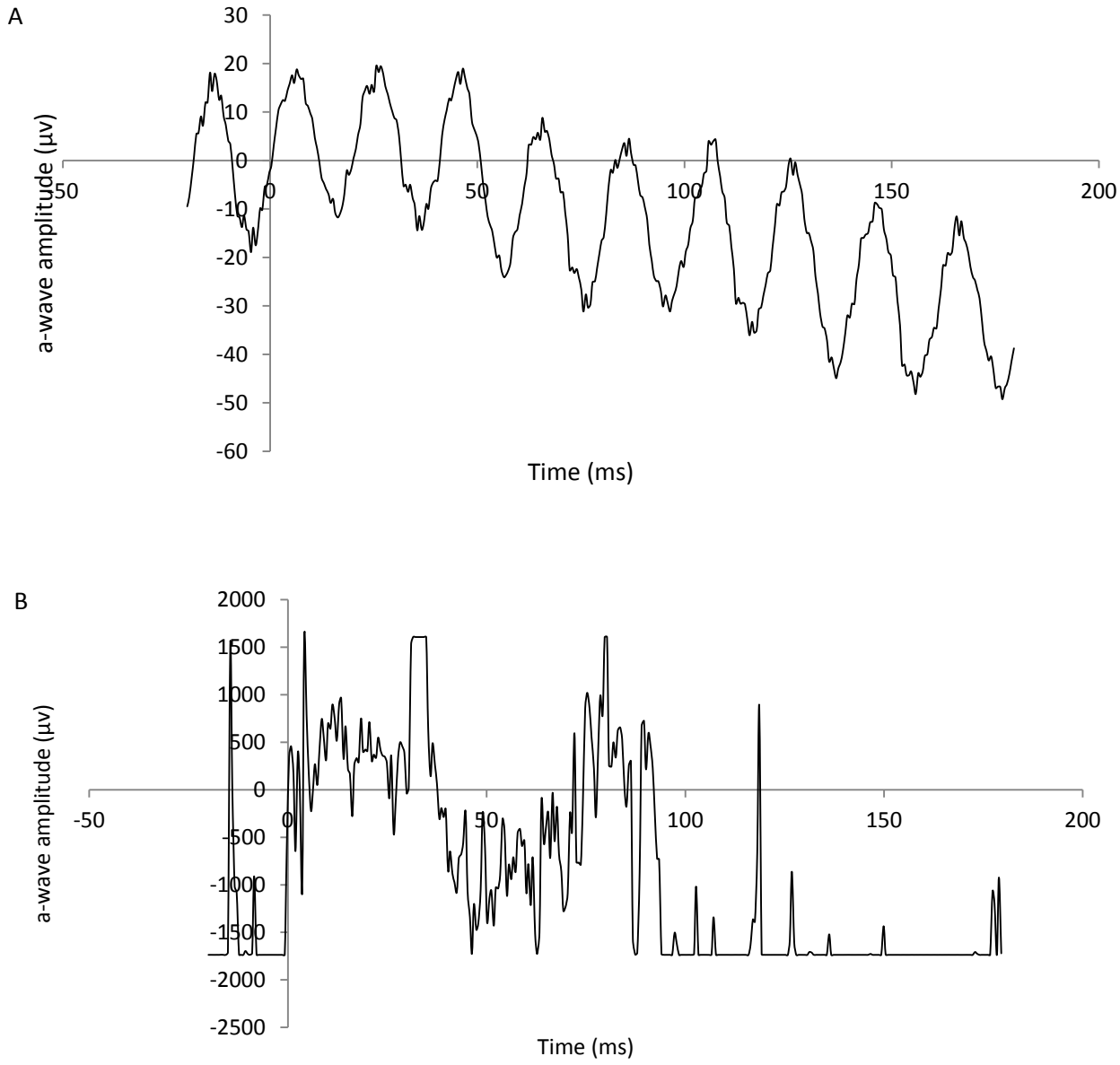

Figure 7.4.3.1. A. ERG trace obtained with inadequate earthing of apparatus causing 50Hz noise from mains electricity. B. Poor ERG trace obtained before optimisation of electrode placement with high amplitude noise.

The following modifications were made to improve recording:

- All metal components of the heating and recording apparatus were earthed.
- ERG were recorded in a Faraday cage.

These modifications allowed clean and reproducible traces to be obtained. Corneal DTL fibre electrodes and metal loop electrodes with hydroxypropylmethylcellulose, hyaluronate (Optive – Allergan, Marlow, UK) and PBS coupling medium, with and without aclar contact lens coverage were

all tried. The cleanest traces were obtained with metal loop corneal electrodes/hydroxypropylmethylcellulose and with DTL fibre electrodes/hydroxypropylmethylcellulose/aclar contact lenses. Some eye movements occur under anaesthesia and the animal moves with breathing and during advancement of the rat into the Ganzfeld stimulator, making corneal loop electrodes prone to change position. DTL fibres were therefore the best option for corneal electrodes. An example of the traces obtained with this recording protocol is shown in Figure 1.5.1. and repeated below in Figure 7.4.3.2.

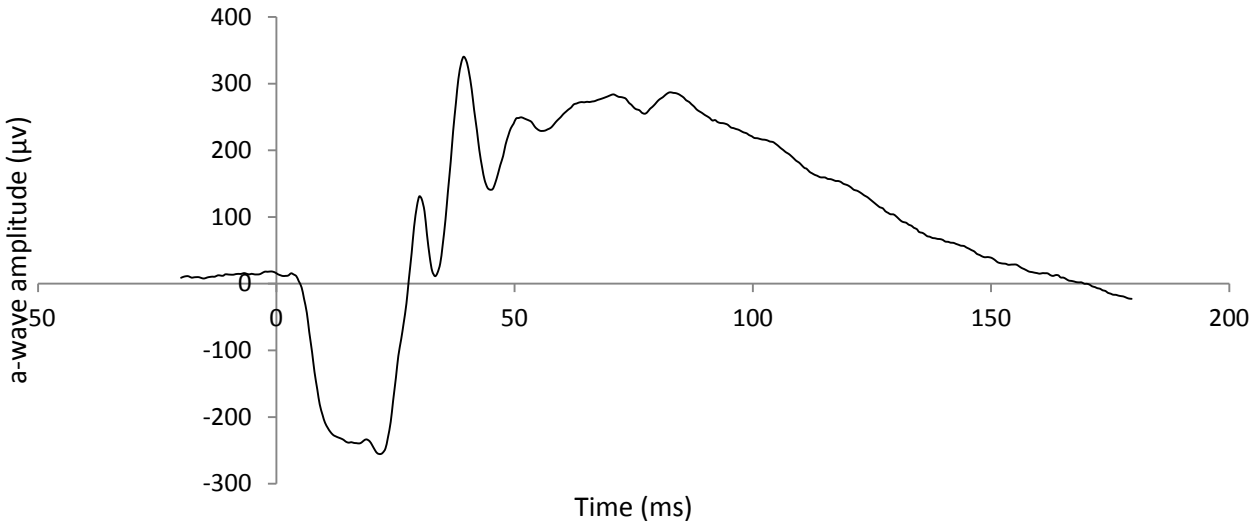

Figure 7.4.3.2. Normal rat ERG obtained after optimisation of recording protocol.

7.4.4.Conclusions

Clean and clear rat ERG were obtained using the optimised recording protocol, which was deemed suitable to use in subsequent studies to assess, (1), the reproducibility of ERG recording in the rat and, (2), the functional effects of the ballistic injury model.

7.5. ERG assessment of blunt ocular trauma

7.5.1.Hypotheses

I. The optimised ERG recording protocol described in Section 7.4. reproducibly assesses rat retinal function.

II. Ballistic retinal injury reduces a-wave amplitude without affecting the b/a wave ratio.

7.5.2.Aim

To characterise the ERG features of ballistic retinal injury.

7.5.3.Materials and Methods

Eight female Lister-hooded rats were injured under recovery anaesthesia (see Section 6.6.7.) and ERG recorded from both eyes at 2, 7 and 14 d after ballistic injury under general anaesthesia with intraperitoneal ketamine/medetomidine. Scotopic flash ERG were recorded at -2.5, 0 and +0.5 log units with respect to standard flash and photopic flash ERG at 0 and +0.5 log units as described in Table 7.5.3. Animals were killed by overdose of anaesthetic at 2 weeks and tissues were used for the investigations described in Section 6.6.9.

Stage of testing	Light exposure (log units with respect to standard flash)	Light exposure (mcd.s/m^2)	Number of flashes averaged	Interval between flashes (sec)	Time elapsed (sec)
Dark adaptation					
Low intensity flash	2.5	10	10	2	12
Delay				2	14
Standard flash	0	3000	4	10	54
Delay				30	84
High intensity flash	0.5	10000	4	20	164
Background (BG) light adaptation (remains on for testing)	1	30000		600	764
Standard flash + BG	0 + BG	3000 + BG	32	2	828
Delay + BG	1	30000		2	830
High intensity flash + BG	0.5 + BG	10000 + BG	32	2	894

Table 7.5.3. ERG recording protocol.

7.5.4.Results

There were 2 anaesthetic deaths, 1 immediately on injection of anaesthetic and 1 during ERG recording. These animals were replaced (so n=10 animals with 2 excluded).

The raw a-wave amplitude dataset was heavily right-skewed (Appendix 7, p27-30). The raw residuals after modelling with generalised estimating equations, fail both the Shipiro-Wilk and the Kolmogorov-Smirnov tests for normality ($p<0.001$ for both; Appendix 7). The Pearson residuals fail the Shapiro –Wilk ($p=0.044$) but not the Kolmogorov-Smirnov ($p=0.2$) tests. The variance of the residuals increases with their means (Appendix 7 p31). All of these features are consistent with the gamma distribution, which was used to model the data instead of the normal distribution.

The amplitude and latency of all components were intensity dependent, though only amplitude was injury dependent. Scotopic a-wave amplitude was significantly reduced by injury (Figure 7.5.4.1., $p<0.001$) and there was a borderline significant 3-way interaction between time, injury and stimulus intensity ($p=0.056$, see Appendix 7). Since b-wave onset can obscure the a-wave, the gradient of the a-wave's linear portion (leading edge) was measured, giving a similar trend as that observed for

Figure 7.5.4.1. Quantification of the relevant components of the ERG at 2, 7 and 14 days after ballistic injury displayed as mean amplitude +/- standard error of the mean (SEM) at increasing stimulus intensity. A. Scotopic (dark-apapted) a-wave amplitude is significantly reduced by injury at all time points and stimulus intensities. B. Test of model effects from generalised estimating equations modelling scotopic a wave-amplitude. The term modelling the 3-way interaction flashintensity*timepoint*Injured was borderline significant at p=0.056 and so was excluded from the model. C. Photopic (light-adapted) b-wave amplitude is similarly reduced. C. Scotopic a/b-wave ratio at increasing stimulus intensity. There is no significant difference between injured and control eyes. a/b-wave ratio is displayed, as b/a wave ratio tends to infinity with small a waves.

A - scotopic

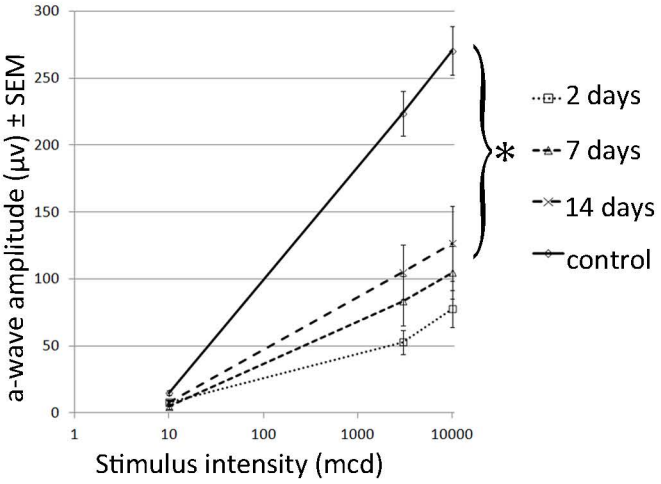

B - scotopic

Source	Type III		
	Wald Chi-Square	df	Sig.
(Intercept)	4569.188	1	0.000
timepoint	13.094	2	.001
flashintensity	443.504	2	0.000
Injured	58.947	1	.000
timepoint * flashintensity	11.561	4	.021
flashintensity * Injured	14.143	2	.001

C - photopic

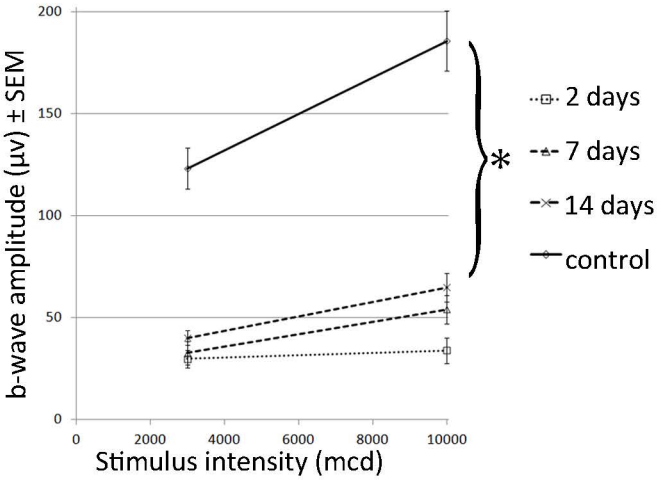

D - scotopic a/b

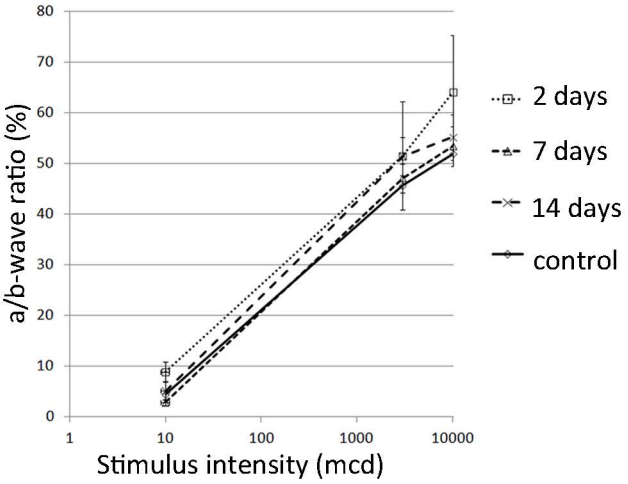

amplitude, except that the 3-way interaction between time, injury and stimulus intensity was significant (p=0.021; see Appendix 8). There was no significant effect of injury on the scotopic b-/a-wave ratio (Figure 7.5.4.1.; Appendix 9). Photopic a-waves were frequently undetectable in injured and control eyes, so b-wave amplitude was analysed and was shown to be significantly reduced by injury (Figure 3.5.2.3.1.; p<0.001; Appendix 10), consistent with commotio retinae affecting both cones and rods equally.

7.6. Discussion

The a-wave is routinely used to measure photoreceptor function. The b-wave is generated by the activity of second order neurons. The b-wave is therefore dependent on photoreceptor activation and synaptic transmission in addition to inner retinal function. ERG of the injured eyes showed a significant reduction in a- wave amplitude compared to the control eyes without any change in implicit time. The b-/a-wave ratio is a measure of how much of the variation in b-wave amplitude is attributable to variation in the magnitude of photoreceptor, compared to second order neuron, activation. The b/a wave ratio was normal and similar between injured and control eyes, indicating that the variation in b-wave amplitude is caused by variation in the magnitude of the photoreceptor response. The reductions in ERG amplitude occurred under both scotopic and photopic conditions consistent with damage primarily to the photoreceptor layer and affecting both rods and cones.

Rods make up 99% of rat photoreceptors (Szel and Rohlich 1992) and, in our model, scotopic a-wave amplitude (which reflects rod function) was reduced by > 50% (Figure 5), although only 18% of photoreceptors died (Section 6.6.9.). The degree of ERG reduction was therefore disproportionate to the amount of histological photoreceptor death, suggesting reduced function in the surviving photoreceptors and may be explained by either outer segment damage beyond the zone of cell death that would not be expected to have recovered completely by 14 d or other photoreceptor remodelling, similar to that seen after retinal detachment (Fisher, Lewis, Linberg, and Verardo 2005). Additionally, the photoreceptor component (leading edge) of the a-wave is sensitive to extracellular

Ca2+ and K+ levels (Vinberg, Strandman, and Koskelainen 2009), which may be affected by altered Müller glial function or local structural changes.

The effect of time in all the analyses is seen in 3 ways: (1), there is a change in a-wave amplitude over time in both the injured and control eyes (p=0.001 for scotopic a-wave amplitude); (2), there is a 2-way interaction between time and flash intensity, i.e. the greater the stimulus intensity, the greater the effect of time (p=0.021 for scotopic a-wave amplitude); (3), there is a borderline significant 3-way interaction between time, injury and stimulus intensity, i.e. the difference in the response of the injured and control eyes to increasing stimulus intensity varies with time in that the effect of injury on this relationship is greater at 14 than at 2 d after injury (see "Estimated Marginal Means timepoint* flashintensity* Injured" in Appendix 7, p16). Similarly, there is a statistically significant 2-way interaction between stimulus intensity and injury because the effect of injury is greater at high stimulus intensities.

Anaesthetic deaths whilst recording ERG may have been due to hypoxia, exacerbated by a flexed neck position as the animal overhangs the edge of the warming plate. To address this, the animals were given oxygen supplementation and the head supported to prevent neck flexion in subsequent experiments. Future experiments used inhalational anaesthetic to reduce the risk of anaesthetic death.

7.7. Conclusion

ERG assessment of the ballistic injury model generated results that were consistent with the retinal pathology observed in Section 6.6. and which were internally consistent in injured and in control eyes with reproducibility evidenced by the tight error bars (Figure 7.5.4.1.).

Ballistic ocular injury causing commotio retinae consistently reduced a-wave amplitude without affecting b/a ratio indicating that the observed reduction in b wave amplitude was related to a reduction in function of photoreceptors rather than second order neurons. ERG a-wave amplitude can therefore be used to assess functional outcomes after ballistic ocular injury.

8. Mechanisms of cell death following blunt ocular trauma

Parts of the work in this section have been prepared for submission to Cell Death and Differentiation, the manuscript is presented in Appendix 11.

8.1. Rationale

The rat ballistic injury model of commotio retinae shares clinical and ultrastructural features with the human condition and the current studies have revealed photoreceptor apoptosis reducing visual function, measured using ERG a-wave amplitude. The observation of photoreceptor apoptosis suggests that regulated apoptotic signalling mediates photoreceptor death and that antiapoptotic neuroprotective therapies have a potential role in the treatment of commotio retinae. Subsequent studies examined apoptotic signalling in order to generate potential translational neuroprotective therapies.

8.2. Hypotheses

I. In experimental commotio retinae, photoreceptor apoptosis is caspase-dependent.

II. Caspase-dependent apoptosis in experimental commotio retinae occurs through the intrinsic pathway.

III. Interfering with caspase function after induction of experimental commotio retinae prevents photoreceptor apoptosis and improves retinal function assessed by ERG.

8.3. Aims

I. To assess which caspase-dependent cell death pathways are active after blunt ocular trauma.

II. To assess the neuroprotective effects of interfering with caspase function after induction of commotio retinae in an experimental model.

8.4. Western Blotting Study of Ballistic Ocular Injury

8.4.1.Hypothesis

The retinal levels of activated caspase 9 and 3 will be increased in a time-dependent manner after ballistic ocular injury (initially caspase 9 then the executioner caspase 3).

8.4.2.Aim

To study which caspase-dependent cell death pathways are active after ballistic ocular injury.

8.4.3.Materials and Methods

At 5, 24 and 48 hr post-injury and in an uninjured control group 3 Lister-hooded rats were killed and both retinae removed and processed for Western blotting. Blots were probed with antibodies to caspases 3, 6 (Cell Signalling), 7, 8 and 9 (Cell Signalling) and to α-tubulin (loading control).

8.4.4.Results

8.4.4.1. Initiator Caspases

Western blotting results are presented in Figure 8.4.1. Retinal levels of both activated caspase 8 and 9 were increased after injury. The retinal levels of activated caspase 9 increased by 5 hr and decreased to basal levels by 24 hr after ballistic injury ($p=0.018$, 1-way ANOVA). The retinal levels of activated caspase 8 p16/18 fragments increased by 5 hr and did not show a significant decrease at 24 hr or 48 hr ($p=0.041$, 1-way ANOVA). The retinal levels of activated caspase 8 p10 fragment increased by 48 hr compared to the levels at 5 and 24 hr ($p=0.004$, 1-way ANOVA). The changes in levels of caspase 9 were qualitatively larger than those of caspase 8. Full length caspase 9 was also increased at 48 hr with respect to all other time points ($p<0.001$, one way ANOVA); full length caspase 8 was not detected.

Figure 8.4.1. A-B. Retinal levels of full length (49kDa) and cleaved (35-39kDa) caspase 9 after injury assessed by Western blotting showing increased cleaved form at 5 hrs and increased full length form at 48 hrs. *p=0.018, **p<0.001 from Tukey post-hoc tests. C-D. Retinal levels of full length (55kDa) and cleaved (16/18 and 10kDa) caspase 8 after injury assessed by Western blotting showing increased p18 fragment at 5 hrs compared to 5 and 24 hrs. Full length caspase 8 was not detected. *p=0.031, Tukey post-hoc tests.

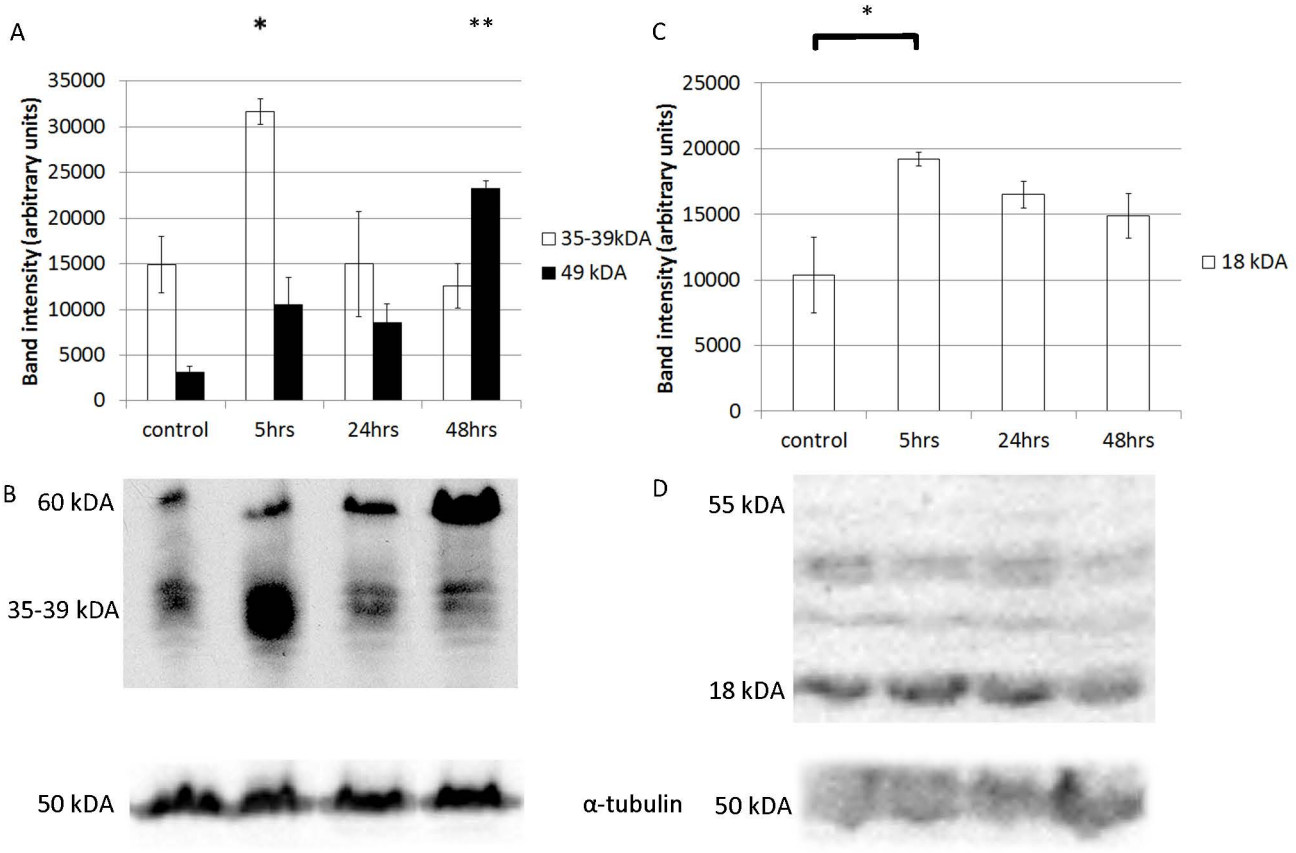

Figure 8.4.2.
A-B. Retinal levels of full length (p33-35) and cleaved (p18) caspase-6 after injury assessed by western blotting showing an increase in levels of p18 up to 48 hours. Note that the level of p18 falls near the lower limit of detection for this assay. (*=0.009) C-D. Retinal levels of full length (32kDA), and cleaved (p17) caspase 3 after injury were unchanged, the p11 fragment was not detected. E-F. Retinal levels of full length caspase 7 (p35) were unchanged after injury, the cleaved form (p20) was not detected.

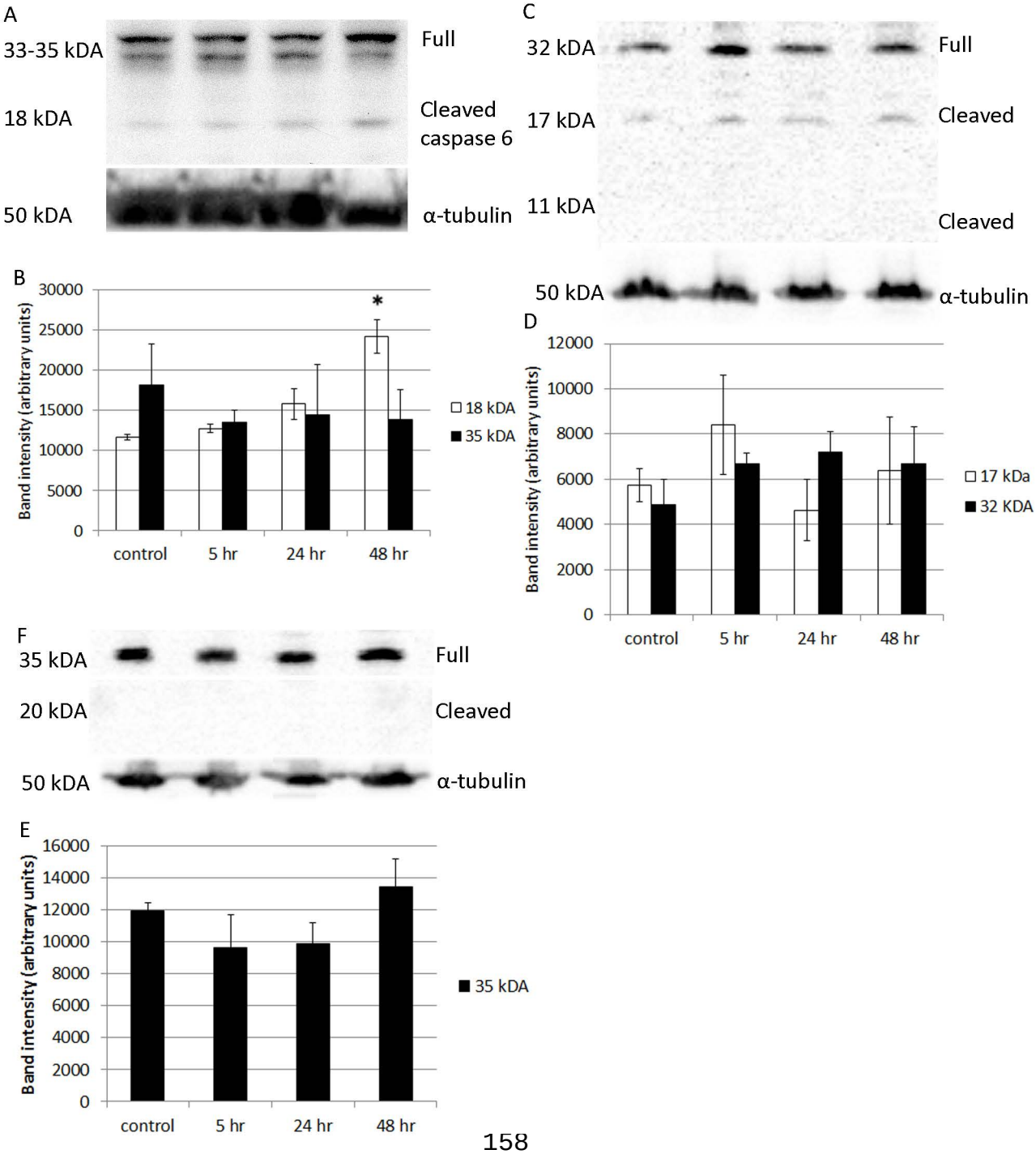

8.4.4.2. Executioner Caspases

Western blotting results are presented in Figure 8.4.2. Retinal levels of the full length (p32) and cleaved (p17) caspase 3 were detectable by western blotting, but were unchanged over the 48 hr after injury (p=0.519, 0.536 respectively; one way ANOVA), whilst the p11 fragment was undetectable (Figure 4C-D). Similarly, western blots detected full length caspase 7 in the retina (p35) that remained unchanged in the 48 hr after injury (p=0.317; one way ANOVA), whilst the p20 cleaved fragment was not detectable (Figure 4E-F). However, western blots showed that retinal levels of cleaved caspase-6 (p18), increased up to 48 hr after injury (p=0.009; one way ANOVA), but the levels of full length caspase-6 (p33-35) were not significantly altered (p=0.059; one way ANOVA) (Figure 4A-B).

8.4.5.Discussion

Western blotting was performed to investigate the expression and processing of initiator caspases in the retina. Compared to uninjured retinae, levels of cleaved caspase-9 were increased by 5 hr and decreased to basal levels by 24 hr after ballistic injury. Caspase-9 is an initiator caspase, and as such usually activates downstream executioner caspases (such as caspase-3, -6, and -7) to bring about apoptosis (Galluzzi, Blomgren, and Kroemer 2009). Western blotting, was used to investigate which executioner caspases were cleaved after ballistic injury and showed that the only active executioner caspase in the retina after ballistic injury is caspase-6.

Subsequent experiments were needed for precise retinal localisation of these caspases and to confirm catalytic activity.

8.4.6.Conclusions

Retinal levels of cleaved caspases 6, 8 and 9 are increased after ballistic ocular injury.

8.5. Immunohistochemical study of high velocity retinal injury

8.5.1.Hypothesis

Cleaved caspases 6, 8 and 9 immunolocalise to photoreceptors after ballistic ocular injury.

8.5.2.Aim

To confirm the precise retinal locations of cleaved caspases within the retina.

8.5.3.Materials and Methods

Two groups of 4 female Lister-hooded rats had unilateral, right ballistic ocular injury under recovery anaesthesia (see Section 6.6.7.) and were killed 5 and 24 hr later. The left eyes were controls. Samples were processed for immunohistochemistry.

Immunohistochemical staining was performed for caspases 3, 6 (Cell Signalling and Santa Cruz), 7, 8 and 9 (Santa Cruz), cone arrestin, ED1 (CD68) and OX42 (CD11b).

8.5.4.Results

Caspase 9 staining was increased in the region of photoreceptor inner segments around the impact site 5 hr after injury and in photoreceptor cell bodies 48 hr after injury (Figure 8.5.1.). Caspase 8 was not detected in the ONL (data not shown).

Cleaved caspase 6 was detected in all photoreceptors 48 hr after injury (Figure 8.5.2.A-D) and in cones (co-staining with cone arrestin; Figure 8.5.2.E-H) around the impact site. Co-staining with ED1 and OX42 confirmed that the observed caspase immunolocalisation was not in inflammatory cells. Cleaved caspases 3 and 7 were not detected in the ONL.

8.5.5.Discussion

Compared to uninjured control retinae, caspase-9 levels were increased in photoreceptor inner segments of injured animals at 5 hr after injury and in photoreceptor cell bodies at 48 hr, indicating

Figure 8.5.1.
Immunohistochemical staining of rat outer retinal layers after injury (DAPI-stained nuclei shown in blue, 50µm scale bar). **A-B**. Caspase-9 (arrows) in photoreceptor inner segments, seen between the DAPI stained outer nuclear layer (ONL) and the autofluorescent outer segments (OS) at 5 hours after injury (A), but not in uninjured control retina (B). **C-F**. Increased caspase-9 levels in photoreceptor cell bodies (arrows) at 2 days in injured (C, blue and green channels in D-E, respectively) but not uninjured control retina (F).

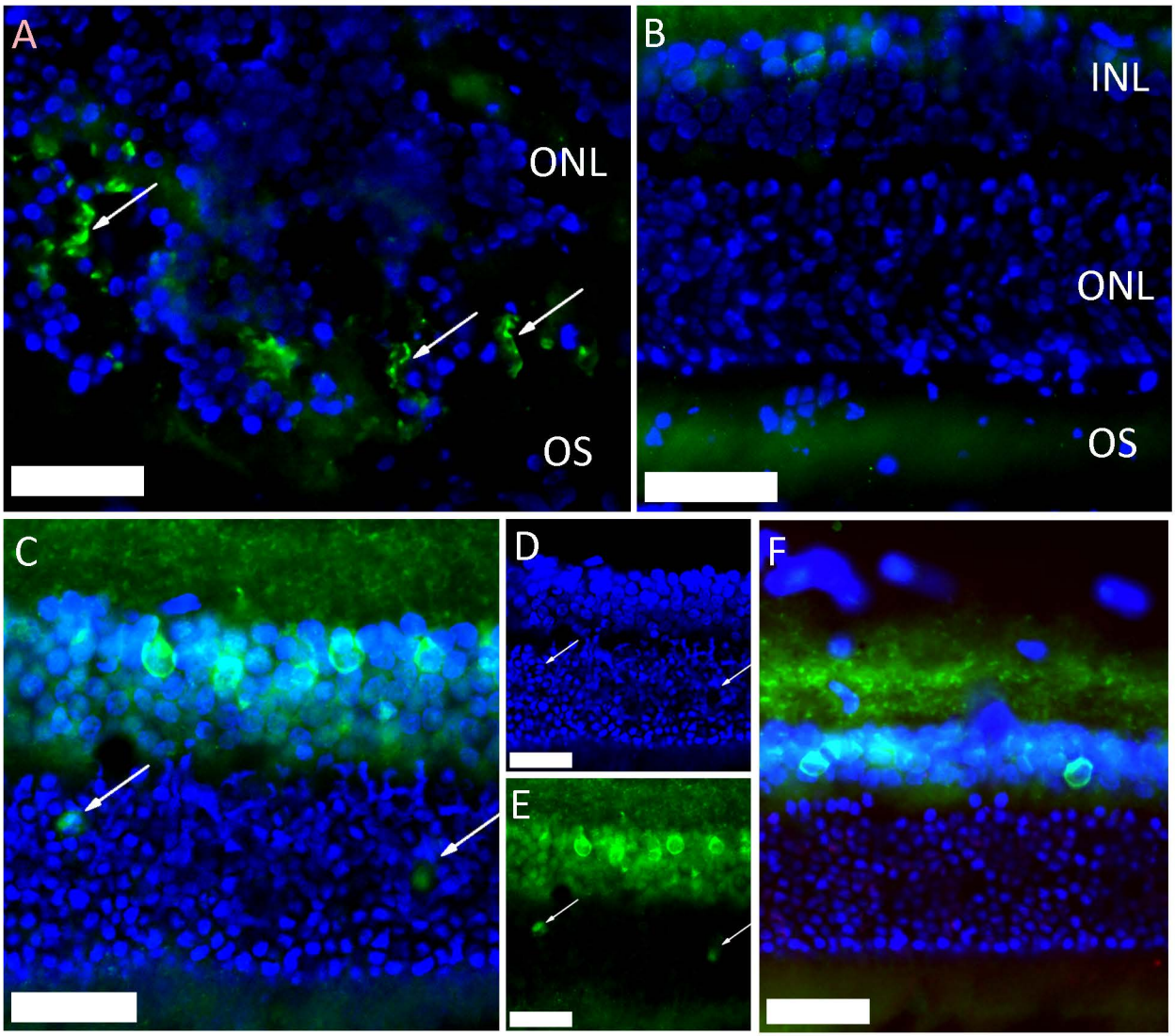

Figure 8.5.2.
A-D. Activated caspase-6 (Cell Signalling, rabbit; arrow) in photoreceptor cell body (green) at 2 days after injury (A, blue and green channels in B-C, respectively), but not in uninjured control tissue (D). Inflammatory cells are stained red by ED1. **E-J-** DAPI-stained nuclei shown in blue, cone arrestin in red and activated caspase-6 (Santa Cruz, goat) in green **E**. 2 days after injury activated caspase-6 colocalised with cone arrestin and so was present in cones in the outer nuclear layer (ONL). **F-G**. Red and green channels of E. **H**. Uninjured control retina with cone arrestin staining cones green (example cell body arrowed), but no caspase-6 staining (red). **I-J**. Red and green channels of H.

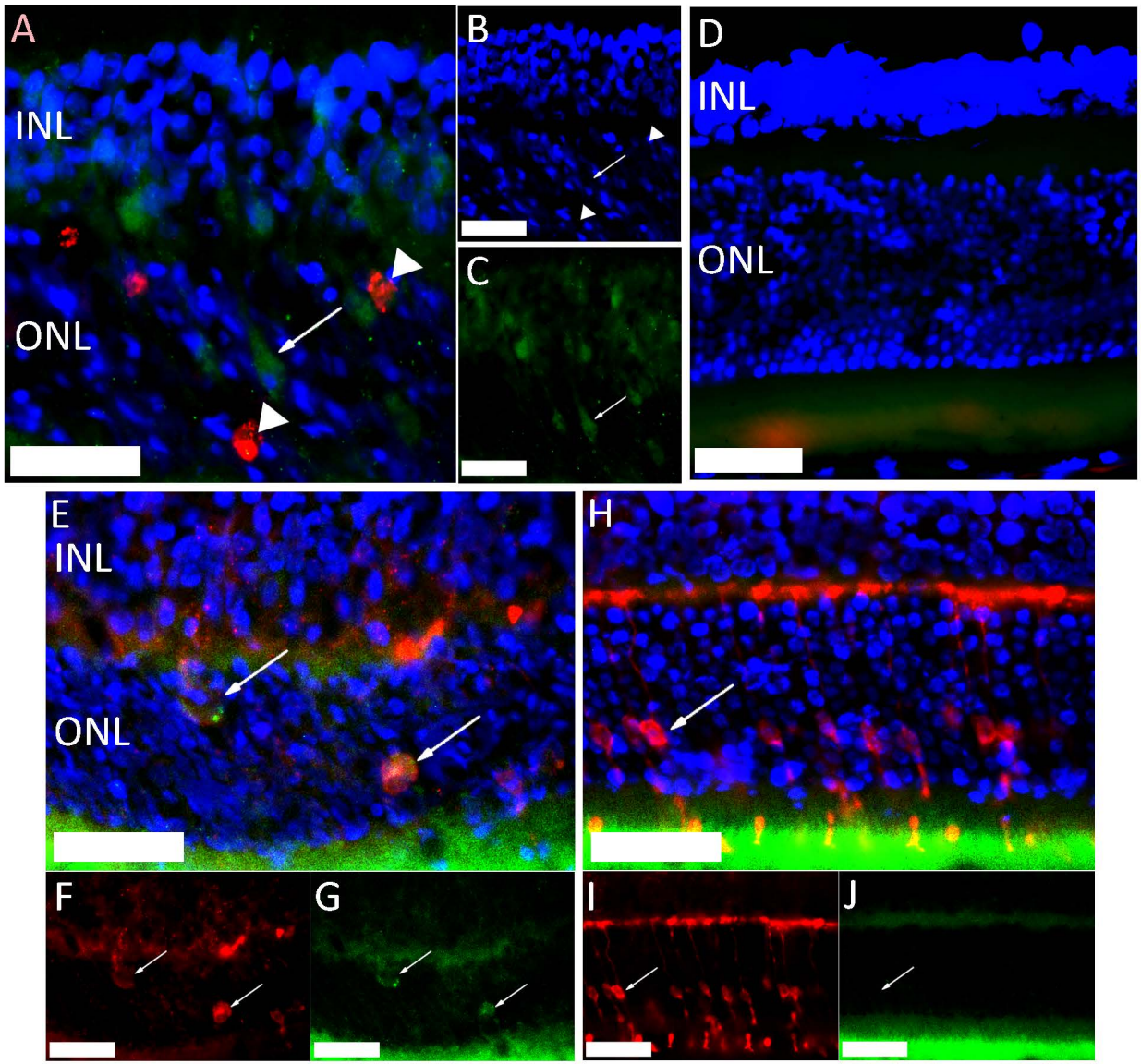

that cleaved active caspase-9 was present in photoreceptors 5 hr after injury, consistent with its function as an initiator and full length caspase-9 was upregulated by 48 hr, correlating with photoreceptor apoptosis.

Despite being advertised as specific for the cleaved form, the antibodies against caspase 9 may have limited ability to distinguish between cleaved and full length enzyme, evidenced by the fact that on western blotting, levels of cleaved enzyme are increased at 5 hr and full length enzyme at 48 hr, yet the same antibody immunohistochemically detected increased levels of caspase 9 at 5 and 48 hr after injury. An alternative explanation is that cleaved caspase 9 immunolocalised in photoreceptor cell bodies 48 hr after injury, but that cells with active caspase 9 represented too few of the total number of retinal cells for increased cleaved caspase 9 levels to be detected by western blotting. It is therefore not possible from these data be certain that photoreceptors expressed the transcriptionally upregulated full-length caspase 9. However, the immunolocalisation of cleaved caspase 9 to the mitochondria-rich outer segments 5 hr after injury is consistent with activation linked to MOMP and the immunolocalisation of caspase 9 to the cell body 48 hr after injury is consistent with synthesis there, suggesting that the antibody detected both cleaved and full length caspase 9, though possibly with different affinities for the 2 forms.

Of the 3 executioner caspases (3, 6 and 7), only cleaved caspase 6 was immunolocalised in photoreceptors and increased in the retina assessed by western blotting. Thus the only active executioner caspase present in photoreceptors after ballistic injury is caspase-6 and therefore we hypothesised that caspase-6 executes the apoptotic programme in photoreceptors after initiation by caspase-9..

8.5.6.Conclusion

There is cleaved caspase 6 and 9 in photoreceptors after ballistic ocular trauma. This suggests that cell death could be prevented by caspase 6 and 9 inhibition.

8.6. Demonstration of Catalytically Active Caspase 9 in Photoreceptor Apoptosis

8.6.1.Rationale

Cleaved caspase 9 levels increased in the retina 5 hr after ballistic injury and immunolocalised to photoreceptors.

Valine-Alanine-Aspartate-fluoromethyl ketone (VAD-fmk) is a pan-caspase inhibitor that covalently binds and, in its biotinlyated form (bVAD-fmk), isolates caspases-1, -2, -3, -8 and -9 through interaction with immobilised streptavidin (Tu et al. 2006), (Moulin and Arrigo 2008). Because binding is initiated by the catalytic activity of the caspase, bVAD-fmk isolates only catalytically active enzyme.

8.6.2.Hypothesis

I. Caspase 9 is catalytically active within the first 5 hr after ballistic ocular injury.

II. Caspase 6 is catalytically active 48 hr after ballistic injury.

8.6.3.Aim

I. To demonstrate catalytically active caspase 9 in the retina within the first 5 hr after ballistic ocular injury.

II. To demonstrate catalytically active caspase 6 in the retina 48 hr after ballistic ocular injury.

8.6.4.Materials and Methods

In 2 groups of 6 animals, bVAD-fmk was injected intravitreally into both eyes, 3 of which were bilaterally ballistically injured. To capture the active initiator caspase 9 (group 1), injuries were induced 2 hr after injection and all animals were killed 5 hr after injury. To capture the active executioner caspase 6 (group 2), injuries were induced 43 hr before injection and all animals were killed 5 hr after injection and retinae processed for caspase pull-down assay. The blot for group 1 was probed with an antibody to caspase 9 (Cell Signalling) and the blot for group 2 with an antibody to caspase 6 (Cell Signalling).

Figure 8.6.
Caspase capture assay. A-B. Pull-down 5 hr after ballistic injury, probed for caspase 9 (Cell Signalling) and showing increased levels of catalytically active caspase 9 in the injured compared to the control retinae (p=0.028). B-C. Pull-down 48 hr after injury probed for caspase 6 (Cell Signalling) and showing increased levels of catalytically active caspase 6 in the injured compared to the control retinae (p=0.003). Note the faint band, that required a long (10 min) exposure time.

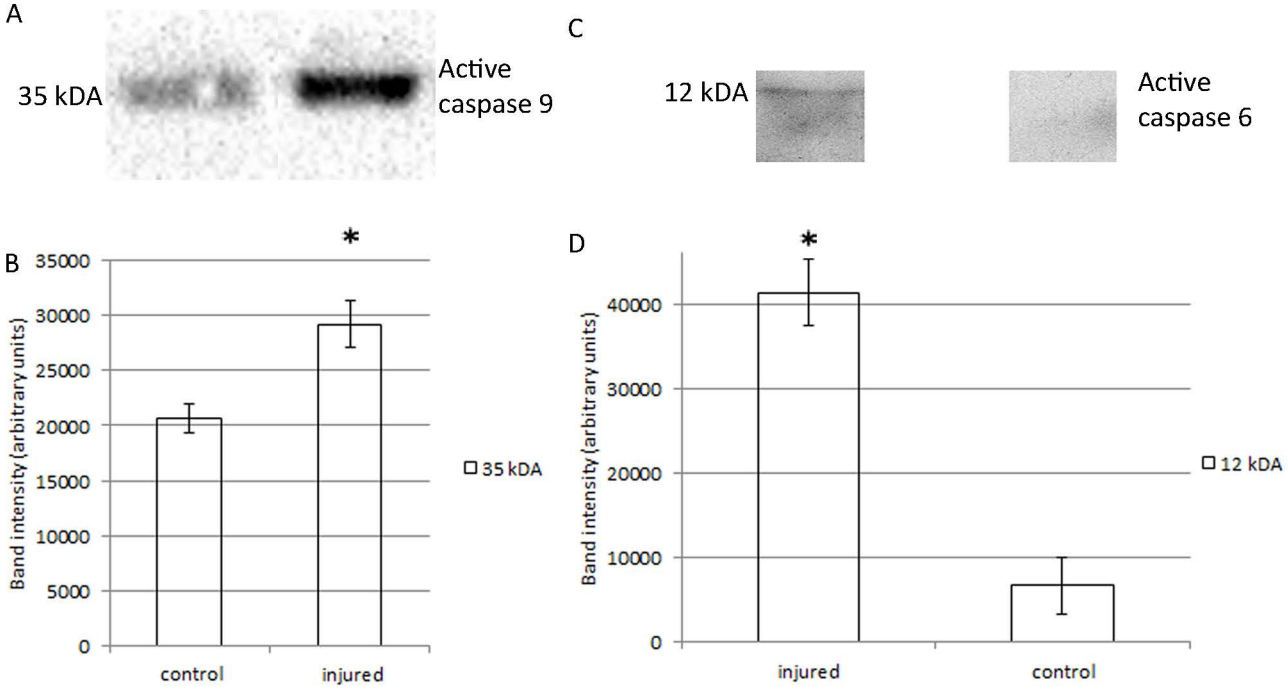

8.6.5.Results

8.6.5.1. Caspase 9 Capture

Higher levels of active caspase-9 were isolated from injured than from uninjured retinae (Figure 8.6.; p=0.028, 2 sample t-test).

8.6.5.2. Caspase 6 Capture

Higher levels of active caspase-9 were isolated from injured than from uninjured retinae (Figure 8.6.; p=0.003, 2 sample t-test;).

8.6.6.Discussion

bVAD-fmk was used to isolate active caspase 9 within the first 5 hr after ballistic ocular injury, which is the first demonstration of catalytically active caspase 9 after eye injury.

8.6.7.Conclusion

Caspase 9 was catalytically active within 5 hr after ballistic ocular injury.

8.7. Demonstration of the Role of Caspase 9 in Photoreceptor Apoptosis

8.7.1.Rationale

Caspase 9 was active in photoreceptors within 5 hr of injury. It is therefore likely that caspase 9 initiates apoptosis in a proportion of photoreceptors after ballistic ocular injury.

8.7.2.Hypothesis

Caspase 9 inhibition decreases cell death and preserves retinal function after ballistic ocular injury.

8.7.3.Aim

To assess the importance of caspase 9 as a mediator of cell death in photoreceptors after ballistic ocular injury.

8.7.4.Materials and Methods

Eight rats were subjected to bilateral ballistic ocular injury. The highly specific caspase-9 inhibitor, X-linked inhibitor of apoptosis (IAP)-baculoviral IAP repeat 3 domain (XBIR3), linked to a cell transduction peptide Penetratin 1 (Pen1; PolyPeptide Laboratories,Torrance, CA USA) (Eckelman et al. 2006) was prepared as previously described (kindly supplied by Carol Troy, Columbia University, USA) (Sun et al. 2000), and 5µl of 5µM solution was delivered by unilateral intravitreal injection to inhibit caspase-9 in 8 rats (n=8 eyes). Contralateral eyes were given control treatment with Pen1 alone. Scotopic and photopic ERG series with stimuli ranging from -2.5 to + 1 log units with respect to a standard flash were recorded at 7 and 14 d after injury as shown in Table 8.7.4. Animals were killed at 14 d and eyes prepared as for immunohistochemistry. Sections were taken through the optic disc (and centre of the impact site) and 600, 1200 and 1800µm either side for H&E staining and quantification of cell death.

H&E stained slides were scanned on a Mirax slide scanner (Zeiss) and the ONL manually segmented using the magnetic lasso tool in Adobe Photoshop by an observer blind to treatment allocation (Figure 8.6.1.). To measure average ONL thickness without incorporating cryosection fragmentation artefact, the outer nuclear layer was then converted to 8 bit grayscale and thresholded to level 160 in ImageJ (http://rsbweb.nih.gov/ij). Pixels above threshold were counted using the automatic pixel counting function of ImageJ and total section length was measured using the segmented line tool. Average ONL thickness (in pixels) was calculated as number of above threshold ONL pixels divided by the length of the section (Figure 8.7.1.).

Figure 8.7.1. A. Cut-out outer nuclear layer from B. **B** whole H&E stained rat retinal section with illustrative line showing the measurement of section length.

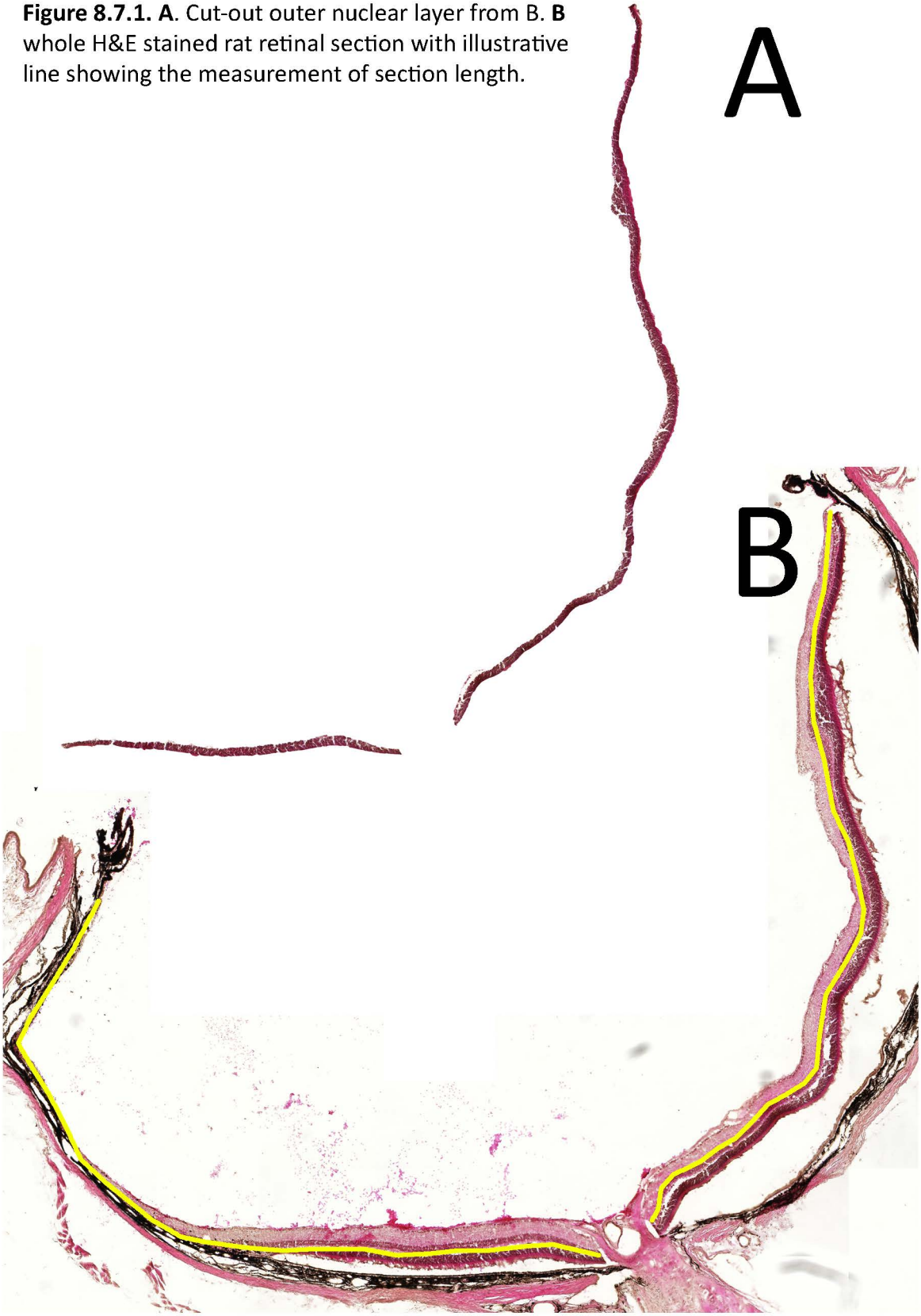

Stage of testing	Light exposure (log units with respect to standard flash)	Light exposure (mcd.s/m^2)	Number of flashes averaged	Interval between flashes (sec)	Time elapsed (sec)
Dark adaptation					
Scotopic Flash	-2.5	10	10	2	20
Delay				2	22
Scotopic Flash	-2	30	4	5	42
Delay				5	47
Scotopic Flash	-1.5	100	4	10	87
Delay				10	97
Scotopic Flash	-1	300	4	10	137
Delay				10	147
Scotopic Flash	-0.5	1000	4	10	187
Delay				10	197
Scotopic Flash	0	3000	4	10	237
Delay				10	247
Scotopic Flash	0.5	10000	4	15	307
Delay				15	322
Scotopic Flash	1	25000	4	20	402
Background (BG) light adaptation (remains on for testing)	1	30000		600	1002
Photopic Flash (+ BG)	-2.5	10	10	0.5	1007
Delay + BG	1	30000		0.5	1007.5
Photopic Flash (+ BG)	-2	30	10	0.5	1012.5
Delay + BG	1	30000		0.5	1013
Photopic Flash (+ BG)	-1.5	100	10	0.5	1018
Delay + BG	1	30000		0.5	1018.5
Photopic Flash (+ BG)	-1	300	10	0.5	1023.5
Delay + BG	1	30000		0.5	1024
Photopic Flash (+ BG)	-0.5	1000	10	0.5	1029
Delay + BG	1	30000		0.5	1029.5
Photopic Flash (+ BG)	0	3000	10	0.5	1034.5
Delay + BG	1	30000		0.5	1035
Photopic Flash (+ BG)	0.5	10000	10	0.5	1040
Delay + BG	1	30000		0.5	1040.5
Photopic Flash (+ BG)	1	25000	10	0.5	1045.5

Table 8.7.4. Scotopic and photopic ERG recording protocol

8.7.5.Results

8.7.5.1. Structural Neuroprotection

Caspase-9 inhibition reduced photoreceptor death, demonstrated by preserved outer nuclear layer (ONL) thickness on retinal sections (Figure 8.6.2.A-B). The effect of treatment on ONL thickness was modelled using generalised estimating equations (Appendix 12) showing: (1), a non-significant effect

Figure 8.7.2. **A**. Outer nuclear layer (ONL) thickness as a function of distance from the impact site. **B**. Test of model effects after analysis of ONL thickness including treatment, distance from the impact site and a term to model their interaction. **C** Scotopic a-wave amplitude as a function of stimulus intensity. **D**. Test of model effects after analysis of scotopic a-wave amplitude including time after injury (timepointdays), stimulus intensity (flashintensitymcd), Pen1-XBIR3 compared to Pen1 alone (TreatedXBIR3vspen) and terms to model all 2 and 3 way interactions. **E**. Photopic b-wave amplitude as a function of stimulus intensity. **F**. Test of model effects after analysis of photopic b-wave amplitude including time after injury, stimulus intensity, treatment and terms to model all 2- and 3-way interactions. Caspase-9 inhibition by Pen1-XBIR3 increases scotopic a- and photopic b-wave amplitudes with an effect that is more pronounced at higher stimulus intensities and at 14 as opposed to 7 days after injury. Caspase-9 inhibition also increased ONL thickness peripheral but not central to the impact site.

A

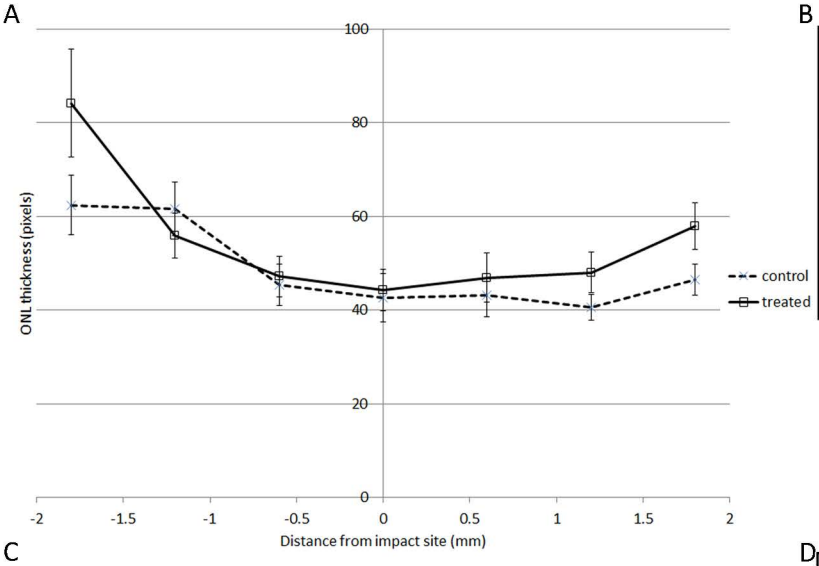

B

Source	Type III Wald Chi-Square	df	Sig.
(Intercept)	6286.697	1	0.000
TreatedXBIR3vspen	1.121	1	0.290
Distanceimpactsite	81.447	6	0.000
TreatedXBIR3vspen * Distanceimpactsite	15.115	6	0.019

C

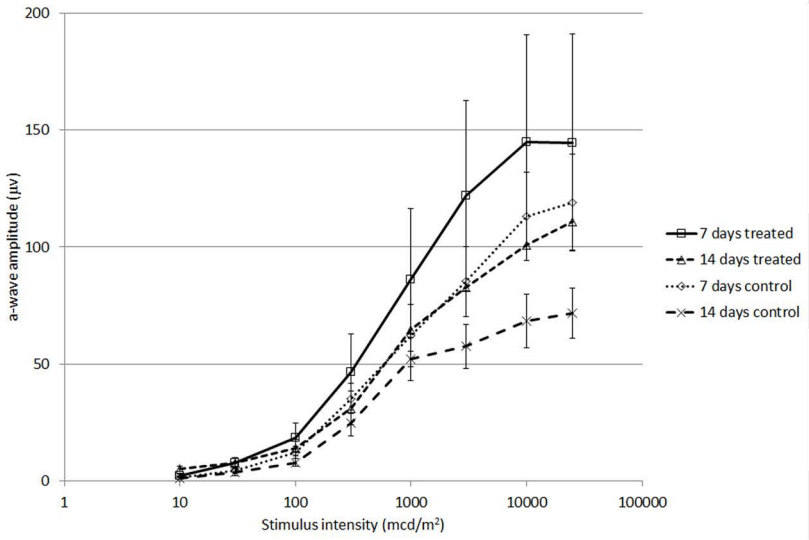

D

Source	Type III Wald Chi-Square	df	Sig.
(Intercept)	1298.494	1	0.000
timepointdays	1.751	1	0.201
flashintensitymcd	9095.097	5	0.000
TreatedXBIR3vspen	3.576	1	0.070
timepointdays * flashintensitymcd	151.653	4	0.000
timepointdays * TreatedXBIR3vspen	.981	1	0.414
flashintensitymcd * TreatedXBIR3vspen	308.048	4	0.000
timepointdays * flashintensitymcd * TreatedXBIR3vspen	30.131	4	0.000

E

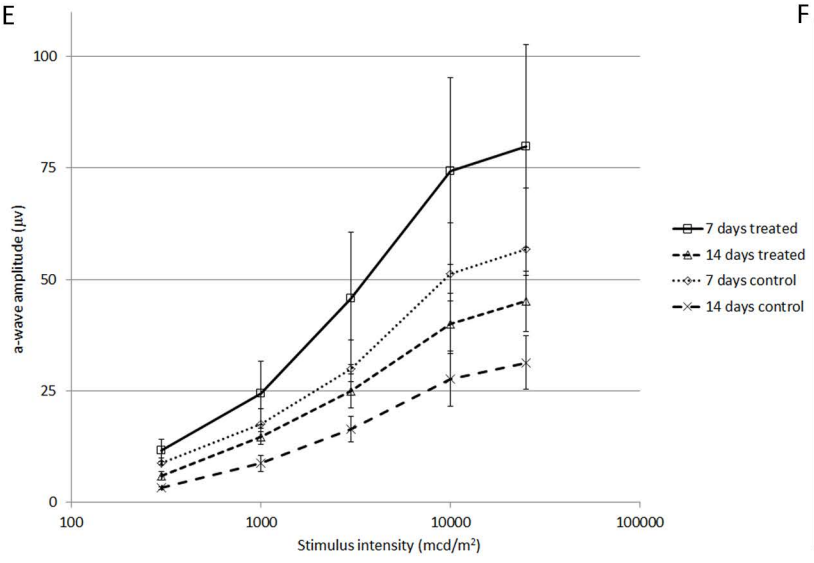

F

Source	Type III Wald Chi-Square	df	Sig.
(Intercept)	364.679	1	0.000
timepointdays	18.175	1	0.000
flashintensitymcd	32807.582	5	0.000
TreatedXBIR3vspen	1.690	1	0.194
timepointdays * flashintensitymcd	36.289	4	0.000
timepointdays * TreatedXBIR3vspen	.411	1	0.522
flashintensitymcd * TreatedXBIR3vspen	40.477	4	0.000
timepointdays * flashintensitymcd * TreatedXBIR3vspen	28.365	4	0.000

of caspase-9 inhibition across all distances from the impact site (p=0.29); (2), a highly significant effect of distance from the centre of the impact site, i.e. the outer nuclear layer was thinner towards the centre of the impact site (p<0.001), as we have previously reported (Blanch et al. 2012a); (3), a significantly thicker ONL peripheral, but not central, to the impact site in caspase-9-suppressed than in Pen1-treated eyes (p=0.019 for the 2-way interaction distance*caspase-9 inhibition).

8.7.5.2. Functional Neuroprotection

Compared to eyes injected with intravitreal Pen1 alone, caspase-9 inhibition improved rod and cone function, assessed by scotopic a-and photopic b-wave amplitude respectively, and this benefit increased with time after injury (Figure 8.6.2.C-F). The effect of treatment on scotopic a-wave amplitude was modelled using generalised estimating equations (Figure 8.6.2.D and Appendix 13) showing: (1), a borderline significant increase in a-wave amplitude after caspase-9 inhibition across all stimulus intensities and time points (p=0.070); (2), a positive effect of caspase-9 inhibition on a-wave amplitude that increases with stimulus intensity (p<0.001 for 2-way interaction caspase-9 inhibition*stimulus intensity); (3), a significant difference in the effect of caspase-9 inhibition between the 2 time points with a more pronounced positive effect (with smaller error bars) at 14 than at 7 d (p<0.001 for the 3-way interaction caspase-9 inhibition*stimulus intensity*time). Photopic b-wave analysis showed similar effects (Figure 8.6.2.E-F; Appendix 14).

8.7.6.Discussion

Use of peptide pharmacological inhibitors (like VAD-fmk) to study caspase activity is common. However, overlap in cleavage motifs means that these inhibitors are non-specific. XBIR3 –the BIR3 domain of XIAP – is a highly specific inhibitor of caspase-9 (Srinivasula et al. 2001) and so the observed neuroprotective effects of caspase-9 inhibition are unlikely to be XBIR3 off-target effects (Akpan et al. 2011).

As 98% of rat photoreceptors are rods and the ONL contains exclusively photoreceptors, ONL thickness reflects rod survival (Blanch et al. 2012b). Caspase-9 inhibition after blunt ocular trauma

most affected ONL thickness peripheral to the impact site, where the highest proportion of apoptotic cells are found, as opposed to central to the impact site, where most cell death is necrotic and therefore less susceptible to modulation by altered caspase activity (Blanch et al. 2012a). Consistent with caspase-9's function as an initiator caspase, the spike in retinal levels of activated caspase-9 was recorded 5 hr after injury and was followed by compensatory upregulation of full length caspase-9 by 48 hr. The western blotting, immunohistochemical and survival data therefore demonstrate that caspase-9 initiates rod and cone apoptosis in a proportion of photoreceptors after blunt ocular trauma causing commotio retinae.

The a-wave is the first negative deflection on the ERG, caused by photoreceptor hyperpolarisation, and its amplitude is routinely measured to assess photoreceptor function. Commotio retinae reduces photoreceptor function (assessed by a-wave amplitude) out of proportion to the extent of photoreceptor death (Blanch et al. 2012a). Scotopic a-wave amplitude in rats reflects rod function and was increased by caspase-9 inhibition, indicating that the increased survival seen on ONL thickness measurements was accompanied by increased rod function.

Photopic ERG are recorded under conditions of light adaptation, which bleaches rod photoreceptors and ensures that the ERG response is cone-mediated. In rats, the photopic a-waves are small and often undetectable after injury (Blanch et al. 2012a). The b-wave is the first positive deflection, immediately following the a-wave and is generated by the activity of second order neurons (such as ON bipolar cells in the inner nuclear layer). The b-wave is therefore dependent on photoreceptor activation and synaptic transmission in addition to inner retinal function. In addition, the b-wave is measured from the base of the a-wave and thus incorporates both responses. The b- to a-wave ratio is a measure of how much of the variation in b-wave amplitude is due to variation in the magnitude of photoreceptor activation compared to the function of second order neurons. In rats, the b- to a-wave ratio is unaffected by commotio retinae (Blanch et al. 2012a), indicating that any variation in b-wave amplitude is due to variation in the magnitude of the photoreceptor response. The observed changes in photopic b-wave amplitude therefore reflect cone photoreceptor function, which was

increased by caspase-9 inhibition, indicating that caspase-9 also initiates cone apoptosis after blunt ocular trauma.

The most commonly reported ultrastructural feature of acute commotio retinae is photoreceptor outer segment disruption (Blight and Hart 1977), (Souza-Santos et al. 2012). In mild cases of commotio retinae there is visual recovery, correlated with outer segment regeneration over weeks to months (Blight and Hart 1977), (Souza-Santos et al. 2012). The effect of caspase-9 inhibition on cone and rod function was greater at 14 than at 7 d, consistent with functional regeneration of damaged outer segments of photoreceptors rescued from apoptosis by caspase-9 inhibition. demonstrating that caspase-9 mediates photoreceptor apoptosis after ballistic injury. indicating that caspase-9 mediates both rod and cone apoptosis after ballistic injury and its inhibition is functionally neuroprotective

This study clearly shows that after high velocity blunt ocular trauma causing retinal injury, inhibition of caspase 9 function with Pen1-XBIR3 delivered intravitreally, (1), reduces photoreceptor death over 2 weeks and, (2), improves photoreceptor function, as assessed by ERG a-wave amplitude.

P values are not significant for an overall effect of treatment but only for interactions with other factors. In the analysis of ONL thickness, this is because the sections through the centre of the impact site feature predominantly necrotic cells, which will not survive as a result of caspase 9 inhibition. If the zone of apoptotic cells is viewed as a peripheral ring of potentially salvageable cells around the necrotic zone at the impact site, the sections through the centre cut radially through this ring and have a minority of salvageable cells. The sections through the peripherally of the impact site have few necrotic cells, but cut tangentially through this ring of salvageable cells. So a neuroprotective effect of sufficient magnitude to achieve statistical significance is only seen in the peripheral sections and this is reflected as an interaction between the effects of distance from the impact site and treatment. Similarly for the ERG data, the a-wave is low amplitude or absent at low

stimulus intensities, so an effect of treatment is only apparent at higher stimulus intensities and this is reflected as an interaction between the effects of stimulus intensity and treatment.

8.7.7.Conclusions

Caspase 9 initiates rod and cone apoptosis after ballistic ocular injury.

8.8. Demonstration of the Role of Caspase 6 in Photoreceptor Apoptosis

8.8.1.Hypothesis

Caspase 6 inhibition decreases cell death and preserves retinal function after ballistic ocular injury.

8.8.2.Aim

To assess the importance of caspase 6 as a mediator of cell death in photoreceptors after ballistic ocular injury.

8.8.3.Materials and Methods

Eight rats were subjected to bilateral ballistic ocular injury. Inhibition of caspase-6 activity used a caspase-6 (Cys163Ala) dominant negative (C6DN) protein linked to Pen1 (kindly supplied by Carol Troy, Columbia University, USA). The C6DN construct was a gift from G. S. Salvesen, Sanford-Burnham Institute, La Jolla, CA and C6DN was purified as previously described (Denault and Salvesen 2003), and 5µl of 5mM solution was delivered by unilateral intravitreal injection in 8 rats (n=8 eyes). Contralateral eyes were given control treatment with Pen1 alone. Scotopic and photopic ERG series with stimuli ranging from -2.5 to + 1 log units with respect to a standard flash in half log unit steps were recorded at 7 and 14 d after injury as shown in Table 8.7.4. and animals killed at 14 d and eyes prepared as for immunohistochemistry. ONL thickness was measured as described in Section 8.6.3.

Figure 8.8. **A**. Outer nuclear layer thickness as a function of distance from the impact site. **B**. Test of model effects after analysis of ONL thickness including treatment and distance from the impact site, with non-significant terms removed (before removal, p=0.345 for normalisedslidenumber*TreatedCasp6DNvspen and p=0.689 for TreatedCasp6DNvspen). **C**. Scotopic a-wave amplitude as a function of stimulus intensity. **D**. Test of model effects after analysis of scotopic a-wave amplitude including time after injury (timepointdays), stimulus intensity (flashintensitymcd), Pen1-C6DN compared to Pen1 alone (TreatedCasp6DNvspen) and terms to model all 2- and 3-way interactions. **E**. Photopic b-wave amplitude as a function of stimulus intensity. **F**. Test of model effects after analysis of photopic b-wave amplitude including time after injury, stimulus intensity, treatment and terms to model significant interactions only. Caspase-6 inhibition using Pen1-C6DN had no effect on ONL thickness, but reduced scotopic a- and photopic b-wave amplitudes with an effect that was more pronounced at higher stimulus intensities.

A

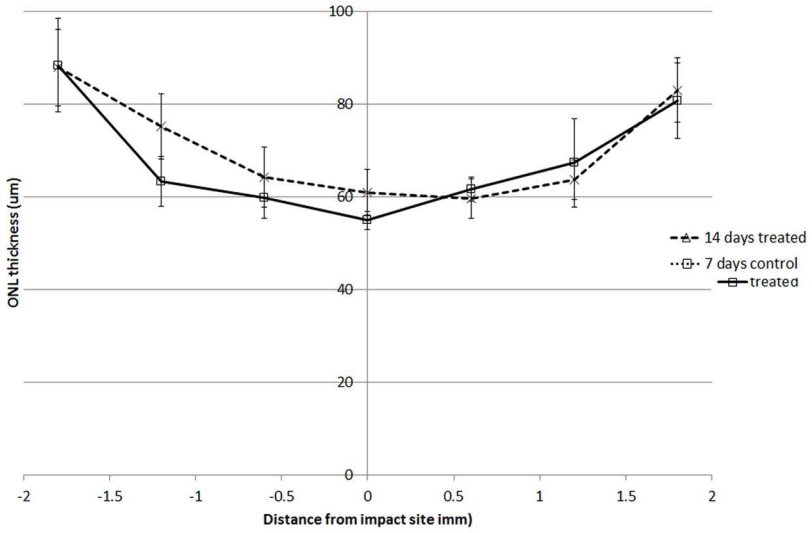

B

Source	Type III Wald Chi-Square	df	Sig.
(Intercept)	13373.411	1	0.000
normalisedslidenumber	1841.301	6	0.000

C

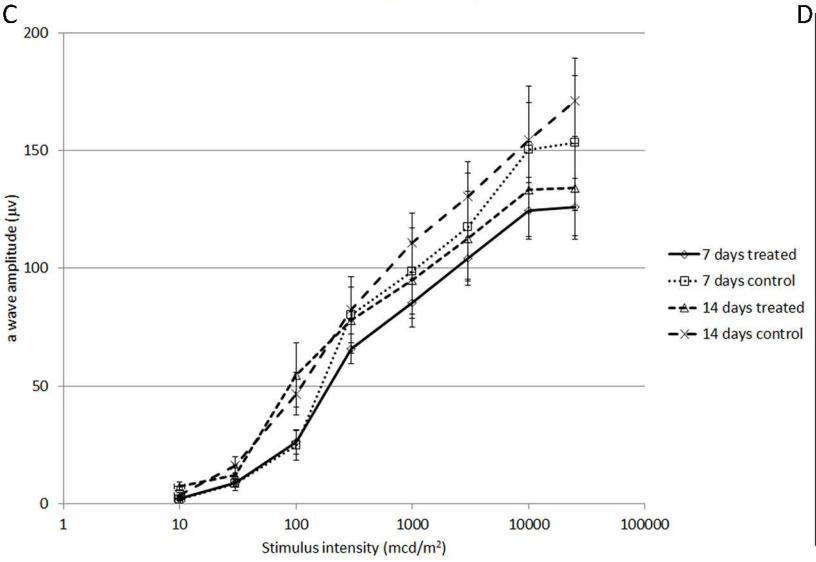

D

Source	Type III Wald Chi-Square	df	Sig.
(Intercept)	3872.703	1	0.000
timepointdays	4.613	1	0.032
flashintensitymcd	71302.045	7	0.000
TreatedCasp6DNvspen	0.070	1	0.791
timepointdays * flashintensitymcd	138.081	7	0.000
timepointdays * TreatedCasp6DNvspen	0.252	1	0.616
flashintensitymcd * TreatedCasp6DNvspen	46.727	7	0.000
timepointdays * flashintensitymcd * TreatedCasp6DNvspen	177.273	7	0.000

E

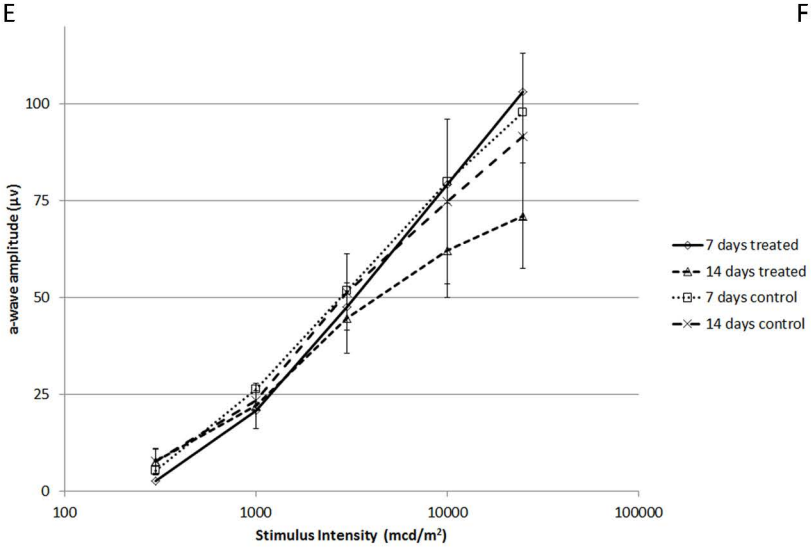

F

Source	Type III Wald Chi-Square	df	Sig.
(Intercept)	1108.201	1	0.000
timepointdays	13.349	1	.000
flashintensitymcd	4630.683	4	0.000
TreatedCasp6DNvspen	.293	1	.589
flashintensitymcd * TreatedCasp6DNvspen	10.650	4	.031

8.8.4.Results

8.8.4.1. Structural Assessment

The effect of caspase-6 inhibition on ONL thickness was modelled using generalised estimating equations (Appendix 15) and did not show any significant differences compared to control eyes in main effects or interaction terms (Figure 8.7.A-B), indicating that caspase-6 inhibition did not reduce rod death after ballistic injury.

8.8.4.2. Functional Assessment

Caspase-6 inhibition reduced rod and cone photoreceptor function, assessed by scotopic a- and photopic b-wave amplitude (Figure 8.7.C-F). The effect of caspase-6 inhibition on scotopic a-wave amplitude was modelled using generalised estimating equations (Figure 8.7.D; Appendix 16) and showed: (1), a non-significant effect of caspase-6 inhibition across all stimulus intensities and time-points ($p=0.791$); (2), a negative effect of caspase-6 inhibition on a-wave amplitude that increases with stimulus intensity ($p<0.001$ for the 2-way interaction caspase-6 inhibition*stimulus intensity); (3), a significant difference in the effect of caspase-6 inhibition between the 2 time points, with a greater negative effect at 14 than at 7 d ($p<0.001$ for the 3-way interaction caspase-6 inhibition*stimulus intensity*time). Photopic ERG assessment of cone function showed similar effects, except that there was no significant difference between 7 and 14 d (Figure 8.7.E-F; Appendix 17).

8.8.5.Discussion

The unexpected failure of caspase 6 inhibition to affect photoreceptor death may represent a significant negative or an underpowered study. In general post-hoc power calculations are not helpful in determining whether an observed non-significant effect reflects the absence of a population effect or a lack of power because the estimate of effect size derived from the (non-significant) data is necessarily imprecise. The use of confidence intervals is more appropriate in this context in defining the range of effect size consistent with the data. However, the interpretation of

confidence intervals for interaction terms derived from repeated measures data such as this is not clear. Looking at the error bars in Figure 8.7.F, the data seems to be consistent with a positive effect of similar magnitude to that presented after caspase 9 inhibition in Section 8.7. However, the finding of a statistically significant detrimental effect on retinal function would suggest that insufficient power is an unlikely explanation for these findings.

Of the three executioner caspases (-3, -6 and -7), only caspase-6 activity was increased after ballistic injury. Caspase-6 was active in both rods and cones after injury, but does not seem to serve as an executioner in this model. Although caspase-6 inhibition did not affect ONL thickness, it did reduce both scotopic and photopic ERG amplitudes, indicating that caspase-6 inhibition is detrimental to retinal function after blunt ocular trauma. Caspase-6 has been implicated in cell death after ischaemic stroke (Akpan et al. 2011), in axonal degeneration in vitro and after optic nerve crush (Nikolaev, McLaughlin, O'Leary, and Tessier-Lavigne 2009), (Monnier et al. 2011), and in cleavage of microtubules and cytoskeletal proteins in Alzheimer's disease (Guo et al. 2004), (Klaiman, Petzke, Hammond, and Leblanc 2008). That ONL thickness was not affected, suggests that the observed functional effects do not relate to caspase-6's role in cell death. It may be that caspase-6's role in microtubule processing is required for photoreceptor outer segment survival or regeneration after commotio retinae.

The role of caspase 6 in apoptosis is incompletely understood and caspase 6 activation does not necessarily induce cell death (Klaiman, Champagne, and LeBlanc 2009). It is also possible that in the ballistic injury model, caspase 6 has a role in preventing necroptotic cell death through RIP cleavage and that inhibiting caspase 6 in the current study increased the number of cells undergoing a necrotic form of cell death (van Raam, Ehrnhoefer, Hayden, and Salvesen 2013). If decreased RIP cleavage caused necroptotic cell death after caspase 6 treatment, then future studies using the RIP1 inhibitor necrostatin in addition to caspase 6 inhibition or in isolation would be expected to demonstrate neuroprotective effects.

8.8.6.Conclusions

Caspase 6 does not mediate rod or cone apoptosis after ballistic ocular injury and caspase 6 inhibition is detrimental to retinal function.

8.9. General Discussion/Conclusions

The experiments described in this section indicate that rod and cone apoptosis after blunt ocular trauma occur through the intrinsic pathway, initiated by caspase-9. Despite the presence of catalytically active caspase-6 in rods and cones after injury, its inhibition using a highly specific inhibitor did not prevent photoreceptor apoptosis but instead was detrimental to retinal function. In contrast, active caspase trapping assays revealed that caspase-9 is an early mediator of photoreceptor death and its inhibition reduced photoreceptor death and preserved visual function in both rods and cones, inducing structural and functional neuroprotection that was sustained at 2 weeks post-injury.

bVAD-fmk was used to isolate active caspase-9 within the first 5 hr after trauma, which is the first demonstration of catalytically active caspase-9 after eye injury. Caspase-6 was also isolated by this method 48 hr after ballistic injury, which is the first report of catalytically active caspase-6 isolation using bVAD-fmk. Activated caspase-6 levels detected by Western blotting and bVAD-fmk increased up to 48 hr after injury, but were near the lower limits of detection of the assays, suggesting that although caspase-6 is active after ballistic injury, it is present in only a small number of photoreceptors.

The high levels of cleaved caspase 9 observed 5 hr after injury are consistent with its function as an initiator caspase. For caspase 9 inhibition to be a translational therapy for eye injury, there would need to be a time window after injury in which initiation of treatment retained therapeutic benefit. There would also need to be a sustained benefit after discontinuing treatment. Future studies should therefore investigate how delayed administration of and duration of treatment with XBIR3 affect its neuroprotective benefits.

Caspase 2 shares substrate specificities with the executioner caspases (Troy and Ribe 2008), thus further investigations should examine the role of caspase 2 as a potential, novel, executioner caspase in the ballistic injury model. The role of caspase 6 in the ballistic ocular injury model is still unclear and further work should include an assessment of the effects of caspase 9 inhibition on caspase 6 activation and investigation of the RIP necroptotic cell death pathway and its interaction with caspase 6.

9. The neuroprotective Effect of Progesterone After High Velocity Injury

Parts of the work in this section have been prepared for submission to PLOS One, a draft manuscript is presented in Appendix 18.

9.1. Study of Progesterone-induced Neuroprotection

9.1.1.Rationale

9.1.1.1. Progesterone in Traumatic Brain Injury

Female rats have better functional outcomes and develop less cerebral oedema after traumatic brain injury than male rats, and this effect is more pronounced in pseudo-pregnant rats, which have high circulating progesterone and low oestrogen (Attella, Nattinville, and Stein 1987), (Roof, Duvdevani, and Stein 1993). In contrast, female gender in humans is associated with a worse outcome after traumatic brain injury (TBI) (Farace and Alves 2000). Nonetheless, the beneficial effects of female gender in animal studies of CNS trauma have been attributed to the higher levels of circulating progesterone compared to male rats and, in humans, phase II trials of progesterone treatment after traumatic brain injury have shown promising results (Xiao et al. 2008).

9.1.1.2. Mechanisms of progesterone-induced neuroprotection

Progesterone has transcriptional, translational and post-translational effects which limit lipid peroxidation, oxidative stress, inflammatory cytokine release, excitotoxicity and apoptosis.

9.1.1.2.1. Intracellular signaling

The progesterone receptor is a nuclear transcription factor associated with progesterone response elements in the promoter region of neurotrophin genes such as BDNF, upregulation of which mediates progesterone-induced neuroprotection (Jodhka et al. 2009) (Kaur et al. 2007) (Singh and Su 2013b). In addition, progesterone binding to the neuronal progesterone receptor membrane component-1 (PGRMC1) releases BDNF (Singh and Su 2013b) (Singh and Su 2013a). Membrane

receptor binding activates a number of intracellular signalling pathways including MAPK/ERK and PI-3-kinase/Akt/mTOR (Singh and Su 2013b) (Singh and Su 2013a), and inhibition of these pathways blocks progesterone's neuroprotective effects (Kaur et al. 2007). Progesterone upregulates anti-apoptotic Bcl-2 expression and activates Akt to phosphorylate pro-apoptotic Bad, inactivating it. Akt also phosphorylates forkhead transcription factor (FKHR), which inhibits Fas pathway activation (Zhao, Sapolsky, and Steinberg 2006) (Sugawara et al. 2004). Progesterone has some conflicting effects on cell death pathways though, upregulating uterine caspase 3 expression in pregnancy (when caspase 3 has functional, non-apoptotic effects), indirectly downregulating anti-apoptotic factors including NF-κB and complexing with the NFκB p65 subunit to prevent its action (Pettus, Wright, Stein, and Hoffman 2005), (Jeyasuria et al. 2009).

9.1.1.2.2. Anti-oxidant

Lipid peroxidation disrupts plasma membranes and contributes to blood-brain barrier breakdown after TBI. Progesterone reduces lipid peroxidation and free radical production and enhances free radical scavenging systems (Stein 2008a), (Roof, Hoffman, and Stein 1997), (Subramanian, Pusphendran, Tarachand, and Devasagayam 1993). Clinical evidence showing that the lipid peroxidation marker, F (2)-isoprostane is higher in male than female cerebral spinal fluid after TBI supports the membrane-stabilising effects progesterone (Bayir et al. 2004) (Stein 2007).

9.1.1.2.3. Anti-inflammatory

Progesterone downregulates synthesis and inhibits release of inflammatory factors and cytokines such as IL-1β, TNFα, complement factors C3, 5, macrophage-inducing factor-1, CDs 24 and 74 and iNOS reducing cerebral oedema and improving functional outcomes in TBI models (Pettus, Wright, Stein, and Hoffman 2005), (Djebaili et al. 2005), (Nilsen and Brinton 2002a), (Drew and Chavis 2000) (Gibson et al. 2005). Progesterone also reduces astrocytosis, gliosis and microglial activation after TBI (Garcia-Estrada, Luquin, Fernandez, and Garcia-Segura 1999) (Garcia-Estrada et al. 1993).

9.1.1.2.4. Progesterone metabolites

Progesterone metabolites may mediate neuroprotection. Progesterone is broken down to dihydroprogesterone (DHP) by 5α-reductase and then to 3α, 5α-tetrahydroprogesterone (THP). THP administration reduced oedema and apoptosis and improved functional outcomes after experimental TBI (Djebaili et al. 2005), (Djebaili, Hoffman, and Stein 2004), (He et al. 2004). THP binds to the GABA receptor, potentiating chloride conductance and counteracting glutamate-induced excitotoxicity. THP also inhibits MPTP opening and upregulates BDNF (Sayeed et al. 2009), (Wang et al. 2008) (Nin et al. 2011).

The synthetic progestin medroxyprogesterone acetate has not been found to be neuroprotective in excitotoxic models, actually reducing BDNF levels, and administration of the 5α-reductase inhibitor finasteride blocked progesterone's neuroprotective effects (Jodhka et al. 2009), (Nilsen and Brinton 2002b), (Ciriza, Carrero, Frye, and Garcia-Segura 2006).

9.1.1.3. Progesterone in Photoreceptor Death

Results from preclinical studies of progesterone in photoreceptor cell death models are variable. In Sprague-Dawley rats exposed to 2700 lux for 24 hr, progesterone was not neuroprotective when given IP at a dose of 60mg/kg daily in benzyl alcohol whereas, the synthetic progestin Norgestrel was neuroprotective when given IP to both Balb/c mice exposed to 5000 lux for 2 hr and rd10 retinal degeneration mice (Kaldi and Berta 2004), (Doonan, O'Driscoll, Kenna, and Cotter 2011). The efficacy of Norgestrel conflicts with previous work suggesting that metabolites are responsible for the neuroprotective effect (Ciriza, Carrero, Frye, and Garcia-Segura 2006) and there were more TUNEL-positive cells in the Norgestrel-treated animals 14 d after injury (Doonan, O'Driscoll, Kenna, and Cotter 2011), suggesting that apoptosis had been delayed rather than prevented. One other pre-clinical study in phototoxicity models did not show a beneficial effect of progesterone, but instead showed that ovariectomy (which lowers serum progesterone) was neuroprotective (O'Steen 1977).

Another study using rd1 mice (a retinitis pigmentosa model) showed reduced photoreceptor death with progesterone treatment (Sánchez-Vallejo et al. 2012).

The investigations reported in Chapter 5 have identified a possible protective effect of female gender after commotio retinae, suggesting that progesterone should be considered as a potential neuroprotective therapy after retinal injury.

There are limited pharmacokinetic data on progesterone in rats, reporting a half-life from 0.5 to 10 hr (Gangrade, Boudinot, and Price 1992), (Petroff and Mizinga 2003). Therapeutic dosing range of progesterone in rats has not been reported, though peak plasma progesterone concentrations in pregnant mice range from 45.5 - 81.9ng/ml (McCormack and Greenwald 1974), (Virgo and Bellward 1974) and these values were taken as the upper limit of the physiological range.

Progesterone therefore has a track record of being a successful neuroprotective agent in pre-clinical and clinical studies of traumatic brain injury and there is some evidence for a gender difference in visual outcomes after commotio retinae, implying that progesterone may affect recovery after eye injury. In addition progesterone has been reported to be neuroprotective in some (though not all) other experimental models of photoreceptor death and there is rat data that allows calculation of a dosing regimen for the current study.

9.1.2.Hypothesis

I. Progesterone reduces photoreceptor death after ballistic retinal injury.

II. Progesterone preserves retinal function after ballistic retinal injury assessed by ERG a-wave amplitude.

9.1.3.Aim

To test the neuroprotective efficacy of progesterone after ballistic retinal injury using structural and functional outcome measures.

9.1.4.Materials and Methods

9.1.4.1. Dosage calculations

Progesterone was administered in ethyl oleate vehicle, as an 8mg/kg IP loading dose immediately after injury and then by continuous subcutaneous infusion of 100µg/h/kg from a primed osmotic minipump (Charles River) for the duration of the study. Using data from Gangrade et al. (1992) this would be expected to give a steady state plasma concentration of 36.4ng/ml (infusion rate = steady state concentration x clearance; clearance = 2.75l/kg/hr) or 263ng/ml using data from Petroff et al. (2003; clearance = 0.38l/kg/hr).

9.1.4.2. Experimental Protocol

The right eyes of 16 anaesthetised male Lister-hooded rats (170-200g) was injured by ballistic trauma (as described in Section 6.6.7.). Eight rats were treated with progesterone as above and 8 with ethyl oleate vehicle. Scotopic ERG only were recorded under inhalational anaesthesia at stimulus intensities ranging from -2.5 to +1 log units with respect to standard flash at 7 and 14 d after injury, as shown in Table 8.7.4. Animals were killed 14 d after injury and the right eyes processed as described in Section 8.7.4. for measurement of ONL thickness.

9.1.4.3. Enzyme-linked Immunosorbant Assay (ELISA)

Blood samples were taken from the tail vein at 2 hr after progesterone injection and from the jugular vein at the time of perfusion fixation (at 14 d) for measurement of serum progesterone concentration.

Blood was centrifuged for 5 min at 10,000 rpm and the serum removed and frozen to -80°c for storage. Uninjured eyes were removed after perfusion fixation and frozen to -80°c for storage. To extract retinal progesterone, eyes were thawed and the retinae removed, weighed and homogenised in 200µl of methanol, left to stand for 20 min and then centrifuged at 13,000g for 10 min. The supernatent was removed and kept and the pellet resuspended in 200µl methanol and then mixed

by gentle rotation for 30 min before centrifuging at 13,000g for 10 min. The supernatent was removed and combined with the earlier supernatent before being dried in a vacuum centrifuge at 37°c. Two retinae from an uninjured male Wistar rat were used as positive control by being combined then processed in the same way except that 2µl of 2µg/ml progesterone in water was added to the methanol before homogenisation. After drying, the extracted solutes were resuspended in 40µl of dH_2O, which should have given a measured progesterone concentration of 50ng/ml in the positive control.

Serum and retinal progesterone concentration was measured by competitive ELISA according to the manufacturer's instructions. Briefly, 20µl of diluted serum at 1/4 and 1/10 dilutions was loaded into the wells, 200µl of progesterone-HRP conjugate added to each well and the plate incubated for 1 hr at 37°C before adding 100µl of tetramethylbenzidine/H_2O_2 substrate, incubating for 15 min and stopping the reaction by adding 100µl 0.15M sulphuric acid. Absorbance was measured at 450nm. In addition to the standard solutions supplied by the manufacturer, 1 ng/ml, 10ng/ml, 100ng/ml and 1000ng/ml standards were created by serial dilution of progesterone dissolved in DMSO at 10mg/ml.

Processing of tissues and image analysis for measurement of ONL thickness was performed by a BMedSci student, Ellie McCance.

9.1.5.Results

9.1.5.1. Structural Assessment

The effects of treatment with progesterone on ONL thickness were analysed using generalised estimating equations (Appendix 19). The ONL thickness in the injured eyes was significantly reduced in animals treated with progesterone compared to the vehicle-treated control animals (p=0.002; Figure 9.1.1.A-B), an effect that was greater further away from the impact site (p=0.051; Figure 9.1.1.A-B).

Figure 9.1.1. Effect of progesterone treatment on outcomes after ballistic ocular trauma in rat assessed by ONL thickness 14 days after injury (A-B) and ERG a-wave amplitude at 7 and 14 days after injury (C-D).

A

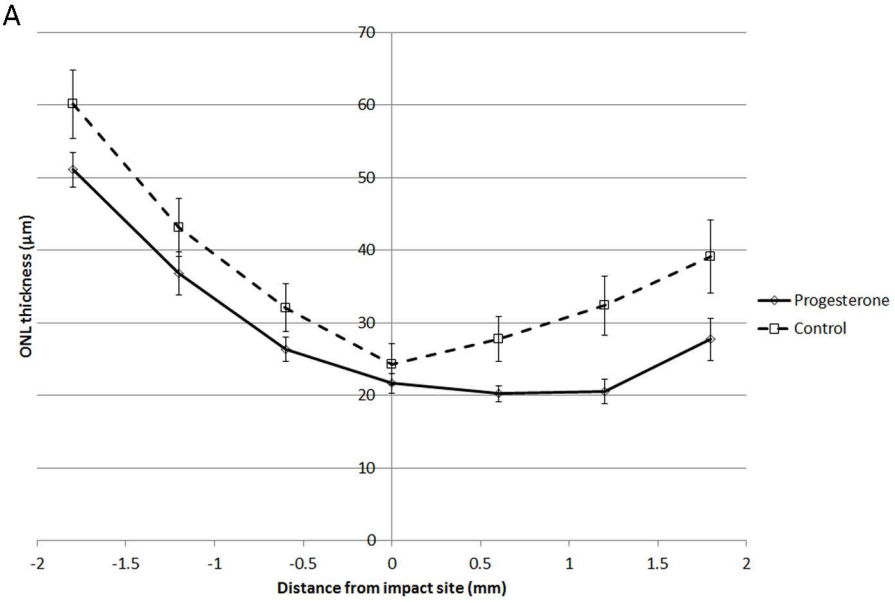

B

Source	Type III		
	Wald Chi-Square	df	Sig.
(Intercept)	7620.857	1	0.000
TreatedProgesteronevsControl	9.838	1	0.002
DistanceImpactSite	256.968	6	0.000
TreatedProgesteronevsControl * DistanceImpactSite	12.526	6	0.051

A-B. ONL thickness in injured eyes is lower at all distances from the impact site ($p<0.001$) in animals treated with progesterone than in controls. The borderline significant 2-way interaction between treatment and distance from the impact site ($p=0.051$) indicates that the negative effect of treatment increases (i.e. the difference in ONL thickness between treated and control animals is greater) with increasing distance from the impact site.

Figure 9.1.2. A. a-wave amplitude in the injured eyes only plotted against stimulus intensity. B. a-wave amplitude in the uninjured eyes only plotted againsts stimulus intensity. C. Test of model effects after analysis of a-wave amplitude using generalised estimating equations to construct a fully factorial model including time after injury (timepointdays), stimulus intensity (flashintensitymcd), treatment with progesterone compared to vehicle (TreatedProgesteronevsControl), injured or uninjured eye (Eye) and terms to model all 2-,3- and 4-way interactions

a-wave amplitude increased with increasing stimulus intensity ($p<0.001$ for flashintensitymcd) and was lower in injured than in uninjured eyes ($p=0.001$ for Eye; data not shown on graph).

On average, treatment with progesterone decreased a-wave amplitude at higher stimulus intensities more than at lower intensities ($p<0.001$ for the 2-way interaction flashintensitymcd * TreatedProgesteronevsControl; see parts A and B), i.e. the lines of the graph are further separated with increasing stimulus intensity. Treatment with progesterone had a different effect at 7 compared to 14 days ($p=0.001$ for the 3-way interaction timepointdays * flashintensitymcd * TreatedProgesteronevsControl, see parts A and B) , increasing a-wave amplitude compared to controls at 7 days, whilst decreasing it at 14 days.

On average, the negative effect of progesterone was greater in uninjured than in injured eyes ($p=0.018$ for the 3-way interaction flashintensitymcd * TreatedProgesteronevsControl * Eye; see part B). i.e. the effect of progesterone on a wave amplitude seen in this Figure was not related to the observed photoreceptor death caused by injury (see Figure 9.1.1.).

A

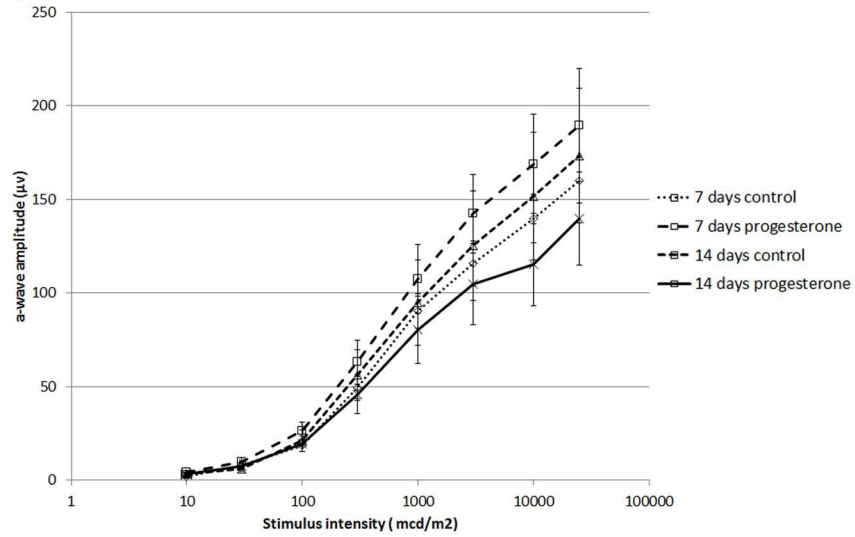

Progesterone reduced a-wave amplitude compared to vehicle treated controls at 14 days and increased it at 7 days in both injured and uninjured eyes, but this difference was greater in the uninjured eyes ($p=0.002$ for the 4 way interaction timepointdays * flashintensitymcd * TreatedProgesteronevsControl * Eye; see part B).

In summary, progestesterone treatment decreased a-wave amplitude in both injured and uninjured eyes, but had the greatest effect on uninjured eyes.

B

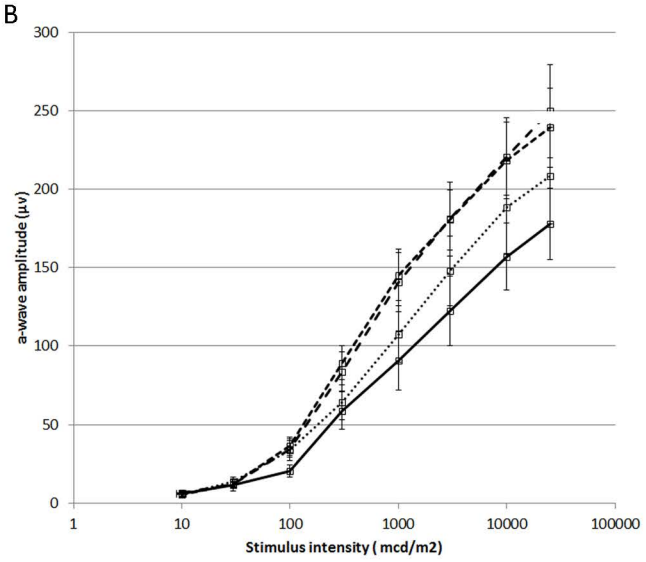

C

Source	Type III		
	Wald Chi-Square	df	Sig.
(Intercept)	8914.011	1	0.000
timepointdays	.517	1	0.472
flashintensitymcd	13543.551	7	0.000
TreatedProgesteronevsControl	.000	1	0.998
Eye	12.032	1	0.001
timepointdays * flashintensitymcd	7.459	7	0.383
timepointdays * TreatedProgesteronevsControl	3.006	1	0.083
timepointdays * Eye	0.006	1	0.936
flashintensitymcd * TreatedProgesteronevsControl	29.230	7	0.000
flashintensitymcd * Eye	25.888	7	0.001
TreatedProgesteronevsControl * Eye	.512	1	0.474
timepointdays * flashintensitymcd * TreatedProgesteronevsControl	24.007	7	0.001
timepointdays * flashintensitymcd * Eye	7.746	7	0.356
timepointdays * TreatedProgesteronevsControl * Eye	0.000	1	0.986
flashintensitymcd * TreatedProgesteronevsControl * Eye	16.844	7	0.018
timepointdays * flashintensitymcd * TreatedProgesteronevsControl * Eye	22.618	7	0.002

9.1.5.2. Functional Assessment

ERG data are presented in Figures 9.1.2. The effects of treatment with progesterone on the ERG were analysed using generalised estimating equations (Appendix 19). Combining data from both 7 and 14 d, progesterone reduced a-wave amplitude compared to vehicle-treated controls ($p<0.001$ for flashintensitymcd * TreatedProgesteronevsControl). However, progesterone increased a-wave amplitude at 7 d, whilst reducing it at 14 d after injury ($p=0.001$ for timepointdays * flashintensitymcd * TreatedProgesteronevsControl). These changes in a-wave amplitude caused by progesterone were greater in the uninjured left eyes than the injured right eyes (Figure 9.1.2.).

9.1.5.3. Serum ELISA

The serum progesterone concentration at 14 d in the progesterone-treated group was 6.04ng/ml. This result allowed clearance to be calculated: infusion rate = steady state concentration x clearance, infusion rate = 100µg/kg/hr, so clearance = 16.667l/kg/hr, assuming that steady state had been reached, i.e. half-life was <2.8 d, as time taken to reach steady state is 5 half-lives. The serum progesterone in control animals was 2.1ng/ml.

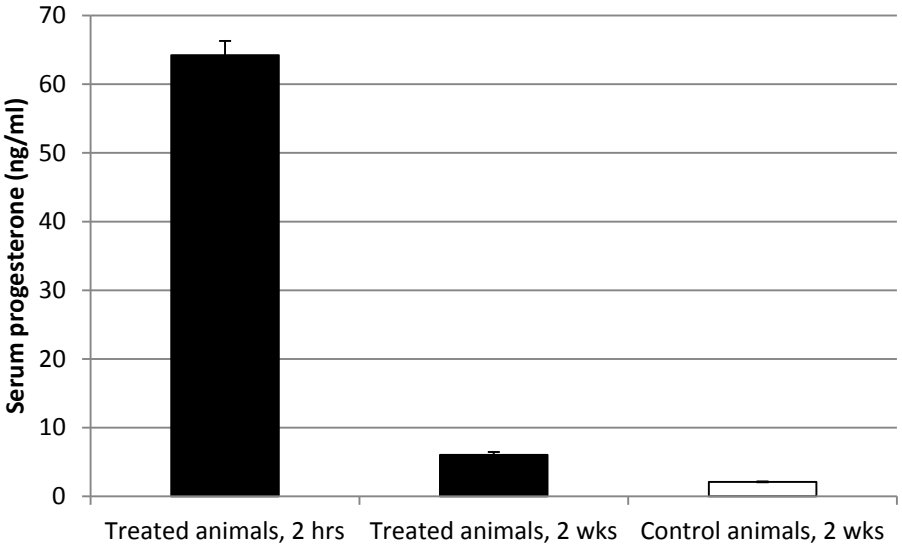

Figure 9.1.4. Mean serum progesterone concentrations after ballistic injury ± standard error of the mean.

9.1.5.4. Retinal ELISA

No progesterone was detected in either the treated or untreated retinae. Progesterone at an average of 42.6ng/ml was detected in the positive control samples, giving an efficiency of recovery of 85.2%.

9.1.6.Discussion

Treatment with progesterone increased photoreceptor death after ballistic injury and depressed a-wave amplitude in both the injured and uninjured eyes. However, the serum progesterone levels at 14 d after injury were significantly lower than the intended 50-100ng/ml. There are 2 possible explanations for this observation of unexpectedly low circulating progesterone: (1), the clearance of progesterone from the rat plasma was much higher than has previously been reported or, (2), the osmotic minipumps did not deliver progesterone at the intended rate of 5µl/hr (or at all).

Methanol extraction failed to detect any progesterone in any of the retinal tissue samples, which could be because retinal levels were very low, or because extraction failed. The lower limit of sensitivity of the ELISA assay is 0.2ng/ml, which would be expected to detect retinal levels 5x lower than serum levels in control animals (20µg retinal weight resuspended in 40µl dH_2O compared to 2.1ng/ml in control animals) and 15x lower than serum levels in progesterone-treated animals, suggesting that extraction failed. The positive control showed that supplementing the retina with aqueous progesterone allowed good recovery of added progesterone, indicating that extraction did not fail because of either adherence to the tubes used for drying or because of trapping in precipitated lipid. Though methanol extraction of faecal progesterone has been previously reported (Korndorfer, Meirelles, Bueno, and Abdalla 1998), it is likely that retinal extraction failed because methanol (a polar solute) failed to solubilise progesterone from the retinal lipid components. It is concluded that any future attempt should use ether extraction, which is more commonly reported but also more hazardous due to the risk of ether combustion.

To aid interpretation of the results, it was decided that the pharmacokinetics of progesterone in 200g male Lister-hooded rats was required.

9.2. Pharmacokinetic Study of Progesterone

9.2.1.Rationale

It was unclear whether the lower-than-intended 14 d serum progesterone data presented in Section 9.1. occurred because the clearance of progesterone in the rat was higher than previously reported or because the osmotic minipumps did not function correctly, so a study was designed to measure the pharmacokinetics of progesterone in the rat.

9.2.2.Hypothesis

The clearance of progesterone in approx. 200g male Lister-hooded rats is 16.6l/kg/hr.

9.2.3.Aim

To determine the pharmacokinetics of progesterone in 200g male Lister-hooded rats.

9.2.4.Methods

Three 215-200g male Lister-hooded rats were given IP injections of 8mg/kg progesterone in ethyl oleate vehicle. Blood samples were taken from the tail veins at 2, 6, 24 and 72 hr after injection, centrifuged for 5 min at 10,000 rpm and the serum removed and frozen to -80°C for storage. Serum progesterone concentration was measured by competitive ELISA according to the manufacturer's instructions (see Section 9.1.4.3.).

9.2.5.ELISA Results

The serum progesterone measured 2 hr after injection was 67.1ng/ml and at 6 hr it was 25.9ng/ml. The half-life derived from these measurements is 2.91 hr. Working the levels back from a 2 hr level of 67.1ng/ml gives an initial serum progesterone concentration of 108ng/ml. Initial concentration =

dose/volume of distribution and, with a dose of 8mg/kg, the volume of distribution = 74.1l/kg. The elimination rate constant, k_e = ln2/half life = 0.238/hr and clearance = volume of distribution x k_e, so clearance = 17.6l/kg/hr.

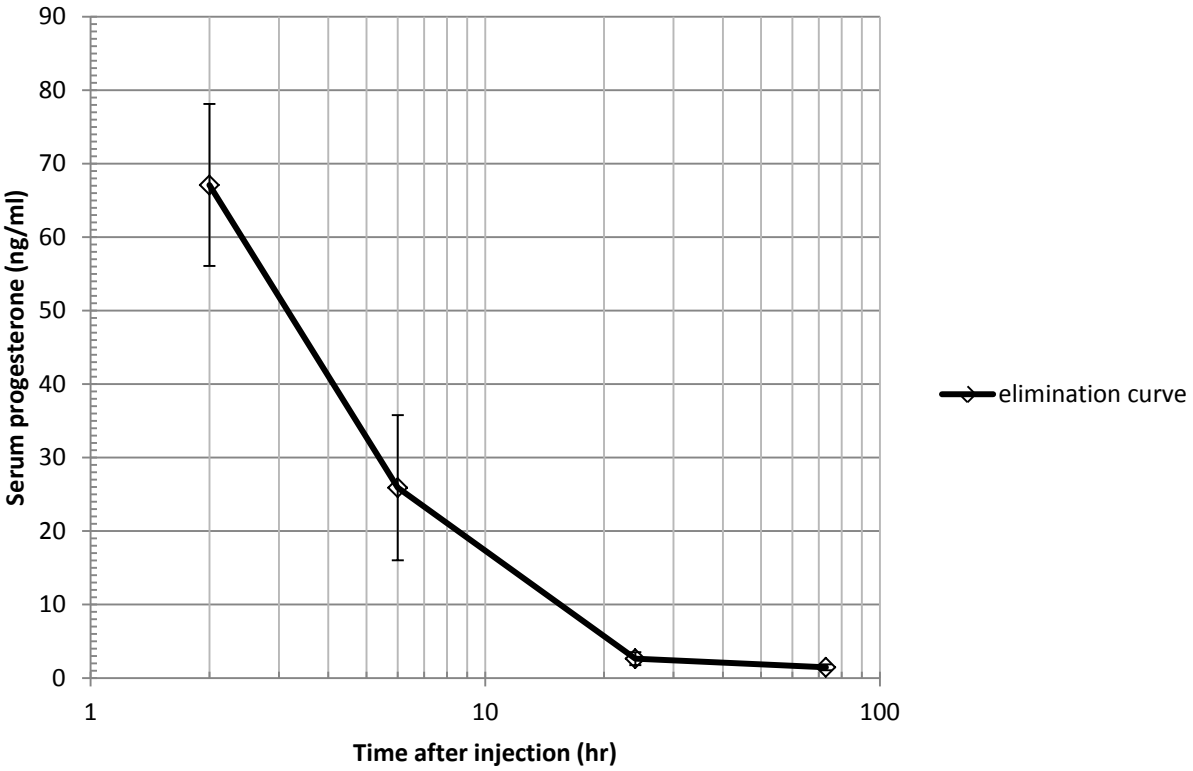

Figure 9.2. Serum progesterone against time after IP injection ± SEM.

9.2.6.Discussion

The calculated half-life of progesterone in the current experiment was 2.91 hr and the calculated clearance was 17.6l/kg/hr, which is similar to the figure of 16.667l calculated from the ELISA data obtained in samples from animals with osmotic minipumps implanted (Section 9.1.5.3.), indicating that the osmotic minipumps delivered the intended dose.

9.2.7.Conclusions

I. The clearance of progesterone in approx. 200g male Lister-hooded rats is 17l/kg/hr.

II. The osmotic minipumps used in Section 9.1. functioned correctly and delivered the intended dose of progesterone.

9.3. General Discussion

9.3.1.Pharmacokinetics

In this experiment, after a single bolus IP injection, progesterone was delivered by continuous subcutaneous infusion. The dose for the bolus injection was derived from previous studies in which 8mg/kg bolus doses were used successfully to treat traumatic brain injury (Goss, Hoffman, and Stein 2003). The rate of progesterone infusion of 100µg/kg/hr was derived from data suggesting that, in rats, the half-life of progesterone is 0.6-10.5 hr and the volume of distribution is 2.75-5.62l (Gangrade, Boudinot, and Price 1992), (Petroff and Mizinga 2003), which would have caused plasma levels of 36.4-236ng/ml. The half-life in the current study was 2.91 hr (in the range previously reported); however, the volume of distribution was 74l/kg, which is considerably higher than has been reported in rats and mice (Gangrade, Boudinot, and Price 1992), (Petroff and Mizinga 2003), (Wong, Ray, and Kendall 2012).

On data from the current study (clearance = 17l/kg/hr), an infusion rate of 850µg/kg/hr or 20.4mg/kg/d would be required to maintain plasma progesterone at 50ng/ml, which is significantly higher than has been administered in most studies of the neuroprotective effects of progesterone (which administer intermittent doses of 4-16mg/kg/d after the initial bolus) (Goss, Hoffman, and Stein 2003). Were the commonly used intermittent dosing regimen of 0, 6, 24, 48. 72, 96 and 120 hr after injury administered to 200g Lister-hooded rats, plasma progesterone levels would be at baseline from 18-24, 36-48, 59-72, 73-96 and 107-120 hr after injury (Goss, Hoffman, and Stein 2003). Male Sprague-Dawley rats weighing approx. 300g are commonly used for traumatic brain injury studies and – though we do not have data on their pharmacokinetics – it seems unlikely that Sprague-Dawley rats would have radically different pharmacokinetics than the Lister-hooded rats used in the current studies.

Three days of daily dosing progesterone after traumatic brain injury is less effective than 5 at improving functional outcomes and reducing lesion size, suggesting that intermittent therapeutic serum levels of progesterone do not preclude a therapeutic effect (Shear, Galani, Hoffman, and Stein 2002). Cutler et al. (2005) found that tapering progesterone dosing over 2 d reduced levels of inflammatory markers, apoptotic markers and behavioural tests for anxiety compared to an abrupt withdrawal after a daily dosing regimen continued for the same length of time, thus either, (1), the beneficial effects of progesterone in the brain do not directly relate to its persistence in the plasma which would contradict the mouse data of Wong et al. (2012) that brain progesterone levels drop below plasma levels approx. 2hr post-dosing, or (2), in the tapered dose group the beneficial effect was seen because levels became sub-therapeutic after 5 d whereas in the abrupt withdrawal group, therapeutic levels continued for 7 d and this prolonged dosing was damaging (Cutler, Pettus, Hoffman, and Stein 2005).

9.3.2. The Effect of Progesterone on Functional and Structural Outcomes After Ballistic Ocular Trauma

9.3.2.1. Structural effects

Progesterone treatment significantly reduced ONL thickness after injury compared to vehicle-treated controls, an apparently detrimental effect. As 98% of rat photoreceptors are rods and the ONL contains photoreceptor somata only, ONL thickness reflects rod survival (Blanch et al. 2012b). After traumatic brain injury, progesterone treatment reduces oedema and lesion size (Stein 2008b). It is possible that a reduction in ONL thickness could occur because of reduced oedema; however, (1), the ONL thickness measurement assessed only haematoxylin-stained nuclei, thus excluding any oedema and, (2), the ONL is not oedematous 14 d after ballistic injury (Blanch et al. 2012a). Thus, it is likely that the reduction in ONL thickness occurred because treatment with progesterone increased the number of photoreceptors that died after ballistic injury.

With a half-life of 2.9 hr, serum progesterone levels would have peaked at near to 100ng/ml and reached steady-state at 6ng/ml 11.6-14.5 hr after injury, which could be considered an abrupt withdrawal of treatment. After traumatic brain injury, abrupt withdrawal of progesterone treatment increases the expression of cell death markers and worsens outcome compared to tapered withdrawal; however, both treatment regimens are still beneficial compared to placebo (Cutler, Pettus, Hoffman, and Stein 2005), (Stein 2008b). Thus, abrupt withdrawal is unlikely to explain the increase in cell death observed in the current study.

Too short a duration of therapeutic plasma levels might explain the observed increase in photoreceptor death. A mechanism for increased cell death could be that brief inhibition of programmed cell death pathways causes cells to undergo less regulated and more inflammatory necrotic cell death, with bystander damage to healthy cells.

Another possibility is that progesterone treatment increased the animals' core temperature (Forman, Chapman, and Steptoe 1987), increasing the metabolic demands of photoreceptors, a cell type with a high requirement for energy and oxygen that lack a functional reserve in terms of excess oxygen supply under normal conditions (Linsenmeier and Padnick-Silver 2000).

9.3.2.2. Functional effects

The a-wave is the first negative deflection on ERG after a light stimulus and is commonly used to assess photoreceptor function. Progesterone treatment significantly reduced ERG a-wave amplitude in both injured and uninjured eyes. An effect of sex steroids on the ERG has been previously reported (Brule et al. 2007); however, an effect of progesterone on the ERG in the uninjured eye makes it difficult to assess the functional effects of treatment with respect to injury. Considering data from both eyes, progesterone reduced a-wave amplitude differently in the injured and uninjured eyes, but the reduction was greater in the uninjured eyes. An interaction between progesterone treatment and injury is possible, for example injury could cause paracrine changes that prime the retina to decrease a-wave amplitude less in response to progesterone treatment than

uninjured retina. It is also possible that changes in core temperature could have caused that observed ERG effects of progesterone, as ERG amplitude is dependent on temperature (Heckenlively and Arden 2006) and temperature, though controlled, was not specifically measured during the experiments.

The current studies of the neuroprotective effects of progesterone used a non-standard dosing regimen and found treatment to be detrimental to retinal structure and function. Repeating the study using a previously reported intermittent regimen would clarify whether the detrimental effect is specific to the current dosing regimen (Stein 2008b). However, a significant detrimental effect after administration of low dose treatment is not encouraging with respect to the translational potential of progesterone in ocular injury and is consistent with past studies that did not find that progesterone reduced photoreceptor death (Doonan, O'Driscoll, Kenna, and Cotter 2011), (Kaldi and Berta 2004) (O'Steen 1977).

9.4. Conclusions

I. Progesterone clearance in 200g male Lister-hooded rats is 17l/kg/hr and the half-life is 2.91 hr.

II. Progesterone treatment administered as a high dose bolus followed by a low-dose infusion to maintain serum levels 3x baseline increased rod death and reduced rod function 14 d after injury.

III. Progesterone is not a translatable treatment for ballistic ocular injury, due to the potential for a detrimental effect with low dose treatment.

10.Summary

Commotio retinae is a closed globe retinal injury caused by blunt ocular trauma characterised by retinal whitening and loss of vision when the macula is affected.

In retrospective clinical studies, commotio retinae affected 16% of British soldiers with an eye injury and 0.4% of civilians with an eye injury (Jones et al. 1986). Macular commotio retinae constituted 31% of civilian cases 55-73% of military cases (Weichel et al. 2008) and was associated with reduced visual acuity. In 26% of patients vision remained ≤6/9, though the proportion with some visual impairment was higher because: (1), a deterioration from 6/4 to 6/9 would be significant to many patients and; (2), paracentral visual field defects may not affect VA. Commotio retinae is predominantly an injury to photoreceptors and permanent visual impairment was associated with photoreceptor degeneration.

In order to investigate the mechanisms of photoreceptor degeneration after commotio retinae, an experimental model was developed. In rats, high velocity ocular impact by a light weight induced commotio retinae more readily than low velocity impact by a relatively heavy weight despite lower delivered kinetic energy.

In an experimental rat model of commotio retinae induced by ballistic ocular injury, photoreceptors died by a combination of necrosis and apoptosis. Visual function, assessed by ERG a-wave amplitude, was reduced out of proportion to the extent of photoreceptor death. Apoptosis was mediated by active caspase 9 present in photoreceptors 5 hr after injury and inhibiting caspase 9 by intravitreal injection of Pen1-XBIR3 reduced photoreceptor death and improved retinal function.

Of the 3 executioner caspases (3, 6 and 7), only caspase 6's activity was increased in the retina after commotio retinae. Despite immunolocalisation of active caspase 6 in photoreceptors 48 hr after injury, caspase 6 inhibition by intravitreal injection of Pen1-C6DN did not prevent photoreceptor death and was detrimental to retinal function, suggesting that caspase 6 does not mediate apoptosis in this model.

Because clinical studies suggested a possible protective effect of female gender in commotio retinae, progesterone was assessed in the rat ballistic injury model as a potential neuroprotective treatment. However, progesterone treatment significantly increased photoreceptor death. This surprising result may be explained by the observation that the clearance of progesterone from the rat plasma was significantly higher than previous reports (Gangrade, Boudinot, and Price 1992), which meant that plasma levels after treatment were lower than intended. Nonetheless, increased cell death after progesterone administration (whether subtherapeutic dosing or not) is discouraging with respect to the potential for progesterone to be a translatable treatment for ocular injury.

References

Abbotts, R., S. E. Harrison, and G. L. Cooper. 2007. "Primary blast injuries to the eye: a review of the evidence." *J R Army Med Corps* 153:119-123.

Agrawal, R. N., S. He, C. Spee, J. Z. Cui, S. J. Ryan, and D. R. Hinton. 2007. "In vivo models of proliferative vitreoretinopathy." *Nat Protoc* 2:67-77.

Agudo, M., M. C. Perez-Marin, U. Lonngren, P. Sobrado, A. Conesa, I. Canovas, M. Salinas-Navarro, J. Miralles-Imperial, F. Hallbook, and M. Vidal-Sanz. 2008. "Time course profiling of the retinal transcriptome after optic nerve transection and optic nerve crush." *Mol Vis* 14:1050-1063.

Ahmed, Z., H. Kalinski, M. Berry, M. Almasieh, H. Ashush, N. Slager, A. Brafman, I. Spivak, N. Prasad, I. Mett, E. Shalom, E. Alpert, A. Di Polo, E. Feinstein, and A. Logan. 2011. "Ocular Neuroprotection by siRNA Targeting Caspase-2." *Cell Death Dis* 2:e173.

Ahmed, Z., M. Aslam, B. Lorber, E. L. Suggate, M. Berry, and A. Logan. 2010. "Optic nerve and vitreal inflammation are both RGC neuroprotective but only the latter is RGC axogenic." *Neurobiol Dis* 37:441-454.

Akpan, N., E. Serrano-Saiz, B. E. Zacharia, M. L. Otten, A. F. Ducruet, S. J. Snipas, W. Liu, J. Velloza, G. Cohen, S. A. Sosunov, 2. nd. Frey WH, G. S. Salvesen, E. S. Connolly, Jr., and C. M. Troy. 2011. "Intranasal delivery of caspase-9 inhibitor reduces caspase-6-dependent axon/neuron loss and improves neurological function after stroke." *J Neurosci* 31:8894-904 LID - 10.1523/JN.

Alamouti, B. and J. Funk. 2003. "Retinal thickness decreases with age: an OCT study." *Br J Ophthalmol* 87:899-901.

Al-Hussaini, H., J. H. Kam, A. Vugler, M. Semo, and G. Jeffery. 2008. "Mature retinal pigment epithelium cells are retained in the cell cycle and proliferate in vivo." *Mol Vis* 14:1784-1791.

An, M. X., X. F. Zhang, and J. S. Zhang. 2004. "(Oxidative damage and photoreceptor cell apoptosis in contusion injury of the rabbit retina) (Chinese)." *Zhonghua yan ke za zhi (Chin J Ophthalmol)* 40:118.

Antelava, J. N. 1969. "Morpho-histological evidence of the clinical picture of the retina in eye contusion." *Ophthalmologica* 158 Suppl:329-331.

Applebury, M. L., M. P. Antoch, L. C. Baxter, L. L. Chun, J. D. Falk, F. Farhangfar, K. Kage, M. G. Krzystolik, L. A. Lyass, and J. T. Robbins. 2000. "The murine cone photoreceptor: a single cone type expresses both S and M opsins with retinal spatial patterning." *Neuron* 27:513-523.

Arnold, J.L., P. Halpern, M.C. Tsai, and H. Smithline. 2004. "Mass casualty terrorist bombings: a comparison of outcomes by bombing type." *Ann Emerg Med* 43:263-273.

Arnoult, D., B. Gaume, M. Karbowski, J. C. Sharpe, F. Cecconi, and R. J. Youle. 2003. "Mitochondrial release of AIF and EndoG requires caspase activation downstream of Bax/Bak-mediated permeabilization." *EMBO J* 22:4385-4399.

Attella, M. J., A. Nattinville, and D. G. Stein. 1987. "Hormonal state affects recovery from frontal cortex lesions in adult female rats." *Behav Neural Biol* 48:352-367.

Bayir, H., D. W. Marion, A. M. Puccio, S. R. Wisniewski, K. L. Janesko, R. S. Clark, and P. M. Kochanek. 2004. "Marked gender effect on lipid peroxidation after severe traumatic brain injury in adult patients." *J Neurotrauma* 21:1-8.

Becker, C. G. and T. Becker. 2008. "Adult zebrafish as a model for successful central nervous system regeneration." *Restor Neurol Neurosci* 26:71-80.

Beiran, I. and B. Miller. 1992. "Pure ocular blast injury." *Am J Ophthalmol* 114:504-505.

Belkin, M. 1983. "Ocular injuries in the Yom Kippur war." *J Ocul Ther Surg* 2:40-49.

Bellows, J. G. 1947. "Observations on 300 consecutive cases of ocular war injuries." *Am J Ophthalmol* 30:309-323.

Benowitz, L. I. and Y. Yin. 2010. "Optic nerve regeneration." *Arch Ophthalmol* 128:1059-1064.

Berkelaar, M., D. B. Clarke, Y. C. Wang, G. M. Bray, and A. J. Aguayo. 1994. "Axotomy results in delayed death and apoptosis of retinal ganglion cells in adult rats." *J Neurosci* 14:4368-4374.

Berlin, R. 1873. "Zur sogenannten commotio retinae." *Klin Monatsbl Augenheilkd* 1:42-78.

Bernal, A., J. M. Parel, and F. Manns. 2006. "Evidence for posterior zonular fiber attachment on the anterior hyaloid membrane." *Invest Ophthalmol Vis Sci* 47:4708-4713.

Bernardos, R. L., L. K. Barthel, J. R. Meyers, and P. A. Raymond. 2007. "Late-stage neuronal progenitors in the retina are radial Muller glia that function as retinal stem cells." *J Neurosci* 27:7028-7040.

Berry, M., J. Carlile, A. Hunter, W. Tsang, P. Rosenstiel, and J. Sievers. 1999. "Optic nerve regeneration after intravitreal peripheral nerve implants: trajectories of axons regrowing through the optic chiasm into the optic tracts." *J Neurocytol* 28:721-741.

Berry, M., J. Carlile, and A. Hunter. 1996. "Peripheral nerve explants grafted into the vitreous body of the eye promote the regeneration of retinal ganglion cell axons severed in the optic nerve." *J Neurocytol* 25:147-170.

Berry, M., Z. Ahmed, B. Lorber, M. Douglas, and A. Logan. 2008. "Regeneration of axons in the visual system." *Restor Neurol Neurosci* 26:147-174.

Besirli, C. G., N. D. Chinskey, Q. D. Zheng, and D. N. Zacks. 2010. "Inhibition of retinal detachment-induced apoptosis in photoreceptors by a small peptide inhibitor of the fas receptor." *Invest Ophthalmol Vis Sci* 51:2177-2184.

Bhutto, I. A. and T. Amemiya. 1995. "Corrosion cast demonstration of retinal vasculature of normal Wistar-Kyoto rats." *Acta Anat (Basel)* 153:290-300.

Bignami, A. and D. Dahl. 1979. "The radial glia of Muller in the rat retina and their response to injury. An immunofluorescence study with antibodies to the glial fibrillary acidic (GFA) protein." *Exp Eye Res* 28:63-69.

Blanch, R. J., M.S. Bindra, A.S. Jacks, and R.A.H. Scott. 2011. "Ophthalmic Injuries in British Armed Forces in Iraq and Afghanistan." *Eye* 25:218-223.

Blanch, R. J., P. A. Good, P. Shah, J. R. B. Bishop, A. Logan, and R. A. H. Scott. 2013. "Visual outcomes after blunt ocular trauma." *Ophthalmol* 120:1588-1591.

Blanch, R. J., Z. Ahmed, A. Sik, D. R. Snead, P. A. Good, J. O'Neill, M. Berry, R. A. Scott, and A. Logan. 2012a. "Neuroretinal cell death in a murine model of closed globe injury; pathological and functional characterisation." *Invest Ophthalmol Vis Sci* 53:7220-7226.

Blanch, R. J., Z. Ahmed, M. Berry, R. A. H. Scott, and A. Logan. 2012b. "Animal Models of Retinal Injury." *Invest Ophthalmol Vis Sci* 53:2913-2920.

Blanch, R. J. and R. A. Scott. 2008. "Primary blast injury of the eye." *J R Army Med Corps* 154:76.

Blanch, R. J. and R.A.H. Scott. 2010. "Military Ocular Injury: Presentation, Assessment and Management." *J R Army Med Corps* 155:279-284.

Blight, R. and J. C. Hart. 1977. "Structural changes in the outer retinal layers following blunt mechanical non-perforating trauma to the globe: an experimental study." *Br J Ophthalmol* 61:573.

—1978. "Histological changes in the internal retinal layers produced by concussive injuries to the globe. An experimental study." *Trans Ophthalmol Soc UK* 98:270-277.

Borutaite, V. 2010. "Mitochondria as decision-makers in cell death." *Environ Mol Mutagen* 51:406-16 LID - 10.1002/em..

Bozzola, J.J. and L.D. Russell. 1999. *Electron Microscopy*: Jones and Barlett Publishers, Inc.

Brule, J., M. P. Lavoie, C. Casanova, P. Lachapelle, and M. Hebert. 2007. "Evidence of a possible impact of the menstrual cycle on the reproducibility of scotopic ERGs in women." *Doc Ophthalmol* 114:125-134.

Bunt-Milam, A. H., R. A. Black, and R. E. Bensinger. 1986. "Breakdown of the outer blood-retinal barrier in experimental commotio retinae." *Exp Eye Res* 43:397-412.

Burgi, H., T. H. Schaffner, and J. P. Seiler. 2001. "The toxicology of iodate: a review of the literature." *Thyroid* 11:449-456.

Burnham, G., R. Lafta, F. Doocy, and L. Roberts. 2006. "Mortality after the 2003 invasion of Iraq: a cross-sectional cluster sample survey." *Lancet* 368:1421-1428.

Campbell, D. R. 1941. "Ophthalmic Casualties resulting from Air Raids." *Br Med J* 1:966.

Carley, S. D. and K. Mackway-Jones. 1997. "The casualty profile from the Manchester bombing 1996: a proposal for the construction and dissemination of casualty profiles from major incidents." *J Accid Emerg Med* 14:76-80.

Carmody, R. J. and T. G. Cotter. 2000. "Oxidative stress induces caspase-independent retinal apoptosis in vitro." *Cell Death Differ* 7:282-291.

Chakravarthy, U., C. J. Maguire, and D. B. Archer. 1986. "Experimental posterior perforating ocular injury: a controlled study of the gross effects of localised gamma irradiation." *Br J Ophthalmol* 70:561-569.

Chakravarthy, U., J. H. Biggart, T. A. Gardiner, D. B. Archer, and C. J. Maguire. 1989. "Focal irradiation of perforating eye injuries." *Curr Eye Res* 8:1241-1250.

Chalioulias, K., K. T. Sim, and R. Scott. 2007. "Retinal sequelae of primary ocular blast injuries." *J R Army Med Corps* 153:124-125.

Chaum, E. 2003. "Retinal neuroprotection by growth factors: a mechanistic perspective." *J Cell Biochem* 88:57-75.

Chen, S., Z. Huang, L. Wang, T. Jiang, B. Wu, and G. Sun. 2003. "Study on retinal ganglion cell apoptosis after explosive injury of eyeballs in rabbits." *Yan Ke Xue Bao (Eye Science)* 19:187.

Cheng, L., P. Sapieha, P. Kittlerova, W. W. Hauswirth, and A. Di Polo. 2002. "TrkB gene transfer protects retinal ganglion cells from axotomy-induced death in vivo." *J Neurosci* 22:3977-3986.

Ciriza, I., P. Carrero, C. A. Frye, and L. M. Garcia-Segura. 2006. "Reduced metabolites mediate neuroprotective effects of progesterone in the adult rat hippocampus. The synthetic progestin medroxyprogesterone acetate (Provera) is not neuroprotective." *J Neurobiol* 66:916-928.

Cleary, P. E., G. Jarus, and S. J. Ryan. 1980. "Experimental posterior penetrating eye injury in the rhesus monkey: vitreous-lens admixture." *Br J Ophthalmol* 64:801-808.

Cleary, P. E. and S. J. Ryan. 1979. "Experimental posterior penetrating eye injury in the rabbit. I. Method of production and natural history." *Br J Ophthalmol* 63:306-311.

—1981. "Vitrectomy in penetrating eye injury: results of a controlled trial of vitrectomy in an experimental posterior penetrating eye injury in the rhesus monkey." *Arch Ophthalmol* 99:287-292.

Close, J. L., B. Gumuscu, and T. A. Reh. 2005. "Retinal neurons regulate proliferation of postnatal progenitors and Muller glia in the rat retina via TGF beta signaling." *Development* 132:3015-3026.

Colyer, M. H., D. W. Chun, K. S. Bower, J. S.B. Dick, and E. D. Weichel. 2008. "Perforating Globe Injuries during Operation Iraqi Freedom." *Ophthalmol* 115:2087-2093.

Courtney, M. and B. Edwards. 2006. "Measuring Bullet Velocity with a PC Soundcard." *Arxiv preprint physics/0601102* 2011.

Cox, M. S. 1980. "Retinal breaks caused by blunt nonperforating trauma at the point of impact." *Trans Am Ophthalmol Soc* 78:414-466.

Cui, Q., Y. Yin, and L. I. Benowitz. 2009. "The role of macrophages in optic nerve regeneration." *Neurosci* 158:1039-1048.

Cullinane, A. B., P. O'Callaghan, K. McDermott, C. Keohane, and P. E. Cleary. 2002. "Effects of autologous platelet concentrate and serum on retinal wound healing in an animal model." *Graefes Arch Clin Exp Ophthalmol* 240:35-41.

Cullis, I. G. 2001. "Blast waves and how they interact with structures." *J R Army Med Corps* 147:16-26.

Cuthbertson, R. A. and T. E. Mandel. 1986. "Anatomy of the mouse retina. Endothelial cell-pericyte ratio and capillary distribution." *Invest Ophthalmol Vis Sci* 27:1659-1664.

Cutler, S. M., E. H. Pettus, S. W. Hoffman, and D. G. Stein. 2005. "Tapered progesterone withdrawal enhances behavioral and molecular recovery after traumatic brain injury." *Exp Neurol* 195:423-429.

Das, A. V., K. B. Mallya, X. Zhao, F. Ahmad, S. Bhattacharya, W. B. Thoreson, G. V. Hegde, and I. Ahmad. 2006. "Neural stem cell properties of Muller glia in the mammalian retina: regulation by Notch and Wnt signaling." *Dev Biol* 299:283-302.

De Monasterio, F. M. 1978. "Spectral interactions in horizontal and ganglion cells of the isolated and arterially-perfused rabbit retina." *Brain Res* 150:239-258.

Dean Hart, J. C. and R. Blight. 1978. "Changes occuring in the nerve fibre layer of pigs' retinae following concussive injuries to the globe." *Bull Soc Ophtalmol Fr* 78:69-70.

Del Priore, L. V., H. J. Kaplan, R. Hornbeck, Z. Jones, and M. Swinn. 1996. "Retinal pigment epithelial debridement as a model for the pathogenesis and treatment of macular degeneration." *Am J Ophthalmol* 122:629-643.

Del Priore, L. V., R. Hornbeck, H. J. Kaplan, Z. Jones, T. L. Valentino, J. Mosinger-Ogilvie, and M. Swinn. 1995. "Debridement of the pig retinal pigment epithelium in vivo." *Arch Ophthalmol* 113:939-944.

Delori, F., O. Pomerantzeff, and M. S. Cox. 1969. "Deformation of the globe under high-speed impact: it relation to contusion injuries." *Invest Ophthalmol* 8:290-301.

Denault, J. B. and G. S. Salvesen. 2003. "Expression, purification, and characterization of caspases." *Curr Protoc Protein Sci* Chapter 21:Unit 21.13 LID-10.1002/0471140864.p.

DePalma, R. G., D. G. Burris, H. R. Champion, and M. J. Hodgson. 2005. "Blast injuries." *New Eng J Med* 352:1335.

Djebaili, M., Q. Guo, E. H. Pettus, S. W. Hoffman, and D. G. Stein. 2005. "The neurosteroids progesterone and allopregnanolone reduce cell death, gliosis, and functional deficits after traumatic brain injury in rats." *J Neurotrauma* 22:106-118.

Djebaili, M., S. W. Hoffman, and D. G. Stein. 2004. "Allopregnanolone and progesterone decrease cell death and cognitive deficits after a contusion of the rat pre-frontal cortex." *Neuroscience* 123:349-359.

Donovan, M., R. J. Carmody, and T. G. Cotter. 2001. "Light-induced photoreceptor apoptosis in vivo requires neuronal nitric-oxide synthase and guanylate cyclase activity and is caspase-3-independent." *J Biol Chem* 276:23000-23008.

Doonan, F., C. O'Driscoll, P. Kenna, and T. G. Cotter. 2011. "Enhancing survival of photoreceptor cells in vivo using the synthetic progestin Norgestrel." *J Neurochem* 118:915-27 LID - 10.1111/j.1.

Doonan, F., M. Donovan, and T. G. Cotter. 2003. "Caspase-independent photoreceptor apoptosis in mouse models of retinal degeneration." *J Neurosci* 23:5723-5731.

Drew, P. D. and J. A. Chavis. 2000. "Female sex steroids: effects upon microglial cell activation." *J Neuroimmunol* 111:77-85.

Dyer, M. A., R. Martins, F. ilho M. da Silva, J. A. Muniz, L. C. Silveira, C. L. Cepko, and B. L. Finlay. 2009. "Developmental sources of conservation and variation in the evolution of the primate eye." *Proc Natl Acad Sci U S A* 106:8963-8968.

Eagling, E. M. 1974. "Ocular damage after blunt trauma to the eye. Its relationship to the nature of the injury." *Br J Ophthalmol* 58:126-140.

Eckelman, B. P., G. S. Salvesen, and F. L. Scott. 2006. "Human inhibitor of apoptosis proteins: why XIAP is the black sheep of the family." *EMBO Rep* 7:988-994.

Elkington, A. R., H. J. Frank, and M. J. Greaney. 1999. *Clinical Optics*. Oxford, UK: Blackwell Science Ltd.

Elmore, S. 2007. "Apoptosis: a review of programmed cell death." *Toxicol Pathol* 35:495-516.

Faktorovich, E. G., R. H. Steinberg, D. Yasumura, M. T. Matthes, and M. M. LaVail. 1992. "Basic fibroblast growth factor and local injury protect photoreceptors from light damage in the rat." *J Neurosci* 12:3554-3567.

Famiglietti, E. V. and S. J. Sharpe. 1995. "Regional topography of rod and immunocytochemically characterized "blue" and "green" cone photoreceptors in rabbit retina." *Vis Neurosci* 12:1151-1175.

Farace, E. and W. M. Alves. 2000. "Do women fare worse: a metaanalysis of gender differences in traumatic brain injury outcome." *J Neurosurg* 93:539-545.

Fatehee, N., P. K. Yu, W. H. Morgan, S. J. Cringle, and D. Y. Yu. 2011. "Correlating morphometric parameters of the porcine optic nerve head in spectral domain optical coherence tomography with histological sections." *Br J Ophthalmol* 95:585-589.

Fischer, A. J. and R. Bongini. 2010. "Turning Muller glia into neural progenitors in the retina." *Mol Neurobiol* 42:199-209.

Fischer, D., M. Pavlidis, and S. Thanos. 2000. "Cataractogenic lens injury prevents traumatic ganglion cell death and promotes axonal regeneration both in vivo and in culture." *Invest Ophthalmol Vis Sci* 41:3943-3954.

Fischer, D., Z. He, and L. I. Benowitz. 2004. "Counteracting the Nogo receptor enhances optic nerve regeneration if retinal ganglion cells are in an active growth state." *J Neurosci* 24:1646-1651.

Fischer, H. 2008. "Iraqi civilian death estimates." Congressional Research Service.

Fisher, S. K., G. P. Lewis, K. A. Linberg, and M. R. Verardo. 2005. "Cellular remodeling in mammalian retina: results from studies of experimental retinal detachment." *Prog Retin Eye Res* 24:395-431.

Fontainhas, A. M. and E. Townes-Anderson. 2011. "RhoA inactivation prevents photoreceptor axon retraction in an in vitro model of acute retinal detachment." *Invest Ophthalmol Vis Sci* 52:579-587.

Forman, R. G., M. C. Chapman, and P. C. Steptoe. 1987. "The effect of endogenous progesterone on basal body temperature in stimulated ovarian cycles." *Hum Reprod* 2:631-634.

Forrester, J. V., A. D. Dick, P. McMenamin, and W. R. Lee. 2003. *The Eye: Basic Sciences in Practice*. Philadelphia, PA, USA: W.B. Saunders.

Galluzzi, L, I. Vitale, J. M. Abrams, . S. Alnemri, E. H. Baehrecke, M. V. Blagosklonny, T. M. Dawson, V. L. Dawson, W. S. El-Deiry, S. Fulda, E. Gottlieb, D. R. Green, M. O. Hengartner, O. Kepp, R. A. Knight, S. Kumar, and S. A. Lipton. 2012. "Molecular definitions of cell death subroutines: recommendations of the Nomenclature Committee on Cell Death 2012." 19:107-120.

Galluzzi, L., K. Blomgren, and G. Kroemer. 2009. "Mitochondrial membrane permeabilization in neuronal injury." *Nat Rev Neurosci* 10:481-94 LID - 10.1038/nrn.

Gallyas, F., G. Zoltay, and W. Dames. 1992. "Formation of "dark" (argyrophilic) neurons of various origin proceeds with a common mechanism of biophysical nature (a novel hypothesis)." *Acta Neuropathol* 83:504-509.

Gallyas, F., M. Hsu, and G. Buzsaki. 1993. "Four modified silver methods for thick sections of formaldehyde-fixed mammalian central nervous tissue: 'dark' neurons, perikarya of all neurons, microglial cells and capillaries." *J Neurosci Methods* 50:159-164.

Gangrade, N. K., F. D. Boudinot, and J. C. Price. 1992. "Pharmacokinetics of progesterone in ovariectomized rats after single dose intravenous administration." *Biopharm Drug Dispos* 13:703-709.

Garcia-Estrada, J., J. A. Del Rio, S. Luquin, E. Soriano, and L. M. Garcia-Segura. 1993. "Gonadal hormones down-regulate reactive gliosis and astrocyte proliferation after a penetrating brain injury." *Brain Res* 628:271-278.

Garcia-Estrada, J., S. Luquin, A. M. Fernandez, and L. M. Garcia-Segura. 1999. "Dehydroepiandrosterone, pregnenolone and sex steroids down-regulate reactive astroglia in the male rat brain after a penetrating brain injury." *Int J Dev Neurosci* 17:145-151.

Garner, J. P., S. Watts, C. Parry, J. Bird, and E. Kirkman. 2009. "Development of a Large Animal Model for Investigating Resuscitation After Blast and Hemorrhage." *World J Surg* 33:2194-2202.

Gerke, C. G., Y. Hao, and F. Wong. 1995. "Topography of rods and cones in the retina of the domestic pig." *Hong Kong Med J* 1:302-308.

Gibson, C. L., D. Constantin, M. J. Prior, P. M. Bath, and S. P. Murphy. 2005. "Progesterone suppresses the inflammatory response and nitric oxide synthase-2 expression following cerebral ischemia." *Exp Neurol* 193:522-530.

Glickstein, M. and M. Millodot. 1970. "Retinoscopy and eye size." *Science* 168:605.

Gloesmann, M., B. Hermann, C. Schubert, H. Sattmann, P. K. Ahnelt, and W. Drexler. 2003. "Histologic correlation of pig retina radial stratification with ultrahigh-resolution optical coherence tomography." *Invest Ophthalmol Vis Sci* 44:1696.

Gomez-Vicente, V., M. Donovan, and T. G. Cotter. 2005. "Multiple death pathways in retina-derived 661W cells following growth factor deprivation: crosstalk between caspases and calpains." *Cell Death Differ* 12:796-804.

Goss, C. W., S. W. Hoffman, and D. G. Stein. 2003. "Behavioral effects and anatomic correlates after brain injury: a progesterone dose-response study." *Pharmacol Biochem Behav* 76:231-242.

Gregor, Z. and S. J. Ryan. 1982a. "Blood-retinal barrier after blunt trauma to the eye." *Graefe's Arch Clin Exp Ophthalmol* 219:205-208.

—1982b. "Combined posterior contusion and penetrating injury in the pig eye. I. A natural history study." *Br J Ophthalmol* 66:793-798.

—1982c. "Combined posterior contusion and penetrating injury in the pig eye. II. Histological features." *Br J Ophthalmol* 66:799-804.

—1983a. "Combined posterior contusion and penetrating injury in the pig eye. III. A controlled treatment trial of vitrectomy." *Br J Ophthalmol* 67:282-285.

—1983b. "Complete and core vitrectomies in the treatment of experimental posterior penetrating eye injury in the rhesus monkey. II. Histologic features." *Arch Ophthalmol* 101:446-450.

Guo, H., S. Albrecht, M. Bourdeau, T. Petzke, C. Bergeron, and A. C. LeBlanc. 2004. "Active caspase-6 and caspase-6-cleaved tau in neuropil threads, neuritic plaques, and neurofibrillary tangles of Alzheimer's disease." *Am J Pathol* 165:523-531.

Gwon, A. 2008. "The Rabbit in Cataract/IOL Surgery." Pp. 184-201 in *Animal models in eye research* edited by P. Tsonis. San Diego, CA: Academic Press.

Hamasaki, D. I. 1967. "An anatomical and electrophysiological study of the retina of the owl monkey, Aotes trivirgatus." *J Comp Neurol* 130:163-174.

Harada, C., X. Guo, K. Namekata, A. Kimura, K. Nakamura, K. Tanaka, L. F. Parada, and T. Harada. 2011. "Glia- and neuron-specific functions of TrkB signalling during retinal degeneration and regeneration." *Nat Commun* 2:189.

Hart, J. C., R. Blight, R. Cooper, and D. Papakostopoulos. 1975. "Electrophysiological and pathological investigation of concussional injury. An Experimental study." *Trans Ophthalmol Soc UK* 95:326.

Hart, J. C., V. E. Natsikos, E. R. Raistrick, and R. M. Doran. 1980. "Chorioretinitis sclopetaria." *Trans Ophthalmol Soc UK* 100:276.

Hart, J. C. and H. J. Frank. 1975. "Retinal opacification after blunt non-perforating concussional injuries to the globe. A clinical and retinal fluorescein angiographic study." *Trans Ophthalmol Soc U K* 95:94-100.

Hart, J. C. and R. Blight. 1979a. "Early changes in peripheral retina following concussive ocular injuries: an experimental study." *J R Soc Med* 72:180-184.

Hart, JCD and R. Blight. 1979b. "Commotio retinae. To the editor." *Arch Ophthalmol* 97:1738.

Hayashi, A., A. B. Majji, S. Fujioka, H. C. Kim, I. Fukushima, and E. de Juan, Jr. 1999. "Surgically induced degeneration and regeneration of the choriocapillaris in rabbit." *Graefes Arch Clin Exp Ophthalmol* 237:668-677.

He, J., C. O. Evans, S. W. Hoffman, N. M. Oyesiku, and D. G. Stein. 2004. "Progesterone and allopregnanolone reduce inflammatory cytokines after traumatic brain injury." *Exp Neurol* 189:404-412.

Heckenlively, J. R. and G. B. Arden. 2006. "Principles and Practice of Clinical Electrophysiology of Vision.".

Hendrickson, A. and D. Hicks. 2002. "Distribution and density of medium- and short-wavelength selective cones in the domestic pig retina." *Exp Eye Res* 74:435-444.

Heriot, W. J. and R. Machemer. 1992. "Pigment epithelial repair." *Graefes Arch Clin Exp Ophthalmol* 230:91-100.

Hines-Beard, J., J. Marchetta, S. Gordon, E. Chaum, E. E. Geisert, and T. S. Rex. 2012. "A mouse model of ocular blast injury that induces closed globe anterior and posterior pole damage." *Exp Eye Res* 99:63-70 LID - 10.1016/j.e.

Hisatomi, T., T. Nakazawa, K. Noda, L. Almulki, S. Miyahara, S. Nakao, Y. Ito, H. She, R. Kohno, N. Michaud, and others. 2008. "HIV protease inhibitors provide neuroprotection through inhibition of mitochondrial apoptosis in mice." *J Clin Invest* 118:2025.

Hou, B., S. W. You, M. M. Wu, F. Kuang, H. L. Liu, X. Y. Jiao, and G. Ju. 2004. "Neuroprotective effect of inosine on axotomized retinal ganglion cells in adult rats." *Invest Ophthalmol Vis Sci* 45:662-667.

Hughes, A. 1977. "The refractive state of the rat eye." *Vision Res* 17:927-939.

—1979. "A schematic eye for the rat." *Vision Res* 19:569-588.

Hui, Y. N., Y. Q. Wu, Q. S. Xiao, B. Kirchhof, and K. Heimann. 1993. "Repair of outer blood-retinal barrier after severe ocular blunt trauma in rabbits." *Graefes Arch Clin Exp Ophthalmol* 231:365-369.

Jacobs, G. H. 1998. "Photopigments and seeing--lessons from natural experiments: the Proctor lecture." *Invest Ophthalmol Vis Sci* 39:2204-2216.

—2008. "Primate color vision: a comparative perspective." *Vis Neurosci* 25:619-633.

Jeon, C. J., E. Strettoi, and R. H. Masland. 1998. "The major cell populations of the mouse retina." *J Neurosci* 18:8936-8946.

Jeyasuria, P., J. Wetzel, M. Bradley, K Subedi, and J. C. Condon. 2009. "Progesterone-regulated caspase-3 action in the mouse may play a role in uterine quiescence during pregnancy through fragmentation of uterine myocyte contractile proteins." *Biol Reprod* 80:928-934.

Jo, S. A., E. Wang, and L. I. Benowitz. 1999. "Ciliary neurotrophic factor is an axogenesis factor for retinal ganglion cells." *Neuroscience* 89:579-591.

Jodhka, P. K., P. Kaur, W. Underwood, J. P. Lydon, and M. Singh. 2009. "The differences in neuroprotective efficacy of progesterone and medroxyprogesterone acetate correlate with their effects on brain-derived neurotrophic factor expression." *Endocrinology* 150:3162-8 LID - 10.1210/en.2.

Jones, N. P., J. M. Hayward, P. T. Khaw, C. M. Claoue, and A. R. Elkington. 1986. "Function of an ophthalmic "accident and emergency" department: results of a six month survey." *Br Med J* 292:188-190.

Kaldi, I. and A. Berta. 2004. "Progesterone administration fails to protect albino male rats against photostress-induced retinal degeneration." *Eur J Ophthalmol* 14:306-314.

Karl, M. O., S. Hayes, B. R. Nelson, K. Tan, B. Buckingham, and T. A. Reh. 2008. "Stimulation of neural regeneration in the mouse retina." *Proc Natl Acad Sci U S A* 105:19508-19513.

Kassen, S. C., R. Thummel, L. A. Campochiaro, M. J. Harding, N. A. Bennett, and D. R. Hyde. 2009. "CNTF induces photoreceptor neuroprotection and Muller glial cell proliferation through two different signaling pathways in the adult zebrafish retina." *Exp Eye Res* 88:1051-1064.

Katai, N., T. Kikuchi, H. Shibuki, S. Kuroiwa, J. A. T. Kurokawa, and N. Yoshimura. 1999. "Caspaselike Proteases activated in apoptotic photoreceptors of Royal College of Surgeons rats." *Invest Ophthalmol Vis Sci* 40:1802-1807.

Kaur, P., P. K. Jodhka, W. A. Underwood, C. A. Bowles, N. C. de Fiebre, C. M. de Fiebre, and M. Singh. 2007. "Progesterone increases brain-derived neuroptrophic factor expression and protects against glutamate toxicity in a mitogen-activated protein kinase- and phosphoinositide-3 kinase-dependent manner in cerebral cortical explants." *J Neurosci Res* 85:2441-2449.

Kayama, M., T. Nakazawa, A. Thanos, Y. Morizane, Y. Murakami, S. Theodoropoulou, T. Abe, D. Vavvas, and J. W. Miller. 2011. "Heat shock protein 70 (HSP70) is critical for the photoreceptor stress response after retinal detachment via modulating anti-apoptotic Akt kinase." *Am J Pathol* 178:1080-1091.

Kermer, P., N. Klocker, M. Labes, and M. Bahr. 1998. "Inhibition of CPP32-like proteases rescues axotomized retinal ganglion cells from secondary cell death in vivo." *J Neurosci* 18:4656-4662.

Kermer, P., N. Klocker, M. Labes, S. Thomsen, A. Srinivasan, and M. Bahr. 1999. "Activation of caspase-3 in axotomized rat retinal ganglion cells in vivo." *FEBS Lett* 453:361-364.

Kigerl, K. A., J. C. Gensel, D. P. Ankeny, J. K. Alexander, D. J. Donnelly, and P. G. Popovich. 2009. "Identification of two distinct macrophage subsets with divergent effects causing either neurotoxicity or regeneration in the injured mouse spinal cord." *J Neurosci* 29:13435-13444.

Kiilgaard, J. F., J. U. Prause, M. Prause, E. Scherfig, M. H. Nissen, and M. la Cour. 2007. "Subretinal posterior pole injury induces selective proliferation of RPE cells in the periphery in in vivo studies in pigs." *Invest Ophthalmol Vis Sci* 48:355-360.

Kimizuka, Y., T. Yamada, and M. Tamai. 1997. "Quantitative study on regenerated retinal pigment epithelium and the effects of growth factor." *Curr Eye Res* 16:1081-1087.

Klaiman, G., N. Champagne, and A. C. LeBlanc. 2009. "Self-activation of Caspase-6 in vitro and in vivo: Caspase-6 activation does not induce cell death in HEK293T cells." *Biochim Biophys Acta* 1793:592-601 LID - 10.1016/j..

Klaiman, G., T. L. Petzke, J. Hammond, and A. C. Leblanc. 2008. "Targets of caspase-6 activity in human neurons and Alzheimer disease." *Mol Cell Proteomics* 7:1541-55 LID - 10.1074/mcp.

Klassen, H., D. S. Sakaguchi, and M. J. Young. 2004. "Stem cells and retinal repair." *Prog Ret Eye Res* 23:149-181.

Klocker, N., P. Kermer, J. H. Weishaupt, M. Labes, R. Ankerhold, and M. Bahr. 2000. "Brain-derived neurotrophic factor-mediated neuroprotection of adult rat retinal ganglion cells in vivo does not exclusively depend on phosphatidyl-inositol-3'-kinase/protein kinase B signaling." *J Neurosci* 20:6962-6967.

Knighton, R. W. and G. W. Blankenship. 1980. "Electrophysiological evaluation of eyes with opaque media." *Int Ophthalmol Clin* 20:1-19.

Koeberle, P. D., A. Tura, N. G. Tassew, L. C. Schlichter, and P. P. Monnier. 2010. "The repulsive guidance molecule, RGMa, promotes retinal ganglion cell survival in vitro and in vivo." *Neuroscience* 169:495-504.

Koeberle, P. D. and A. K. Ball. 1998. "Effects of GDNF on retinal ganglion cell survival following axotomy." *Vision Res* 38:1505-1515.

—2002. "Neurturin enhances the survival of axotomized retinal ganglion cells in vivo: combined effects with glial cell line-derived neurotrophic factor and brain-derived neurotrophic factor." *Neuroscience* 110:555-567.

Kohno, T., T. Ishibashi, H. Inomata, H. Ikui, and Y. Taniguchi. 1983. "Experimental macular edema of commotio retinae: preliminary report." *Jpn J Ophthalmol* 27:149.

Kohno, T., T. Miki, and K. Hayashi. 1998. "Choroidopathy after blunt trauma to the eye: a fluorescein and indocyanine green angiographic study." *Am J Ophthalmol* 126:248-260.

Koopmans, S. A., T. Terwee, H. J. Haitjema, H. Deuring, S. Aarle, and A. C. Kooijman. 2004. "Relation between injected volume and optical parameters in refilled isolated porcine lenses." *Ophthalmic Physiol Opt* 24:572-579.

Korndorfer, C. N., C. F. Meirelles, I. C. S. Bueno, and A. L. Abdalla. 1998. "Evaluation of extraction methods for progesterone determination in rabbit (Oryctolagus cuniculus) feces by radioimmunoassay." *Braz. J. Vet. Res. Anim. Sci.* 35:115-119.

Kugler, S., N. Klocker, P. Kermer, S. Isenmann, and M. Bahr. 1999. "Transduction of axotomized retinal ganglion cells by adenoviral vector administration at the optic nerve stump: an in vivo model system for the inhibition of neuronal apoptotic cell death." *Gene Ther* 6:1759-1767.

Kuhn, F., R. Maisiak, L. Mann, V. Mester, R. Morris, and C. D. Witherspoon. 2002. "The Ocular Trauma Score (OTS)." *Ophthalmol Clin N Am* 15:163-165.

Lai, T. Y., W. W. Yip, V. W. Wong, and D. S. Lam. 2005. "Multifocal electroretinogram and optical coherence tomography of commotio retinae and traumatic macular hole." *Eye* 19:219-221.

Lamkanfi, M., W. Declercq, M. Kalai, X. Saelens, and P. Vandenabeele. 2002. "Alice in caspase land. A phylogenetic analysis of caspases from worm to man." *Cell Death Differ* 9:358-361.

Latanza, L., D. V. Alfaro, R. Bockman, T. Iwamoto, M. H. Heinemann, and S. Chang. 1988. "Leukotrienes levels in the aqueous humor following experimental ocular trauma." *Retina* 8:199-204.

Lee, V., R. L. Ford, W. Xing, C. Bunce, and B. Foot. 2010. "Surveillance of traumatic optic neuropathy in the UK." *Eye* 24:240-250.

Leon, S., Y. Yin, J. Nguyen, N. Irwin, and L. I. Benowitz. 2000. "Lens injury stimulates axon regeneration in the mature rat optic nerve." *J Neurosci* 20:4615-4626.

Leonard, D. S., X. G. Zhang, G. Panozzo, I. K. Sugino, and M. A. Zarbin. 1997. "Clinicopathologic correlation of localized retinal pigment epithelium debridement." *Invest Ophthalmol Vis Sci* 38:1094-1109.

Lewis, G. P., E. A. Chapin, G. Luna, K. A. Linberg, and S. K. Fisher. 2010. "The fate of Muller's glia following experimental retinal detachment: nuclear migration, cell division, and subretinal glial scar formation." *Mol Vis* 16:1361.

Lewis, G. P., E. A. Chapin, J. Byun, G. Luna, D. Sherris, and S. K. Fisher. 2009. "Muller cell reactivity and photoreceptor cell death are reduced after experimental retinal detachment using an inhibitor of the Akt/mTOR pathway." *Invest Ophthalmol Vis Sci* 50:4429-4435.

Liem, A. T., J. E. Keunen, and D. van Norren. 1995. "Reversible cone photoreceptor injury in commotio retinae of the macula." *Retina* 15:58-61.

Lim, M. N., T. Umapathy, P. J. Baharuddin, and Z. Zubaidah. 2011. "Characterization and safety assessment of bioengineered limbal epithelium." *Med J Malaysia* 66:335-341.

Linsenmeier, R. A. and L. Padnick-Silver. 2000. "Metabolic dependence of photoreceptors on the choroid in the normal and detached retina." *Invest Ophthalmol Vis Sci* 41:3117-3123.

Lloyd, C. M., A. R. Phillips, G. J. Cooper, and P. R. Dunbar. 2008. "Double immunofluorescent labeling using sequential application of two rat primary antibodies." *J Immunol Methods* 334:70-71.

Lopez, P. F., Q. Yan, L. Kohen, N. A. Rao, C. Spee, J. Black, and A. Oganesian. 1995. "Retinal pigment epithelial wound healing in vivo." *Arch Ophthalmol* 113:1437-1446.

Lorber, B., M. Berry, and A. Logan. 2008. "Different factors promote axonal regeneration of adult rat retinal ganglion cells after lens injury and intravitreal peripheral nerve grafting." *J Neurosci Res* 86:894-903.

Lorber, B., M. L. Howe, L. I. Benowitz, and N. Irwin. 2009. "Mst3b, an Ste20-like kinase, regulates axon regeneration in mature CNS and PNS pathways." *Nat Neurosci* 12:1407-1414.

Luna, G., G. P. Lewis, C. D. Banna, O. Skalli, and S. K. Fisher. 2010. "Expression profiles of nestin and synemin in reactive astrocytes and Muller cells following retinal injury: a comparison with glial fibrillar acidic protein and vimentin." *Mol Vis* 16:2511.

Luo, J. M., L. P. Cen, X. M. Zhang, S. W. Chiang, Y. Huang, D. Lin, Y. M. Fan, N. van Rooijen, D. S. Lam, C. P. Pang, and Q. Cui. 2007. "PI3K/akt, JAK/STAT and MEK/ERK pathway inhibition protects retinal ganglion cells via different mechanisms after optic nerve injury." *Eur J Neurosci* 26:828-842.

Lutjen-Drecoll, E., P. L. Kaufman, R. Wasielewski, L. Ting-Li, and M. A. Croft. 2010. "Morphology and accommodative function of the vitreous zonule in human and monkey eyes." *Invest Ophthalmol Vis Sci* 51:1554-1564.

Mac Donald, C. L., A. M. Johnson, D. Cooper, E. C. Nelson, N. J. Werner, J. S. Shimony, A. Z. Snyder, M. E. Raichle, J. R. Witherow, R. Fang, S. F. Flaherty, and D. L. Brody. 2011. "Detection of blast-related traumatic brain injury in U.S. military personnel." *N Engl J Med* 364:2091-2100.

Mader, T. H., R. D. Carroll, C. S. Slade, R. K. George, J. P. Ritchey, and S. P. Neville. 2006. "Ocular war injuries of the Iraqi Insurgency,January-September 2004." *Ophthalmol* 113:97-104.

Malik, J. M., Z. Shevtsova, M. Bahr, and S. Kugler. 2005. "Long-term in vivo inhibition of CNS neurodegeneration by Bcl-XL gene transfer." *Mol Ther* 11:373-381.

Mallonee, S., S. Shariat, G. Stennies, R. Waxweiler, D. Hogan, and F. Jordan. 1996. "Physical injuries and fatalities resulting from the Oklahoma City bombing." *J Am Med Assoc* 276:382-387.

Matsumoto, B., J. C. Blanks, and S. J. Ryan. 1984. "Topographic variations in the rabbit and primate internal limiting membrane." *Invest Ophthalmol Vis Sci* 25:71-82.

McConnell, P. and M. Berry. 1982. "Regeneration of ganglion cell axons in the adult mouse retina." *Brain Res* 241:362-365.

McCormack, J. T. and G. S. Greenwald. 1974. "Progesterone and oestradiol-17beta concentrations in the peripheral plasma during pregnancy in the mouse." *J Endocrinol* 62:101-107.

Meyer, C. H., E. B. Rodrigues, and S. Mennel. 2003. "Acute commotio retinae determined by cross-sectional optical coherence tomography." *Eur J Ophthalmol* 13:816-818.

Miki, T., K. Kitashoji, and T. Kohno. 1992. "Intrachoroidal dye leakage in indocyanine green fundus angiography after experimental commotio retinae." *Eur J Ophthalmol* 2:79-82.

Miller, B., H. Miller, R. Patterson, and S. J. Ryan. 1986. "Retinal wound healing. Cellular activity at the vitreoretinal interface." *Arch Ophthalmol* 104:281-285.

Mo, X., A. Yokoyama, T. Oshitari, H. Negishi, M. Dezawa, A. Mizota, and E. Adachi-Usami. 2002. "Rescue of axotomized retinal ganglion cells by BDNF gene electroporation in adult rats." *Invest Ophthalmol Vis Sci* 43:2401-2405.

Monnier, P. P., P. M. D'Onofrio, M. Magharious, A. C. Hollander, N. Tassew, K. Szydlowska, M. Tymianski, and P. D. Koeberle. 2011. "Involvement of caspase-6 and caspase-8 in neuronal apoptosis and the regenerative failure of injured retinal ganglion cells." *J Neurosci* 31:10494-10505.

Morris, A. C., T. Scholz, and J. M. Fadool. 2008. "Rod progenitor cells in the mature zebrafish retina." *Adv Exp Med Biol* 613:361-368.

Moulin, M. and A. P. Arrigo. 2008. "Caspases activation in hyperthermia-induced stimulation of TRAIL apoptosis." *Cell Stress Chaperones* 13:313-26 LID - 10.1007/s12.

Muller, A., T. G. Hauk, and D. Fischer. 2007. "Astrocyte-derived CNTF switches mature RGCs to a regenerative state following inflammatory stimulation." *Brain* 130:3308-3320.

Nakazawa, T., M. Kayama, M. Ryu, H. Kunikata, R. Watanabe, M. Yasuda, J. Kinugawa, D. Vavvas, and J. W. Miller. 2011. "Tumor necrosis factor-alpha mediates photoreceptor death in a rodent model of retinal detachment." *Invest Ophthalmol Vis Sci* 52:1384-1391.

Nangia, V., J. B. Jonas, A. Sinha, A. Matin, M. Kulkarni, and S. Panda-Jonas. 2010. "Ocular axial length and its associations in an adult population of central rural India: the Central India Eye and Medical Study." *Ophthalmology* 117:1360-1366.

Nathans, J. 1992. "Rhodopsin: structure, function, and genetics." *Biochemistry* 31:4923-4931.

National Centre for the Replacement Refinement and Reduction of Animals in Research. . "Species Selection." 2011.

Nicotera, P., M. Leist, and L. Manzo. 1999. "Neuronal cell death: a demise with different shapes." *Trends Pharmacol Sci* 20:46-51.

Nikolaev, A., T. McLaughlin, D. D. O'Leary, and M. Tessier-Lavigne. 2009. "APP binds DR6 to trigger axon pruning and neuron death via distinct caspases." *Nature* 457:981-9 LID - 10.1038/natu.

Nilsen, J. and R. D. Brinton. 2002a. "Impact of progestins on estradiol potentiation of the glutamate calcium response." *Neuroreport* 13:825-830.

—2002b. "Impact of progestins on estrogen-induced neuroprotection: synergy by progesterone and 19-norprogesterone and antagonism by medroxyprogesterone acetate." *Endocrinology* 143:205-212.

Nin, M. S., L. A. Martinez, F. Pibiri, M. Nelson, and G. Pinna. 2011. "Neurosteroids reduce social isolation-induced behavioral deficits: a proposed link with neurosteroid-mediated upregulation of BDNF expression." *Front Endocrinol (Lausanne)* 2:73 LID-10.3389/fendo.2011.0.

Ninomiya, H. and H. Kuno. 2001. "Microvasculature of the rat eye: scanning electron microscopy of vascular corrosion casts." *Vet Ophthalmol* 4:55-59.

Nishida, A., M. Takahashi, H. Tanihara, I. Nakano, J. B. Takahashi, A. Mizoguchi, C. Ide, and Y. Honda. 2000. "Incorporation and differentiation of hippocampus-derived neural stem cells transplanted in injured adult rat retina." *Invest Ophthalmol Vis Sci* 41:4268-4274.

Noia Lda, C., A. Berezovsky, D. Freitas, P. Y. Sacai, and S. R. Salomao. 2006. "[Clinical and electroretinographic profile of commotio retinae.]." *Arq Bras Oftalmol* 69:895-906.

Odhiambo, W.A., S.W. Guthua, F.G. Macigo, and M.K. Ahama. 2002. "Maxillofacial injuries caused by terrorist bomb attack in Nairobi, Kenya." *Int J Oral Maxillofac Surg* 31:374-377.

Oganesian, A., E. Bueno, Q. Yan, C. Spee, J. Black, N. A. Rao, and P. F. Lopez. 1997. "Scanning and transmission electron microscopic findings during RPE wound healing in vivo." *Int Ophthalmol* 21:165-175.

Ogino, H., M. Ito, K. Matsumoto, S. Yagyu, H. Tsuda, I. Hirono, C. P. Wild, and R. Montesano. 1993. "Retinal degeneration induced by N-methyl-N-nitrosourea and detection of 7-methyldeoxyguanosine in the rat retina." *Toxicol Pathol* 21:21-25.

Oh, J., J. H. Jung, S. W. Moon, S. J. Song, H. G. Yu, and H. Y. Cho. 2011. "Commotio retinae with spectral-domain optical coherence tomography." *Retina* 31:2044-2049.

Ohki, K., K. Yoshida, A. Yamakawa, T. Harada, H. Matsuda, and J. Imaki. 1995. "jun-B gene expression in rat retinal cells following focal retinal injury." *Curr Eye Res* 14:1021-1024.

Ohta, K., A. Ito, and H. Tanaka. 2008. "Neuronal stem/progenitor cells in the vertebrate eye." *Dev Growth Differ* 50:253-259.

Oishi, A., M. Hata, M. Shimozono, M. Mandai, A. Nishida, and Y. Kurimoto. 2010. "The significance of external limiting membrane status for visual acuity in age-related macular degeneration." *Am J Ophthalmol* 150:27-32.e1.

Oliveira, C., N. Harizman, C. A. Girkin, A. Xie, C. Tello, J. M. Liebmann, and R. Ritch. 2007. "Axial length and optic disc size in normal eyes." *Br J Ophthalmol* 91:37.

Ooto, S., T. Akagi, R. Kageyama, J. Akita, M. Mandai, Y. Honda, and M. Takahashi. 2004. "Potential for neural regeneration after neurotoxic injury in the adult mammalian retina." *Proc Natl Acad Sci USA* 101:13654-13659.

Organisciak, D. T. and D. K. Vaughan. 2010. "Retinal light damage: mechanisms and protection." *Prog Retin Eye Res* 29:113-134.

Osakada, F., S. Ooto, T. Akagi, M. Mandai, A. Akaike, and M. Takahashi. 2007. "Wnt signaling promotes regeneration in the retina of adult mammals." *J Neurosci* 27:4210-4219.

O'Steen, W. K. 1977. "Ovarian steroid effects on light-induced retinal photoreceptor damage." *Exp Eye Res* 25:361-369.

Otteson, D. C. and P. F. Hitchcock. 2003. "Stem cells in the teleost retina: persistent neurogenesis and injury-induced regeneration." *Vision Res* 43:927-936.

Ozaki, S., M. J. Radeke, and D. H. Anderson. 2000. "Rapid upregulation of fibroblast growth factor receptor 1 (flg) by rat photoreceptor cells after injury." *Invest Ophthalmol Vis Sci* 41:568-579.

Ozaki, S., M. Kita, T. Yamana, A. Negi, and Y. Honda. 1997. "Influence of the sensory retina on healing of the rabbit retinal pigment epithelium." *Curr Eye Res* 16:349-358.

Ozerdem, U., B. Mach-Hofacre, K. Keefe, T. Pham, K. Soules, K. Appelt, and W. R. Freeman. 2001. "The effect of prinomastat (AG3340), a synthetic inhibitor of matrix metalloproteinases, on posttraumatic proliferative vitreoretinopathy." *Ophthalmic Res* 33:20-23.

Ozerdem, U., B. Mach-Hofacre, L. Cheng, S. Chaidhawangul, K. Keefe, C. D. McDermott, G. Bergeron-Lynn, K. Appelt, and W. R. Freeman. 2000. "The effect of prinomastat (AG3340), a potent inhibitor of matrix metalloproteinases, on a subacute model of proliferative vitreoretinopathy." *Curr Eye Res* 20:447-453.

Paquet-Durand, F., D. Sanges, J. McCall, J. Silva, T. van Veen, V. Marigo, and P. Ekstrom. 2010. "Photoreceptor rescue and toxicity induced by different calpain inhibitors." *J Neurochem* 115:930-940.

Park, C. M. and M. J. Hollenberg. 1993. "Growth factor-induced retinal regeneration in vivo." *Int Rev Cytol* 146:49-74.

Park, J. Y., W. H. Nam, S. H. Kim, S. Y. Jang, Y. H. Ohn, and T. K. Park. 2011. "Evaluation of the central macula in commotio retinae not associated with other types of traumatic retinopathy." *Korean J Ophthalmol* 25:262-267.

Park, K., J. M. Luo, S. Hisheh, A. R. Harvey, and Q. Cui. 2004. "Cellular mechanisms associated with spontaneous and ciliary neurotrophic factor-cAMP-induced survival and axonal regeneration of adult retinal ganglion cells." *J Neurosci* 24:10806-10815.

Park, K. K., K. Liu, Y. Hu, P. D. Smith, C. Wang, B. Cai, B. Xu, L. Connolly, I. Kramvis, M. Sahin, and Z. He. 2008. "Promoting axon regeneration in the adult CNS by modulation of the PTEN/mTOR pathway." *Science* 322:963-966.

Parrilla-Reverter, G., M. Agudo, P. Sobrado-Calvo, M. Salinas-Navarro, M. P. Villegas-Perez, and M. Vidal-Sanz. 2009. "Effects of different neurotrophic factors on the survival of retinal ganglion cells after a complete intraorbital nerve crush injury: a quantitative in vivo study." *Exp Eye Res* 89:32-41.

Peinado-Ramon, P., M. Salvador, M. P. Villegas-Perez, and M. Vidal-Sanz. 1996. "Effects of axotomy and intraocular administration of NT-4, NT-3, and brain-derived neurotrophic factor on the survival of adult rat retinal ganglion cells. A quantitative in vivo study." *Invest Ophthalmol Vis Sci* 37:489-500.

Penn, J. S., G. W. McCollum, J. M. Barnett, X. Q. Werdich, K. A. Koepke, and V. S. Rajaratnam. 2006. "Angiostatic effect of penetrating ocular injury: role of pigment epithelium-derived factor." *Invest Ophthalmol Vis Sci* 47:405-414.

Petras, J. M., R. A. Bauman, and N. M. Elsayed. 1997. "Visual system degeneration induced by blast overpressure." *Toxicol* 121:41-49.

Petroff, B. K. and K. M. Mizinga. 2003. "Pharmacokinetics of ovarian steroids in Sprague-Dawley rats after acute exposure to 2,3,7,8-tetrachlorodibenzo-p-dioxin (TCDD)." *Reprod Biol* 3:131-141.

Pettus, E. H., D. W. Wright, D. G. Stein, and S. W. Hoffman. 2005. "Progesterone treatment inhibits the inflammatory agents that accompany traumatic brain injury." *Brain Res* 1049:112-119.

Pieramici, D. J., P. Sternberg, Jr., S. r. Aaberg TM, W. Z. Bridges, Jr., A. Capone, Jr., J. A. Cardillo, E. de Juan, Jr., F. Kuhn, T. A. Meredith, W. F. Mieler, T. W. Olsen, P. Rubsamen, and T. Stout. 1997. "A system for classifying mechanical injuries of the eye (globe). The Ocular Trauma Classification Group." *Am J Ophthalmol* 123:820-831.

Pradelli, L. A., M. Beneteau, and J. E. Ricci. 2010. "Mitochondrial control of caspase-dependent and -independent cell death." *Cell Mol Life Sci* 67:1589-1597.

Prusky, G. T., K. T. Harker, R. M. Douglas, and I. Q. Whishaw. 2002. "Variation in visual acuity within pigmented, and between pigmented and albino rat strains." *Behav Brain Res* 136:339-348.

Pulido, J. S., I. Sugaya, J. Comstock, and K. Sugaya. 2007. "Reelin expression is upregulated following ocular tissue injury." *Graefes Arch Clin Exp Ophthalmol* 245:889-893.

Pulido, J. S. and N. P. Blair. 1987. "The blood-retinal barrier in Berlin's edema." *Retina* 7:233-236.

Remtulla, S. and P. E. Hallett. 1985. "A schematic eye for the mouse, and comparisons with the rat." *Vision Res* 25:21-31.

Rhodes, R. H. 1982. "An ultrastructural study of the complex carbohydrates of the mouse posterior vitreoretinal juncture." *Invest Ophthalmol Vis Sci* 22:460-477.

—1983. "A comparative study of vitreous-body and zonular glycoconjugates that bind to the lectin from Ulex europaeus." *Histochemistry* 78:349-360.

—1985. "An ultrastructural study of complex carbohydrates in the posterior chamber and vitreous base of the mouse." *Histochem J* 17:291-312.

Richmond, D. R., D. E. Pratt, and C. S. White. 1962. "Orbital 'Blow-Out' Fractures in Dogs Produced by Air Blast. Formal Progress Report to Defence Atomic Support Agency 1316." Lovelace Foundation for Medical Education and Research, Albuquerque, N. Mex., Washington DC.

Roof, R. L., R. Duvdevani, and D. G. Stein. 1993. "Gender influences outcome of brain injury: progesterone plays a protective role." *Brain Res* 607:333-336.

Roof, R. L., S. W. Hoffman, and D. G. Stein. 1997. "Progesterone protects against lipid peroxidation following traumatic brain injury in rats." *Mol Chem Neuropathol* 31:1-11.

Roof, R. L. and E. D. Hall. 2000. "Gender differences in acute CNS trauma and stroke: neuroprotective effects of estrogen and progesterone." *J Neurotrauma* 17:367-388.

Sánchez-Vallejo, V., I. Almansa, R. López-Pedrajas, F. J. Romero, and M. Miranda. 2012. "The effect of progesterone on retinitis pigmentosa." *The International Society for Eye Research, Berlin*.

Saika, S., S. Kono-Saika, T. Tanaka, O. Yamanaka, Y. Ohnishi, M. Sato, Y. Muragaki, A. Ooshima, J. Yoo, K. C. Flanders, and A. B. Roberts. 2004. "Smad3 is required for dedifferentiation of retinal pigment epithelium following retinal detachment in mice." *Lab Invest* 84:1245-1258.

Sanchez, I., R. Martin, F. Ussa, and I. Fernandez-Bueno. 2011. "The parameters of the porcine eyeball." *Graefes Arch Clin Exp Ophthalmol* 249:475-482.

Sandvig, A., M. Berry, L. B. Barrett, A. Butt, and A. Logan. 2004. "Myelin-, reactive glia-, and scar-derived CNS axon growth inhibitors: expression, receptor signaling, and correlation with axon regeneration." *Glia* 46:225-251.

Sayeed, I., S. Parvez, B. Wali, D. Siemen, and D. G. Stein. 2009. "Direct inhibition of the mitochondrial permeability transition pore: a possible mechanism for better neuroprotective effects of allopregnanolone over progesterone." *Brain Res* 1263:165-73 LID - 10.1016/j.b.

Schulze-Bonsel, K., N. Feltgen, H. Burau, L. Hansen, and M. Bach. 2006. "Visual acuities "hand motion" and "counting fingers" can be quantified with the freiburg visual acuity test." *Invest Ophthalmol Vis Sci* 47:1236-1240.

Schwab, M. E. 2010. "Functions of Nogo proteins and their receptors in the nervous system." *Nat Rev Neurosci* 11:799-811.

Scott, W. R., W. C. Lloyd, J. V. Benedict, and R. Meredith. 2000. "Ocular injuries due to projectile impacts." *Annu Proc Assoc Adv Automot Med* 44:205-217.

Sebag, J. 1992. "Anatomy and pathology of the vitreo-retinal interface." *Eye* 6:541-552.

Sebag, J. and K.M.P. Yee. 2007. "Vitreous: From Biochemistry to Clinical Relevance." Pp. Chap 16; 13 and 22 in *Duane's Foundations of Clinical Ophthalmology*, vol. 1 edited by W. Tasman and E. Jaeger. Philadelphia, PA: Lippincott Williams & Wilkins.

Sharma, A. K. and B. Rohrer. 2004. "Calcium-induced calpain mediates apoptosis via caspase-3 in a mouse photoreceptor cell line." *J Biol Chem* 279:35564-35572.

Sharpnack, D. D., A. J. Johnson, and Y. Y. Phillips. 1991. "The pathology of primary blast injury." Pp. 272-294 in *Conventional Warfare--Ballistic, Blast and Burn Injuries* edited by R. Zajtchuk, P. Jenkins, R. Bellamy, and C. Quick. Washington, DC: Office of the Surgeon General at TMM publications.

Shear, D. A., R. Galani, S. W. Hoffman, and D. G. Stein. 2002. "Progesterone protects against necrotic damage and behavioral abnormalities caused by traumatic brain injury." *Exp Neurol* 178:59-67.

Silver, J. and J. H. Miller. 2004. "Regeneration beyond the glial scar." *Nat Rev Neurosci* 5:146-156.

Simoens, P., L. De Schaepdrijver, and H. Lauwers. 1992. "Morphologic and clinical study of the retinal circulation in the miniature pig. A: Morphology of the retinal microvasculature." *Exp Eye Res* 54:965-973.

Singh, M. and C. Su. 2013a. "Progesterone and neuroprotection." *Horm Behav* 63:284-290.

—2013b. "Progesterone, brain-derived neurotrophic factor and neuroprotection." *Neuroscience* 239:84-91 LID - 10.1016/j.n.

Sipperley, J. O., H. A. Quigley, and J. D.M. Gass. 1978. "Traumatic retinopathy in primates: the explanation of commotio retinae." *Arch Ophthalmol* 96:2267.

Slabe, T. J., S. T. Rasmussen, and B. Tandler. 1990. "A simple method for improving glass knives." *J Electron Microsc Tech* 15:316-317.

Sloop, G. D., J. C. Roa, A. G. Delgado, J. T. Balart, 3. rd. Hines MO, and J. M. Hill. 1999. "Histologic sectioning produces TUNEL reactivity. A potential cause of false-positive staining." *Arch Pathol Lab Med* 123:529-532.

Smiddy, W. E., S. L. Fine, H. A. Quigley, G. Dunkelberger, R. M. Hohman, and E. M. Addicks. 1986. "Cell proliferation after laser photocoagulation in primate retina. An autoradiographic study." *Arch Ophthalmol* 104:1065-1069.

Smith, P. D., F. Sun, K. K. Park, B. Cai, C. Wang, K. Kuwako, I. Martinez-Carrasco, L. Connolly, and Z. He. 2009. "SOCS3 deletion promotes optic nerve regeneration in vivo." *Neuron* 64:617-623.

Snead, D. R., N. Cullen, S. James, A. V. Poulson, A. H. Morris, A. Lukaris, J. D. Scott, A. J. Richards, and M. P. Snead. 2004. "Hyperconvolution of the inner limiting membrane in vitreomaculopathies." *Graefes Arch Clin Exp Ophthalmol* 242:853-862.

Snell, R. S., M. A. Lemp, and I. Grunther. 1998. *Clinical anatomy of the eye*. Oxford, UK: Blackwell Science.

Snodderly, D. M. and R. S. Weinhaus. 1990. "Retinal vasculature of the fovea of the squirrel monkey, Saimiri sciureus: three-dimensional architecture, visual screening, and relationships to the neuronal layers." *J Comp Neurol* 297:145-163.

Sony, P., P. Venkatesh, S. Gadaginamath, and S. P. Garg. 2006. "Optical coherence tomography findings in commotio retina." *Clin Exp Ophthalmol* 34:621.

Souza-Santos, F., D. Lavinsky, N. S. Moraes, A. R. Castro, J. A. Cardillo, and M. E. Farah. 2012. "Spectral-domain optical coherence tomography in patients with commotio retinae." *Retina* 32:711-718.

Srinivasula, S. M., R. Hegde, A. Saleh, P. Datta, E. Shiozaki, J. Chai, R. A. Lee, P. D. Robbins, T. Fernandes-Alnemri, Y. Shi, and E. S. Alnemri. 2001. "A conserved XIAP-interaction motif in caspase-9 and Smac/DIABLO regulates caspase activity and apoptosis." *Nature* 410:112-116.

Stein, D. G. 2007. "Sex differences in brain damage and recovery of function: experimental and clinical findings." *Prog Brain Res* 161:339-351.

—2008a. "Progesterone exerts neuroprotective effects after brain injury." *Brain Res Rev* 57:386-397.

—2008b. "Progesterone exerts neuroprotective effects after brain injury." *Brain Res Rev* 57:386-397.

Stenkamp, D. L. 2007. "Neurogenesis in the fish retina." *Int Rev Cytol* 259:173-224.

Streit. 2005. *Microglia*, Edited by H. Kettenmann and B. R. Ransom. New York: Oxford University Press.

Subramanian, M., C. K. Pusphendran, U. Tarachand, and T. P. Devasagayam. 1993. "Gestation confers temporary resistance to peroxidation in the maternal rat brain." *Neurosci Lett* 155:151-154.

Sugawara, T., M. Fujimura, N. Noshita, G. W. Kim, A. Saito, T. Hayashi, P. Narasimhan, C. M. Maier, and P. H. Chan. 2004. "Neuronal death/survival signaling pathways in cerebral ischemia." *NeuroRx* 1:17-25.

Sun, C., M. Cai, R. P. Meadows, N. Xu, A. H. Gunasekera, J. Herrmann, J. C. Wu, and S. W. Fesik. 2000. "NMR structure and mutagenesis of the third Bir domain of the inhibitor of apoptosis protein XIAP." *J Biol Chem* 275:33777-33781.

Susin, S. A., H. K. Lorenzo, N. Zamzami, I. Marzo, B. E. Snow, G. M. Brothers, J. Mangion, E. Jacotot, P. Costantini, M. Loeffler, N. Larochette, D. R. Goodlett, R. Aebersold, D. P. Siderovski, J. M. Penninger, and G. Kroemer. 1999. "Molecular characterization of mitochondrial apoptosis-inducing factor." *Nature* 397:441-446.

Szel, A. and P. Rohlich. 1992. "Two cone types of rat retina detected by anti-visual pigment antibodies." *Exp Eye Res* 55:47-52.

Thach, A. B., A. J. Johnson, R. B. Carroll, A. Huchun, D. J. Ainbinder, R. D. Stutzman, S. M. Blaydon, S. L. Demartelaere, T. H. Mader, C. S. Slade, R. K. George, J. P. Ritchey, S. D. Barnes, and L. A. Fannin. 2008. "Severe eye injuries in the war in Iraq, 2003-2005." *Ophthalmol* 115:377-382.

Thach, A. B., T. P. Ward, R. D. Hollifield, K. Cockerham, R. Birdsong, and K. K. Kramer. 2000. "Eye injuries in a terrorist bombing: Dhahran, Saudi Arabia, June 25, 1996." *Ophthalmology* 107:844-847.

Thanos, S., J. Mey, and M. Wild. 1993. "Treatment of the adult retina with microglia-suppressing factors retards axotomy-induced neuronal degradation and enhances axonal regeneration in vivo and in vitro." *J Neurosci* 13:455-466.

Thomas, R., J. G. McManus, A. Johnson, P. Mayer, C. Wade, and J. B. Holcomb. 2009. "Ocular injury reduction from ocular protection use in current combat operations." *J Trauma* 66:S99-103.

Thummel, R., S. C. Kassen, J. M. Enright, C. M. Nelson, J. E. Montgomery, and D. R. Hyde. 2008. "Characterization of Muller glia and neuronal progenitors during adult zebrafish retinal regeneration." *Exp Eye Res* 87:433-444.

Topping, T. M., G. W. Abrams, and R. Machemer. 1979. "Experimental double-perforating injury of the posterior segment in rabbit eyes: the natural history of intraocular proliferation." *Arch Ophthalmol* 97:735-742.

Trichonas, G., Y. Murakami, A. Thanos, Y. Morizane, M. Kayama, C. M. Debouck, T. Hisatomi, J. W. Miller, and D. G. Vavvas. 2010. "Receptor interacting protein kinases mediate retinal detachment-induced photoreceptor necrosis and compensate for inhibition of apoptosis." *Proc Natl Acad Sci U S A* 107:21695-21700.

Troy, C. M., L. Stefanis, A. Prochiantz, L. A. Greene, and M. L. Shelanski. 1996. "The contrasting roles of ICE family proteases and interleukin-1beta in apoptosis induced by trophic factor withdrawal and by copper/zinc superoxide dismutase down-regulation." *Proc Natl Acad Sci U S A* 93:5635-5640.

Troy, C. M., L. Stefanis, L. A. Greene, and M. L. Shelanski. 1997. "Nedd2 is required for apoptosis after trophic factor withdrawal, but not superoxide dismutase (SOD1) downregulation, in sympathetic neurons and PC12 cells." *J Neurosci* 17:1911-1918.

Troy, C. M. and E. M. Ribe. 2008. "Caspase-2: vestigial remnant or master regulator?" *Sci Signal* 1.

Tu, S., G. P. McStay, L. M. Boucher, T. Mak, H. M. Beere, and D. R. Green. 2006. "In situ trapping of activated initiator caspases reveals a role for caspase-2 in heat shock-induced apoptosis." *Nat Cell Biol* 8:72-77.

Turner, J. E., J. R. Blair, and E. T. Chappell. 1986. "Peripheral nerve implantation into a penetrating lesion of the eye: stimulation of the damaged retina." *Brain Res* 376:246-254.

Valentino, T. L., H. J. Kaplan, L. V. Del Priore, S. R. Fang, A. Berger, and M. S. Silverman. 1995. "Retinal pigment epithelial repopulation in monkeys after submacular surgery." *Arch Ophthalmol* 113:932-938.

van Adel, B. A., C. Kostic, N. Deglon, A. K. Ball, and Y. Arsenijevic. 2003. "Delivery of ciliary neurotrophic factor via lentiviral-mediated transfer protects axotomized retinal ganglion cells for an extended period of time." *Hum Gene Ther* 14:103-115.

van Lookeren, C. ampagne M. and R. Gill. 1996. "Ultrastructural morphological changes are not characteristic of apoptotic cell death following focal cerebral ischaemia in the rat." *Neurosci Lett* 213:111-114.

van Raam, B. J., D. E. Ehrnhoefer, M. R. Hayden, and G. S. Salvesen. 2013. "Intrinsic cleavage of receptor-interacting protein kinase-1 by caspase-6." *Cell Death Differ* 20:86-96 LID - 10.1038/cdd.

Vazquez-Chona, F., B. K. Song, and E. E. Geisert, Jr. 2004. "Temporal changes in gene expression after injury in the rat retina." *Invest Ophthalmol Vis Sci* 45:2737-2746.

Vazquez-Chona, F. R., A. N. Khan, C. K. Chan, A. N. Moore, P. K. Dash, M. R. Hernandez, L. Lu, E. J. Chesler, K. F. Manly, R. W. Williams, and E. E. Geisert, Jr. 2005. "Genetic networks controlling retinal injury." *Mol Vis* 11:958-970.

Vernon, S. A. 1983. "Analysis of all new cases seen in a busy regional centre ophthalmic casualty department during 24-week period." *J R Soc Med* 76:279-282.

Vinberg, F. J., S. Strandman, and A. Koskelainen. 2009. "Origin of the fast negative ERG component from isolated aspartate-treated mouse retina." *J Vis* 9:9.1-17.

Virgo, B. B. and G. D. Bellward. 1974. "Serum progesterone levels in the pregnant and postpartum laboratory mouse." *Endocrinology* 95:1486-1490.

von Leithner, P. L., C. Ciurtin, and G. Jeffery. 2010. "Microscopic mammalian retinal pigment epithelium lesions induce widespread proliferation with differences in magnitude between center and periphery." *Mol Vis* 16:570-581.

Wan, J., H. Zheng, Z. L. Chen, H. L. Xiao, Z. J. Shen, and G. M. Zhou. 2008. "Preferential regeneration of photoreceptor from Muller glia after retinal degeneration in adult rat." *Vision Res* 48:223-234.

Wang, J., C. K. Chan, J. S. Taylor, and S. O. Chan. 2008. "Localization of Nogo and its receptor in the optic pathway of mouse embryos." *J Neurosci Res* 86:1721-1733.

Wang, J. M., L. Liu, R. W. Irwin, S. Chen, and R. D. Brinton. 2008. "Regenerative potential of allopregnanolone." *Brain Res Rev* 57:398-409.

Weichel, E. D., M. H. Colyer, S. E. Ludlow, K. S. Bower, and A. S. Eiseman. 2008. "Combat ocular trauma visual outcomes during operations Iraqi and Enduring Freedom." *Ophthalmol* 115:2235-2245.

Weidenthal, D. T. and C. L. Schepens. 1966. "Peripheral fundus changes associated with ocular contusion." *Am J Ophthalmol* 62:465-477.

Weishaupt, J. H., G. Rohde, E. Polking, A. L. Siren, H. Ehrenreich, and M. Bahr. 2004. "Effect of erythropoietin axotomy-induced apoptosis in rat retinal ganglion cells." *Invest Ophthalmol Vis Sci* 45:1514-1522.

Wen, R., Y. Song, T. Cheng, M. T. Matthes, D. Yasumura, M. M. LaVail, and R. H. Steinberg. 1995. "Injury-induced upregulation of bFGF and CNTF mRNAS in the rat retina." *J Neurosci* 15:7377-7385.

Westra, I., S. G. Robbins, D. J. Wilson, J. E. Robertson, L. M. O'Rourke, C. E. Hart, and J. T. Rosenbaum. 1995. "Time course of growth factor staining in a rabbit model of traumatic tractional retinal detachment." *Graefes Arch Clin Exp Ophthalmol* 233:573-581.

Wikler, K. C. and P. Rakic. 1990. "Distribution of photoreceptor subtypes in the retina of diurnal and nocturnal primates." *J Neurosci* 10:3390-3401.

Wong, K. H., S. A. Koopmans, T. Terwee, and A. C. Kooijman. 2007. "Changes in spherical aberration after lens refilling with a silicone oil." *Invest Ophthalmol Vis Sci* 48:1261-1267.

Wong, R., D. Ray, and D. A. Kendall. 2012. "Progesterone pharmacokinetics in the mouse: implications for potential stroke therapy." *J Pharm Pharmacol* 64:1614-20 LID - 10.1111/j.2.

Wong, T. Y., B. E. Klein, and R. Klein. 2000. "The prevalence and 5-year incidence of ocular trauma. The Beaver Dam Eye Study." *Ophthalmol* 107:2196.

Wong, T. Y., M. B. Seet, and C. L. Ang. 1997. "Eye injuries in twentieth century warfare: a historical perspective." *Surv Ophthalmol* 41:433-459.

Xiao, G., J. Wei, W. Yan, W. Wang, and Z. Lu. 2008. "Improved outcomes from the administration of progesterone for patients with acute severe traumatic brain injury: a randomized controlled trial." *Crit Care* 12:R61 LID-10.1186/cc6887 [doi].

Yin, Y., M. T. Henzl, B. Lorber, T. Nakazawa, T. T. Thomas, F. Jiang, R. Langer, and L. I. Benowitz. 2006. "Oncomodulin is a macrophage-derived signal for axon regeneration in retinal ganglion cells." *Nat Neurosci* 9:843-852.

Yoshida, K., Y. Muraki, K. Ohki, T. Harada, T. Ohashi, H. Matsuda, and J. Imaki. 1995. "C-fos gene expression in rat retinal cells after focal retinal injury." *Invest Ophthalmol Vis Sci* 36:251-254.

Yoshizawa, K., H. Nambu, J. Yang, Y. Oishi, H. Senzaki, N. Shikata, H. Miki, and A. Tsubura. 1999. "Mechanisms of photoreceptor cell apoptosis induced by N-methyl-N-nitrosourea in Sprague-Dawley rats." *Lab Invest* 79:1359-1367.

Yoshizawa, K., J. Yang, H. Senzaki, Y. Uemura, Y. Kiyozuka, N. Shikata, Y. Oishi, H. Miki, and A. Tsubura. 2000. "Caspase-3 inhibitor rescues N -methyl- N -nitrosourea-induced retinal degeneration in Sprague-Dawley rats." *Exp Eye Res* 71:629-635.

Zacks, D. N., V. Hanninen, M. Pantcheva, E. Ezra, C. Grosskreutz, and J. W. Miller. 2003. "Caspase activation in an experimental model of retinal detachment." *Invest Ophthalmol Vis Sci* 44:1262-1267.

Zadro-Lamoureux, L. A., D. N. Zacks, A. N. Baker, Q. D. Zheng, W. W. Hauswirth, and C. Tsilfidis. 2009. "XIAP effects on retinal detachment-induced photoreceptor apoptosis [corrected]." *Invest Ophthalmol Vis Sci* 50:1448-1453.

Zhang, T., Y. Hu, Y. Li, J. Wu, L. Zhao, C. Wang, Y. Liu, Z. Yin, and Z. Ma. 2009a. "Photoreceptors repair by autologous transplantation of retinal pigment epithelium and partial-thickness choroid graft in rabbits." *Invest Ophthalmol Vis Sci* 50:2982-2988.

Zhang, Z., S. F. Larner, M. C. Liu, W. Zheng, R. L. Hayes, and K. K. Wang. 2009b. "Multiple alphaII-spectrin breakdown products distinguish calpain and caspase dominated necrotic and apoptotic cell death pathways." *Apoptosis* 14:1289-1298.

Zhao, H., R. M. Sapolsky, and G. K. Steinberg. 2006. "Phosphoinositide-3-kinase/akt survival signal pathways are implicated in neuronal survival after stroke." *Mol Neurobiol* 34:249-270.

Zhi, Y., Q. Lu, C. W. Zhang, H. K. Yip, K. F. So, and Q. Cui. 2005. "Different optic nerve injury sites result in different responses of retinal ganglion cells to brain-derived neurotrophic factor but not neurotrophin-4/5." *Brain Res* 1047:224-232.

Ziegler, U. and P. Groscurth. 2004. "Morphological features of cell death." *News Physiol Sci* 19:124-128.

Zuckerman, S. 1941. "Ocular injuries resulting from the war." *Trans Ophthal Soc U K* 61:45-60.

APPENDIX 1

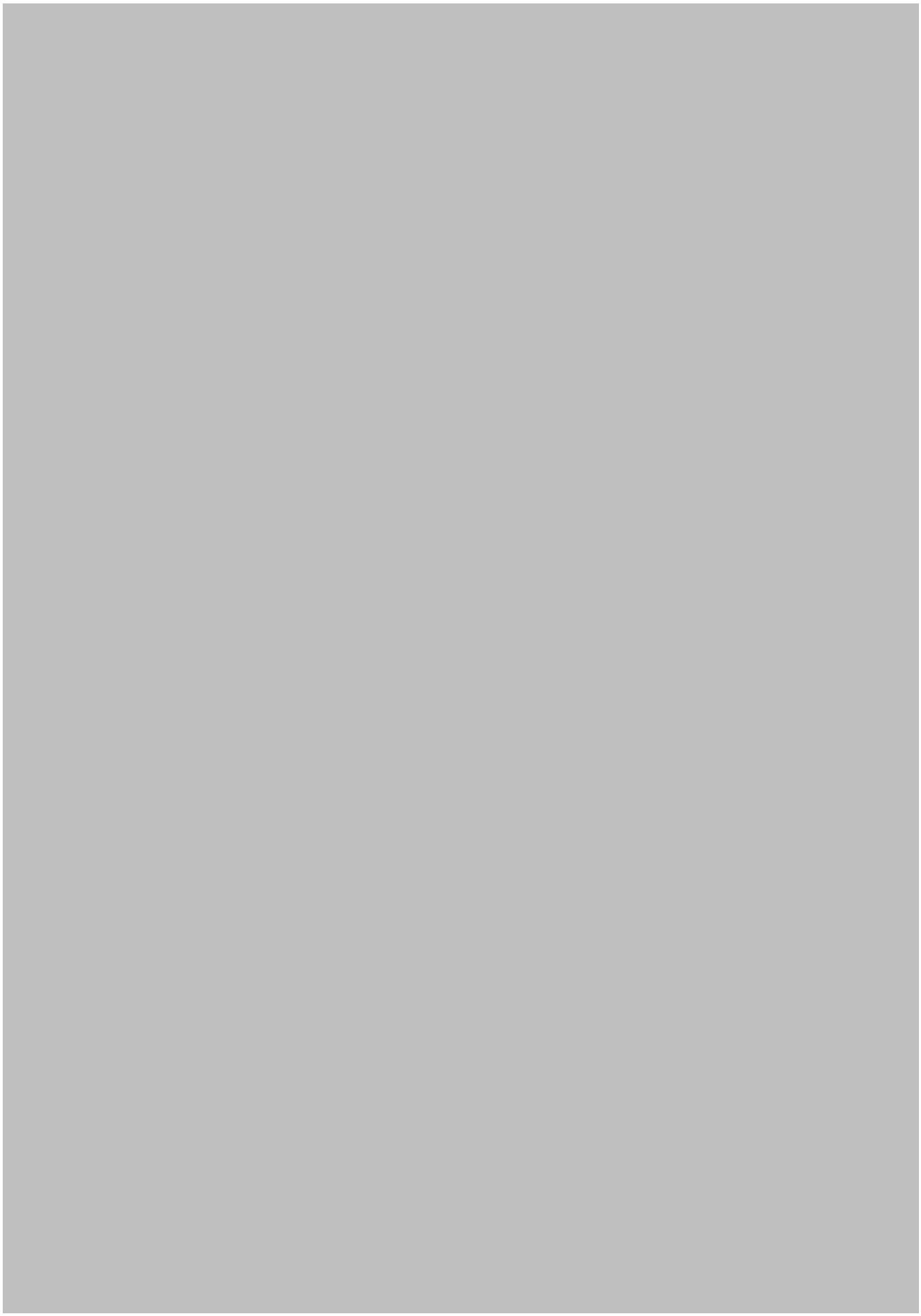

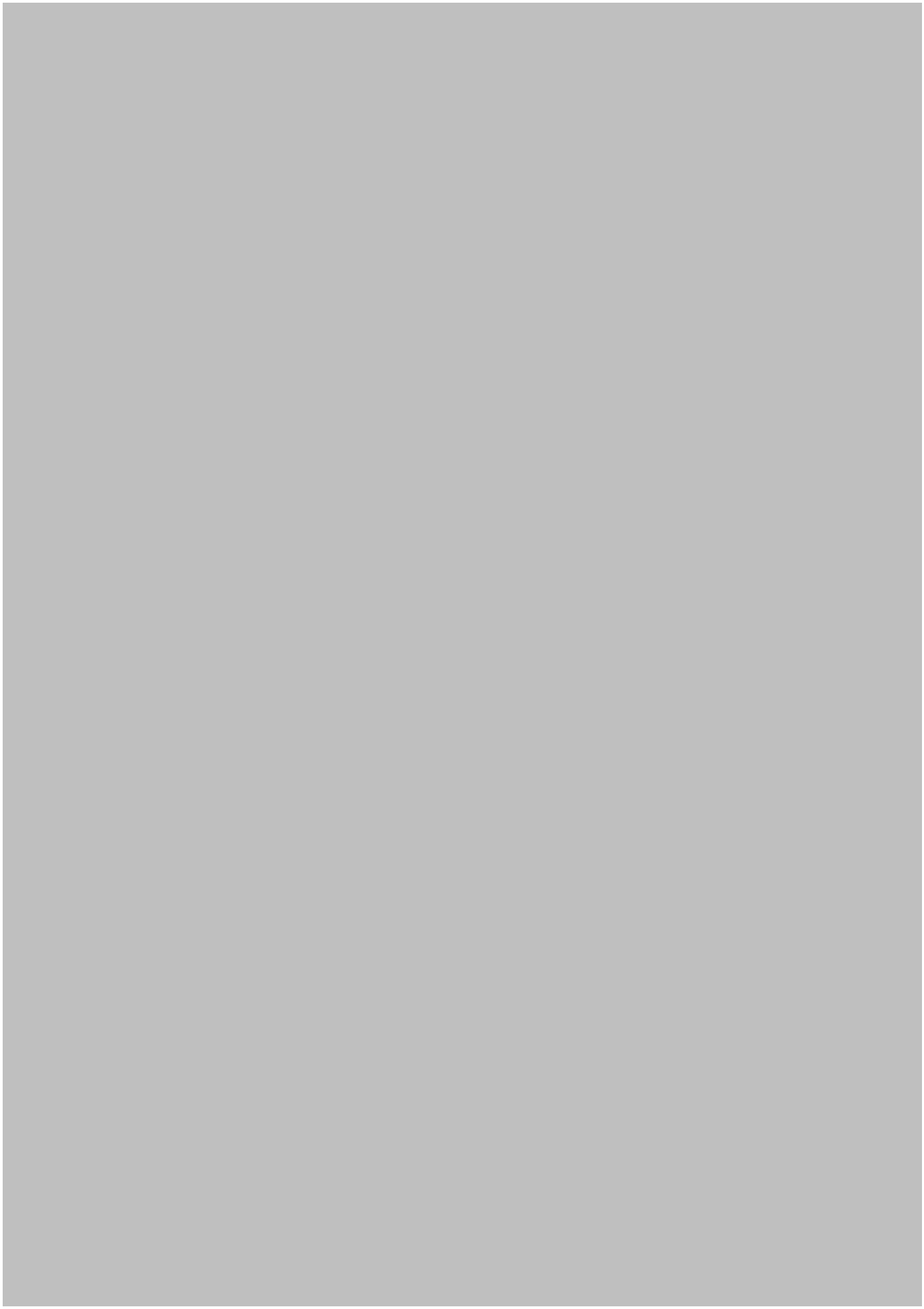

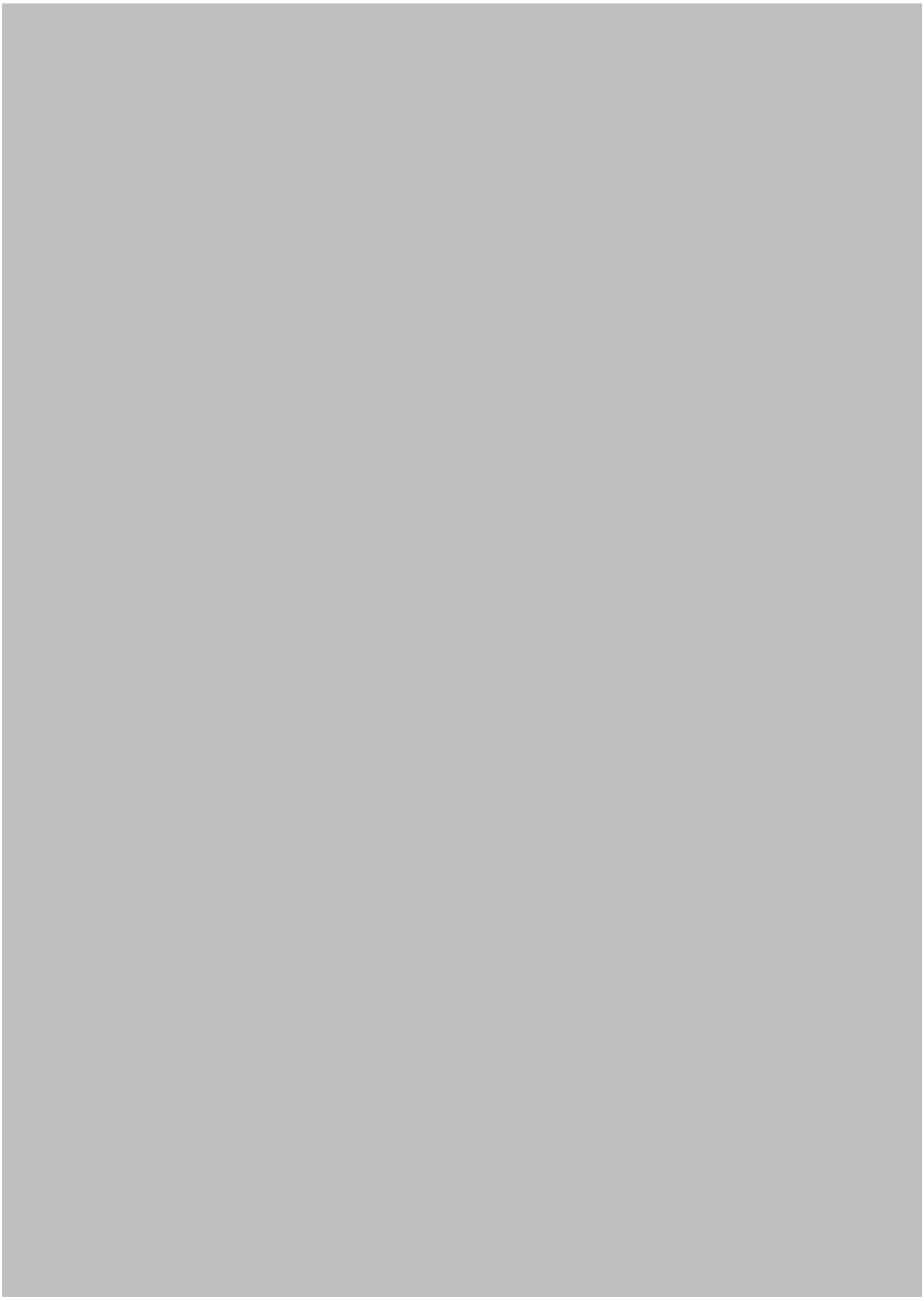

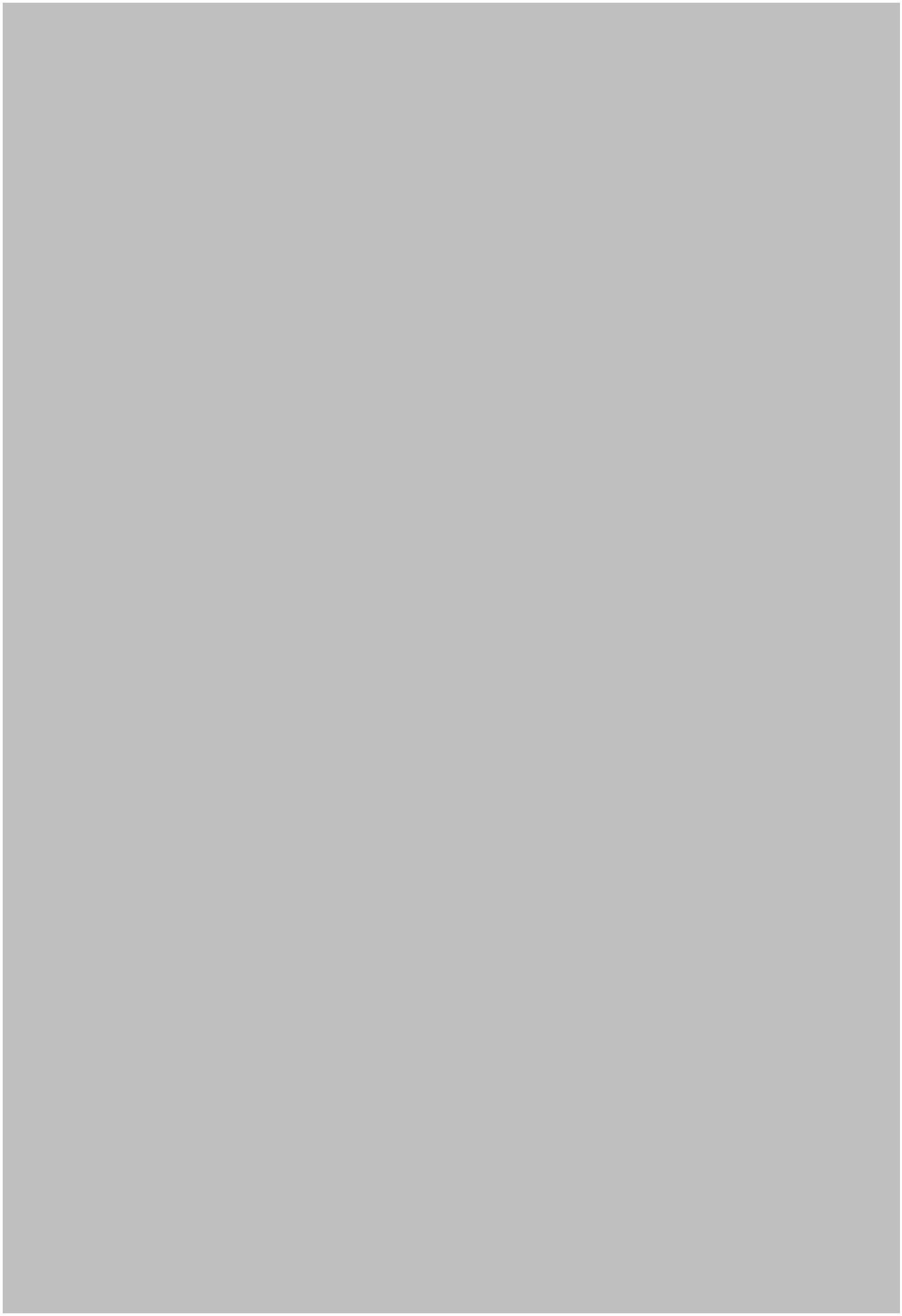

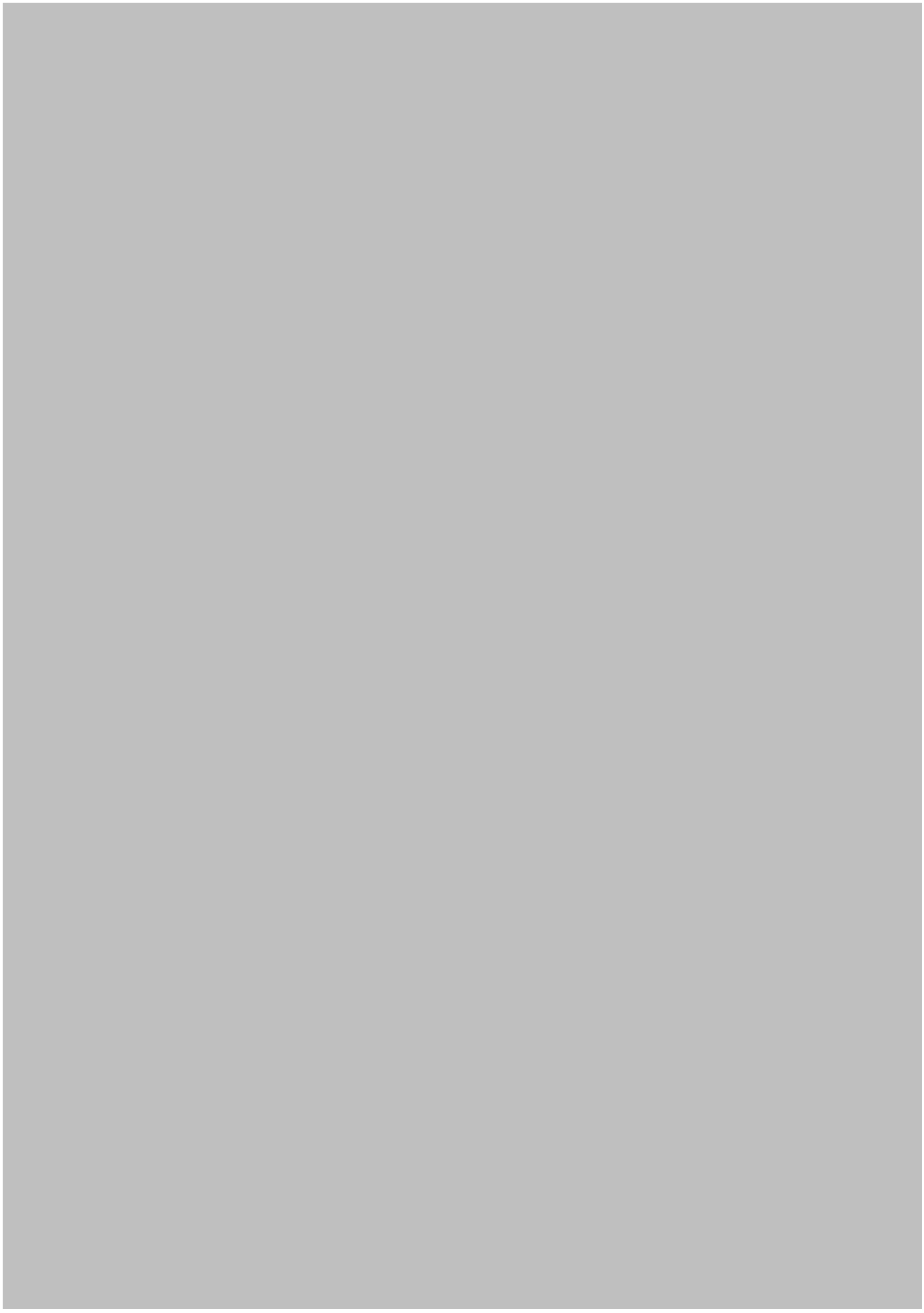

APPENDIX 2

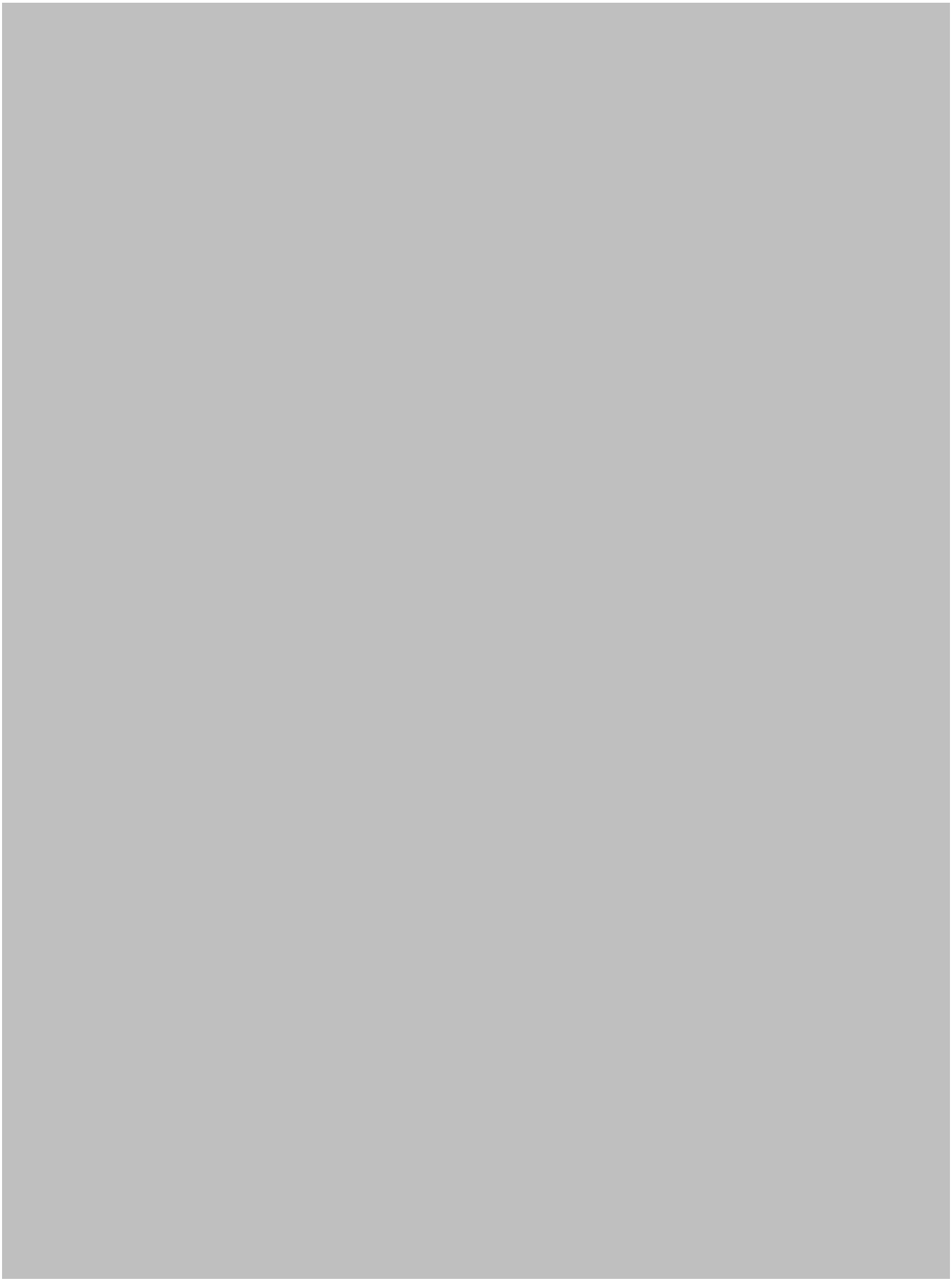

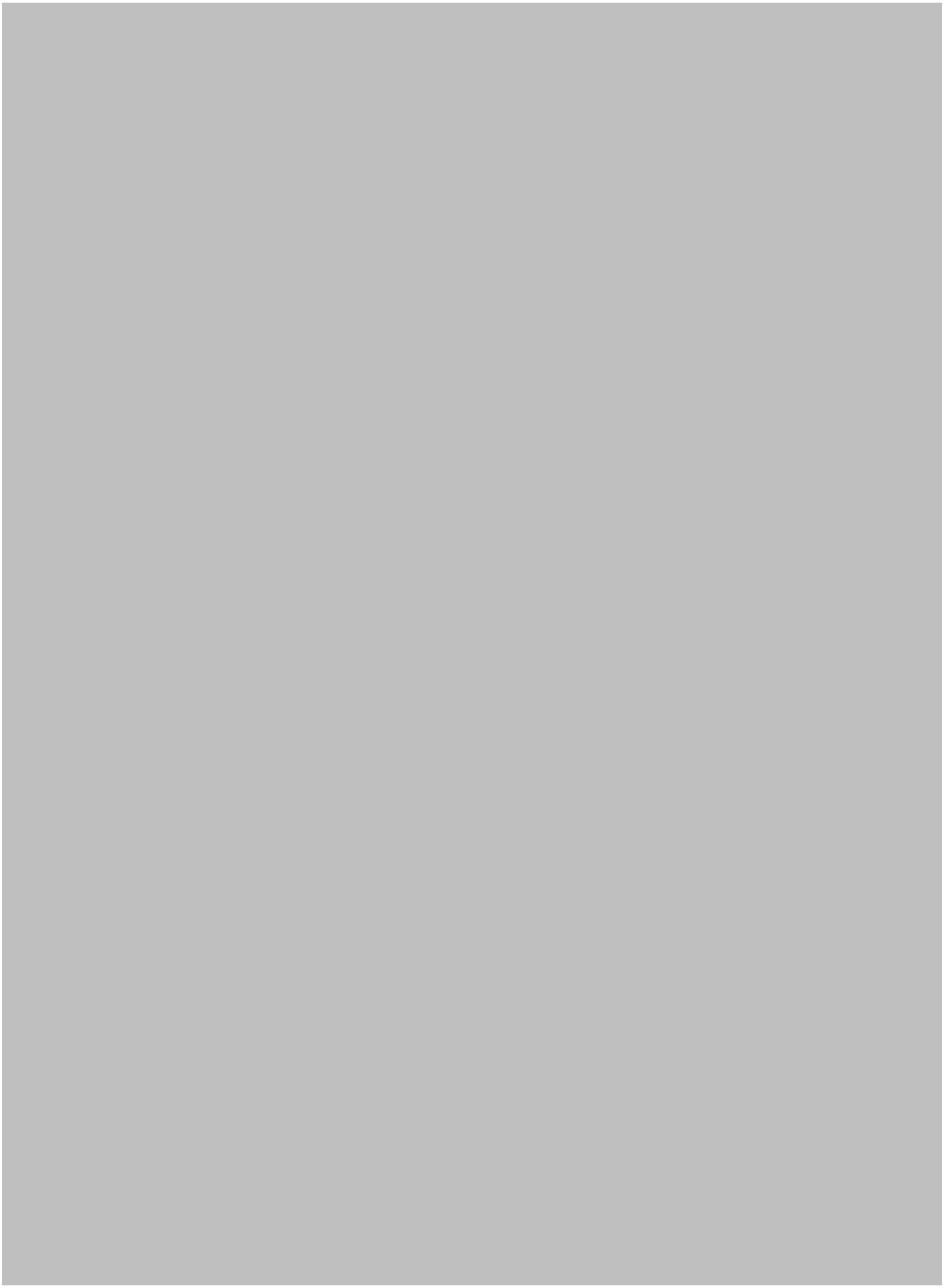

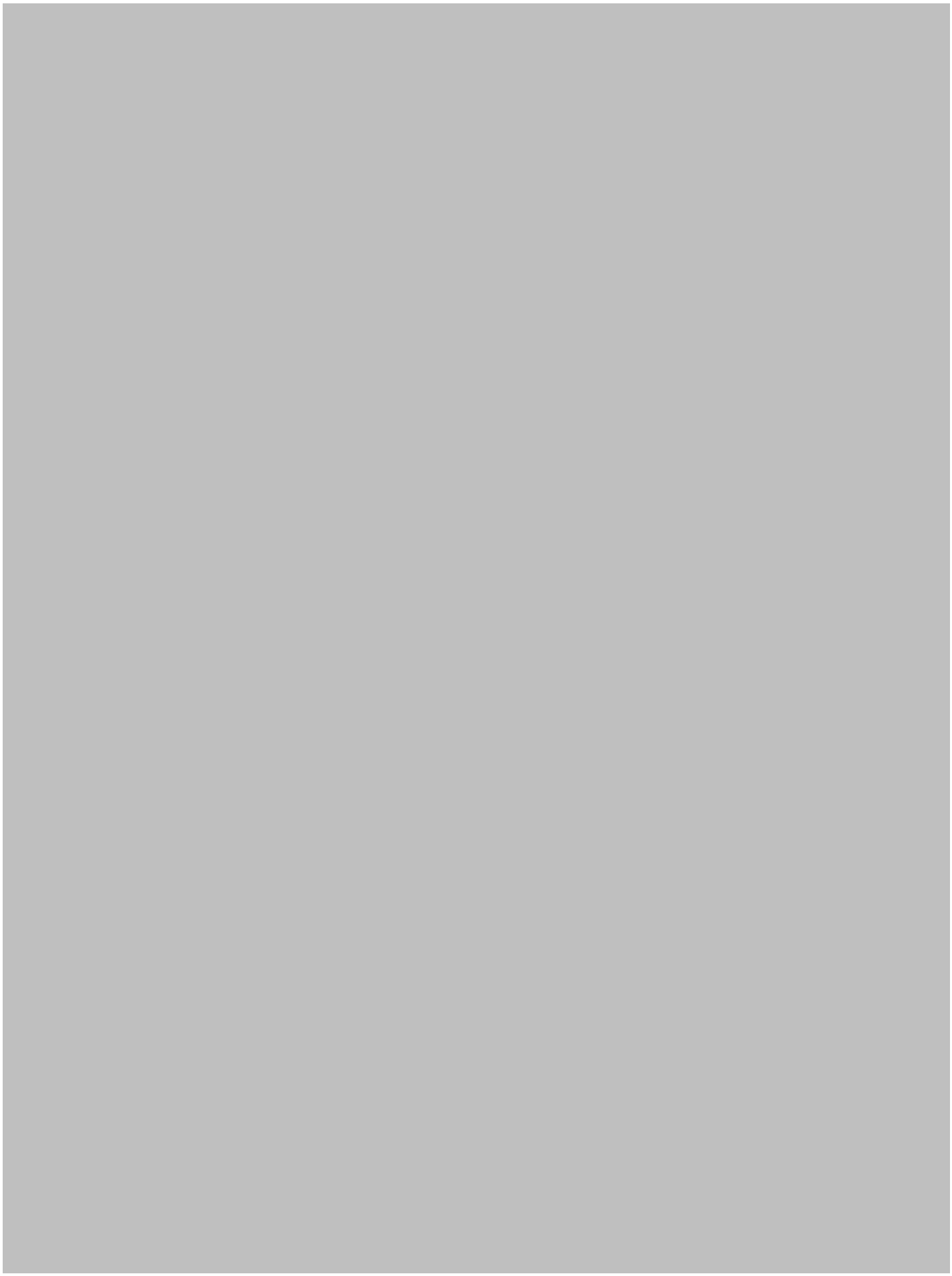

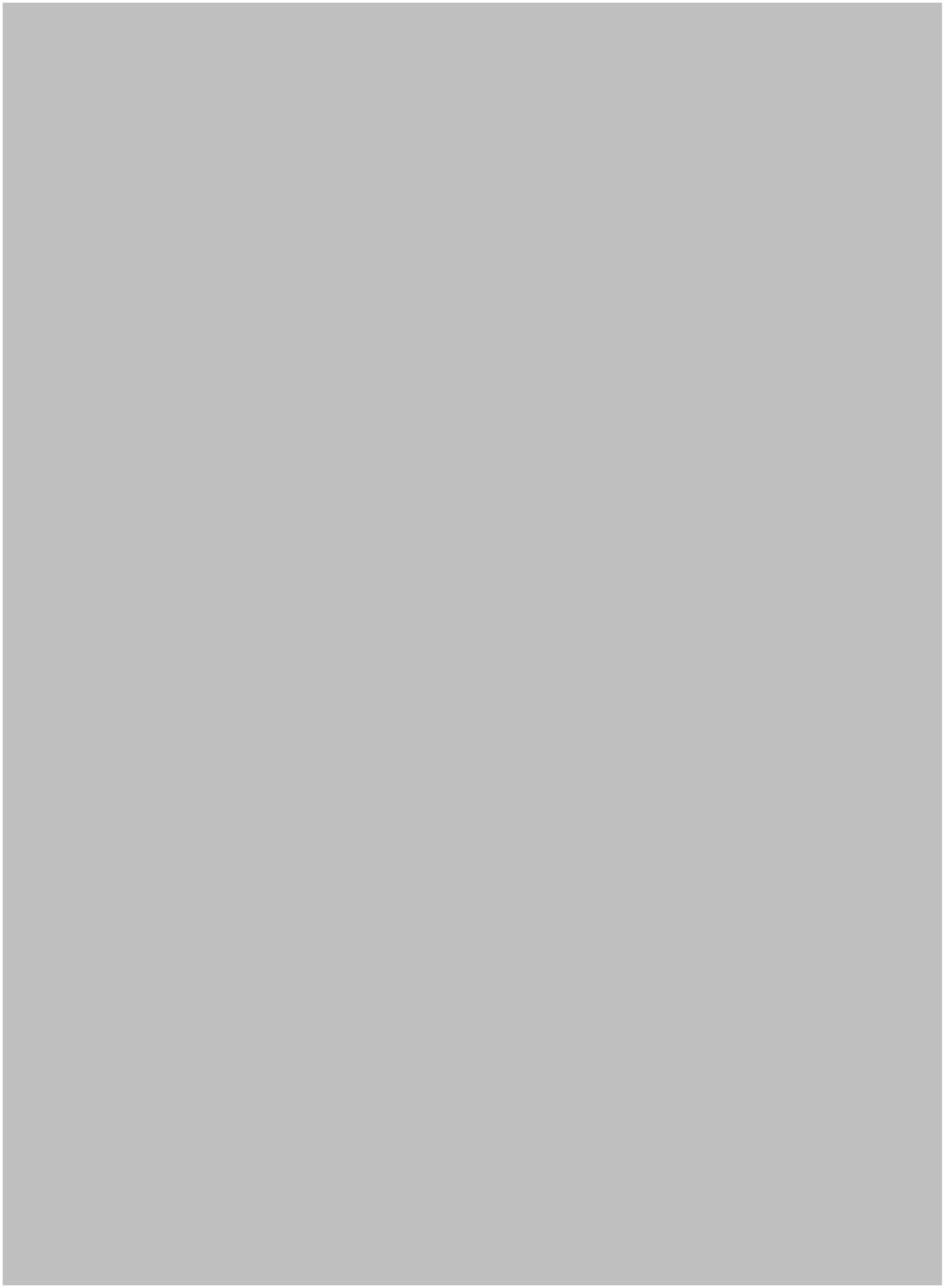

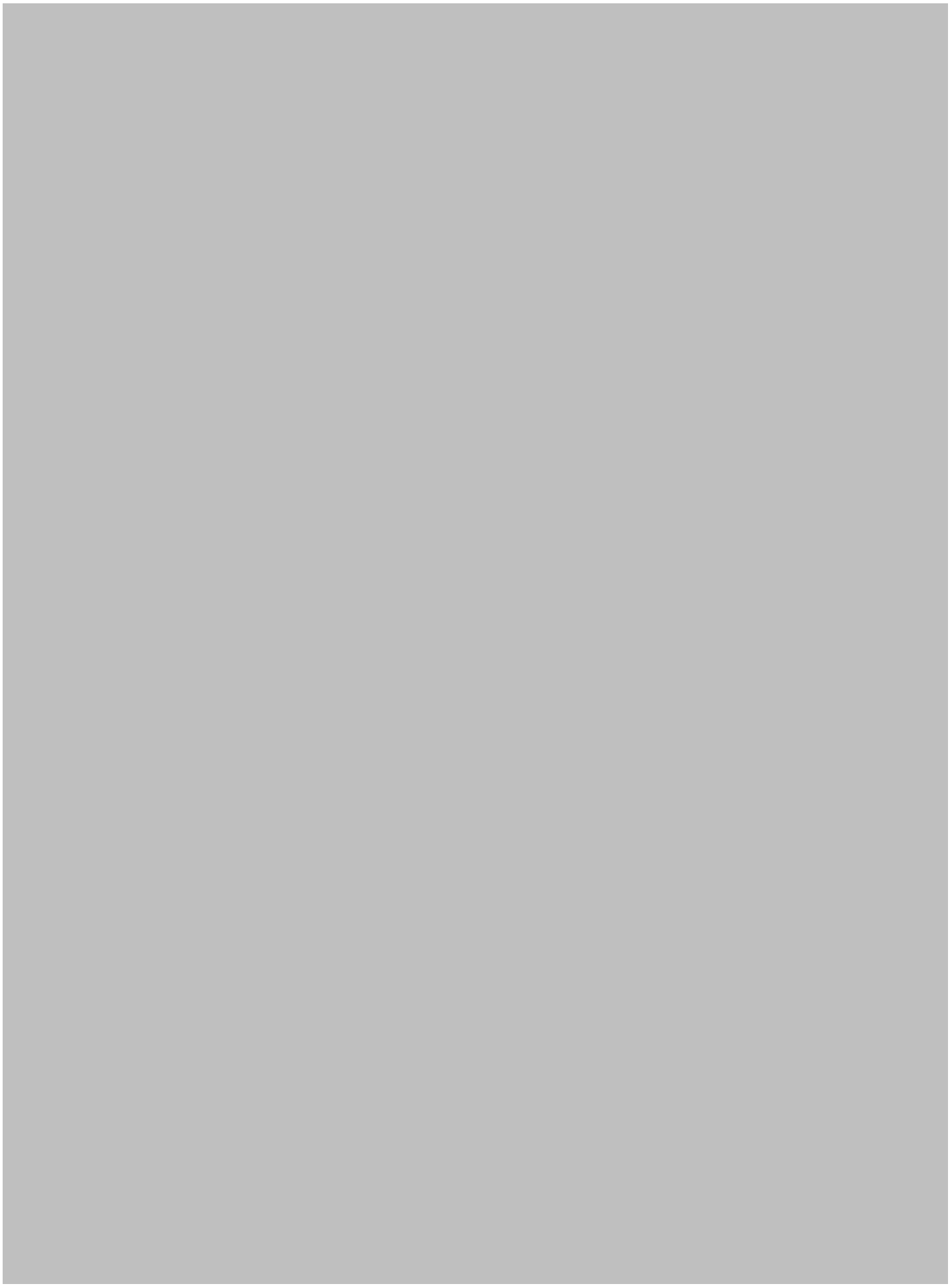

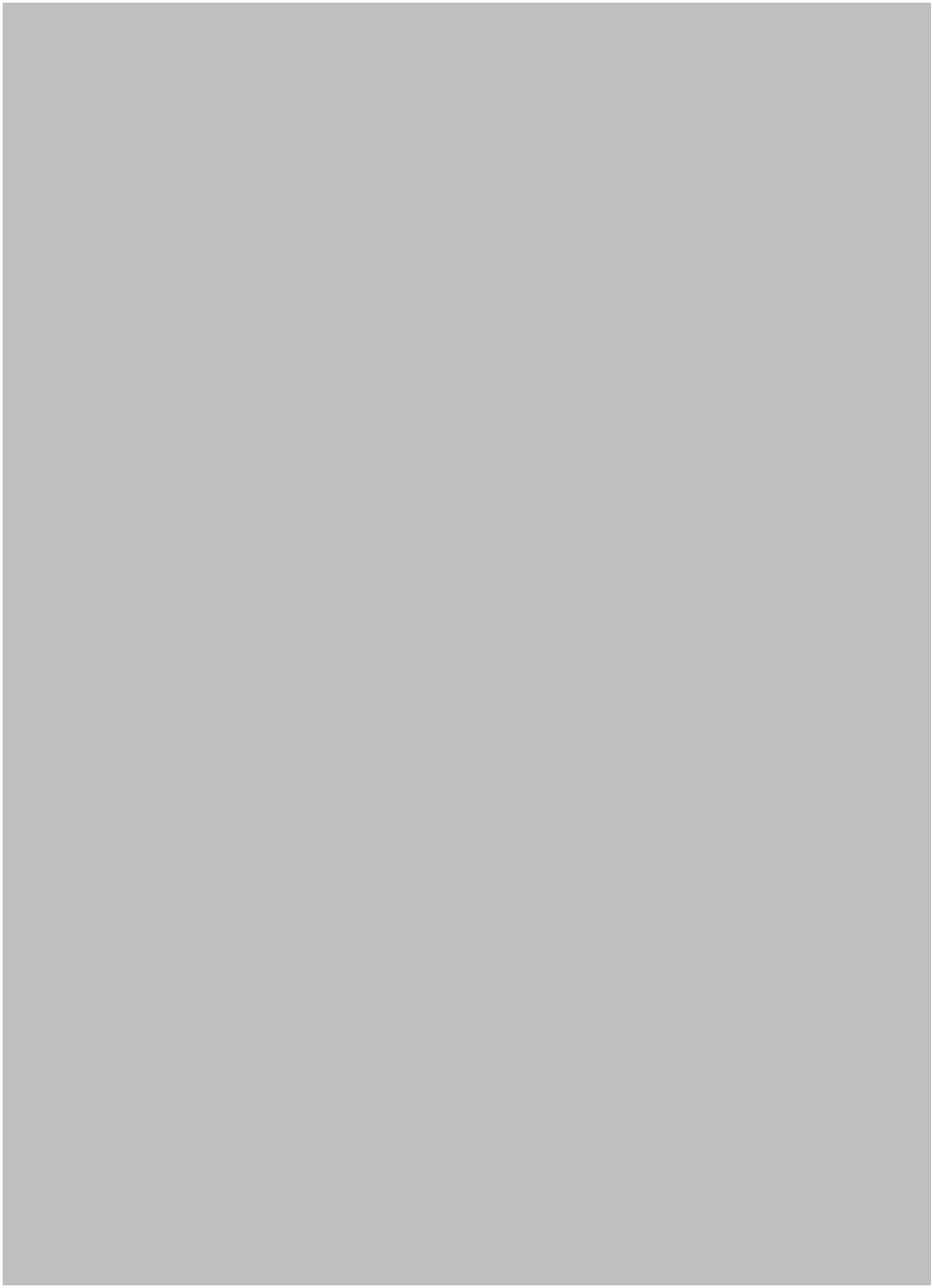

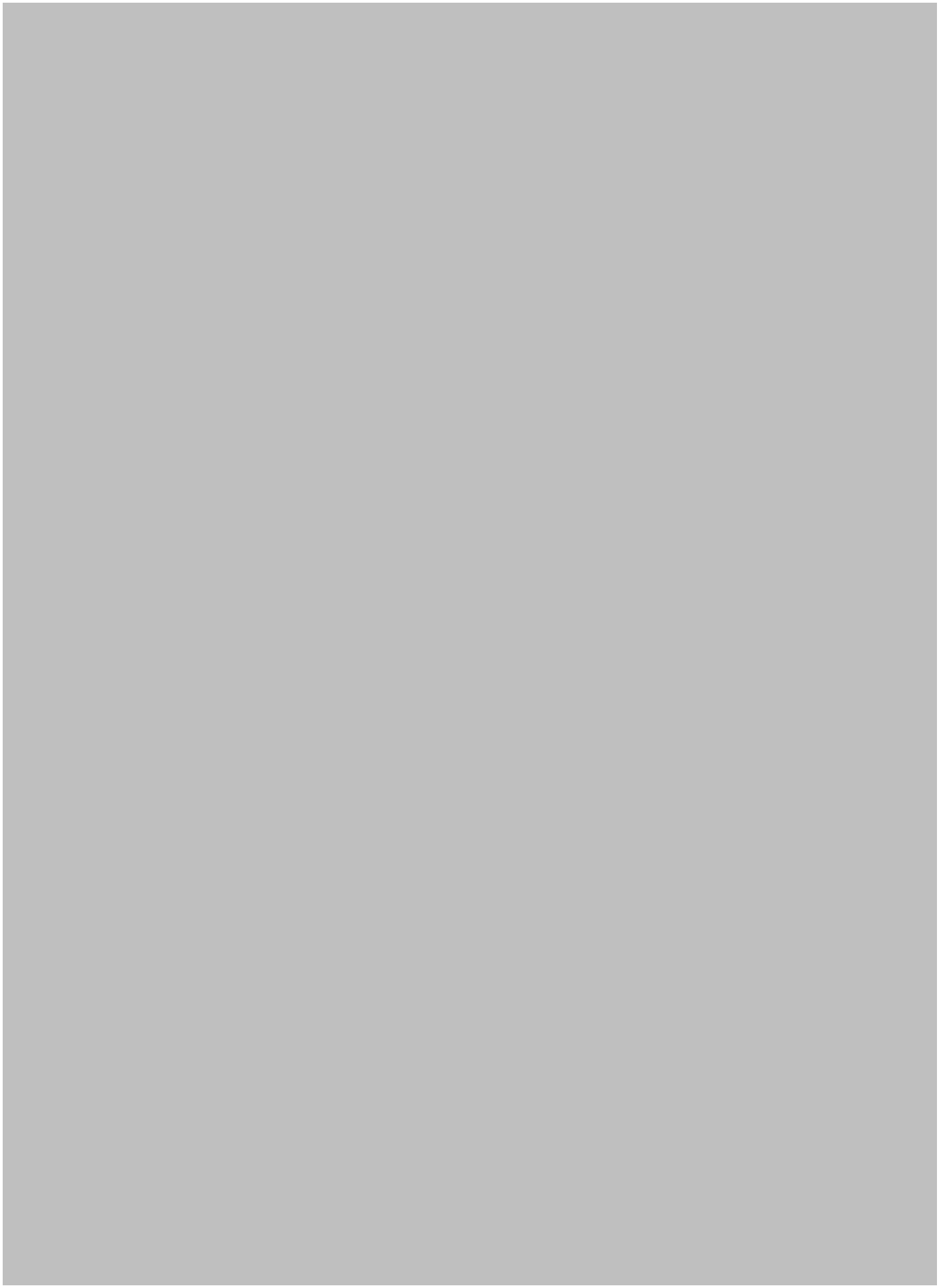

APPENDIX 3

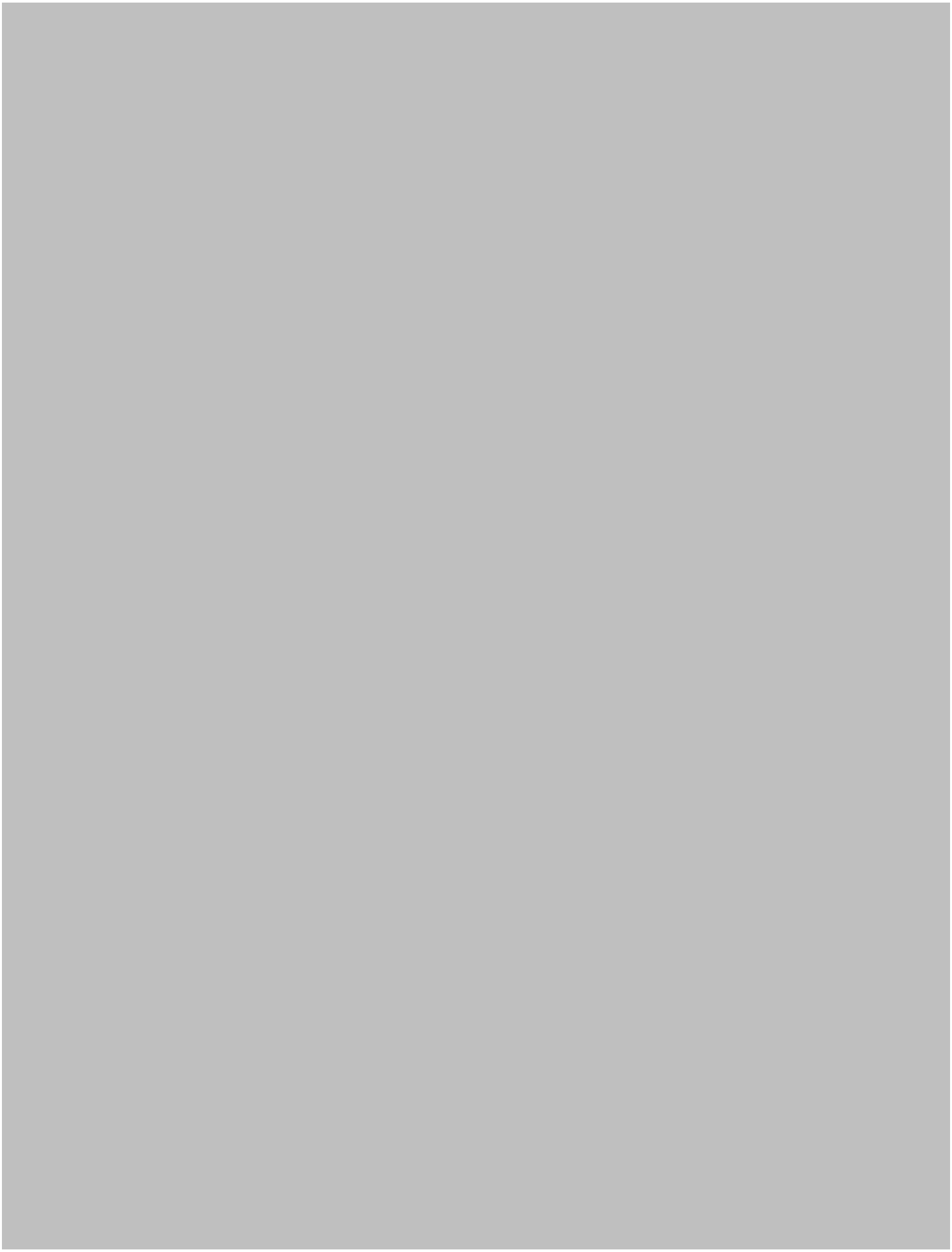

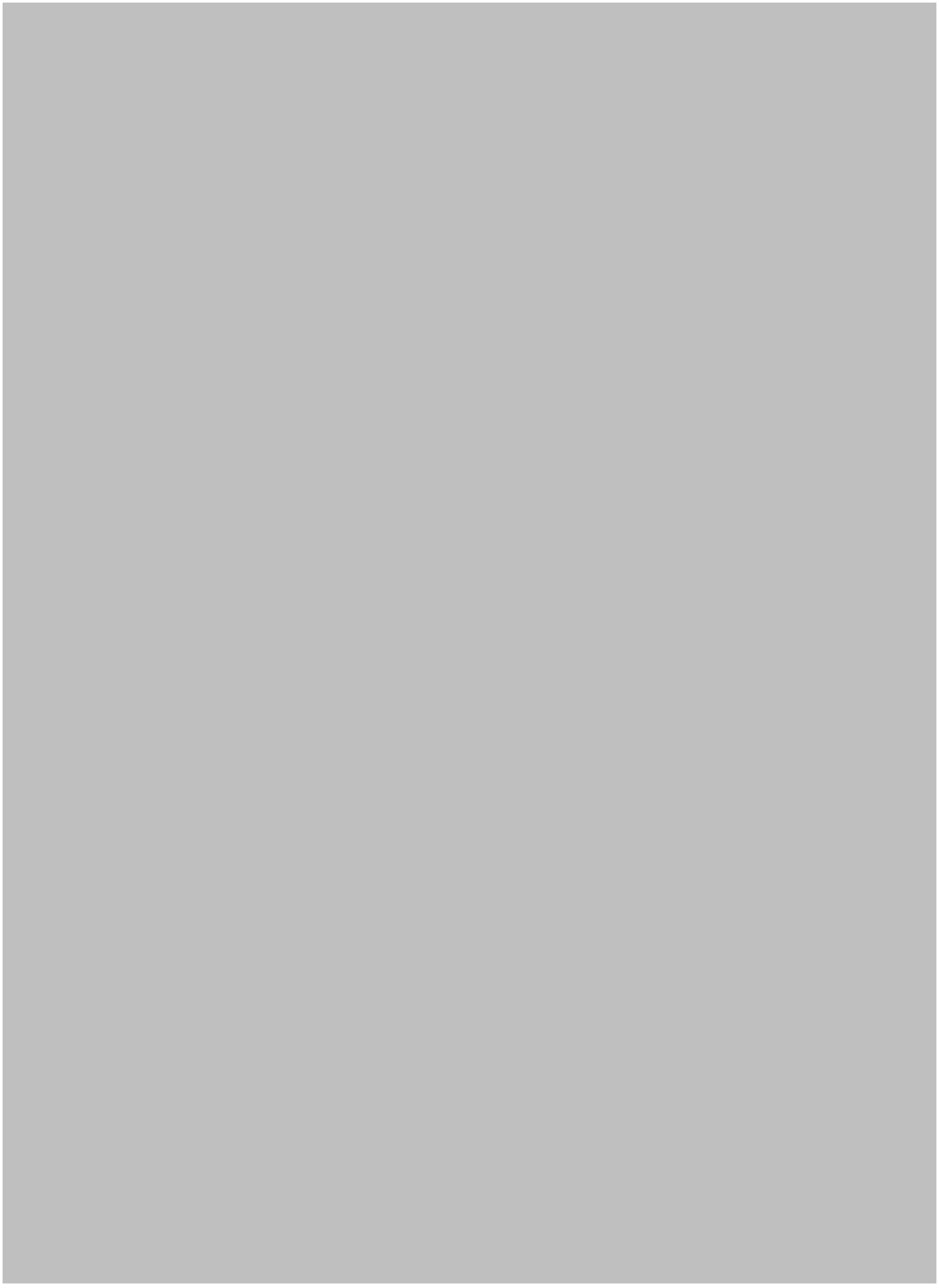

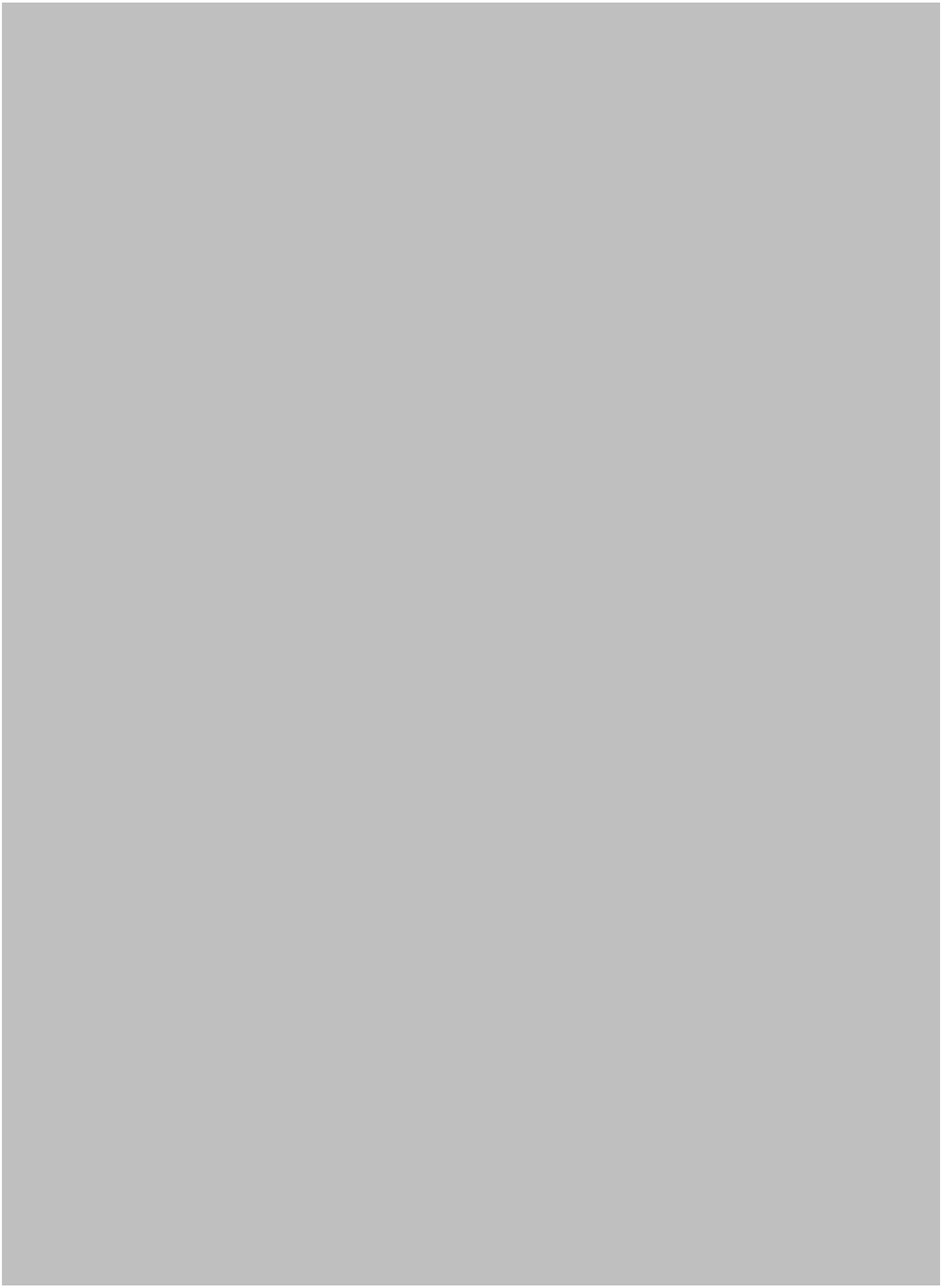

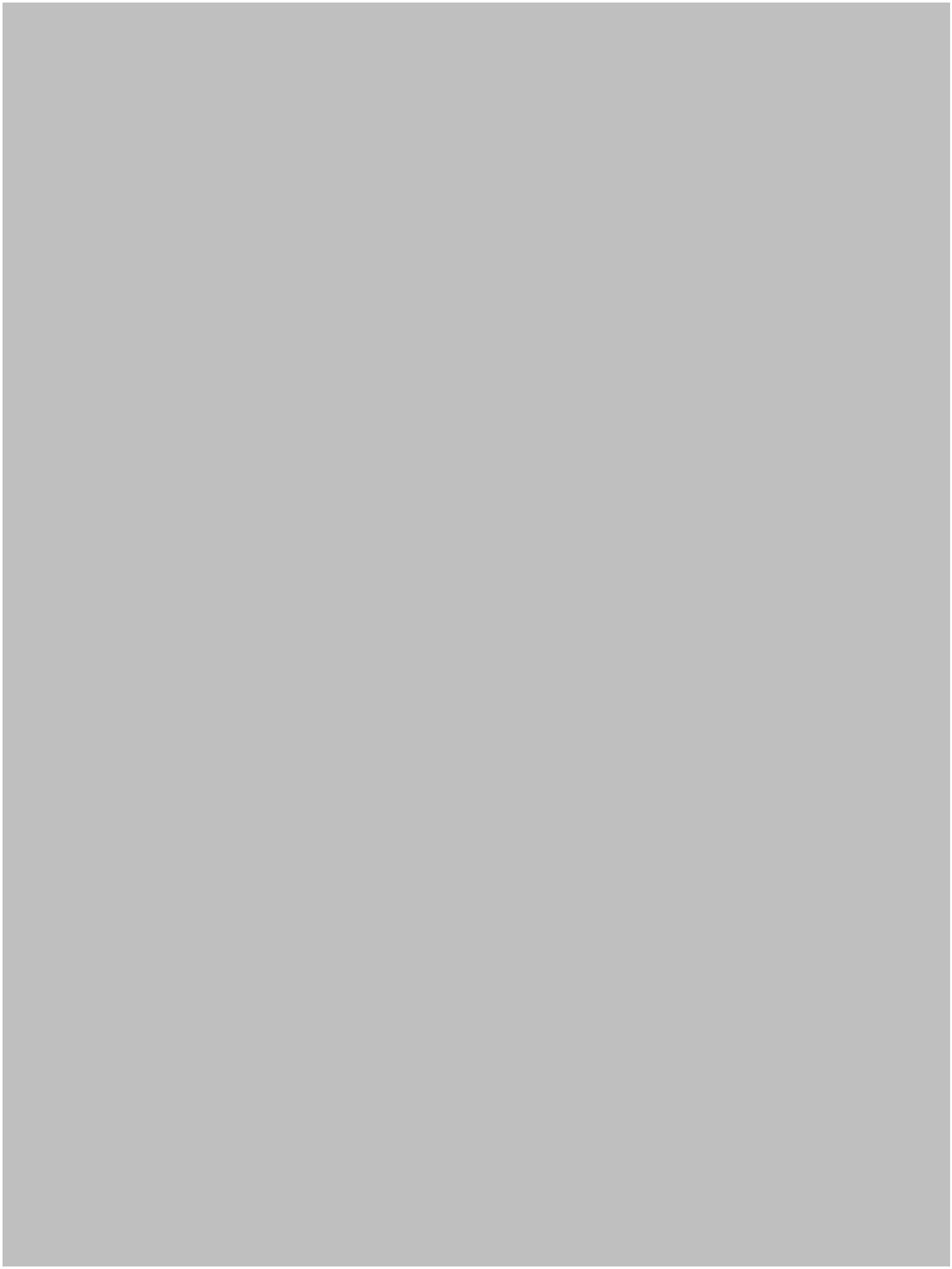

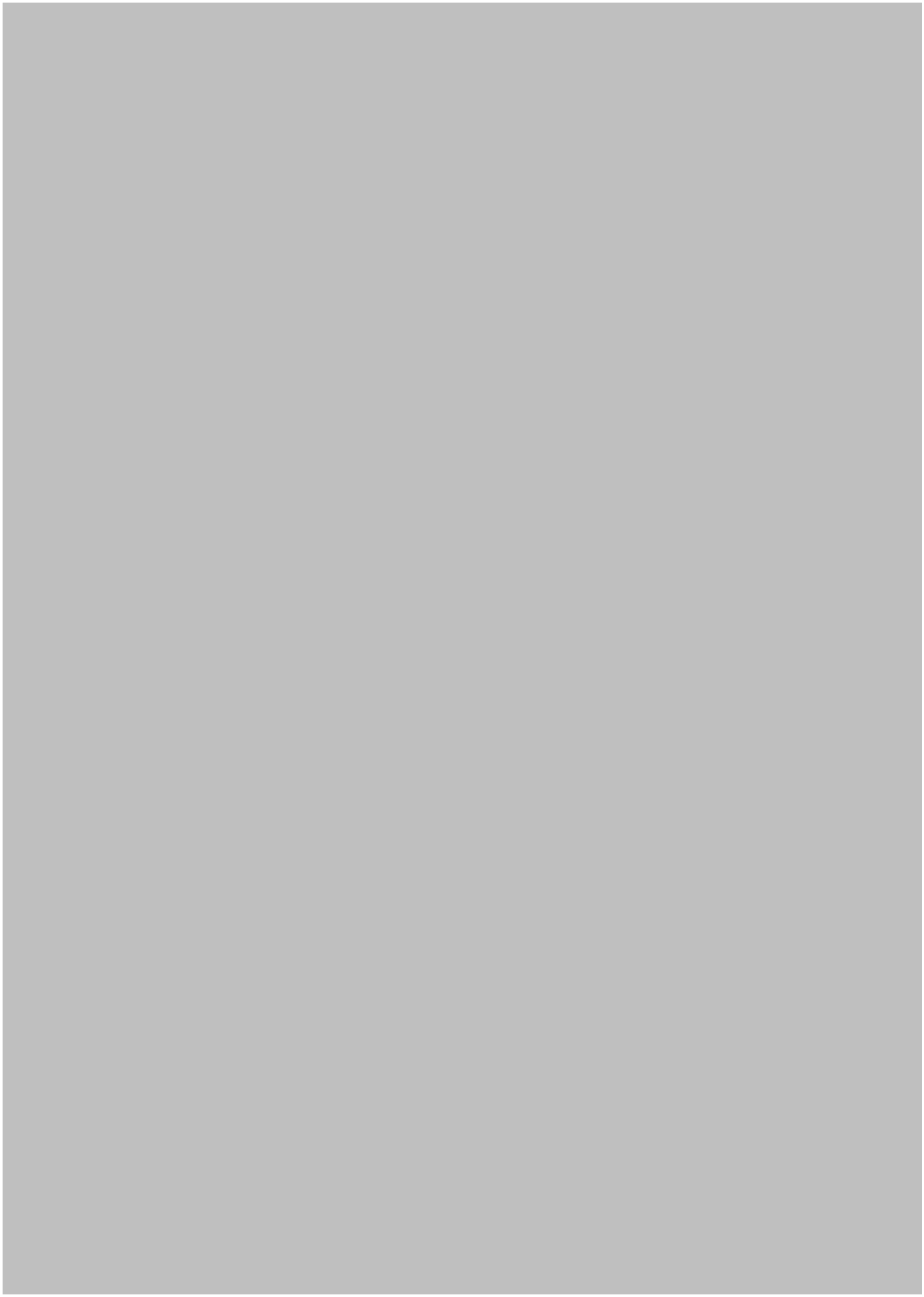

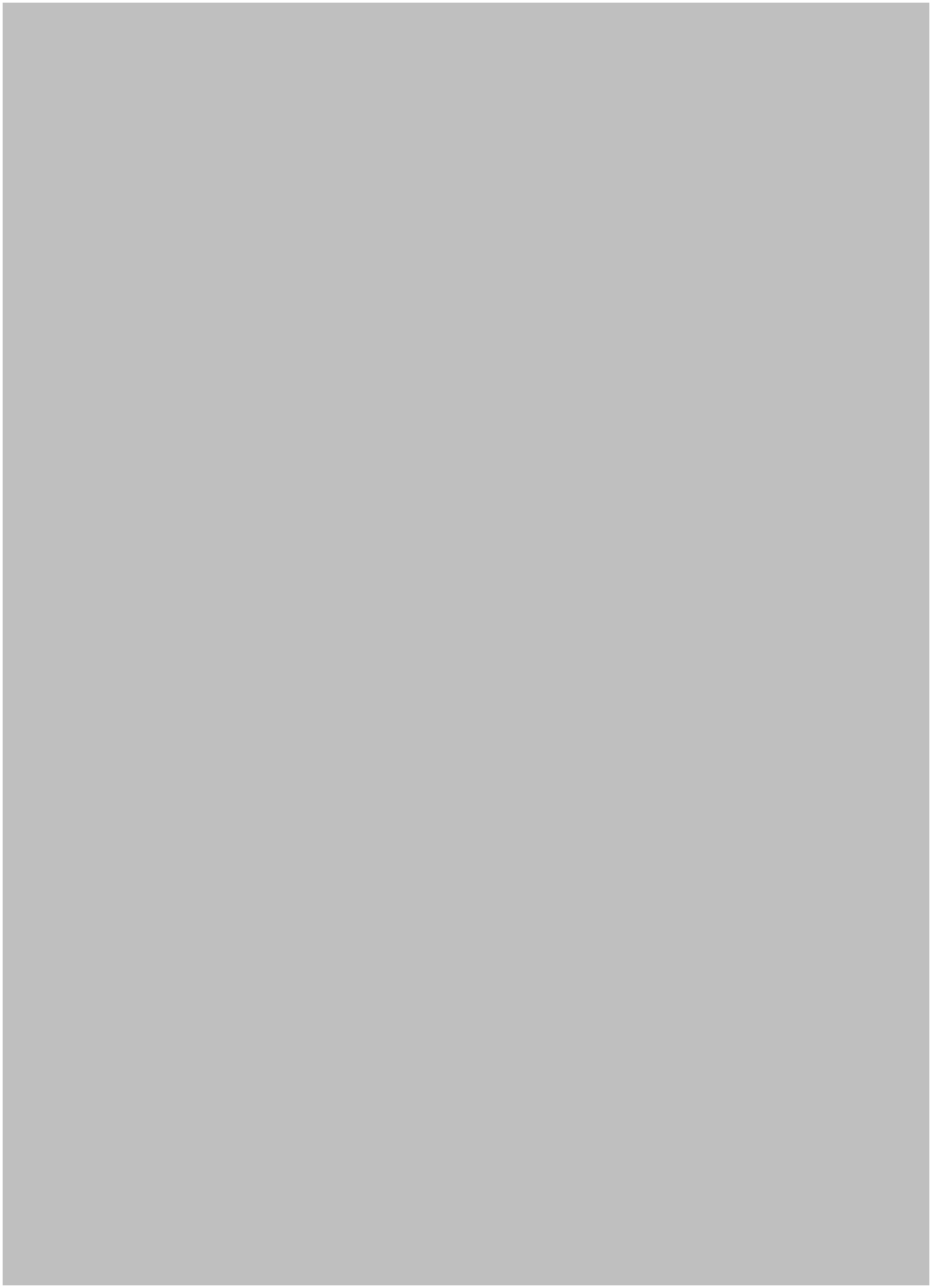

APPENDIX 4

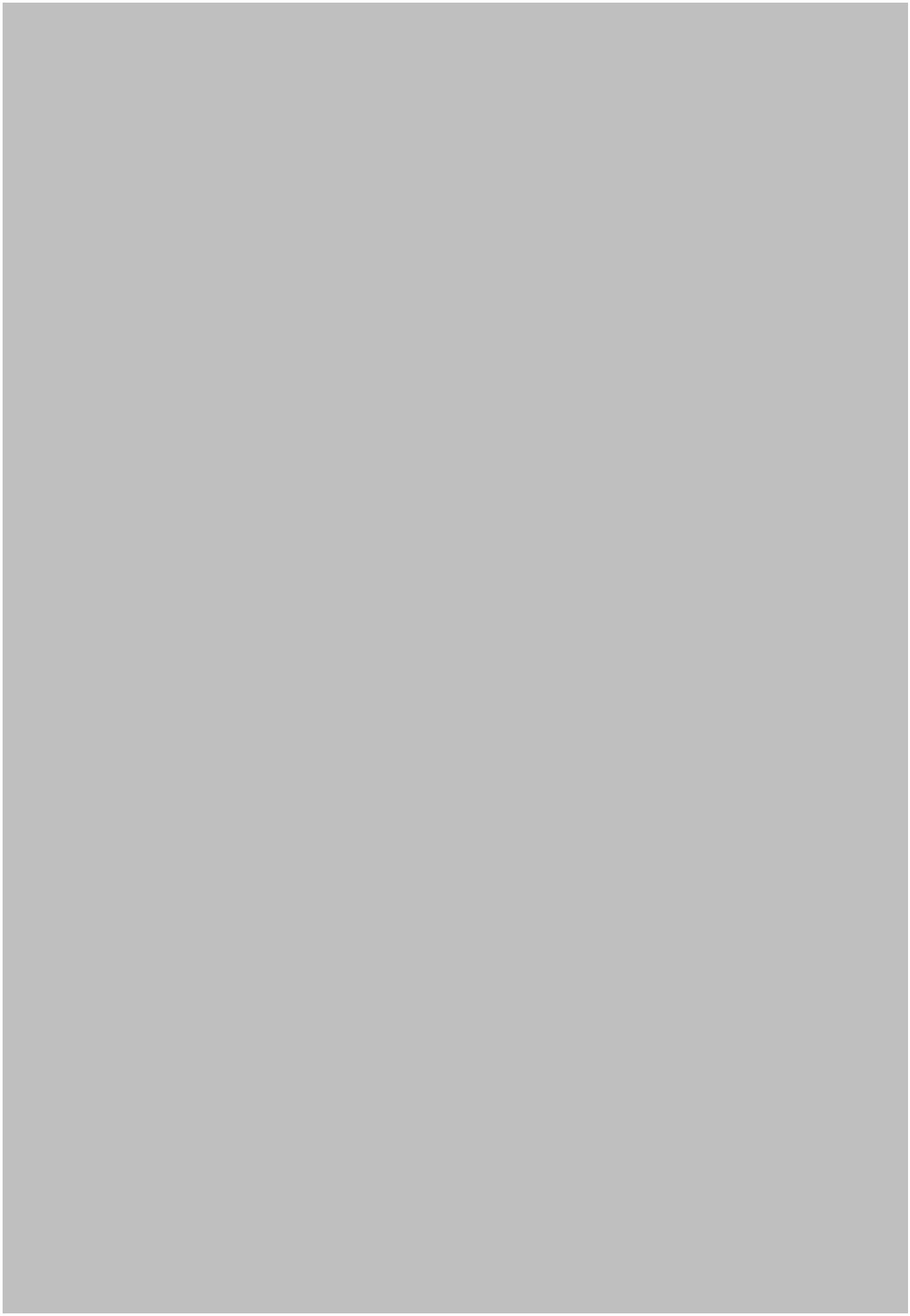

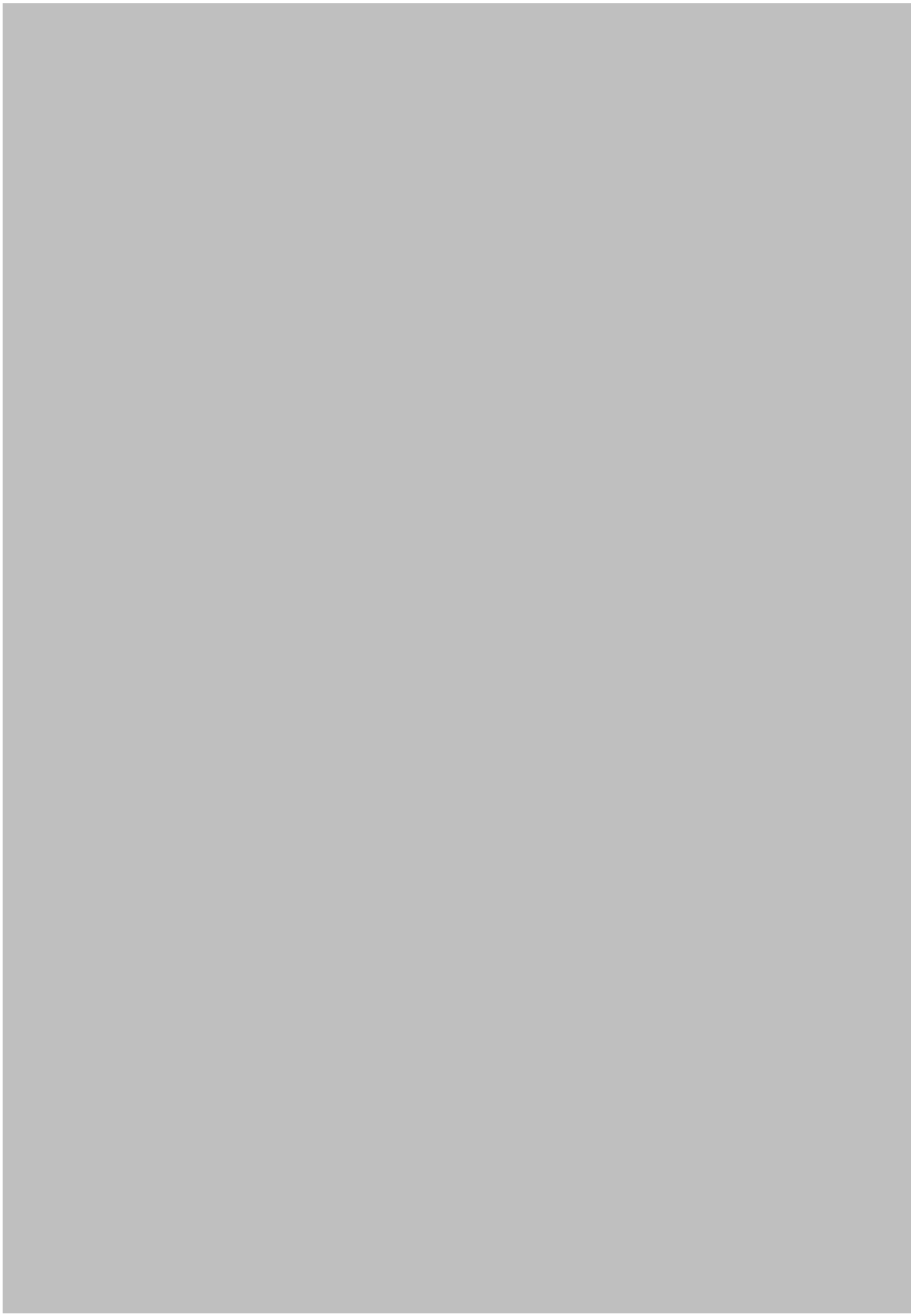

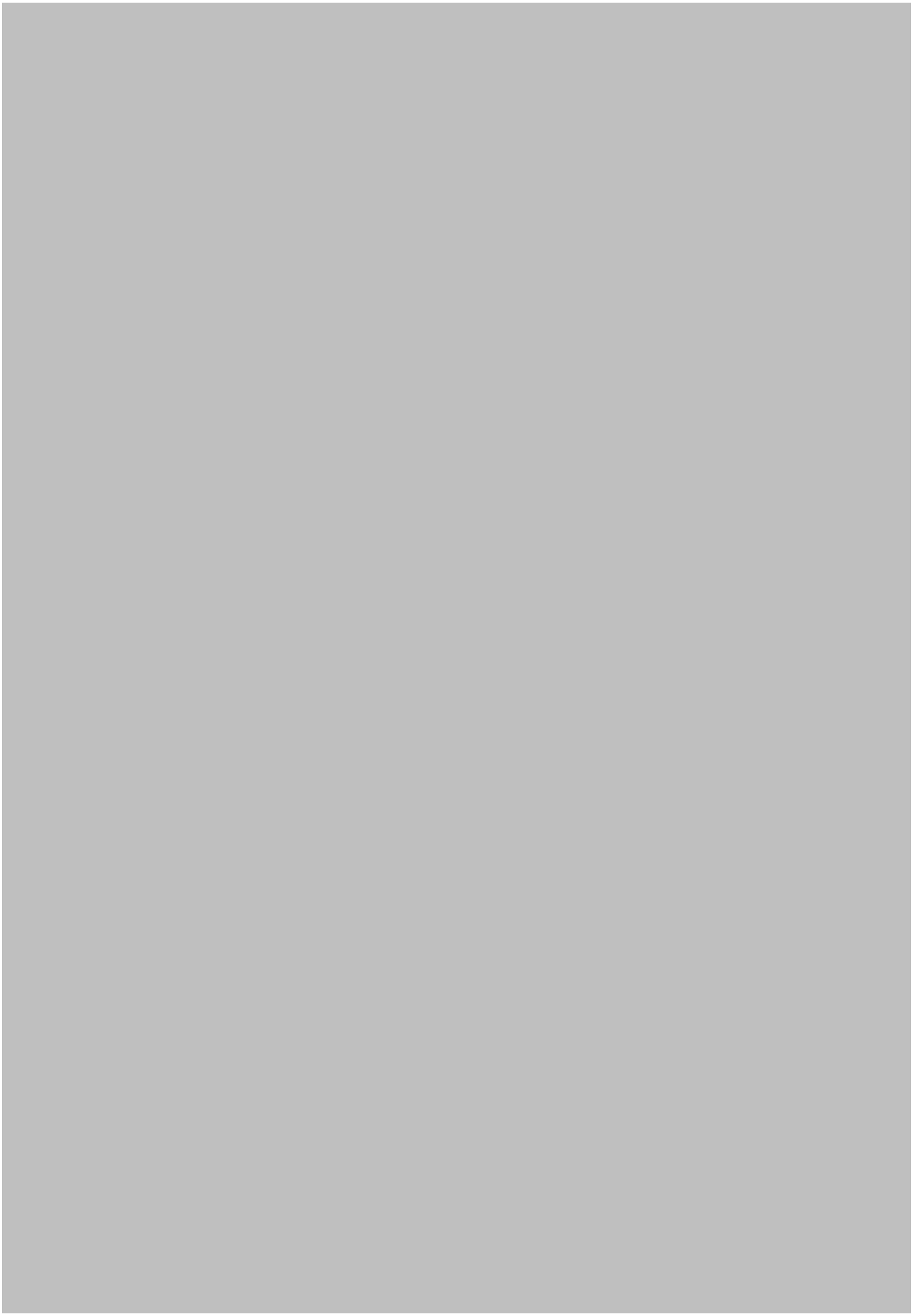

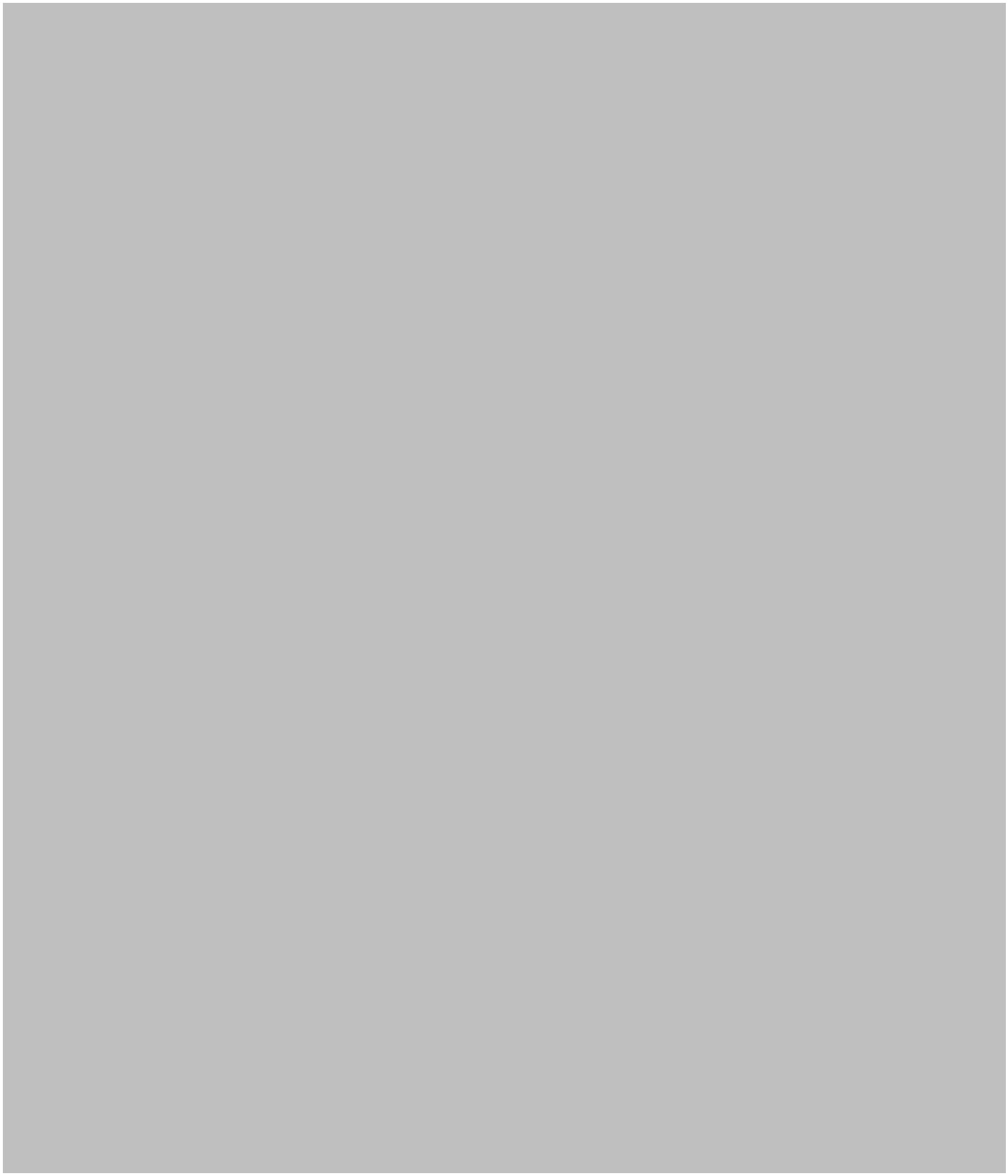

APPENDIX 5

Welcome to the Integrated Research Application System

IRAS Project Filter

The integrated dataset required for your project will be created from the answers you give to the following questions. The system will generate only those questions and sections which (a) apply to your study type and (b) are required by the bodies reviewing your study. Please ensure you answer all the questions before proceeding with your applications.

Please enter a short title for this project (maximum 70 characters)
Characterising commotio retinae: a retrospective study

1. Is your project research?

☐ Yes ☐ No

2. Select one category from the list below:

☐ Clinical trial of an investigational medicinal product
☐ Clinical investigation or other study of a medical device
☐ Combined trial of an investigational medicinal product and an investigational medical device
☐ Other clinical trial or clinical investigation
☐ Study administering questionnaires/interviews for quantitative analysis, or using mixed quantitative/qualitative methodology
☐ Study involving qualitative methods only
☐ Study limited to working with human tissue samples, other human biological samples and/or data *(specific project only)*
☐ Research tissue bank
☐ Research database

If your work does not fit any of these categories, select the option below:

☐ Other study

2a. Please answer the following question(s):

a) Will you be taking new samples primarily for research purposes (i.e. not surplus or existing stored samples)?	☐ Yes	☐ No
b) Will you be using surplus tissue or existing stored samples identifiable to the researcher?	☐ Yes	☐ No
c) Will you be using only surplus tissue or existing stored samples not identifiable to the researcher?	☐ Yes	☐ No
d) Will you be processing identifiable data at any stage of the research (including in the identification of participants)?	☐ Yes	☐ No

3. In which countries of the UK will the research sites be located?*(Tick all that apply)*

☐ England
☐ Scotland
☐ Wales
☐ Northern Ireland

3a. In which country of the UK will the lead NHS R&D office be located:

- England
- Scotland
- Wales
- Northern Ireland
- This study does not involve the NHS

4. Which review bodies are you applying to?

- NHS/HSC Research and Development offices
- Social Care Research Ethics Committee
- Research Ethics Committee
- National Information Governance Board for Health and Social Care (NIGB)
- Ministry of Justice (MoJ)
- National Offender Management System (NOMS)

4a. Will you be seeking data from Hospital Episode Statistics (HES) or the Secondary Uses Service (SUS)?

Yes No

5. Will any research sites in this study be NHS organisations?

Yes No

5a. Do you want your application to be processed through the NIHR Coordinated System for gaining NHS Permission?

Yes No

If yes, you must complete and submit the NIHR CSP Application Form immediately after completing this project filter, before proceeding with completing and submitting other applications.

6. Do you plan to include any participants who are children?

Yes No

7. Do you plan to include any participants who are adults unable to consent for themselves through physical or mental incapacity? *The guidance notes explain how an adult is defined for this purpose.*

Yes No

8. Do you plan to include any participants who are prisoners or young offenders in the custody of HM Prison Service or who are offenders supervised by the probation service in England or Wales?

Yes No

9. Is the study, or any part of the study, being undertaken as an educational project?

Yes No

9a. Is the project being undertaken in part fulfilment of a PhD or other doctorate?

Yes No

10. Is this project financially supported by the United States Department for Health and Human Services?

Yes No

11. Will identifiable patient data be accessed outside the clinical care team without prior consent at any stage of the project (including identification of potential participants)?

Yes No

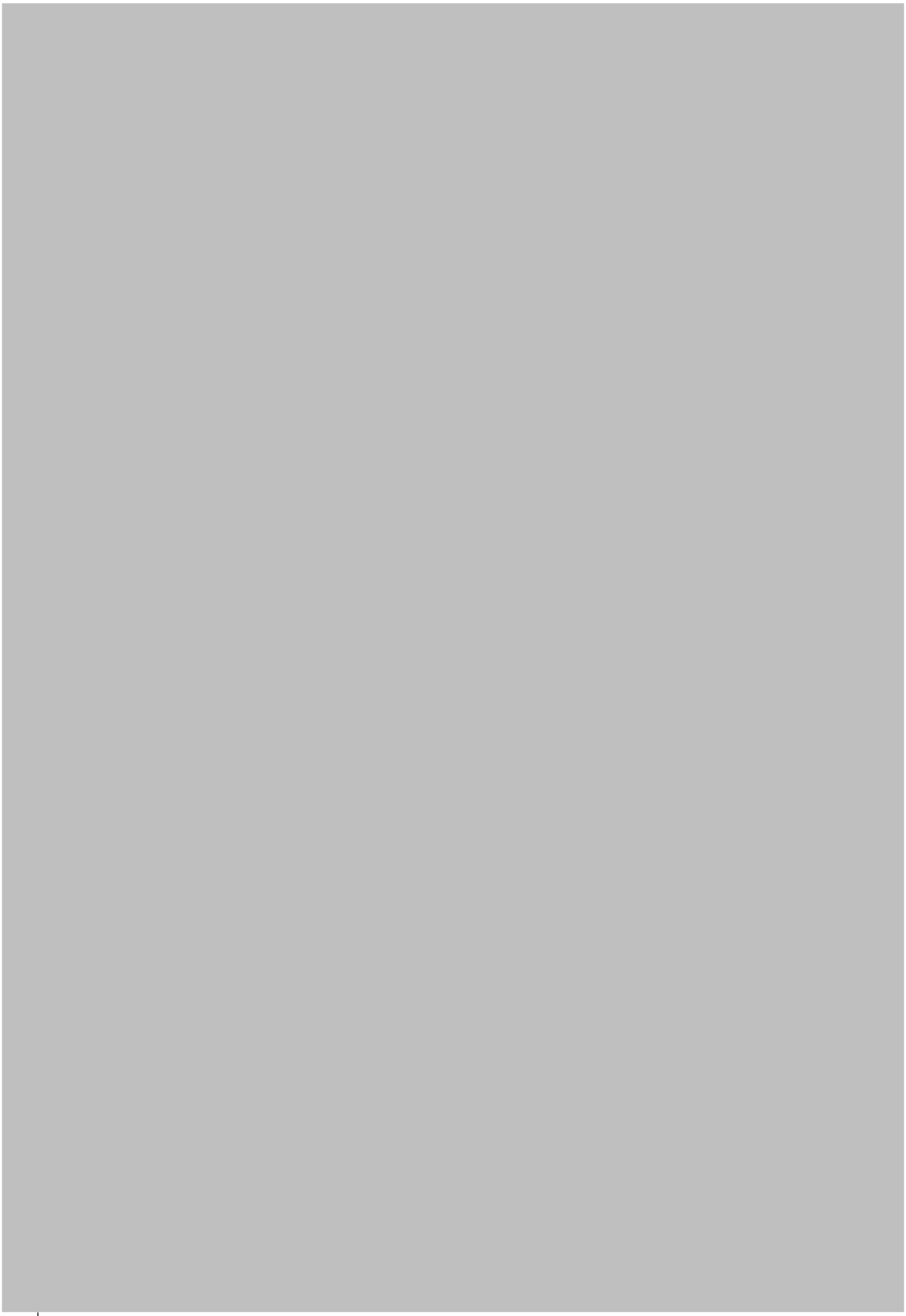

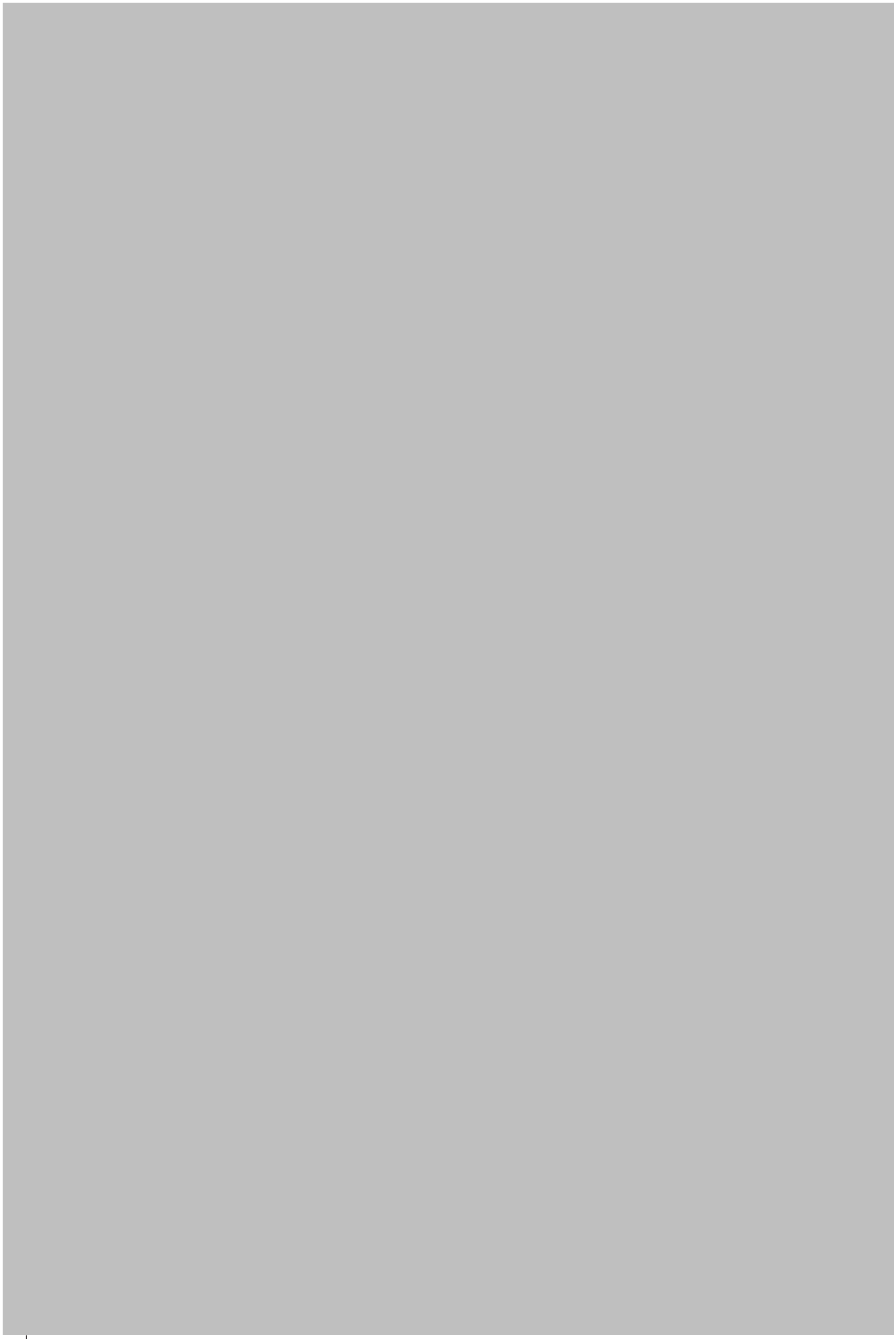

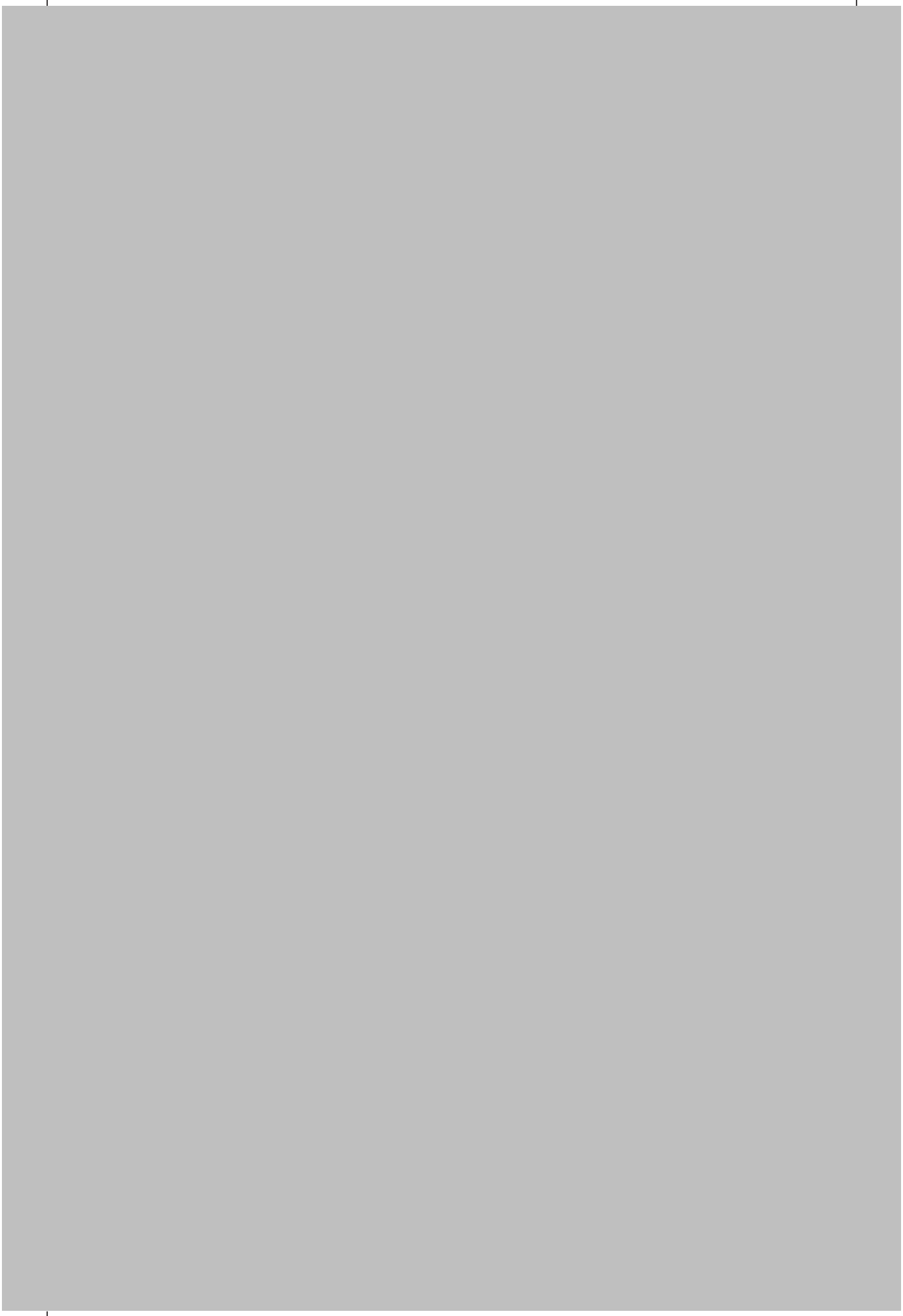

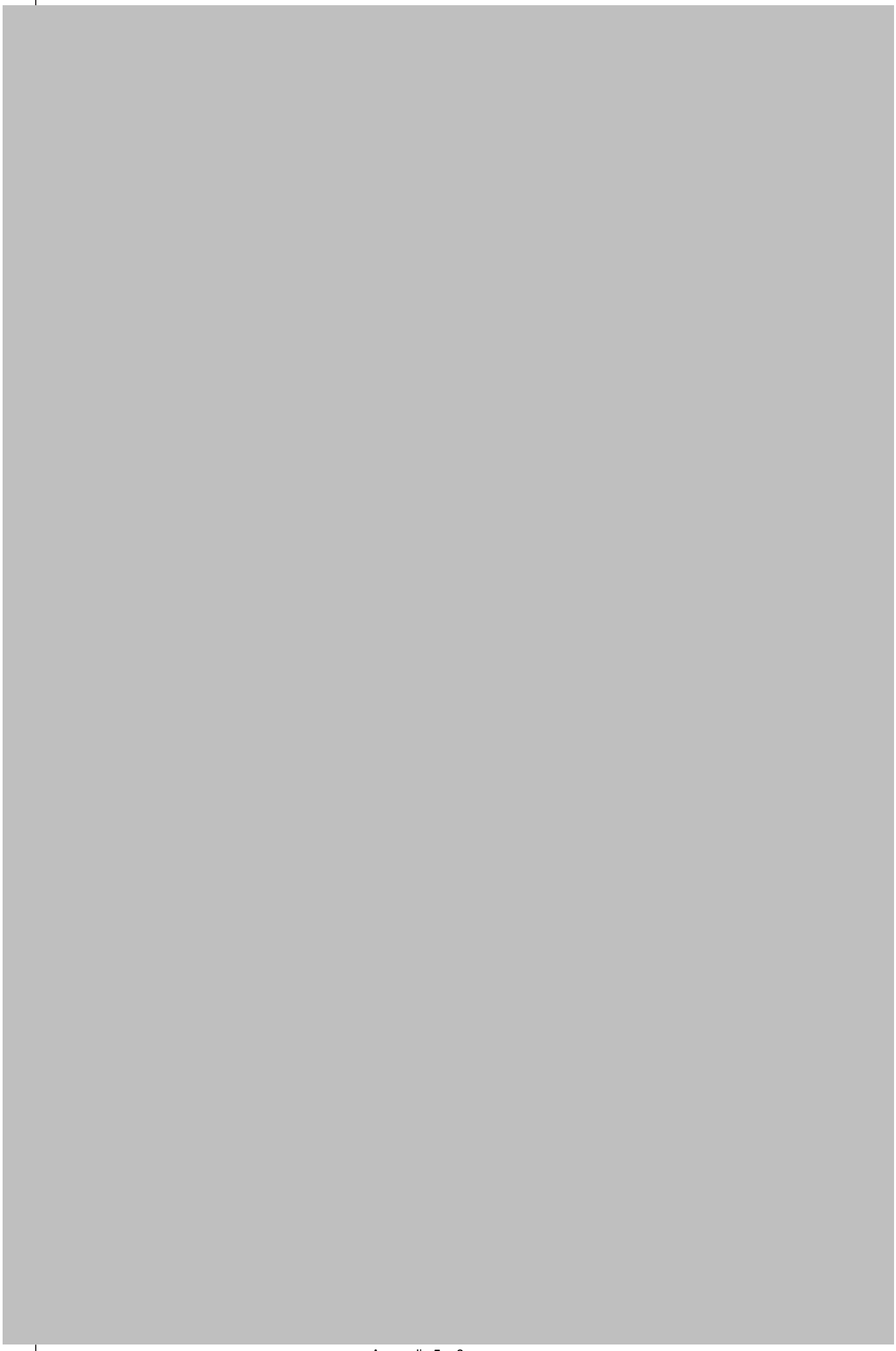

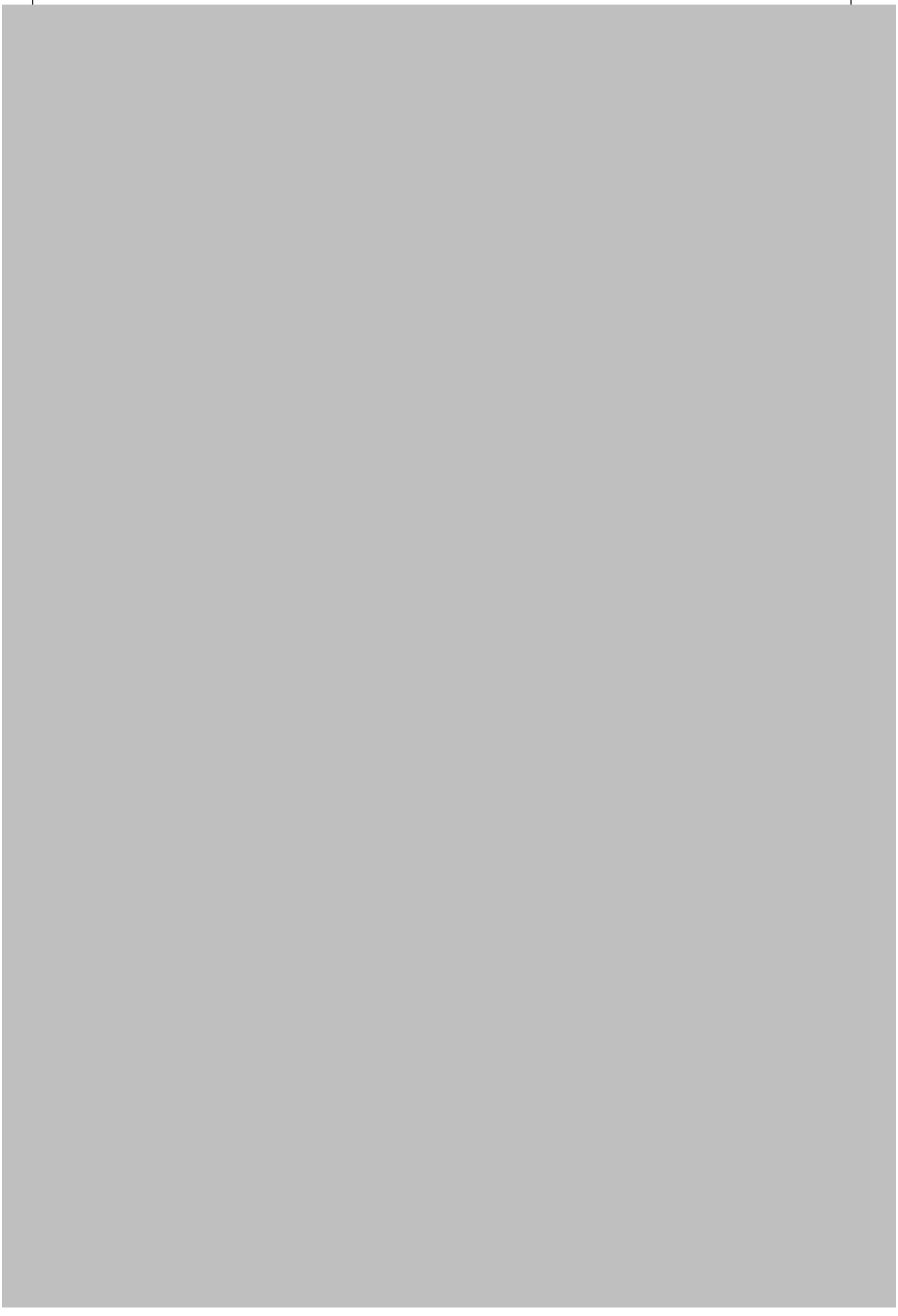

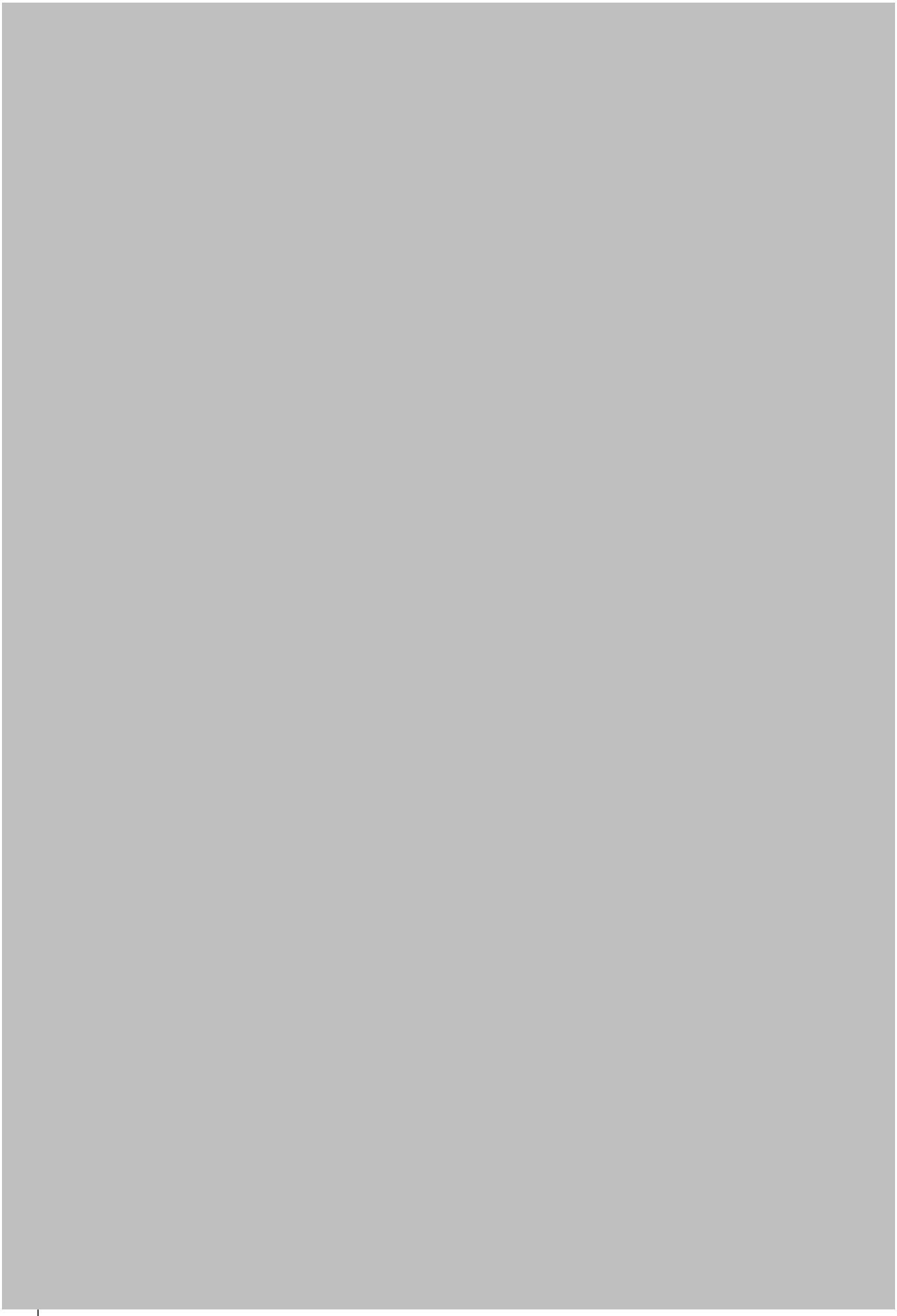

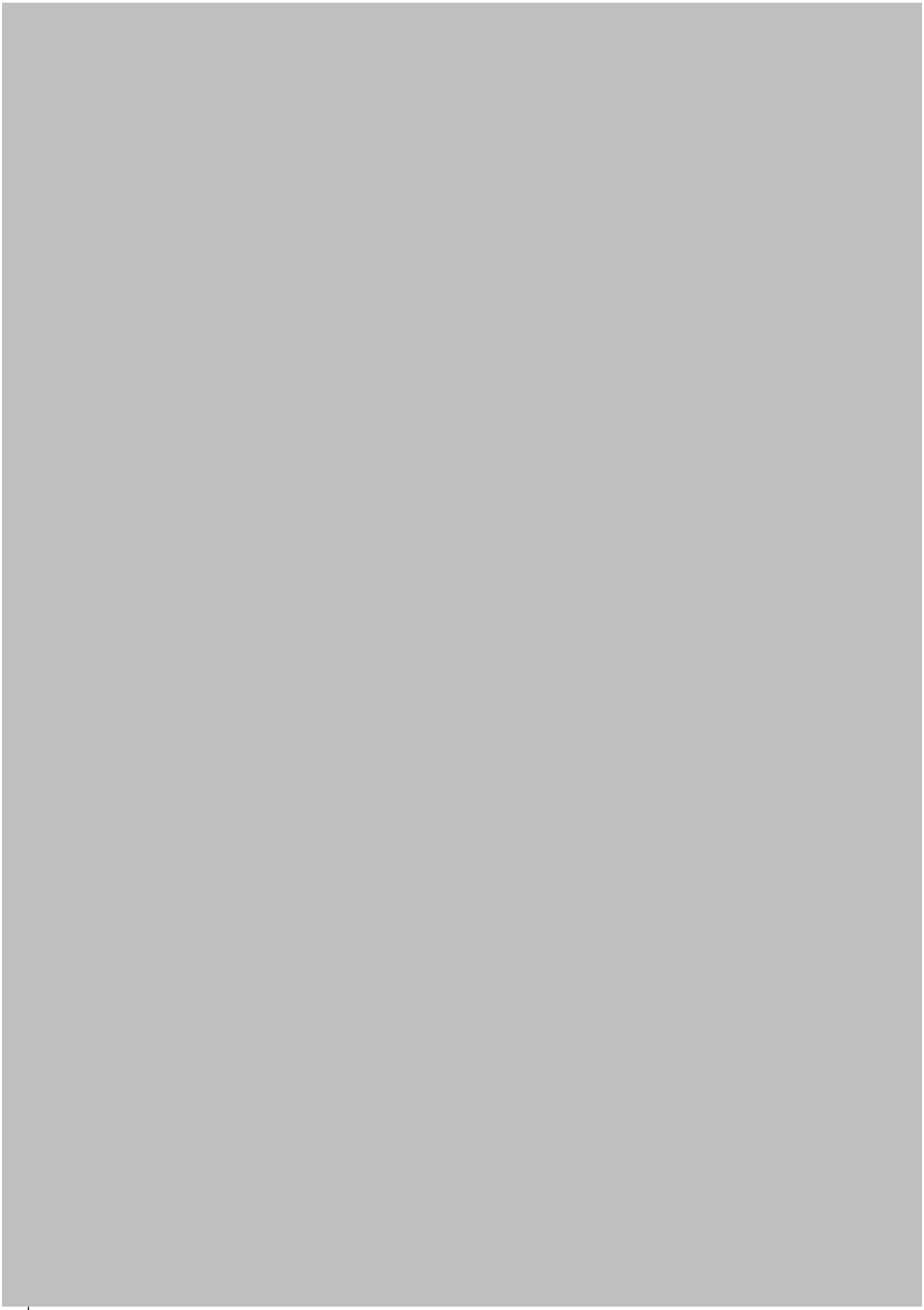

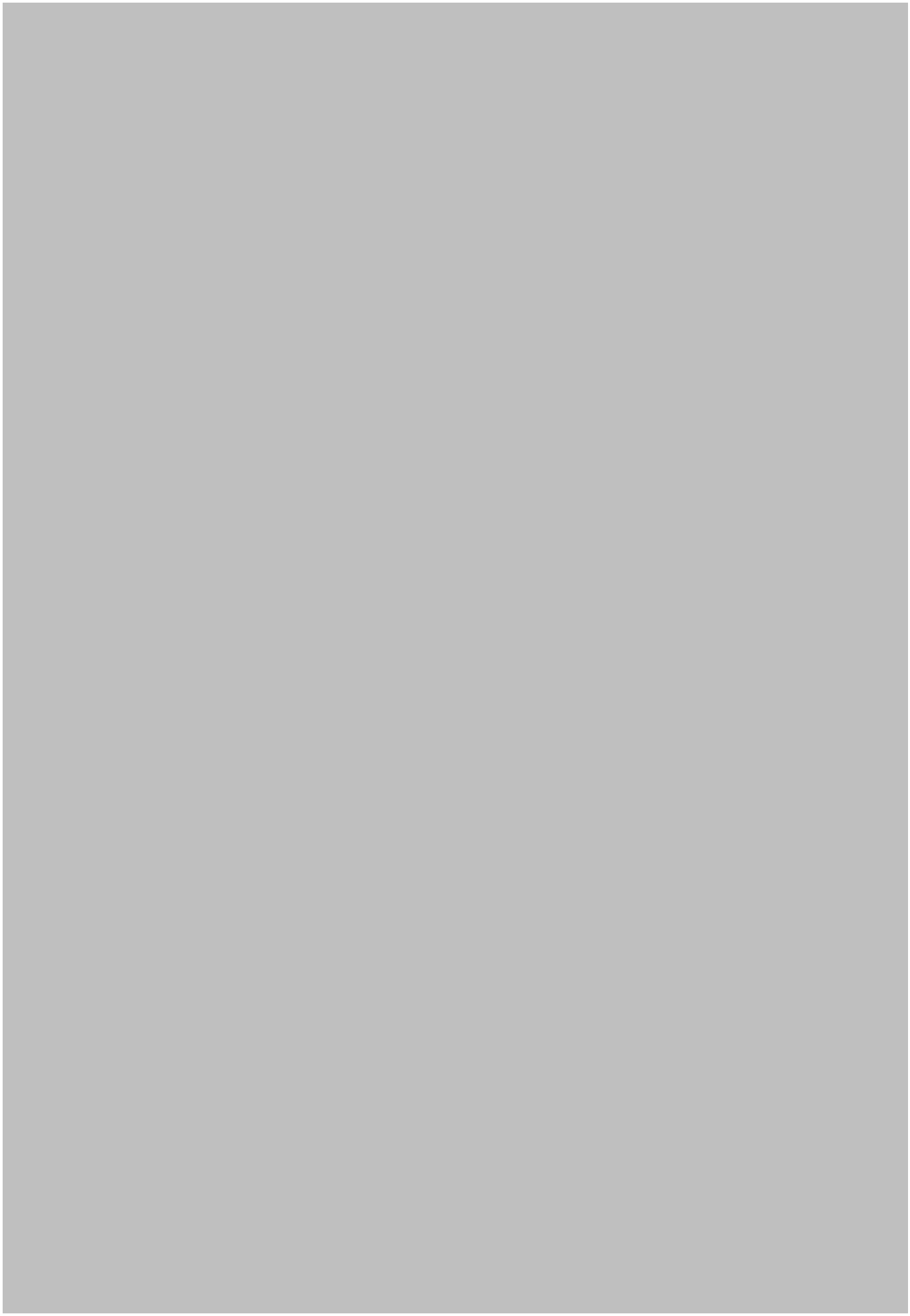

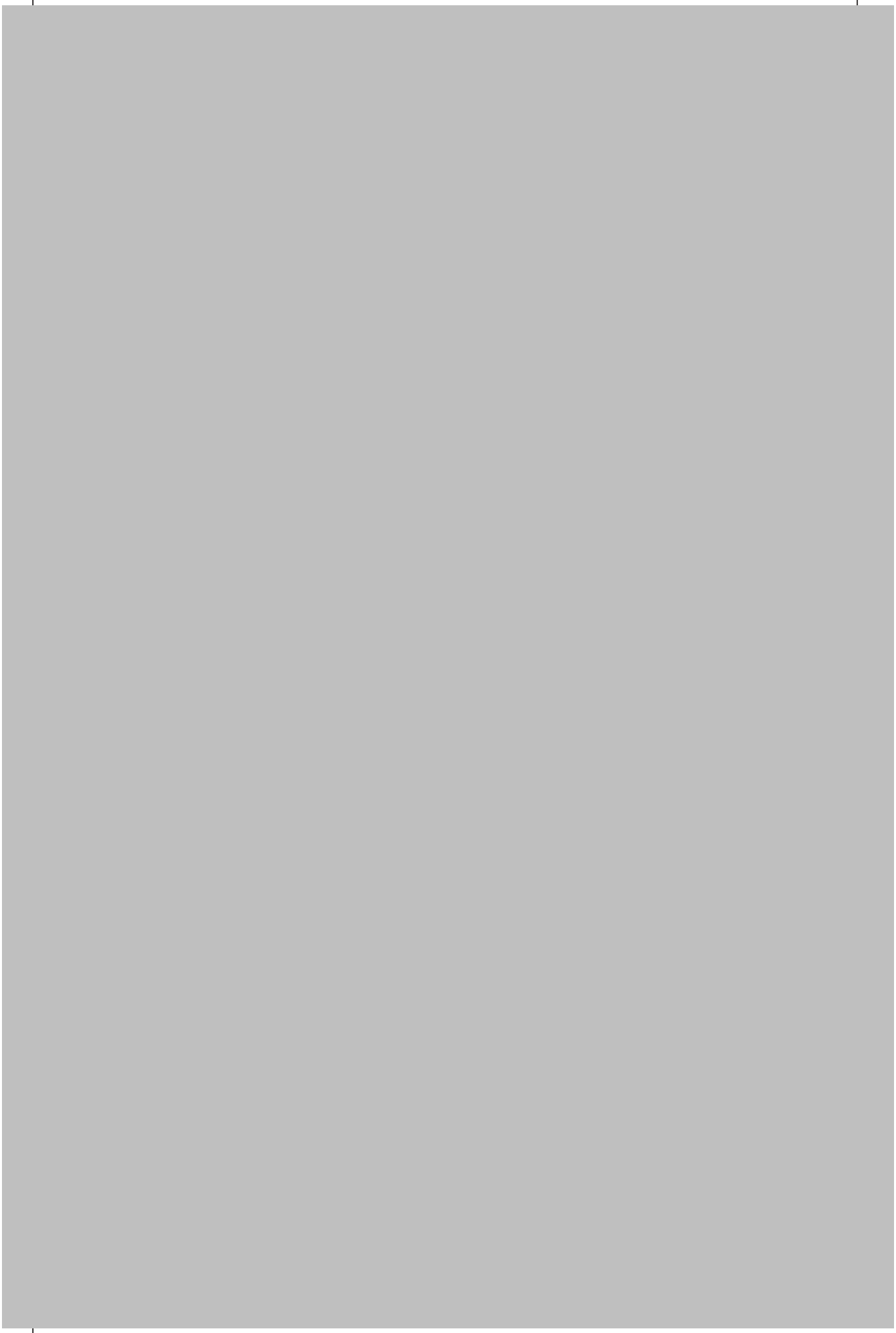

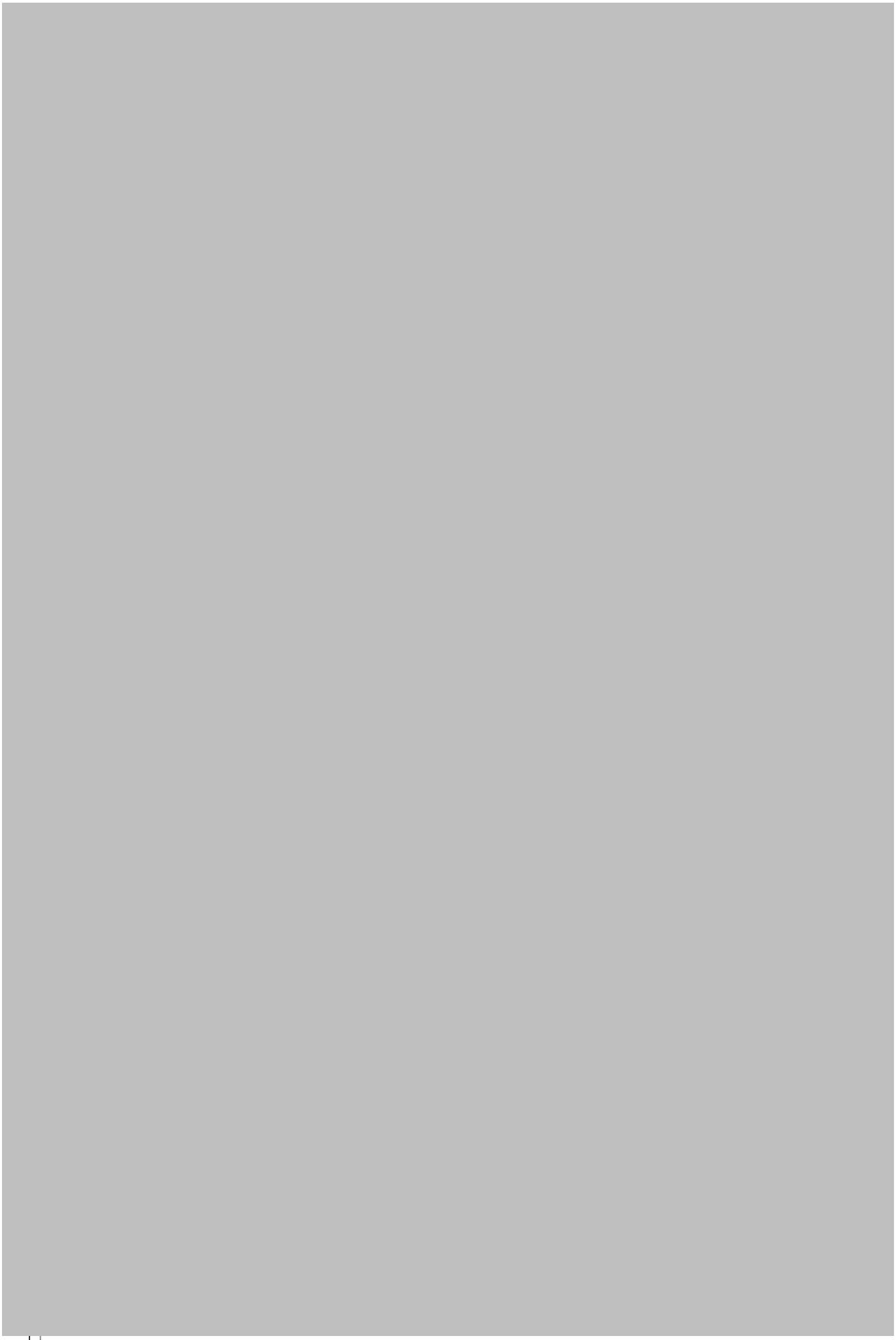

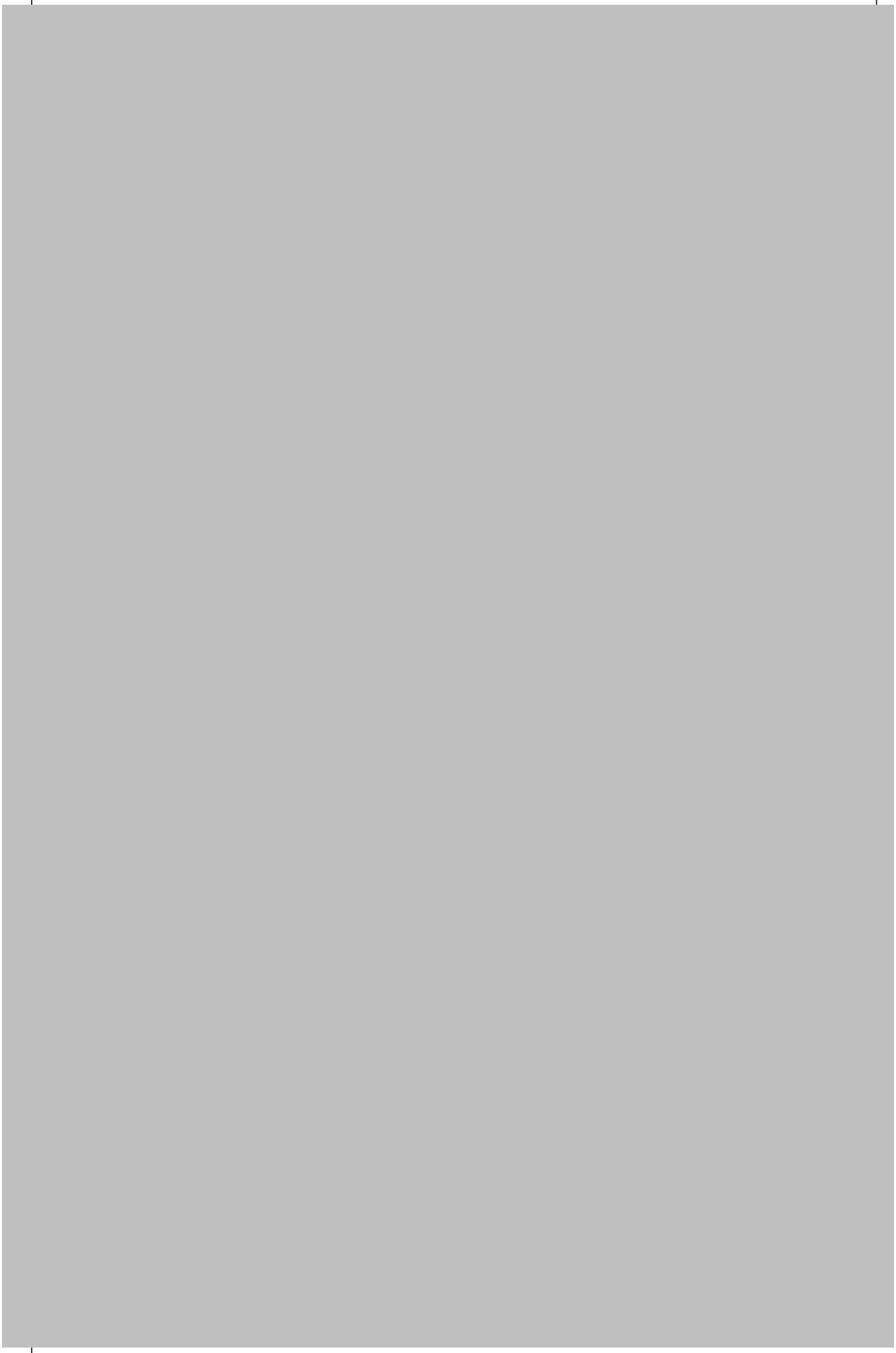

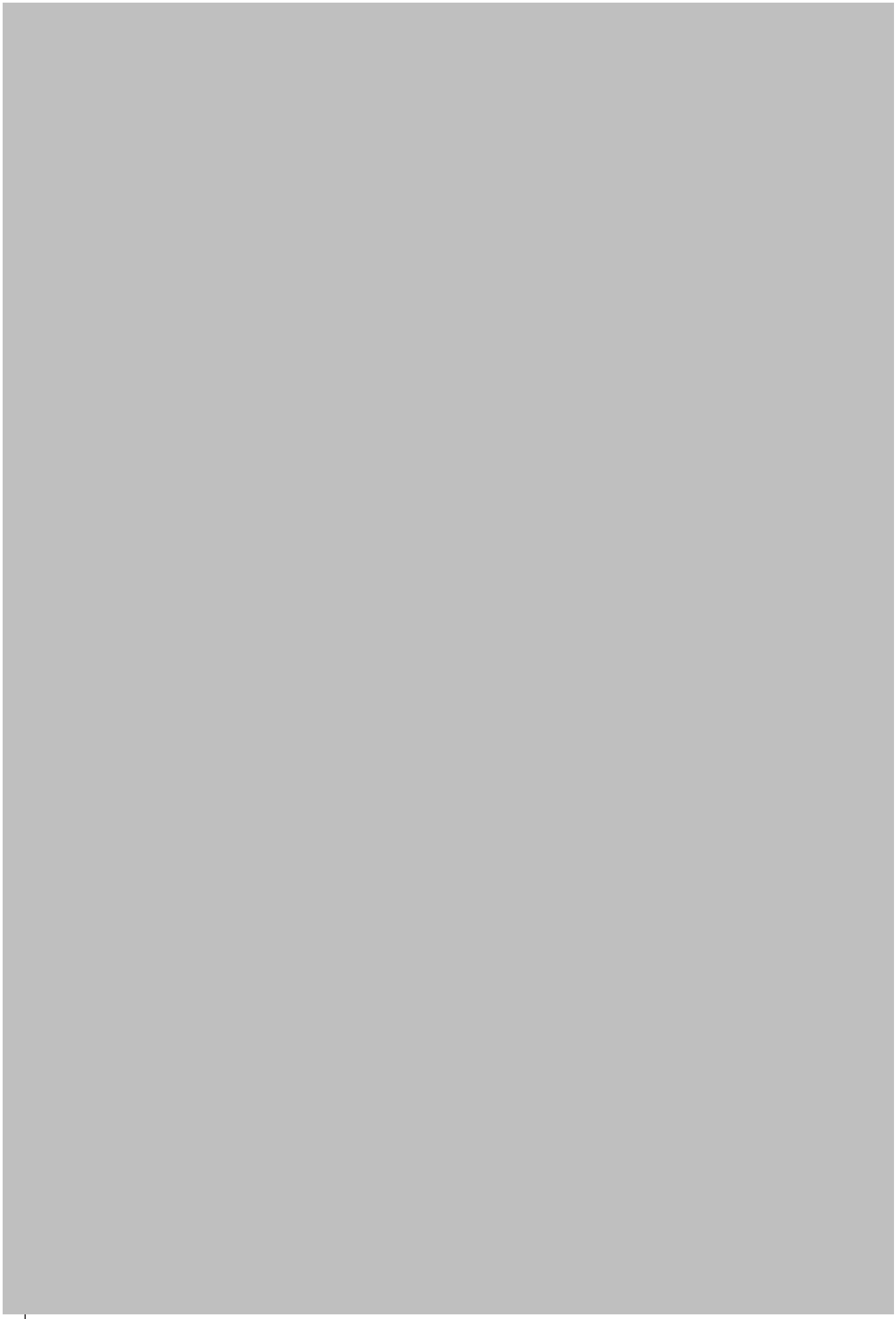

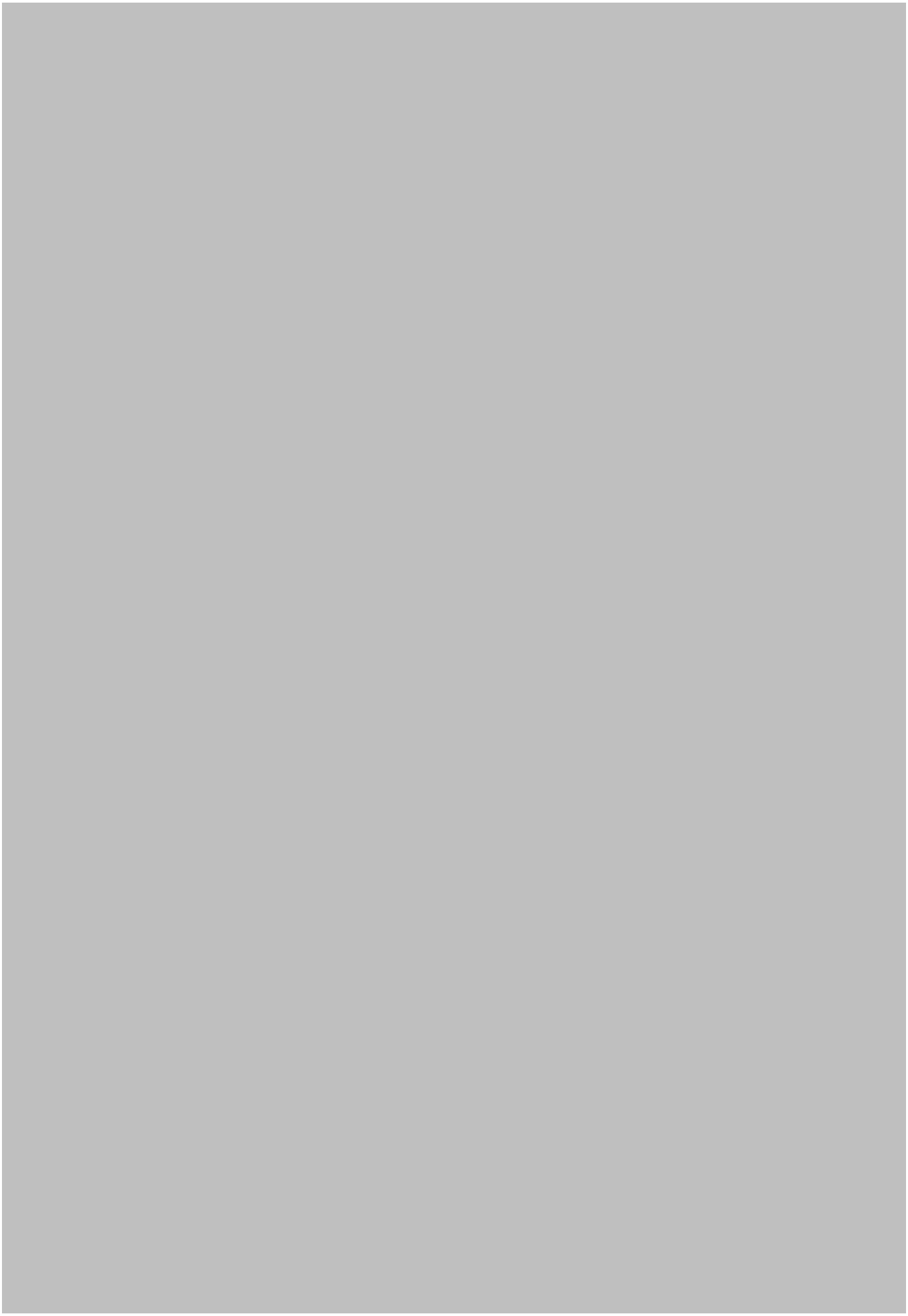

PART C: Overview of research sites

Please enter details of the host organisations (Local Authority, NHS or other) in the UK that will be responsible for the research sites. *For NHS sites, the host organisation is the Trust or Health Board. Where the research site is a primary care site, e.g. GP practice, please insert the host organisation (PCT or Health Board) in the Institution row and insert the research site (e.g. GP practice) in the Department row.*

Research site		Investigator/ Collaborator/ Contact	
Institution name	Sandwell and West Birmingham Hospitals NHS Trust	Title	Mr
Department name		First name/ Initials	Richard J
Street address	Dudley Road	Surname	Blanch
Town/city	Birmingham		
Post Code	B18 7QH		

PART D: Declarations

D1. Declaration by Chief Investigator

1. The information in this form is accurate to the best of my knowledge and belief and I take full responsibility for it.

2. I undertake to abide by the ethical principles underlying the Declaration of Helsinki and good practice guidelines on the proper conduct of research.

3. If the research is approved I undertake to adhere to the study protocol, the terms of the full application as approved and any conditions set out by review bodies in giving approval.

4. I undertake to notify review bodies of substantial amendments to the protocol or the terms of the approved application, and to seek a favourable opinion from the main REC before implementing the amendment.

5. I undertake to submit annual progress reports setting out the progress of the research, as required by review bodies.

6. I am aware of my responsibility to be up to date and comply with the requirements of the law and relevant guidelines relating to security and confidentiality of patient or other personal data, including the need to register when necessary with the appropriate Data Protection Officer. I understand that I am not permitted to disclose identifiable data to third parties unless the disclosure has the consent of the data subject or, in the case of patient data in England and Wales, the disclosure is covered by the terms of an approval under Section 251 of the NHS Act 2006.

7. I understand that research records/data may be subject to inspection by review bodies for audit purposes if required.

8. I understand that any personal data in this application will be held by review bodies and their operational managers and that this will be managed according to the principles established in the Data Protection Act 1998.

9. I understand that the information contained in this application, any supporting documentation and all correspondence with review bodies or their operational managers relating to the application:

    - Will be held by the main REC or the GTAC (as applicable) until at least 3 years after the end of the study; and by NHS R&D offices (where the research requires NHS management permission) in accordance with the NHS Code of Practice on Records Management.
    - May be disclosed to the operational managers of review bodies, or the appointing authority for the main REC, in order to check that the application has been processed correctly or to investigate any complaint.
    - May be seen by auditors appointed to undertake accreditation of RECs.
    - Will be subject to the provisions of the Freedom of Information Acts and may be disclosed in response to requests made under the Acts except where statutory exemptions apply.

10. I understand that information relating to this research, including the contact details on this application, may be held on national research information systems, and that this will be managed according to the principles established in the Data Protection Act 1998.

11. I understand that the summary of this study will be published on the website of the National Research Ethics Service (NRES), together with the contact point for enquiries named below. Publication will take place no earlier than 3 months after issue of the ethics committee's final opinion or the withdrawal of the application.

Contact point for publication*(Not applicable for R&D Forms)*

NRES would like to include a contact point with the published summary of the study for those wishing to seek further information. We would be grateful if you would indicate one of the contact points below.

- [ ] Chief Investigator
- [ ] Sponsor
- [ ] Study co-ordinator

☐ Student

☐ Other – please give details

☐ None

Access to application for training purposes *(Not applicable for R&D Forms)*

Optional – please tick as appropriate:

☐ I would be content for members of other RECs to have access to the information in the application in confidence for training purposes. All personal identifiers and references to sponsors, funders and research units would be removed.

This section was signed electronically by Mr Richard Blanch on 12/11/2010 09:35.

Job Title/Post:	Specialty Registrar in Ophthalmology
Organisation:	Sandwell and West Birmingham Hospitals NHS Trust
Email:	richard.blanch@tiscali.co.uk
Signature:	.....
Print Name:	Richard Blanch
Date:	11/11/2010 *(dd/mm/yyyy)*

D2. Declaration by the sponsor's representative

If there is more than one sponsor, this declaration should be signed on behalf of the co−sponsors by a representative of the lead sponsor named at A64-1.

I confirm that:

1. This research proposal has been discussed with the Chief Investigator and agreement in principle to sponsor the research is in place.

2. An appropriate process of scientific critique has demonstrated that this research proposal is worthwhile and of high scientific quality.

3. Any necessary indemnity or insurance arrangements, as described in question A76, will be in place before this research starts. Insurance or indemnity policies will be renewed for the duration of the study where necessary.

4. Arrangements will be in place before the study starts for the research team to access resources and support to deliver the research as proposed.

5. Arrangements to allocate responsibilities for the management, monitoring and reporting of the research will be in place before the research starts.

6. The duties of sponsors set out in the Research Governance Framework for Health and Social Care will be undertaken in relation to this research.

7. I understand that the summary of this study will be published on the website of the National Research Ethics Service (NRES), together with the contact point for enquiries named in this application. Publication will take place no earlier than 3 months after issue of the ethics committee's final opinion or the withdrawal of the application.

Signature: .....

Print Name: Prof Carl Clarke

Post: Professor of Clinical Neurology & Director of Research and Development

Organisation: Sandwell and West Birmingham Hospitals NHS Trust

Date: *(dd/mm/yyyy)*

D3. Declaration for student projects by academic supervisor

1. I have read and approved both the research proposal and this application. I am satisfied that the scientific content of the research is satisfactory for an educational qualification at this level.

2. I undertake to fulfil the responsibilities of the Chief Investigator and the supervisor for this study as set out in the Research Governance Framework for Health and Social Care.

3. I take responsibility for ensuring that this study is conducted in accordance with the ethical principles underlying the Declaration of Helsinki and good practice guidelines on the proper conduct of research, in conjunction with clinical supervisors as appropriate.

4. I take responsibility for ensuring that the applicant is up to date and complies with the requirements of the law and relevant guidelines relating to security and confidentiality of patient and other personal data, in conjunction with clinical supervisors as appropriate.

This section was signed electronically by Mr Robert Scott on 13/11/2010 10:58.

Job Title/Post:	Consultant Ophthalmologist
Organisation:	Birmingham and Midland Eye Centre
Email:	rahscott@btinternet.com

APPENDIX 6

Neuroretinal Cell Death in a Murine Model of Closed Globe Injury: Pathological and Functional Characterization

Richard J. Blanch,[1,2] *Zubair Ahmed,*[1] *Attila Sik,*[1] *David R. J. Snead,*[3] *Peter A. Good,*[4] *Jenna O'Neill,*[1] *Martin Berry,*[1] *Robert A. H. Scott,*[2,4,5] *and Ann Logan*[1,5]

Purpose. Blunt ocular trauma causes severe retinal injury with death of neuroretinal tissue, scarring, and permanent visual loss. The mechanisms of cell death are not known, and there are no therapeutic interventions that improve visual outcome. We aimed to study the extent, distribution, and functional consequences of cell death by developing and characterizing a rat model of retinal injury caused by blunt ocular trauma.

Methods. The eyes of anesthetized adult rats were injured by either weight drop or low-velocity ballistic trauma and assessed by clinical examination, electroretinography, light microscopy, electron microscopy, and TUNEL. Projectile velocity was measured and standardized.

Results. Weight drop did not cause reproducible retinal injury, and the energy threshold for retinal injury was similar to that for rupture. Low-velocity ballistic trauma to the inferior sclera created a reproducible retinal injury, with central sclopetaria retinae, retinal necrosis, and surrounding commotio retinae with specific photoreceptor cell death and sparing of cells in the other retinal layers. The extent of photoreceptor cell death declined and necrosis progressed to apoptosis with increasing distance from the impact site.

Conclusions. This is the only murine model of closed globe injury and the only model of retinal trauma with specific photoreceptor cell death. The clinical appearance mirrors that in severe retinal injury after blunt ocular trauma in humans, and the ultrastructural features are consistent with human and animal studies of commotio retinae. After ocular trauma, photoreceptor apoptosis may be prevented and visual outcomes improved by blocking of the cell death pathways. (*Invest Ophthalmol Vis Sci.* 2012;53:7220–7226) DOI: 10.1167/iovs.12-9887

From the [1]Neurotrauma and Neurodegeneration Section, Clinical and Experimental Medicine, University of Birmingham, Birmingham, United Kingdom; the [2]Academic Department of Military Surgery and Trauma, Royal Centre for Defence Medicine, Birmingham, United Kingdom; the [3]University Hospitals Coventry and Warwickshire NHS Trust, Coventry, United Kingdom; and the [4]Birmingham and Midland Eye Centre, Birmingham, United Kingdom.

[5]These authors are joint senior authors.

Supported by the Ministry of Defence, United Kingdom; the Drummond Foundation, United Kingdom; and the Sir Ian Fraser Foundation, Blind Veterans UK.

Submitted for publication March 20, 2012; revised July 28, 2012; accepted September 11, 2012.

Disclosure: **R.J. Blanch**, None; **Z. Ahmed**, None; **A. Sik**, None; **D.R.J. Snead**, None; **P.A. Good**, None; **J. O'Neill**, None; **M. Berry**, None; **R.A.H. Scott**, None; **A. Logan**, None

Corresponding author: Richard J. Blanch, Molecular Neuroscience Research Group, IBR West (2nd Floor), Medical School, University of Birmingham, Edgbaston, Birmingham B15 2TT, United Kingdom; rjb017@bham.ac.uk.

Ocular trauma affects 20% of Americans during their lifetime, and 0.6% to 1% of these suffer retinal injury.[1–3] Personnel in war zones are at much higher risk, and up to 13% of soldiers wounded in action sustain an ocular injury, of whom 50% to 60% have retinal injuries.[4,5] Retinal trauma occurs with penetrating and perforating globe injuries, ruptures, and contusion-type closed globe injuries including those caused by blast.[6,7]

Retinal injury caused by blunt trauma is characterized clinically as commotio retinae (Berlin's edema) or the more severe sclopetaria retinae.[8,9] Commotio retinae describes gray-white opacification of the neuroretina caused by blunt ocular trauma and covers a spectrum of injury from self-limiting to severe with permanent visual loss.[10,11] Commotio retinae has been modeled in pigs, rabbits, cats, and rhesus and owl monkeys, demonstrating traumatic disruption of the photoreceptor outer segments,[12–14] which is also seen on optical coherence tomography (OCT) and fundus reflection densitometry in humans.[11,15] The outer segments are phagocytosed by retinal pigment epithelium (RPE) cells. The RPE becomes a multilayered disorganized structure, sometimes directly opposed to the inner segments.[14] Though photoreceptor cell death has been noted in animal models, the focus of previous studies was disruption and subsequent recovery of photoreceptor outer segments; the extent, distribution, and type of cell death have not been reported.[14,16] After severe blunt ocular trauma in humans, commotio retinae features disruption of the inner–outer segment junction and progresses to outer retinal atrophy with degeneration of photoreceptors.[17]

Rats are an ideal species in which to model ocular trauma due to the similarities of their retina with that of humans, the ready availability of antibodies for immunohistochemical studies, the low capital costs, and the ease of husbandry and surgical interventions.[12] Previous animal studies of commotio retinae used modified air guns or a catapult to deliver high-velocity (20-50 m/s) projectiles to the eye,[12] but such methods cannot precisely control and calibrate the energy delivered. For the pig, 0.49 J is sufficient to cause commotio retinae, and thus we hypothesized that a lower energy would be required in the smaller, more delicate rat eye.[12]

We report a rat model of retinal injury induced by low-energy blunt ocular trauma, which features commotio retinae and sclopetaria retinae with specific photoreceptor cell death. This correlates well with reported loss of the outer nuclear layer (ONL) observed by OCT in patients with long-term visual loss after commotio retinae.[17]

Materials and Methods

Animal Care and Procedures

Animal procedures were evaluated and licensed by the UK Home Office, approved by the University of Birmingham's Biomedical Ethics Review Sub-Committee, and conducted in accordance with the ARVO Statement

Investigative Ophthalmology & Visual Science, October 2012, Vol. 53, No. 11

for the Use of Animals in Ophthalmic and Vision Research. Female rats weighing 170 to 200 g were purchased from Charles River Laboratories (Margate, UK), kept on a 12-hour light/dark cycle with a daytime luminance of 80 lux, and fed and watered ad libitum (as in all our previous studies of central nervous system injury[18]). Wistar rats were used for studies of weight drop and Lister hooded rats for studies of ballistic injury, except where otherwise stated. All injuries were induced under general anesthesia with inhaled isofluorane in oxygen. For electron microscopy (EM) and terminal deoxynucleotidyl transferase-mediated dUTP nick-end labeling (TUNEL), animals were killed by perfusion with fixative under terminal anesthesia with intraperitoneal ketamine/medetomidine. Electroretinograms (ERG) were recorded under general anesthesia with intraperitoneal ketamine/medetomidine, and animals were killed by intraperitoneal overdose of pentobarbitone for retinal whole mounts.

Weight Drop Injury

Weights were dropped from a height of 50 cm onto the lateral sclera. Six groups of rats were injured by weight drop (2–6 eyes of 2–4 rats per group). Weights of 22.6 g (0.111 J) and 31.3 g (0.154 J) with 6 mm flat tips were dropped onto the central cornea, and rats were killed at 2 hours after injury. Weights of 17.6 g (0.086 J) and 23.0 g (0.113 J) with 3 mm flat tips and 22.6 and 31.3 g with 6 mm flat tips were dropped onto the lateral sclera, and animals were killed at 2 days after injury. To increase the energy of the weight drop method, a 7 cm doubled section of catapult latex (Match System superpower catapult latex; Middy Tackle International, Heanor, UK), stretched by 7 cm, was used to propel a 22.6 g/6 mm tip weight downward; animals were killed at 2 days after injury. Additional Lister hooded rats were injured with a 31.3 g weight/6 mm tip plus catapult latex. The catapult latex gave a measured impact energy of 0.6 J for both 22.6 and 31.3 g weights due to inefficiencies in the system. Velocity was calculated for weight drop as gravitational potential energy; the additional energy of the catapult latex was calculated by distance traveled when fired horizontally from a known height.

Ballistic Injury

Injury was created by firing a dome-headed (air gun pellet) or spherical (ball bearing) weight down a 5.5 × 300 mm steel barrel using compressed air held in a 500 mL reservoir with pressure monitoring, released by a solenoid-actuated valve (response time <5 ms, flow coefficient [Cv] 491 NL/min; SMC Pneumatics, Milton Keynes, UK). Projectiles were plastic ball bearings (0.095 g), plastic 0.22-caliber pellets (0.5 g), and metal 0.22-caliber air gun pellets (0.91 g). Projectile velocity was measured using a PC sound card.[19] Briefly, a Dell Studio XPS (Dell Corporation Ltd., Berkshire, UK) laptop was used to record the sound of the compressed air device being fired using MAGIX Music Editor 3 (MAGIX AG, Reno, NV) at a metal plate at known distance from the muzzle. The resultant waveform was then viewed and the time between air first leaving the barrel and the impact with the metal plate recorded at 1, 10.5, 22, 31.5, and 42 cm for 10 iterations at each distance. Mean velocity was calculated at the different time points.

Wistar rats ($n = 13$ rats, 26 eyes) were used for cadaveric studies to determine the risk of rupture. Female Lister hooded rats were used to study the effects of a 0.095 g projectile delivered at 20 m/s to the sclera: (1) bilaterally for EM studies before killing at 2 hours (lateral scleral impact; $n = 4$ animals), 2 days (inferior scleral impact; $n = 4$ animals), and 14 days (inferior scleral impact; $n = 4$ animals) after injury; (2) unilaterally to inferior sclera for TUNEL and immunohistochemical studies before killing at 2 days ($n = 4$ animals); and (3) unilaterally to inferior sclera for ERG studies and retinal whole mounts before killing at 2 weeks ($n = 8$ animals).

In Vivo Imaging

Animals were examined immediately after injury, at 2 days, and at 14 days by indirect ophthalmoscopy.

Electroretinography

ERG were recorded (HMsERG; Ocuscience, Kansas City, MO) at 2, 7, and 14 days after ballistic injury and interpreted using ERGView (Ocuscience). Animals were dark adapted overnight and prepared for ERG under dim red light (>630 nm). Scotopic flash ERG were recorded at −2.5, 0, and +0.5 log units with respect to standard flash and photopic flash ERG with background illumination of 30,000 mcd/m^2 at 0 and +0.5 log units, using DTL fiber (Unimed Electrode Supplies, Farnham, UK) corneal electrodes with pressure-molded Aclar (Agar Scientific, Stansted, UK) contact lenses and needle skin electrodes (Unimed).

Electron Microscopy

The primary tissue fixative was 4% gluteraldehyde in 0.1 M phosphate buffer (PB; pH 7.3) as used in previous studies of commotio retinae.[13,14] Eyes were removed and the cornea incised before 24 hours postfixation in the primary fixative at room temperature. A section of injured retina was dissected out, washed in 0.1 M PB, postfixed in 1% osmium tetroxide in 0.1 M PB for 45 minutes, washed in PB, dehydrated in ascending concentrations of ethanol, and immersed in propylene oxide before infiltrating in resin (Durcupan; Electron Microscopy Sciences, Hatfield, PA) for 24 hours and polymerizing at 56°C for 24 hours. Semithin sections (1 μm thick) were cut using glass knives on an "ultracut" ultramicrotome (Reichert-Jung, Vienna, Austria). Sections were stained with toludine blue. Ultrathin gold sections (70–90 nm) were cut with a glass or diamond knife, floated on distilled water, mounted on formvar-coated 50-mesh copper grids, stained with uranyl acetate and lead citrate, and examined on a JEOL 1200 EX transmission electron microscope (JEOL [UK] Ltd., Welwyn Garden City, UK) fitted with a LaB6 filament at an operating voltage of 80 keV.

TUNEL and Immunohistochemistry

The tissue fixative was 4% paraformaldehyde (PFA) in phosphate-buffered saline. Eyes were removed, and the cornea was incised before 24 hours postfixation at 4°C. Specimens were cryoprotected in ascending concentrations of sucrose in phosphate-buffered saline (PBS) at 4°C; the anterior segments were removed, and the retinal cup was embedded in OCT and stored at −80°C. Sections 15 μm thick were cut using a cryostat (Bright Instruments, Huntingdon, UK) and adhered onto SuperfrostTM (Fisher, Loughborough, UK)-coated glass microscope slides. TUNEL FragEL DNA Fragmentation Detection Kit (Merck, Nottingham, UK) was used per manufacturer's instructions, except that proteinase K was omitted and replaced by 15 minutes in Triton X-100 0.1% in PBS. Immunohistochemistry was performed using primary antibodies to ED1 (1/400, monoclonal; ABD Serotec, Kidlington, UK) and OX42 (1/400, monoclonal; ABD Serotec; and 1/100, polyclonal; Santa Cruz Biotechnology, Inc., Heidelberg, Germany) with Texas red anti-mouse and Alexa Fluor 488 anti-rabbit IgG (both 1/400; Invitrogen, Grand Island, NY) secondary antibodies.

Retinal Whole Mounts and Counting of Photoreceptors

Anterior segments and vitreous were removed; eye cups were fixed in 4% PFA in PBS, and the neuroretina was dissected from the RPE except when it was adherent, in which case the RPE was dissected from the choroid. Retinae were permeabilized in 0.1% Triton X-100/4′,6-diamidino-2-phenylindole (DAPI) in PBS for 2 hours and mounted with DAPI mountant for cell counting. Images were captured at 63× magnification using a confocal laser scanning microscope (Zeiss, Hertfordshire, UK) running the LSM 510 software version 3.2 (Zeiss). Images were captured from three different areas (at 1/6, 3/6, and 5/6 of the radius) of each quadrant (total = 12 counts per eye) in the middle of the outer nuclear layer, to account for variation of photoreceptor

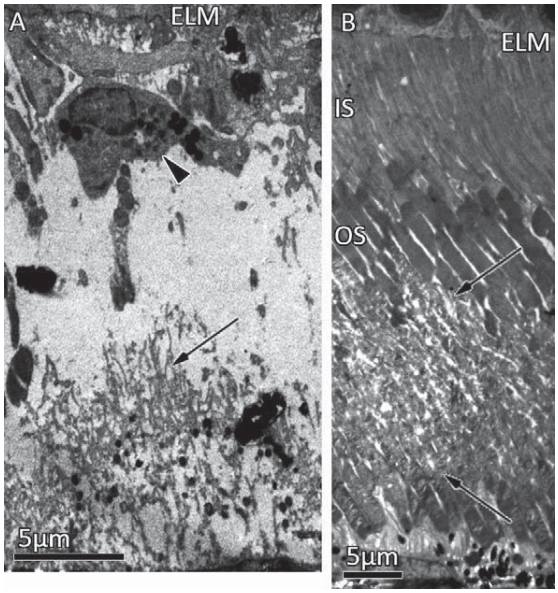

Figure 1. Electron micrographs of rat outer retina. (**A**) Two days after 22.6 g (0.6 J) weight drop to lateral sclera; absent photoreceptor inner segments (IS) and outer segments (OS) with RPE response (*arrowed*), disrupted external limiting membrane (ELM), and a macrophage (*arrowhead*). (**B**) Immediately after 31.3 g (0.6 J) weight drop to lateral sclera. Disrupted photoreceptor outer segments (OS; *arrowed above* and *below*).

numbers in the different areas, and quantified using the built-in particle counting facilities in ImagePro (Media Cybernetics, Bethesda, MD). Mean photoreceptor density per high-power field (0.146×0.146 mm) was expressed as a percentage of the mean value for uninjured control tissue.

Semithin (1 µm) toludine blue–stained retinal sections were cut 2 weeks after injury from the optic disc to the ciliary body through the center of the impact site; control tissue was taken from the (uninjured) inferior retina of animals killed at 2 hours after impact to the lateral sclera. Images were captured at 40× magnification (0.25×0.3 mm field of view) from five different areas of each section and quantified by a blinded observer using the user-defined manual counting facility in ImagePro. For display, counts were normalized as percentages of the mean value for uninjured control tissue in the same retinal area.

Statistical Analysis

Cell count and ERG data were normally distributed and analyzed with parametric tests in SPSS 19 (IBM, Armonk, NY). Means ± standard error were calculated for all samples. Electrophysiological data were analyzed using either three-way (time, intensity, injury) repeated measures ANOVA or generalized estimating equations for sets missing data (type III sum of squares). Nonsignificant interactions were removed from the models, and normality was assessed using residual plots.

Results

Weight Drop Did Not Create a Reproducible Retinal Injury

Two hours after impact to the central cornea, no injury was seen by clinical examination or light or electron microscopy. After direct scleral impact, retinal pathology was clinically occult, as the clinical examination and macroscopic appearances were normal. Photoreceptor outer segment disruption

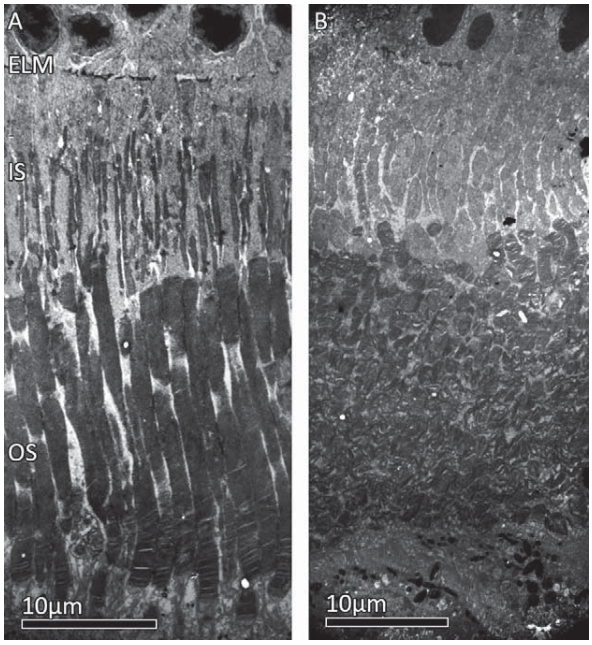

Figure 2. Electron micrographs of rat outer retina. (**A**) Normal control retina. (**B**) Disrupted photoreceptor inner (IS) and outer segments (OS) and external limiting membrane (ELM) 2 hours after ballistic injury.

was induced in two of nine eyes to which 0.6 J was delivered; and, at this energy level, globe rupture occurred in two of nine eyes (Fig. 1).

Ballistic Trauma Created a Reproducible Retinal Injury

In cadaveric studies, a chamber pressure of $\geq$0.15 bar caused rupture in >50% of eyes. Weights of 0.91, 0.50, 0.16 (air gun pellets), and 0.095 g (ball bearing) were tested; 0.095 g was chosen to give the highest-velocity injury, 20 m/s at chamber pressure of 0.125 bar.

Immediately after injury, there was retinal pallor underlying the injury site in all eyes and variable vitreous hemorrhage. The pallor resolved over the next 2 weeks to leave an area of retinal atrophy revealing the choroidal vasculature.

Light and electron microscopy of resin-embedded retinal sections at 2 hours after injury showed disruption of photoreceptor outer and inner segments in all eight eyes and disruption of the external limiting membrane (ELM) in three eyes (Fig. 2).

Specific Photoreceptor Death Developed after Ballistic Blunt Ocular Trauma

By 2 weeks after ballistic injury, a large area of retinal and RPE atrophy developed. There was progressive loss of the ONL approaching the center of the impact site but relative preservation of the inner nuclear and ganglion cell layers, with hypopigmentation and irregularity of the underlying RPE (Figs. 3A, 3B). At the center of the impact site, all neuroretinal layers were absent.

The proportion of photoreceptors surviving increased at increasing distances from the center of the impact site, demonstrated by ONL cell counts on toludine blue–stained resin sections of the retina radially from the optic disc to the ciliary body, through the center of the lesion site (Fig. 3C).

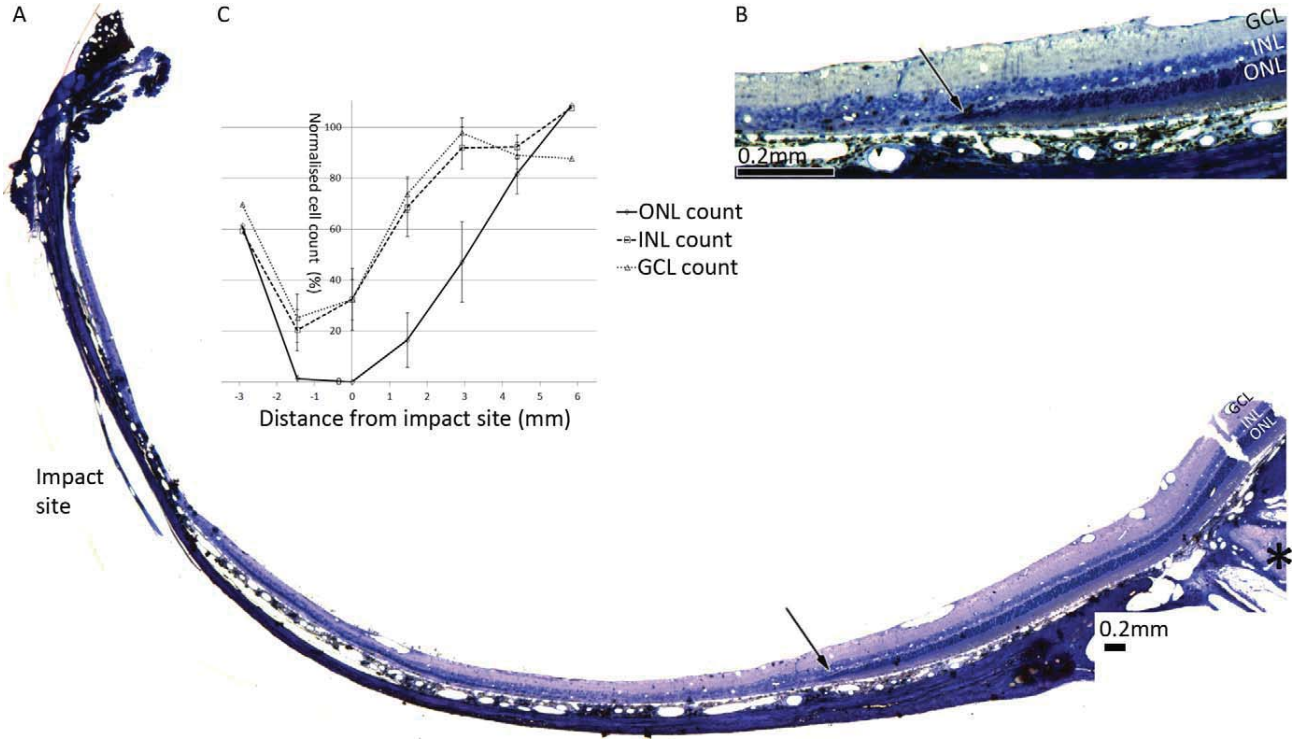

Figure 3. Light micrograph of rat retina 2 weeks after ballistic injury. (**A**) Outer nuclear layer (ONL) around the optic disc (*asterisk*) is normal. Approaching the impact site it thins (*arrowed*) and then disappears, leaving the inner retina relatively intact. (**B**) Line graph showing normalized retinal cell counts at distance from the impact site ± standard error of the mean. ONL survival is lowest, with the inner nuclear layer (INL) and ganglion cell layer (GCL) relatively spared. (**C**) Higher-power cutout of (**A**) showing thinning and loss of the ONL.

ONL cell counting on retinal whole mounts confirmed that 18.4 ± 4.6% of photoreceptors had died.

Photoreceptors Died by Necrosis and Apoptosis

By 2 hours after injury, there were occasional apoptotic nuclei in the ONL with chromatin condensation and nuclear blebbing (Fig. 4A). Two days after injury, in the center of the impact site, there was infiltration of macrophages (histiocytic, ED1-positive, OX42-negative; Figs. 4B, 4I–K, Supplementary Material and Supplementary Figs. S1C–H, http://www.iovs.org/lookup/suppl/doi:10.1167/iovs.12-9887/-/DCSupplemental),[20] edema, and necrotic nuclei in the ONL (Figs. 4B–E). In the perilesional area there was disruption of outer segments with inflammatory cell infiltration. There were fewer necrotic photoreceptor nuclei at increasing distances from the lesion site but more apoptotic photoreceptor nuclei (Figs. 4E–H; see Supplementary Material and Supplementary Figs. S1A, S1B http://www.iovs.org/lookup/suppl/doi:10.1167/iovs.12-9887/-/DCSupplemental). Centrally in the impact site, many cells with diffuse nuclear and cytoplasmic TUNEL staining were observed (Fig. 4L), probably because direct cellular injury caused necrotic death.[21] However, in areas away from the impact site, the presence of specific TUNEL-positive photoreceptor cell nuclei confirmed apoptosis of these cells (Figs. 4L–O).

Electrophysiological Assessment of Ballistic Injury

To assess retinal function, scotopic and photopic flash ERG series were recorded and the major components (a- and b-waves) observed. The a- and b-wave amplitudes were quantified and compared between injured and control eyes at 2, 7, and 14 days postinjury. The magnitude and latency of all components were intensity dependent, though only amplitude was injury dependent. ANOVA was used to compare scotopic (dark adapted) a-wave amplitudes. Scotopic a-wave amplitude was significantly reduced by injury (Fig. 5A; 1 *df*, $F = 59.7$, $P < 0.001$, $\eta = 0.895$), and there was no significant change between the three time points (2 *df*, $F = 2.706$, $P = 0.129$, $\eta = 0.279$). Since b-wave onset can obscure the a-wave, gradient of the a-wave's linear portion (leading edge) was measured, giving a trend similar to that observed for amplitude (1 *df*, $F = 40.9$, $P < 0.001$, $\eta = 0.854$). Scotopic b-wave amplitude was significantly reduced by injury (2 *df*, $F = 39.9$, $P < 0.001$, $\eta = 0.851$), though there was no significant effect on the scotopic b-/a-wave ratio (see Supplementary Material and Supplementary Fig. S2, http://www.iovs.org/lookup/suppl/doi:10.1167/iovs.12-9887/-/DCSupplemental; 1 *df*, $F = 4.917$, $P = 0.062$, $\eta = 0.413$). Photopic a-waves were frequently undetectable in injured and control eyes, and some data points were missing. Generalized estimating equations were therefore used to analyze photopic b-wave amplitudes, which were significantly reduced by injury (Fig. 5B; unstructured correlation matrix, 1 *df*, $P < 0.001$), consistent with the outer retinal injury affecting both cones and rods equally.

Discussion

This is the first murine model of closed globe injury to show that low-velocity ballistic trauma creates reproducible commotio retinae, with pathological features that mirror the clinical and OCT findings in humans after severe blunt ocular trauma.[17] At the impact site, there was necrosis of photoreceptors, and centrally there was death of all retinal cells

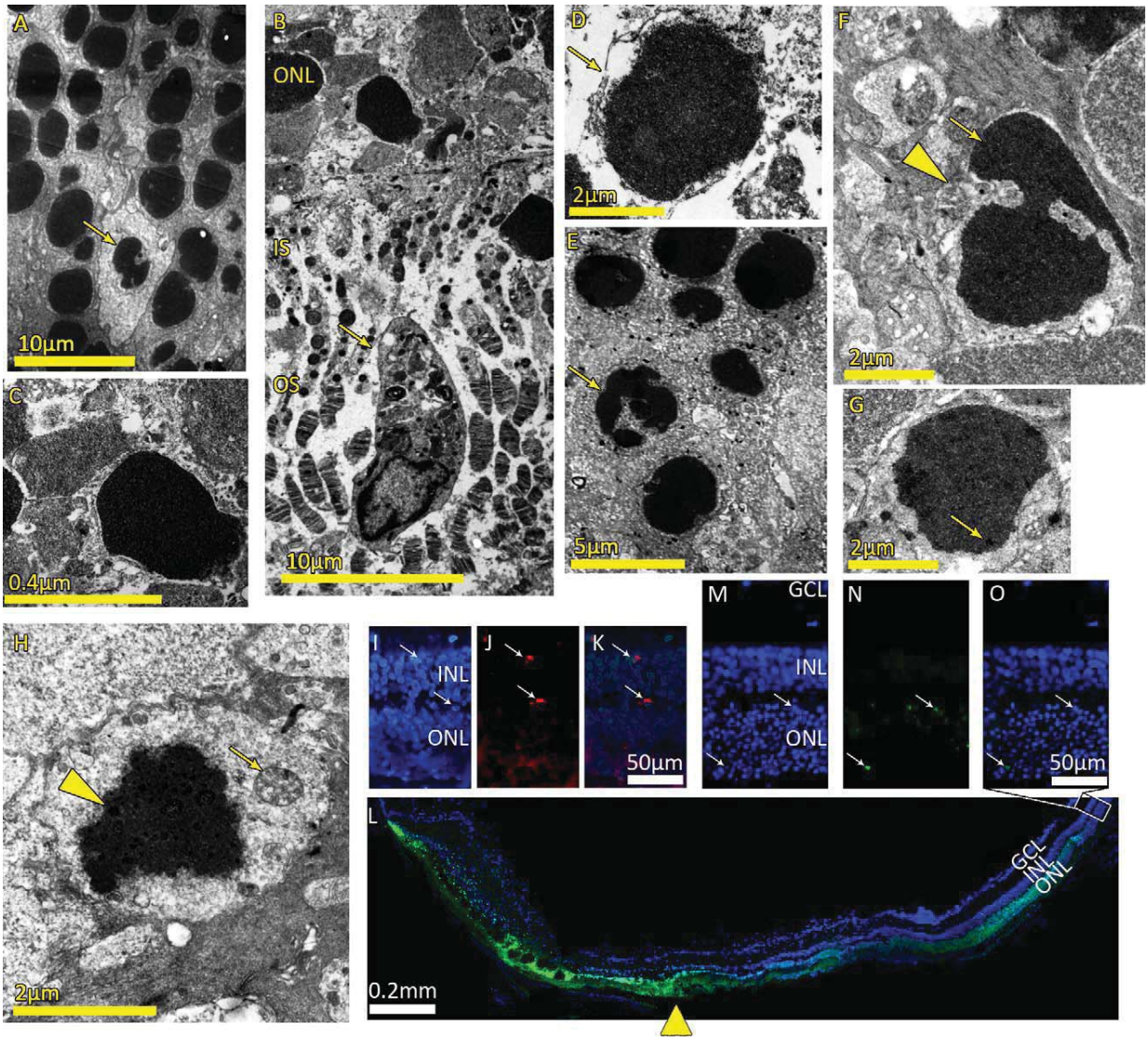

Figure 4. (**A–G**) Electron micrographs of rat outer retina. (**A**) Outer nuclear layer (ONL) 2 hours after ballistic injury; blebbed (apoptotic) photoreceptor nucleus *arrowed*. (**B–G**) Two days after ballistic injury. (**B**) Close to the impact site, macrophage removing disrupted photoreceptor outer and inner segments (*arrowed*) and nonspecific cell death with condensed and fragmented photoreceptor nuclei in the ONL, shown at higher magnification in (**C**). (**D**) Close to the impact site, necrotic photoreceptor nucleus in an edematous ONL with ruptured cell membranes (*arrowed*). (**E–H**) Apoptotic photoreceptor nuclei farther away from the impact site. (**E**) Nuclear blebbing (*arrowed*); (**F**) nuclear blebbing (*arrowed*) with invasion of the photoreceptor cytoplasm by Müller cell processes (*arrowhead*); (**G**) a condensed photoreceptor nucleus with chromatin condensation at the periphery of the nucleus, typical of apoptosis; (**H**) chromatin aggregates (*arrowhead*) dispersed throughout the condensed photoreceptor nucleus (rather than peripherally), but the intact mitochodrion (*arrowed*) is suggestive of apoptosis. (**I–K**) ED1 staining showing DAPI-stained nuclei (**I**), *red* ED1-positive macrophages (*arrowed*) in the inner nuclear layer (INL) and ONL (**J**), and combined image (**K**). (**L**) TUNEL staining. The frequency of TUNEL-positive cells is highest in the ONL centrally to the impact site (*arrowhead*), reducing in frequency with increasing distance. (**M–O**) High-power cutout of (**L**): DAPI-stained nuclei (**M**), apoptotic photoreceptor nuclei (*arrowed*, **N**), combined image (**O**).

(sclopetaria retinae). Away from the impact site, photoreceptor death occurred by a combination of apoptosis and necrosis. Preservation of the inner retinal layers, together with specific photoreceptor cell death, mirrored human OCT findings. The reason this injury predominantly affects photoreceptors is unclear, but we suggest that shearing forces at the neuroretina–RPE junction during globe deformation make them particularly vulnerable.

The spectrum of cell death ranges between apoptosis and necrosis, with significant overlap. We have shown cells that are clearly necrotic (Figs. 4C, 4D) and cells that exhibit features consistent with apoptosis (Figs. 4E–H, 4L–O; see Supplementary Material and Supplementary Figs. S1A, S1B, http://www.iovs.org/lookup/suppl/doi:10.1167/iovs.12-9887/-/DCSupplemental), though it is likely that many photoreceptors undergo a mixed form of cell death. While necrosis is an unregulated form of cell death, apoptosis is mediated by specific cell death signaling pathways, as is the mixed form of cell death, termed necroptosis, and these pathways can be modulated to increase cell survival.[18,22] Thus, our results imply that in a proportion of photoreceptors after ballistic retinal injury, cell death is mediated by apoptotic or necroptotic

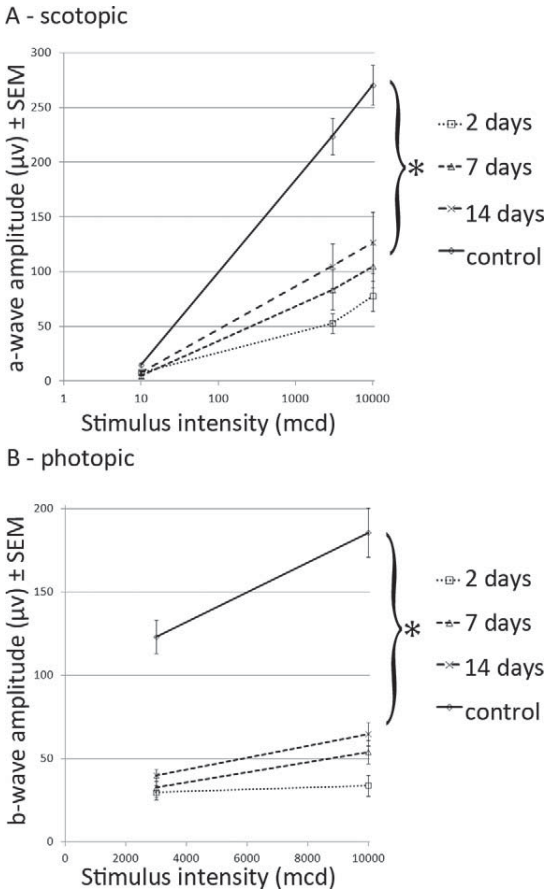

Figure 5. Quantification of the relevant components of the ERG at 2, 7, and 14 days after injury displayed as amplitude ± standard error of the mean (SEM) at increasing stimulus intensity. (**A**) Scotopic (dark adapted) a-wave amplitude was significantly reduced by injury at all time points and stimulus intensities (*$P < 0.001$), and (**B**) photopic (light adapted) b-wave amplitude was similarly reduced.

regulated signaling pathways, with a potential for successful neuroprotective therapies.

In human studies, mild commotio retinae associated with photoreceptor recovery is characterized by outer segment disruption, whereas severe commotio retinae is associated with photoreceptor inner and outer segment disruption observed by OCT.[17] Inner segment disruption was also present in our model, but has not been reported in other (mild, recovering) animal models of commotio retinae. The RPE and photoreceptor outer and inner segments appear as three bands on spectral-domain OCT. The thinner line above them may represent the ELM or the myoid portion of the cone inner segments.[23] Loss of this line on OCT may be a marker of severe photoreceptor damage in commotio retinae and age-related macular degeneration.[17,24] If it represents cone inner segments, we speculate that disruption of these mitochondria-rich structures (seen in our model) is a lethal injury to photoreceptors, while outer segment disruption is less likely to cause photoreceptor death.

In our hands, the severity of weight drop–induced retinal injuries was inconsistent in rats. The energy threshold for inducing commotio retinae is close to that causing rupture (approximately 0.6 J). That low-velocity injury does not usually cause commotio retinae is consistent with the body of literature on commotio retinae induced by high-velocity impact.[12] In contrast, a lower-energy injury with a 0.095 g pellet traveling at 20 m/s (0.019 J) reproducibly created central sclopetaria retinae at the impact site and surrounding commotio retinae. High-velocity impact of a low-weight projectile creates more injury than low-velocity impact by a heavy projectile, despite similar kinetic energies[25]; and the curved profile of ball bearings used for ballistic trauma in this study resulted in a higher area-normalized impact energy (lower with a larger projectile), which is a better predictor of corneoscleral stress and vitreous pressure than impact energy alone.[26] The ultrastructural features of our ballistic retinal injury model are consistent with other studies of commotio retinae, showing disruption of photoreceptor outer segments.

The rat lens accounts for 60% of axial length.[27] With such a small vitreous cavity, it is likely that the lens impacted the retina during injury in our experiments with potential crushing of the retina. This is also the case in larger animals in which ocular dimensions are similar to those in humans,[12] though with the larger lens this crushing will be more extensive in the rat.

The a-wave is the initial negative deflection caused by photoreceptor activation (rods in scotopic series, cones in photopic series) and is routinely used to measure photoreceptor function. The b-wave is the first positive deflection, immediately following the a-wave, and is generated by the activity of second-order neurons (such as ON bipolar cells in the inner nuclear layer). The b-wave is therefore dependent on photoreceptor activation and synaptic transmission in addition to inner retinal function. The ERG in the injured eyes showed a significant reduction in a- and b-wave amplitude compared to the control eyes without any change in implicit time. The b-/a-wave ratio is a measure of how much of the variation in b-wave amplitude is explained by variation in the magnitude of photoreceptor activation compared to the function of second-order neurons; this ratio was normal and similar between injured and control eyes. These reductions in ERG amplitude occurred under both scotopic and photopic conditions and would be consistent with damage primarily to the photoreceptor layer.

Rods make up 99% of rat photoreceptors[28] and, in our model, scotopic a-wave amplitude (which reflects rod function) was reduced by >50% (Fig. 5), although only 18% of photoreceptors died. The degree of ERG reduction was therefore disproportionate to the amount of histological photoreceptor death. Either outer segment damage or photoreceptor remodeling (similar to that seen after retinal detachment[29]) could reduce the a-wave. Additionally, the photoreceptor component (leading edge) of the a-wave is sensitive to extracellular Ca^{2+} and K^{+} levels,[30] which may be affected either by altered Müller glial function or by local structural changes.

In conclusion, we report an animal model of the outer retinal changes that occur after severe commotio retinae in humans, which is the first murine rodent model of blunt ocular trauma. Our results suggest that outer retinal atrophy occurs as a result of photoreceptor apoptosis and necrosis due to a terminal injury to photoreceptor inner segments. The observed photoreceptor apoptosis is translationally relevant because there is the potential to prevent neuronal death and improve visual outcomes with use of antiapoptotic neuroprotective therapies. This model provides an opportunity for both mechanistic and translational therapeutic studies.

Acknowledgments

We thank Peter Nightingale (Queen Elizabeth Hospital, Birmingham, UK) for statistical advice and Theresa Morris and Katharine Griffiths (University of Birmingham) for technical support.

References

1. Wong TY, Klein BE, Klein R. The prevalence and 5-year incidence of ocular trauma. The Beaver Dam Eye Study. *Ophthalmol*. 2000;107:2196–2202.
2. Jones NP, Hayward JM, Khaw PT, Claoue CM, Elkington AR. Function of an ophthalmic "accident and emergency" department: results of a six month survey. *Br Med J*. 1986; 292:188–190.
3. Vernon SA. Analysis of all new cases seen in a busy regional centre ophthalmic casualty department during 24-week period. *J R Soc Med*. 1983;76:279–282.
4. Blanch RJ, Scott R. Military ocular injury: Presentation, assessment and management. *J R Army Med Corps*. 2010; 155:279–284.
5. Weichel ED, Colyer MH, Ludlow SE, Bower KS, Eiseman AS. Combat ocular trauma visual outcomes during operations Iraqi and Enduring Freedom. *Ophthalmol*. 2008;115:2235–2245.
6. Pieramici DJ, Sternberg P Jr, Aaberg TM Sr, et al. A system for classifying mechanical injuries of the eye (globe). The Ocular Trauma Classification Group. *Am J Ophthalmol*. 1997;123: 820–831.
7. Chalioulias K, Sim KT, Scott R. Retinal sequelae of primary ocular blast injuries. *J R Army Med Corps*. 2007;153:124–125.
8. Berlin R. Zur sogenannten commotio retinae. *Klin Monatsbl Augenheilkd*. 1873;1:42–78.
9. Hart JC, Natsikos VE, Raistrick ER, Doran RM. Chorioretinitis sclopetaria. *Trans Ophthalmol Soc U K*. 1980;100:276–281.
10. Eagling EM. Ocular damage after blunt trauma to the eye. Its relationship to the nature of the injury. *Br J Ophthalmol*. 1974;58:126–140.
11. Saleh M, Letsch J, Bourcier T, Munsch C, Speeg-Schatz C, Gaucher D. Long-term outcomes of acute traumatic maculopathy. *Retina*. 2011;31:2037–2043.
12. Blanch RJ, Ahmed Z, Berry M, Scott RAH, Logan A. Animal models of retinal injury. *Invest Ophthalmol Vis Sci*. 2012;53: 2913–2920.
13. Hart JC, Blight R, Cooper R, Papakostopoulos D. Electrophysiological and pathological investigation of concussional injury. An experimental study. *Trans Ophthalmol Soc U K*. 1975;95: 326–334.
14. Sipperley JO, Quigley HA, Gass JD. Traumatic retinopathy in primates: the explanation of commotio retinae. *Arch Ophthalmol*. 1978;96:2267–2273.
15. Liem AT, Keunen JE, van Norren D. Reversible cone photoreceptor injury in commotio retinae of the macula. *Retina*. 1995;15:58–61.
16. An MX, Zhang XF, Zhang JS. Oxidative damage and photoreceptor cell apoptosis in contusion injury of the rabbit retina [in Chinese]. *Zhonghua yan ke za zhi [Chin J Ophthalmol]*. 2004;40:118–121.
17. Souza-Santos F, Lavinsky D, Moraes NS, Castro AR, Cardillo JA, Farah ME. Spectral-domain optical coherence tomography in patients with commotio retinae. *Retina*. 2011;32:711–718.
18. Ahmed Z, Kalinski H, Berry M, et al. Ocular neuroprotection by siRNA targeting caspase-2. *Cell Death Dis*. 2011;2:e173.
19. Courtney M, Edwards B. Measuring bullet velocity with a PC soundcard. ArXiv preprint physics/0601102. 2006.
20. Streit WJ. Microglia. In Kettenmann H, Ransom BR, eds. *Neuroglia*. 2nd ed. New York, NY: Oxford University Press; 2005:63.
21. van Lookeren Campagne M, Gill R. Ultrastructural morphological changes are not characteristic of apoptotic cell death following focal cerebral ischaemia in the rat. *Neurosci Lett*. 1996;213:111–114.
22. Trichonas G, Murakami Y, Thanos A, et al. Receptor interacting protein kinases mediate retinal detachment-induced photoreceptor necrosis and compensate for inhibition of apoptosis. *Proc Natl Acad Sci U S A*. 2010;107:21695–21700.
23. Gloesmann M, Hermann B, Schubert C, Sattmann H, Ahnelt PK, Drexler W. Histologic correlation of pig retina radial stratification with ultrahigh-resolution optical coherence tomography. *Invest Ophthalmol Vis Sci*. 2003;44:1696–1703.
24. Oishi A, Hata M, Shimozono M, Mandai M, Nishida A, Kurimoto Y. The significance of external limiting membrane status for visual acuity in age-related macular degeneration. *Am J Ophthalmol*. 2010;150:27–32.e1.
25. Scott WR, Lloyd WC, Benedict JV, Meredith R. Ocular injuries due to projectile impacts. *Annu Proc Assoc Adv Automot Med*. 2000;44:205–217.
26. Weaver AA, Kennedy EA, Duma SM, Stitzel JD. Evaluation of different projectiles in matched experimental eye impact simulations. *J Biomech Eng*. 2011;133:031002.
27. Hughes A. A schematic eye for the rat. *Vision Res*. 1979;19: 569–588.
28. Szel A, Rohlich P. Two cone types of rat retina detected by anti-visual pigment antibodies. *Exp Eye Res*. 1992;55:47–52.
29. Fisher SK, Lewis GP, Linberg KA, Verardo MR. Cellular remodeling in mammalian retina: results from studies of experimental retinal detachment. *Prog Retin Eye Res*. 2005; 24:395–431.
30. Vinberg FJ, Strandman S, Koskelainen A. Origin of the fast negative ERG component from isolated aspartate-treated mouse retina. *J Vis*. 2009;9:9.1–17.

APPENDIX 7

```
 GET
  FILE='C:\Users\Public\Documents\PhD\ERG\Results\T-CEM423-6\scotopic data T.sav'.
DATASET NAME DataSet1 WINDOW=FRONT.
EXAMINE VARIABLES=awaveamplitudev
  /PLOT BOXPLOT STEMLEAF NPPLOT
  /COMPARE GROUPS
  /STATISTICS DESCRIPTIVES
  /CINTERVAL 95
  /MISSING LISTWISE
  /NOTOTAL.


 * Generalized Estimating Equations.
GENLIN awaveamplitudev BY timepoint flashintensitymcd Injured (ORDER=ASCENDING)
  /MODEL timepoint flashintensitymcd Injured timepoint*flashintensitymcd timepoint*Injured f
 DISTRIBUTION=GAMMA LINK=LOG
  /CRITERIA METHOD=FISHER(1) SCALE=MLE MAXITERATIONS=100 MAXSTEPHALVING=5 PCONVERGE=1E-006(A
  /REPEATED SUBJECT=animal WITHINSUBJECT=Injured*timepoint*flashintensitymcd SORT=YES CORRTY
(ABSOLUTE) UPDATECORR=1
  /MISSING CLASSMISSING=EXCLUDE
  /PRINT CPS DESCRIPTIVES MODELINFO FIT SUMMARY.
```

Generalized Linear Models

[DataSet1] C:\Users\Public\Documents\PhD\ERG\Results\T-CEM423-6\scotopic data T.sav

Warnings

One or more cases were found with dependent variable data values that are less than or equal to zero. These values are invalid for the gamma probability distribution, and the cases are not used in the analysis.

Model Information

Dependent Variable		awaveamplitudev
Probability Distribution		Gamma
Link Function		Log
Subject Effect	1	animal
Within-Subject Effect	1	Injured
	2	timepoint
	3	flashintensitymcd
Working Correlation Matrix Structure		AR(1)

Case Processing Summary

	N	Percent
Included	134	88.2%
Excluded	18	11.8%
Total	152	100.0%

Correlated Data Summary

Number of Levels	Subject Effect	animal	8
	Within-Subject Effect	Injured	2
		timepoint	3
		flashintensitymcd	3
Number of Subjects			8
Number of Measurements per Subject	Minimum		13
	Maximum		18
Correlation Matrix Dimension			18

Categorical Variable Information

			N	Percent
Factor	timepoint	2	47	35.1%
		7	42	31.3%
		14	45	33.6%
		Total	134	100.0%
	flashintensitymcd	10	38	28.4%
		3000	48	35.8%
		10000	48	35.8%
		Total	134	100.0%
	Injured	0	69	51.5%
		1	65	48.5%
		Total	134	100.0%

Continuous Variable Information

		N	Minimum	Maximum	Mean
Dependent Variable	awaveamplitudev	134	1.6	440.5	128.900

Continuous Variable Information

		Std. Deviation
Dependent Variable	awaveamplitudev	117.9479

Goodness of Fit[a]

	Value
Quasi Likelihood under Independence Model Criterion (QIC)[b]	59.414
Corrected Quasi Likelihood under Independence Model Criterion (QICC)[b]	61.584

Dependent Variable: awaveamplitudev
Model: (Intercept), timepoint, flashintensitymcd, Injured, timepoint * flashintensitymcd, timepoint * Injured, flashintensitymcd * Injured, timepoint * flashintensitymcd * Injured

a. Information criteria are in small-is-better form.

b. Computed using the full log quasi-likelihood function.

Tests of Model Effects

Source	Type III		
	Wald Chi-Square	df	Sig.
(Intercept)	4435.076	1	.000
timepoint	12.739	2	.002
flashintensitymcd	466.775	2	.000
Injured	114.068	1	.000
timepoint * flashintensitymcd	10.396	4	.034
timepoint * Injured	2.246	2	.325
flashintensitymcd * Injured	9.226	2	.010
timepoint * flashintensitymcd * Injured	9.195	4	.056

Dependent Variable: awaveamplitudev
Model: (Intercept), timepoint, flashintensitymcd, Injured, timepoint * flashintensitymcd, timepoint * Injured, flashintensitymcd * Injured, timepoint * flashintensitymcd * Injured

```
 * Generalized Estimating Equations.
GENLIN awaveamplitudev BY timepoint flashintensitymcd Injured (ORDER=ASCENDING)
  /MODEL timepoint flashintensitymcd Injured timepoint*flashintensitymcd timepoint*Injured f
 DISTRIBUTION=GAMMA LINK=LOG
  /CRITERIA METHOD=FISHER(1) SCALE=MLE MAXITERATIONS=100 MAXSTEPHALVING=5 PCONVERGE=1E-006(A
012 ANALYSISTYPE=3(WALD) CILEVEL=95 LIKELIHOOD=FULL
  /REPEATED SUBJECT=animal WITHINSUBJECT=Injured*timepoint*flashintensitymcd SORT=YES CORRTY
```

```
(1) ADJUSTCORR=YES COVB=ROBUST MAXITERATIONS=100 PCONVERGE=1e-006(ABSOLUTE) UPDATECORR=1
  /MISSING CLASSMISSING=EXCLUDE
  /PRINT CPS DESCRIPTIVES MODELINFO FIT SUMMARY.
```

Generalized Linear Models

[DataSet1] C:\Users\Public\Documents\PhD\ERG\Results\T-CEM423-6\scotopic data T.sav

Warnings

One or more cases were found with dependent variable data values that are less than or equal to zero. These values are invalid for the gamma probability distribution, and the cases are not used in the analysis.

Model Information

Dependent Variable		awaveamplitudev
Probability Distribution		Gamma
Link Function		Log
Subject Effect	1	animal
Within-Subject Effect	1	Injured
	2	timepoint
	3	flashintensitymcd
Working Correlation Matrix Structure		AR(1)

Case Processing Summary

	N	Percent
Included	134	88.2%
Excluded	18	11.8%
Total	152	100.0%

Correlated Data Summary

Number of Levels	Subject Effect	animal	8
	Within-Subject Effect	Injured	2
		timepoint	3
		flashintensitymcd	3
Number of Subjects			8
Number of Measurements per Subject	Minimum		13
	Maximum		18
Correlation Matrix Dimension			18

Categorical Variable Information

			N	Percent
Factor	timepoint	2	47	35.1%
		7	42	31.3%
		14	45	33.6%
		Total	134	100.0%
	flashintensitymcd	10	38	28.4%
		3000	48	35.8%
		10000	48	35.8%
		Total	134	100.0%
	Injured	0	69	51.5%
		1	65	48.5%
		Total	134	100.0%

Continuous Variable Information

		N	Minimum	Maximum	Mean
Dependent Variable	awaveamplitudev	134	1.6	440.5	128.900

Continuous Variable Information

		Std. Deviation
Dependent Variable	awaveamplitudev	117.9479

Goodness of Fit[a]

	Value
Quasi Likelihood under Independence Model Criterion (QIC)[b]	58.126
Corrected Quasi Likelihood under Independence Model Criterion (QICC)[b]	54.352

Dependent Variable: awaveamplitudev

Model: (Intercept), timepoint, flashintensitymcd, Injured, timepoint * flashintensitymcd, timepoint * Injured, flashintensitymcd * Injured

a. Information criteria are in small-is-better form.

b. Computed using the full log quasi-likelihood function.

Tests of Model Effects

Source	Type III		
	Wald Chi-Square	df	Sig.
(Intercept)	4675.918	1	.000
timepoint	11.620	2	.003
flashintensitymcd	466.202	2	.000
Injured	73.306	1	.000
timepoint * flashintensitymcd	11.029	4	.026
timepoint * Injured	2.581	2	.275
flashintensitymcd * Injured	15.387	2	.000

Dependent Variable: awaveamplitudev
Model: (Intercept), timepoint, flashintensitymcd, Injured, timepoint * flashintensitymcd, timepoint * Injured, flashintensitymcd * Injured

```
 * Generalized Estimating Equations.
GENLIN awaveamplitudev BY timepoint flashintensitymcd Injured (ORDER=ASCENDING)
  /MODEL timepoint flashintensitymcd Injured timepoint*flashintensitymcd flashintensitymcd*I
 DISTRIBUTION=GAMMA LINK=LOG
  /CRITERIA METHOD=FISHER(1) SCALE=MLE MAXITERATIONS=100 MAXSTEPHALVING=5 PCONVERGE=1E-006
(ABSOLUTE) SINGULAR=1E-012 ANALYSISTYPE=3(WALD) CILEVEL=95 LIKELIHOOD=FULL
  /EMMEANS TABLES=timepoint*flashintensitymcd*Injured SCALE=ORIGINAL
  /REPEATED SUBJECT=animal WITHINSUBJECT=Injured*timepoint*flashintensitymcd SORT=YES CORRTY
(1) ADJUSTCORR=YES COVB=ROBUST MAXITERATIONS=100 PCONVERGE=1e-006(ABSOLUTE) UPDATECORR=1
  /MISSING CLASSMISSING=EXCLUDE
  /PRINT CPS DESCRIPTIVES MODELINFO FIT SUMMARY WORKINGCORR
  /SAVE RESID PEARSONRESID.
```

Generalized Linear Models

```
[DataSet1] C:\Users\Public\Documents\PhD\ERG\Results\T-CEM423-6\scotopic
data T.sav
```

Warnings

One or more cases were found with dependent variable data values that are less than or equal to zero. These values are invalid for the gamma probability distribution, and the cases are not used in the analysis.

Model Information

Dependent Variable		awaveamplitudev
Probability Distribution		Gamma
Link Function		Log
Subject Effect	1	animal
Within-Subject Effect	1	Injured
	2	timepoint
	3	flashintensitymcd
Working Correlation Matrix Structure		AR(1)

Case Processing Summary

	N	Percent
Included	134	88.2%
Excluded	18	11.8%
Total	152	100.0%

Correlated Data Summary

Number of Levels	Subject Effect	animal	8
	Within-Subject Effect	Injured	2
		timepoint	3
		flashintensitymcd	3
Number of Subjects			8
Number of Measurements per Subject	Minimum		13
	Maximum		18
Correlation Matrix Dimension			18

Categorical Variable Information

			N	Percent
Factor	timepoint	2	47	35.1%
		7	42	31.3%
		14	45	33.6%
		Total	134	100.0%
	flashintensitymcd	10	38	28.4%
		3000	48	35.8%
		10000	48	35.8%
		Total	134	100.0%
	Injured	0	69	51.5%
		1	65	48.5%
		Total	134	100.0%

Continuous Variable Information

		N	Minimum	Maximum	Mean
Dependent Variable	awaveamplitudev	134	1.6	440.5	128.900

Continuous Variable Information

		Std. Deviation
Dependent Variable	awaveamplitudev	117.9479

Goodness of Fit[a]

	Value
Quasi Likelihood under Independence Model Criterion (QIC)[b]	53.508
Corrected Quasi Likelihood under Independence Model Criterion (QICC)[b]	50.798

Dependent Variable: awaveamplitudev
Model: (Intercept), timepoint, flashintensitymcd, Injured, timepoint * flashintensitymcd, flashintensitymcd * Injured

a. Information criteria are in small-is-better form.

b. Computed using the full log quasi-likelihood function.

Tests of Model Effects

Source	Type III		
	Wald Chi-Square	df	Sig.
(Intercept)	4569.188	1	.000
timepoint	13.094	2	.001
flashintensitymcd	443.504	2	.000
Injured	58.947	1	.000
timepoint * flashintensitymcd	11.561	4	.021
flashintensitymcd * Injured	14.143	2	.001

Dependent Variable: awaveamplitudev
Model: (Intercept), timepoint, flashintensitymcd, Injured, timepoint * flashintensitymcd, flashintensitymcd * Injured

Working Correlation Matrix[a]

Measurement	Measurement			
	[Injured = 0]* [timepoint = 2]* [flashintensity mcd = 10]	[Injured = 0]* [timepoint = 2]* [flashintensity mcd = 3000]	[Injured = 0]* [timepoint = 2]* [flashintensity mcd = 10000]	[Injured = 0]* [timepoint = 7]* [flashintensity mcd = 10]
[Injured = 0]* [timepoint = 2]* [flashintensitymcd = 10]	1.000	.479	.229	.110
[Injured = 0]* [timepoint = 2]* [flashintensitymcd = 3000]	.479	1.000	.479	.229
[Injured = 0]* [timepoint = 2]* [flashintensitymcd = 10000]	.229	.479	1.000	.479
[Injured = 0]* [timepoint = 7]* [flashintensitymcd = 10]	.110	.229	.479	1.000
[Injured = 0]* [timepoint = 7]* [flashintensitymcd = 3000]	.053	.110	.229	.479
[Injured = 0]* [timepoint = 7]* [flashintensitymcd = 10000]	.025	.053	.110	.229
[Injured = 0]* [timepoint = 14]* [flashintensitymcd = 10]	.012	.025	.053	.110
[Injured = 0]* [timepoint = 14]* [flashintensitymcd = 3000]	.006	.012	.025	.053
[Injured = 0]* [timepoint = 14]* [flashintensitymcd = 10000]	.003	.006	.012	.025
[Injured = 1]* [timepoint = 2]* [flashintensitymcd = 10]	.001	.003	.006	.012
[Injured = 1]* [timepoint = 2]* [flashintensitymcd = 3000]	.001	.001	.003	.006
[Injured = 1]* [timepoint = 2]* [flashintensitymcd = 10000]	.000	.001	.001	.003
[Injured = 1]* [timepoint = 7]* [flashintensitymcd = 10]	.000	.000	.001	.001
[Injured = 1]* [timepoint = 7]* [flashintensitymcd = 3000]	.000	.000	.000	.001

Working Correlation Matrix[a]

Measurement	Measurement			
	[Injured = 0]* [timepoint = 7]* [flashintensity mcd = 3000]	[Injured = 0]* [timepoint = 7]* [flashintensity mcd = 10000]	[Injured = 0]* [timepoint = 14]* [flashintensity mcd = 10]	[Injured = 0]* [timepoint = 14]* [flashintensity mcd = 3000]
[Injured = 0]* [timepoint = 2]* [flashintensitymcd = 10]	.053	.025	.012	.006
[Injured = 0]* [timepoint = 2]* [flashintensitymcd = 3000]	.110	.053	.025	.012
[Injured = 0]* [timepoint = 2]* [flashintensitymcd = 10000]	.229	.110	.053	.025
[Injured = 0]* [timepoint = 7]* [flashintensitymcd = 10]	.479	.229	.110	.053
[Injured = 0]* [timepoint = 7]* [flashintensitymcd = 3000]	1.000	.479	.229	.110
[Injured = 0]* [timepoint = 7]* [flashintensitymcd = 10000]	.479	1.000	.479	.229
[Injured = 0]* [timepoint = 14]* [flashintensitymcd = 10]	.229	.479	1.000	.479
[Injured = 0]* [timepoint = 14]* [flashintensitymcd = 3000]	.110	.229	.479	1.000
[Injured = 0]* [timepoint = 14]* [flashintensitymcd = 10000]	.053	.110	.229	.479
[Injured = 1]* [timepoint = 2]* [flashintensitymcd = 10]	.025	.053	.110	.229
[Injured = 1]* [timepoint = 2]* [flashintensitymcd = 3000]	.012	.025	.053	.110
[Injured = 1]* [timepoint = 2]* [flashintensitymcd = 10000]	.006	.012	.025	.053
[Injured = 1]* [timepoint = 7]* [flashintensitymcd = 10]	.003	.006	.012	.025
[Injured = 1]* [timepoint = 7]* [flashintensitymcd = 3000]	.001	.003	.006	.012

Working Correlation Matrix[a]

Measurement	Measurement			
	[Injured = 0]* [timepoint = 14]* [flashintensity mcd = 10000]	[Injured = 1]* [timepoint = 2]* [flashintensity mcd = 10]	[Injured = 1]* [timepoint = 2]* [flashintensity mcd = 3000]	[Injured = 1]* [timepoint = 2]* [flashintensity mcd = 10000]
[Injured = 0]* [timepoint = 2]* [flashintensitymcd = 10]	.003	.001	.001	.000
[Injured = 0]* [timepoint = 2]* [flashintensitymcd = 3000]	.006	.003	.001	.001
[Injured = 0]* [timepoint = 2]* [flashintensitymcd = 10000]	.012	.006	.003	.001
[Injured = 0]* [timepoint = 7]* [flashintensitymcd = 10]	.025	.012	.006	.003
[Injured = 0]* [timepoint = 7]* [flashintensitymcd = 3000]	.053	.025	.012	.006
[Injured = 0]* [timepoint = 7]* [flashintensitymcd = 10000]	.110	.053	.025	.012
[Injured = 0]* [timepoint = 14]* [flashintensitymcd = 10]	.229	.110	.053	.025
[Injured = 0]* [timepoint = 14]* [flashintensitymcd = 3000]	.479	.229	.110	.053
[Injured = 0]* [timepoint = 14]* [flashintensitymcd = 10000]	1.000	.479	.229	.110
[Injured = 1]* [timepoint = 2]* [flashintensitymcd = 10]	.479	1.000	.479	.229
[Injured = 1]* [timepoint = 2]* [flashintensitymcd = 3000]	.229	.479	1.000	.479
[Injured = 1]* [timepoint = 2]* [flashintensitymcd = 10000]	.110	.229	.479	1.000
[Injured = 1]* [timepoint = 7]* [flashintensitymcd = 10]	.053	.110	.229	.479
[Injured = 1]* [timepoint = 7]* [flashintensitymcd = 3000]	.025	.053	.110	.229

Working Correlation Matrix[a]

Measurement	Measurement			
	[Injured = 1]* [timepoint = 7]* [flashintensity mcd = 10]	[Injured = 1]* [timepoint = 7]* [flashintensity mcd = 3000]	[Injured = 1]* [timepoint = 7]* [flashintensity mcd = 10000]	[Injured = 1]* [timepoint = 14]* [flashintensity mcd = 10]
[Injured = 0]* [timepoint = 2]* [flashintensitymcd = 10]	.000	.000	.000	.000
[Injured = 0]* [timepoint = 2]* [flashintensitymcd = 3000]	.000	.000	.000	.000
[Injured = 0]* [timepoint = 2]* [flashintensitymcd = 10000]	.001	.000	.000	.000
[Injured = 0]* [timepoint = 7]* [flashintensitymcd = 10]	.001	.001	.000	.000
[Injured = 0]* [timepoint = 7]* [flashintensitymcd = 3000]	.003	.001	.001	.000
[Injured = 0]* [timepoint = 7]* [flashintensitymcd = 10000]	.006	.003	.001	.001
[Injured = 0]* [timepoint = 14]* [flashintensitymcd = 10]	.012	.006	.003	.001
[Injured = 0]* [timepoint = 14]* [flashintensitymcd = 3000]	.025	.012	.006	.003
[Injured = 0]* [timepoint = 14]* [flashintensitymcd = 10000]	.053	.025	.012	.006
[Injured = 1]* [timepoint = 2]* [flashintensitymcd = 10]	.110	.053	.025	.012
[Injured = 1]* [timepoint = 2]* [flashintensitymcd = 3000]	.229	.110	.053	.025
[Injured = 1]* [timepoint = 2]* [flashintensitymcd = 10000]	.479	.229	.110	.053
[Injured = 1]* [timepoint = 7]* [flashintensitymcd = 10]	1.000	.479	.229	.110
[Injured = 1]* [timepoint = 7]* [flashintensitymcd = 3000]	.479	1.000	.479	.229

Working Correlation Matrix[a]

Measurement	Measurement	
	[Injured = 1]* [timepoint = 14]* [flashintensity mcd = 3000]	[Injured = 1]* [timepoint = 14]* [flashintensity mcd = 10000]
[Injured = 0]* [timepoint = 2]* [flashintensitymcd = 10]	.000	.000
[Injured = 0]* [timepoint = 2]* [flashintensitymcd = 3000]	.000	.000
[Injured = 0]* [timepoint = 2]* [flashintensitymcd = 10000]	.000	.000
[Injured = 0]* [timepoint = 7]* [flashintensitymcd = 10]	.000	.000
[Injured = 0]* [timepoint = 7]* [flashintensitymcd = 3000]	.000	.000
[Injured = 0]* [timepoint = 7]* [flashintensitymcd = 10000]	.000	.000
[Injured = 0]* [timepoint = 14]* [flashintensitymcd = 10]	.001	.000
[Injured = 0]* [timepoint = 14]* [flashintensitymcd = 3000]	.001	.001
[Injured = 0]* [timepoint = 14]* [flashintensitymcd = 10000]	.003	.001
[Injured = 1]* [timepoint = 2]* [flashintensitymcd = 10]	.006	.003
[Injured = 1]* [timepoint = 2]* [flashintensitymcd = 3000]	.012	.006
[Injured = 1]* [timepoint = 2]* [flashintensitymcd = 10000]	.025	.012
[Injured = 1]* [timepoint = 7]* [flashintensitymcd = 10]	.053	.025
[Injured = 1]* [timepoint = 7]* [flashintensitymcd = 3000]	.110	.053

Working Correlation Matrix[a]

Measurement	Measurement			
	[Injured = 0]* [timepoint = 2]* [flashintensity mcd = 10]	[Injured = 0]* [timepoint = 2]* [flashintensity mcd = 3000]	[Injured = 0]* [timepoint = 2]* [flashintensity mcd = 10000]	[Injured = 0]* [timepoint = 7]* [flashintensity mcd = 10]
[Injured = 1]* [timepoint = 7]* [flashintensitymcd = 10000]	.000	.000	.000	.000
[Injured = 1]* [timepoint = 14]* [flashintensitymcd = 10]	.000	.000	.000	.000
[Injured = 1]* [timepoint = 14]* [flashintensitymcd = 3000]	.000	.000	.000	.000
[Injured = 1]* [timepoint = 14]* [flashintensitymcd = 10000]	.000	.000	.000	.000

Working Correlation Matrix[a]

Measurement	Measurement			
	[Injured = 0]* [timepoint = 7]* [flashintensity mcd = 3000]	[Injured = 0]* [timepoint = 7]* [flashintensity mcd = 10000]	[Injured = 0]* [timepoint = 14]* [flashintensity mcd = 10]	[Injured = 0]* [timepoint = 14]* [flashintensity mcd = 3000]
[Injured = 1]* [timepoint = 7]* [flashintensitymcd = 10000]	.001	.001	.003	.006
[Injured = 1]* [timepoint = 14]* [flashintensitymcd = 10]	.000	.001	.001	.003
[Injured = 1]* [timepoint = 14]* [flashintensitymcd = 3000]	.000	.000	.001	.001
[Injured = 1]* [timepoint = 14]* [flashintensitymcd = 10000]	.000	.000	.000	.001

Working Correlation Matrix[a]

Measurement	Measurement			
	[Injured = 0]* [timepoint = 14]* [flashintensity mcd = 10000]	[Injured = 1]* [timepoint = 2]* [flashintensity mcd = 10]	[Injured = 1]* [timepoint = 2]* [flashintensity mcd = 3000]	[Injured = 1]* [timepoint = 2]* [flashintensity mcd = 10000]
[Injured = 1]* [timepoint = 7]* [flashintensitymcd = 10000]	.012	.025	.053	.110
[Injured = 1]* [timepoint = 14]* [flashintensitymcd = 10]	.006	.012	.025	.053
[Injured = 1]* [timepoint = 14]* [flashintensitymcd = 3000]	.003	.006	.012	.025
[Injured = 1]* [timepoint = 14]* [flashintensitymcd = 10000]	.001	.003	.006	.012

Working Correlation Matrix[a]

Measurement	Measurement			
	[Injured = 1]* [timepoint = 7]* [flashintensity mcd = 10]	[Injured = 1]* [timepoint = 7]* [flashintensity mcd = 3000]	[Injured = 1]* [timepoint = 7]* [flashintensity mcd = 10000]	[Injured = 1]* [timepoint = 14]* [flashintensity mcd = 10]
[Injured = 1]* [timepoint = 7]* [flashintensitymcd = 10000]	.229	.479	1.000	.479
[Injured = 1]* [timepoint = 14]* [flashintensitymcd = 10]	.110	.229	.479	1.000
[Injured = 1]* [timepoint = 14]* [flashintensitymcd = 3000]	.053	.110	.229	.479
[Injured = 1]* [timepoint = 14]* [flashintensitymcd = 10000]	.025	.053	.110	.229

Working Correlation Matrix[a]

Measurement	Measurement	
	[Injured = 1]* [timepoint = 14]* [flashintensity mcd = 3000]	[Injured = 1]* [timepoint = 14]* [flashintensity mcd = 10000]
[Injured = 1]* [timepoint = 7]* [flashintensitymcd = 10000]	.229	.110
[Injured = 1]* [timepoint = 14]* [flashintensitymcd = 10]	.479	.229
[Injured = 1]* [timepoint = 14]* [flashintensitymcd = 3000]	1.000	.479
[Injured = 1]* [timepoint = 14]* [flashintensitymcd = 10000]	.479	1.000

Dependent Variable: awaveamplitudev
Model: (Intercept), timepoint, flashintensitymcd, Injured, timepoint * flashintensitymcd, flashintensitymcd * Injured

a. The AR(1) working correlation matrix structure is computed assuming the measurements are equally spaced for all subjects.

Estimated Marginal Means: timepoint* flashintensitymcd* Injured

Estimates

timepoint	flashintensitymcd	Injured	Mean	Std. Error	95% Wald Confidence Interval	
					Lower	Upper
2	10	0	15.494	1.5642	12.713	18.884
		1	8.205	.9912	6.476	10.397
	3000	0	176.086	26.6687	130.860	236.942
		1	62.891	8.0637	48.916	80.859
	10000	0	224.350	26.8911	177.378	283.761
		1	83.104	8.9128	67.349	102.544
7	10	0	16.761	3.0466	11.738	23.935
		1	8.876	2.0411	5.656	13.930
	3000	0	240.090	30.5745	187.058	308.156
		1	85.750	14.7053	61.272	120.007
	10000	0	280.907	32.1364	224.483	351.514
		1	104.054	16.8664	75.733	142.966
14	10	0	19.160	2.7818	14.415	25.467
		1	10.147	1.8597	7.085	14.532
	3000	0	281.935	17.8812	248.979	319.252
		1	100.696	13.9219	76.794	132.037
	10000	0	321.952	25.6459	275.414	376.353
		1	119.257	18.5496	87.920	161.764

```
EXAMINE VARIABLES=Residual PearsonResidual
  /PLOT BOXPLOT HISTOGRAM NPPLOT
  /COMPARE GROUPS
  /STATISTICS DESCRIPTIVES
  /CINTERVAL 95
  /MISSING LISTWISE
  /NOTOTAL.
```

Explore

[DataSet1] C:\Users\Public\Documents\PhD\ERG\Results\T-CEM423-6\scotopic data T.sav

Case Processing Summary

	Cases					
	Valid		Missing		Total	
	N	Percent	N	Percent	N	Percent
Raw Residual	134	88.2%	18	11.8%	152	100.0%
Pearson Residual	134	88.2%	18	11.8%	152	100.0%

Descriptives

			Statistic	Std. Error
Raw Residual	Mean		.83261	4.998476
	95% Confidence Interval for Mean	Lower Bound	-9.05418	
		Upper Bound	10.71940	
	5% Trimmed Mean		.64777	
	Median		-.48135	
	Variance		3347.958	
	Std. Deviation		57.861543	
	Minimum		-168.752	
	Maximum		157.243	
	Range		325.994	
	Interquartile Range		44.021	
	Skewness		.157	.209
	Kurtosis		1.199	.416
Pearson Residual	Mean		.01414	.036701
	95% Confidence Interval for Mean	Lower Bound	-.05845	
		Upper Bound	.08673	
	5% Trimmed Mean		-.00164	
	Median		-.01573	
	Variance		.180	
	Std. Deviation		.424844	
	Minimum		-.842	
	Maximum		1.319	
	Range		2.161	

Descriptives

		Statistic	Std. Error
	Interquartile Range	.560	
	Skewness	.478	.209
	Kurtosis	.219	.416

Tests of Normality

	Kolmogorov-Smirnov[a]			Shapiro-Wilk		
	Statistic	df	Sig.	Statistic	df	Sig.
Raw Residual	.152	134	.000	.938	134	.000
Pearson Residual	.048	134	.200*	.980	134	.044

*. This is a lower bound of the true significance.

a. Lilliefors Significance Correction

Raw Residual

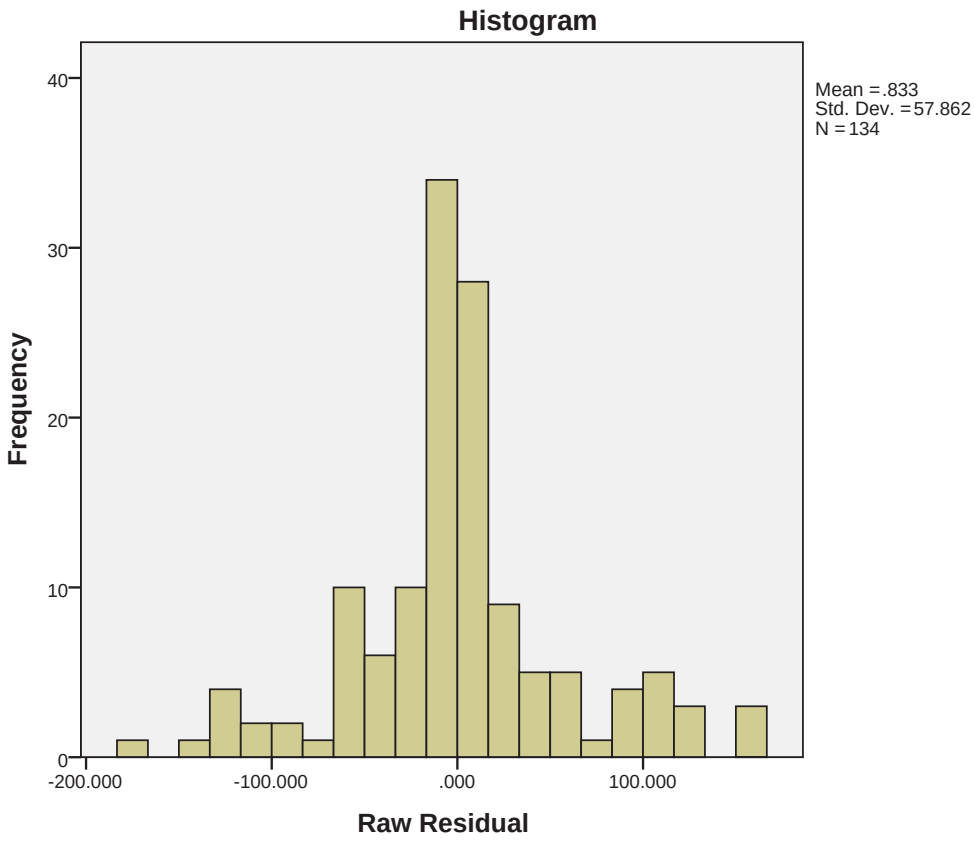

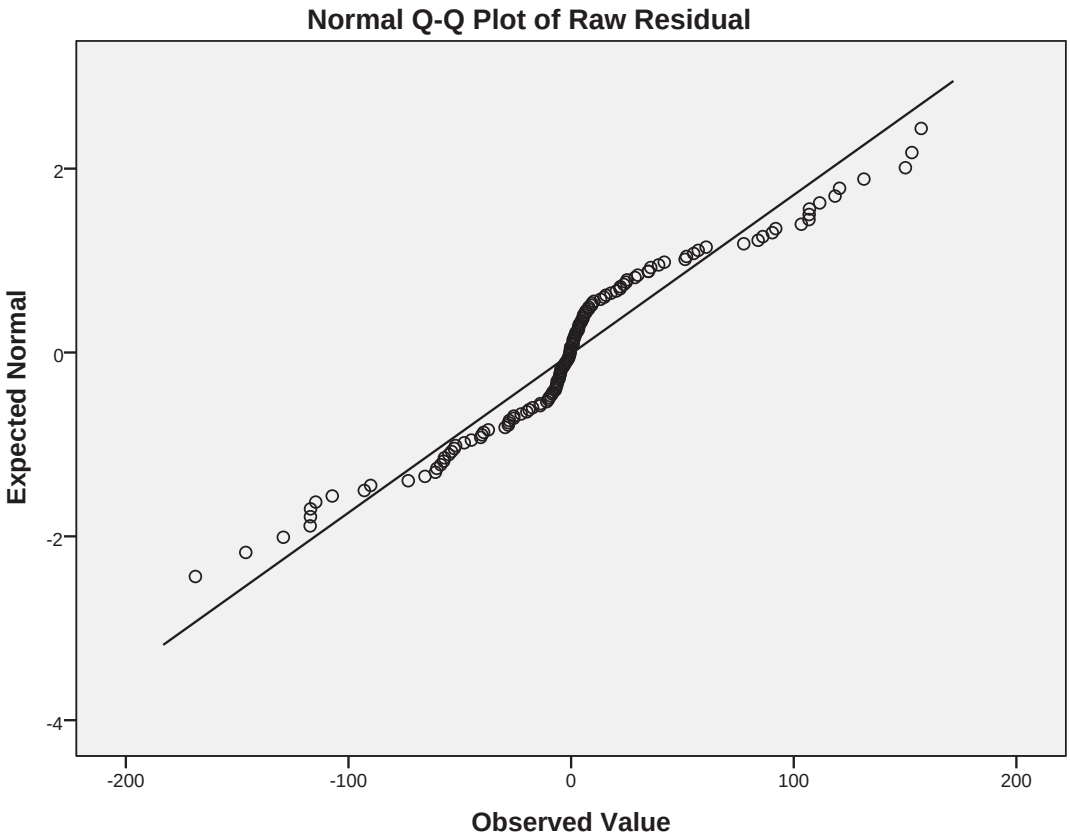
Normal Q-Q Plot of Raw Residual
Expected Normal
2
0
-2
-4
-200
-100
0
100
200
Observed Value

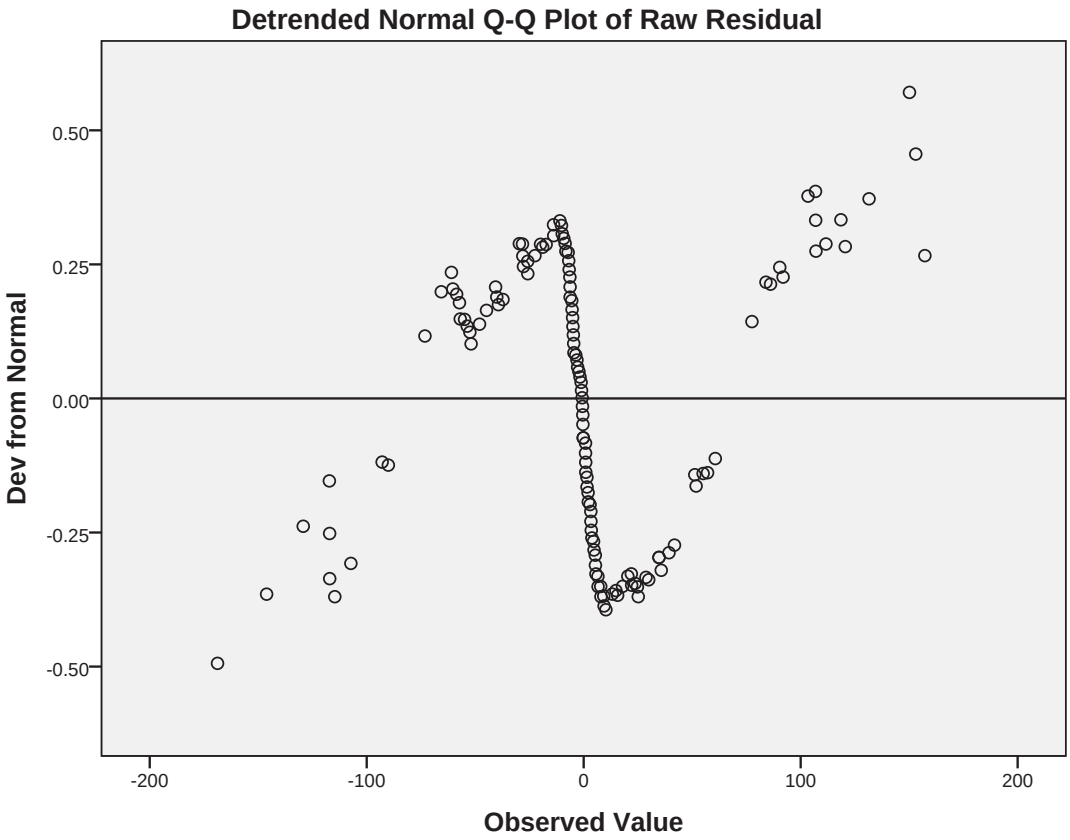
Detrended Normal Q-Q Plot of Raw Residual
Dev from Normal
0.50
0.25
0.00
-0.25
-0.50
-200
-100
0
100
200
Observed Value

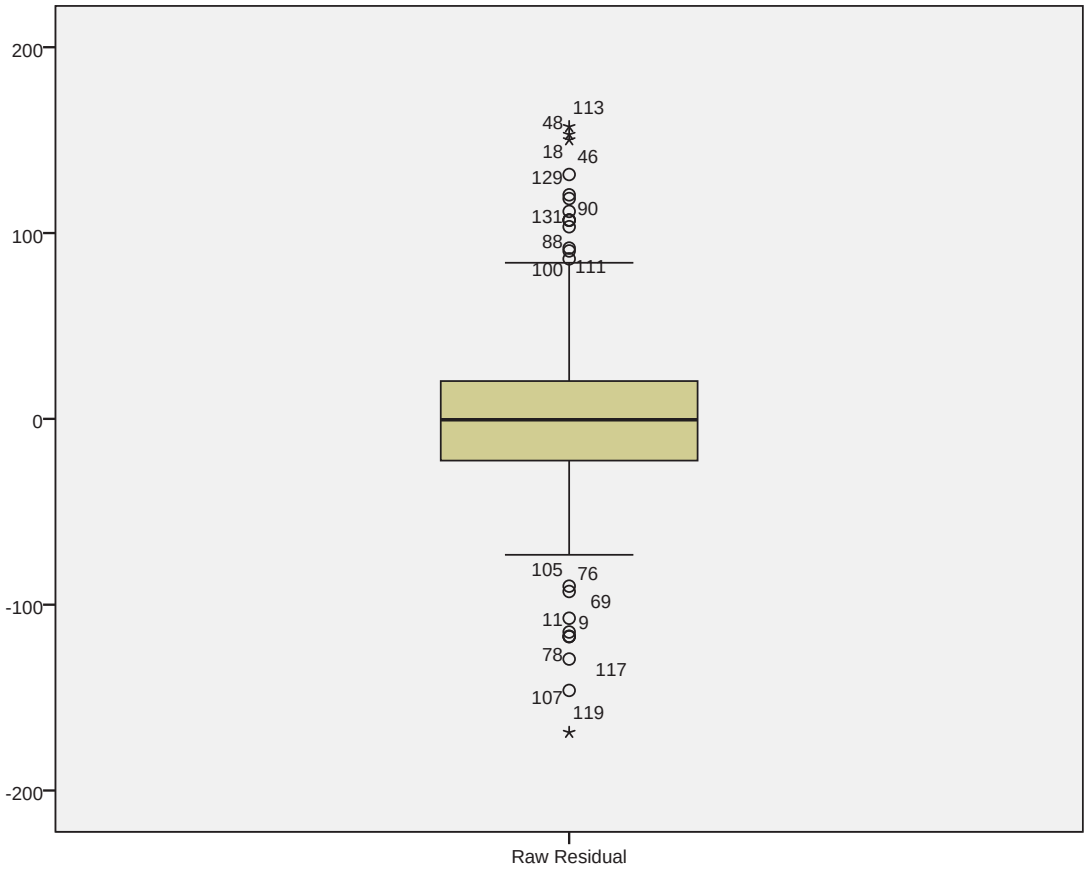

Pearson Residual

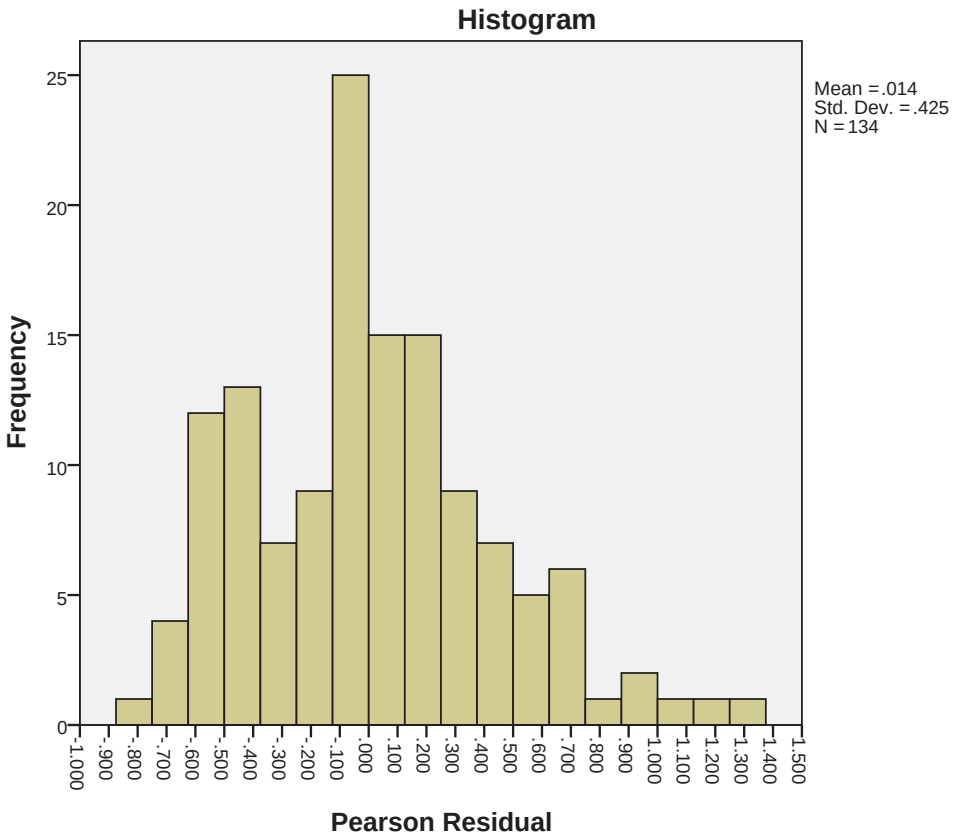
Histogram
Mean =.014
Std. Dev. =.425
N =134
Frequency
Pearson Residual
0
5
10
15
20
25
-1.000
-.900
-.800
-.700
-.600
-.500
-.400
-.300
-.200
-.100
.000
.100
.200
.300
.400
.500
.600
.700
.800
.900
1.000
1.100
1.200
1.300
1.400
1.500

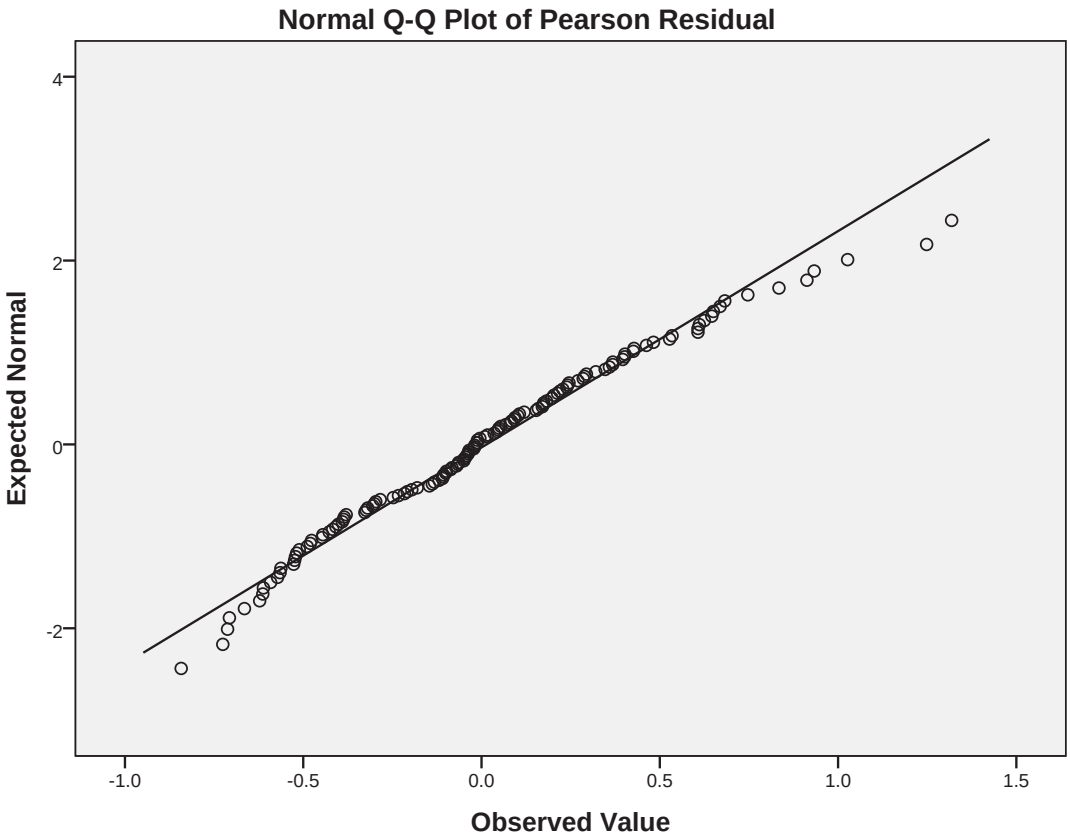
Normal Q-Q Plot of Pearson Residual
Expected Normal
4
2
0
-2
-1.0
-0.5
0.0
0.5
1.0
1.5
Observed Value

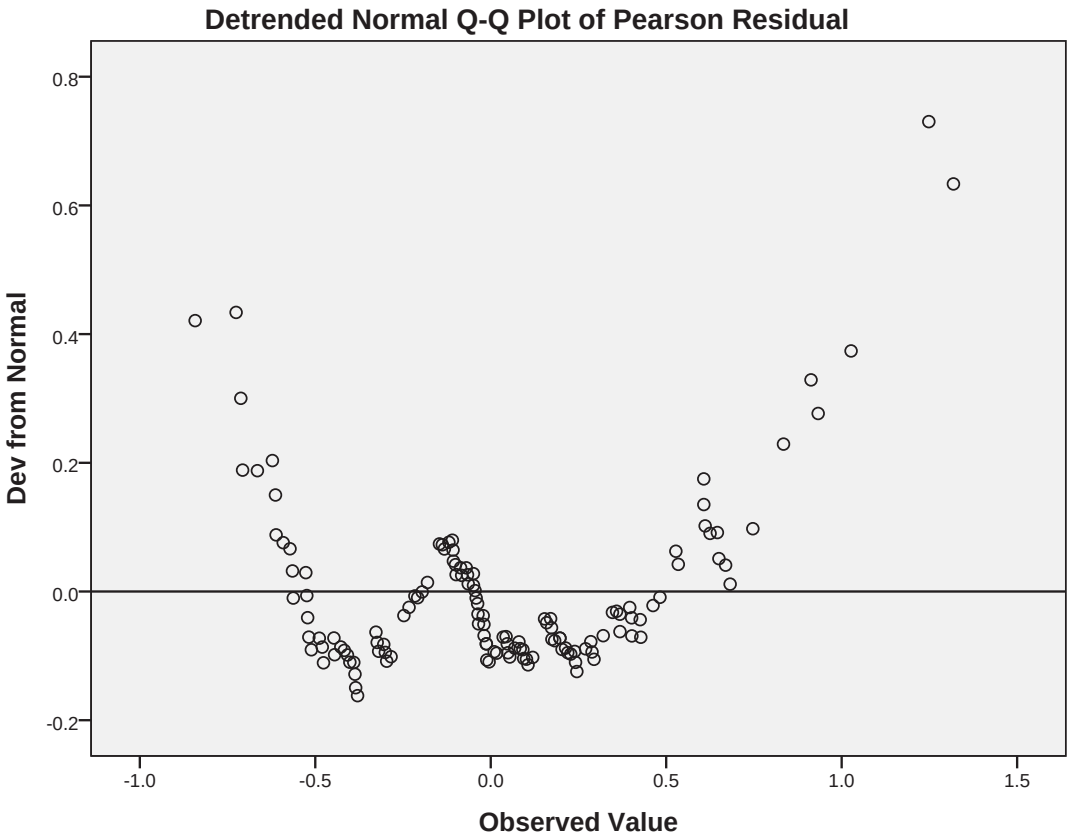
Detrended Normal Q-Q Plot of Pearson Residual
Dev from Normal
0.8
0.6
0.4
0.2
0.0
-0.2
-1.0
-0.5
0.0
0.5
1.0
1.5
Observed Value

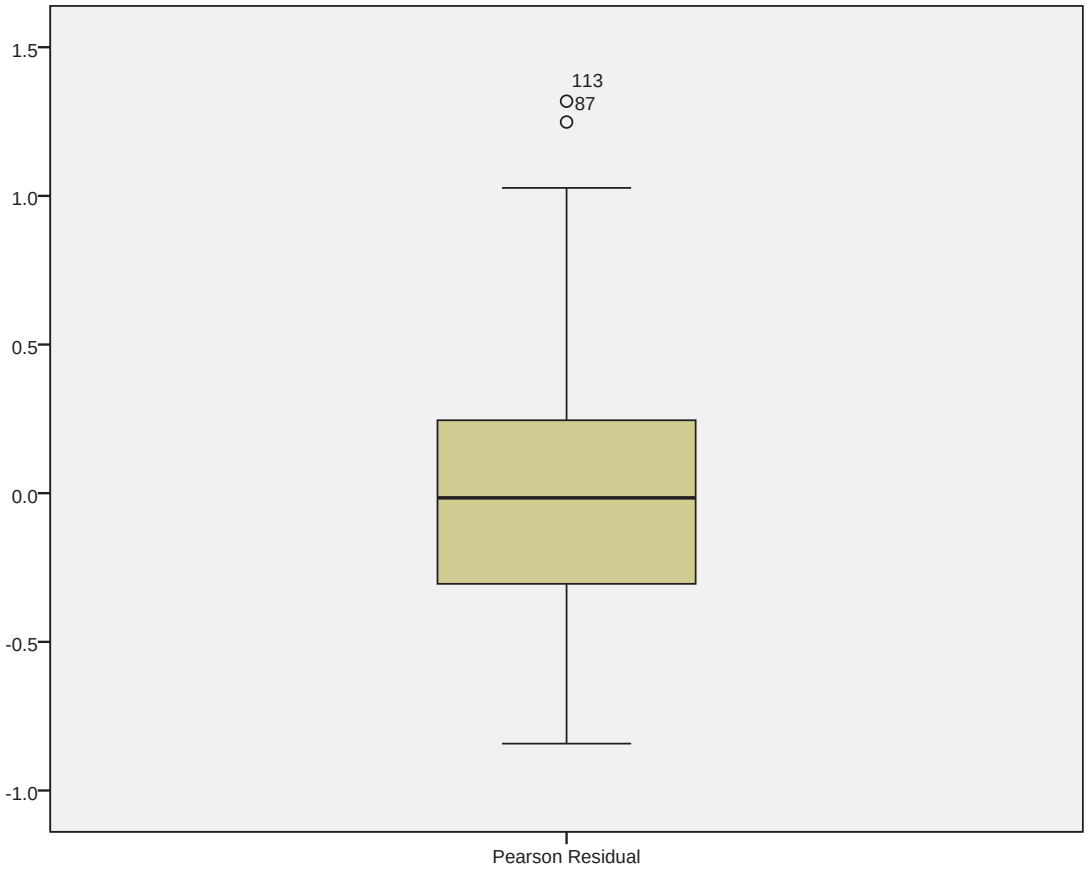


```
EXAMINE VARIABLES=awaveamplitudev
  /PLOT BOXPLOT HISTOGRAM NPPLOT
  /COMPARE GROUPS
  /STATISTICS DESCRIPTIVES
  /CINTERVAL 95
  /MISSING LISTWISE
  /NOTOTAL.
```

Explore

[DataSet1] C:\Users\Public\Documents\PhD\ERG\Results\T-CEM423-6\scotopic data T.sav

Case Processing Summary

	Cases					
	Valid		Missing		Total	
	N	Percent	N	Percent	N	Percent
awaveamplitudev	144	94.7%	8	5.3%	152	100.0%

Descriptives

			Statistic	Std. Error
awaveamplitudev	Mean		119.949	9.8672
	95% Confidence Interval for Mean	Lower Bound	100.444	
		Upper Bound	139.453	
	5% Trimmed Mean		111.256	
	Median		76.250	
	Variance		14020.079	
	Std. Deviation		118.4064	
	Minimum		.0	
	Maximum		440.5	
	Range		440.5	
	Interquartile Range		192.0	
	Skewness		.883	.202
	Kurtosis		-.332	.401

Tests of Normality

	Kolmogorov-Smirnov[a]			Shapiro-Wilk		
	Statistic	df	Sig.	Statistic	df	Sig.
awaveamplitudev	.162	144	.000	.870	144	.000

a. Lilliefors Significance Correction

awaveamplitudev

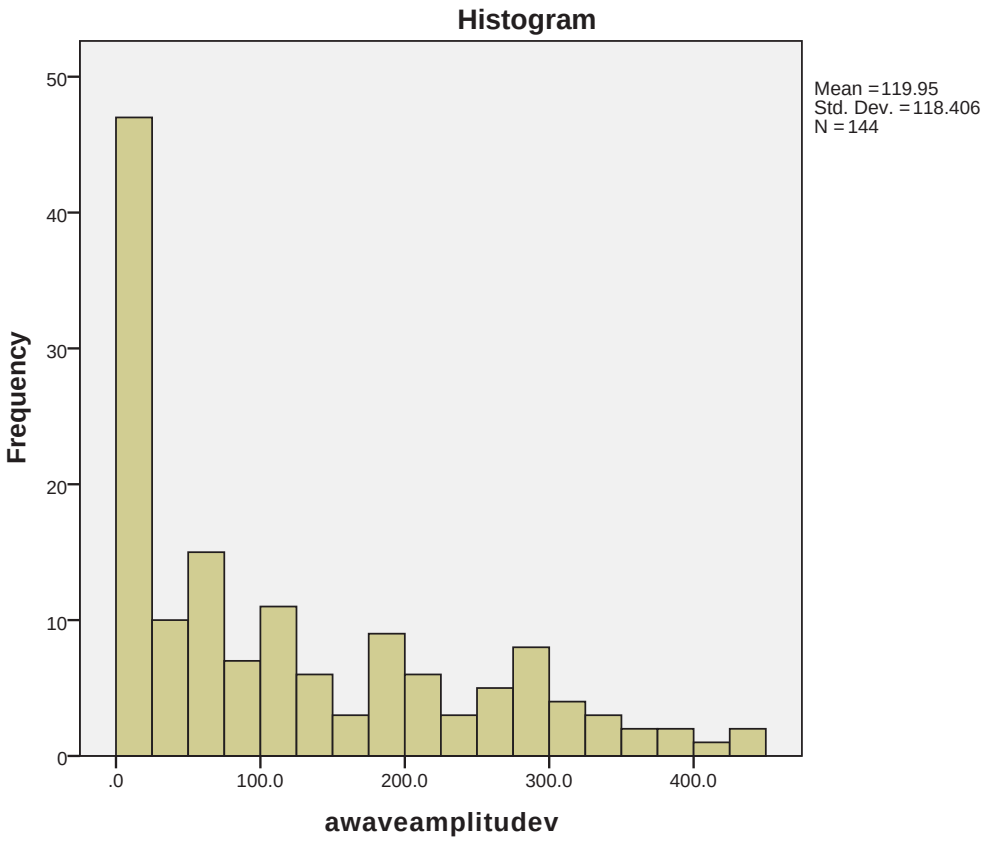
Histogram
Mean =119.95
Std. Dev. =118.406
N =144
Frequency
50
40
30
20
10
0
.0
100.0
200.0
300.0
400.0
awaveamplitudev

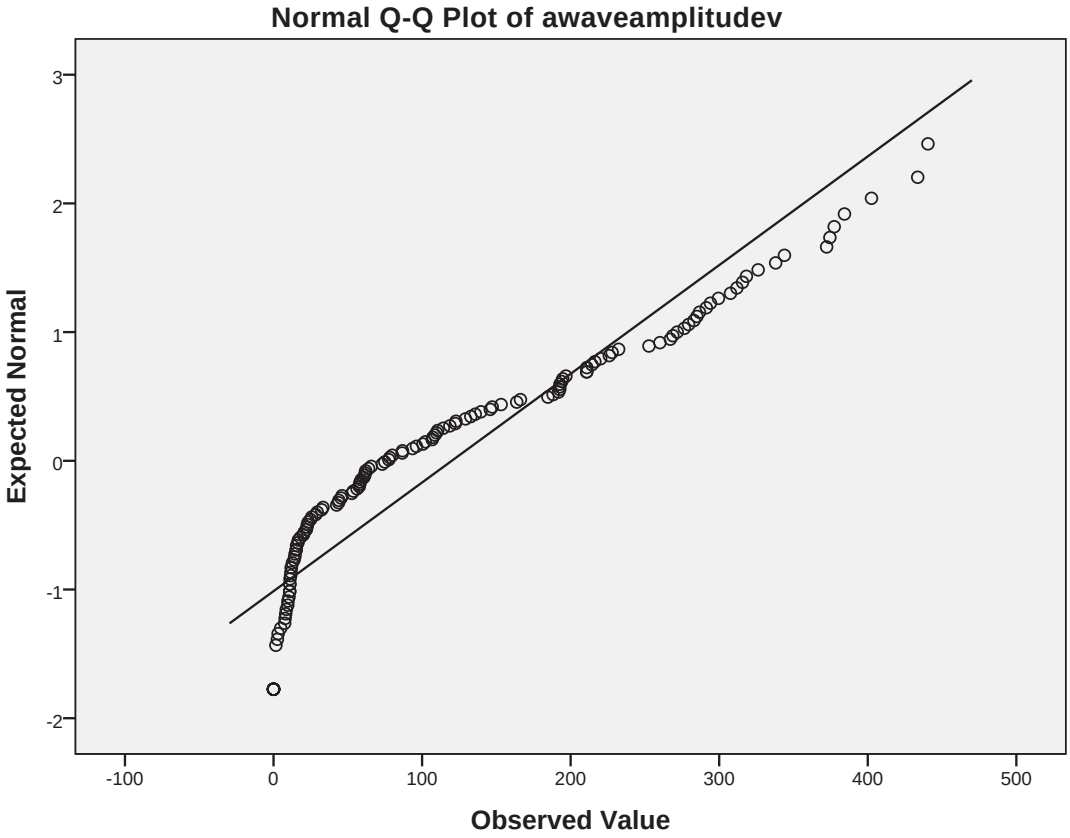
Normal Q-Q Plot of awaveamplitudev
Expected Normal
3
2
1
0
-1
-2
-100
0
100
200
300
400
500
Observed Value

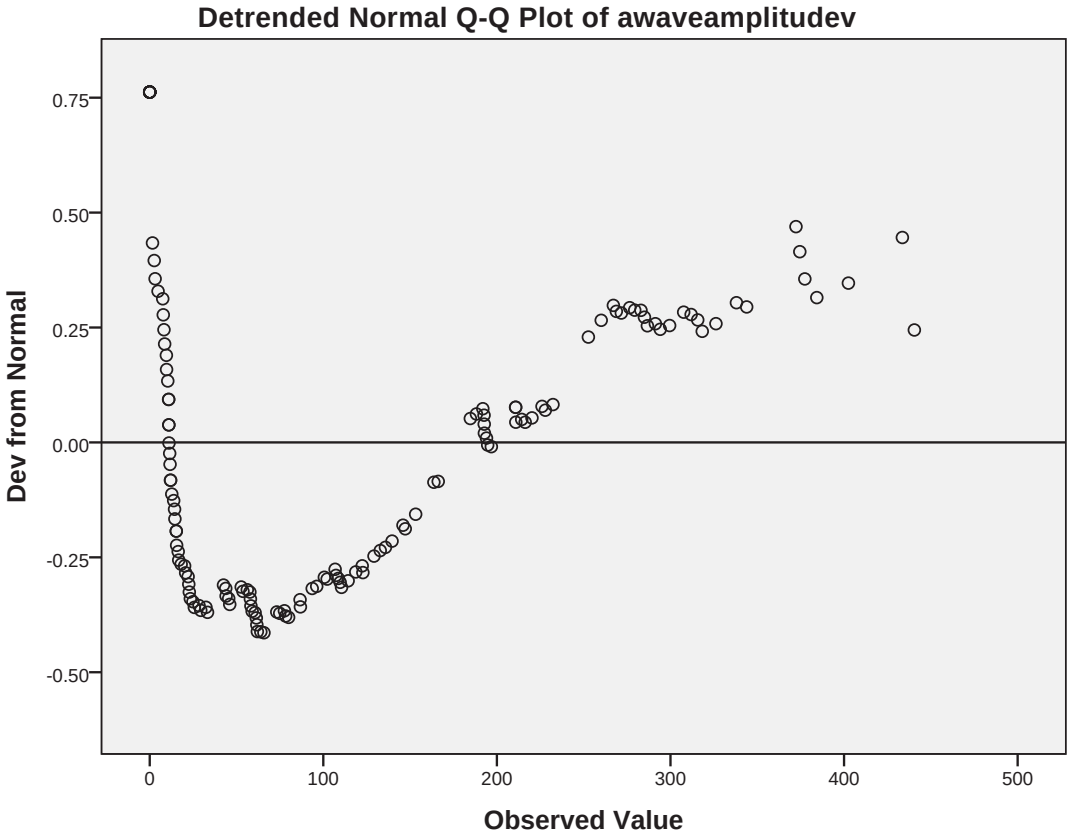
Detrended Normal Q-Q Plot of awaveamplitudev
Dev from Normal
0.75
0.50
0.25
0.00
-0.25
-0.50
0
100
200
300
400
500
Observed Value

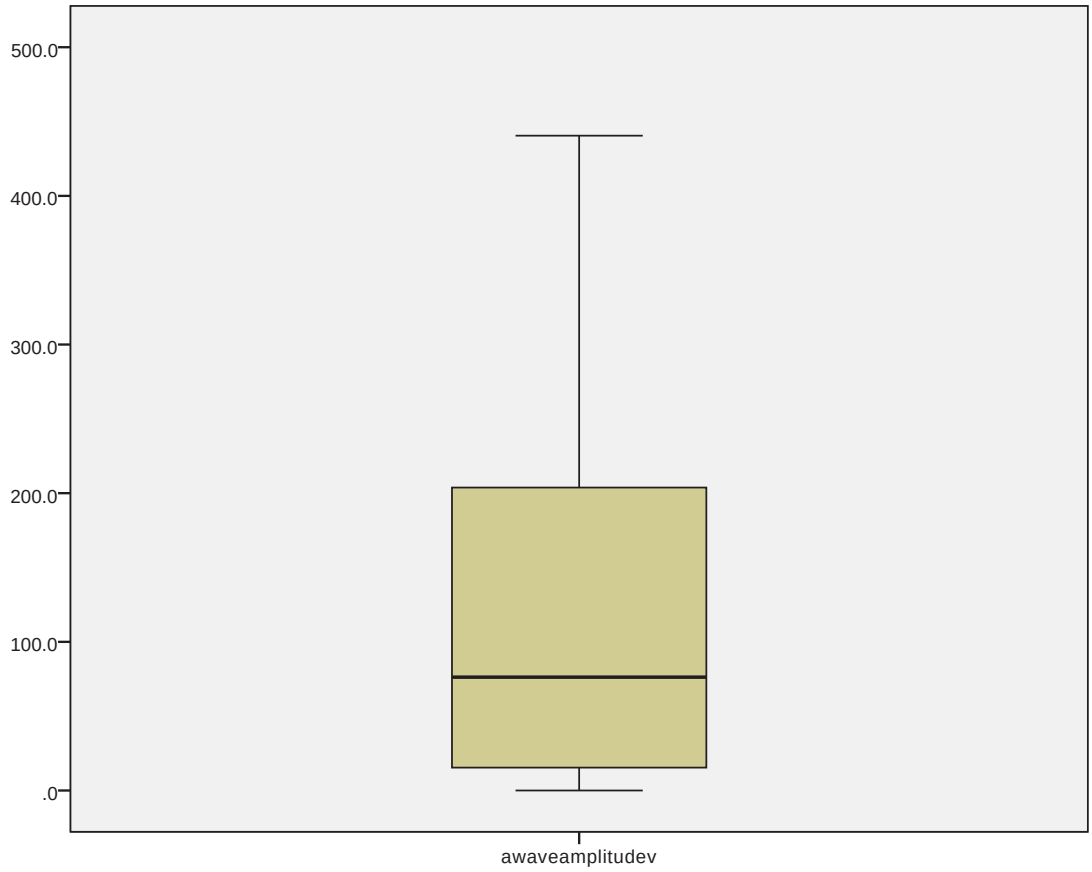


```
 * Chart Builder.
GGRAPH
  /GRAPHDATASET NAME="graphdataset" VARIABLES=MeanPredicted MEAN(Residual)[name="MEAN_Residu
  /GRAPHSPEC SOURCE=INLINE.
BEGIN GPL
  SOURCE: s=userSource(id("graphdataset"))
  DATA: MeanPredicted=col(source(s), name("MeanPredicted"))
  DATA: MEAN_Residual=col(source(s), name("MEAN_Residual"))
  GUIDE: axis(dim(1), label("Predicted Value of Mean of Response"))
  GUIDE: axis(dim(2), label("Mean Raw Residual"))
  ELEMENT: point(position(MeanPredicted*MEAN_Residual))
END GPL.
```

```
 * Chart Builder.
GGRAPH
  /GRAPHDATASET NAME="graphdataset" VARIABLES=MeanPredicted_1 Residual_2 MISSING=LISTWISE RE
  /GRAPHSPEC SOURCE=INLINE.
BEGIN GPL
  SOURCE: s=userSource(id("graphdataset"))
  DATA: MeanPredicted_1=col(source(s), name("MeanPredicted_1"))
  DATA: Residual_2=col(source(s), name("Residual_2"))
```

```
  GUIDE: axis(dim(1), label("Predicted Value of Mean of Response"))
  GUIDE: axis(dim(2), label("Raw Residual"))
  ELEMENT: point(position(MeanPredicted_1*Residual_2))
END GPL.
```

GGraph

[DataSet1] C:\Users\Public\Documents\PhD\ERG\Results\T-CEM423-6\scotopic data T.sav

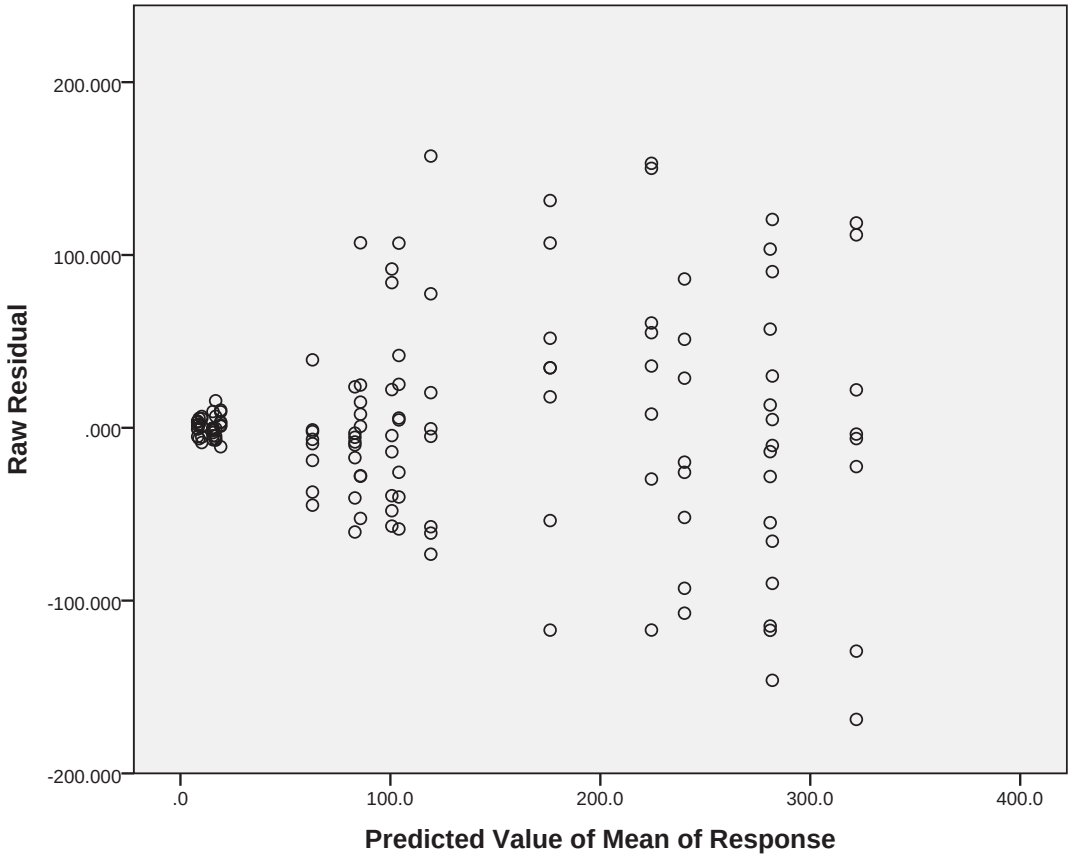


```
 * Chart Builder.
GGRAPH
  /GRAPHDATASET NAME="graphdataset" VARIABLES=MeanPredicted_1 PearsonResidual_2 MISSING=LIST
  /GRAPHSPEC SOURCE=INLINE.
BEGIN GPL
  SOURCE: s=userSource(id("graphdataset"))
  DATA: MeanPredicted_1=col(source(s), name("MeanPredicted_1"))
  DATA: PearsonResidual_2=col(source(s), name("PearsonResidual_2"))
  GUIDE: axis(dim(1), label("Predicted Value of Mean of Response"))
  GUIDE: axis(dim(2), label("Pearson Residual"))
  ELEMENT: point(position(MeanPredicted_1*PearsonResidual_2))
END GPL.
```

GGraph

[DataSet1] C:\Users\Public\Documents\PhD\ERG\Results\T-CEM423-6\scotopic data T.sav

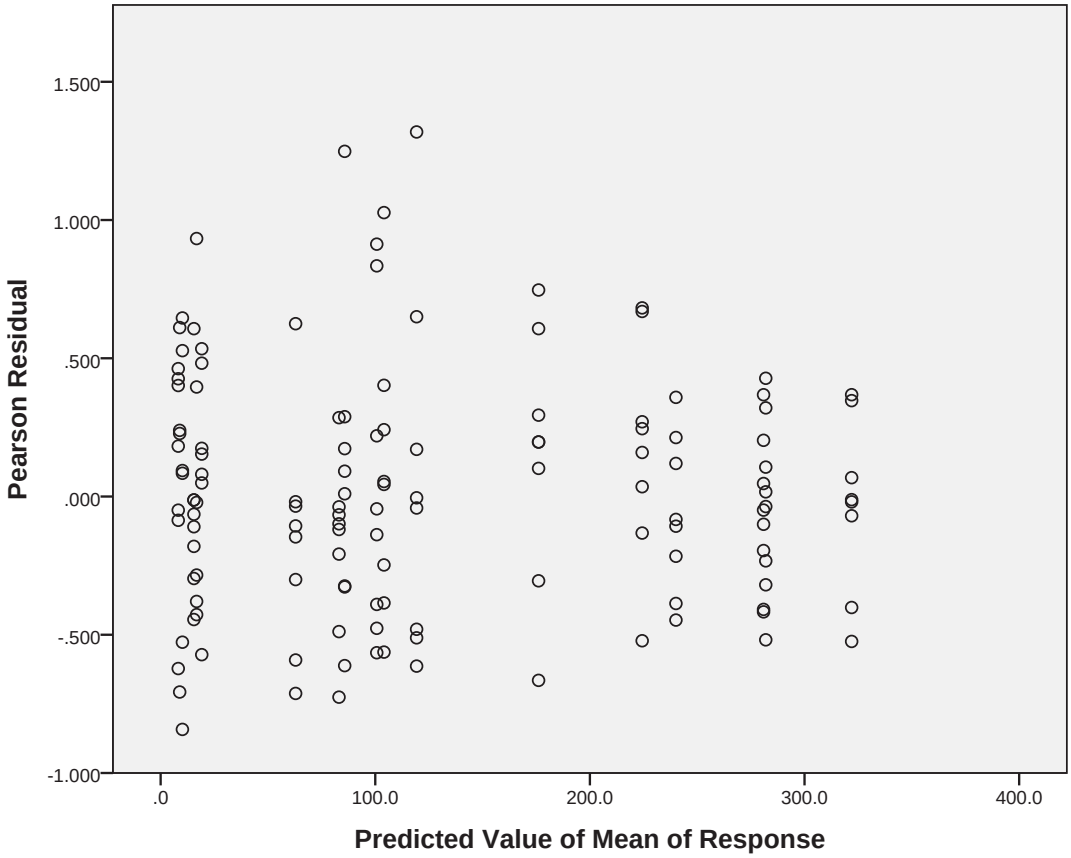

APPENDIX 8

```
 DATASET ACTIVATE DataSet5.
* Generalized Estimating Equations.
GENLIN awaveslopevms BY timepoint flashintensitymcd Injured (ORDER=DATA)
  /MODEL timepoint flashintensitymcd Injured timepoint*flashintensitymcd flashintensitymcd*I
 DISTRIBUTION=GAMMA LINK=LOG
  /CRITERIA METHOD=FISHER(1) SCALE=MLE MAXITERATIONS=100 MAXSTEPHALVING=5 PCONVERGE=1E-006
(ABSOLUTE) SINGULAR=1E-012 ANALYSISTYPE=3(WALD) CILEVEL=95 LIKELIHOOD=FULL
  /EMMEANS TABLES=timepoint*flashintensitymcd*Injured SCALE=ORIGINAL
  /REPEATED SUBJECT=animal WITHINSUBJECT=Injured*timepoint*flashintensitymcd SORT=YES CORRTY
(1) ADJUSTCORR=YES COVB=ROBUST MAXITERATIONS=100 PCONVERGE=1e-006(ABSOLUTE) UPDATECORR=1
  /MISSING CLASSMISSING=EXCLUDE
  /PRINT CPS DESCRIPTIVES MODELINFO FIT SUMMARY WORKINGCORR.


 * Generalized Estimating Equations.
GENLIN awaveslopevms BY timepoint flashintensitymcd Injured (ORDER=DATA)
  /MODEL timepoint flashintensitymcd Injured timepoint*flashintensitymcd timepoint*Injured f
 DISTRIBUTION=GAMMA LINK=LOG
  /CRITERIA METHOD=FISHER(1) SCALE=MLE MAXITERATIONS=100 MAXSTEPHALVING=5 PCONVERGE=1E-006(A
  /EMMEANS TABLES=timepoint*flashintensitymcd*Injured SCALE=ORIGINAL
  /REPEATED SUBJECT=animal WITHINSUBJECT=Injured*timepoint*flashintensitymcd SORT=YES CORRTY
(ABSOLUTE) UPDATECORR=1
  /MISSING CLASSMISSING=EXCLUDE
  /PRINT CPS DESCRIPTIVES MODELINFO FIT SUMMARY WORKINGCORR.
```

Generalized Linear Models

Notes

Output Created		02-MAY-2013 09:59:00
Comments		
Input	Data	C:\Users\Public\Documents\PhD\ERG\Results\T-CEM423-6\scotopic data T.sav
	Active Dataset	DataSet5
	Filter	<none>
	Weight	<none>
	Split File	<none>
	N of Rows in Working Data File	152
Missing Value Handling	Definition of Missing	User-defined missing values for factor, subject and within-subject variables are treated as missing.
	Cases Used	Statistics are based on cases with valid data for all variables in the model.
Weight Handling		not applicable
Syntax		GENLIN awaveslopevms BY timepoint flashintensitymcd Injured (ORDER=DATA) /MODEL timepoint flashintensitymcd Injured timepoint*flashintensitymcd timepoint*Injured flashintensitymcd*Injured timepoint*flashintensitymcd*Injured INTERCEPT=YES DISTRIBUTION=GAMMA LINK=LOG /CRITERIA METHOD=FISHER(1) SCALE=MLE MAXITERATIONS=100 MAXSTEPHALVING=5 PCONVERGE=1E-006(ABSOLUTE) SINGULAR=1E-012 ANALYSISTYPE=3(WALD) CILEVEL=95 LIKELIHOOD=FULL /EMMEANS TABLES=timepoint*flashintensitymcd*Injured SCALE=ORIGINAL /REPEATED SUBJECT=animal WITHINSUBJECT=Injured*timepoint*flashintensitymcd SORT=YES CORRTYPE=AR(1) ADJUSTCORR=YES COVB=ROBUST MAXITERATIONS=100 PCONVERGE=1e-006(ABSOLUTE) UPDATECORR=1 /MISSING CLASSMISSING=EXCLUDE /PRINT CPS DESCRIPTIVES...

Notes

Resources	Processor Time	00:00:00.11
	Elapsed Time	00:00:00.14

[DataSet5] C:\Users\Public\Documents\PhD\ERG\Results\T-CEM423-6\scotopic data T.sav

Warnings

One or more cases were found with dependent variable data values that are less than or equal to zero. These values are invalid for the gamma probability distribution, and the cases are not used in the analysis.

Model Information

Dependent Variable		awaveslopevms
Probability Distribution		Gamma
Link Function		Log
Subject Effect	1	animal
Within-Subject Effect	1	Injured
	2	timepoint
	3	flashintensitymcd
Working Correlation Matrix Structure		AR(1)

Case Processing Summary

	N	Percent
Included	142	93.4%
Excluded	10	6.6%
Total	152	100.0%

Correlated Data Summary

Number of Levels	Subject Effect	animal	8
	Within-Subject Effect	Injured	2
		timepoint	3
		flashintensitymcd	3
Number of Subjects			8
Number of Measurements per Subject	Minimum		17
	Maximum		18
Correlation Matrix Dimension			18

Categorical Variable Information

			N	Percent
Factor	timepoint	2	48	33.8%
		7	46	32.4%
		14	48	33.8%
		Total	142	100.0%
	flashintensitymcd	10	46	32.4%
		3000	48	33.8%
		10000	48	33.8%
		Total	142	100.0%
	Injured	1	70	49.3%
		0	72	50.7%
		Total	142	100.0%

Continuous Variable Information

		N	Minimum	Maximum	Mean
Dependent Variable	awaveslopevms	142	.019	93.300	19.45224

Continuous Variable Information

		Std. Deviation
Dependent Variable	awaveslopevms	21.003468

Goodness of Fit[a]

	Value
Quasi Likelihood under Independence Model Criterion (QIC)[b]	87.520
Corrected Quasi Likelihood under Independence Model Criterion (QICC)[b]	92.409

Dependent Variable: awaveslopevms
Model: (Intercept), timepoint, flashintensitymcd, Injured, timepoint * flashintensitymcd, timepoint * Injured, flashintensitymcd * Injured, timepoint * flashintensitymcd * Injured

a. Information criteria are in small-is-better form.

b. Computed using the full log quasi-likelihood function.

Tests of Model Effects

Source	Type III		
	Wald Chi-Square	df	Sig.
(Intercept)	489.916	1	.000
timepoint	14.093	2	.001
flashintensitymcd	1042.949	2	.000
Injured	61.656	1	.000
timepoint * flashintensitymcd	10.404	4	.034
timepoint * Injured	.883	2	.643
flashintensitymcd * Injured	12.648	2	.002
timepoint * flashintensitymcd * Injured	11.543	4	.021

Dependent Variable: awaveslopevms
Model: (Intercept), timepoint, flashintensitymcd, Injured, timepoint * flashintensitymcd, timepoint * Injured, flashintensitymcd * Injured, timepoint * flashintensitymcd * Injured

Working Correlation Matrix[a]

Measurement	Measurement			
	[Injured = 0]* [timepoint = 2]* [flashintensitymcd = 10]	[Injured = 0]* [timepoint = 2]* [flashintensitymcd = 3000]	[Injured = 0]* [timepoint = 2]* [flashintensitymcd = 10000]	[Injured = 0]* [timepoint = 7]* [flashintensitymcd = 10]
[Injured = 0]* [timepoint = 2]* [flashintensitymcd = 10]	1.000	.506	.256	.129
[Injured = 0]* [timepoint = 2]* [flashintensitymcd = 3000]	.506	1.000	.506	.256
[Injured = 0]* [timepoint = 2]* [flashintensitymcd = 10000]	.256	.506	1.000	.506
[Injured = 0]* [timepoint = 7]* [flashintensitymcd = 10]	.129	.256	.506	1.000
[Injured = 0]* [timepoint = 7]* [flashintensitymcd = 3000]	.065	.129	.256	.506
[Injured = 0]* [timepoint = 7]* [flashintensitymcd = 10000]	.033	.065	.129	.256

Working Correlation Matrix[a]

Measurement	Measurement			
	[Injured = 0]* [timepoint = 7]* [flashintensity mcd = 3000]	[Injured = 0]* [timepoint = 7]* [flashintensity mcd = 10000]	[Injured = 0]* [timepoint = 14]* [flashintensity mcd = 10]	[Injured = 0]* [timepoint = 14]* [flashintensity mcd = 3000]
[Injured = 0]* [timepoint = 2]* [flashintensitymcd = 10]	.065	.033	.017	.008
[Injured = 0]* [timepoint = 2]* [flashintensitymcd = 3000]	.129	.065	.033	.017
[Injured = 0]* [timepoint = 2]* [flashintensitymcd = 10000]	.256	.129	.065	.033
[Injured = 0]* [timepoint = 7]* [flashintensitymcd = 10]	.506	.256	.129	.065
[Injured = 0]* [timepoint = 7]* [flashintensitymcd = 3000]	1.000	.506	.256	.129
[Injured = 0]* [timepoint = 7]* [flashintensitymcd = 10000]	.506	1.000	.506	.256

Working Correlation Matrix[a]

Measurement	Measurement			
	[Injured = 0]* [timepoint = 14]* [flashintensity mcd = 10000]	[Injured = 1]* [timepoint = 2]* [flashintensity mcd = 10]	[Injured = 1]* [timepoint = 2]* [flashintensity mcd = 3000]	[Injured = 1]* [timepoint = 2]* [flashintensity mcd = 10000]
[Injured = 0]* [timepoint = 2]* [flashintensitymcd = 10]	.004	.002	.001	.001
[Injured = 0]* [timepoint = 2]* [flashintensitymcd = 3000]	.008	.004	.002	.001
[Injured = 0]* [timepoint = 2]* [flashintensitymcd = 10000]	.017	.008	.004	.002
[Injured = 0]* [timepoint = 7]* [flashintensitymcd = 10]	.033	.017	.008	.004
[Injured = 0]* [timepoint = 7]* [flashintensitymcd = 3000]	.065	.033	.017	.008
[Injured = 0]* [timepoint = 7]* [flashintensitymcd = 10000]	.129	.065	.033	.017

Working Correlation Matrix[a]

Measurement	Measurement			
	[Injured = 1]* [timepoint = 7]* [flashintensity mcd = 10]	[Injured = 1]* [timepoint = 7]* [flashintensity mcd = 3000]	[Injured = 1]* [timepoint = 7]* [flashintensity mcd = 10000]	[Injured = 1]* [timepoint = 14]* [flashintensity mcd = 10]
[Injured = 0]* [timepoint = 2]* [flashintensitymcd = 10]	.000	.000	.000	.000
[Injured = 0]* [timepoint = 2]* [flashintensitymcd = 3000]	.001	.000	.000	.000
[Injured = 0]* [timepoint = 2]* [flashintensitymcd = 10000]	.001	.001	.000	.000
[Injured = 0]* [timepoint = 7]* [flashintensitymcd = 10]	.002	.001	.001	.000
[Injured = 0]* [timepoint = 7]* [flashintensitymcd = 3000]	.004	.002	.001	.001
[Injured = 0]* [timepoint = 7]* [flashintensitymcd = 10000]	.008	.004	.002	.001

Working Correlation Matrix[a]

Measurement	Measurement	
	[Injured = 1]* [timepoint = 14]* [flashintensity mcd = 3000]	[Injured = 1]* [timepoint = 14]* [flashintensity mcd = 10000]
[Injured = 0]* [timepoint = 2]* [flashintensitymcd = 10]	.000	.000
[Injured = 0]* [timepoint = 2]* [flashintensitymcd = 3000]	.000	.000
[Injured = 0]* [timepoint = 2]* [flashintensitymcd = 10000]	.000	.000
[Injured = 0]* [timepoint = 7]* [flashintensitymcd = 10]	.000	.000
[Injured = 0]* [timepoint = 7]* [flashintensitymcd = 3000]	.000	.000
[Injured = 0]* [timepoint = 7]* [flashintensitymcd = 10000]	.001	.000

Working Correlation Matrix[a]

Measurement	Measurement			
	[Injured = 0]* [timepoint = 2]* [flashintensity mcd = 10]	[Injured = 0]* [timepoint = 2]* [flashintensity mcd = 3000]	[Injured = 0]* [timepoint = 2]* [flashintensity mcd = 10000]	[Injured = 0]* [timepoint = 7]* [flashintensity mcd = 10]
[Injured = 0]* [timepoint = 14]* [flashintensitymcd = 10]	.017	.033	.065	.129
[Injured = 0]* [timepoint = 14]* [flashintensitymcd = 3000]	.008	.017	.033	.065
[Injured = 0]* [timepoint = 14]* [flashintensitymcd = 10000]	.004	.008	.017	.033
[Injured = 1]* [timepoint = 2]* [flashintensitymcd = 10]	.002	.004	.008	.017
[Injured = 1]* [timepoint = 2]* [flashintensitymcd = 3000]	.001	.002	.004	.008
[Injured = 1]* [timepoint = 2]* [flashintensitymcd = 10000]	.001	.001	.002	.004
[Injured = 1]* [timepoint = 7]* [flashintensitymcd = 10]	.000	.001	.001	.002
[Injured = 1]* [timepoint = 7]* [flashintensitymcd = 3000]	.000	.000	.001	.001
[Injured = 1]* [timepoint = 7]* [flashintensitymcd = 10000]	.000	.000	.000	.001
[Injured = 1]* [timepoint = 14]* [flashintensitymcd = 10]	.000	.000	.000	.000
[Injured = 1]* [timepoint = 14]* [flashintensitymcd = 3000]	.000	.000	.000	.000
[Injured = 1]* [timepoint = 14]* [flashintensitymcd = 10000]	.000	.000	.000	.000

Working Correlation Matrix[a]

Measurement	Measurement			
	[Injured = 0]* [timepoint = 7]* [flashintensity mcd = 3000]	[Injured = 0]* [timepoint = 7]* [flashintensity mcd = 10000]	[Injured = 0]* [timepoint = 14]* [flashintensity mcd = 10]	[Injured = 0]* [timepoint = 14]* [flashintensity mcd = 3000]
[Injured = 0]* [timepoint = 14]* [flashintensitymcd = 10]	.256	.506	1.000	.506
[Injured = 0]* [timepoint = 14]* [flashintensitymcd = 3000]	.129	.256	.506	1.000
[Injured = 0]* [timepoint = 14]* [flashintensitymcd = 10000]	.065	.129	.256	.506
[Injured = 1]* [timepoint = 2]* [flashintensitymcd = 10]	.033	.065	.129	.256
[Injured = 1]* [timepoint = 2]* [flashintensitymcd = 3000]	.017	.033	.065	.129
[Injured = 1]* [timepoint = 2]* [flashintensitymcd = 10000]	.008	.017	.033	.065
[Injured = 1]* [timepoint = 7]* [flashintensitymcd = 10]	.004	.008	.017	.033
[Injured = 1]* [timepoint = 7]* [flashintensitymcd = 3000]	.002	.004	.008	.017
[Injured = 1]* [timepoint = 7]* [flashintensitymcd = 10000]	.001	.002	.004	.008
[Injured = 1]* [timepoint = 14]* [flashintensitymcd = 10]	.001	.001	.002	.004
[Injured = 1]* [timepoint = 14]* [flashintensitymcd = 3000]	.000	.001	.001	.002
[Injured = 1]* [timepoint = 14]* [flashintensitymcd = 10000]	.000	.000	.001	.001

Working Correlation Matrix[a]

Measurement	Measurement			
	[Injured = 0]* [timepoint = 14]* [flashintensity mcd = 10000]	[Injured = 1]* [timepoint = 2]* [flashintensity mcd = 10]	[Injured = 1]* [timepoint = 2]* [flashintensity mcd = 3000]	[Injured = 1]* [timepoint = 2]* [flashintensity mcd = 10000]
[Injured = 0]* [timepoint = 14]* [flashintensitymcd = 10]	.256	.129	.065	.033
[Injured = 0]* [timepoint = 14]* [flashintensitymcd = 3000]	.506	.256	.129	.065
[Injured = 0]* [timepoint = 14]* [flashintensitymcd = 10000]	1.000	.506	.256	.129
[Injured = 1]* [timepoint = 2]* [flashintensitymcd = 10]	.506	1.000	.506	.256
[Injured = 1]* [timepoint = 2]* [flashintensitymcd = 3000]	.256	.506	1.000	.506
[Injured = 1]* [timepoint = 2]* [flashintensitymcd = 10000]	.129	.256	.506	1.000
[Injured = 1]* [timepoint = 7]* [flashintensitymcd = 10]	.065	.129	.256	.506
[Injured = 1]* [timepoint = 7]* [flashintensitymcd = 3000]	.033	.065	.129	.256
[Injured = 1]* [timepoint = 7]* [flashintensitymcd = 10000]	.017	.033	.065	.129
[Injured = 1]* [timepoint = 14]* [flashintensitymcd = 10]	.008	.017	.033	.065
[Injured = 1]* [timepoint = 14]* [flashintensitymcd = 3000]	.004	.008	.017	.033
[Injured = 1]* [timepoint = 14]* [flashintensitymcd = 10000]	.002	.004	.008	.017

Working Correlation Matrix[a]

Measurement	Measurement			
	[Injured = 1]* [timepoint = 7]* [flashintensity mcd = 10]	[Injured = 1]* [timepoint = 7]* [flashintensity mcd = 3000]	[Injured = 1]* [timepoint = 7]* [flashintensity mcd = 10000]	[Injured = 1]* [timepoint = 14]* [flashintensity mcd = 10]
[Injured = 0]* [timepoint = 14]* [flashintensitymcd = 10]	.017	.008	.004	.002
[Injured = 0]* [timepoint = 14]* [flashintensitymcd = 3000]	.033	.017	.008	.004
[Injured = 0]* [timepoint = 14]* [flashintensitymcd = 10000]	.065	.033	.017	.008
[Injured = 1]* [timepoint = 2]* [flashintensitymcd = 10]	.129	.065	.033	.017
[Injured = 1]* [timepoint = 2]* [flashintensitymcd = 3000]	.256	.129	.065	.033
[Injured = 1]* [timepoint = 2]* [flashintensitymcd = 10000]	.506	.256	.129	.065
[Injured = 1]* [timepoint = 7]* [flashintensitymcd = 10]	1.000	.506	.256	.129
[Injured = 1]* [timepoint = 7]* [flashintensitymcd = 3000]	.506	1.000	.506	.256
[Injured = 1]* [timepoint = 7]* [flashintensitymcd = 10000]	.256	.506	1.000	.506
[Injured = 1]* [timepoint = 14]* [flashintensitymcd = 10]	.129	.256	.506	1.000
[Injured = 1]* [timepoint = 14]* [flashintensitymcd = 3000]	.065	.129	.256	.506
[Injured = 1]* [timepoint = 14]* [flashintensitymcd = 10000]	.033	.065	.129	.256

Working Correlation Matrix[a]

Measurement	Measurement	
	[Injured = 1]* [timepoint = 14]* [flashintensity mcd = 3000]	[Injured = 1]* [timepoint = 14]* [flashintensity mcd = 10000]
[Injured = 0]* [timepoint = 14]* [flashintensitymcd = 10]	.001	.001
[Injured = 0]* [timepoint = 14]* [flashintensitymcd = 3000]	.002	.001
[Injured = 0]* [timepoint = 14]* [flashintensitymcd = 10000]	.004	.002
[Injured = 1]* [timepoint = 2]* [flashintensitymcd = 10]	.008	.004
[Injured = 1]* [timepoint = 2]* [flashintensitymcd = 3000]	.017	.008
[Injured = 1]* [timepoint = 2]* [flashintensitymcd = 10000]	.033	.017
[Injured = 1]* [timepoint = 7]* [flashintensitymcd = 10]	.065	.033
[Injured = 1]* [timepoint = 7]* [flashintensitymcd = 3000]	.129	.065
[Injured = 1]* [timepoint = 7]* [flashintensitymcd = 10000]	.256	.129
[Injured = 1]* [timepoint = 14]* [flashintensitymcd = 10]	.506	.256
[Injured = 1]* [timepoint = 14]* [flashintensitymcd = 3000]	1.000	.506
[Injured = 1]* [timepoint = 14]* [flashintensitymcd = 10000]	.506	1.000

Dependent Variable: awaveslopevms
Model: (Intercept), timepoint, flashintensitymcd, Injured, timepoint * flashintensitymcd, timepoint * Injured, flashintensitymcd * Injured, timepoint * flashintensitymcd * Injured

a. The AR(1) working correlation matrix structure is computed assuming the measurements are equally spaced for all subjects.

Estimated Marginal Means: timepoint* flashintensitymcd* Injured

Estimates

timepoint	flashintensitymcd	Injured	Mean	Std. Error	95% Wald Confidence Interval	
					Lower	Upper
2	10	1	.61438	.146839	.38458	.98147
		0	1.17313	.273227	.74318	1.85180
	3000	1	6.31875	1.561073	3.89348	10.25472
		0	24.55375	3.871302	18.02652	33.44442
	10000	1	11.80500	2.492307	7.80473	17.85559
		0	41.61250	6.477327	30.67096	56.45733
7	10	1	.79120	.259321	.41620	1.50409
		0	1.79063	.565919	.96380	3.32677
	3000	1	11.99125	2.683348	7.73368	18.59270
		0	32.72500	4.375241	25.18120	42.52878
	10000	1	20.11125	3.380244	14.46677	27.95804
		0	49.28750	6.143046	38.60518	62.92569
14	10	1	1.12350	.217217	.76913	1.64113
		0	2.41375	.366802	1.79201	3.25120
	3000	1	15.01375	3.046657	10.08694	22.34698
		0	39.30000	4.976131	30.66297	50.36988
	10000	1	25.07000	4.849224	17.15966	36.62689
		0	59.68750	6.720920	47.86704	74.42695

APPENDIX 9

```
 * Generalized Estimating Equations.
GENLIN abwaveratio BY timepoint flashintensitymcd Injured (ORDER=DATA)
  /MODEL timepoint flashintensitymcd Injured timepoint*flashintensitymcd timepoint*Injured f
 DISTRIBUTION=GAMMA LINK=LOG
  /CRITERIA METHOD=FISHER(1) SCALE=MLE MAXITERATIONS=100 MAXSTEPHALVING=5 PCONVERGE=1E-006(A
  /EMMEANS TABLES=timepoint*flashintensitymcd*Injured SCALE=ORIGINAL
  /REPEATED SUBJECT=animal WITHINSUBJECT=Injured*timepoint*flashintensitymcd SORT=YES CORRTY
  /MISSING CLASSMISSING=EXCLUDE
  /PRINT CPS DESCRIPTIVES MODELINFO FIT SUMMARY WORKINGCORR.
```

Generalized Linear Models

Notes

Output Created		02-MAY-2013 10:13:14
Comments		
Input	Data	C:\Users\Public\Documents\PhD\ERG\Results\T-CEM423-6\scotopic data T.sav
	Active Dataset	DataSet5
	Filter	<none>
	Weight	<none>
	Split File	<none>
	N of Rows in Working Data File	152
Missing Value Handling	Definition of Missing	User-defined missing values for factor, subject and within-subject variables are treated as missing.
	Cases Used	Statistics are based on cases with valid data for all variables in the model.
Weight Handling		not applicable

Notes

Syntax		GENLIN V12 BY timepoint flashintensitymcd Injured (ORDER=DATA) /MODEL timepoint flashintensitymcd Injured timepoint*flashintensitymcd timepoint*Injured flashintensitymcd*Injured timepoint*flashintensitymcd*Injured INTERCEPT=YES DISTRIBUTION=GAMMA LINK=LOG /CRITERIA METHOD=FISHER(1) SCALE=MLE MAXITERATIONS=100 MAXSTEPHALVING=5 PCONVERGE=1E-006(ABSOLUTE) SINGULAR=1E-012 ANALYSISTYPE=3(WALD) CILEVEL=95 LIKELIHOOD=FULL /EMMEANS TABLES=timepoint*flashintensitymcd*Injured SCALE=ORIGINAL /REPEATED SUBJECT=animal WITHINSUBJECT=Injured*timepoint*flashintensitymcd SORT=YES CORRTYPE=AR(1) ADJUSTCORR=YES COVB=ROBUST MAXITERATIONS=100 PCONVERGE=1e-006(ABSOLUTE) UPDATECORR=1 /MISSING CLASSMISSING=EXCLUDE /PRINT CPS DESCRIPTIVES...
Resources	Processor Time	00:00:00.08
	Elapsed Time	00:00:00.15

[DataSet5] C:\Users\Public\Documents\PhD\ERG\Results\T-CEM423-6\scotopic data T.sav

Model Information

Dependent Variable		V12
Probability Distribution		Gamma
Link Function		Log
Subject Effect	1	animal
Within-Subject Effect	1	Injured
	2	timepoint
	3	flashintensitymcd
Working Correlation Matrix Structure		AR(1)

Case Processing Summary

	N	Percent
Included	144	94.7%
Excluded	8	5.3%
Total	152	100.0%

Correlated Data Summary

Number of Levels	Subject Effect	animal	8
	Within-Subject Effect	Injured	2
		timepoint	3
		flashintensitymcd	3
Number of Subjects			8
Number of Measurements per Subject	Minimum		18
	Maximum		18
Correlation Matrix Dimension			18

Categorical Variable Information

			N	Percent
Factor	timepoint	2	48	33.3%
		7	48	33.3%
		14	48	33.3%
		Total	144	100.0%
	flashintensitymcd	10	48	33.3%
		3000	48	33.3%
		10000	48	33.3%
		Total	144	100.0%
	Injured	1	72	50.0%
		0	72	50.0%
		Total	144	100.0%

Continuous Variable Information

		N	Minimum	Maximum	Mean	Std. Deviation
Dependent Variable	V12	144	1	3436	119.25	472.496

Goodness of Fit[a]

	Value
Quasi Likelihood under Independence Model Criterion (QIC)[b]	185.896
Corrected Quasi Likelihood under Independence Model Criterion (QICC)[b]	197.166

Dependent Variable: V12
Model: (Intercept), timepoint, flashintensitymcd, Injured, timepoint * flashintensitymcd, timepoint * Injured, flashintensitymcd * Injured, timepoint * flashintensitymcd * Injured

a. Information criteria are in small-is-better form.

b. Computed using the full log quasi-likelihood function.

Tests of Model Effects

Source	Type III		
	Wald Chi-Square	df	Sig.
(Intercept)	217.835	1	.000
timepoint	19.098	2	.000
flashintensitymcd	175.955	2	.000
Injured	1.028	1	.311
timepoint * flashintensitymcd	237.445	4	.000
timepoint * Injured	1.056	2	.590
flashintensitymcd * Injured	9.009	2	.011
timepoint * flashintensitymcd * Injured	6.612	4	.158

Dependent Variable: V12
Model: (Intercept), timepoint, flashintensitymcd, Injured, timepoint * flashintensitymcd, timepoint * Injured, flashintensitymcd * Injured, timepoint * flashintensitymcd * Injured

Working Correlation Matrix[a]

Measurement	Measurement			
	[Injured = 0]* [timepoint = 2]* [flashintensity mcd = 10]	[Injured = 0]* [timepoint = 2]* [flashintensity mcd = 3000]	[Injured = 0]* [timepoint = 2]* [flashintensity mcd = 10000]	[Injured = 0]* [timepoint = 7]* [flashintensity mcd = 10]
[Injured = 0]* [timepoint = 2]* [flashintensitymcd = 10]	1.000	.041	.002	.000
[Injured = 0]* [timepoint = 2]* [flashintensitymcd = 3000]	.041	1.000	.041	.002
[Injured = 0]* [timepoint = 2]* [flashintensitymcd = 10000]	.002	.041	1.000	.041
[Injured = 0]* [timepoint = 7]* [flashintensitymcd = 10]	.000	.002	.041	1.000
[Injured = 0]* [timepoint = 7]* [flashintensitymcd = 3000]	.000	.000	.002	.041
[Injured = 0]* [timepoint = 7]* [flashintensitymcd = 10000]	.000	.000	.000	.002
[Injured = 0]* [timepoint = 14]* [flashintensitymcd = 10]	.000	.000	.000	.000
[Injured = 0]* [timepoint = 14]* [flashintensitymcd = 3000]	.000	.000	.000	.000
[Injured = 0]* [timepoint = 14]* [flashintensitymcd = 10000]	.000	.000	.000	.000
[Injured = 1]* [timepoint = 2]* [flashintensitymcd = 10]	.000	.000	.000	.000
[Injured = 1]* [timepoint = 2]* [flashintensitymcd = 3000]	.000	.000	.000	.000
[Injured = 1]* [timepoint = 2]* [flashintensitymcd = 10000]	.000	.000	.000	.000
[Injured = 1]* [timepoint = 7]* [flashintensitymcd = 10]	.000	.000	.000	.000
[Injured = 1]* [timepoint = 7]* [flashintensitymcd = 3000]	.000	.000	.000	.000

Working Correlation Matrix[a]

Measurement	Measurement			
	[Injured = 0]* [timepoint = 7]* [flashintensity mcd = 3000]	[Injured = 0]* [timepoint = 7]* [flashintensity mcd = 10000]	[Injured = 0]* [timepoint = 14]* [flashintensity mcd = 10]	[Injured = 0]* [timepoint = 14]* [flashintensity mcd = 3000]
[Injured = 0]* [timepoint = 2]* [flashintensitymcd = 10]	.000	.000	.000	.000
[Injured = 0]* [timepoint = 2]* [flashintensitymcd = 3000]	.000	.000	.000	.000
[Injured = 0]* [timepoint = 2]* [flashintensitymcd = 10000]	.002	.000	.000	.000
[Injured = 0]* [timepoint = 7]* [flashintensitymcd = 10]	.041	.002	.000	.000
[Injured = 0]* [timepoint = 7]* [flashintensitymcd = 3000]	1.000	.041	.002	.000
[Injured = 0]* [timepoint = 7]* [flashintensitymcd = 10000]	.041	1.000	.041	.002
[Injured = 0]* [timepoint = 14]* [flashintensitymcd = 10]	.002	.041	1.000	.041
[Injured = 0]* [timepoint = 14]* [flashintensitymcd = 3000]	.000	.002	.041	1.000
[Injured = 0]* [timepoint = 14]* [flashintensitymcd = 10000]	.000	.000	.002	.041
[Injured = 1]* [timepoint = 2]* [flashintensitymcd = 10]	.000	.000	.000	.002
[Injured = 1]* [timepoint = 2]* [flashintensitymcd = 3000]	.000	.000	.000	.000
[Injured = 1]* [timepoint = 2]* [flashintensitymcd = 10000]	.000	.000	.000	.000
[Injured = 1]* [timepoint = 7]* [flashintensitymcd = 10]	.000	.000	.000	.000
[Injured = 1]* [timepoint = 7]* [flashintensitymcd = 3000]	.000	.000	.000	.000

Working Correlation Matrix[a]

Measurement	Measurement			
	[Injured = 0]* [timepoint = 14]* [flashintensity mcd = 10000]	[Injured = 1]* [timepoint = 2]* [flashintensity mcd = 10]	[Injured = 1]* [timepoint = 2]* [flashintensity mcd = 3000]	[Injured = 1]* [timepoint = 2]* [flashintensity mcd = 10000]
[Injured = 0]* [timepoint = 2]* [flashintensitymcd = 10]	.000	.000	.000	.000
[Injured = 0]* [timepoint = 2]* [flashintensitymcd = 3000]	.000	.000	.000	.000
[Injured = 0]* [timepoint = 2]* [flashintensitymcd = 10000]	.000	.000	.000	.000
[Injured = 0]* [timepoint = 7]* [flashintensitymcd = 10]	.000	.000	.000	.000
[Injured = 0]* [timepoint = 7]* [flashintensitymcd = 3000]	.000	.000	.000	.000
[Injured = 0]* [timepoint = 7]* [flashintensitymcd = 10000]	.000	.000	.000	.000
[Injured = 0]* [timepoint = 14]* [flashintensitymcd = 10]	.002	.000	.000	.000
[Injured = 0]* [timepoint = 14]* [flashintensitymcd = 3000]	.041	.002	.000	.000
[Injured = 0]* [timepoint = 14]* [flashintensitymcd = 10000]	1.000	.041	.002	.000
[Injured = 1]* [timepoint = 2]* [flashintensitymcd = 10]	.041	1.000	.041	.002
[Injured = 1]* [timepoint = 2]* [flashintensitymcd = 3000]	.002	.041	1.000	.041
[Injured = 1]* [timepoint = 2]* [flashintensitymcd = 10000]	.000	.002	.041	1.000
[Injured = 1]* [timepoint = 7]* [flashintensitymcd = 10]	.000	.000	.002	.041
[Injured = 1]* [timepoint = 7]* [flashintensitymcd = 3000]	.000	.000	.000	.002

Working Correlation Matrix[a]

Measurement	Measurement			
	[Injured = 1]* [timepoint = 7]* [flashintensity mcd = 10]	[Injured = 1]* [timepoint = 7]* [flashintensity mcd = 3000]	[Injured = 1]* [timepoint = 7]* [flashintensity mcd = 10000]	[Injured = 1]* [timepoint = 14]* [flashintensity mcd = 10]
[Injured = 0]* [timepoint = 2]* [flashintensitymcd = 10]	.000	.000	.000	.000
[Injured = 0]* [timepoint = 2]* [flashintensitymcd = 3000]	.000	.000	.000	.000
[Injured = 0]* [timepoint = 2]* [flashintensitymcd = 10000]	.000	.000	.000	.000
[Injured = 0]* [timepoint = 7]* [flashintensitymcd = 10]	.000	.000	.000	.000
[Injured = 0]* [timepoint = 7]* [flashintensitymcd = 3000]	.000	.000	.000	.000
[Injured = 0]* [timepoint = 7]* [flashintensitymcd = 10000]	.000	.000	.000	.000
[Injured = 0]* [timepoint = 14]* [flashintensitymcd = 10]	.000	.000	.000	.000
[Injured = 0]* [timepoint = 14]* [flashintensitymcd = 3000]	.000	.000	.000	.000
[Injured = 0]* [timepoint = 14]* [flashintensitymcd = 10000]	.000	.000	.000	.000
[Injured = 1]* [timepoint = 2]* [flashintensitymcd = 10]	.000	.000	.000	.000
[Injured = 1]* [timepoint = 2]* [flashintensitymcd = 3000]	.002	.000	.000	.000
[Injured = 1]* [timepoint = 2]* [flashintensitymcd = 10000]	.041	.002	.000	.000
[Injured = 1]* [timepoint = 7]* [flashintensitymcd = 10]	1.000	.041	.002	.000
[Injured = 1]* [timepoint = 7]* [flashintensitymcd = 3000]	.041	1.000	.041	.002

Working Correlation Matrix[a]

Measurement	Measurement	
	[Injured = 1]* [timepoint = 14]* [flashintensity mcd = 3000]	[Injured = 1]* [timepoint = 14]* [flashintensity mcd = 10000]
[Injured = 0]* [timepoint = 2]* [flashintensitymcd = 10]	.000	.000
[Injured = 0]* [timepoint = 2]* [flashintensitymcd = 3000]	.000	.000
[Injured = 0]* [timepoint = 2]* [flashintensitymcd = 10000]	.000	.000
[Injured = 0]* [timepoint = 7]* [flashintensitymcd = 10]	.000	.000
[Injured = 0]* [timepoint = 7]* [flashintensitymcd = 3000]	.000	.000
[Injured = 0]* [timepoint = 7]* [flashintensitymcd = 10000]	.000	.000
[Injured = 0]* [timepoint = 14]* [flashintensitymcd = 10]	.000	.000
[Injured = 0]* [timepoint = 14]* [flashintensitymcd = 3000]	.000	.000
[Injured = 0]* [timepoint = 14]* [flashintensitymcd = 10000]	.000	.000
[Injured = 1]* [timepoint = 2]* [flashintensitymcd = 10]	.000	.000
[Injured = 1]* [timepoint = 2]* [flashintensitymcd = 3000]	.000	.000
[Injured = 1]* [timepoint = 2]* [flashintensitymcd = 10000]	.000	.000
[Injured = 1]* [timepoint = 7]* [flashintensitymcd = 10]	.000	.000
[Injured = 1]* [timepoint = 7]* [flashintensitymcd = 3000]	.000	.000

Working Correlation Matrix[a]

Measurement	Measurement			
	[Injured = 0]* [timepoint = 2]* [flashintensity mcd = 10]	[Injured = 0]* [timepoint = 2]* [flashintensity mcd = 3000]	[Injured = 0]* [timepoint = 2]* [flashintensity mcd = 10000]	[Injured = 0]* [timepoint = 7]* [flashintensity mcd = 10]
[Injured = 1]* [timepoint = 7]* [flashintensitymcd = 10000]	.000	.000	.000	.000
[Injured = 1]* [timepoint = 14]* [flashintensitymcd = 10]	.000	.000	.000	.000
[Injured = 1]* [timepoint = 14]* [flashintensitymcd = 3000]	.000	.000	.000	.000
[Injured = 1]* [timepoint = 14]* [flashintensitymcd = 10000]	.000	.000	.000	.000

Working Correlation Matrix[a]

Measurement	Measurement			
	[Injured = 0]* [timepoint = 7]* [flashintensity mcd = 3000]	[Injured = 0]* [timepoint = 7]* [flashintensity mcd = 10000]	[Injured = 0]* [timepoint = 14]* [flashintensity mcd = 10]	[Injured = 0]* [timepoint = 14]* [flashintensity mcd = 3000]
[Injured = 1]* [timepoint = 7]* [flashintensitymcd = 10000]	.000	.000	.000	.000
[Injured = 1]* [timepoint = 14]* [flashintensitymcd = 10]	.000	.000	.000	.000
[Injured = 1]* [timepoint = 14]* [flashintensitymcd = 3000]	.000	.000	.000	.000
[Injured = 1]* [timepoint = 14]* [flashintensitymcd = 10000]	.000	.000	.000	.000

Working Correlation Matrix[a]

Measurement	Measurement			
	[Injured = 0]* [timepoint = 14]* [flashintensity mcd = 10000]	[Injured = 1]* [timepoint = 2]* [flashintensity mcd = 10]	[Injured = 1]* [timepoint = 2]* [flashintensity mcd = 3000]	[Injured = 1]* [timepoint = 2]* [flashintensity mcd = 10000]
[Injured = 1]* [timepoint = 7]* [flashintensitymcd = 10000]	.000	.000	.000	.000
[Injured = 1]* [timepoint = 14]* [flashintensitymcd = 10]	.000	.000	.000	.000
[Injured = 1]* [timepoint = 14]* [flashintensitymcd = 3000]	.000	.000	.000	.000
[Injured = 1]* [timepoint = 14]* [flashintensitymcd = 10000]	.000	.000	.000	.000

Working Correlation Matrix[a]

Measurement	Measurement			
	[Injured = 1]* [timepoint = 7]* [flashintensity mcd = 10]	[Injured = 1]* [timepoint = 7]* [flashintensity mcd = 3000]	[Injured = 1]* [timepoint = 7]* [flashintensity mcd = 10000]	[Injured = 1]* [timepoint = 14]* [flashintensity mcd = 10]
[Injured = 1]* [timepoint = 7]* [flashintensitymcd = 10000]	.002	.041	1.000	.041
[Injured = 1]* [timepoint = 14]* [flashintensitymcd = 10]	.000	.002	.041	1.000
[Injured = 1]* [timepoint = 14]* [flashintensitymcd = 3000]	.000	.000	.002	.041
[Injured = 1]* [timepoint = 14]* [flashintensitymcd = 10000]	.000	.000	.000	.002

Working Correlation Matrix[a]

Measurement	Measurement	
	[Injured = 1]* [timepoint = 14]* [flashintensity mcd = 3000]	[Injured = 1]* [timepoint = 14]* [flashintensity mcd = 10000]
[Injured = 1]* [timepoint = 7]* [flashintensitymcd = 10000]	.002	.000
[Injured = 1]* [timepoint = 14]* [flashintensitymcd = 10]	.041	.002
[Injured = 1]* [timepoint = 14]* [flashintensitymcd = 3000]	1.000	.041
[Injured = 1]* [timepoint = 14]* [flashintensitymcd = 10000]	.041	1.000

Dependent Variable: V12
Model: (Intercept), timepoint, flashintensitymcd, Injured, timepoint * flashintensitymcd, timepoint * Injured, flashintensitymcd * Injured, timepoint * flashintensitymcd * Injured

a. The AR(1) working correlation matrix structure is computed assuming the measurements are equally spaced for all subjects.

Estimated Marginal Means: timepoint* flashintensitymcd* Injured

Estimates

timepoint	flashintensitymcd	Injured	Mean	Std. Error	95% Wald Confidence Interval	
					Lower	Upper
2	10	1	70.77	53.084	16.27	307.85
		0	26.29	4.798	18.38	37.59
	3000	1	3.06	.864	1.76	5.32
		0	3.09	.602	2.11	4.52
	10000	1	2.03	.414	1.36	3.03
		0	2.31	.329	1.74	3.05
7	10	1	568.73	219.566	266.86	1212.06
		0	732.16	445.344	222.26	2411.90
	3000	1	2.25	.192	1.91	2.66
		0	2.23	.170	1.92	2.59
	10000	1	1.96	.135	1.71	2.24
		0	1.98	.135	1.73	2.26
14	10	1	404.43	257.622	116.04	1409.49
		0	316.96	271.867	59.01	1702.57
	3000	1	2.02	.140	1.77	2.32
		0	2.09	.132	1.85	2.37
	10000	1	1.89	.134	1.65	2.17
		0	2.24	.324	1.69	2.98

```
 * Generalized Estimating Equations.
GENLIN V12 BY timepoint flashintensitymcd Injured (ORDER=DATA)
  /MODEL timepoint flashintensitymcd Injured timepoint*flashintensitymcd timepoint*Injured f
 DISTRIBUTION=GAMMA LINK=LOG
  /CRITERIA METHOD=FISHER(1) SCALE=MLE MAXITERATIONS=100 MAXSTEPHALVING=5 PCONVERGE=1E-006(A
  /EMMEANS TABLES=timepoint*flashintensitymcd*Injured SCALE=ORIGINAL
  /REPEATED SUBJECT=animal WITHINSUBJECT=Injured*timepoint*flashintensitymcd SORT=YES CORRTY
  /MISSING CLASSMISSING=EXCLUDE
  /PRINT CPS DESCRIPTIVES MODELINFO FIT SUMMARY WORKINGCORR.
```

Generalized Linear Models

Notes

Output Created		02-MAY-2013 10:14:49
Comments		
Input	Data	C:\Users\Public\Documents\PhD\ERG\Results\T-CEM423-6\scotopic data T.sav
	Active Dataset	DataSet5
	Filter	<none>
	Weight	<none>
	Split File	<none>
	N of Rows in Working Data File	152
Missing Value Handling	Definition of Missing	User-defined missing values for factor, subject and within-subject variables are treated as missing.
	Cases Used	Statistics are based on cases with valid data for all variables in the model.
Weight Handling		not applicable

Notes

Syntax		GENLIN V12 BY timepoint flashintensitymcd Injured (ORDER=DATA) /MODEL timepoint flashintensitymcd Injured timepoint*flashintensitymcd timepoint*Injured flashintensitymcd*Injured INTERCEPT=YES DISTRIBUTION=GAMMA LINK=LOG /CRITERIA METHOD=FISHER(1) SCALE=MLE MAXITERATIONS=100 MAXSTEPHALVING=5 PCONVERGE=1E-006(ABSOLUTE) SINGULAR=1E-012 ANALYSISTYPE=3(WALD) CILEVEL=95 LIKELIHOOD=FULL /EMMEANS TABLES=timepoint*flashintensitymcd*Injured SCALE=ORIGINAL /REPEATED SUBJECT=animal WITHINSUBJECT=Injured*timepoint*flashintensitymcd SORT=YES CORRTYPE=AR(1) ADJUSTCORR=YES COVB=ROBUST MAXITERATIONS=100 PCONVERGE=1e-006(ABSOLUTE) UPDATECORR=1 /MISSING CLASSMISSING=EXCLUDE /PRINT CPS DESCRIPTIVES...
Resources	Processor Time	00:00:00.08
	Elapsed Time	00:00:00.14

[DataSet5] C:\Users\Public\Documents\PhD\ERG\Results\T-CEM423-6\scotopic data T.sav

Model Information

Dependent Variable		V12
Probability Distribution		Gamma
Link Function		Log
Subject Effect	1	animal
Within-Subject Effect	1	Injured
	2	timepoint
	3	flashintensitymcd
Working Correlation Matrix Structure		AR(1)

Case Processing Summary

	N	Percent
Included	144	94.7%
Excluded	8	5.3%
Total	152	100.0%

Correlated Data Summary

Number of Levels	Subject Effect	animal	8
	Within-Subject Effect	Injured	2
		timepoint	3
		flashintensitymcd	3
Number of Subjects			8
Number of Measurements per Subject	Minimum		18
	Maximum		18
Correlation Matrix Dimension			18

Categorical Variable Information

			N	Percent
Factor	timepoint	2	48	33.3%
		7	48	33.3%
		14	48	33.3%
		Total	144	100.0%
	flashintensitymcd	10	48	33.3%
		3000	48	33.3%
		10000	48	33.3%
		Total	144	100.0%
	Injured	1	72	50.0%
		0	72	50.0%
		Total	144	100.0%

Continuous Variable Information

		N	Minimum	Maximum	Mean	Std. Deviation
Dependent Variable	V12	144	1	3436	119.25	472.496

Goodness of Fit[a]

	Value
Quasi Likelihood under Independence Model Criterion (QIC)[b]	203.605
Corrected Quasi Likelihood under Independence Model Criterion (QICC)[b]	191.457

Dependent Variable: V12
Model: (Intercept), timepoint, flashintensitymcd, Injured, timepoint * flashintensitymcd, timepoint * Injured, flashintensitymcd * Injured

a. Information criteria are in small-is-better form.

b. Computed using the full log quasi-likelihood function.

Tests of Model Effects

	Type III		
Source	Wald Chi-Square	df	Sig.
(Intercept)	194.038	1	.000
timepoint	19.726	2	.000
flashintensitymcd	145.029	2	.000
Injured	.740	1	.390
timepoint * flashintensitymcd	248.600	4	.000
timepoint * Injured	.700	2	.705
flashintensitymcd * Injured	6.425	2	.040

Dependent Variable: V12
Model: (Intercept), timepoint, flashintensitymcd, Injured, timepoint * flashintensitymcd, timepoint * Injured, flashintensitymcd * Injured

Working Correlation Matrix[a]

Measurement	Measurement			
	[Injured = 0]* [timepoint = 2]* [flashintensity mcd = 10]	[Injured = 0]* [timepoint = 2]* [flashintensity mcd = 3000]	[Injured = 0]* [timepoint = 2]* [flashintensity mcd = 10000]	[Injured = 0]* [timepoint = 7]* [flashintensity mcd = 10]
[Injured = 0]* [timepoint = 2]* [flashintensitymcd = 10]	1.000	.030	.001	.000
[Injured = 0]* [timepoint = 2]* [flashintensitymcd = 3000]	.030	1.000	.030	.001
[Injured = 0]* [timepoint = 2]* [flashintensitymcd = 10000]	.001	.030	1.000	.030
[Injured = 0]* [timepoint = 7]* [flashintensitymcd = 10]	.000	.001	.030	1.000
[Injured = 0]* [timepoint = 7]* [flashintensitymcd = 3000]	.000	.000	.001	.030
[Injured = 0]* [timepoint = 7]* [flashintensitymcd = 10000]	.000	.000	.000	.001
[Injured = 0]* [timepoint = 14]* [flashintensitymcd = 10]	.000	.000	.000	.000
[Injured = 0]* [timepoint = 14]* [flashintensitymcd = 3000]	.000	.000	.000	.000
[Injured = 0]* [timepoint = 14]* [flashintensitymcd = 10000]	.000	.000	.000	.000
[Injured = 1]* [timepoint = 2]* [flashintensitymcd = 10]	.000	.000	.000	.000
[Injured = 1]* [timepoint = 2]* [flashintensitymcd = 3000]	.000	.000	.000	.000
[Injured = 1]* [timepoint = 2]* [flashintensitymcd = 10000]	.000	.000	.000	.000
[Injured = 1]* [timepoint = 7]* [flashintensitymcd = 10]	.000	.000	.000	.000
[Injured = 1]* [timepoint = 7]* [flashintensitymcd = 3000]	.000	.000	.000	.000

Working Correlation Matrix[a]

Measurement	Measurement			
	[Injured = 0]* [timepoint = 7]* [flashintensity mcd = 3000]	[Injured = 0]* [timepoint = 7]* [flashintensity mcd = 10000]	[Injured = 0]* [timepoint = 14]* [flashintensity mcd = 10]	[Injured = 0]* [timepoint = 14]* [flashintensity mcd = 3000]
[Injured = 0]* [timepoint = 2]* [flashintensitymcd = 10]	.000	.000	.000	.000
[Injured = 0]* [timepoint = 2]* [flashintensitymcd = 3000]	.000	.000	.000	.000
[Injured = 0]* [timepoint = 2]* [flashintensitymcd = 10000]	.001	.000	.000	.000
[Injured = 0]* [timepoint = 7]* [flashintensitymcd = 10]	.030	.001	.000	.000
[Injured = 0]* [timepoint = 7]* [flashintensitymcd = 3000]	1.000	.030	.001	.000
[Injured = 0]* [timepoint = 7]* [flashintensitymcd = 10000]	.030	1.000	.030	.001
[Injured = 0]* [timepoint = 14]* [flashintensitymcd = 10]	.001	.030	1.000	.030
[Injured = 0]* [timepoint = 14]* [flashintensitymcd = 3000]	.000	.001	.030	1.000
[Injured = 0]* [timepoint = 14]* [flashintensitymcd = 10000]	.000	.000	.001	.030
[Injured = 1]* [timepoint = 2]* [flashintensitymcd = 10]	.000	.000	.000	.001
[Injured = 1]* [timepoint = 2]* [flashintensitymcd = 3000]	.000	.000	.000	.000
[Injured = 1]* [timepoint = 2]* [flashintensitymcd = 10000]	.000	.000	.000	.000
[Injured = 1]* [timepoint = 7]* [flashintensitymcd = 10]	.000	.000	.000	.000
[Injured = 1]* [timepoint = 7]* [flashintensitymcd = 3000]	.000	.000	.000	.000

Working Correlation Matrix[a]

Measurement	Measurement			
	[Injured = 0]* [timepoint = 14]* [flashintensity mcd = 10000]	[Injured = 1]* [timepoint = 2]* [flashintensity mcd = 10]	[Injured = 1]* [timepoint = 2]* [flashintensity mcd = 3000]	[Injured = 1]* [timepoint = 2]* [flashintensity mcd = 10000]
[Injured = 0]* [timepoint = 2]* [flashintensitymcd = 10]	.000	.000	.000	.000
[Injured = 0]* [timepoint = 2]* [flashintensitymcd = 3000]	.000	.000	.000	.000
[Injured = 0]* [timepoint = 2]* [flashintensitymcd = 10000]	.000	.000	.000	.000
[Injured = 0]* [timepoint = 7]* [flashintensitymcd = 10]	.000	.000	.000	.000
[Injured = 0]* [timepoint = 7]* [flashintensitymcd = 3000]	.000	.000	.000	.000
[Injured = 0]* [timepoint = 7]* [flashintensitymcd = 10000]	.000	.000	.000	.000
[Injured = 0]* [timepoint = 14]* [flashintensitymcd = 10]	.001	.000	.000	.000
[Injured = 0]* [timepoint = 14]* [flashintensitymcd = 3000]	.030	.001	.000	.000
[Injured = 0]* [timepoint = 14]* [flashintensitymcd = 10000]	1.000	.030	.001	.000
[Injured = 1]* [timepoint = 2]* [flashintensitymcd = 10]	.030	1.000	.030	.001
[Injured = 1]* [timepoint = 2]* [flashintensitymcd = 3000]	.001	.030	1.000	.030
[Injured = 1]* [timepoint = 2]* [flashintensitymcd = 10000]	.000	.001	.030	1.000
[Injured = 1]* [timepoint = 7]* [flashintensitymcd = 10]	.000	.000	.001	.030
[Injured = 1]* [timepoint = 7]* [flashintensitymcd = 3000]	.000	.000	.000	.001

Working Correlation Matrix[a]

Measurement	Measurement			
	[Injured = 1]* [timepoint = 7]* [flashintensity mcd = 10]	[Injured = 1]* [timepoint = 7]* [flashintensity mcd = 3000]	[Injured = 1]* [timepoint = 7]* [flashintensity mcd = 10000]	[Injured = 1]* [timepoint = 14]* [flashintensity mcd = 10]
[Injured = 0]* [timepoint = 2]* [flashintensitymcd = 10]	.000	.000	.000	.000
[Injured = 0]* [timepoint = 2]* [flashintensitymcd = 3000]	.000	.000	.000	.000
[Injured = 0]* [timepoint = 2]* [flashintensitymcd = 10000]	.000	.000	.000	.000
[Injured = 0]* [timepoint = 7]* [flashintensitymcd = 10]	.000	.000	.000	.000
[Injured = 0]* [timepoint = 7]* [flashintensitymcd = 3000]	.000	.000	.000	.000
[Injured = 0]* [timepoint = 7]* [flashintensitymcd = 10000]	.000	.000	.000	.000
[Injured = 0]* [timepoint = 14]* [flashintensitymcd = 10]	.000	.000	.000	.000
[Injured = 0]* [timepoint = 14]* [flashintensitymcd = 3000]	.000	.000	.000	.000
[Injured = 0]* [timepoint = 14]* [flashintensitymcd = 10000]	.000	.000	.000	.000
[Injured = 1]* [timepoint = 2]* [flashintensitymcd = 10]	.000	.000	.000	.000
[Injured = 1]* [timepoint = 2]* [flashintensitymcd = 3000]	.001	.000	.000	.000
[Injured = 1]* [timepoint = 2]* [flashintensitymcd = 10000]	.030	.001	.000	.000
[Injured = 1]* [timepoint = 7]* [flashintensitymcd = 10]	1.000	.030	.001	.000
[Injured = 1]* [timepoint = 7]* [flashintensitymcd = 3000]	.030	1.000	.030	.001

Working Correlation Matrix[a]

Measurement	Measurement	
	[Injured = 1]* [timepoint = 14]* [flashintensity mcd = 3000]	[Injured = 1]* [timepoint = 14]* [flashintensity mcd = 10000]
[Injured = 0]* [timepoint = 2]* [flashintensitymcd = 10]	.000	.000
[Injured = 0]* [timepoint = 2]* [flashintensitymcd = 3000]	.000	.000
[Injured = 0]* [timepoint = 2]* [flashintensitymcd = 10000]	.000	.000
[Injured = 0]* [timepoint = 7]* [flashintensitymcd = 10]	.000	.000
[Injured = 0]* [timepoint = 7]* [flashintensitymcd = 3000]	.000	.000
[Injured = 0]* [timepoint = 7]* [flashintensitymcd = 10000]	.000	.000
[Injured = 0]* [timepoint = 14]* [flashintensitymcd = 10]	.000	.000
[Injured = 0]* [timepoint = 14]* [flashintensitymcd = 3000]	.000	.000
[Injured = 0]* [timepoint = 14]* [flashintensitymcd = 10000]	.000	.000
[Injured = 1]* [timepoint = 2]* [flashintensitymcd = 10]	.000	.000
[Injured = 1]* [timepoint = 2]* [flashintensitymcd = 3000]	.000	.000
[Injured = 1]* [timepoint = 2]* [flashintensitymcd = 10000]	.000	.000
[Injured = 1]* [timepoint = 7]* [flashintensitymcd = 10]	.000	.000
[Injured = 1]* [timepoint = 7]* [flashintensitymcd = 3000]	.000	.000

Working Correlation Matrix[a]

Measurement	Measurement			
	[Injured = 0]* [timepoint = 2]* [flashintensity mcd = 10]	[Injured = 0]* [timepoint = 2]* [flashintensity mcd = 3000]	[Injured = 0]* [timepoint = 2]* [flashintensity mcd = 10000]	[Injured = 0]* [timepoint = 7]* [flashintensity mcd = 10]
[Injured = 1]* [timepoint = 7]* [flashintensitymcd = 10000]	.000	.000	.000	.000
[Injured = 1]* [timepoint = 14]* [flashintensitymcd = 10]	.000	.000	.000	.000
[Injured = 1]* [timepoint = 14]* [flashintensitymcd = 3000]	.000	.000	.000	.000
[Injured = 1]* [timepoint = 14]* [flashintensitymcd = 10000]	.000	.000	.000	.000

Working Correlation Matrix[a]

Measurement	Measurement			
	[Injured = 0]* [timepoint = 7]* [flashintensity mcd = 3000]	[Injured = 0]* [timepoint = 7]* [flashintensity mcd = 10000]	[Injured = 0]* [timepoint = 14]* [flashintensity mcd = 10]	[Injured = 0]* [timepoint = 14]* [flashintensity mcd = 3000]
[Injured = 1]* [timepoint = 7]* [flashintensitymcd = 10000]	.000	.000	.000	.000
[Injured = 1]* [timepoint = 14]* [flashintensitymcd = 10]	.000	.000	.000	.000
[Injured = 1]* [timepoint = 14]* [flashintensitymcd = 3000]	.000	.000	.000	.000
[Injured = 1]* [timepoint = 14]* [flashintensitymcd = 10000]	.000	.000	.000	.000

Working Correlation Matrix[a]

Measurement	Measurement			
	[Injured = 0]* [timepoint = 14]* [flashintensity mcd = 10000]	[Injured = 1]* [timepoint = 2]* [flashintensity mcd = 10]	[Injured = 1]* [timepoint = 2]* [flashintensity mcd = 3000]	[Injured = 1]* [timepoint = 2]* [flashintensity mcd = 10000]
[Injured = 1]* [timepoint = 7]* [flashintensitymcd = 10000]	.000	.000	.000	.000
[Injured = 1]* [timepoint = 14]* [flashintensitymcd = 10]	.000	.000	.000	.000
[Injured = 1]* [timepoint = 14]* [flashintensitymcd = 3000]	.000	.000	.000	.000
[Injured = 1]* [timepoint = 14]* [flashintensitymcd = 10000]	.000	.000	.000	.000

Working Correlation Matrix[a]

Measurement	Measurement			
	[Injured = 1]* [timepoint = 7]* [flashintensity mcd = 10]	[Injured = 1]* [timepoint = 7]* [flashintensity mcd = 3000]	[Injured = 1]* [timepoint = 7]* [flashintensity mcd = 10000]	[Injured = 1]* [timepoint = 14]* [flashintensity mcd = 10]
[Injured = 1]* [timepoint = 7]* [flashintensitymcd = 10000]	.001	.030	1.000	.030
[Injured = 1]* [timepoint = 14]* [flashintensitymcd = 10]	.000	.001	.030	1.000
[Injured = 1]* [timepoint = 14]* [flashintensitymcd = 3000]	.000	.000	.001	.030
[Injured = 1]* [timepoint = 14]* [flashintensitymcd = 10000]	.000	.000	.000	.001

Working Correlation Matrix[a]

Measurement	Measurement	
	[Injured = 1]* [timepoint = 14]* [flashintensity mcd = 3000]	[Injured = 1]* [timepoint = 14]* [flashintensity mcd = 10000]
[Injured = 1]* [timepoint = 7]* [flashintensitymcd = 10000]	.001	.000
[Injured = 1]* [timepoint = 14]* [flashintensitymcd = 10]	.030	.001
[Injured = 1]* [timepoint = 14]* [flashintensitymcd = 3000]	1.000	.030
[Injured = 1]* [timepoint = 14]* [flashintensitymcd = 10000]	.030	1.000

Dependent Variable: V12
Model: (Intercept), timepoint, flashintensitymcd, Injured, timepoint * flashintensitymcd, timepoint * Injured, flashintensitymcd * Injured

a. The AR(1) working correlation matrix structure is computed assuming the measurements are equally spaced for all subjects.

Estimated Marginal Means: timepoint* flashintensitymcd* Injured

Estimates

timepoint	flashintensitymcd	Injured	Mean	Std. Error	95% Wald Confidence Interval	
					Lower	Upper
2	10	1	58.01	38.001	16.07	209.46
		0	33.70	10.308	18.50	61.37
	3000	1	3.43	.914	2.03	5.78
		0	2.79	.807	1.58	4.92
	10000	1	2.32	.407	1.64	3.27
		0	2.05	.569	1.19	3.53
7	10	1	718.53	263.253	350.42	1473.35
		0	605.85	356.328	191.31	1918.65
	3000	1	2.07	.197	1.72	2.50
		0	2.45	.353	1.85	3.25
	10000	1	1.75	.156	1.47	2.08
		0	2.25	.265	1.79	2.83
14	10	1	409.02	303.826	95.38	1754.00
		0	313.44	233.939	72.59	1353.50
	3000	1	1.99	.200	1.63	2.42
		0	2.13	.198	1.78	2.56
	10000	1	1.90	.198	1.55	2.33
		0	2.22	.284	1.73	2.85

```
 * Generalized Estimating Equations.
GENLIN V12 BY timepoint flashintensitymcd Injured (ORDER=DATA)
  /MODEL timepoint flashintensitymcd Injured timepoint*flashintensitymcd flashintensitymcd*I
 DISTRIBUTION=GAMMA LINK=LOG
  /CRITERIA METHOD=FISHER(1) SCALE=MLE MAXITERATIONS=100 MAXSTEPHALVING=5 PCONVERGE=1E-006(A
  /EMMEANS TABLES=timepoint*flashintensitymcd*Injured SCALE=ORIGINAL
  /REPEATED SUBJECT=animal WITHINSUBJECT=Injured*timepoint*flashintensitymcd SORT=YES CORRTY
  /MISSING CLASSMISSING=EXCLUDE
  /PRINT CPS DESCRIPTIVES MODELINFO FIT SUMMARY WORKINGCORR.
```

Generalized Linear Models

Notes

Output Created		02-MAY-2013 10:15:22
Comments		
Input	Data	C:\Users\Public\Documents\PhD\ERG\Results\T-CEM423-6\scotopic data T.sav
	Active Dataset	DataSet5
	Filter	<none>
	Weight	<none>
	Split File	<none>
	N of Rows in Working Data File	152
Missing Value Handling	Definition of Missing	User-defined missing values for factor, subject and within-subject variables are treated as missing.
	Cases Used	Statistics are based on cases with valid data for all variables in the model.
Weight Handling		not applicable

Notes

Syntax		GENLIN V12 BY timepoint flashintensitymcd Injured (ORDER=DATA) /MODEL timepoint flashintensitymcd Injured timepoint*flashintensitymcd flashintensitymcd*Injured INTERCEPT=YES DISTRIBUTION=GAMMA LINK=LOG /CRITERIA METHOD=FISHER(1) SCALE=MLE MAXITERATIONS=100 MAXSTEPHALVING=5 PCONVERGE=1E-006(ABSOLUTE) SINGULAR=1E-012 ANALYSISTYPE=3(WALD) CILEVEL=95 LIKELIHOOD=FULL /EMMEANS TABLES=timepoint*flashintensitymcd*Injured SCALE=ORIGINAL /REPEATED SUBJECT=animal WITHINSUBJECT=Injured*timepoint*flashintensitymcd SORT=YES CORRTYPE=AR(1) ADJUSTCORR=YES COVB=ROBUST MAXITERATIONS=100 PCONVERGE=1e-006(ABSOLUTE) UPDATECORR=1 /MISSING CLASSMISSING=EXCLUDE /PRINT CPS DESCRIPTIVES...
Resources	Processor Time	00:00:00.13
	Elapsed Time	00:00:00.14

[DataSet5] C:\Users\Public\Documents\PhD\ERG\Results\T-CEM423-6\scotopic data T.sav

Model Information

Dependent Variable		V12
Probability Distribution		Gamma
Link Function		Log
Subject Effect	1	animal
Within-Subject Effect	1	Injured
	2	timepoint
	3	flashintensitymcd
Working Correlation Matrix Structure		AR(1)

Case Processing Summary

	N	Percent
Included	144	94.7%
Excluded	8	5.3%
Total	152	100.0%

Correlated Data Summary

Number of Levels	Subject Effect	animal	8
	Within-Subject Effect	Injured	2
		timepoint	3
		flashintensitymcd	3
Number of Subjects			8
Number of Measurements per Subject	Minimum		18
	Maximum		18
Correlation Matrix Dimension			18

Categorical Variable Information

			N	Percent
Factor	timepoint	2	48	33.3%
		7	48	33.3%
		14	48	33.3%
		Total	144	100.0%
	flashintensitymcd	10	48	33.3%
		3000	48	33.3%
		10000	48	33.3%
		Total	144	100.0%
	Injured	1	72	50.0%
		0	72	50.0%
		Total	144	100.0%

Continuous Variable Information

		N	Minimum	Maximum	Mean	Std. Deviation
Dependent Variable	V12	144	1	3436	119.25	472.496

Goodness of Fit[a]

	Value
Quasi Likelihood under Independence Model Criterion (QIC)[b]	202.567
Corrected Quasi Likelihood under Independence Model Criterion (QICC)[b]	188.305

Dependent Variable: V12
Model: (Intercept), timepoint, flashintensitymcd, Injured, timepoint * flashintensitymcd, flashintensitymcd * Injured

a. Information criteria are in small-is-better form.

b. Computed using the full log quasi-likelihood function.

Tests of Model Effects

	Type III		
Source	Wald Chi-Square	df	Sig.
(Intercept)	183.994	1	.000
timepoint	19.088	2	.000
flashintensitymcd	132.105	2	.000
Injured	.676	1	.411
timepoint * flashintensitymcd	244.249	4	.000
flashintensitymcd * Injured	5.393	2	.067

Dependent Variable: V12
Model: (Intercept), timepoint, flashintensitymcd, Injured, timepoint * flashintensitymcd, flashintensitymcd * Injured

Working Correlation Matrix[a]

Measurement	Measurement			
	[Injured = 0]* [timepoint = 2]* [flashintensity mcd = 10]	[Injured = 0]* [timepoint = 2]* [flashintensity mcd = 3000]	[Injured = 0]* [timepoint = 2]* [flashintensity mcd = 10000]	[Injured = 0]* [timepoint = 7]* [flashintensity mcd = 10]
[Injured = 0]* [timepoint = 2]* [flashintensitymcd = 10]	1.000	.026	.001	.000
[Injured = 0]* [timepoint = 2]* [flashintensitymcd = 3000]	.026	1.000	.026	.001
[Injured = 0]* [timepoint = 2]* [flashintensitymcd = 10000]	.001	.026	1.000	.026
[Injured = 0]* [timepoint = 7]* [flashintensitymcd = 10]	.000	.001	.026	1.000
[Injured = 0]* [timepoint = 7]* [flashintensitymcd = 3000]	.000	.000	.001	.026
[Injured = 0]* [timepoint = 7]* [flashintensitymcd = 10000]	.000	.000	.000	.001
[Injured = 0]* [timepoint = 14]* [flashintensitymcd = 10]	.000	.000	.000	.000
[Injured = 0]* [timepoint = 14]* [flashintensitymcd = 3000]	.000	.000	.000	.000
[Injured = 0]* [timepoint = 14]* [flashintensitymcd = 10000]	.000	.000	.000	.000
[Injured = 1]* [timepoint = 2]* [flashintensitymcd = 10]	.000	.000	.000	.000
[Injured = 1]* [timepoint = 2]* [flashintensitymcd = 3000]	.000	.000	.000	.000
[Injured = 1]* [timepoint = 2]* [flashintensitymcd = 10000]	.000	.000	.000	.000
[Injured = 1]* [timepoint = 7]* [flashintensitymcd = 10]	.000	.000	.000	.000
[Injured = 1]* [timepoint = 7]* [flashintensitymcd = 3000]	.000	.000	.000	.000

Working Correlation Matrix[a]

Measurement	Measurement			
	[Injured = 0]* [timepoint = 7]* [flashintensity mcd = 3000]	[Injured = 0]* [timepoint = 7]* [flashintensity mcd = 10000]	[Injured = 0]* [timepoint = 14]* [flashintensity mcd = 10]	[Injured = 0]* [timepoint = 14]* [flashintensity mcd = 3000]
[Injured = 0]* [timepoint = 2]* [flashintensitymcd = 10]	.000	.000	.000	.000
[Injured = 0]* [timepoint = 2]* [flashintensitymcd = 3000]	.000	.000	.000	.000
[Injured = 0]* [timepoint = 2]* [flashintensitymcd = 10000]	.001	.000	.000	.000
[Injured = 0]* [timepoint = 7]* [flashintensitymcd = 10]	.026	.001	.000	.000
[Injured = 0]* [timepoint = 7]* [flashintensitymcd = 3000]	1.000	.026	.001	.000
[Injured = 0]* [timepoint = 7]* [flashintensitymcd = 10000]	.026	1.000	.026	.001
[Injured = 0]* [timepoint = 14]* [flashintensitymcd = 10]	.001	.026	1.000	.026
[Injured = 0]* [timepoint = 14]* [flashintensitymcd = 3000]	.000	.001	.026	1.000
[Injured = 0]* [timepoint = 14]* [flashintensitymcd = 10000]	.000	.000	.001	.026
[Injured = 1]* [timepoint = 2]* [flashintensitymcd = 10]	.000	.000	.000	.001
[Injured = 1]* [timepoint = 2]* [flashintensitymcd = 3000]	.000	.000	.000	.000
[Injured = 1]* [timepoint = 2]* [flashintensitymcd = 10000]	.000	.000	.000	.000
[Injured = 1]* [timepoint = 7]* [flashintensitymcd = 10]	.000	.000	.000	.000
[Injured = 1]* [timepoint = 7]* [flashintensitymcd = 3000]	.000	.000	.000	.000

Working Correlation Matrix[a]

Measurement	Measurement			
	[Injured = 0]* [timepoint = 14]* [flashintensity mcd = 10000]	[Injured = 1]* [timepoint = 2]* [flashintensity mcd = 10]	[Injured = 1]* [timepoint = 2]* [flashintensity mcd = 3000]	[Injured = 1]* [timepoint = 2]* [flashintensity mcd = 10000]
[Injured = 0]* [timepoint = 2]* [flashintensitymcd = 10]	.000	.000	.000	.000
[Injured = 0]* [timepoint = 2]* [flashintensitymcd = 3000]	.000	.000	.000	.000
[Injured = 0]* [timepoint = 2]* [flashintensitymcd = 10000]	.000	.000	.000	.000
[Injured = 0]* [timepoint = 7]* [flashintensitymcd = 10]	.000	.000	.000	.000
[Injured = 0]* [timepoint = 7]* [flashintensitymcd = 3000]	.000	.000	.000	.000
[Injured = 0]* [timepoint = 7]* [flashintensitymcd = 10000]	.000	.000	.000	.000
[Injured = 0]* [timepoint = 14]* [flashintensitymcd = 10]	.001	.000	.000	.000
[Injured = 0]* [timepoint = 14]* [flashintensitymcd = 3000]	.026	.001	.000	.000
[Injured = 0]* [timepoint = 14]* [flashintensitymcd = 10000]	1.000	.026	.001	.000
[Injured = 1]* [timepoint = 2]* [flashintensitymcd = 10]	.026	1.000	.026	.001
[Injured = 1]* [timepoint = 2]* [flashintensitymcd = 3000]	.001	.026	1.000	.026
[Injured = 1]* [timepoint = 2]* [flashintensitymcd = 10000]	.000	.001	.026	1.000
[Injured = 1]* [timepoint = 7]* [flashintensitymcd = 10]	.000	.000	.001	.026
[Injured = 1]* [timepoint = 7]* [flashintensitymcd = 3000]	.000	.000	.000	.001

Working Correlation Matrix[a]

Measurement	Measurement			
	[Injured = 1]* [timepoint = 7]* [flashintensity mcd = 10]	[Injured = 1]* [timepoint = 7]* [flashintensity mcd = 3000]	[Injured = 1]* [timepoint = 7]* [flashintensity mcd = 10000]	[Injured = 1]* [timepoint = 14]* [flashintensity mcd = 10]
[Injured = 0]* [timepoint = 2]* [flashintensitymcd = 10]	.000	.000	.000	.000
[Injured = 0]* [timepoint = 2]* [flashintensitymcd = 3000]	.000	.000	.000	.000
[Injured = 0]* [timepoint = 2]* [flashintensitymcd = 10000]	.000	.000	.000	.000
[Injured = 0]* [timepoint = 7]* [flashintensitymcd = 10]	.000	.000	.000	.000
[Injured = 0]* [timepoint = 7]* [flashintensitymcd = 3000]	.000	.000	.000	.000
[Injured = 0]* [timepoint = 7]* [flashintensitymcd = 10000]	.000	.000	.000	.000
[Injured = 0]* [timepoint = 14]* [flashintensitymcd = 10]	.000	.000	.000	.000
[Injured = 0]* [timepoint = 14]* [flashintensitymcd = 3000]	.000	.000	.000	.000
[Injured = 0]* [timepoint = 14]* [flashintensitymcd = 10000]	.000	.000	.000	.000
[Injured = 1]* [timepoint = 2]* [flashintensitymcd = 10]	.000	.000	.000	.000
[Injured = 1]* [timepoint = 2]* [flashintensitymcd = 3000]	.001	.000	.000	.000
[Injured = 1]* [timepoint = 2]* [flashintensitymcd = 10000]	.026	.001	.000	.000
[Injured = 1]* [timepoint = 7]* [flashintensitymcd = 10]	1.000	.026	.001	.000
[Injured = 1]* [timepoint = 7]* [flashintensitymcd = 3000]	.026	1.000	.026	.001

Working Correlation Matrix[a]

Measurement	Measurement	
	[Injured = 1]* [timepoint = 14]* [flashintensity mcd = 3000]	[Injured = 1]* [timepoint = 14]* [flashintensity mcd = 10000]
[Injured = 0]* [timepoint = 2]* [flashintensitymcd = 10]	.000	.000
[Injured = 0]* [timepoint = 2]* [flashintensitymcd = 3000]	.000	.000
[Injured = 0]* [timepoint = 2]* [flashintensitymcd = 10000]	.000	.000
[Injured = 0]* [timepoint = 7]* [flashintensitymcd = 10]	.000	.000
[Injured = 0]* [timepoint = 7]* [flashintensitymcd = 3000]	.000	.000
[Injured = 0]* [timepoint = 7]* [flashintensitymcd = 10000]	.000	.000
[Injured = 0]* [timepoint = 14]* [flashintensitymcd = 10]	.000	.000
[Injured = 0]* [timepoint = 14]* [flashintensitymcd = 3000]	.000	.000
[Injured = 0]* [timepoint = 14]* [flashintensitymcd = 10000]	.000	.000
[Injured = 1]* [timepoint = 2]* [flashintensitymcd = 10]	.000	.000
[Injured = 1]* [timepoint = 2]* [flashintensitymcd = 3000]	.000	.000
[Injured = 1]* [timepoint = 2]* [flashintensitymcd = 10000]	.000	.000
[Injured = 1]* [timepoint = 7]* [flashintensitymcd = 10]	.000	.000
[Injured = 1]* [timepoint = 7]* [flashintensitymcd = 3000]	.000	.000

Working Correlation Matrix[a]

Measurement	Measurement			
	[Injured = 0]* [timepoint = 2]* [flashintensity mcd = 10]	[Injured = 0]* [timepoint = 2]* [flashintensity mcd = 3000]	[Injured = 0]* [timepoint = 2]* [flashintensity mcd = 10000]	[Injured = 0]* [timepoint = 7]* [flashintensity mcd = 10]
[Injured = 1]* [timepoint = 7]* [flashintensitymcd = 10000]	.000	.000	.000	.000
[Injured = 1]* [timepoint = 14]* [flashintensitymcd = 10]	.000	.000	.000	.000
[Injured = 1]* [timepoint = 14]* [flashintensitymcd = 3000]	.000	.000	.000	.000
[Injured = 1]* [timepoint = 14]* [flashintensitymcd = 10000]	.000	.000	.000	.000

Working Correlation Matrix[a]

Measurement	Measurement			
	[Injured = 0]* [timepoint = 7]* [flashintensity mcd = 3000]	[Injured = 0]* [timepoint = 7]* [flashintensity mcd = 10000]	[Injured = 0]* [timepoint = 14]* [flashintensity mcd = 10]	[Injured = 0]* [timepoint = 14]* [flashintensity mcd = 3000]
[Injured = 1]* [timepoint = 7]* [flashintensitymcd = 10000]	.000	.000	.000	.000
[Injured = 1]* [timepoint = 14]* [flashintensitymcd = 10]	.000	.000	.000	.000
[Injured = 1]* [timepoint = 14]* [flashintensitymcd = 3000]	.000	.000	.000	.000
[Injured = 1]* [timepoint = 14]* [flashintensitymcd = 10000]	.000	.000	.000	.000

Working Correlation Matrix[a]

Measurement	Measurement			
	[Injured = 0]* [timepoint = 14]* [flashintensity mcd = 10000]	[Injured = 1]* [timepoint = 2]* [flashintensity mcd = 10]	[Injured = 1]* [timepoint = 2]* [flashintensity mcd = 3000]	[Injured = 1]* [timepoint = 2]* [flashintensity mcd = 10000]
[Injured = 1]* [timepoint = 7]* [flashintensitymcd = 10000]	.000	.000	.000	.000
[Injured = 1]* [timepoint = 14]* [flashintensitymcd = 10]	.000	.000	.000	.000
[Injured = 1]* [timepoint = 14]* [flashintensitymcd = 3000]	.000	.000	.000	.000
[Injured = 1]* [timepoint = 14]* [flashintensitymcd = 10000]	.000	.000	.000	.000

Working Correlation Matrix[a]

Measurement	Measurement			
	[Injured = 1]* [timepoint = 7]* [flashintensity mcd = 10]	[Injured = 1]* [timepoint = 7]* [flashintensity mcd = 3000]	[Injured = 1]* [timepoint = 7]* [flashintensity mcd = 10000]	[Injured = 1]* [timepoint = 14]* [flashintensity mcd = 10]
[Injured = 1]* [timepoint = 7]* [flashintensitymcd = 10000]	.001	.026	1.000	.026
[Injured = 1]* [timepoint = 14]* [flashintensitymcd = 10]	.000	.001	.026	1.000
[Injured = 1]* [timepoint = 14]* [flashintensitymcd = 3000]	.000	.000	.001	.026
[Injured = 1]* [timepoint = 14]* [flashintensitymcd = 10000]	.000	.000	.000	.001

Working Correlation Matrix[a]

Measurement	Measurement	
	[Injured = 1]* [timepoint = 14]* [flashintensity mcd = 3000]	[Injured = 1]* [timepoint = 14]* [flashintensity mcd = 10000]
[Injured = 1]* [timepoint = 7]* [flashintensitymcd = 10000]	.001	.000
[Injured = 1]* [timepoint = 14]* [flashintensitymcd = 10]	.026	.001
[Injured = 1]* [timepoint = 14]* [flashintensitymcd = 3000]	1.000	.026
[Injured = 1]* [timepoint = 14]* [flashintensitymcd = 10000]	.026	1.000

Dependent Variable: V12
Model: (Intercept), timepoint, flashintensitymcd, Injured, timepoint * flashintensitymcd, flashintensitymcd * Injured

a. The AR(1) working correlation matrix structure is computed assuming the measurements are equally spaced for all subjects.

Estimated Marginal Means: timepoint* flashintensitymcd* Injured

Estimates

timepoint	flashintensitymcd	Injured	Mean	Std. Error	95% Wald Confidence Interval	
					Lower	Upper
2	10	1	53.53	30.159	17.74	161.50
		0	38.73	18.248	15.38	97.52
	3000	1	3.06	.799	1.83	5.10
		0	3.09	.660	2.04	4.70
	10000	1	2.06	.341	1.49	2.85
		0	2.27	.403	1.60	3.21
7	10	1	790.32	335.884	343.59	1817.86
		0	571.83	314.181	194.80	1678.58
	3000	1	2.23	.171	1.92	2.59
		0	2.26	.193	1.91	2.67
	10000	1	1.88	.124	1.65	2.14
		0	2.07	.139	1.81	2.36
14	10	1	421.25	338.481	87.21	2034.68
		0	304.79	210.675	78.64	1181.31
	3000	1	2.05	.138	1.79	2.34
		0	2.07	.133	1.83	2.35
	10000	1	1.96	.168	1.66	2.32
		0	2.15	.217	1.77	2.62

```
 * Generalized Estimating Equations.
GENLIN V12 BY timepoint flashintensitymcd Injured (ORDER=DATA)
  /MODEL timepoint flashintensitymcd Injured timepoint*flashintensitymcd INTERCEPT=YES
 DISTRIBUTION=GAMMA LINK=LOG
  /CRITERIA METHOD=FISHER(1) SCALE=MLE MAXITERATIONS=100 MAXSTEPHALVING=5 PCONVERGE=1E-006(A
  /EMMEANS TABLES=timepoint*flashintensitymcd*Injured SCALE=ORIGINAL
  /REPEATED SUBJECT=animal WITHINSUBJECT=Injured*timepoint*flashintensitymcd SORT=YES CORRTY
  /MISSING CLASSMISSING=EXCLUDE
  /PRINT CPS DESCRIPTIVES MODELINFO FIT SUMMARY WORKINGCORR.
```

Generalized Linear Models

Notes

Output Created		02-MAY-2013 10:16:02
Comments		
Input	Data	C:\Users\Public\Documents\PhD\ERG\Results\T-CEM423-6\scotopic data T.sav
	Active Dataset	DataSet5
	Filter	<none>
	Weight	<none>
	Split File	<none>
	N of Rows in Working Data File	152
Missing Value Handling	Definition of Missing	User-defined missing values for factor, subject and within-subject variables are treated as missing.
	Cases Used	Statistics are based on cases with valid data for all variables in the model.
Weight Handling		not applicable

Notes

Syntax		GENLIN V12 BY timepoint flashintensitymcd Injured (ORDER=DATA) /MODEL timepoint flashintensitymcd Injured timepoint*flashintensitymcd INTERCEPT=YES DISTRIBUTION=GAMMA LINK=LOG /CRITERIA METHOD=FISHER(1) SCALE=MLE MAXITERATIONS=100 MAXSTEPHALVING=5 PCONVERGE=1E-006(ABSOLUTE) SINGULAR=1E-012 ANALYSISTYPE=3(WALD) CILEVEL=95 LIKELIHOOD=FULL /EMMEANS TABLES=timepoint*flashintensitymcd*Injured SCALE=ORIGINAL /REPEATED SUBJECT=animal WITHINSUBJECT=Injured*timepoint*flashintensitymcd SORT=YES CORRTYPE=AR(1) ADJUSTCORR=YES COVB=ROBUST MAXITERATIONS=100 PCONVERGE=1e-006(ABSOLUTE) UPDATECORR=1 /MISSING CLASSMISSING=EXCLUDE /PRINT CPS DESCRIPTIVES...
Resources	Processor Time	00:00:00.06
	Elapsed Time	00:00:00.13

[DataSet5] C:\Users\Public\Documents\PhD\ERG\Results\T-CEM423-6\scotopic data T.sav

Model Information

Dependent Variable		V12
Probability Distribution		Gamma
Link Function		Log
Subject Effect	1	animal
Within-Subject Effect	1	Injured
	2	timepoint
	3	flashintensitymcd
Working Correlation Matrix Structure		AR(1)

Case Processing Summary

	N	Percent
Included	144	94.7%
Excluded	8	5.3%
Total	152	100.0%

Correlated Data Summary

Number of Levels	Subject Effect	animal	8
	Within-Subject Effect	Injured	2
		timepoint	3
		flashintensitymcd	3
Number of Subjects			8
Number of Measurements per Subject	Minimum		18
	Maximum		18
Correlation Matrix Dimension			18

Categorical Variable Information

			N	Percent
Factor	timepoint	2	48	33.3%
		7	48	33.3%
		14	48	33.3%
		Total	144	100.0%
	flashintensitymcd	10	48	33.3%
		3000	48	33.3%
		10000	48	33.3%
		Total	144	100.0%
	Injured	1	72	50.0%
		0	72	50.0%
		Total	144	100.0%

Continuous Variable Information

		N	Minimum	Maximum	Mean	Std. Deviation
Dependent Variable	V12	144	1	3436	119.25	472.496

Goodness of Fit[a]

	Value
Quasi Likelihood under Independence Model Criterion (QIC)[b]	202.668
Corrected Quasi Likelihood under Independence Model Criterion (QICC)[b]	185.470

Dependent Variable: V12
Model: (Intercept), timepoint, flashintensitymcd, Injured, timepoint * flashintensitymcd

a. Information criteria are in small-is-better form.

b. Computed using the full log quasi-likelihood function.

Tests of Model Effects

	Type III		
Source	Wald Chi-Square	df	Sig.
(Intercept)	184.414	1	.000
timepoint	19.216	2	.000
flashintensitymcd	122.411	2	.000
Injured	.425	1	.514
timepoint * flashintensitymcd	227.503	4	.000

Dependent Variable: V12
Model: (Intercept), timepoint, flashintensitymcd, Injured, timepoint * flashintensitymcd

Working Correlation Matrix[a]

Measurement	Measurement			
	[Injured = 0]* [timepoint = 2]* [flashintensity mcd = 10]	[Injured = 0]* [timepoint = 2]* [flashintensity mcd = 3000]	[Injured = 0]* [timepoint = 2]* [flashintensity mcd = 10000]	[Injured = 0]* [timepoint = 7]* [flashintensity mcd = 10]
[Injured = 0]* [timepoint = 2]* [flashintensitymcd = 10]	1.000	.026	.001	.000
[Injured = 0]* [timepoint = 2]* [flashintensitymcd = 3000]	.026	1.000	.026	.001
[Injured = 0]* [timepoint = 2]* [flashintensitymcd = 10000]	.001	.026	1.000	.026
[Injured = 0]* [timepoint = 7]* [flashintensitymcd = 10]	.000	.001	.026	1.000
[Injured = 0]* [timepoint = 7]* [flashintensitymcd = 3000]	.000	.000	.001	.026
[Injured = 0]* [timepoint = 7]* [flashintensitymcd = 10000]	.000	.000	.000	.001
[Injured = 0]* [timepoint = 14]* [flashintensitymcd = 10]	.000	.000	.000	.000
[Injured = 0]* [timepoint = 14]* [flashintensitymcd = 3000]	.000	.000	.000	.000
[Injured = 0]* [timepoint = 14]* [flashintensitymcd = 10000]	.000	.000	.000	.000
[Injured = 1]* [timepoint = 2]* [flashintensitymcd = 10]	.000	.000	.000	.000
[Injured = 1]* [timepoint = 2]* [flashintensitymcd = 3000]	.000	.000	.000	.000
[Injured = 1]* [timepoint = 2]* [flashintensitymcd = 10000]	.000	.000	.000	.000
[Injured = 1]* [timepoint = 7]* [flashintensitymcd = 10]	.000	.000	.000	.000
[Injured = 1]* [timepoint = 7]* [flashintensitymcd = 3000]	.000	.000	.000	.000

Working Correlation Matrix[a]

Measurement	Measurement			
	[Injured = 0]* [timepoint = 7]* [flashintensity mcd = 3000]	[Injured = 0]* [timepoint = 7]* [flashintensity mcd = 10000]	[Injured = 0]* [timepoint = 14]* [flashintensity mcd = 10]	[Injured = 0]* [timepoint = 14]* [flashintensity mcd = 3000]
[Injured = 0]* [timepoint = 2]* [flashintensitymcd = 10]	.000	.000	.000	.000
[Injured = 0]* [timepoint = 2]* [flashintensitymcd = 3000]	.000	.000	.000	.000
[Injured = 0]* [timepoint = 2]* [flashintensitymcd = 10000]	.001	.000	.000	.000
[Injured = 0]* [timepoint = 7]* [flashintensitymcd = 10]	.026	.001	.000	.000
[Injured = 0]* [timepoint = 7]* [flashintensitymcd = 3000]	1.000	.026	.001	.000
[Injured = 0]* [timepoint = 7]* [flashintensitymcd = 10000]	.026	1.000	.026	.001
[Injured = 0]* [timepoint = 14]* [flashintensitymcd = 10]	.001	.026	1.000	.026
[Injured = 0]* [timepoint = 14]* [flashintensitymcd = 3000]	.000	.001	.026	1.000
[Injured = 0]* [timepoint = 14]* [flashintensitymcd = 10000]	.000	.000	.001	.026
[Injured = 1]* [timepoint = 2]* [flashintensitymcd = 10]	.000	.000	.000	.001
[Injured = 1]* [timepoint = 2]* [flashintensitymcd = 3000]	.000	.000	.000	.000
[Injured = 1]* [timepoint = 2]* [flashintensitymcd = 10000]	.000	.000	.000	.000
[Injured = 1]* [timepoint = 7]* [flashintensitymcd = 10]	.000	.000	.000	.000
[Injured = 1]* [timepoint = 7]* [flashintensitymcd = 3000]	.000	.000	.000	.000

Working Correlation Matrix[a]

Measurement	Measurement			
	[Injured = 0]* [timepoint = 14]* [flashintensity mcd = 10000]	[Injured = 1]* [timepoint = 2]* [flashintensity mcd = 10]	[Injured = 1]* [timepoint = 2]* [flashintensity mcd = 3000]	[Injured = 1]* [timepoint = 2]* [flashintensity mcd = 10000]
[Injured = 0]* [timepoint = 2]* [flashintensitymcd = 10]	.000	.000	.000	.000
[Injured = 0]* [timepoint = 2]* [flashintensitymcd = 3000]	.000	.000	.000	.000
[Injured = 0]* [timepoint = 2]* [flashintensitymcd = 10000]	.000	.000	.000	.000
[Injured = 0]* [timepoint = 7]* [flashintensitymcd = 10]	.000	.000	.000	.000
[Injured = 0]* [timepoint = 7]* [flashintensitymcd = 3000]	.000	.000	.000	.000
[Injured = 0]* [timepoint = 7]* [flashintensitymcd = 10000]	.000	.000	.000	.000
[Injured = 0]* [timepoint = 14]* [flashintensitymcd = 10]	.001	.000	.000	.000
[Injured = 0]* [timepoint = 14]* [flashintensitymcd = 3000]	.026	.001	.000	.000
[Injured = 0]* [timepoint = 14]* [flashintensitymcd = 10000]	1.000	.026	.001	.000
[Injured = 1]* [timepoint = 2]* [flashintensitymcd = 10]	.026	1.000	.026	.001
[Injured = 1]* [timepoint = 2]* [flashintensitymcd = 3000]	.001	.026	1.000	.026
[Injured = 1]* [timepoint = 2]* [flashintensitymcd = 10000]	.000	.001	.026	1.000
[Injured = 1]* [timepoint = 7]* [flashintensitymcd = 10]	.000	.000	.001	.026
[Injured = 1]* [timepoint = 7]* [flashintensitymcd = 3000]	.000	.000	.000	.001

Working Correlation Matrix[a]

Measurement	Measurement			
	[Injured = 1]* [timepoint = 7]* [flashintensity mcd = 10]	[Injured = 1]* [timepoint = 7]* [flashintensity mcd = 3000]	[Injured = 1]* [timepoint = 7]* [flashintensity mcd = 10000]	[Injured = 1]* [timepoint = 14]* [flashintensity mcd = 10]
[Injured = 0]* [timepoint = 2]* [flashintensitymcd = 10]	.000	.000	.000	.000
[Injured = 0]* [timepoint = 2]* [flashintensitymcd = 3000]	.000	.000	.000	.000
[Injured = 0]* [timepoint = 2]* [flashintensitymcd = 10000]	.000	.000	.000	.000
[Injured = 0]* [timepoint = 7]* [flashintensitymcd = 10]	.000	.000	.000	.000
[Injured = 0]* [timepoint = 7]* [flashintensitymcd = 3000]	.000	.000	.000	.000
[Injured = 0]* [timepoint = 7]* [flashintensitymcd = 10000]	.000	.000	.000	.000
[Injured = 0]* [timepoint = 14]* [flashintensitymcd = 10]	.000	.000	.000	.000
[Injured = 0]* [timepoint = 14]* [flashintensitymcd = 3000]	.000	.000	.000	.000
[Injured = 0]* [timepoint = 14]* [flashintensitymcd = 10000]	.000	.000	.000	.000
[Injured = 1]* [timepoint = 2]* [flashintensitymcd = 10]	.000	.000	.000	.000
[Injured = 1]* [timepoint = 2]* [flashintensitymcd = 3000]	.001	.000	.000	.000
[Injured = 1]* [timepoint = 2]* [flashintensitymcd = 10000]	.026	.001	.000	.000
[Injured = 1]* [timepoint = 7]* [flashintensitymcd = 10]	1.000	.026	.001	.000
[Injured = 1]* [timepoint = 7]* [flashintensitymcd = 3000]	.026	1.000	.026	.001

Working Correlation Matrix[a]

Measurement	Measurement	
	[Injured = 1]* [timepoint = 14]* [flashintensity mcd = 3000]	[Injured = 1]* [timepoint = 14]* [flashintensity mcd = 10000]
[Injured = 0]* [timepoint = 2]* [flashintensitymcd = 10]	.000	.000
[Injured = 0]* [timepoint = 2]* [flashintensitymcd = 3000]	.000	.000
[Injured = 0]* [timepoint = 2]* [flashintensitymcd = 10000]	.000	.000
[Injured = 0]* [timepoint = 7]* [flashintensitymcd = 10]	.000	.000
[Injured = 0]* [timepoint = 7]* [flashintensitymcd = 3000]	.000	.000
[Injured = 0]* [timepoint = 7]* [flashintensitymcd = 10000]	.000	.000
[Injured = 0]* [timepoint = 14]* [flashintensitymcd = 10]	.000	.000
[Injured = 0]* [timepoint = 14]* [flashintensitymcd = 3000]	.000	.000
[Injured = 0]* [timepoint = 14]* [flashintensitymcd = 10000]	.000	.000
[Injured = 1]* [timepoint = 2]* [flashintensitymcd = 10]	.000	.000
[Injured = 1]* [timepoint = 2]* [flashintensitymcd = 3000]	.000	.000
[Injured = 1]* [timepoint = 2]* [flashintensitymcd = 10000]	.000	.000
[Injured = 1]* [timepoint = 7]* [flashintensitymcd = 10]	.000	.000
[Injured = 1]* [timepoint = 7]* [flashintensitymcd = 3000]	.000	.000

Working Correlation Matrix[a]

Measurement	Measurement			
	[Injured = 0]* [timepoint = 2]* [flashintensity mcd = 10]	[Injured = 0]* [timepoint = 2]* [flashintensity mcd = 3000]	[Injured = 0]* [timepoint = 2]* [flashintensity mcd = 10000]	[Injured = 0]* [timepoint = 7]* [flashintensity mcd = 10]
[Injured = 1]* [timepoint = 7]* [flashintensitymcd = 10000]	.000	.000	.000	.000
[Injured = 1]* [timepoint = 14]* [flashintensitymcd = 10]	.000	.000	.000	.000
[Injured = 1]* [timepoint = 14]* [flashintensitymcd = 3000]	.000	.000	.000	.000
[Injured = 1]* [timepoint = 14]* [flashintensitymcd = 10000]	.000	.000	.000	.000

Working Correlation Matrix[a]

Measurement	Measurement			
	[Injured = 0]* [timepoint = 7]* [flashintensity mcd = 3000]	[Injured = 0]* [timepoint = 7]* [flashintensity mcd = 10000]	[Injured = 0]* [timepoint = 14]* [flashintensity mcd = 10]	[Injured = 0]* [timepoint = 14]* [flashintensity mcd = 3000]
[Injured = 1]* [timepoint = 7]* [flashintensitymcd = 10000]	.000	.000	.000	.000
[Injured = 1]* [timepoint = 14]* [flashintensitymcd = 10]	.000	.000	.000	.000
[Injured = 1]* [timepoint = 14]* [flashintensitymcd = 3000]	.000	.000	.000	.000
[Injured = 1]* [timepoint = 14]* [flashintensitymcd = 10000]	.000	.000	.000	.000

Working Correlation Matrix[a]

Measurement	Measurement			
	[Injured = 0]* [timepoint = 14]* [flashintensity mcd = 10000]	[Injured = 1]* [timepoint = 2]* [flashintensity mcd = 10]	[Injured = 1]* [timepoint = 2]* [flashintensity mcd = 3000]	[Injured = 1]* [timepoint = 2]* [flashintensity mcd = 10000]
[Injured = 1]* [timepoint = 7]* [flashintensitymcd = 10000]	.000	.000	.000	.000
[Injured = 1]* [timepoint = 14]* [flashintensitymcd = 10]	.000	.000	.000	.000
[Injured = 1]* [timepoint = 14]* [flashintensitymcd = 3000]	.000	.000	.000	.000
[Injured = 1]* [timepoint = 14]* [flashintensitymcd = 10000]	.000	.000	.000	.000

Working Correlation Matrix[a]

Measurement	Measurement			
	[Injured = 1]* [timepoint = 7]* [flashintensity mcd = 10]	[Injured = 1]* [timepoint = 7]* [flashintensity mcd = 3000]	[Injured = 1]* [timepoint = 7]* [flashintensity mcd = 10000]	[Injured = 1]* [timepoint = 14]* [flashintensity mcd = 10]
[Injured = 1]* [timepoint = 7]* [flashintensitymcd = 10000]	.001	.026	1.000	.026
[Injured = 1]* [timepoint = 14]* [flashintensitymcd = 10]	.000	.001	.026	1.000
[Injured = 1]* [timepoint = 14]* [flashintensitymcd = 3000]	.000	.000	.001	.026
[Injured = 1]* [timepoint = 14]* [flashintensitymcd = 10000]	.000	.000	.000	.001

Working Correlation Matrix[a]

Measurement	Measurement	
	[Injured = 1]* [timepoint = 14]* [flashintensity mcd = 3000]	[Injured = 1]* [timepoint = 14]* [flashintensity mcd = 10000]
[Injured = 1]* [timepoint = 7]* [flashintensitymcd = 10000]	.001	.000
[Injured = 1]* [timepoint = 14]* [flashintensitymcd = 10]	.026	.001
[Injured = 1]* [timepoint = 14]* [flashintensitymcd = 3000]	1.000	.026
[Injured = 1]* [timepoint = 14]* [flashintensitymcd = 10000]	.026	1.000

Dependent Variable: V12
Model: (Intercept), timepoint, flashintensitymcd, Injured, timepoint * flashintensitymcd

a. The AR(1) working correlation matrix structure is computed assuming the measurements are equally spaced for all subjects.

Estimated Marginal Means: timepoint* flashintensitymcd* Injured

Estimates

timepoint	flashintensitymcd	Injured	Mean	Std. Error	95% Wald Confidence Interval	
					Lower	Upper
2	10	1	49.37	28.610	15.86	153.72
		0	46.16	23.500	17.02	125.20
	3000	1	3.18	.739	2.02	5.02
		0	2.98	.744	1.82	4.86
	10000	1	2.25	.362	1.64	3.08
		0	2.10	.398	1.45	3.05
7	10	1	675.93	303.673	280.21	1630.49
		0	631.93	295.786	252.50	1581.57
	3000	1	2.32	.236	1.90	2.83
		0	2.17	.179	1.85	2.55
	10000	1	2.04	.181	1.71	2.42
		0	1.90	.141	1.65	2.20
14	10	1	371.73	283.966	83.17	1661.37
		0	347.53	238.505	90.54	1334.02
	3000	1	2.13	.178	1.81	2.51
		0	1.99	.150	1.72	2.31
	10000	1	2.13	.228	1.73	2.63
		0	2.00	.220	1.61	2.48

```
 * Generalized Estimating Equations.
GENLIN V12 BY timepoint flashintensitymcd Injured (ORDER=DATA)
  /MODEL timepoint flashintensitymcd timepoint*flashintensitymcd INTERCEPT=YES
 DISTRIBUTION=GAMMA LINK=LOG
  /CRITERIA METHOD=FISHER(1) SCALE=MLE MAXITERATIONS=100 MAXSTEPHALVING=5 PCONVERGE=1E-006(A
  /EMMEANS TABLES=timepoint*flashintensitymcd*Injured SCALE=ORIGINAL
  /REPEATED SUBJECT=animal WITHINSUBJECT=Injured*timepoint*flashintensitymcd SORT=YES CORRTY
  /MISSING CLASSMISSING=EXCLUDE
```

Generalized Linear Models

Notes

Output Created		02-MAY-2013 10:16:13
Comments		
Input	Data	C:\Users\Public\Documents\PhD\ERG\Results\T-CEM423-6\scotopic data T.sav
	Active Dataset	DataSet5
	Filter	<none>
	Weight	<none>
	Split File	<none>
	N of Rows in Working Data File	152
Missing Value Handling	Definition of Missing	User-defined missing values for factor, subject and within-subject variables are treated as missing.
	Cases Used	Statistics are based on cases with valid data for all variables in the model.
Weight Handling		not applicable

Notes

Syntax		GENLIN V12 BY timepoint flashintensitymcd Injured (ORDER=DATA) /MODEL timepoint flashintensitymcd timepoint*flashintensitymcd INTERCEPT=YES DISTRIBUTION=GAMMA LINK=LOG /CRITERIA METHOD=FISHER(1) SCALE=MLE MAXITERATIONS=100 MAXSTEPHALVING=5 PCONVERGE=1E-006(ABSOLUTE) SINGULAR=1E-012 ANALYSISTYPE=3(WALD) CILEVEL=95 LIKELIHOOD=FULL /EMMEANS TABLES=timepoint*flashintensitymcd*Injured SCALE=ORIGINAL /REPEATED SUBJECT=animal WITHINSUBJECT=Injured*timepoint*flashintensitymcd SORT=YES CORRTYPE=AR(1) ADJUSTCORR=YES COVB=ROBUST MAXITERATIONS=100 PCONVERGE=1e-006(ABSOLUTE) UPDATECORR=1 /MISSING CLASSMISSING=EXCLUDE /PRINT CPS DESCRIPTIVES...
Resources	Processor Time	00:00:00.11
	Elapsed Time	00:00:00.14

[DataSet5] C:\Users\Public\Documents\PhD\ERG\Results\T-CEM423-6\scotopic data T.sav

Model Information

Dependent Variable		V12
Probability Distribution		Gamma
Link Function		Log
Subject Effect	1	animal
Within-Subject Effect	1	Injured
	2	timepoint
	3	flashintensitymcd
Working Correlation Matrix Structure		AR(1)

Case Processing Summary

	N	Percent
Included	144	94.7%
Excluded	8	5.3%
Total	152	100.0%

Correlated Data Summary

Number of Levels	Subject Effect	animal	8
	Within-Subject Effect	Injured	2
		timepoint	3
		flashintensitymcd	3
Number of Subjects			8
Number of Measurements per Subject	Minimum		18
	Maximum		18
Correlation Matrix Dimension			18

Categorical Variable Information

			N	Percent
Factor	timepoint	2	48	33.3%
		7	48	33.3%
		14	48	33.3%
		Total	144	100.0%
	flashintensitymcd	10	48	33.3%
		3000	48	33.3%
		10000	48	33.3%
		Total	144	100.0%
	Injured	1	72	50.0%
		0	72	50.0%
		Total	144	100.0%

Continuous Variable Information

		N	Minimum	Maximum	Mean	Std. Deviation
Dependent Variable	V12	144	1	3436	119.25	472.496

Goodness of Fit[a]

	Value
Quasi Likelihood under Independence Model Criterion (QIC)[b]	202.080
Corrected Quasi Likelihood under Independence Model Criterion (QICC)[b]	183.615

Dependent Variable: V12
Model: (Intercept), timepoint, flashintensitymcd, timepoint * flashintensitymcd

a. Information criteria are in small-is-better form.

b. Computed using the full log quasi-likelihood function.

Tests of Model Effects

	Type III		
Source	Wald Chi-Square	df	Sig.
(Intercept)	184.459	1	.000
timepoint	18.828	2	.000
flashintensitymcd	126.078	2	.000
timepoint * flashintensitymcd	216.733	4	.000

Dependent Variable: V12
Model: (Intercept), timepoint, flashintensitymcd, timepoint * flashintensitymcd

Working Correlation Matrix[a]

Measurement	Measurement			
	[Injured = 0]* [timepoint = 2]* [flashintensity mcd = 10]	[Injured = 0]* [timepoint = 2]* [flashintensity mcd = 3000]	[Injured = 0]* [timepoint = 2]* [flashintensity mcd = 10000]	[Injured = 0]* [timepoint = 7]* [flashintensity mcd = 10]
[Injured = 0]* [timepoint = 2]* [flashintensitymcd = 10]	1.000	.024	.001	.000
[Injured = 0]* [timepoint = 2]* [flashintensitymcd = 3000]	.024	1.000	.024	.001
[Injured = 0]* [timepoint = 2]* [flashintensitymcd = 10000]	.001	.024	1.000	.024
[Injured = 0]* [timepoint = 7]* [flashintensitymcd = 10]	.000	.001	.024	1.000
[Injured = 0]* [timepoint = 7]* [flashintensitymcd = 3000]	.000	.000	.001	.024
[Injured = 0]* [timepoint = 7]* [flashintensitymcd = 10000]	.000	.000	.000	.001
[Injured = 0]* [timepoint = 14]* [flashintensitymcd = 10]	.000	.000	.000	.000
[Injured = 0]* [timepoint = 14]* [flashintensitymcd = 3000]	.000	.000	.000	.000
[Injured = 0]* [timepoint = 14]* [flashintensitymcd = 10000]	.000	.000	.000	.000
[Injured = 1]* [timepoint = 2]* [flashintensitymcd = 10]	.000	.000	.000	.000
[Injured = 1]* [timepoint = 2]* [flashintensitymcd = 3000]	.000	.000	.000	.000
[Injured = 1]* [timepoint = 2]* [flashintensitymcd = 10000]	.000	.000	.000	.000
[Injured = 1]* [timepoint = 7]* [flashintensitymcd = 10]	.000	.000	.000	.000
[Injured = 1]* [timepoint = 7]* [flashintensitymcd = 3000]	.000	.000	.000	.000

Working Correlation Matrix[a]

Measurement	Measurement			
	[Injured = 0]* [timepoint = 7]* [flashintensity mcd = 3000]	[Injured = 0]* [timepoint = 7]* [flashintensity mcd = 10000]	[Injured = 0]* [timepoint = 14]* [flashintensity mcd = 10]	[Injured = 0]* [timepoint = 14]* [flashintensity mcd = 3000]
[Injured = 0]* [timepoint = 2]* [flashintensitymcd = 10]	.000	.000	.000	.000
[Injured = 0]* [timepoint = 2]* [flashintensitymcd = 3000]	.000	.000	.000	.000
[Injured = 0]* [timepoint = 2]* [flashintensitymcd = 10000]	.001	.000	.000	.000
[Injured = 0]* [timepoint = 7]* [flashintensitymcd = 10]	.024	.001	.000	.000
[Injured = 0]* [timepoint = 7]* [flashintensitymcd = 3000]	1.000	.024	.001	.000
[Injured = 0]* [timepoint = 7]* [flashintensitymcd = 10000]	.024	1.000	.024	.001
[Injured = 0]* [timepoint = 14]* [flashintensitymcd = 10]	.001	.024	1.000	.024
[Injured = 0]* [timepoint = 14]* [flashintensitymcd = 3000]	.000	.001	.024	1.000
[Injured = 0]* [timepoint = 14]* [flashintensitymcd = 10000]	.000	.000	.001	.024
[Injured = 1]* [timepoint = 2]* [flashintensitymcd = 10]	.000	.000	.000	.001
[Injured = 1]* [timepoint = 2]* [flashintensitymcd = 3000]	.000	.000	.000	.000
[Injured = 1]* [timepoint = 2]* [flashintensitymcd = 10000]	.000	.000	.000	.000
[Injured = 1]* [timepoint = 7]* [flashintensitymcd = 10]	.000	.000	.000	.000
[Injured = 1]* [timepoint = 7]* [flashintensitymcd = 3000]	.000	.000	.000	.000

Working Correlation Matrix[a]

Measurement	Measurement			
	[Injured = 0]* [timepoint = 14]* [flashintensity mcd = 10000]	[Injured = 1]* [timepoint = 2]* [flashintensity mcd = 10]	[Injured = 1]* [timepoint = 2]* [flashintensity mcd = 3000]	[Injured = 1]* [timepoint = 2]* [flashintensity mcd = 10000]
[Injured = 0]* [timepoint = 2]* [flashintensitymcd = 10]	.000	.000	.000	.000
[Injured = 0]* [timepoint = 2]* [flashintensitymcd = 3000]	.000	.000	.000	.000
[Injured = 0]* [timepoint = 2]* [flashintensitymcd = 10000]	.000	.000	.000	.000
[Injured = 0]* [timepoint = 7]* [flashintensitymcd = 10]	.000	.000	.000	.000
[Injured = 0]* [timepoint = 7]* [flashintensitymcd = 3000]	.000	.000	.000	.000
[Injured = 0]* [timepoint = 7]* [flashintensitymcd = 10000]	.000	.000	.000	.000
[Injured = 0]* [timepoint = 14]* [flashintensitymcd = 10]	.001	.000	.000	.000
[Injured = 0]* [timepoint = 14]* [flashintensitymcd = 3000]	.024	.001	.000	.000
[Injured = 0]* [timepoint = 14]* [flashintensitymcd = 10000]	1.000	.024	.001	.000
[Injured = 1]* [timepoint = 2]* [flashintensitymcd = 10]	.024	1.000	.024	.001
[Injured = 1]* [timepoint = 2]* [flashintensitymcd = 3000]	.001	.024	1.000	.024
[Injured = 1]* [timepoint = 2]* [flashintensitymcd = 10000]	.000	.001	.024	1.000
[Injured = 1]* [timepoint = 7]* [flashintensitymcd = 10]	.000	.000	.001	.024
[Injured = 1]* [timepoint = 7]* [flashintensitymcd = 3000]	.000	.000	.000	.001

Working Correlation Matrix[a]

Measurement	Measurement			
	[Injured = 1]* [timepoint = 7]* [flashintensity mcd = 10]	[Injured = 1]* [timepoint = 7]* [flashintensity mcd = 3000]	[Injured = 1]* [timepoint = 7]* [flashintensity mcd = 10000]	[Injured = 1]* [timepoint = 14]* [flashintensity mcd = 10]
[Injured = 0]* [timepoint = 2]* [flashintensitymcd = 10]	.000	.000	.000	.000
[Injured = 0]* [timepoint = 2]* [flashintensitymcd = 3000]	.000	.000	.000	.000
[Injured = 0]* [timepoint = 2]* [flashintensitymcd = 10000]	.000	.000	.000	.000
[Injured = 0]* [timepoint = 7]* [flashintensitymcd = 10]	.000	.000	.000	.000
[Injured = 0]* [timepoint = 7]* [flashintensitymcd = 3000]	.000	.000	.000	.000
[Injured = 0]* [timepoint = 7]* [flashintensitymcd = 10000]	.000	.000	.000	.000
[Injured = 0]* [timepoint = 14]* [flashintensitymcd = 10]	.000	.000	.000	.000
[Injured = 0]* [timepoint = 14]* [flashintensitymcd = 3000]	.000	.000	.000	.000
[Injured = 0]* [timepoint = 14]* [flashintensitymcd = 10000]	.000	.000	.000	.000
[Injured = 1]* [timepoint = 2]* [flashintensitymcd = 10]	.000	.000	.000	.000
[Injured = 1]* [timepoint = 2]* [flashintensitymcd = 3000]	.001	.000	.000	.000
[Injured = 1]* [timepoint = 2]* [flashintensitymcd = 10000]	.024	.001	.000	.000
[Injured = 1]* [timepoint = 7]* [flashintensitymcd = 10]	1.000	.024	.001	.000
[Injured = 1]* [timepoint = 7]* [flashintensitymcd = 3000]	.024	1.000	.024	.001

Working Correlation Matrix[a]

Measurement	Measurement	
	[Injured = 1]* [timepoint = 14]* [flashintensity mcd = 3000]	[Injured = 1]* [timepoint = 14]* [flashintensity mcd = 10000]
[Injured = 0]* [timepoint = 2]* [flashintensitymcd = 10]	.000	.000
[Injured = 0]* [timepoint = 2]* [flashintensitymcd = 3000]	.000	.000
[Injured = 0]* [timepoint = 2]* [flashintensitymcd = 10000]	.000	.000
[Injured = 0]* [timepoint = 7]* [flashintensitymcd = 10]	.000	.000
[Injured = 0]* [timepoint = 7]* [flashintensitymcd = 3000]	.000	.000
[Injured = 0]* [timepoint = 7]* [flashintensitymcd = 10000]	.000	.000
[Injured = 0]* [timepoint = 14]* [flashintensitymcd = 10]	.000	.000
[Injured = 0]* [timepoint = 14]* [flashintensitymcd = 3000]	.000	.000
[Injured = 0]* [timepoint = 14]* [flashintensitymcd = 10000]	.000	.000
[Injured = 1]* [timepoint = 2]* [flashintensitymcd = 10]	.000	.000
[Injured = 1]* [timepoint = 2]* [flashintensitymcd = 3000]	.000	.000
[Injured = 1]* [timepoint = 2]* [flashintensitymcd = 10000]	.000	.000
[Injured = 1]* [timepoint = 7]* [flashintensitymcd = 10]	.000	.000
[Injured = 1]* [timepoint = 7]* [flashintensitymcd = 3000]	.000	.000

Working Correlation Matrix[a]

Measurement	Measurement			
	[Injured = 0]* [timepoint = 2]* [flashintensity mcd = 10]	[Injured = 0]* [timepoint = 2]* [flashintensity mcd = 3000]	[Injured = 0]* [timepoint = 2]* [flashintensity mcd = 10000]	[Injured = 0]* [timepoint = 7]* [flashintensity mcd = 10]
[Injured = 1]* [timepoint = 7]* [flashintensitymcd = 10000]	.000	.000	.000	.000
[Injured = 1]* [timepoint = 14]* [flashintensitymcd = 10]	.000	.000	.000	.000
[Injured = 1]* [timepoint = 14]* [flashintensitymcd = 3000]	.000	.000	.000	.000
[Injured = 1]* [timepoint = 14]* [flashintensitymcd = 10000]	.000	.000	.000	.000

Working Correlation Matrix[a]

Measurement	Measurement			
	[Injured = 0]* [timepoint = 7]* [flashintensity mcd = 3000]	[Injured = 0]* [timepoint = 7]* [flashintensity mcd = 10000]	[Injured = 0]* [timepoint = 14]* [flashintensity mcd = 10]	[Injured = 0]* [timepoint = 14]* [flashintensity mcd = 3000]
[Injured = 1]* [timepoint = 7]* [flashintensitymcd = 10000]	.000	.000	.000	.000
[Injured = 1]* [timepoint = 14]* [flashintensitymcd = 10]	.000	.000	.000	.000
[Injured = 1]* [timepoint = 14]* [flashintensitymcd = 3000]	.000	.000	.000	.000
[Injured = 1]* [timepoint = 14]* [flashintensitymcd = 10000]	.000	.000	.000	.000

Working Correlation Matrix[a]

Measurement	Measurement			
	[Injured = 0]* [timepoint = 14]* [flashintensity mcd = 10000]	[Injured = 1]* [timepoint = 2]* [flashintensity mcd = 10]	[Injured = 1]* [timepoint = 2]* [flashintensity mcd = 3000]	[Injured = 1]* [timepoint = 2]* [flashintensity mcd = 10000]
[Injured = 1]* [timepoint = 7]* [flashintensitymcd = 10000]	.000	.000	.000	.000
[Injured = 1]* [timepoint = 14]* [flashintensitymcd = 10]	.000	.000	.000	.000
[Injured = 1]* [timepoint = 14]* [flashintensitymcd = 3000]	.000	.000	.000	.000
[Injured = 1]* [timepoint = 14]* [flashintensitymcd = 10000]	.000	.000	.000	.000

Working Correlation Matrix[a]

Measurement	Measurement			
	[Injured = 1]* [timepoint = 7]* [flashintensity mcd = 10]	[Injured = 1]* [timepoint = 7]* [flashintensity mcd = 3000]	[Injured = 1]* [timepoint = 7]* [flashintensity mcd = 10000]	[Injured = 1]* [timepoint = 14]* [flashintensity mcd = 10]
[Injured = 1]* [timepoint = 7]* [flashintensitymcd = 10000]	.001	.024	1.000	.024
[Injured = 1]* [timepoint = 14]* [flashintensitymcd = 10]	.000	.001	.024	1.000
[Injured = 1]* [timepoint = 14]* [flashintensitymcd = 3000]	.000	.000	.001	.024
[Injured = 1]* [timepoint = 14]* [flashintensitymcd = 10000]	.000	.000	.000	.001

Working Correlation Matrix[a]

Measurement	Measurement	
	[Injured = 1]* [timepoint = 14]* [flashintensity mcd = 3000]	[Injured = 1]* [timepoint = 14]* [flashintensity mcd = 10000]
[Injured = 1]* [timepoint = 7]* [flashintensitymcd = 10000]	.001	.000
[Injured = 1]* [timepoint = 14]* [flashintensitymcd = 10]	.024	.001
[Injured = 1]* [timepoint = 14]* [flashintensitymcd = 3000]	1.000	.024
[Injured = 1]* [timepoint = 14]* [flashintensitymcd = 10000]	.024	1.000

Dependent Variable: V12
Model: (Intercept), timepoint, flashintensitymcd, timepoint * flashintensitymcd

a. The AR(1) working correlation matrix structure is computed assuming the measurements are equally spaced for all subjects.

Estimated Marginal Means: timepoint* flashintensitymcd* Injured

Estimates

timepoint	flashintensitymcd	Injured	Mean	Std. Error	95% Wald Confidence Interval	
					Lower	Upper
2	10	1	48.48	26.805	16.40	143.28
		0	48.48	26.805	16.40	143.28
	3000	1	3.08	.729	1.93	4.89
		0	3.08	.729	1.93	4.89
	10000	1	2.17	.366	1.56	3.02
		0	2.17	.366	1.56	3.02
7	10	1	650.44	293.415	268.68	1574.66
		0	650.44	293.415	268.68	1574.66
	3000	1	2.24	.173	1.93	2.61
		0	2.24	.173	1.93	2.61
	10000	1	1.97	.125	1.74	2.23
		0	1.97	.125	1.74	2.23
14	10	1	360.69	259.935	87.84	1481.02
		0	360.69	259.935	87.84	1481.02
	3000	1	2.06	.125	1.83	2.32
		0	2.06	.125	1.83	2.32
	10000	1	2.06	.193	1.71	2.47
		0	2.06	.193	1.71	2.47

APPENDIX 10

```
 DATASET ACTIVATE DataSet2.

GET DATA
  /TYPE=XLS
  /FILE='C:\Users\Public\Documents\PhD\ERG\Results\T-CEM423-6\photopic b wave amplitude for
  /SHEET=name 'Sheet1'
  /CELLRANGE=full
  /READNAMES=on
  /ASSUMEDSTRWIDTH=32767.

>Error.  Command name: GET DATA
>(2054) The file is not in a recognized Excel file format.
>* File: "C:\Users\Public\Documents\PhD\ERG\Results\T-CEM423-6\photopic b wave amplitude for
>Execution of this command stops.
EXECUTE.

>Error # 105.  Command name: EXECUTE
>This command is not valid before a working file has been defined.
>Execution of this command stops.
DATASET NAME DataSet7 WINDOW=FRONT.
DATASET ACTIVATE DataSet2.
DATASET CLOSE DataSet7.

GET DATA
  /TYPE=XLS
  /FILE='C:\Users\Public\Documents\PhD\ERG\Results\T-CEM423-6\photopic b wave amplitude for
  /SHEET=name 'Sheet1'
  /CELLRANGE=full
  /READNAMES=on
  /ASSUMEDSTRWIDTH=32767.
EXECUTE.
DATASET NAME DataSet8 WINDOW=FRONT.
* Generalized Estimating Equations.
GENLIN bwaveamplitudevdependentvariable BY Injured timepoint flashintensity (ORDER=ASCENDIN
  /MODEL Injured timepoint flashintensity Injured*timepoint Injured*flashintensity timepoint
 DISTRIBUTION=GAMMA LINK=LOG
  /CRITERIA METHOD=FISHER(1) SCALE=MLE MAXITERATIONS=100 MAXSTEPHALVING=5 PCONVERGE=1E-006(A
(WALD) CILEVEL=95 LIKELIHOOD=FULL
  /EMMEANS TABLES=Injured*timepoint*flashintensity SCALE=ORIGINAL
  /REPEATED SUBJECT=animal WITHINSUBJECT=Injured*timepoint*flashintensity SORT=YES CORRTYPE=
(1) ADJUSTCORR=YES COVB=ROBUST MAXITERATIONS=100 PCONVERGE=1e-006(ABSOLUTE) UPDATECORR=1
  /MISSING CLASSMISSING=EXCLUDE
  /PRINT CPS DESCRIPTIVES MODELINFO FIT SUMMARY WORKINGCORR.
```

Generalized Linear Models

Notes

Output Created		02-MAY-2013 09:55:19
Comments		
Input	Active Dataset	DataSet8
	Filter	<none>
	Weight	<none>
	Split File	<none>
	N of Rows in Working Data File	96
Missing Value Handling	Definition of Missing	User-defined missing values for factor, subject and within-subject variables are treated as missing.
	Cases Used	Statistics are based on cases with valid data for all variables in the model.
Weight Handling		not applicable
Syntax		GENLIN bwaveamplitudevdependentvariable BY Injured timepoint flashintensity (ORDER=ASCENDING) /MODEL Injured timepoint flashintensity Injured*timepoint Injured*flashintensity timepoint*flashintensity Injured*timepoint*flashintensity INTERCEPT=YES DISTRIBUTION=GAMMA LINK=LOG /CRITERIA METHOD=FISHER(1) SCALE=MLE MAXITERATIONS=100 MAXSTEPHALVING=5 PCONVERGE=1E-006(ABSOLUTE) SINGULAR=1E-012 ANALYSISTYPE=3(WALD) CILEVEL=95 LIKELIHOOD=FULL /EMMEANS TABLES=Injured*timepoint*flashintensity SCALE=ORIGINAL /REPEATED SUBJECT=animal WITHINSUBJECT=Injured*timepoint*flashintensity SORT=YES CORRTYPE=AR(1) ADJUSTCORR=YES COVB=ROBUST MAXITERATIONS=100 PCONVERGE=1e-006(ABSOLUTE) UPDATECORR=1 /MISSING CLASSMISSING=EXCLUDE /PRINT CPS DESCRIPTIVES...
Resources	Processor Time	00:00:00.05
	Elapsed Time	00:00:00.13

[DataSet8]

Model Information

Dependent Variable		b wave amplitude (v; dependent variable)
Probability Distribution		Gamma
Link Function		Log
Subject Effect	1	animal
Within-Subject Effect	1	injury condition (1=injured, 2=control)
	2	time point (days)
	3	stimulus intensity (mcd)
Working Correlation Matrix Structure		AR(1)

Case Processing Summary

	N	Percent
Included	83	86.5%
Excluded	13	13.5%
Total	96	100.0%

Correlated Data Summary

Number of Levels	Subject Effect	animal	8
	Within-Subject Effect	injury condition (1=injured, 2=control)	2
		time point (days)	3
		stimulus intensity (mcd)	2
Number of Subjects			8
Number of Measurements per Subject	Minimum		4
	Maximum		12
Correlation Matrix Dimension			12

Categorical Variable Information

			N	Percent
Factor	injury condition (1=injured, 2=control)	1	39	47.0%
		2	44	53.0%
		Total	83	100.0%
	time point (days)	2	27	32.5%
		7	32	38.6%
		14	24	28.9%
		Total	83	100.0%
	stimulus intensity (mcd)	3000	42	50.6%
		10000	41	49.4%
		Total	83	100.0%

Continuous Variable Information

		N	Minimum	Maximum	Mean
Dependent Variable	b wave amplitude (v; dependent variable)	83	11	357	101.93

Continuous Variable Information

		Std. Deviation
Dependent Variable	b wave amplitude (v; dependent variable)	75.874

Goodness of Fit[a]

	Value
Quasi Likelihood under Independence Model Criterion (QIC)[b]	40.328
Corrected Quasi Likelihood under Independence Model Criterion (QICC)[b]	41.070

Dependent Variable: b wave amplitude (v; dependent variable)
Model: (Intercept), Injured, timepoint, flashintensity, Injured * timepoint, Injured * flashintensity, timepoint * flashintensity, Injured * timepoint * flashintensity

a. Information criteria are in small-is-better form.

b. Computed using the full log quasi-likelihood function.

Tests of Model Effects

	Type III		
Source	Wald Chi-Square	df	Sig.
(Intercept)	4275.570	1	.000
Injured	56.740	1	.000
timepoint	5.751	2	.056
flashintensity	41.645	1	.000
Injured * timepoint	1.512	2	.470
Injured * flashintensity	5.074	1	.024
timepoint * flashintensity	1.340	2	.512
Injured * timepoint * flashintensity	21.273	2	.000

Dependent Variable: b wave amplitude (v; dependent variable)
Model: (Intercept), Injured, timepoint, flashintensity, Injured * timepoint, Injured * flashintensity, timepoint * flashintensity, Injured * timepoint * flashintensity

Working Correlation Matrix[a]

Measurement	Measurement			
	[Injured = 1]* [timepoint = 2]* [flashintensity = 3000]	[Injured = 1]* [timepoint = 2]* [flashintensity = 10000]	[Injured = 1]* [timepoint = 7]* [flashintensity = 3000]	[Injured = 1]* [timepoint = 7]* [flashintensity = 10000]
[Injured = 1]* [timepoint = 2]* [flashintensity = 3000]	1.000	.692	.479	.332
[Injured = 1]* [timepoint = 2]* [flashintensity = 10000]	.692	1.000	.692	.479
[Injured = 1]* [timepoint = 7]* [flashintensity = 3000]	.479	.692	1.000	.692
[Injured = 1]* [timepoint = 7]* [flashintensity = 10000]	.332	.479	.692	1.000
[Injured = 1]* [timepoint = 14]* [flashintensity = 3000]	.229	.332	.479	.692
[Injured = 1]* [timepoint = 14]* [flashintensity = 10000]	.159	.229	.332	.479
[Injured = 2]* [timepoint = 2]* [flashintensity = 3000]	.110	.159	.229	.332
[Injured = 2]* [timepoint = 2]* [flashintensity = 10000]	.076	.110	.159	.229
[Injured = 2]* [timepoint = 7]* [flashintensity = 3000]	.053	.076	.110	.159
[Injured = 2]* [timepoint = 7]* [flashintensity = 10000]	.036	.053	.076	.110
[Injured = 2]* [timepoint = 14]* [flashintensity = 3000]	.025	.036	.053	.076
[Injured = 2]* [timepoint = 14]* [flashintensity = 10000]	.017	.025	.036	.053

Working Correlation Matrix[a]

Measurement	Measurement			
	[Injured = 1]* [timepoint = 14]* [flashintensity = 3000]	[Injured = 1]* [timepoint = 14]* [flashintensity = 10000]	[Injured = 2]* [timepoint = 2]* [flashintensity = 3000]	[Injured = 2]* [timepoint = 2]* [flashintensity = 10000]
[Injured = 1]* [timepoint = 2]* [flashintensity = 3000]	.229	.159	.110	.076
[Injured = 1]* [timepoint = 2]* [flashintensity = 10000]	.332	.229	.159	.110
[Injured = 1]* [timepoint = 7]* [flashintensity = 3000]	.479	.332	.229	.159
[Injured = 1]* [timepoint = 7]* [flashintensity = 10000]	.692	.479	.332	.229
[Injured = 1]* [timepoint = 14]* [flashintensity = 3000]	1.000	.692	.479	.332
[Injured = 1]* [timepoint = 14]* [flashintensity = 10000]	.692	1.000	.692	.479
[Injured = 2]* [timepoint = 2]* [flashintensity = 3000]	.479	.692	1.000	.692
[Injured = 2]* [timepoint = 2]* [flashintensity = 10000]	.332	.479	.692	1.000
[Injured = 2]* [timepoint = 7]* [flashintensity = 3000]	.229	.332	.479	.692
[Injured = 2]* [timepoint = 7]* [flashintensity = 10000]	.159	.229	.332	.479
[Injured = 2]* [timepoint = 14]* [flashintensity = 3000]	.110	.159	.229	.332
[Injured = 2]* [timepoint = 14]* [flashintensity = 10000]	.076	.110	.159	.229

Working Correlation Matrix[a]

Measurement	Measurement			
	[Injured = 2]* [timepoint = 7]* [flashintensity = 3000]	[Injured = 2]* [timepoint = 7]* [flashintensity = 10000]	[Injured = 2]* [timepoint = 14]* [flashintensity = 3000]	[Injured = 2]* [timepoint = 14]* [flashintensity = 10000]
[Injured = 1]* [timepoint = 2]* [flashintensity = 3000]	.053	.036	.025	.017
[Injured = 1]* [timepoint = 2]* [flashintensity = 10000]	.076	.053	.036	.025
[Injured = 1]* [timepoint = 7]* [flashintensity = 3000]	.110	.076	.053	.036
[Injured = 1]* [timepoint = 7]* [flashintensity = 10000]	.159	.110	.076	.053
[Injured = 1]* [timepoint = 14]* [flashintensity = 3000]	.229	.159	.110	.076
[Injured = 1]* [timepoint = 14]* [flashintensity = 10000]	.332	.229	.159	.110
[Injured = 2]* [timepoint = 2]* [flashintensity = 3000]	.479	.332	.229	.159
[Injured = 2]* [timepoint = 2]* [flashintensity = 10000]	.692	.479	.332	.229
[Injured = 2]* [timepoint = 7]* [flashintensity = 3000]	1.000	.692	.479	.332
[Injured = 2]* [timepoint = 7]* [flashintensity = 10000]	.692	1.000	.692	.479
[Injured = 2]* [timepoint = 14]* [flashintensity = 3000]	.479	.692	1.000	.692
[Injured = 2]* [timepoint = 14]* [flashintensity = 10000]	.332	.479	.692	1.000

Dependent Variable: b wave amplitude (v; dependent variable)
Model: (Intercept), Injured, timepoint, flashintensity, Injured * timepoint, Injured * flashintensity, timepoint * flashintensity, Injured * timepoint * flashintensity

a. The AR(1) working correlation matrix structure is computed assuming the measurements are equally spaced for all subjects.

Estimated Marginal Means: injury condition (1=injured, 2=control)* t ime point (days)* stimulus intensity (mcd)

Estimates

injury condition (1=injured, 2=control)	time point (days)	stimulus intensity (mcd)	Mean	Std. Error
1	2	3000	32.16	5.436
		10000	37.75	7.032
	7	3000	32.58	5.254
		10000	53.99	6.421
	14	3000	53.48	14.235
		10000	74.82	15.520
2	2	3000	122.10	20.663
		10000	178.98	22.468
	7	3000	119.53	14.682
		10000	176.39	28.050
	14	3000	116.42	20.201
		10000	190.55	29.118

Estimates

injury condition (1=injured, 2=control)	time point (days)	stimulus intensity (mcd)	95% Wald ...
			Lower
1	2	3000	23.09
		10000	26.20
	7	3000	23.75
		10000	42.76
	14	3000	31.74
		10000	49.83
2	2	3000	87.63
		10000	139.94
	7	3000	93.95
		10000	129.15
	14	3000	82.86
		10000	141.23

Estimates

injury condition (1=injured, 2=control)	time point (days)	stimulus intensity (mcd)	95% Wald ... Upper
1	2	3000	44.79
		10000	54.38
	7	3000	44.69
		10000	68.16
	14	3000	90.10
		10000	112.35
2	2	3000	170.12
		10000	228.91
	7	3000	152.06
		10000	240.90
	14	3000	163.58
		10000	257.09

APPENDIX 11

Title: Caspase-9-Mediates Photoreceptor Apoptosis After Blunt Ocular Trauma

Authors: Maj Richard J Blanch BSc(Hons) MBChB(Hons) MRCS(Ed) RAMC[1,2]
Dr Zubair Ahmed BSc(Hons) PhD[1]
Dr Nsikan Akpan PhD[3]
Dr David RJ Snead FRCPath[4]
Prof Martin Berry MD DSc FRCPath[1]
Asst Prof Carol Troy MD PhD[3]
Prof Robert AH Scott MBBS FRCS(Ed) FRCOphth DM[2,5,6]
Prof Ann Logan BSc PhD[1,6]

1. Neurotrauma and Neurodegeneration Section, Clinical and Experimental Medicine, University of Birmingham, Birmingham, UK
2. Academic Department of Military Surgery and Trauma, Royal Centre for Defence Medicine, Birmingham, UK
3. Department of Pathology & Cell Biology, Columbia University, New York, NY, USA
4. University Hospitals Coventry and Warwickshire NHS Trust, Coventry
5. Birmingham and Midland Eye Centre, Birmingham, UK
6. Joint senior authors

Correspondence Address:
Richard Blanch
Molecular Neuroscience Research Group
IBR West (2nd Floor)
Medical School
University of Birmingham
Edgbaston
Birmingham
B15 2TT

Email: rjb017@bham.ac.uk

Tel: +44(7973)770061

Word Count: 4386 + figure legends and references

Funding: Ministry of Defence, UK

Drummond Foundation, UK

Sir Ian Fraser Foundation, Blind Veterans UK

Programmed cell death by apoptosis occurs in developing tissues, but in the mature animal, dysregulated apoptosis is induced after injury and the ensuing cell loss often causes permanent functional impairment[1]. Different cells exhibit differential biochemical and cellular responses to injury and multiple mechanisms of cell death may co-exist in the same tissue[1]. Cell death by apoptosis is mediated by initiator caspases belonging to either the intrinsic or extrinsic signalling pathways, both of which converge to activate the executioner caspases, 3, 6 and 7. Intracellular damage initiates the intrinsic pathway in which mitochondrial outer membrane permeabilisation (MOMP) causes the intermembrane spaces to release cytochrome c, which complexes with apoptosis activating factor-1 (apaf-1) forming an apoptosome. The apoptosome recruits and activates initiator caspase-9, which activates the executioner caspases. The extrinsic pathway is activated by cell surface "death receptor" ligation and activates caspase 8, which activates the executioner caspases[1].

Ocular trauma is common in military personnel and civilians, with a civilian lifetime prevalence of 20%[2,3]. The condition of commotio retinae is characterised by photoreceptor damage after blunt ocular trauma and has an incidence of 15% of military and 0.4% in civilian eye injuries [2,4], affecting the macula in 73% of military and 31% of civilian cases[2,5]. In cases of macular commotio, 26% of cases stabilise with a visual acuity <6/9 and persistent, visually debilitating, paracentral scotomas are common, with visual impairment caused by photoreceptor degeneration[5,6]. In animal models of commotio retinae, photoreceptors die by apoptosis and necrosis [7,8]. Thus, regulated apoptotic signalling mediates cell death in a proportion of photoreceptors, implying that antiapoptotic neuroprotective therapies have a potential role in the treatment of commotio retinae. In animal models of retinal detachment, for example, photoreceptor death is correlated with raised levels of caspase 3, 7 and 9 and detachment-induced photoreceptor death is partially reversed when the intrinsic pathway is inhibited by over-expression of an AAV-transduced X-linked inhibitor of apoptosis, inhibition of MOMP and heat shock protein (HSP70) down regulation of the mTOR pathway [9,10,11,12]. Extrinsic pathway inhibition by Fas receptor blockade, TNF-α blockade and TNF-α knockout [13,14] also protect photoreceptors, implicating both the intrinsic and extrinsic apoptotic pathways.

Inhibiting apoptosis by neuroprotective therapies improves structural and functional outcomes in pre-clinical studies of acute neuronal injury [1,15], and recent phase 2 clinical studies in traumatic brain injury have shown promising results[16]. In this report, using a rat model of commotio retinae[7], we demonstrate that the intrinsic apoptotic pathway predominantly mediates photoreceptor death and that inhibition of caspase-9 using X-linked inhibitor of apoptosis (IAP)-baculoviral IAP repeat 3 domain (XBIR3), a highly specific caspase-9 inhibitor linked to a cell transduction peptide Penetratin 1 (Pen1) [17] prevents photoreceptor death and preserves their function. In contrast, inhibition of caspase-6 activity using a dominant negative molecule (C6DN) linked to Pen1 was detrimental to photoreceptor function.

Results

Activated caspase-9 was present in photoreceptors after injury

We have previously demonstrated photoreceptor apoptosis after ballistic injury [Blanch,2012]. However, in the current experiments TUNEL+ cells were localised in the outer nuclear layer (ONL; Figure 1A-D) in sections of eyes assayed 2 days after ballistic injury, confirming photoreceptor apoptosis. Western blotting was performed to investigate the expression and processing of caspase-

9 in the retina. Compared to uninjured retinae, levels of cleaved caspase-9 were increased by 5 hours and decreased to basal levels by 24 hours after ballistic injury (Figure 2A-B; p=0.018, one way ANOVA). Levels of full length caspase-9 were upregulated by 48 hours after injury (Figure 1A-B; p<0.001, one way ANOVA). To determine whether caspase-9 was active after ballistic injury, we used the biotinylated caspase activity probe bVAD-fmk, a broad spectrum inhibitor which covalently binds active caspases. To capture initiator caspases, we injected bVAD-fmk intravitreally 2 hours before injury and harvested retinae at 5 hours, then used streptavidin-coated beads to pull out the biotinylated inhibitor-bound caspase. In this way, higher levels of active caspase-9 were isolated from injured than from uninjured retinae (Figure 2C-D; p=0.028, 2 sample t-test), indicating that the increased levels of cleaved caspase-9 seen by western blotting reflects active enzyme. To localise caspase-9 within the retina, we performed immunohistochemistry on the eyes of animals killed at 5 and 48 hours after injury. Compared to uninjured control retinae, caspase-9 levels were increased in photoreceptor inner segments of injured animals at 5 hours after injury (Figure 1E-F) and in photoreceptor cell bodies at 48 hours after injury (Figure 1G-J), indicating that cataytically active caspase-9 was present in photoreceptors 5 hours after injury, consistent with its function as an initiator and full length caspase-9 was upregulated in photoreceptors by 48 hours, correlating with photoreceptor apoptosis.

Caspase-9 inhibition induced structural neuroprotection

To determine the contribution of caspase-9 to photoreceptor death in commotio retinae, we treated animals with unilateral intravitreal injections of the highly specific caspase-9 inhibitor Pen1-XBIR3 after ballistic injury. Contralateral eyes received control injections of Pen1. Caspase-9 inhibition reduced photoreceptor death, demonstrated by preserved ONL thickness on retinal sections (Figure 3A-B). The effect of treatment on ONL thickness was modelled using generalised estimating equations showing: (1), a non-significant effect of caspase-9 inhibition across all distances from the impact site (p=0.29); (2), a highly significant effect of distance from the centre of the impact site, i.e. the outer nuclear layer was thinner towards the centre of the impact site (p<0.001), as we have previously reported[7]; (3), a significantly thicker ONL peripheral, but not central, to the impact site in caspase-9-suppressed than in Pen1-treated eyes (p=0.019 for the 2-way interaction distance*caspase-9 inhibition), demonstrating that caspase-9 mediates photoreceptor apoptosis after ballistic injury.

Caspase-9 inhibition induced functional neuroprotection

At 7 and 14 days after ballistic injury and unilateral intravitreal Pen1-XBIR3 injections, we recorded scotopic (dark-adapted) and photopic (light-adapted) electroretinograms (ERG) to assess rod and cone function respectively. The effect of treatment on scotopic a-wave amplitude was modelled using generalised estimating equations (Figure 3D) showing: (1), a borderline significant increase in a-wave amplitude after caspase-9 inhibition across all stimulus intensities and time points (p=0.059); (2), a positive effect of caspase-9 inhibition on a-wave amplitude that increases with stimulus intensity (p<0.001 for 2-way interaction caspase-9 inhibition*stimulus intensity); (3), a significant difference in the effect of caspase-9 inhibition between the 2 time points with a more pronounced positive effect (with smaller error bars) at 14 than at 7 days (p<0.001 for the 3-way interaction caspase-9 inhibition*stimulus intensity*time). In summary, compared to eyes injected with intravitreal Pen1 alone, caspase-9 inhibition improved rod and cone function, demonstrated by increased scotopic a-wave amplitude and photopic b-wave amplitude, and this benefit increased

with time after injury (Figure 3C-F). Photopic b-wave analysis showed similar effects (Figure 3E-F), indicating that caspase-9 mediates both rod and cone apoptosis after ballistic injury and its inhibition is functionally neuroprotective.

Assessment of executioner caspases in photoreceptors after injury

Caspase-9 is an initiator caspase, and as such usually activates downstream executioner caspases (such as caspase-3, -6, and -7) to bring about apoptosis[1]. Western blotting, immunohistochemistry and the bVAD pulldown assay were used to investigate which executioner caspases were cleaved and activated after ballistic injury. Retinal levels of the full length (p32) and cleaved (p17) caspase 3 were detectable by western blotting, but were unchanged over the 48 hours after injury (p=0.519, 0.536 respectively; one way ANOVA), whilst the p11 fragment was undetectable (Figure 4C-D). Cleaved caspase 3 was not detectable in the ONL by immunohistochemistry (data not shown). Similarly, western blots detected full length caspase 7 in the retina (p35) that remained unchanged in the 48 hours after injury (p=0.317; one way ANOVA), whilst the p20 cleaved fragment was not detectable (Figure 4E-F). Cleaved caspase 7 was also not detectable in the ONL by immunohistochemistry (data not shown). However, western blots showed that retinal levels of cleaved caspase-6 (p18), increased up to 48 hours after injury (p=0.009; one way ANOVA), but the levels of full length caspase-6 (p33-35) were not significantly altered (p=0.059; one way ANOVA) (Figure 4A-B). Cleaved caspase-6 was also immunolocalised in cones and rods at 48 hours after injury (Figure 2C-F showing all photoreceptors; Supplementary Figure 1 showing co-staining with cone-arrestin). To determine whether caspase-6 was active after ballistic injury, we injected bVAD-fmk intravitreally 43 hours after injury and killed animals 5 hours later, demonstrating active caspase-6 at 48 hours after injury (p=0.003, 2 sample t-test; Figure 4G-H). Thus the only active executioner caspase present in photoreceptors after ballistic injury is caspase-6 and therefore we hypothesised that caspase-6 executes the apoptotic programme in photoreceptors after initiation by caspase-9.

Inhibition of caspase-6 did not prevent photoreceptor death and was detrimental to photoreceptor function

To investigate whether caspase-6 mediates photoreceptor apoptosis, we treated animals with unilateral intravitreal injections of Pen1-C6DN after ballistic injury. Contralateral eyes received control injections of Pen1. The effect of caspase-6 inhibition on ONL thickness was modelled using generalised estimating equations and did not show any significant differences compared to control eyes in main effects or interaction terms (Figure 5A-B), indicating that caspase-6 inhibition did not reduce rod death after ballistic injury compared to Pen1-treated control eyes. The effect of caspase-6 inhibition on scotopic a-wave amplitude was modelled using generalised estimating equations (Figure 5D) and showed: (1), a non-significant effect of caspase-6 inhibition across all stimulus intensities and time-points (p=0.983); (2), a negative effect of caspase-6 inhibition on a-wave amplitude that increases with stimulus intensity (p<0.001 for the 2-way interaction caspase-6 inhibition*stimulus intensity); (3), a significant difference in the effect of caspase-6 inhibition between the 2 time points, with a greater negative effect at 7 than at 14 days (p<0.001 for the 3-way interaction caspase-6 inhibition*stimulus intensity*time). Surprisingly, caspase-6 inhibition reduced rod and cone photoreceptor function, demonstrated by reduced scotopic a- and photopic b-wave amplitude (Figure 5C-F). Photopic ERG assessment of cone function showed similar effects, with reduced b-wave amplitudes in eyes injected with Pen1-C6DN, but there was no significant difference in b wave amplitudes between those recorded at 7 compared to 14 days after injury (Figure 5E-F).

Discussion

To our knowledge, this is the first report elucidating the mechanisms of photoreceptor apoptosis after blunt ocular trauma and highlights a new therapeutic angle in the treatment of this condition. We demonstrate that rod and cone apoptosis after blunt ocular trauma occur through the intrinsic pathway, initiated by caspase-9. Despite the presence of catalytically active caspase-6 in rods and cones after injury, its inhibition using a highly specific inhibitor did not prevent photoreceptor apoptosis but instead was detrimental to retinal function. In contrast, active caspase trapping assays revealed that caspase-9 is an early mediator of photoreceptor death and its inhibition reduced photoreceptor death and preserved visual function in both rods and cones, inducing structural and functional neuroprotection that was sustained at 2 weeks post-injury.

VAD-fmk is a pan-caspase inhibitor that covalently binds and, in its biotinlyated form (bVAD-fmk), isolates caspases-1, -2, -3, -8 and -9 through interaction with immobilised streptavidin[18,19]. In this study, we used bVAD-fmk to isolate active caspase-9 within the first 5 hours after trauma, which is the first demonstration of catalytically active caspase-9 after eye injury. Caspase-6 was also isolated by this method 48 hours after ballistic injury, which is the first report of catalytically active caspase-6 isolation using bVAD-fmk. Activated caspase-6 levels detected by Western blotting and bVAD-fmk increased up to 48 hours after injury, but were near the lower limits of detection of the assays, suggesting that although caspase-6 is active after ballistic injury, it is present in only a small number of photoreceptors.

Use of peptide pharmacological inhibitors (like VAD-fmk) to study caspase activity is common. However, overlap in cleavage motifs means that these inhibitors are non-specific[20]. XBIR3 –the BIR3 domain of XIAP – is a highly specific inhibitor of caspase-9[21] and so the observed neuroprotective effects of caspase-9 inhibition were not XBIR3 off-target effects [22].

As 98% of rat photoreceptors are rods and the ONL contains exclusively photoreceptors, ONL thickness reflects rod survival[15]. Caspase-9 inhibition after blunt ocular trauma most affected ONL thickness peripheral to the impact site, where the highest proportion of apoptotic cells are found, as opposed to central to the impact site, where most cell death is necrotic and therefore less susceptible to modulation by altered caspase activity[7]. Consistent with the function of caspase-9 as an initiator caspase, the spike in retinal levels of activated caspase-9 was recorded 5 hours after injury and was followed by compensatory upregulation of full length caspase-9 by 48 hours. The western blotting, immunohistochemical and survival data therefore demonstrate unequivocally that caspase-9 initiates rod apoptosis after commotio retinae caused by blunt ocular trauma.

The a-wave is the first negative deflection on the ERG, caused by photoreceptor hyperpolarisation, and its amplitude is routinely measured to assess photoreceptor function. Commotio retinae reduces photoreceptor function (demonstrated by reduced a-wave amplitude) out of proportion to the extent of photoreceptor death[7]. Scotopic a-wave amplitude in rats reflects rod function and was increased by caspase-9 inhibition, indicating that the increased survival seen on ONL thickness measurements was accompanied by increased rod function.

Photopic ERG are recorded under conditions of light adaptation, which bleaches rod photoreceptors and ensures that the ERG response is cone-mediated. In rats, the photopic a-waves are small and often undetectable after injury[7]. The b-wave is the first positive deflection, immediately following the a-wave and is generated by the activity of second order neurons (such as ON bipolar cells in the

inner nuclear layer). The b-wave is therefore dependent on photoreceptor activation and synaptic transmission in addition to inner retinal function. In addition, the b-wave is measured from the base of the a-wave and thus incorporates both responses. The b- to a-wave ratio is a measure of how much of the variation in b-wave amplitude is due to variation in the magnitude of photoreceptor activation compared to the function of second order neurons. In rats, the b- to a-wave ratio is unaffected by commotio retinae[7], indicating that any variation in b-wave amplitude is due to variation in the magnitude of the photoreceptor response. The observed changes in photopic b-wave amplitude therefore reflect cone photoreceptor function, which was increased by caspase-9 inhibition, indicating that caspase-9 also initiates cone apoptosis after blunt ocular trauma.

The most commonly reported ultrastructural feature of acute commotio retinae is photoreceptor outer segment disruption[23,6]. In mild cases of commotio retinae there is visual recovery, correlated with outer segment regeneration over weeks to months[23,6]. The effect of caspase-9 inhibition on cone and rod function was greater at 14 than at 7 days, consistent with functional regeneration of damaged outer segments of photoreceptors rescued from apoptosis by caspase-9 inhibition.

Of the three executioner caspases (-3, -6 and -7), only caspase-6 activity was increased after ballistic injury. Caspase-6 was active in both rods and cones after injury, but does not seem to serve as an executioner in this model. Although caspase-6 inhibition did not affect ONL thickness compared to Pen1 injected control eyes, it did reduce both scotopic and photopic ERG amplitudes, indicating that caspase-6 inhibition is detrimental to retinal function after blunt ocular trauma. Caspase-6 has been implicated in cell death after ischaemic stroke[22], in axonal degeneration *in vitro* and after optic nerve crush[24,25], and in cleavage of microtubules and cytoskeletal proteins in Alzheimer's disease [26,27]. That ONL thickness was not affected, suggests that the observed functional effects do not relate to the role of caspase-6 in apoptosis. It may be that caspase-6's role in microtubule processing is required for photoreceptor outer segment survival or regeneration after commotio retinae.

In conclusion, we show that after ballistic ocular trauma, caspase-9 initiated photoreceptor apoptosis and caspase-9 inhibition reduced photoreceptor death with preservation of both rod and cone function. In contrast, though catalytically active caspase-6 was present in rods and cones after ballistic injury, cspase-6 inhibition did not reduce cell death and was detrimental to both rod and cone function.

Materials and Methods

Animal Care and Procedures

Animal procedures were licensed by the UK Home Office, approved by the University of Birmingham's Biomedical Ethics Review Sub-Committee and conducted in accordance with the ARVO Statement for the Use of Animals in Ophthalmic and Vision Research. Female Lister-hooded rats weighing 170-200g were purchased from Charles River Laboratories (Margate, UK), kept on a 12 hour light-dark cycle with a daytime luminance of 80 lux and fed and watered *ad libitum*. Surgery and ERG recording were performed under inhalation anaesthesia with 2.5% isofluorane in oxygen. Ballistic injury was induced as previously described[7]: a spherical 0.095g spherical plastic pellet was fired using compressed air to directly impact the inferior scleral surface at 20m/s.

Western Blotting

At 5, 24 and 48 hours post-ballistic injury and in uninjured controls, 3 rats were killed by overdose of anaesthetic, both retinae were removed, protein was extracted in lysis buffer (150mM NaCl, 20mM Tris, 1mM EDTA, 0.5mM EGTA, 1% NP-40, pH 7.4) supplemented with protease inhibitor cocktail (Sigma, Gillingham, UK) denatured by heating to 90°C for 5 minutes, separated on a tris-glycine gel with 80µg protein/lane and transferred to a Polyvinylidene fluoride membrane (Millipore, Watford, UK). After probing with primary and secondary antibodies, specific protein bands were detected using an enhanced chemiluminescence system (GE Healthcare, Little Chalfont, UK) membranes were read on a digital imaging system (ChemiDocTM MP System, Bio-Rad, Hemel Hempstead, UK) for short exposure times (<5 minutes) and exposed to photographic film when longer exposure times were required.

Caspase Pull-down Assay

To capture active caspases, 5µl of 1mM bVAD-fmk (MP Biomedicals, Cambridge, UK) in 10% DMSO/PBS was injected intravitreally into both eyes of 6 animals, 3 of which were bilaterally ballistically injured. To capture active caspase-9, injuries were induced 2 hours after injection and all animals were killed 5 hours after injury. To capture active caspase-6, injuries were induced 43 hours before injection and all animals were killed 5 hours after injection. Retinal protein was extracted in CHAPS lysis buffer (150mM KCl, 50mM HEPES, 0.1% CHAPS pH 8.5). Active caspase was extracted by incubation overnight at 4°C with 2mg of streptavidin-coated dynabeads (Invitrogen) and then prepared and run as for western blotting.

Immunohistochemistry and TUNEL

At 5 and 48 hours after unilateral ballistic injury, 4 rats in each group were killed by perfusion with 4% paraformaldehyde in phosphate buffered saline (PBS), both eyes were removed, cryoprotected in ascending concentrations of sucrose in phosphate buffered saline (PBS) at 4°C, the anterior segments removed and the retinal cup embedded in OCT and stored at -80°C until required. Sections were cut at 15µm thick using a cryostat (Bright Instruments, Huntingdon, UK) and adhered onto SuperfrostTM (Fisher, UK) coated glass microscope slides. The TUNEL FragEL™ DNA Fragmentation Detection Kit (Merck, Nottingham, UK) was used as per manufacturer's instructions, except that proteinase K permeabilisation was replaced by immersion in Triton-X 100 0.1% in PBS for 15 minutes.

Antibodies

The polyclonal primary antibodies used were against: activated caspase-6 to detect both the active (p18) and full length (p35) fragments by Western blotting (rabbit, New England Biolabs, Hitchin, UK) and the p18 fragment by immunohistochemistry (rabbit, New England Biolabs; goat, Santa Cruz Biotechnology, Dallas, TX, USA); activated caspase 7, to detect the full length (p35) and active (p20) fragments by Western blotting (rabbit, New England Biolabs); α-tubulin as a Western blotting loading control (rabbit,); caspase 3 (goat, Santa Cruz Biotechnology); caspase-9 to detect the full length (p60) and cleaved (p35-39) fragments by Western blotting (rabbit, New England Biolabs and immunohistochemistry (rabbit, Santa Cruz). Monoclonal ED1 (mouse, Serotec Kidlington, UK) was used to detect inflammatory cells. Secondary antibodies used were species-specific peroxidase-conjugated for Western blotting (GE Healthcare) and Alexa Fluor 488 or Texas red-conjugated for immunohistochemistry (Invitrogen, Paisley, UK).

Caspase Inhibition

Pen1-XBIR3 was prepared as previously described[28], and 5µl of 5µM solution was delivered by unilateral intravitreal injection to inhibit caspase-9 in 8 rats (n=8 eyes). Contralateral eyes were given control treatment with Pen1 (PolyPeptide Laboratories,Torrance, CA USA) alone. Caspase-6 (Cys163Ala) dominant negative (C6DN) construct was a gift from G. S. Salvesen, Sanford-Burnham Institute, La Jolla, CA and C6DN was purified as previously described[29]. Pen-1 and C6DN/XBIR3 were linked by incubating equimolar concentrations at 37°C for 24 hours and linkage was confirmed by nonreducing 20% PAGE with western blotting using anti-his antibodies. Pen1-C6DN was used to inhibit caspase-6 by 5µl of 5µM solution unilateral intravitreal injection to 8 rats, contralateral control eyes were treated with Pen1 alone. Validation of efficacy/specificity?

Electroretinography (ERG)

ERG were recorded (HMsERG – Ocuscience, Kansas City, MO USA) at 7 and 14 days after injury and interpreted using ERGView (Ocuscience). Animals were dark-adapted overnight and prepared for ERG under dim red light (>630nm). Scotopic flash ERG were recorded from -2.5 to +1 log units with respect to standard flash in half log unit steps and photopic flash ERG were recorded with background illumination of 30,000mcd/m2 over the same range. DTL fibre (Unimed Electrode Supplies, Farnham, UK) corneal electrodes with pressure-moulded Aclar (Agar scientific, Stansted, UK) contact lenses were used with needle skin electrodes (Unimed).

Assessment of Photoreceptor Survival

Animals were killed and eyes processed as for immunohistochemistry. Sections were cut through the optic disc and centre of the impact site and at 600, 1200 and 1800µm to either side of this plane. Haematoxyllin and eosin (H&E) stained slides were scanned on a MIrax slide scanner (Zeiss, Cambridge, UK) and the ONL manually segmented in Adobe Photoshop by a blinded observer. ONL images were thresholded and average thickness measured as area of above threshold pixels divided by section length using ImageJ (http://rsbweb.nih.gov/ij).

Statistics

All statistical analysis was performed in SPSS 21. One way ANOVA with Tukey *post-hoc* testing was used to analyse Western blotting results and 2 sample t-tests assuming equal variances were used to analyse pull down assays. ERG and ONL thickness data were analysed using generalised estimating equations (type III sum of squares; autoregressive correlation matrix; gamma distribution with log link) and model fit assessed by plotting residuals and calculating quasi-likelihood information criteria.

Figure Legends

Figure 1. Immunohistochemical staining of rat outer retinal layers after injury (DAPI-stained nuclei shown in blue, 50µm scale bar). **A-D**. TUNEL stained photoreceptor nuclei in green (arrowed) at 2 days after injury (A, blue and green channels in B-C, respectively), but not in uninjured control retina (D). **E-F**. Caspase-9 (arrows) in photoreceptor inner segments, seen between the DAPI stained outer nuclear layer (ONL) and the autofluorescent outer segments (OS) at 5 hours after injury (E), but not in uninjured control retina (F). **G-J**. Increased caspase-9 levels in photoreceptor cell bodies (arrows) at 2 days in injured (G, blue and green channels in H-I, respectively) but not uninjured control retina

(J). **K-N**. Activated caspase-6 (Cell Signalling, rabbit; arrow) in photoreceptor cell body (green) at 2 days after injury (K, blue and green channels in L-M, respectively), but not in uninjured control tissue (N). Inflammatory cells are stained red by ED1.

Figure 2. A-B. Retinal levels of full length (p60) and cleaved (p35-39) caspase-9 after ballistic injury assessed by western blotting showing increased p35-39 at 5 hours and increased p60 at 48 hours. (*p=0.018, **p<0.001) **C-D**. Increased retinal levels of catalytically active caspase-9 at 5 hours detected by bVAD-fmk pull-down. (*=0.028)

Figure 3. A. Outer nuclear layer (ONL) thickness as a function of distance from the impact site. **B**. Test of model effects after analysis of ONL thickness including treatment, distance from the impact site and a term to model their interaction. **C** Scotopic a-wave amplitude as a function of stimulus intensity. **D**. Test of model effects after analysis of scotopic a-wave amplitude including time after injury (timepointdays), stimulus intensity (flashintensitymcd), Pen1-XBIR3 compared to Pen1 alone (TreatedXBIR3vspen) and terms to model all 2 and 3 way interactions. **E**. Photopic b-wave amplitude as a function of stimulus intensity. **F**. Test of model effects after analysis of photopic b-wave amplitude including time after injury, stimulus intensity, treatment and terms to model all 2- and 3-way interactions. Caspase-9 inhibition by dominant negative protein increases scotopic a- and photopic b-wave amplitudes with an effect that is more pronounced at higher stimulus intensities and at 14 as opposed to 7 days after injury. Caspase-9 inhibition also increased ONL thickness peripheral but not central to the impact site.

Figure 4. A-B. Retinal levels of full length (p33-35) and cleaved (p18) caspase-6 after injury assessed by western blotting showing an increase in levels of p18 up to 48 hours. Note that the level of p18 falls near the lower limit of detection for this assay. (*=0.009) **C-D**. Retinal levels of full length (32kDA), and cleaved (p17) caspase 3 after injury were unchanged, the p11 fragment was not detected. **E-F**. Retinal levels of full length caspase 7 (p35) were unchanged after injury, the cleaved form (p20) was not detected. **G-H**. Increased retinal levels of catalytically active caspase-6 (p18) at 48 hours detected by bVAD-fmk pull-down. (*=0.003)

Figure 5. A. Outer nuclear layer (ONL) thickness as a function of distance from the impact site. **B**. Test of model effects after analysis of ONL thickness including treatment and distance from the impact site, with non-significant terms removed (before removal, p=0.345 for normalisedslidenumber*TreatedCasp6DNvspen and p=0.689 for TreatedCasp6DNvspen). **C.** Scotopic a-wave amplitude as a function of stimulus intensity. **D**. Test of model effects after analysis of scotopic a-wave amplitude including time after injury (timepointdays), stimulus intensity (flashintensitymcd), Pen1-C6DN compared to Pen1 alone (TreatedCasp6DNvspen) and terms to model all 2- and 3-way interactions. **E**. Photopic b-wave amplitude as a function of stimulus intensity. **F**. Test of model effects after analysis of photopic b-wave amplitude including time after injury, stimulus intensity, treatment and terms to model significant interactions only. Caspase-6 inhibition using Pen1-C6DN had no effect on ONL thickness, but reduced scotopic a- and photopic b-wave amplitudes with an effect that was more pronounced at higher stimulus intensities.

Supplementary Figure 1. Immunohistochemical staining of rat outer retina with DAPI-stained nuclei shown in blue, cone arrestin in red and activated caspase-6 (Santa Cruz, goat) in green. Scale bar is 50μm. **A**. 2 days after injury activated caspase-6 colocalised with cone arrestin and so was present in cones in the outer nuclear layer (ONL). **B-C.** Red and green channels of A. **D**. Uninjured control retina with cone arrestin staining cones green (example cell body arrowed), but no caspase-6

staining (red). **E-F**. Red and green channels of D.

Full length caspase 6 has multiple high molecular weight forms between 30 and 36 kDA [30]. The 2 bands seen for full-length caspase 6 on western blotting in the current study may reflect a suppressed, phosphorylated form with altered mobility, or deletion of the N-terminal pro-domain from aberrant processing [31,32].

References:

1. Galluzzi L, Blomgren K, Kroemer G. Mitochondrial membrane permeabilization in neuronal injury. Advances.in Experimental.Medicine &.Biology. 2009;10(7):481-94 LID - 10.1038/nrn.

2. Weichel ED, Colyer MH, Ludlow SE, et al. Combat ocular trauma visual outcomes during operations Iraqi and Enduring Freedom. Advances.in Experimental.Medicine &.Biology. 2008;115(12):2235-45.

3. Wong TY, Klein BE, Klein R. The prevalence and 5-year incidence of ocular trauma. The Beaver Dam Eye Study. Advances.in Experimental.Medicine &.Biology. 2000;107(12):2196.

4. Jones NP, Hayward JM, Khaw PT, et al. Function of an ophthalmic "accident and emergency" department: results of a six month survey. Advances.in Experimental.Medicine &.Biology. 1986;292(6514):188-90.

5. Blanch RJ, Good PA, Shah P, et al. Visual outcomes after blunt ocular trauma. http://dx.doi.org/10.1016/j.ophtha.2013.01.009. Advances.in Experimental.Medicine &.Biology. 2013.

6. Souza-Santos F, Lavinsky D, Moraes NS, et al. Spectral-domain optical coherence tomography in patients with commotio retinae. Advances.in Experimental.Medicine &.Biology. 2012;32:711-8.

7. Blanch RJ, Ahmed Z, Sik A, et al. Neuroretinal cell death in a murine model of closed globe injury; pathological and functional characterisation. Advances.in Experimental.Medicine &.Biology. 2012.

8. Sipperley JO, Quigley HA, Gass JD. Traumatic retinopathy in primates: the explanation of commotio retinae. Advances.in Experimental.Medicine &.Biology. 1978;96(12):2267.

9. Zadro-Lamoureux LA, Zacks DN, Baker AN, et al. XIAP effects on retinal detachment-induced photoreceptor apoptosis [corrected]. Advances.in Experimental.Medicine &.Biology. 2009;50(3):1448-53.

10. Kayama M, Nakazawa T, Thanos A, et al. Heat shock protein 70 (HSP70) is critical for the photoreceptor stress response after retinal detachment via modulating anti-apoptotic Akt kinase. Advances.in Experimental.Medicine &.Biology. 2011;178(3):1080-91.

11. Hisatomi T, Nakazawa T, Noda K, et al. HIV protease inhibitors provide neuroprotection through inhibition of mitochondrial apoptosis in mice. Advances.in Experimental.Medicine &.Biology. 2008;118(6):2025.

12. Zacks DN, Hanninen V, Pantcheva M, et al. Caspase activation in an experimental model of retinal detachment. Advances.in Experimental.Medicine &.Biology. 2003;44(3):1262-7.

13. Besirli CG, Chinskey ND, Zheng QD, Zacks DN. Inhibition of retinal detachment-induced apoptosis in photoreceptors by a small peptide inhibitor of the fas receptor. Advances.in Experimental.Medicine &.Biology. 2010;51(4):2177-84.

14. Nakazawa T, Kayama M, Ryu M, et al. Tumor necrosis factor-alpha mediates photoreceptor death in a rodent model of retinal detachment. Advances.in Experimental.Medicine &.Biology. 2011;52(3):1384-91.

15. Blanch RJ, Ahmed Z, Berry M, et al. Animal Models of Retinal Injury. Advances.in Experimental.Medicine &.Biology. 2012;53(6):2913-20.

16. Xiao G, Wei J, Yan W, et al. Improved outcomes from the administration of progesterone for patients with acute severe traumatic brain injury: a randomized controlled trial. Advances.in Experimental.Medicine &.Biology. 2008;12(2):R61 LID-10.1186/cc6887 [doi].

17. Eckelman BP, Salvesen GS, Scott FL. Human inhibitor of apoptosis proteins: why XIAP is the black sheep of the family. Advances.in Experimental.Medicine &.Biology. 2006;7(10):988-94.

18. Tu S, McStay GP, Boucher LM, et al. In situ trapping of activated initiator caspases reveals a role for caspase-2 in heat shock-induced apoptosis. Advances.in Experimental.Medicine &.Biology. 2006;8(1):72-7.

19. Moulin M, Arrigo AP. Caspases activation in hyperthermia-induced stimulation of TRAIL apoptosis. Advances.in Experimental.Medicine &.Biology. 2008;13(3):313-26 LID - 10.1007/s12.

20. McStay GP, Salvesen GS, Green DR. Overlapping cleavage motif selectivity of caspases: implications for analysis of apoptotic pathways. Advances.in Experimental.Medicine &.Biology. 2008;15(2):322-31.

21. Srinivasula SM, Hegde R, Saleh A, et al. A conserved XIAP-interaction motif in caspase-9 and Smac/DIABLO regulates caspase activity and apoptosis. Nature 2001;410(6824):112-6.

22. Akpan N, Serrano-Saiz E, Zacharia BE, et al. Intranasal delivery of caspase-9 inhibitor reduces caspase-6-dependent axon/neuron loss and improves neurological function after stroke. J Neurosci 2011;31(24):8894-904 LID - 10.1523/JN.

23. Blight R, Hart JC. Structural changes in the outer retinal layers following blunt mechanical non-perforating trauma to the globe: an experimental study. Br J Ophthalmol 1977;61(9):573.

24. Nikolaev A, McLaughlin T, O'Leary DD, Tessier-Lavigne M. APP binds DR6 to trigger axon pruning and neuron death via distinct caspases. Nature 2009;457(7232):981- LID - 10.1038/natu.

25. Monnier PP, D'Onofrio PM, Magharious M, et al. Involvement of caspase-6 and caspase-8 in neuronal apoptosis and the regenerative failure of injured retinal ganglion cells. J Neurosci 2011;31(29):10494-505.

26. Guo H, Albrecht S, Bourdeau M, et al. Active caspase-6 and caspase-6-cleaved tau in neuropil threads, neuritic plaques, and neurofibrillary tangles of Alzheimer's disease. Am J Pathol 2004;165(2):523-31.

27. Klaiman G, Petzke TL, Hammond J, Leblanc AC. Targets of caspase-6 activity in human neurons and Alzheimer disease. Mol Cell Proteomics 2008;7(8):1541-55 LID - 10.1074/mcp.

28. Sun C, Cai M, Meadows RP, et al. NMR structure and mutagenesis of the third Bir domain of the inhibitor of apoptosis protein XIAP. J Biol Chem 2000;275(43):33777-81.

29. Denault JB, Salvesen GS. Expression, purification, and characterization of caspases. Curr Protoc Protein Sci 2003;Chapter 21:Unit 21.13 LID-10.1002/0471140864.p.

30. Edgington LE, van Raam BJ, Verdoes M, et al. An optimized activity-based probe for the study of caspase-6 activation. Chem Biol 2012;19(3):340-52 LID - 10.1016/j.c.

31. Lee VM, Balin BJ, Otvos L, Jr., Trojanowski JQ. A68: a major subunit of paired helical filaments and derivatized forms of normal Tau. Science 1991;251(4994):675-8.

32. Velazquez-Delgado EM, Hardy JA. Phosphorylation regulates assembly of the caspase-6 substrate-binding groove. Structure 2012;20(4):742-51 LID - 10.1016/j.s.

APPENDIX 12

```
 DATASET ACTIVATE DataSet1.
* Generalized Estimating Equations.
GENLIN AvgONLthickness BY Treated1nottreated0 normalisedslidenumber (ORDEI
  /MODEL Treated1nottreated0 normalisedslidenumber Treated1nottreated0*noi
 DISTRIBUTION=GAMMA LINK=LOG
  /CRITERIA METHOD=FISHER(1) SCALE=MLE MAXITERATIONS=100 MAXSTEPHALVING=5
  /EMMEANS TABLES=Treated1nottreated0 SCALE=ORIGINAL
  /EMMEANS TABLES=normalisedslidenumber SCALE=ORIGINAL
  /EMMEANS TABLES=Treated1nottreated0*normalisedslidenumber SCALE=ORIGINAI
  /REPEATED SUBJECT=Animal WITHINSUBJECT=Treated1nottreated0*normalisedsli
  /MISSING CLASSMISSING=EXCLUDE
  /PRINT CPS DESCRIPTIVES MODELINFO FIT SUMMARY WORKINGCORR.
```

Generalized Linear Models

Notes

Output Created		26-JUL-2013 23:40:06
Comments		
Input	Active Dataset	DataSet1
	Filter	<none>
	Weight	<none>
	Split File	<none>
	N of Rows in Working Data File	112
Missing Value Handling	Definition of Missing	User-defined missing values for factor, subject and within-subject variables are treated as missing.
	Cases Used	Statistics are based on cases with valid data for all variables in the model.
Weight Handling		not applicable

Notes

Syntax		GENLIN AvgONLthickness BY Treated1nottreated0 normalisedslidenumber (ORDER=ASCENDING) /MODEL Treated1nottreated0 normalisedslidenumber Treated1nottreated0*normalisedslidenumber INTERCEPT=YES DISTRIBUTION=GAMMA LINK=LOG /CRITERIA METHOD=FISHER(1) SCALE=MLE MAXITERATIONS=100 MAXSTEPHALVING=5 PCONVERGE=1E-006 (ABSOLUTE) SINGULAR=1E-012 ANALYSISTYPE=3(WALD) CILEVEL=95 LIKELIHOOD=FULL /EMMEANS TABLES=Treated1nottreated0 SCALE=ORIGINAL /EMMEANS TABLES=normalisedslidenumber SCALE=ORIGINAL /EMMEANS TABLES=Treated1nottreated0*normalisedslidenumber SCALE=ORIGINAL /REPEATED SUBJECT=Animal WITHINSUBJECT=Treated1nottreated0*normalisedslidenumber SORT=YES CORRTYPE=AR(1) ADJUSTCORR=YES COVB=ROBUST MAXITERATIONS=100 PCONVERGE=1e-006 (ABSOLUTE) UPDATECORR=1 /MISSING CLASSMISSING=EXCLUDE /PRINT CPS DESCRIPTIVES MODELINFO FIT SUMMARY WORKINGCORR.
Resources	Processor Time	00:00:00.25
	Elapsed Time	00:00:00.27

[DataSet1]

Model Information

Dependent Variable		AvgONLthickness
Probability Distribution		Gamma
Link Function		Log
Subject Effect	1	Animal
Within-Subject Effect	1	Treated1nottreated0
	2	normalisedslidenumber
Working Correlation Matrix Structure		AR(1)

Case Processing Summary

	N	Percent
Included	110	98.2%
Excluded	2	1.8%
Total	112	100.0%

Correlated Data Summary

Number of Levels	Subject Effect	Animal	8
	Within-Subject Effect	Treated1nottreated0	2
		normalisedslidenumber	7
Number of Subjects			8
Number of Measurements per Subject	Minimum		13
	Maximum		14
Correlation Matrix Dimension			14

Categorical Variable Information

			N	Percent
Factor	Treated1nottreated0	.0	54	49.1%
		1.0	56	50.9%
		Total	110	100.0%
	normalisedslidenumber	1.0	14	12.7%
		2.0	16	14.5%
		3.0	16	14.5%
		4.0	16	14.5%
		5.0	16	14.5%
		6.0	16	14.5%
		7.0	16	14.5%
		Total	110	100.0%

Continuous Variable Information

		N	Minimum	Maximum	Mean
Dependent Variable	AvgONLthickness	110	24.50923623	134.3101555	51.94469764

Continuous Variable Information

		Std. Deviation
Dependent Variable	AvgONLthickness	17.82410798

Goodness of Fit[a]

	Value
Quasi Likelihood under Independence Model Criterion (QIC)[b]	34.977
Corrected Quasi Likelihood under Independence Model Criterion (QICC)[b]	35.937

Dependent Variable: AvgONLthickness
Model: (Intercept), Treated1nottreated0, normalisedslidenumber, Treated1nottreated0 * normalisedslidenumber

a. Information criteria are in small-is-better form.

b. Computed using the full log quasi-likelihood function.

Tests of Model Effects

Source	Type III		
	Wald Chi-Square	df	Sig.
(Intercept)	6286.697	1	.000
Treated1nottreated0	1.121	1	.290
normalisedslidenumber	81.447	6	.000
Treated1nottreated0 * normalisedslidenumber	15.115	6	.019

Dependent Variable: AvgONLthickness
Model: (Intercept), Treated1nottreated0, normalisedslidenumber, Treated1nottreated0 * normalisedslidenumber

Working Correlation Matrix[a]

Measurement	Measurement			
	[Treated1nottreated0 = .0]* [normalisedslidenumber = 1.0]	[Treated1nottreated0 = .0]* [normalisedslidenumber = 2.0]	[Treated1nottreated0 = .0]* [normalisedslidenumber = 3.0]	[Treated1nottreated0 = .0]* [normalisedslidenumber = 4.0]
[Treated1nottreated0 = .0]* [normalisedslidenumber = 1.0]	1.000	.692	.479	.332
[Treated1nottreated0 = .0]* [normalisedslidenumber = 2.0]	.692	1.000	.692	.479
[Treated1nottreated0 = .0]* [normalisedslidenumber = 3.0]	.479	.692	1.000	.692
[Treated1nottreated0 = .0]* [normalisedslidenumber = 4.0]	.332	.479	.692	1.000
[Treated1nottreated0 = .0]* [normalisedslidenumber = 5.0]	.230	.332	.479	.692
[Treated1nottreated0 = .0]* [normalisedslidenumber = 6.0]	.159	.230	.332	.479
[Treated1nottreated0 = .0]* [normalisedslidenumber = 7.0]	.110	.159	.230	.332
[Treated1nottreated0 = 1.0]* [normalisedslidenumber = 1.0]	.076	.110	.159	.230
[Treated1nottreated0 = 1.0]* [normalisedslidenumber = 2.0]	.053	.076	.110	.159
[Treated1nottreated0 = 1.0]* [normalisedslidenumber = 3.0]	.036	.053	.076	.110

Working Correlation Matrix[a]

Measurement	Measurement			
	[Treated1nottreated0 = .0]* [normalisedslidenumber = 5.0]	[Treated1nottreated0 = .0]* [normalisedslidenumber = 6.0]	[Treated1nottreated0 = .0]* [normalisedslidenumber = 7.0]	[Treated1nottreated0 = 1.0] * [normalisedslidenumber = 1.0]
[Treated1nottreated0 = .0]* [normalisedslidenumber = 1.0]	.230	.159	.110	.076
[Treated1nottreated0 = .0]* [normalisedslidenumber = 2.0]	.332	.230	.159	.110
[Treated1nottreated0 = .0]* [normalisedslidenumber = 3.0]	.479	.332	.230	.159
[Treated1nottreated0 = .0]* [normalisedslidenumber = 4.0]	.692	.479	.332	.230
[Treated1nottreated0 = .0]* [normalisedslidenumber = 5.0]	1.000	.692	.479	.332
[Treated1nottreated0 = .0]* [normalisedslidenumber = 6.0]	.692	1.000	.692	.479
[Treated1nottreated0 = .0]* [normalisedslidenumber = 7.0]	.479	.692	1.000	.692
[Treated1nottreated0 = 1.0]* [normalisedslidenumber = 1.0]	.332	.479	.692	1.000
[Treated1nottreated0 = 1.0]* [normalisedslidenumber = 2.0]	.230	.332	.479	.692
[Treated1nottreated0 = 1.0]* [normalisedslidenumber = 3.0]	.159	.230	.332	.479

Working Correlation Matrix[a]

Measurement	Measurement			
	[Treated1nottreated0 = 1.0] * [normalisedslidenumber = 2.0]	[Treated1nottreated0 = 1.0] * [normalisedslidenumber = 3.0]	[Treated1nottreated0 = 1.0] * [normalisedslidenumber = 4.0]	[Treated1nottreated0 = 1.0] * [normalisedslidenumber = 5.0]
[Treated1nottreated0 = .0]* [normalisedslidenumber = 1.0]	.053	.036	.025	.017
[Treated1nottreated0 = .0]* [normalisedslidenumber = 2.0]	.076	.053	.036	.025
[Treated1nottreated0 = .0]* [normalisedslidenumber = 3.0]	.110	.076	.053	.036
[Treated1nottreated0 = .0]* [normalisedslidenumber = 4.0]	.159	.110	.076	.053
[Treated1nottreated0 = .0]* [normalisedslidenumber = 5.0]	.230	.159	.110	.076
[Treated1nottreated0 = .0]* [normalisedslidenumber = 6.0]	.332	.230	.159	.110
[Treated1nottreated0 = .0]* [normalisedslidenumber = 7.0]	.479	.332	.230	.159
[Treated1nottreated0 = 1.0]* [normalisedslidenumber = 1.0]	.692	.479	.332	.230
[Treated1nottreated0 = 1.0]* [normalisedslidenumber = 2.0]	1.000	.692	.479	.332
[Treated1nottreated0 = 1.0]* [normalisedslidenumber = 3.0]	.692	1.000	.692	.479

Working Correlation Matrix[a]

Measurement	Measurement	
	[Treated1nottreated0 = 1.0] * [normalisedslidenumber = 6.0]	[Treated1nottreated0 = 1.0] * [normalisedslidenumber = 7.0]
[Treated1nottreated0 = .0]* [normalisedslidenumber = 1.0]	.012	.008
[Treated1nottreated0 = .0]* [normalisedslidenumber = 2.0]	.017	.012
[Treated1nottreated0 = .0]* [normalisedslidenumber = 3.0]	.025	.017
[Treated1nottreated0 = .0]* [normalisedslidenumber = 4.0]	.036	.025
[Treated1nottreated0 = .0]* [normalisedslidenumber = 5.0]	.053	.036
[Treated1nottreated0 = .0]* [normalisedslidenumber = 6.0]	.076	.053
[Treated1nottreated0 = .0]* [normalisedslidenumber = 7.0]	.110	.076
[Treated1nottreated0 = 1.0]* [normalisedslidenumber = 1.0]	.159	.110
[Treated1nottreated0 = 1.0]* [normalisedslidenumber = 2.0]	.230	.159
[Treated1nottreated0 = 1.0]* [normalisedslidenumber = 3.0]	.332	.230

Working Correlation Matrix[a]

Measurement	Measurement			
	[Treated1nottreated0 = .0]* [normalisedslidenumber = 1.0]	[Treated1nottreated0 = .0]* [normalisedslidenumber = 2.0]	[Treated1nottreated0 = .0]* [normalisedslidenumber = 3.0]	[Treated1nottreated0 = .0]* [normalisedslidenumber = 4.0]
[Treated1nottreated0 = 1.0]* [normalisedslidenumber = 4.0]	.025	.036	.053	.076
[Treated1nottreated0 = 1.0]* [normalisedslidenumber = 5.0]	.017	.025	.036	.053
[Treated1nottreated0 = 1.0]* [normalisedslidenumber = 6.0]	.012	.017	.025	.036
[Treated1nottreated0 = 1.0]* [normalisedslidenumber = 7.0]	.008	.012	.017	.025

Working Correlation Matrix[a]

Measurement	Measurement			
	[Treated1nottreated0 = .0]* [normalisedslidenumber = 5.0]	[Treated1nottreated0 = .0]* [normalisedslidenumber = 6.0]	[Treated1nottreated0 = .0]* [normalisedslidenumber = 7.0]	[Treated1nottreated0 = 1.0] * [normalisedslidenumber = 1.0]
[Treated1nottreated0 = 1.0]* [normalisedslidenumber = 4.0]	.110	.159	.230	.332
[Treated1nottreated0 = 1.0]* [normalisedslidenumber = 5.0]	.076	.110	.159	.230
[Treated1nottreated0 = 1.0]* [normalisedslidenumber = 6.0]	.053	.076	.110	.159
[Treated1nottreated0 = 1.0]* [normalisedslidenumber = 7.0]	.036	.053	.076	.110

Working Correlation Matrix[a]

Measurement	Measurement			
	[Treated1nottreated0 = 1.0] * [normalisedslidenumber = 2.0]	[Treated1nottreated0 = 1.0] * [normalisedslidenumber = 3.0]	[Treated1nottreated0 = 1.0] * [normalisedslidenumber = 4.0]	[Treated1nottreated0 = 1.0] * [normalisedslidenumber = 5.0]
[Treated1nottreated0 = 1.0]* [normalisedslidenumber = 4.0]	.479	.692	1.000	.692
[Treated1nottreated0 = 1.0]* [normalisedslidenumber = 5.0]	.332	.479	.692	1.000
[Treated1nottreated0 = 1.0]* [normalisedslidenumber = 6.0]	.230	.332	.479	.692
[Treated1nottreated0 = 1.0]* [normalisedslidenumber = 7.0]	.159	.230	.332	.479

Working Correlation Matrix[a]

Measurement	Measurement	
	[Treated1nottreated0 = 1.0] * [normalisedslidenumber = 6.0]	[Treated1nottreated0 = 1.0] * [normalisedslidenumber = 7.0]
[Treated1nottreated0 = 1.0]* [normalisedslidenumber = 4.0]	.479	.332
[Treated1nottreated0 = 1.0]* [normalisedslidenumber = 5.0]	.692	.479
[Treated1nottreated0 = 1.0]* [normalisedslidenumber = 6.0]	1.000	.692
[Treated1nottreated0 = 1.0]* [normalisedslidenumber = 7.0]	.692	1.000

Dependent Variable: AvgONLthickness
Model: (Intercept), Treated1nottreated0, normalisedslidenumber, Treated1nottreated0 * normalisedslidenumber

a. The AR(1) working correlation matrix structure is computed assuming the measurements are equally spaced for all subjects.

Estimated Marginal Means 1: Treated1nottreated0

Estimates

Treated1nottreated0	Mean	Std. Error	95% Wald Confidence Interval	
			Lower	Upper
.0	48.84507977	3.219693032	42.92523294	55.58133654
1.0	53.84267315	3.737703466	46.99342192	61.69019691

Estimated Marginal Means 2: normalisedslidenumber

Estimates

normalisedslidenumber	Mean	Std. Error	95% Wald Confidence Interval	
			Lower	Upper
1.0	71.51399022	5.624644645	61.29755958	83.43318777
2.0	58.71404010	2.865181543	53.35857860	64.60701532
3.0	47.08120376	3.025788110	41.50907161	53.40133281
4.0	42.95773618	3.038166234	37.39732571	49.34489465
5.0	45.53504641	4.132473989	38.11501484	54.39957089
6.0	45.81437743	2.967122283	40.35288351	52.01504817
7.0	52.65583867	3.131803527	46.86188415	59.16615168

Estimated Marginal Means 3: Treated1nottreated0* normalisedslide number

Estimates

Treated1nottreated0	normalisedslidenumber	Mean	Std. Error	95% Wald ... Lower
.0	1.0	62.82405868	6.580160368	51.16483381
	2.0	61.64259335	5.333373256	52.02764516
	3.0	47.03576127	5.158831753	37.93755227
	4.0	41.69684928	4.139168856	34.32464404
	5.0	44.22580609	4.990641931	35.45049372
	6.0	43.09146323	3.583208566	36.61093353
	7.0	45.82900780	2.885258598	40.50898175
1.0	1.0	81.40592800	9.692137710	64.46329794
	2.0	55.92461832	4.450519461	47.84800409
	3.0	47.12669016	4.102280900	39.73485252
	4.0	44.25675151	4.119621723	36.87616789
	5.0	46.88304488	4.875191438	38.23865111
	6.0	48.70935035	3.616756567	42.11231315
	7.0	60.49961540	4.749351773	51.87181402

Estimates

Treated1nottreated0	normalisedslidenumber	95% Wald ... Upper
.0	1.0	77.14013817
	2.0	73.03442819
	3.0	58.31590879
	4.0	50.65244779
	5.0	55.17333383
	6.0	50.71911651
	7.0	51.84771043
1.0	1.0	102.8015216
	2.0	65.36454329
	3.0	55.89362447
	4.0	53.11452265
	5.0	57.48162744
	6.0	56.33983588
	7.0	70.56247277

APPENDIX 13

```
 * Generalized Estimating Equations.
GENLIN awaveamplitudev BY timepointdays flashintensitymcd Treated1casp9DN
  /MODEL timepointdays flashintensitymcd Treated1casp9DN0pen1 timepointday
 DISTRIBUTION=GAMMA LINK=LOG
  /CRITERIA METHOD=FISHER(1) SCALE=MLE MAXITERATIONS=100 MAXSTEPHALVING=5
  /EMMEANS TABLES=Treated1casp9DN0pen1 SCALE=ORIGINAL
  /EMMEANS TABLES=timepointdays*flashintensitymcd*Treated1casp9DN0pen1 SCA
  /REPEATED SUBJECT=animal WITHINSUBJECT=Treated1casp9DN0pen1*timepointday
  /MISSING CLASSMISSING=EXCLUDE
  /PRINT CPS DESCRIPTIVES MODELINFO FIT SUMMARY WORKINGCORR.
```

Generalized Linear Models

Notes

Output Created		27-JUL-2013 00:00:34
Comments		
Input	Active Dataset	DataSet3
	Filter	<none>
	Weight	<none>
	Split File	<none>
	N of Rows in Working Data File	413
Missing Value Handling	Definition of Missing	User-defined missing values for factor, subject and within-subject variables are treated as missing.
	Cases Used	Statistics are based on cases with valid data for all variables in the model.
Weight Handling		not applicable

Notes

Syntax		GENLIN awaveamplitudev BY timepointdays flashintensitymcd Treated1casp9DN0pen1 (ORDER=ASCENDING) /MODEL timepointdays flashintensitymcd Treated1casp9DN0pen1 timepointdays*flashintensitymcd timepointdays*Treated1casp9DN0pen1 flashintensitymcd*Treated1casp9DN0pen1 timepointdays*flashintensitymcd*Treated1casp9DN0pen1 INTERCEPT=YES DISTRIBUTION=GAMMA LINK=LOG /CRITERIA METHOD=FISHER(1) SCALE=MLE MAXITERATIONS=100 MAXSTEPHALVING=5 PCONVERGE=1E-006 (ABSOLUTE) SINGULAR=1E-012 ANALYSISTYPE=3(WALD) CILEVEL=95 LIKELIHOOD=FULL /EMMEANS TABLES=Treated1casp9DN0pen1 SCALE=ORIGINAL /EMMEANS TABLES=timepointdays*flashintensitymcd*Treated1casp9DN0pen1 SCALE=ORIGINAL /REPEATED SUBJECT=animal WITHINSUBJECT=Treated1casp9DN0pen1*timepointdays*flashintensitymcd SORT=YES CORRTYPE=AR(1) ADJUSTCORR=YES COVB=ROBUST MAXITERATIONS=100 PCONVERGE=1e-006(ABSOLUTE) UPDATECORR=1 /MISSING CLASSMISSING=EXCLUDE /PRINT CPS DESCRIPTIVES MODELINFO FIT SUMMARY WORKINGCORR.
Resources	Processor Time	00:00:00.70
	Elapsed Time	00:00:00.70

[DataSet3]

Model Information

Dependent Variable		awaveamplitudev
Probability Distribution		Gamma
Link Function		Log
Subject Effect	1	animal
Within-Subject Effect	1	Treated1casp9DN0pen1
	2	timepointdays
	3	flashintensitymcd
Working Correlation Matrix Structure		AR(1)

Case Processing Summary

	N	Percent
Included	249	60.3%
Excluded	164	39.7%
Total	413	100.0%

Correlated Data Summary

Number of Levels	Subject Effect	animal	8
	Within-Subject Effect	Treated1casp9DN0pen1	2
		timepointdays	2
		flashintensitymcd	8
Number of Subjects			8
Number of Measurements per Subject	Minimum		28
	Maximum		32
Correlation Matrix Dimension			32

Categorical Variable Information

			N	Percent
Factor	timepointdays	7.0	128	51.4%
		14.0	121	48.6%
		Total	249	100.0%
	flashintensitymcd	10.0	32	12.9%
		30.0	32	12.9%
		100.0	32	12.9%
		300.0	32	12.9%
		1000.0	31	12.4%
		3000.0	30	12.0%
		10000.0	30	12.0%
		25000.0	30	12.0%
		Total	249	100.0%
	Treated1casp9DN0pen1	.0	125	50.2%
		1.0	124	49.8%
		Total	249	100.0%

Continuous Variable Information

		N	Minimum	Maximum	Mean
Dependent Variable	awaveamplitudev	249	.1	454.2	52.737

Continuous Variable Information

		Std. Deviation
Dependent Variable	awaveamplitudev	65.0063

Goodness of Fit[a]

	Value
Quasi Likelihood under Independence Model Criterion (QIC)[b]	183.955
Corrected Quasi Likelihood under Independence Model Criterion (QICC)[b]	188.537

Dependent Variable: awaveamplitudev
Model: (Intercept), timepointdays, flashintensitymcd, Treated1casp9DN0pen1, timepointdays * flashintensitymcd, timepointdays * Treated1casp9DN0pen1, flashintensitymcd * Treated1casp9DN0pen1, timepointdays * flashintensitymcd * Treated1casp9DN0pen1

a. Information criteria are in small-is-better form.

b. Computed using the full log quasi-likelihood function.

Tests of Model Effects

Source	Type III		
	Wald Chi-Square	df	Sig.
(Intercept)	1254.985	1	.000
timepointdays	1.634	1	.201
flashintensitymcd	5178.626	7	.000
Treated1casp9DN0pen1	3.283	1	.070
timepointdays * flashintensitymcd	12087.487	7	.000
timepointdays * Treated1casp9DN0pen1	.666	1	.414
flashintensitymcd * Treated1casp9DN0pen1	242.964	7	.000
timepointdays * flashintensitymcd * Treated1casp9DN0pen1	99.442	7	.000

Dependent Variable: awaveamplitudev
Model: (Intercept), timepointdays, flashintensitymcd, Treated1casp9DN0pen1, timepointdays * flashintensitymcd, timepointdays * Treated1casp9DN0pen1, flashintensitymcd * Treated1casp9DN0pen1, timepointdays * flashintensitymcd * Treated1casp9DN0pen1

Estimated Marginal Means 1: Treated1casp9DN0pen1

Estimates

Treated1casp9DN0pen1	Mean	Std. Error	95% Wald Confidence Interval	
			Lower	Upper
.0	22.271	2.7174	17.534	28.288
1.0	34.124	5.9471	24.250	48.018

Estimated Marginal Means 2: timepointdays* flashintensitymcd* Treated1casp9DN0pen1

Estimates

timepointdays	flashintensitymcd	Treated1casp9DN0pen1	Mean	Std. Error	95% Wald ...
					Lower
7.0	10.0	.0	1.463	.5043	.744
		1.0	2.375	.4785	1.600
	30.0	.0	4.663	1.1910	2.826
		1.0	7.700	2.2721	4.318
	100.0	.0	12.175	2.4543	8.201
		1.0	18.675	5.7044	10.263
	300.0	.0	35.263	5.9799	25.291
		1.0	46.525	15.2154	24.508
	1000.0	.0	62.188	12.3717	42.108
		1.0	85.950	28.5355	44.838
	3000.0	.0	85.225	13.8615	61.962
		1.0	122.000	37.9968	66.260
	10000.0	.0	113.013	17.6965	83.145
		1.0	144.713	42.8324	81.015
	25000.0	.0	119.075	19.1849	86.832
		1.0	144.500	43.3475	80.264
14.0	10.0	.0	1.250	.2537	.840
		1.0	5.313	1.1526	3.472
	30.0	.0	3.975	1.3971	1.996
		1.0	7.775	2.2643	4.393
	100.0	.0	8.000	1.6203	5.379
		1.0	14.250	3.1733	9.210
	300.0	.0	24.788	5.1928	16.440
		1.0	31.150	6.7671	20.349
	1000.0	.0	52.138	8.5893	37.750
		1.0	61.010	9.6612	44.731
	3000.0	.0	61.633	9.4848	45.585
		1.0	80.129	11.4102	60.615
	10000.0	.0	72.447	11.6880	52.807
		1.0	99.013	13.4938	75.804

Estimates

timepointdays	flashintensitymcd	Treated1casp9DN0pen1	95% Wald ... Upper
7.0	10.0	.0	2.875
		1.0	3.525
	30.0	.0	7.692
		1.0	13.730
	100.0	.0	18.074
		1.0	33.983
	300.0	.0	49.166
		1.0	88.320
	1000.0	.0	91.842
		1.0	164.758
	3000.0	.0	117.223
		1.0	224.629
	10000.0	.0	153.609
		1.0	258.492
	25000.0	.0	163.291
		1.0	260.144
14.0	10.0	.0	1.861
		1.0	8.128
	30.0	.0	7.916
		1.0	13.759
	100.0	.0	11.898
		1.0	22.048
	300.0	.0	37.373
		1.0	47.684
	1000.0	.0	72.008
		1.0	83.213
	3000.0	.0	83.331
		1.0	105.925
	10000.0	.0	99.391
		1.0	129.330

Estimates

timepointdays	flashintensitymcd	Treated1casp9DN0pen1	Mean	Std. Error	95% Wald ... Lower
	25000.0	.0	76.503	11.5244	56.945
		1.0	109.340	15.3044	83.107

Estimates

timepointdays	flashintensitymcd	Treated1casp9DN0pen1	95% Wald ... Upper
	25000.0	.0	102.778
		1.0	143.854

APPENDIX 14

```
 SORT CASES BY awaveamplitude(A).
* Generalized Estimating Equations.
GENLIN bwaveamplitudev BY timepointdays flashintensitymcd Treated1casp9DN
  /MODEL timepointdays flashintensitymcd Treated1casp9DN0pen1 timepointday
 DISTRIBUTION=GAMMA LINK=LOG
  /CRITERIA METHOD=FISHER(1) SCALE=MLE MAXITERATIONS=100 MAXSTEPHALVING=5
  /EMMEANS TABLES=Treated1casp9DN0pen1 SCALE=ORIGINAL
  /EMMEANS TABLES=timepointdays*flashintensitymcd*Treated1casp9DN0pen1 SCA
  /REPEATED SUBJECT=animal WITHINSUBJECT=Treated1casp9DN0pen1*timepointday
  /MISSING CLASSMISSING=EXCLUDE
  /PRINT CPS DESCRIPTIVES MODELINFO FIT SUMMARY WORKINGCORR.
```

Generalized Linear Models

Notes

Output Created		27-JUL-2013 00:17:37
Comments		
Input	Active Dataset	DataSet4
	Filter	<none>
	Weight	<none>
	Split File	<none>
	N of Rows in Working Data File	112
Missing Value Handling	Definition of Missing	User-defined missing values for factor, subject and within-subject variables are treated as missing.
	Cases Used	Statistics are based on cases with valid data for all variables in the model.
Weight Handling		not applicable

Notes

Syntax		GENLIN bwaveamplitudev BY timepointdays flashintensitymcd Treated1casp9DN0pen1 (ORDER=ASCENDING) /MODEL timepointdays flashintensitymcd Treated1casp9DN0pen1 timepointdays*flashintensitymcd timepointdays*Treated1casp9DN0pen1 flashintensitymcd*Treated1casp9DN0pen1 timepointdays*flashintensitymcd*Treated1casp9DN0pen1 INTERCEPT=YES DISTRIBUTION=GAMMA LINK=LOG /CRITERIA METHOD=FISHER(1) SCALE=MLE MAXITERATIONS=100 MAXSTEPHALVING=5 PCONVERGE=1E-006 (ABSOLUTE) SINGULAR=1E-012 ANALYSISTYPE=3(WALD) CILEVEL=95 LIKELIHOOD=FULL /EMMEANS TABLES=Treated1casp9DN0pen1 SCALE=ORIGINAL /EMMEANS TABLES=timepointdays*flashintensitymcd*Treated1casp9DN0pen1 SCALE=ORIGINAL /REPEATED SUBJECT=animal WITHINSUBJECT=Treated1casp9DN0pen1*timepointdays*flashintensitymcd SORT=YES CORRTYPE=AR(1) ADJUSTCORR=YES COVB=ROBUST MAXITERATIONS=100 PCONVERGE=1e-006(ABSOLUTE) UPDATECORR=1 /MISSING CLASSMISSING=EXCLUDE /PRINT CPS DESCRIPTIVES MODELINFO FIT SUMMARY WORKINGCORR.
Resources	Processor Time	00:00:00.59
	Elapsed Time	00:00:00.60

[DataSet4]

Model Information

Dependent Variable		bwaveamplitudev
Probability Distribution		Gamma
Link Function		Log
Subject Effect	1	animal
Within-Subject Effect	1	Treated1casp9DN0pen1
	2	timepointdays
	3	flashintensitymcd
Working Correlation Matrix Structure		AR(1)

Case Processing Summary

	N	Percent
Included	112	100.0%
Excluded	0	0.0%
Total	112	100.0%

Correlated Data Summary

Number of Levels	Subject Effect	animal	8
	Within-Subject Effect	Treated1casp9DN0pen1	2
		timepointdays	2
		flashintensitymcd	6
Number of Subjects			8
Number of Measurements per Subject	Minimum		8
	Maximum		19
Correlation Matrix Dimension			21

Categorical Variable Information

			N	Percent
Factor	timepointdays	7.0	63	56.3%
		14.0	49	43.8%
		Total	112	100.0%
	flashintensitymcd	100.0	1	0.9%
		300.0	14	12.5%
		1000.0	22	19.6%
		3000.0	25	22.3%
		10000.0	25	22.3%
		25000.0	25	22.3%
		Total	112	100.0%
	Treated1casp9DN0pen1	.0	47	42.0%
		1.0	65	58.0%
		Total	112	100.0%

Continuous Variable Information

		N	Minimum	Maximum	Mean
Dependent Variable	bwaveamplitudev	112	2.4	216.7	35.407

Continuous Variable Information

		Std. Deviation
Dependent Variable	bwaveamplitudev	36.3579

Goodness of Fit[a]

	Value
Quasi Likelihood under Independence Model Criterion (QIC)[b]	83.778
Corrected Quasi Likelihood under Independence Model Criterion (QICC)[b]	82.546

Dependent Variable: bwaveamplitudev
Model: (Intercept), timepointdays, flashintensitymcd, Treated1casp9DN0pen1, timepointdays * flashintensitymcd, timepointdays * Treated1casp9DN0pen1, flashintensitymcd * Treated1casp9DN0pen1, timepointdays * flashintensitymcd * Treated1casp9DN0pen1

a. Information criteria are in small-is-better form.

b. Computed using the full log quasi-likelihood function.

Tests of Model Effects

Source	Type III		
	Wald Chi-Square	df	Sig.
(Intercept)	364.679	1	.000
timepointdays	18.175	1	.000
flashintensitymcd	32807.582	5	.000
Treated1casp9DN0pen1	1.690	1	.194
timepointdays * flashintensitymcd	36.289	4	.000
timepointdays * Treated1casp9DN0pen1	.411	1	.522
flashintensitymcd * Treated1casp9DN0pen1	40.477	4	.000
timepointdays * flashintensitymcd * Treated1casp9DN0pen1	28.365	4	.000

Dependent Variable: bwaveamplitudev
Model: (Intercept), timepointdays, flashintensitymcd, Treated1casp9DN0pen1, timepointdays * flashintensitymcd, timepointdays * Treated1casp9DN0pen1, flashintensitymcd * Treated1casp9DN0pen1, timepointdays * flashintensitymcd * Treated1casp9DN0pen1

Working Correlation Matrix[a]

Measurement	Measurement			
	[Treated1casp 9DN0pen1 = . 0]* [timepointdays = 7.0]* [flashintensity mcd = 300.0]	[Treated1casp 9DN0pen1 = . 0]* [timepointdays = 7.0]* [flashintensity mcd = 1000.0]	[Treated1casp 9DN0pen1 = . 0]* [timepointdays = 7.0]* [flashintensity mcd = 3000.0]	[Treated1casp 9DN0pen1 = . 0]* [timepointdays = 7.0]* [flashintensity mcd = 10000.0]
[Treated1casp9DN0pen1 = .0]* [timepointdays = 7.0]* [flashintensitymcd = 300.0]	1.000	1.000	1.000	1.000
[Treated1casp9DN0pen1 = .0]* [timepointdays = 7.0]* [flashintensitymcd = 1000.0]	1.000	1.000	1.000	1.000
[Treated1casp9DN0pen1 = .0]* [timepointdays = 7.0]* [flashintensitymcd = 3000.0]	1.000	1.000	1.000	1.000
[Treated1casp9DN0pen1 = .0]* [timepointdays = 7.0]* [flashintensitymcd = 10000.0]	1.000	1.000	1.000	1.000
[Treated1casp9DN0pen1 = .0]* [timepointdays = 7.0]* [flashintensitymcd = 25000.0]	1.000	1.000	1.000	1.000
[Treated1casp9DN0pen1 = .0]* [timepointdays = 14.0]* [flashintensitymcd = 300.0]	1.000	1.000	1.000	1.000
[Treated1casp9DN0pen1 = .0]* [timepointdays = 14.0]* [flashintensitymcd = 1000.0]	.999	1.000	1.000	1.000
[Treated1casp9DN0pen1 = .0]* [timepointdays = 14.0]* [flashintensitymcd = 3000.0]	.999	.999	1.000	1.000
[Treated1casp9DN0pen1 = .0]* [timepointdays = 14.0]* [flashintensitymcd = 10000.0]	.999	.999	.999	1.000
[Treated1casp9DN0pen1 = .0]* [timepointdays = 14.0]* [flashintensitymcd = 25000.0]	.999	.999	.999	.999

Working Correlation Matrix[a]

Measurement	Measurement			
	[Treated1casp9DN0pen1 = .0]* [timepointdays = 7.0]* [flashintensitymcd = 25000.0]	[Treated1casp9DN0pen1 = .0]* [timepointdays = 14.0]* [flashintensitymcd = 300.0]	[Treated1casp9DN0pen1 = .0]* [timepointdays = 14.0]* [flashintensitymcd = 1000.0]	[Treated1casp9DN0pen1 = .0]* [timepointdays = 14.0]* [flashintensitymcd = 3000.0]
[Treated1casp9DN0pen1 = .0]* [timepointdays = 7.0]* [flashintensitymcd = 300.0]	1.000	1.000	.999	.999
[Treated1casp9DN0pen1 = .0]* [timepointdays = 7.0]* [flashintensitymcd = 1000.0]	1.000	1.000	1.000	.999
[Treated1casp9DN0pen1 = .0]* [timepointdays = 7.0]* [flashintensitymcd = 3000.0]	1.000	1.000	1.000	1.000
[Treated1casp9DN0pen1 = .0]* [timepointdays = 7.0]* [flashintensitymcd = 10000.0]	1.000	1.000	1.000	1.000
[Treated1casp9DN0pen1 = .0]* [timepointdays = 7.0]* [flashintensitymcd = 25000.0]	1.000	1.000	1.000	1.000
[Treated1casp9DN0pen1 = .0]* [timepointdays = 14.0]* [flashintensitymcd = 300.0]	1.000	1.000	1.000	1.000
[Treated1casp9DN0pen1 = .0]* [timepointdays = 14.0]* [flashintensitymcd = 1000.0]	1.000	1.000	1.000	1.000
[Treated1casp9DN0pen1 = .0]* [timepointdays = 14.0]* [flashintensitymcd = 3000.0]	1.000	1.000	1.000	1.000
[Treated1casp9DN0pen1 = .0]* [timepointdays = 14.0]* [flashintensitymcd = 10000.0]	1.000	1.000	1.000	1.000
[Treated1casp9DN0pen1 = .0]* [timepointdays = 14.0]* [flashintensitymcd = 25000.0]	1.000	1.000	1.000	1.000

Working Correlation Matrix[a]

Measurement	Measurement			
	[Treated1casp9DN0pen1 = .0]* [timepointdays = 14.0]* [flashintensitymcd = 10000.0]	[Treated1casp9DN0pen1 = .0]* [timepointdays = 14.0]* [flashintensitymcd = 25000.0]	[Treated1casp9DN0pen1 = 1.0]* [timepointdays = 7.0]* [flashintensitymcd = 100.0]	[Treated1casp9DN0pen1 = 1.0]* [timepointdays = 7.0]* [flashintensitymcd = 300.0]
[Treated1casp9DN0pen1 = .0]* [timepointdays = 7.0]* [flashintensitymcd = 300.0]	.999	.999	.999	.999
[Treated1casp9DN0pen1 = .0]* [timepointdays = 7.0]* [flashintensitymcd = 1000.0]	.999	.999	.999	.999
[Treated1casp9DN0pen1 = .0]* [timepointdays = 7.0]* [flashintensitymcd = 3000.0]	.999	.999	.999	.999
[Treated1casp9DN0pen1 = .0]* [timepointdays = 7.0]* [flashintensitymcd = 10000.0]	1.000	.999	.999	.999
[Treated1casp9DN0pen1 = .0]* [timepointdays = 7.0]* [flashintensitymcd = 25000.0]	1.000	1.000	.999	.999
[Treated1casp9DN0pen1 = .0]* [timepointdays = 14.0]* [flashintensitymcd = 300.0]	1.000	1.000	1.000	.999
[Treated1casp9DN0pen1 = .0]* [timepointdays = 14.0]* [flashintensitymcd = 1000.0]	1.000	1.000	1.000	1.000
[Treated1casp9DN0pen1 = .0]* [timepointdays = 14.0]* [flashintensitymcd = 3000.0]	1.000	1.000	1.000	1.000
[Treated1casp9DN0pen1 = .0]* [timepointdays = 14.0]* [flashintensitymcd = 10000.0]	1.000	1.000	1.000	1.000
[Treated1casp9DN0pen1 = .0]* [timepointdays = 14.0]* [flashintensitymcd = 25000.0]	1.000	1.000	1.000	1.000

Working Correlation Matrix[a]

Measurement	Measurement			
	[Treated1casp9DN0pen1 = 1.0]* [timepointdays = 7.0]* [flashintensitymcd = 1000.0]	[Treated1casp9DN0pen1 = 1.0]* [timepointdays = 7.0]* [flashintensitymcd = 3000.0]	[Treated1casp9DN0pen1 = 1.0]* [timepointdays = 7.0]* [flashintensitymcd = 10000.0]	[Treated1casp9DN0pen1 = 1.0]* [timepointdays = 7.0]* [flashintensitymcd = 25000.0]
[Treated1casp9DN0pen1 = .0]* [timepointdays = 7.0]* [flashintensitymcd = 300.0]	.999	.999	.999	.999
[Treated1casp9DN0pen1 = .0]* [timepointdays = 7.0]* [flashintensitymcd = 1000.0]	.999	.999	.999	.999
[Treated1casp9DN0pen1 = .0]* [timepointdays = 7.0]* [flashintensitymcd = 3000.0]	.999	.999	.999	.999
[Treated1casp9DN0pen1 = .0]* [timepointdays = 7.0]* [flashintensitymcd = 10000.0]	.999	.999	.999	.999
[Treated1casp9DN0pen1 = .0]* [timepointdays = 7.0]* [flashintensitymcd = 25000.0]	.999	.999	.999	.999
[Treated1casp9DN0pen1 = .0]* [timepointdays = 14.0]* [flashintensitymcd = 300.0]	.999	.999	.999	.999
[Treated1casp9DN0pen1 = .0]* [timepointdays = 14.0]* [flashintensitymcd = 1000.0]	.999	.999	.999	.999
[Treated1casp9DN0pen1 = .0]* [timepointdays = 14.0]* [flashintensitymcd = 3000.0]	1.000	.999	.999	.999
[Treated1casp9DN0pen1 = .0]* [timepointdays = 14.0]* [flashintensitymcd = 10000.0]	1.000	1.000	.999	.999
[Treated1casp9DN0pen1 = .0]* [timepointdays = 14.0]* [flashintensitymcd = 25000.0]	1.000	1.000	1.000	.999

Working Correlation Matrix[a]

Measurement	Measurement			
	[Treated1casp 9DN0pen1 = 1.0]* [timepointdays = 14.0]* [flashintensity mcd = 300.0]	[Treated1casp 9DN0pen1 = 1.0]* [timepointdays = 14.0]* [flashintensity mcd = 1000.0]	[Treated1casp 9DN0pen1 = 1.0]* [timepointdays = 14.0]* [flashintensity mcd = 3000.0]	[Treated1casp 9DN0pen1 = 1.0]* [timepointdays = 14.0]* [flashintensity mcd = 10000.0]
[Treated1casp9DN0pen1 = .0]* [timepointdays = 7.0]* [flashintensitymcd = 300.0]	.998	.998	.998	.998
[Treated1casp9DN0pen1 = .0]* [timepointdays = 7.0]* [flashintensitymcd = 1000.0]	.999	.998	.998	.998
[Treated1casp9DN0pen1 = .0]* [timepointdays = 7.0]* [flashintensitymcd = 3000.0]	.999	.999	.998	.998
[Treated1casp9DN0pen1 = .0]* [timepointdays = 7.0]* [flashintensitymcd = 10000.0]	.999	.999	.999	.998
[Treated1casp9DN0pen1 = .0]* [timepointdays = 7.0]* [flashintensitymcd = 25000.0]	.999	.999	.999	.999
[Treated1casp9DN0pen1 = .0]* [timepointdays = 14.0]* [flashintensitymcd = 300.0]	.999	.999	.999	.999
[Treated1casp9DN0pen1 = .0]* [timepointdays = 14.0]* [flashintensitymcd = 1000.0]	.999	.999	.999	.999
[Treated1casp9DN0pen1 = .0]* [timepointdays = 14.0]* [flashintensitymcd = 3000.0]	.999	.999	.999	.999
[Treated1casp9DN0pen1 = .0]* [timepointdays = 14.0]* [flashintensitymcd = 10000.0]	.999	.999	.999	.999
[Treated1casp9DN0pen1 = .0]* [timepointdays = 14.0]* [flashintensitymcd = 25000.0]	.999	.999	.999	.999

Working Correlation Matrix[a]

Measurement	Measurement [Treated1casp9DN0pen1 = 1.0]* [timepointdays = 14.0]* [flashintensitymcd = 25000.0]
[Treated1casp9DN0pen1 = .0]* [timepointdays = 7.0]* [flashintensitymcd = 300.0]	.998
[Treated1casp9DN0pen1 = .0]* [timepointdays = 7.0]* [flashintensitymcd = 1000.0]	.998
[Treated1casp9DN0pen1 = .0]* [timepointdays = 7.0]* [flashintensitymcd = 3000.0]	.998
[Treated1casp9DN0pen1 = .0]* [timepointdays = 7.0]* [flashintensitymcd = 10000.0]	.998
[Treated1casp9DN0pen1 = .0]* [timepointdays = 7.0]* [flashintensitymcd = 25000.0]	.998
[Treated1casp9DN0pen1 = .0]* [timepointdays = 14.0]* [flashintensitymcd = 300.0]	.999
[Treated1casp9DN0pen1 = .0]* [timepointdays = 14.0]* [flashintensitymcd = 1000.0]	.999
[Treated1casp9DN0pen1 = .0]* [timepointdays = 14.0]* [flashintensitymcd = 3000.0]	.999
[Treated1casp9DN0pen1 = .0]* [timepointdays = 14.0]* [flashintensitymcd = 10000.0]	.999
[Treated1casp9DN0pen1 = .0]* [timepointdays = 14.0]* [flashintensitymcd = 25000.0]	.999

Working Correlation Matrix[a]

Measurement	Measurement			
	[Treated1casp 9DN0pen1 = . 0]* [timepointdays = 7.0]* [flashintensity mcd = 300.0]	[Treated1casp 9DN0pen1 = . 0]* [timepointdays = 7.0]* [flashintensity mcd = 1000.0]	[Treated1casp 9DN0pen1 = . 0]* [timepointdays = 7.0]* [flashintensity mcd = 3000.0]	[Treated1casp 9DN0pen1 = . 0]* [timepointdays = 7.0]* [flashintensity mcd = 10000.0]
[Treated1casp9DN0pen1 = 1.0]* [timepointdays = 7.0]* [flashintensitymcd = 100.0]	.999	.999	.999	.999
[Treated1casp9DN0pen1 = 1.0]* [timepointdays = 7.0]* [flashintensitymcd = 300.0]	.999	.999	.999	.999
[Treated1casp9DN0pen1 = 1.0]* [timepointdays = 7.0]* [flashintensitymcd = 1000.0]	.999	.999	.999	.999
[Treated1casp9DN0pen1 = 1.0]* [timepointdays = 7.0]* [flashintensitymcd = 3000.0]	.999	.999	.999	.999
[Treated1casp9DN0pen1 = 1.0]* [timepointdays = 7.0]* [flashintensitymcd = 10000.0]	.999	.999	.999	.999
[Treated1casp9DN0pen1 = 1.0]* [timepointdays = 7.0]* [flashintensitymcd = 25000.0]	.999	.999	.999	.999
[Treated1casp9DN0pen1 = 1.0]* [timepointdays = 14.0]* [flashintensitymcd = 300.0]	.998	.999	.999	.999
[Treated1casp9DN0pen1 = 1.0]* [timepointdays = 14.0]* [flashintensitymcd = 1000.0]	.998	.998	.999	.999
[Treated1casp9DN0pen1 = 1.0]* [timepointdays = 14.0]* [flashintensitymcd = 3000.0]	.998	.998	.998	.999
[Treated1casp9DN0pen1 = 1.0]* [timepointdays = 14.0]* [flashintensitymcd = 10000.0]	.998	.998	.998	.998
[Treated1casp9DN0pen1 = 1.0]* [timepointdays = 14.0]* [flashintensitymcd = 25000.0]	.998	.998	.998	.998

Working Correlation Matrix[a]

Measurement	Measurement			
	[Treated1casp9DN0pen1 = .0]* [timepointdays = 7.0]* [flashintensitymcd = 25000.0]	[Treated1casp9DN0pen1 = .0]* [timepointdays = 14.0]* [flashintensitymcd = 300.0]	[Treated1casp9DN0pen1 = .0]* [timepointdays = 14.0]* [flashintensitymcd = 1000.0]	[Treated1casp9DN0pen1 = .0]* [timepointdays = 14.0]* [flashintensitymcd = 3000.0]
[Treated1casp9DN0pen1 = 1.0]* [timepointdays = 7.0]* [flashintensitymcd = 100.0]	.999	1.000	1.000	1.000
[Treated1casp9DN0pen1 = 1.0]* [timepointdays = 7.0]* [flashintensitymcd = 300.0]	.999	.999	1.000	1.000
[Treated1casp9DN0pen1 = 1.0]* [timepointdays = 7.0]* [flashintensitymcd = 1000.0]	.999	.999	.999	1.000
[Treated1casp9DN0pen1 = 1.0]* [timepointdays = 7.0]* [flashintensitymcd = 3000.0]	.999	.999	.999	.999
[Treated1casp9DN0pen1 = 1.0]* [timepointdays = 7.0]* [flashintensitymcd = 10000.0]	.999	.999	.999	.999
[Treated1casp9DN0pen1 = 1.0]* [timepointdays = 7.0]* [flashintensitymcd = 25000.0]	.999	.999	.999	.999
[Treated1casp9DN0pen1 = 1.0]* [timepointdays = 14.0]* [flashintensitymcd = 300.0]	.999	.999	.999	.999
[Treated1casp9DN0pen1 = 1.0]* [timepointdays = 14.0]* [flashintensitymcd = 1000.0]	.999	.999	.999	.999
[Treated1casp9DN0pen1 = 1.0]* [timepointdays = 14.0]* [flashintensitymcd = 3000.0]	.999	.999	.999	.999
[Treated1casp9DN0pen1 = 1.0]* [timepointdays = 14.0]* [flashintensitymcd = 10000.0]	.999	.999	.999	.999
[Treated1casp9DN0pen1 = 1.0]* [timepointdays = 14.0]* [flashintensitymcd = 25000.0]	.998	.999	.999	.999

Working Correlation Matrix[a]

Measurement	Measurement			
	[Treated1casp9DN0pen1 = .0]* [timepointdays = 14.0]* [flashintensitymcd = 10000.0]	[Treated1casp9DN0pen1 = .0]* [timepointdays = 14.0]* [flashintensitymcd = 25000.0]	[Treated1casp9DN0pen1 = 1.0]* [timepointdays = 7.0]* [flashintensitymcd = 100.0]	[Treated1casp9DN0pen1 = 1.0]* [timepointdays = 7.0]* [flashintensitymcd = 300.0]
[Treated1casp9DN0pen1 = 1.0]* [timepointdays = 7.0]* [flashintensitymcd = 100.0]	1.000	1.000	1.000	1.000
[Treated1casp9DN0pen1 = 1.0]* [timepointdays = 7.0]* [flashintensitymcd = 300.0]	1.000	1.000	1.000	1.000
[Treated1casp9DN0pen1 = 1.0]* [timepointdays = 7.0]* [flashintensitymcd = 1000.0]	1.000	1.000	1.000	1.000
[Treated1casp9DN0pen1 = 1.0]* [timepointdays = 7.0]* [flashintensitymcd = 3000.0]	1.000	1.000	1.000	1.000
[Treated1casp9DN0pen1 = 1.0]* [timepointdays = 7.0]* [flashintensitymcd = 10000.0]	.999	1.000	1.000	1.000
[Treated1casp9DN0pen1 = 1.0]* [timepointdays = 7.0]* [flashintensitymcd = 25000.0]	.999	.999	1.000	1.000
[Treated1casp9DN0pen1 = 1.0]* [timepointdays = 14.0]* [flashintensitymcd = 300.0]	.999	.999	.999	1.000
[Treated1casp9DN0pen1 = 1.0]* [timepointdays = 14.0]* [flashintensitymcd = 1000.0]	.999	.999	.999	.999
[Treated1casp9DN0pen1 = 1.0]* [timepointdays = 14.0]* [flashintensitymcd = 3000.0]	.999	.999	.999	.999
[Treated1casp9DN0pen1 = 1.0]* [timepointdays = 14.0]* [flashintensitymcd = 10000.0]	.999	.999	.999	.999
[Treated1casp9DN0pen1 = 1.0]* [timepointdays = 14.0]* [flashintensitymcd = 25000.0]	.999	.999	.999	.999

Working Correlation Matrix[a]

Measurement	Measurement			
	[Treated1casp9DN0pen1 = 1.0]* [timepointdays = 7.0]* [flashintensitymcd = 1000.0]	[Treated1casp9DN0pen1 = 1.0]* [timepointdays = 7.0]* [flashintensitymcd = 3000.0]	[Treated1casp9DN0pen1 = 1.0]* [timepointdays = 7.0]* [flashintensitymcd = 10000.0]	[Treated1casp9DN0pen1 = 1.0]* [timepointdays = 7.0]* [flashintensitymcd = 25000.0]
[Treated1casp9DN0pen1 = 1.0]* [timepointdays = 7.0]* [flashintensitymcd = 100.0]	1.000	1.000	1.000	1.000
[Treated1casp9DN0pen1 = 1.0]* [timepointdays = 7.0]* [flashintensitymcd = 300.0]	1.000	1.000	1.000	1.000
[Treated1casp9DN0pen1 = 1.0]* [timepointdays = 7.0]* [flashintensitymcd = 1000.0]	1.000	1.000	1.000	1.000
[Treated1casp9DN0pen1 = 1.0]* [timepointdays = 7.0]* [flashintensitymcd = 3000.0]	1.000	1.000	1.000	1.000
[Treated1casp9DN0pen1 = 1.0]* [timepointdays = 7.0]* [flashintensitymcd = 10000.0]	1.000	1.000	1.000	1.000
[Treated1casp9DN0pen1 = 1.0]* [timepointdays = 7.0]* [flashintensitymcd = 25000.0]	1.000	1.000	1.000	1.000
[Treated1casp9DN0pen1 = 1.0]* [timepointdays = 14.0]* [flashintensitymcd = 300.0]	1.000	1.000	1.000	1.000
[Treated1casp9DN0pen1 = 1.0]* [timepointdays = 14.0]* [flashintensitymcd = 1000.0]	1.000	1.000	1.000	1.000
[Treated1casp9DN0pen1 = 1.0]* [timepointdays = 14.0]* [flashintensitymcd = 3000.0]	.999	1.000	1.000	1.000
[Treated1casp9DN0pen1 = 1.0]* [timepointdays = 14.0]* [flashintensitymcd = 10000.0]	.999	.999	1.000	1.000
[Treated1casp9DN0pen1 = 1.0]* [timepointdays = 14.0]* [flashintensitymcd = 25000.0]	.999	.999	.999	1.000

Working Correlation Matrix[a]

Measurement	Measurement			
	[Treated1casp9DN0pen1 = 1.0]* [timepointdays = 14.0]* [flashintensitymcd = 300.0]	[Treated1casp9DN0pen1 = 1.0]* [timepointdays = 14.0]* [flashintensitymcd = 1000.0]	[Treated1casp9DN0pen1 = 1.0]* [timepointdays = 14.0]* [flashintensitymcd = 3000.0]	[Treated1casp9DN0pen1 = 1.0]* [timepointdays = 14.0]* [flashintensitymcd = 10000.0]
[Treated1casp9DN0pen1 = 1.0]* [timepointdays = 7.0]* [flashintensitymcd = 100.0]	.999	.999	.999	.999
[Treated1casp9DN0pen1 = 1.0]* [timepointdays = 7.0]* [flashintensitymcd = 300.0]	1.000	.999	.999	.999
[Treated1casp9DN0pen1 = 1.0]* [timepointdays = 7.0]* [flashintensitymcd = 1000.0]	1.000	1.000	.999	.999
[Treated1casp9DN0pen1 = 1.0]* [timepointdays = 7.0]* [flashintensitymcd = 3000.0]	1.000	1.000	1.000	.999
[Treated1casp9DN0pen1 = 1.0]* [timepointdays = 7.0]* [flashintensitymcd = 10000.0]	1.000	1.000	1.000	1.000
[Treated1casp9DN0pen1 = 1.0]* [timepointdays = 7.0]* [flashintensitymcd = 25000.0]	1.000	1.000	1.000	1.000
[Treated1casp9DN0pen1 = 1.0]* [timepointdays = 14.0]* [flashintensitymcd = 300.0]	1.000	1.000	1.000	1.000
[Treated1casp9DN0pen1 = 1.0]* [timepointdays = 14.0]* [flashintensitymcd = 1000.0]	1.000	1.000	1.000	1.000
[Treated1casp9DN0pen1 = 1.0]* [timepointdays = 14.0]* [flashintensitymcd = 3000.0]	1.000	1.000	1.000	1.000
[Treated1casp9DN0pen1 = 1.0]* [timepointdays = 14.0]* [flashintensitymcd = 10000.0]	1.000	1.000	1.000	1.000
[Treated1casp9DN0pen1 = 1.0]* [timepointdays = 14.0]* [flashintensitymcd = 25000.0]	1.000	1.000	1.000	1.000

Working Correlation Matrix[a]

Measurement	Measurement [Treated1casp9DN0pen1 = 1.0]* [timepointdays = 14.0]* [flashintensitymcd = 25000.0]
[Treated1casp9DN0pen1 = 1.0]* [timepointdays = 7.0]* [flashintensitymcd = 100.0]	.999
[Treated1casp9DN0pen1 = 1.0]* [timepointdays = 7.0]* [flashintensitymcd = 300.0]	.999
[Treated1casp9DN0pen1 = 1.0]* [timepointdays = 7.0]* [flashintensitymcd = 1000.0]	.999
[Treated1casp9DN0pen1 = 1.0]* [timepointdays = 7.0]* [flashintensitymcd = 3000.0]	.999
[Treated1casp9DN0pen1 = 1.0]* [timepointdays = 7.0]* [flashintensitymcd = 10000.0]	.999
[Treated1casp9DN0pen1 = 1.0]* [timepointdays = 7.0]* [flashintensitymcd = 25000.0]	1.000
[Treated1casp9DN0pen1 = 1.0]* [timepointdays = 14.0]* [flashintensitymcd = 300.0]	1.000
[Treated1casp9DN0pen1 = 1.0]* [timepointdays = 14.0]* [flashintensitymcd = 1000.0]	1.000
[Treated1casp9DN0pen1 = 1.0]* [timepointdays = 14.0]* [flashintensitymcd = 3000.0]	1.000
[Treated1casp9DN0pen1 = 1.0]* [timepointdays = 14.0]* [flashintensitymcd = 10000.0]	1.000
[Treated1casp9DN0pen1 = 1.0]* [timepointdays = 14.0]* [flashintensitymcd = 25000.0]	1.000

Dependent Variable: bwaveamplitudev

Model: (Intercept), timepointdays, flashintensitymcd, Treated1casp9DN0pen1, timepointdays * flashintensitymcd, timepointdays * Treated1casp9DN0pen1, flashintensitymcd * Treated1casp9DN0pen1, timepointdays * flashintensitymcd * Treated1casp9DN0pen1

a. The AR(1) working correlation matrix structure is computed assuming the measurements are equally spaced for all subjects.

Estimated Marginal Means 1: Treated1casp9DN0pen1

Estimates

Treated1casp9DN0pen1	Mean	Std. Error	95% Wald Confidence Interval	
			Lower	Upper
.0	14.277	3.6012	8.708	23.407
1.0	21.388	3.9229	14.929	30.640

Estimated Marginal Means 2: timepointdays* flashintensitymcd* Treated1casp9DN0pen1

Estimates

timepointdays	flashintensitymcd	Treated1casp9DN0pen1	Mean	Std. Error	95% Wald ...
					Lower
7.0	100.0	.0	2.841	1.3837	1.094
		1.0	4.001	.6931	2.849
	300.0	.0	6.725	1.2475	4.675
		1.0	8.819	2.7331	4.804
	1000.0	.0	16.884	3.7767	10.891
		1.0	22.204	6.9351	12.039
	3000.0	.0	29.829	7.4697	18.259
		1.0	45.663	13.9157	25.128
	10000.0	.0	51.219	12.8263	31.353
		1.0	74.263	19.6638	44.196
	25000.0	.0	56.729	15.0556	33.721
		1.0	79.888	21.3549	47.309
14.0	300.0	.0	1.916	.4399	1.222
		1.0	4.461	.8865	3.022
	1000.0	.0	7.912	1.8744	4.974
		1.0	13.383	2.0322	9.938
	3000.0	.0	15.247	3.6020	9.596
		1.0	22.659	3.1637	17.234
	10000.0	.0	26.047	8.7760	13.457
		1.0	36.391	7.1692	24.735
	25000.0	.0	29.840	8.9412	16.586
		1.0	40.999	6.6836	29.786

Estimates

timepointdays	flashintensitymcd	Treated1casp9DN0pen1	95% Wald ... Upper
7.0	100.0	.0	7.380
		1.0	5.618
	300.0	.0	9.673
		1.0	16.189
	1000.0	.0	26.175
		1.0	40.954
	3000.0	.0	48.730
		1.0	82.978
	10000.0	.0	83.674
		1.0	124.783
	25000.0	.0	95.435
		1.0	134.901
14.0	300.0	.0	3.005
		1.0	6.585
	1000.0	.0	12.588
		1.0	18.022
	3000.0	.0	24.226
		1.0	29.791
	10000.0	.0	50.414
		1.0	53.541
	25000.0	.0	53.685
		1.0	56.433

APPENDIX 15

```
 * Generalized Estimating Equations.
GENLIN AvgONLthickness BY Treated1nottreated0 normalisedslidenumber (ORDEI
  /MODEL Treated1nottreated0 normalisedslidenumber Treated1nottreated0*noi
 DISTRIBUTION=GAMMA LINK=LOG
  /CRITERIA METHOD=FISHER(1) SCALE=MLE MAXITERATIONS=100 MAXSTEPHALVING=5
  /EMMEANS TABLES=Treated1nottreated0 SCALE=ORIGINAL
  /EMMEANS TABLES=normalisedslidenumber SCALE=ORIGINAL
  /EMMEANS TABLES=Treated1nottreated0*normalisedslidenumber SCALE=ORIGINAI
  /REPEATED SUBJECT=Animal WITHINSUBJECT=Treated1nottreated0*normalisedsli
  /MISSING CLASSMISSING=EXCLUDE
  /PRINT CPS DESCRIPTIVES MODELINFO FIT SUMMARY WORKINGCORR.
```

Generalized Linear Models

Notes

Output Created		26-JUL-2013 23:36:31
Comments		
Input	Active Dataset	DataSet2
	Filter	<none>
	Weight	<none>
	Split File	<none>
	N of Rows in Working Data File	112
Missing Value Handling	Definition of Missing	User-defined missing values for factor, subject and within-subject variables are treated as missing.
	Cases Used	Statistics are based on cases with valid data for all variables in the model.
Weight Handling		not applicable

Notes

Syntax		GENLIN AvgONLthickness BY Treated1nottreated0 normalisedslidenumber (ORDER=ASCENDING) /MODEL Treated1nottreated0 normalisedslidenumber Treated1nottreated0*normalisedslidenumber INTERCEPT=YES DISTRIBUTION=GAMMA LINK=LOG /CRITERIA METHOD=FISHER(1) SCALE=MLE MAXITERATIONS=100 MAXSTEPHALVING=5 PCONVERGE=1E-006 (ABSOLUTE) SINGULAR=1E-012 ANALYSISTYPE=3(WALD) CILEVEL=95 LIKELIHOOD=FULL /EMMEANS TABLES=Treated1nottreated0 SCALE=ORIGINAL /EMMEANS TABLES=normalisedslidenumber SCALE=ORIGINAL /EMMEANS TABLES=Treated1nottreated0*normalisedslidenumber SCALE=ORIGINAL /REPEATED SUBJECT=Animal WITHINSUBJECT=Treated1nottreated0*normalisedslidenumber SORT=YES CORRTYPE=AR(1) ADJUSTCORR=YES COVB=ROBUST MAXITERATIONS=100 PCONVERGE=1e-006 (ABSOLUTE) UPDATECORR=1 /MISSING CLASSMISSING=EXCLUDE /PRINT CPS DESCRIPTIVES MODELINFO FIT SUMMARY WORKINGCORR.
Resources	Processor Time	00:00:00.33
	Elapsed Time	00:00:00.32

[DataSet2]

Model Information

Dependent Variable		AvgONLthickness
Probability Distribution		Gamma
Link Function		Log
Subject Effect	1	Animal
Within-Subject Effect	1	Treated1nottreated0
	2	normalisedslidenumber
Working Correlation Matrix Structure		AR(1)

Case Processing Summary

	N	Percent
Included	111	99.1%
Excluded	1	0.9%
Total	112	100.0%

Correlated Data Summary

Number of Levels	Subject Effect	Animal	8
	Within-Subject Effect	Treated1nottreated0	2
		normalisedslidenumber	7
Number of Subjects			8
Number of Measurements per Subject	Minimum		13
	Maximum		14
Correlation Matrix Dimension			14

Categorical Variable Information

			N	Percent
Factor	Treated1nottreated0	.0	56	50.5%
		1.0	55	49.5%
		Total	111	100.0%
	normalisedslidenumber	1	16	14.4%
		2	16	14.4%
		3	16	14.4%
		4	15	13.5%
		5	16	14.4%
		6	16	14.4%
		7	16	14.4%
		Total	111	100.0%

Continuous Variable Information

		N	Minimum	Maximum	Mean
Dependent Variable	AvgONLthickness	111	39.94070536	123.6170213	69.41941045

Continuous Variable Information

		Std. Deviation
Dependent Variable	AvgONLthickness	20.12078517

Goodness of Fit[a]

	Value
Quasi Likelihood under Independence Model Criterion (QIC)[b]	33.422
Corrected Quasi Likelihood under Independence Model Criterion (QICC)[b]	33.934

Dependent Variable: AvgONLthickness
Model: (Intercept), Treated1nottreated0, normalisedslidenumber, Treated1nottreated0 * normalisedslidenumber

a. Information criteria are in small-is-better form.

b. Computed using the full log quasi-likelihood function.

Tests of Model Effects

Source	Type III		
	Wald Chi-Square	df	Sig.
(Intercept)	17601.120	1	.000
Treated1nottreated0	.313	1	.576
normalisedslidenumber	13709.115	6	.000
Treated1nottreated0 * normalisedslidenumber	6.746	6	.345

Dependent Variable: AvgONLthickness
Model: (Intercept), Treated1nottreated0, normalisedslidenumber, Treated1nottreated0 * normalisedslidenumber

Working Correlation Matrix[a]

Measurement	Measurement			
	[Treated1nottreated0 = .0]* [normalisedslidenumber = 1]	[Treated1nottreated0 = .0]* [normalisedslidenumber = 2]	[Treated1nottreated0 = .0]* [normalisedslidenumber = 3]	[Treated1nottreated0 = .0]* [normalisedslidenumber = 4]
[Treated1nottreated0 = .0]* [normalisedslidenumber = 1]	1.000	.554	.307	.170
[Treated1nottreated0 = .0]* [normalisedslidenumber = 2]	.554	1.000	.554	.307
[Treated1nottreated0 = .0]* [normalisedslidenumber = 3]	.307	.554	1.000	.554
[Treated1nottreated0 = .0]* [normalisedslidenumber = 4]	.170	.307	.554	1.000
[Treated1nottreated0 = .0]* [normalisedslidenumber = 5]	.094	.170	.307	.554
[Treated1nottreated0 = .0]* [normalisedslidenumber = 6]	.052	.094	.170	.307
[Treated1nottreated0 = .0]* [normalisedslidenumber = 7]	.029	.052	.094	.170
[Treated1nottreated0 = 1.0]* [normalisedslidenumber = 1]	.016	.029	.052	.094
[Treated1nottreated0 = 1.0]* [normalisedslidenumber = 2]	.009	.016	.029	.052
[Treated1nottreated0 = 1.0]* [normalisedslidenumber = 3]	.005	.009	.016	.029

Working Correlation Matrix[a]

Measurement	Measurement			
	[Treated1nottreated0 = .0]* [normalisedslidenumber = 5]	[Treated1nottreated0 = .0]* [normalisedslidenumber = 6]	[Treated1nottreated0 = .0]* [normalisedslidenumber = 7]	[Treated1nottreated0 = 1.0] * [normalisedslidenumber = 1]
[Treated1nottreated0 = .0]* [normalisedslidenumber = 1]	.094	.052	.029	.016
[Treated1nottreated0 = .0]* [normalisedslidenumber = 2]	.170	.094	.052	.029
[Treated1nottreated0 = .0]* [normalisedslidenumber = 3]	.307	.170	.094	.052
[Treated1nottreated0 = .0]* [normalisedslidenumber = 4]	.554	.307	.170	.094
[Treated1nottreated0 = .0]* [normalisedslidenumber = 5]	1.000	.554	.307	.170
[Treated1nottreated0 = .0]* [normalisedslidenumber = 6]	.554	1.000	.554	.307
[Treated1nottreated0 = .0]* [normalisedslidenumber = 7]	.307	.554	1.000	.554
[Treated1nottreated0 = 1.0]* [normalisedslidenumber = 1]	.170	.307	.554	1.000
[Treated1nottreated0 = 1.0]* [normalisedslidenumber = 2]	.094	.170	.307	.554
[Treated1nottreated0 = 1.0]* [normalisedslidenumber = 3]	.052	.094	.170	.307

Working Correlation Matrix[a]

Measurement	Measurement			
	[Treated1nottreated0 = 1.0] * [normalisedslidenumber = 2]	[Treated1nottreated0 = 1.0] * [normalisedslidenumber = 3]	[Treated1nottreated0 = 1.0] * [normalisedslidenumber = 4]	[Treated1nottreated0 = 1.0] * [normalisedslidenumber = 5]
[Treated1nottreated0 = .0]* [normalisedslidenumber = 1]	.009	.005	.003	.002
[Treated1nottreated0 = .0]* [normalisedslidenumber = 2]	.016	.009	.005	.003
[Treated1nottreated0 = .0]* [normalisedslidenumber = 3]	.029	.016	.009	.005
[Treated1nottreated0 = .0]* [normalisedslidenumber = 4]	.052	.029	.016	.009
[Treated1nottreated0 = .0]* [normalisedslidenumber = 5]	.094	.052	.029	.016
[Treated1nottreated0 = .0]* [normalisedslidenumber = 6]	.170	.094	.052	.029
[Treated1nottreated0 = .0]* [normalisedslidenumber = 7]	.307	.170	.094	.052
[Treated1nottreated0 = 1.0]* [normalisedslidenumber = 1]	.554	.307	.170	.094
[Treated1nottreated0 = 1.0]* [normalisedslidenumber = 2]	1.000	.554	.307	.170
[Treated1nottreated0 = 1.0]* [normalisedslidenumber = 3]	.554	1.000	.554	.307

Working Correlation Matrix[a]

Measurement	Measurement	
	[Treated1nottreated0 = 1.0] * [normalisedslidenumber = 6]	[Treated1nottreated0 = 1.0] * [normalisedslidenumber = 7]
[Treated1nottreated0 = .0]* [normalisedslidenumber = 1]	.001	.000
[Treated1nottreated0 = .0]* [normalisedslidenumber = 2]	.002	.001
[Treated1nottreated0 = .0]* [normalisedslidenumber = 3]	.003	.002
[Treated1nottreated0 = .0]* [normalisedslidenumber = 4]	.005	.003
[Treated1nottreated0 = .0]* [normalisedslidenumber = 5]	.009	.005
[Treated1nottreated0 = .0]* [normalisedslidenumber = 6]	.016	.009
[Treated1nottreated0 = .0]* [normalisedslidenumber = 7]	.029	.016
[Treated1nottreated0 = 1.0]* [normalisedslidenumber = 1]	.052	.029
[Treated1nottreated0 = 1.0]* [normalisedslidenumber = 2]	.094	.052
[Treated1nottreated0 = 1.0]* [normalisedslidenumber = 3]	.170	.094

Working Correlation Matrix[a]

Measurement	Measurement			
	[Treated1nottreated0 = .0]* [normalisedslidenumber = 1]	[Treated1nottreated0 = .0]* [normalisedslidenumber = 2]	[Treated1nottreated0 = .0]* [normalisedslidenumber = 3]	[Treated1nottreated0 = .0]* [normalisedslidenumber = 4]
[Treated1nottreated0 = 1.0]* [normalisedslidenumber = 4]	.003	.005	.009	.016
[Treated1nottreated0 = 1.0]* [normalisedslidenumber = 5]	.002	.003	.005	.009
[Treated1nottreated0 = 1.0]* [normalisedslidenumber = 6]	.001	.002	.003	.005
[Treated1nottreated0 = 1.0]* [normalisedslidenumber = 7]	.000	.001	.002	.003

Working Correlation Matrix[a]

Measurement	Measurement			
	[Treated1nottreated0 = .0]* [normalisedslidenumber = 5]	[Treated1nottreated0 = .0]* [normalisedslidenumber = 6]	[Treated1nottreated0 = .0]* [normalisedslidenumber = 7]	[Treated1nottreated0 = 1.0]* [normalisedslidenumber = 1]
[Treated1nottreated0 = 1.0]* [normalisedslidenumber = 4]	.029	.052	.094	.170
[Treated1nottreated0 = 1.0]* [normalisedslidenumber = 5]	.016	.029	.052	.094
[Treated1nottreated0 = 1.0]* [normalisedslidenumber = 6]	.009	.016	.029	.052
[Treated1nottreated0 = 1.0]* [normalisedslidenumber = 7]	.005	.009	.016	.029

Working Correlation Matrix[a]

Measurement	Measurement			
	[Treated1nottreated0 = 1.0] * [normalisedslidenumber = 2]	[Treated1nottreated0 = 1.0] * [normalisedslidenumber = 3]	[Treated1nottreated0 = 1.0] * [normalisedslidenumber = 4]	[Treated1nottreated0 = 1.0] * [normalisedslidenumber = 5]
[Treated1nottreated0 = 1.0]* [normalisedslidenumber = 4]	.307	.554	1.000	.554
[Treated1nottreated0 = 1.0]* [normalisedslidenumber = 5]	.170	.307	.554	1.000
[Treated1nottreated0 = 1.0]* [normalisedslidenumber = 6]	.094	.170	.307	.554
[Treated1nottreated0 = 1.0]* [normalisedslidenumber = 7]	.052	.094	.170	.307

Working Correlation Matrix[a]

Measurement	Measurement	
	[Treated1nottreated0 = 1.0] * [normalisedslidenumber = 6]	[Treated1nottreated0 = 1.0] * [normalisedslidenumber = 7]
[Treated1nottreated0 = 1.0]* [normalisedslidenumber = 4]	.307	.170
[Treated1nottreated0 = 1.0]* [normalisedslidenumber = 5]	.554	.307
[Treated1nottreated0 = 1.0]* [normalisedslidenumber = 6]	1.000	.554
[Treated1nottreated0 = 1.0]* [normalisedslidenumber = 7]	.554	1.000

Dependent Variable: AvgONLthickness
Model: (Intercept), Treated1nottreated0, normalisedslidenumber, Treated1nottreated0 * normalisedslidenumber

a. The AR(1) working correlation matrix structure is computed assuming the measurements are equally spaced for all subjects.

Estimated Marginal Means 1: Treated1nottreated0

Estimates

Treated1nottreated0	Mean	Std. Error	95% Wald Confidence Interval	
			Lower	Upper
.0	69.85950532	4.112606223	62.24658782	78.40350217
1.0	67.28871774	1.912681035	63.64244535	71.14389636

Estimated Marginal Means 2: normalisedslidenumber

Estimates

normalisedslidenumber	Mean	Std. Error	95% Wald Confidence Interval	
			Lower	Upper
1	88.05663912	5.944779439	77.14304144	100.5142077
2	68.90674295	2.568269231	64.05249057	74.12887744
3	61.92577866	2.330846939	57.52184284	66.66688466
4	58.43305501	2.075539455	54.50344488	62.64598366
5	60.58101806	3.188380674	54.64341162	67.16381062
6	65.43657841	5.298489468	55.83385658	76.69084775
7	81.82313362	5.509295251	71.70727410	93.36605358

Estimated Marginal Means 3: Treated1nottreated0* normalisedslide number

Estimates

Treated1nottreated0	normalisedslidenumber	Mean	Std. Error	95% Wald ... Lower
.0	1	87.83600910	7.734649320	73.91245454
	2	75.08609738	6.588595422	63.22210814
	3	64.23233662	6.010611476	53.46894330
	4	60.96729483	4.531685000	52.70202596
	5	59.55281837	3.962682303	52.27124317
	6	63.62614070	3.993716958	56.26093476
	7	82.97702642	6.480948218	71.19909739
1.0	1	88.27782333	9.435468440	71.59323193
	2	63.23593034	4.346846787	55.26525751
	3	59.70204828	4.100323017	52.18298330
	4	56.00415644	1.942663635	52.32315348
	5	61.62696996	2.487782598	56.93891208
	6	67.29853088	8.069474740	53.20368349
	7	80.68528705	7.600407484	67.08303596

Estimates

Treated1nottreated0	normalisedslidenumber	95% Wald ... Upper
.0	1	104.3824690
	2	89.17643188
	3	77.16242016
	4	70.52880742
	5	67.84874362
	6	71.95553714
	7	96.70328932
1.0	1	108.8507095
	2	72.35617937
	3	68.30453806
	4	59.94412281
	5	66.70101848
	6	85.12741903
	7	97.04563088

```
 * Generalized Estimating Equations.
GENLIN AvgONLthickness BY Treated1nottreated0 normalisedslidenumber (ORDEI
  /MODEL Treated1nottreated0 normalisedslidenumber INTERCEPT=YES
 DISTRIBUTION=GAMMA LINK=LOG
  /CRITERIA METHOD=FISHER(1) SCALE=MLE MAXITERATIONS=100 MAXSTEPHALVING=5
  /EMMEANS TABLES=Treated1nottreated0 SCALE=ORIGINAL
  /EMMEANS TABLES=normalisedslidenumber SCALE=ORIGINAL
```

```
/EMMEANS TABLES=Treated1nottreated0*normalisedslidenumber SCALE=ORIGINAI
/REPEATED SUBJECT=Animal WITHINSUBJECT=Treated1nottreated0*normalisedsli
/MISSING CLASSMISSING=EXCLUDE
/PRINT CPS DESCRIPTIVES MODELINFO FIT SUMMARY WORKINGCORR.
```

Generalized Linear Models

Notes

Output Created		26-JUL-2013 23:36:58
Comments		
Input	Active Dataset	DataSet2
	Filter	<none>
	Weight	<none>
	Split File	<none>
	N of Rows in Working Data File	112
Missing Value Handling	Definition of Missing	User-defined missing values for factor, subject and within-subject variables are treated as missing.
	Cases Used	Statistics are based on cases with valid data for all variables in the model.
Weight Handling		not applicable
Syntax		GENLIN AvgONLthickness BY Treated1nottreated0 normalisedslidenumber (ORDER=ASCENDING) /MODEL Treated1nottreated0 normalisedslidenumber INTERCEPT=YES DISTRIBUTION=GAMMA LINK=LOG /CRITERIA METHOD=FISHER(1) SCALE=MLE MAXITERATIONS=100 MAXSTEPHALVING=5 PCONVERGE=1E-006 (ABSOLUTE) SINGULAR=1E-012 ANALYSISTYPE=3(WALD) CILEVEL=95 LIKELIHOOD=FULL /EMMEANS TABLES=Treated1nottreated0 SCALE=ORIGINAL /EMMEANS TABLES=normalisedslidenumber SCALE=ORIGINAL /EMMEANS TABLES=Treated1nottreated0*normalisedslidenumber SCALE=ORIGINAL /REPEATED SUBJECT=Animal WITHINSUBJECT=Treated1nottreated0*normalisedslidenumber SORT=YES CORRTYPE=AR(1) ADJUSTCORR=YES COVB=ROBUST MAXITERATIONS=100 PCONVERGE=1e-006 (ABSOLUTE) UPDATECORR=1 /MISSING CLASSMISSING=EXCLUDE /PRINT CPS DESCRIPTIVES MODELINFO FIT SUMMARY WORKINGCORR.
Resources	Processor Time	00:00:00.31
	Elapsed Time	00:00:00.37

[DataSet2]

Model Information

Dependent Variable		AvgONLthickness
Probability Distribution		Gamma
Link Function		Log
Subject Effect	1	Animal
Within-Subject Effect	1	Treated1nottreated0
	2	normalisedslidenumber
Working Correlation Matrix Structure		AR(1)

Case Processing Summary

	N	Percent
Included	111	99.1%
Excluded	1	0.9%
Total	112	100.0%

Correlated Data Summary

Number of Levels	Subject Effect	Animal	8
	Within-Subject Effect	Treated1nottreated0	2
		normalisedslidenumber	7
Number of Subjects			8
Number of Measurements per Subject	Minimum		13
	Maximum		14
Correlation Matrix Dimension			14

Categorical Variable Information

			N	Percent
Factor	Treated1nottreated0	.0	56	50.5%
		1.0	55	49.5%
		Total	111	100.0%
	normalisedslidenumber	1	16	14.4%
		2	16	14.4%
		3	16	14.4%
		4	15	13.5%
		5	16	14.4%
		6	16	14.4%
		7	16	14.4%
		Total	111	100.0%

Continuous Variable Information

		N	Minimum	Maximum	Mean
Dependent Variable	AvgONLthickness	111	39.94070536	123.6170213	69.41941045

Continuous Variable Information

		Std. Deviation
Dependent Variable	AvgONLthickness	20.12078517

Goodness of Fit[a]

	Value
Quasi Likelihood under Independence Model Criterion (QIC)[b]	24.491
Corrected Quasi Likelihood under Independence Model Criterion (QICC)[b]	22.094

Dependent Variable: AvgONLthickness
Model: (Intercept), Treated1nottreated0, normalisedslidenumber

a. Information criteria are in small-is-better form.

b. Computed using the full log quasi-likelihood function.

Tests of Model Effects

	Type III		
Source	Wald Chi-Square	df	Sig.
(Intercept)	13584.325	1	.000
Treated1nottreated0	.160	1	.689
normalisedslidenumber	2007.383	6	.000

Dependent Variable: AvgONLthickness
Model: (Intercept), Treated1nottreated0, normalisedslidenumber

Working Correlation Matrix[a]

Measurement	Measurement			
	[Treated1nottreated0 = .0]* [normalisedslidenumber = 1]	[Treated1nottreated0 = .0]* [normalisedslidenumber = 2]	[Treated1nottreated0 = .0]* [normalisedslidenumber = 3]	[Treated1nottreated0 = .0]* [normalisedslidenumber = 4]
[Treated1nottreated0 = .0]* [normalisedslidenumber = 1]	1.000	.542	.294	.159
[Treated1nottreated0 = .0]* [normalisedslidenumber = 2]	.542	1.000	.542	.294
[Treated1nottreated0 = .0]* [normalisedslidenumber = 3]	.294	.542	1.000	.542
[Treated1nottreated0 = .0]* [normalisedslidenumber = 4]	.159	.294	.542	1.000
[Treated1nottreated0 = .0]* [normalisedslidenumber = 5]	.086	.159	.294	.542
[Treated1nottreated0 = .0]* [normalisedslidenumber = 6]	.047	.086	.159	.294
[Treated1nottreated0 = .0]* [normalisedslidenumber = 7]	.025	.047	.086	.159
[Treated1nottreated0 = 1.0]* [normalisedslidenumber = 1]	.014	.025	.047	.086
[Treated1nottreated0 = 1.0]* [normalisedslidenumber = 2]	.007	.014	.025	.047
[Treated1nottreated0 = 1.0]* [normalisedslidenumber = 3]	.004	.007	.014	.025

Working Correlation Matrix[a]

Measurement	Measurement			
	[Treated1nottreated0 = .0]* [normalisedslidenumber = 5]	[Treated1nottreated0 = .0]* [normalisedslidenumber = 6]	[Treated1nottreated0 = .0]* [normalisedslidenumber = 7]	[Treated1nottreated0 = 1.0] * [normalisedslidenumber = 1]
[Treated1nottreated0 = .0]* [normalisedslidenumber = 1]	.086	.047	.025	.014
[Treated1nottreated0 = .0]* [normalisedslidenumber = 2]	.159	.086	.047	.025
[Treated1nottreated0 = .0]* [normalisedslidenumber = 3]	.294	.159	.086	.047
[Treated1nottreated0 = .0]* [normalisedslidenumber = 4]	.542	.294	.159	.086
[Treated1nottreated0 = .0]* [normalisedslidenumber = 5]	1.000	.542	.294	.159
[Treated1nottreated0 = .0]* [normalisedslidenumber = 6]	.542	1.000	.542	.294
[Treated1nottreated0 = .0]* [normalisedslidenumber = 7]	.294	.542	1.000	.542
[Treated1nottreated0 = 1.0]* [normalisedslidenumber = 1]	.159	.294	.542	1.000
[Treated1nottreated0 = 1.0]* [normalisedslidenumber = 2]	.086	.159	.294	.542
[Treated1nottreated0 = 1.0]* [normalisedslidenumber = 3]	.047	.086	.159	.294

Working Correlation Matrix[a]

Measurement	Measurement			
	[Treated1nottreated0 = 1.0] * [normalisedslidenumber = 2]	[Treated1nottreated0 = 1.0] * [normalisedslidenumber = 3]	[Treated1nottreated0 = 1.0] * [normalisedslidenumber = 4]	[Treated1nottreated0 = 1.0] * [normalisedslidenumber = 5]
[Treated1nottreated0 = .0]* [normalisedslidenumber = 1]	.007	.004	.002	.001
[Treated1nottreated0 = .0]* [normalisedslidenumber = 2]	.014	.007	.004	.002
[Treated1nottreated0 = .0]* [normalisedslidenumber = 3]	.025	.014	.007	.004
[Treated1nottreated0 = .0]* [normalisedslidenumber = 4]	.047	.025	.014	.007
[Treated1nottreated0 = .0]* [normalisedslidenumber = 5]	.086	.047	.025	.014
[Treated1nottreated0 = .0]* [normalisedslidenumber = 6]	.159	.086	.047	.025
[Treated1nottreated0 = .0]* [normalisedslidenumber = 7]	.294	.159	.086	.047
[Treated1nottreated0 = 1.0]* [normalisedslidenumber = 1]	.542	.294	.159	.086
[Treated1nottreated0 = 1.0]* [normalisedslidenumber = 2]	1.000	.542	.294	.159
[Treated1nottreated0 = 1.0]* [normalisedslidenumber = 3]	.542	1.000	.542	.294

Working Correlation Matrix[a]

Measurement	Measurement	
	[Treated1nottreated0 = 1.0] * [normalisedslidenumber = 6]	[Treated1nottreated0 = 1.0] * [normalisedslidenumber = 7]
[Treated1nottreated0 = .0]* [normalisedslidenumber = 1]	.001	.000
[Treated1nottreated0 = .0]* [normalisedslidenumber = 2]	.001	.001
[Treated1nottreated0 = .0]* [normalisedslidenumber = 3]	.002	.001
[Treated1nottreated0 = .0]* [normalisedslidenumber = 4]	.004	.002
[Treated1nottreated0 = .0]* [normalisedslidenumber = 5]	.007	.004
[Treated1nottreated0 = .0]* [normalisedslidenumber = 6]	.014	.007
[Treated1nottreated0 = .0]* [normalisedslidenumber = 7]	.025	.014
[Treated1nottreated0 = 1.0]* [normalisedslidenumber = 1]	.047	.025
[Treated1nottreated0 = 1.0]* [normalisedslidenumber = 2]	.086	.047
[Treated1nottreated0 = 1.0]* [normalisedslidenumber = 3]	.159	.086

Working Correlation Matrix[a]

Measurement	Measurement			
	[Treated1nottreated0 = .0]* [normalisedslidenumber = 1]	[Treated1nottreated0 = .0]* [normalisedslidenumber = 2]	[Treated1nottreated0 = .0]* [normalisedslidenumber = 3]	[Treated1nottreated0 = .0]* [normalisedslidenumber = 4]
[Treated1nottreated0 = 1.0]* [normalisedslidenumber = 4]	.002	.004	.007	.014
[Treated1nottreated0 = 1.0]* [normalisedslidenumber = 5]	.001	.002	.004	.007
[Treated1nottreated0 = 1.0]* [normalisedslidenumber = 6]	.001	.001	.002	.004
[Treated1nottreated0 = 1.0]* [normalisedslidenumber = 7]	.000	.001	.001	.002

Working Correlation Matrix[a]

Measurement	Measurement			
	[Treated1nottreated0 = .0]* [normalisedslidenumber = 5]	[Treated1nottreated0 = .0]* [normalisedslidenumber = 6]	[Treated1nottreated0 = .0]* [normalisedslidenumber = 7]	[Treated1nottreated0 = 1.0]* [normalisedslidenumber = 1]
[Treated1nottreated0 = 1.0]* [normalisedslidenumber = 4]	.025	.047	.086	.159
[Treated1nottreated0 = 1.0]* [normalisedslidenumber = 5]	.014	.025	.047	.086
[Treated1nottreated0 = 1.0]* [normalisedslidenumber = 6]	.007	.014	.025	.047
[Treated1nottreated0 = 1.0]* [normalisedslidenumber = 7]	.004	.007	.014	.025

Working Correlation Matrix[a]

Measurement	Measurement			
	[Treated1nottreated0 = 1.0] * [normalisedslidenumber = 2]	[Treated1nottreated0 = 1.0] * [normalisedslidenumber = 3]	[Treated1nottreated0 = 1.0] * [normalisedslidenumber = 4]	[Treated1nottreated0 = 1.0] * [normalisedslidenumber = 5]
[Treated1nottreated0 = 1.0]* [normalisedslidenumber = 4]	.294	.542	1.000	.542
[Treated1nottreated0 = 1.0]* [normalisedslidenumber = 5]	.159	.294	.542	1.000
[Treated1nottreated0 = 1.0]* [normalisedslidenumber = 6]	.086	.159	.294	.542
[Treated1nottreated0 = 1.0]* [normalisedslidenumber = 7]	.047	.086	.159	.294

Working Correlation Matrix[a]

Measurement	Measurement	
	[Treated1nottreated0 = 1.0] * [normalisedslidenumber = 6]	[Treated1nottreated0 = 1.0] * [normalisedslidenumber = 7]
[Treated1nottreated0 = 1.0]* [normalisedslidenumber = 4]	.294	.159
[Treated1nottreated0 = 1.0]* [normalisedslidenumber = 5]	.542	.294
[Treated1nottreated0 = 1.0]* [normalisedslidenumber = 6]	1.000	.542
[Treated1nottreated0 = 1.0]* [normalisedslidenumber = 7]	.542	1.000

Dependent Variable: AvgONLthickness
Model: (Intercept), Treated1nottreated0, normalisedslidenumber

a. The AR(1) working correlation matrix structure is computed assuming the measurements are equally spaced for all subjects.

Estimated Marginal Means 1: Treated1nottreated0

Estimates

Treated1nottreated0	Mean	Std. Error	95% Wald Confidence Interval	
			Lower	Upper
.0	69.46610242	4.302361785	61.52534042	78.43173808
1.0	67.65685973	2.110143327	63.64492701	71.92168934

Estimated Marginal Means 2: normalisedslidenumber

Estimates

normalisedslidenumber	Mean	Std. Error	95% Wald Confidence Interval	
			Lower	Upper
1	88.14746073	5.436683852	78.11062696	99.47397857
2	69.11241924	2.701752167	64.01486118	74.61590019
3	61.93692772	2.497201673	57.23089293	67.02993469
4	58.55154001	2.297248294	54.21778119	63.23170669
5	60.53309176	3.300297963	54.39824302	67.35980786
6	65.33389186	5.629503867	55.18164337	77.35393809
7	81.45381344	5.655572615	71.09025131	93.32817935

Estimated Marginal Means 3: Treated1nottreated0* normalisedslide number

Estimates

Treated1nottreated0	normalisedslidenumber	Mean	Std. Error	95% Wald ...
				Lower
.0	1	89.31828057	6.104277112	78.12080455
	2	70.03040588	4.703267374	61.39311085
	3	62.75960581	4.159313716	55.11475719
	4	59.32925163	3.695102932	52.51156133
	5	61.33712337	4.976595353	52.31919560
	6	66.20169016	6.614576600	54.42780606
	7	82.53572482	7.070178987	69.77925117
1.0	1	86.99198846	6.221369552	75.61435193
	2	68.20646593	1.834131442	64.70472481
	3	61.12503363	1.967610177	57.38772364
	4	57.78402294	2.144243289	53.73057389
	5	59.73959972	2.343830833	55.31796075
	6	64.47746900	5.411113132	54.69819355
	7	80.38608419	5.381129809	70.50185413

Estimates

Treated1nottreated0	normalisedslidenumber	95% Wald ... Upper
.0	1	102.1207512
	2	79.88286764
	3	71.46485482
	4	67.03209750
	5	71.90941413
	6	80.52251409
	7	97.62423296
1.0	1	100.0816097
	2	71.89771702
	3	65.10573167
	4	62.14326528
	5	64.51466623
	6	76.00514275
	7	91.65606508

APPENDIX 16

```
 DATASET ACTIVATE DataSet3.
DATASET CLOSE DataSet4.
GET DATA /TYPE=XLSX
  /FILE='C:\Users\Public\Documents\PhD\ERG\Results\U-CEM423-43\U - ERG Nur
  /SHEET=name 'Sheet1'
  /CELLRANGE=full
  /READNAMES=on
  /ASSUMEDSTRWIDTH=32767.
EXECUTE.
DATASET NAME DataSet5 WINDOW=FRONT.
* Generalized Estimating Equations.
GENLIN awaveamplitudev BY timepointdays flashintensitymcd Treated1casp6DN
  /MODEL timepointdays flashintensitymcd Treated1casp6DN0pen1 timepointday
 DISTRIBUTION=GAMMA LINK=LOG
  /CRITERIA METHOD=FISHER(1) SCALE=MLE MAXITERATIONS=100 MAXSTEPHALVING=5
  /EMMEANS TABLES=Treated1casp6DN0pen1 SCALE=ORIGINAL
  /EMMEANS TABLES=timepointdays*flashintensitymcd*Treated1casp6DN0pen1 SCA
  /REPEATED SUBJECT=animal WITHINSUBJECT=Treated1casp6DN0pen1*timepointday
  /MISSING CLASSMISSING=EXCLUDE
  /PRINT CPS DESCRIPTIVES MODELINFO FIT SUMMARY WORKINGCORR.
```

Generalized Linear Models

Notes

Output Created		27-JUL-2013 00:23:26
Comments		
Input	Active Dataset	DataSet5
	Filter	<none>
	Weight	<none>
	Split File	<none>
	N of Rows in Working Data File	315
Missing Value Handling	Definition of Missing	User-defined missing values for factor, subject and within-subject variables are treated as missing.
	Cases Used	Statistics are based on cases with valid data for all variables in the model.
Weight Handling		not applicable
Syntax		GENLIN awaveamplitudev BY timepointdays flashintensitymcd Treated1casp6DN0pen1 (ORDER=ASCENDING) /MODEL timepointdays flashintensitymcd Treated1casp6DN0pen1 timepointdays*flashintensitymcd timepointdays*Treated1casp6DN0pen1 flashintensitymcd*Treated1casp6DN0pen1 timepointdays*flashintensitymcd*Treated1casp6DN0pen1 INTERCEPT=YES DISTRIBUTION=GAMMA LINK=LOG /CRITERIA METHOD=FISHER(1) SCALE=MLE MAXITERATIONS=100 MAXSTEPHALVING=5 PCONVERGE=1E-006 (ABSOLUTE) SINGULAR=1E-012 ANALYSISTYPE=3(WALD) CILEVEL=95 LIKELIHOOD=FULL /EMMEANS TABLES=Treated1casp6DN0pen1 SCALE=ORIGINAL /EMMEANS TABLES=timepointdays*flashintensitymcd*Treated1casp6DN0pen1 SCALE=ORIGINAL /REPEATED SUBJECT=animal WITHINSUBJECT=Treated1casp6DN0pen1*timepointdays*flashintensitymcd SORT=YES CORRTYPE=AR(1) ADJUSTCORR=YES COVB=ROBUST MAXITERATIONS=100 PCONVERGE=1e-006(ABSOLUTE) UPDATECORR=1 /MISSING CLASSMISSING=EXCLUDE /PRINT CPS DESCRIPTIVES MODELINFO FIT SUMMARY WORKINGCORR.
Resources	Processor Time	00:00:00.72
	Elapsed Time	00:00:00.68

[DataSet5]

Warnings

One or more cases were found with dependent variable data values that are less than or equal to zero. These values are invalid for the gamma probability distribution, and the cases are not used in the analysis.

Model Information

Dependent Variable		awaveamplitudev
Probability Distribution		Gamma
Link Function		Log
Subject Effect	1	animal
Within-Subject Effect	1	Treated1casp6DN0pen1
	2	timepointdays
	3	flashintensitymcd
Working Correlation Matrix Structure		AR(1)

Case Processing Summary

	N	Percent
Included	222	70.5%
Excluded	93	29.5%
Total	315	100.0%

Correlated Data Summary

Number of Levels	Subject Effect	animal	8
	Within-Subject Effect	Treated1casp6DN0pen1	2
		timepointdays	2
		flashintensitymcd	8
Number of Subjects			8
Number of Measurements per Subject	Minimum		16
	Maximum		32
Correlation Matrix Dimension			32

Categorical Variable Information

			N	Percent
Factor	timepointdays	7.0	125	56.3%
		14.0	97	43.7%
		Total	222	100.0%
	flashintensitymcd	10.0	29	13.1%
		30.0	29	13.1%
		100.0	28	12.6%
		300.0	27	12.2%
		1000.0	27	12.2%
		3000.0	27	12.2%
		10000.0	27	12.2%
		25000.0	28	12.6%
		Total	222	100.0%
	Treated1casp6DN0pen1	.0	112	50.5%
		1.0	110	49.5%
		Total	222	100.0%

Continuous Variable Information

		N	Minimum	Maximum	Mean
Dependent Variable	awaveamplitudev	222	.1	251.5	76.893

Continuous Variable Information

		Std. Deviation
Dependent Variable	awaveamplitudev	64.5519

Goodness of Fit[a]

	Value
Quasi Likelihood under Independence Model Criterion (QIC)[b]	126.584
Corrected Quasi Likelihood under Independence Model Criterion (QICC)[b]	139.601

Dependent Variable: awaveamplitudev
Model: (Intercept), timepointdays, flashintensitymcd, Treated1casp6DN0pen1, timepointdays * flashintensitymcd, timepointdays * Treated1casp6DN0pen1, flashintensitymcd * Treated1casp6DN0pen1, timepointdays * flashintensitymcd * Treated1casp6DN0pen1

a. Information criteria are in small-is-better form.

b. Computed using the full log quasi-likelihood function.

Tests of Model Effects

Source	Type III		
	Wald Chi-Square	df	Sig.
(Intercept)	3872.703	1	.000
timepointdays	4.613	1	.032
flashintensitymcd	71302.045	7	.000
Treated1casp6DN0pen1	.070	1	.791
timepointdays * flashintensitymcd	138.081	7	.000
timepointdays * Treated1casp6DN0pen1	.252	1	.616
flashintensitymcd * Treated1casp6DN0pen1	46.727	7	.000
timepointdays * flashintensitymcd * Treated1casp6DN0pen1	177.273	7	.000

Dependent Variable: awaveamplitudev
Model: (Intercept), timepointdays, flashintensitymcd, Treated1casp6DN0pen1, timepointdays * flashintensitymcd, timepointdays * Treated1casp6DN0pen1, flashintensitymcd * Treated1casp6DN0pen1, timepointdays * flashintensitymcd * Treated1casp6DN0pen1

Estimated Marginal Means 1: Treated1casp6DN0pen1

Estimates

Treated1casp6DN0pen1	Mean	Std. Error	95% Wald Confidence Interval	
			Lower	Upper
.0	49.171	4.6669	40.824	59.224
1.0	47.481	4.1101	40.072	56.260

Estimated Marginal Means 2: timepointdays* flashintensitymcd* Treated1casp6DN0pen1

Estimates

timepointdays	flashintensitymcd	Treated1casp6DN0pen1	Mean	Std. Error	95% Wald ...
					Lower
7.0	10.0	.0	2.190	.8084	1.062
		1.0	2.388	.8034	1.235
	30.0	.0	9.304	2.6850	5.285
		1.0	9.013	1.5275	6.465
	100.0	.0	24.888	6.0880	15.408
		1.0	26.100	4.6984	18.341
	300.0	.0	80.038	15.1649	55.210
		1.0	67.535	5.7025	57.234
	1000.0	.0	98.800	17.1216	70.347
		1.0	85.238	9.4596	68.575
	3000.0	.0	117.538	21.3811	82.288
		1.0	104.113	8.3963	88.891
	10000.0	.0	150.500	25.0738	108.573
		1.0	124.338	11.2748	104.092
	25000.0	.0	153.213	26.7164	108.859
		1.0	126.000	11.3302	105.640
14.0	10.0	.0	3.378	.8886	2.018
		1.0	8.094	1.4520	5.695
	30.0	.0	16.942	3.2639	11.614
		1.0	12.298	2.6421	8.072
	100.0	.0	50.711	8.8159	36.069
		1.0	57.188	13.5872	35.898
	300.0	.0	89.263	12.4667	67.887
		1.0	77.630	15.3078	52.745
	1000.0	.0	107.010	14.2224	82.470
		1.0	98.067	16.5810	70.405
	3000.0	.0	127.873	17.5226	97.755
		1.0	122.410	19.0877	90.176
	10000.0	.0	161.708	22.3359	123.356
		1.0	149.160	19.1002	116.052

Estimates

timepointdays	flashintensitymcd	Treated1casp6DN0pen1	95% Wald ... Upper
7.0	10.0	.0	4.515
		1.0	4.617
	30.0	.0	16.380
		1.0	12.564
	100.0	.0	40.198
		1.0	37.142
	300.0	.0	116.031
		1.0	79.690
	1000.0	.0	138.761
		1.0	105.949
	3000.0	.0	167.887
		1.0	121.941
	10000.0	.0	208.617
		1.0	148.521
	25000.0	.0	215.637
		1.0	150.284
14.0	10.0	.0	5.657
		1.0	11.505
	30.0	.0	24.714
		1.0	18.738
	100.0	.0	71.299
		1.0	91.105
	300.0	.0	117.368
		1.0	114.256
	1000.0	.0	138.853
		1.0	136.598
	3000.0	.0	167.271
		1.0	166.168
	10000.0	.0	211.985
		1.0	191.712

Estimates

timepointdays	flashintensitymcd	Treated1casp6DN0pen1	Mean	Std. Error	95% Wald ... Lower
	25000.0	.0	187.437	35.5042	129.307
		1.0	159.912	22.5498	121.297

Estimates

timepointdays	flashintensitymcd	Treated1casp6DN0pen1	95% Wald ... Upper
	25000.0	.0	271.700
		1.0	210.820

APPENDIX 17

```
 GET DATA /TYPE=XLSX
  /FILE='C:\Users\Public\Documents\PhD\ERG\Results\U-CEM423-43\U - ERG Nur
  /SHEET=name 'photopic numbers'
  /CELLRANGE=full
  /READNAMES=on
  /ASSUMEDSTRWIDTH=32767.
EXECUTE.
DATASET NAME DataSet1 WINDOW=FRONT.
SORT CASES BY awaveamplitudev(A).
* Generalized Estimating Equations.
GENLIN bwaveamplitudev BY timepointdays flashintensitymcd Treated1casp6DN
  /MODEL timepointdays flashintensitymcd Treated1casp6DN0pen1 timepointday
 DISTRIBUTION=GAMMA LINK=LOG
  /CRITERIA METHOD=FISHER(1) SCALE=MLE MAXITERATIONS=100 MAXSTEPHALVING=5
  /EMMEANS TABLES=Treated1casp6DN0pen1 SCALE=ORIGINAL
  /EMMEANS TABLES=timepointdays*flashintensitymcd*Treated1casp6DN0pen1 SCA
  /REPEATED SUBJECT=animal WITHINSUBJECT=Treated1casp6DN0pen1*timepointday
  /MISSING CLASSMISSING=EXCLUDE
  /PRINT CPS DESCRIPTIVES MODELINFO FIT SUMMARY WORKINGCORR.
```

Generalized Linear Models

Notes

Output Created		27-JUL-2013 00:51:47
Comments		
Input	Active Dataset	DataSet1
	Filter	<none>
	Weight	<none>
	Split File	<none>
	N of Rows in Working Data File	72
Missing Value Handling	Definition of Missing	User-defined missing values for factor, subject and within-subject variables are treated as missing.
	Cases Used	Statistics are based on cases with valid data for all variables in the model.
Weight Handling		not applicable
Syntax		GENLIN bwaveamplitudev BY timepointdays flashintensitymcd Treated1casp6DN0pen1 (ORDER=ASCENDING) /MODEL timepointdays flashintensitymcd Treated1casp6DN0pen1 timepointdays*flashintensitymcd timepointdays*Treated1casp6DN0pen1 flashintensitymcd*Treated1casp6DN0pen1 timepointdays*flashintensitymcd*Treated1casp6DN0pen1 INTERCEPT=YES DISTRIBUTION=GAMMA LINK=LOG /CRITERIA METHOD=FISHER(1) SCALE=MLE MAXITERATIONS=100 MAXSTEPHALVING=5 PCONVERGE=1E-006 (ABSOLUTE) SINGULAR=1E-012 ANALYSISTYPE=3(WALD) CILEVEL=95 LIKELIHOOD=FULL /EMMEANS TABLES=Treated1casp6DN0pen1 SCALE=ORIGINAL /EMMEANS TABLES=timepointdays*flashintensitymcd*Treated1casp6DN0pen1 SCALE=ORIGINAL /REPEATED SUBJECT=animal WITHINSUBJECT=Treated1casp6DN0pen1*timepointdays*flashintensitymcd SORT=YES CORRTYPE=AR(1) ADJUSTCORR=YES COVB=ROBUST MAXITERATIONS=100 PCONVERGE=1e-006(ABSOLUTE) UPDATECORR=1 /MISSING CLASSMISSING=EXCLUDE /PRINT CPS DESCRIPTIVES MODELINFO FIT SUMMARY WORKINGCORR.
Resources	Processor Time	00:00:00.39
	Elapsed Time	00:00:00.40

[DataSet1]

Model Information

Dependent Variable		bwaveamplitudev
Probability Distribution		Gamma
Link Function		Log
Subject Effect	1	animal
Within-Subject Effect	1	Treated1casp6DN0pen1
	2	timepointdays
	3	flashintensitymcd
Working Correlation Matrix Structure		AR(1)

Case Processing Summary

	N	Percent
Included	72	100.0%
Excluded	0	0.0%
Total	72	100.0%

Correlated Data Summary

Number of Levels	Subject Effect	animal	8
	Within-Subject Effect	Treated1casp6DN0pen1	2
		timepointdays	2
		flashintensitymcd	5
Number of Subjects			8
Number of Measurements per Subject	Minimum		3
	Maximum		14
Correlation Matrix Dimension			20

Categorical Variable Information

			N	Percent
Factor	timepointdays	7.0	34	47.2%
		14.0	38	52.8%
		Total	72	100.0%
	flashintensitymcd	300.0	9	12.5%
		1000.0	16	22.2%
		3000.0	17	23.6%
		10000.0	16	22.2%
		25000.0	14	19.4%
		Total	72	100.0%
	Treated1casp6DN0pen1	.0	31	43.1%
		1.0	41	56.9%
		Total	72	100.0%

Continuous Variable Information

		N	Minimum	Maximum	Mean
Dependent Variable	bwaveamplitudev	72	5.9	135.8	52.056

Continuous Variable Information

		Std. Deviation
Dependent Variable	bwaveamplitudev	34.4985

Goodness of Fit[a]

	Value
Quasi Likelihood under Independence Model Criterion (QIC)[b]	42.773
Corrected Quasi Likelihood under Independence Model Criterion (QICC)[b]	50.979

Dependent Variable: bwaveamplitudev
Model: (Intercept), timepointdays, flashintensitymcd, Treated1casp6DN0pen1, timepointdays * flashintensitymcd, timepointdays * Treated1casp6DN0pen1, flashintensitymcd * Treated1casp6DN0pen1, timepointdays * flashintensitymcd * Treated1casp6DN0pen1

a. Information criteria are in small-is-better form.

b. Computed using the full log quasi-likelihood function.

Tests of Model Effects

Source	Type III		
	Wald Chi-Square	df	Sig.
(Intercept)	1004.472	1	.000
timepointdays	17.688	1	.000
flashintensitymcd	1547.191	4	.000
Treated1casp6DN0pen1	.523	1	.469
timepointdays * flashintensitymcd	16.279	4	.003
timepointdays * Treated1casp6DN0pen1	.855	1	.355
flashintensitymcd * Treated1casp6DN0pen1	18.163	4	.001
timepointdays * flashintensitymcd * Treated1casp6DN0pen1	5.375	4	.251

Dependent Variable: bwaveamplitudev
Model: (Intercept), timepointdays, flashintensitymcd, Treated1casp6DN0pen1, timepointdays * flashintensitymcd, timepointdays * Treated1casp6DN0pen1, flashintensitymcd * Treated1casp6DN0pen1, timepointdays * flashintensitymcd * Treated1casp6DN0pen1

```
 * Generalized Estimating Equations.
GENLIN bwaveamplitudev BY timepointdays flashintensitymcd Treated1casp6DN
  /MODEL timepointdays flashintensitymcd Treated1casp6DN0pen1 timepointday
 DISTRIBUTION=GAMMA LINK=LOG
  /CRITERIA METHOD=FISHER(1) SCALE=MLE MAXITERATIONS=100 MAXSTEPHALVING=5
  /EMMEANS TABLES=Treated1casp6DN0pen1 SCALE=ORIGINAL
  /EMMEANS TABLES=timepointdays*flashintensitymcd*Treated1casp6DN0pen1 SCA
  /REPEATED SUBJECT=animal WITHINSUBJECT=Treated1casp6DN0pen1*timepointday
(ABSOLUTE) UPDATECORR=1
  /MISSING CLASSMISSING=EXCLUDE
  /PRINT CPS DESCRIPTIVES MODELINFO FIT SUMMARY WORKINGCORR.
```

Generalized Linear Models

Notes

Output Created		27-JUL-2013 00:52:07
Comments		
Input	Active Dataset	DataSet1
	Filter	<none>
	Weight	<none>
	Split File	<none>
	N of Rows in Working Data File	72
Missing Value Handling	Definition of Missing	User-defined missing values for factor, subject and within-subject variables are treated as missing.
	Cases Used	Statistics are based on cases with valid data for all variables in the model.
Weight Handling		not applicable
Syntax		GENLIN bwaveamplitudev BY timepointdays flashintensitymcd Treated1casp6DN0pen1 (ORDER=ASCENDING) /MODEL timepointdays flashintensitymcd Treated1casp6DN0pen1 timepointdays*flashintensitymcd timepointdays*Treated1casp6DN0pen1 flashintensitymcd*Treated1casp6DN0pen1 INTERCEPT=YES DISTRIBUTION=GAMMA LINK=LOG /CRITERIA METHOD=FISHER(1) SCALE=MLE MAXITERATIONS=100 MAXSTEPHALVING=5 PCONVERGE=1E-006 (ABSOLUTE) SINGULAR=1E-012 ANALYSISTYPE=3(WALD) CILEVEL=95 LIKELIHOOD=FULL /EMMEANS TABLES=Treated1casp6DN0pen1 SCALE=ORIGINAL /EMMEANS TABLES=timepointdays*flashintensitymcd*Treated1casp6DN0pen1 SCALE=ORIGINAL /REPEATED SUBJECT=animal WITHINSUBJECT=Treated1casp6DN0pen1*timepointdays*flashintensitymcd SORT=YES CORRTYPE=AR(1) ADJUSTCORR=YES COVB=ROBUST MAXITERATIONS=100 PCONVERGE=1e-006(ABSOLUTE) UPDATECORR=1 /MISSING CLASSMISSING=EXCLUDE /PRINT CPS DESCRIPTIVES MODELINFO FIT SUMMARY WORKINGCORR.
Resources	Processor Time	00:00:00.34
	Elapsed Time	00:00:00.34

[DataSet1]

Model Information

Dependent Variable		bwaveamplitudev
Probability Distribution		Gamma
Link Function		Log
Subject Effect	1	animal
Within-Subject Effect	1	Treated1casp6DN0pen1
	2	timepointdays
	3	flashintensitymcd
Working Correlation Matrix Structure		AR(1)

Case Processing Summary

	N	Percent
Included	72	100.0%
Excluded	0	0.0%
Total	72	100.0%

Correlated Data Summary

Number of Levels	Subject Effect	animal	8
	Within-Subject Effect	Treated1casp6DN0pen1	2
		timepointdays	2
		flashintensitymcd	5
Number of Subjects			8
Number of Measurements per Subject	Minimum		3
	Maximum		14
Correlation Matrix Dimension			20

Categorical Variable Information

			N	Percent
Factor	timepointdays	7.0	34	47.2%
		14.0	38	52.8%
		Total	72	100.0%
	flashintensitymcd	300.0	9	12.5%
		1000.0	16	22.2%
		3000.0	17	23.6%
		10000.0	16	22.2%
		25000.0	14	19.4%
		Total	72	100.0%
	Treated1casp6DN0pen1	.0	31	43.1%
		1.0	41	56.9%
		Total	72	100.0%

Continuous Variable Information

		N	Minimum	Maximum	Mean
Dependent Variable	bwaveamplitudev	72	5.9	135.8	52.056

Continuous Variable Information

		Std. Deviation
Dependent Variable	bwaveamplitudev	34.4985

Goodness of Fit[a]

	Value
Quasi Likelihood under Independence Model Criterion (QIC)[b]	39.926
Corrected Quasi Likelihood under Independence Model Criterion (QICC)[b]	42.835

Dependent Variable: bwaveamplitudev
Model: (Intercept), timepointdays, flashintensitymcd, Treated1casp6DN0pen1, timepointdays * flashintensitymcd, timepointdays * Treated1casp6DN0pen1, flashintensitymcd * Treated1casp6DN0pen1

a. Information criteria are in small-is-better form.

b. Computed using the full log quasi-likelihood function.

Tests of Model Effects

	Type III		
Source	Wald Chi-Square	df	Sig.
(Intercept)	1091.572	1	.000
timepointdays	13.120	1	.000
flashintensitymcd	1594.751	4	.000
Treated1casp6DN0pen1	.575	1	.448
timepointdays * flashintensitymcd	9.007	4	.061
timepointdays * Treated1casp6DN0pen1	.528	1	.467
flashintensitymcd * Treated1casp6DN0pen1	21.912	4	.000

Dependent Variable: bwaveamplitudev
Model: (Intercept), timepointdays, flashintensitymcd, Treated1casp6DN0pen1, timepointdays * flashintensitymcd, timepointdays * Treated1casp6DN0pen1, flashintensitymcd * Treated1casp6DN0pen1

```
* Generalized Estimating Equations.
```

```
GENLIN bwaveamplitudev BY timepointdays flashintensitymcd Treated1casp6DN
  /MODEL timepointdays flashintensitymcd Treated1casp6DN0pen1 timepointday
 DISTRIBUTION=GAMMA LINK=LOG
  /CRITERIA METHOD=FISHER(1) SCALE=MLE MAXITERATIONS=100 MAXSTEPHALVING=5
(WALD) CILEVEL=95 LIKELIHOOD=FULL
  /EMMEANS TABLES=Treated1casp6DN0pen1 SCALE=ORIGINAL
  /EMMEANS TABLES=timepointdays*flashintensitymcd*Treated1casp6DN0pen1 SCA
  /REPEATED SUBJECT=animal WITHINSUBJECT=Treated1casp6DN0pen1*timepointday
(1) ADJUSTCORR=YES COVB=ROBUST MAXITERATIONS=100 PCONVERGE=1e-006(ABSOLUTE
  /MISSING CLASSMISSING=EXCLUDE
  /PRINT CPS DESCRIPTIVES MODELINFO FIT SUMMARY WORKINGCORR.
```

Generalized Linear Models

Notes

Output Created		27-JUL-2013 00:52:27
Comments		
Input	Active Dataset	DataSet1
	Filter	<none>
	Weight	<none>
	Split File	<none>
	N of Rows in Working Data File	72
Missing Value Handling	Definition of Missing	User-defined missing values for factor, subject and within-subject variables are treated as missing.
	Cases Used	Statistics are based on cases with valid data for all variables in the model.
Weight Handling		not applicable

Notes

Syntax		GENLIN bwaveamplitudev BY timepointdays flashintensitymcd Treated1casp6DN0pen1 (ORDER=ASCENDING) /MODEL timepointdays flashintensitymcd Treated1casp6DN0pen1 timepointdays*flashintensitymcd flashintensitymcd*Treated1casp6DN0pen1 INTERCEPT=YES DISTRIBUTION=GAMMA LINK=LOG /CRITERIA METHOD=FISHER(1) SCALE=MLE MAXITERATIONS=100 MAXSTEPHALVING=5 PCONVERGE=1E-006 (ABSOLUTE) SINGULAR=1E-012 ANALYSISTYPE=3(WALD) CILEVEL=95 LIKELIHOOD=FULL /EMMEANS TABLES=Treated1casp6DN0pen1 SCALE=ORIGINAL /EMMEANS TABLES=timepointdays*flashintensitymcd*Treated1casp6DN0pen1 SCALE=ORIGINAL /REPEATED SUBJECT=animal WITHINSUBJECT=Treated1casp6DN0pen1*timepointdays*flashintensitymcd SORT=YES CORRTYPE=AR(1) ADJUSTCORR=YES COVB=ROBUST MAXITERATIONS=100 PCONVERGE=1e-006(ABSOLUTE) UPDATECORR=1 /MISSING CLASSMISSING=EXCLUDE /PRINT CPS DESCRIPTIVES MODELINFO FIT SUMMARY WORKINGCORR.
Resources	Processor Time	00:00:00.33
	Elapsed Time	00:00:00.37

[DataSet1]

Model Information

Dependent Variable		bwaveamplitudev
Probability Distribution		Gamma
Link Function		Log
Subject Effect	1	animal
Within-Subject Effect	1	Treated1casp6DN0pen1
	2	timepointdays
	3	flashintensitymcd
Working Correlation Matrix Structure		AR(1)

Case Processing Summary

	N	Percent
Included	72	100.0%
Excluded	0	0.0%
Total	72	100.0%

Correlated Data Summary

Number of Levels	Subject Effect	animal	8
	Within-Subject Effect	Treated1casp6DN0pen1	2
		timepointdays	2
		flashintensitymcd	5
Number of Subjects			8
Number of Measurements per Subject	Minimum		3
	Maximum		14
Correlation Matrix Dimension			20

Categorical Variable Information

			N	Percent
Factor	timepointdays	7.0	34	47.2%
		14.0	38	52.8%
		Total	72	100.0%
	flashintensitymcd	300.0	9	12.5%
		1000.0	16	22.2%
		3000.0	17	23.6%
		10000.0	16	22.2%
		25000.0	14	19.4%
		Total	72	100.0%
	Treated1casp6DN0pen1	.0	31	43.1%
		1.0	41	56.9%
		Total	72	100.0%

Continuous Variable Information

		N	Minimum	Maximum	Mean
Dependent Variable	bwaveamplitudev	72	5.9	135.8	52.056

Continuous Variable Information

		Std. Deviation
Dependent Variable	bwaveamplitudev	34.4985

Goodness of Fit[a]

	Value
Quasi Likelihood under Independence Model Criterion (QIC)[b]	38.288
Corrected Quasi Likelihood under Independence Model Criterion (QICC)[b]	40.691

Dependent Variable: bwaveamplitudev
Model: (Intercept), timepointdays, flashintensitymcd, Treated1casp6DN0pen1, timepointdays * flashintensitymcd, flashintensitymcd * Treated1casp6DN0pen1

a. Information criteria are in small-is-better form.

b. Computed using the full log quasi-likelihood function.

Tests of Model Effects

Source	Type III		
	Wald Chi-Square	df	Sig.
(Intercept)	1159.385	1	.000
timepointdays	10.563	1	.001
flashintensitymcd	1630.649	4	.000
Treated1casp6DN0pen1	.440	1	.507
timepointdays * flashintensitymcd	7.930	4	.094
flashintensitymcd * Treated1casp6DN0pen1	18.823	4	.001

Dependent Variable: bwaveamplitudev
Model: (Intercept), timepointdays, flashintensitymcd, Treated1casp6DN0pen1, timepointdays * flashintensitymcd, flashintensitymcd * Treated1casp6DN0pen1

```
 * Generalized Estimating Equations.
GENLIN bwaveamplitudev BY timepointdays flashintensitymcd Treated1casp6DN
  /MODEL timepointdays flashintensitymcd Treated1casp6DN0pen1 flashintensi
 DISTRIBUTION=GAMMA LINK=LOG
  /CRITERIA METHOD=FISHER(1) SCALE=MLE MAXITERATIONS=100 MAXSTEPHALVING=5
012 ANALYSISTYPE=3(WALD) CILEVEL=95 LIKELIHOOD=FULL
  /EMMEANS TABLES=Treated1casp6DN0pen1 SCALE=ORIGINAL
  /EMMEANS TABLES=timepointdays*flashintensitymcd*Treated1casp6DN0pen1 SCA
```

```
  /REPEATED SUBJECT=animal WITHINSUBJECT=Treated1casp6DN0pen1*timepointday
(1) ADJUSTCORR=YES COVB=ROBUST MAXITERATIONS=100 PCONVERGE=1e-006(ABSOLUTE
  /MISSING CLASSMISSING=EXCLUDE
  /PRINT CPS DESCRIPTIVES MODELINFO FIT SUMMARY WORKINGCORR.
```

Generalized Linear Models

Notes

Output Created		27-JUL-2013 00:53:08
Comments		
Input	Active Dataset	DataSet1
	Filter	<none>
	Weight	<none>
	Split File	<none>
	N of Rows in Working Data File	72
Missing Value Handling	Definition of Missing	User-defined missing values for factor, subject and within-subject variables are treated as missing.
	Cases Used	Statistics are based on cases with valid data for all variables in the model.
Weight Handling		not applicable
Syntax		GENLIN bwaveamplitudev BY timepointdays flashintensitymcd Treated1casp6DN0pen1 (ORDER=ASCENDING) /MODEL timepointdays flashintensitymcd Treated1casp6DN0pen1 flashintensitymcd*Treated1casp6DN0pen1 INTERCEPT=YES DISTRIBUTION=GAMMA LINK=LOG /CRITERIA METHOD=FISHER(1) SCALE=MLE MAXITERATIONS=100 MAXSTEPHALVING=5 PCONVERGE=1E-006 (ABSOLUTE) SINGULAR=1E-012 ANALYSISTYPE=3(WALD) CILEVEL=95 LIKELIHOOD=FULL /EMMEANS TABLES=Treated1casp6DN0pen1 SCALE=ORIGINAL /EMMEANS TABLES=timepointdays*flashintensitymcd*Treated1casp6DN0pen1 SCALE=ORIGINAL /REPEATED SUBJECT=animal WITHINSUBJECT=Treated1casp6DN0pen1*timepointdays*flashintensitymcd SORT=YES CORRTYPE=AR(1) ADJUSTCORR=YES COVB=ROBUST MAXITERATIONS=100 PCONVERGE=1e-006(ABSOLUTE) UPDATECORR=1 /MISSING CLASSMISSING=EXCLUDE /PRINT CPS DESCRIPTIVES MODELINFO FIT SUMMARY WORKINGCORR.
Resources	Processor Time	00:00:00.34
	Elapsed Time	00:00:00.33

[DataSet1]

Model Information

Dependent Variable		bwaveamplitudev
Probability Distribution		Gamma
Link Function		Log
Subject Effect	1	animal
Within-Subject Effect	1	Treated1casp6DN0pen1
	2	timepointdays
	3	flashintensitymcd
Working Correlation Matrix Structure		AR(1)

Case Processing Summary

	N	Percent
Included	72	100.0%
Excluded	0	0.0%
Total	72	100.0%

Correlated Data Summary

Number of Levels	Subject Effect	animal	8
	Within-Subject Effect	Treated1casp6DN0pen1	2
		timepointdays	2
		flashintensitymcd	5
Number of Subjects			8
Number of Measurements per Subject	Minimum		3
	Maximum		14
Correlation Matrix Dimension			20

Categorical Variable Information

			N	Percent
Factor	timepointdays	7.0	34	47.2%
		14.0	38	52.8%
		Total	72	100.0%
	flashintensitymcd	300.0	9	12.5%
		1000.0	16	22.2%
		3000.0	17	23.6%
		10000.0	16	22.2%
		25000.0	14	19.4%
		Total	72	100.0%
	Treated1casp6DN0pen1	.0	31	43.1%
		1.0	41	56.9%
		Total	72	100.0%

Continuous Variable Information

		N	Minimum	Maximum	Mean
Dependent Variable	bwaveamplitudev	72	5.9	135.8	52.056

Continuous Variable Information

		Std. Deviation
Dependent Variable	bwaveamplitudev	34.4985

Goodness of Fit[a]

	Value
Quasi Likelihood under Independence Model Criterion (QIC)[b]	34.367
Corrected Quasi Likelihood under Independence Model Criterion (QICC)[b]	32.725

Dependent Variable: bwaveamplitudev
Model: (Intercept), timepointdays, flashintensitymcd, Treated1casp6DN0pen1, flashintensitymcd * Treated1casp6DN0pen1

a. Information criteria are in small-is-better form.

b. Computed using the full log quasi-likelihood function.

Tests of Model Effects

	Type III		
Source	Wald Chi-Square	df	Sig.
(Intercept)	1108.201	1	.000
timepointdays	13.349	1	.000
flashintensitymcd	4630.683	4	.000
Treated1casp6DN0pen1	.293	1	.589
flashintensitymcd * Treated1casp6DN0pen1	10.650	4	.031

Dependent Variable: bwaveamplitudev
Model: (Intercept), timepointdays, flashintensitymcd, Treated1casp6DN0pen1, flashintensitymcd * Treated1casp6DN0pen1

Working Correlation Matrix[a]

Measurement	Measurement			
	[Treated1casp6DN0pen1 = .0]* [timepointdays = 7.0]* [flashintensitymcd = 300.0]	[Treated1casp6DN0pen1 = .0]* [timepointdays = 7.0]* [flashintensitymcd = 1000.0]	[Treated1casp6DN0pen1 = .0]* [timepointdays = 7.0]* [flashintensitymcd = 3000.0]	[Treated1casp6DN0pen1 = .0]* [timepointdays = 7.0]* [flashintensitymcd = 10000.0]
[Treated1casp6DN0pen1 = .0]* [timepointdays = 7.0]* [flashintensitymcd = 300.0]	1.000	.929	.863	.801
[Treated1casp6DN0pen1 = .0]* [timepointdays = 7.0]* [flashintensitymcd = 1000.0]	.929	1.000	.929	.863
[Treated1casp6DN0pen1 = .0]* [timepointdays = 7.0]* [flashintensitymcd = 3000.0]	.863	.929	1.000	.929
[Treated1casp6DN0pen1 = .0]* [timepointdays = 7.0]* [flashintensitymcd = 10000.0]	.801	.863	.929	1.000
[Treated1casp6DN0pen1 = .0]* [timepointdays = 7.0]* [flashintensitymcd = 25000.0]	.744	.801	.863	.929
[Treated1casp6DN0pen1 = .0]* [timepointdays = 14.0]* [flashintensitymcd = 300.0]	.691	.744	.801	.863
[Treated1casp6DN0pen1 = .0]* [timepointdays = 14.0]* [flashintensitymcd = 1000.0]	.642	.691	.744	.801
[Treated1casp6DN0pen1 = .0]* [timepointdays = 14.0]* [flashintensitymcd = 3000.0]	.596	.642	.691	.744
[Treated1casp6DN0pen1 = .0]* [timepointdays = 14.0]* [flashintensitymcd = 10000.0]	.553	.596	.642	.691
[Treated1casp6DN0pen1 = .0]* [timepointdays = 14.0]* [flashintensitymcd = 25000.0]	.514	.553	.596	.642

Working Correlation Matrix[a]

Measurement	Measurement			
	[Treated1casp6DN0pen1 = .0]* [timepointdays = 7.0]* [flashintensitymcd = 25000.0]	[Treated1casp6DN0pen1 = .0]* [timepointdays = 14.0]* [flashintensitymcd = 300.0]	[Treated1casp6DN0pen1 = .0]* [timepointdays = 14.0]* [flashintensitymcd = 1000.0]	[Treated1casp6DN0pen1 = .0]* [timepointdays = 14.0]* [flashintensitymcd = 3000.0]
[Treated1casp6DN0pen1 = .0]* [timepointdays = 7.0]* [flashintensitymcd = 300.0]	.744	.691	.642	.596
[Treated1casp6DN0pen1 = .0]* [timepointdays = 7.0]* [flashintensitymcd = 1000.0]	.801	.744	.691	.642
[Treated1casp6DN0pen1 = .0]* [timepointdays = 7.0]* [flashintensitymcd = 3000.0]	.863	.801	.744	.691
[Treated1casp6DN0pen1 = .0]* [timepointdays = 7.0]* [flashintensitymcd = 10000.0]	.929	.863	.801	.744
[Treated1casp6DN0pen1 = .0]* [timepointdays = 7.0]* [flashintensitymcd = 25000.0]	1.000	.929	.863	.801
[Treated1casp6DN0pen1 = .0]* [timepointdays = 14.0]* [flashintensitymcd = 300.0]	.929	1.000	.929	.863
[Treated1casp6DN0pen1 = .0]* [timepointdays = 14.0]* [flashintensitymcd = 1000.0]	.863	.929	1.000	.929
[Treated1casp6DN0pen1 = .0]* [timepointdays = 14.0]* [flashintensitymcd = 3000.0]	.801	.863	.929	1.000
[Treated1casp6DN0pen1 = .0]* [timepointdays = 14.0]* [flashintensitymcd = 10000.0]	.744	.801	.863	.929
[Treated1casp6DN0pen1 = .0]* [timepointdays = 14.0]* [flashintensitymcd = 25000.0]	.691	.744	.801	.863

Working Correlation Matrix[a]

Measurement	Measurement			
	[Treated1casp6DN0pen1 = .0]* [timepointdays = 14.0]* [flashintensitymcd = 10000.0]	[Treated1casp6DN0pen1 = .0]* [timepointdays = 14.0]* [flashintensitymcd = 25000.0]	[Treated1casp6DN0pen1 = 1.0]* [timepointdays = 7.0]* [flashintensitymcd = 300.0]	[Treated1casp6DN0pen1 = 1.0]* [timepointdays = 7.0]* [flashintensitymcd = 1000.0]
[Treated1casp6DN0pen1 = .0]* [timepointdays = 7.0]* [flashintensitymcd = 300.0]	.553	.514	.477	.443
[Treated1casp6DN0pen1 = .0]* [timepointdays = 7.0]* [flashintensitymcd = 1000.0]	.596	.553	.514	.477
[Treated1casp6DN0pen1 = .0]* [timepointdays = 7.0]* [flashintensitymcd = 3000.0]	.642	.596	.553	.514
[Treated1casp6DN0pen1 = .0]* [timepointdays = 7.0]* [flashintensitymcd = 10000.0]	.691	.642	.596	.553
[Treated1casp6DN0pen1 = .0]* [timepointdays = 7.0]* [flashintensitymcd = 25000.0]	.744	.691	.642	.596
[Treated1casp6DN0pen1 = .0]* [timepointdays = 14.0]* [flashintensitymcd = 300.0]	.801	.744	.691	.642
[Treated1casp6DN0pen1 = .0]* [timepointdays = 14.0]* [flashintensitymcd = 1000.0]	.863	.801	.744	.691
[Treated1casp6DN0pen1 = .0]* [timepointdays = 14.0]* [flashintensitymcd = 3000.0]	.929	.863	.801	.744
[Treated1casp6DN0pen1 = .0]* [timepointdays = 14.0]* [flashintensitymcd = 10000.0]	1.000	.929	.863	.801
[Treated1casp6DN0pen1 = .0]* [timepointdays = 14.0]* [flashintensitymcd = 25000.0]	.929	1.000	.929	.863

Working Correlation Matrix[a]

Measurement	Measurement			
	[Treated1casp6DN0pen1 = 1.0]* [timepointdays = 7.0]* [flashintensitymcd = 3000.0]	[Treated1casp6DN0pen1 = 1.0]* [timepointdays = 7.0]* [flashintensitymcd = 10000.0]	[Treated1casp6DN0pen1 = 1.0]* [timepointdays = 7.0]* [flashintensitymcd = 25000.0]	[Treated1casp6DN0pen1 = 1.0]* [timepointdays = 14.0]* [flashintensitymcd = 300.0]
[Treated1casp6DN0pen1 = .0]* [timepointdays = 7.0]* [flashintensitymcd = 300.0]	.412	.382	.355	.330
[Treated1casp6DN0pen1 = .0]* [timepointdays = 7.0]* [flashintensitymcd = 1000.0]	.443	.412	.382	.355
[Treated1casp6DN0pen1 = .0]* [timepointdays = 7.0]* [flashintensitymcd = 3000.0]	.477	.443	.412	.382
[Treated1casp6DN0pen1 = .0]* [timepointdays = 7.0]* [flashintensitymcd = 10000.0]	.514	.477	.443	.412
[Treated1casp6DN0pen1 = .0]* [timepointdays = 7.0]* [flashintensitymcd = 25000.0]	.553	.514	.477	.443
[Treated1casp6DN0pen1 = .0]* [timepointdays = 14.0]* [flashintensitymcd = 300.0]	.596	.553	.514	.477
[Treated1casp6DN0pen1 = .0]* [timepointdays = 14.0]* [flashintensitymcd = 1000.0]	.642	.596	.553	.514
[Treated1casp6DN0pen1 = .0]* [timepointdays = 14.0]* [flashintensitymcd = 3000.0]	.691	.642	.596	.553
[Treated1casp6DN0pen1 = .0]* [timepointdays = 14.0]* [flashintensitymcd = 10000.0]	.744	.691	.642	.596
[Treated1casp6DN0pen1 = .0]* [timepointdays = 14.0]* [flashintensitymcd = 25000.0]	.801	.744	.691	.642

Working Correlation Matrix[a]

Measurement	Measurement			
	[Treated1casp6DN0pen1 = 1.0]* [timepointdays = 14.0]* [flashintensitymcd = 1000.0]	[Treated1casp6DN0pen1 = 1.0]* [timepointdays = 14.0]* [flashintensitymcd = 3000.0]	[Treated1casp6DN0pen1 = 1.0]* [timepointdays = 14.0]* [flashintensitymcd = 10000.0]	[Treated1casp6DN0pen1 = 1.0]* [timepointdays = 14.0]* [flashintensitymcd = 25000.0]
[Treated1casp6DN0pen1 = .0]* [timepointdays = 7.0]* [flashintensitymcd = 300.0]	.306	.285	.264	.245
[Treated1casp6DN0pen1 = .0]* [timepointdays = 7.0]* [flashintensitymcd = 1000.0]	.330	.306	.285	.264
[Treated1casp6DN0pen1 = .0]* [timepointdays = 7.0]* [flashintensitymcd = 3000.0]	.355	.330	.306	.285
[Treated1casp6DN0pen1 = .0]* [timepointdays = 7.0]* [flashintensitymcd = 10000.0]	.382	.355	.330	.306
[Treated1casp6DN0pen1 = .0]* [timepointdays = 7.0]* [flashintensitymcd = 25000.0]	.412	.382	.355	.330
[Treated1casp6DN0pen1 = .0]* [timepointdays = 14.0]* [flashintensitymcd = 300.0]	.443	.412	.382	.355
[Treated1casp6DN0pen1 = .0]* [timepointdays = 14.0]* [flashintensitymcd = 1000.0]	.477	.443	.412	.382
[Treated1casp6DN0pen1 = .0]* [timepointdays = 14.0]* [flashintensitymcd = 3000.0]	.514	.477	.443	.412
[Treated1casp6DN0pen1 = .0]* [timepointdays = 14.0]* [flashintensitymcd = 10000.0]	.553	.514	.477	.443
[Treated1casp6DN0pen1 = .0]* [timepointdays = 14.0]* [flashintensitymcd = 25000.0]	.596	.553	.514	.477

Working Correlation Matrix[a]

Measurement	Measurement			
	[Treated1casp6DN0pen1 = .0]* [timepointdays = 7.0]* [flashintensitymcd = 300.0]	[Treated1casp6DN0pen1 = .0]* [timepointdays = 7.0]* [flashintensitymcd = 1000.0]	[Treated1casp6DN0pen1 = .0]* [timepointdays = 7.0]* [flashintensitymcd = 3000.0]	[Treated1casp6DN0pen1 = .0]* [timepointdays = 7.0]* [flashintensitymcd = 10000.0]
[Treated1casp6DN0pen1 = 1.0]* [timepointdays = 7.0]* [flashintensitymcd = 300.0]	.477	.514	.553	.596
[Treated1casp6DN0pen1 = 1.0]* [timepointdays = 7.0]* [flashintensitymcd = 1000.0]	.443	.477	.514	.553
[Treated1casp6DN0pen1 = 1.0]* [timepointdays = 7.0]* [flashintensitymcd = 3000.0]	.412	.443	.477	.514
[Treated1casp6DN0pen1 = 1.0]* [timepointdays = 7.0]* [flashintensitymcd = 10000.0]	.382	.412	.443	.477
[Treated1casp6DN0pen1 = 1.0]* [timepointdays = 7.0]* [flashintensitymcd = 25000.0]	.355	.382	.412	.443
[Treated1casp6DN0pen1 = 1.0]* [timepointdays = 14.0]* [flashintensitymcd = 300.0]	.330	.355	.382	.412
[Treated1casp6DN0pen1 = 1.0]* [timepointdays = 14.0]* [flashintensitymcd = 1000.0]	.306	.330	.355	.382
[Treated1casp6DN0pen1 = 1.0]* [timepointdays = 14.0]* [flashintensitymcd = 3000.0]	.285	.306	.330	.355
[Treated1casp6DN0pen1 = 1.0]* [timepointdays = 14.0]* [flashintensitymcd = 10000.0]	.264	.285	.306	.330
[Treated1casp6DN0pen1 = 1.0]* [timepointdays = 14.0]* [flashintensitymcd = 25000.0]	.245	.264	.285	.306

Working Correlation Matrix[a]

Measurement	Measurement			
	[Treated1casp6DN0pen1 = .0]* [timepointdays = 7.0]* [flashintensitymcd = 25000.0]	[Treated1casp6DN0pen1 = .0]* [timepointdays = 14.0]* [flashintensitymcd = 300.0]	[Treated1casp6DN0pen1 = .0]* [timepointdays = 14.0]* [flashintensitymcd = 1000.0]	[Treated1casp6DN0pen1 = .0]* [timepointdays = 14.0]* [flashintensitymcd = 3000.0]
[Treated1casp6DN0pen1 = 1.0]* [timepointdays = 7.0]* [flashintensitymcd = 300.0]	.642	.691	.744	.801
[Treated1casp6DN0pen1 = 1.0]* [timepointdays = 7.0]* [flashintensitymcd = 1000.0]	.596	.642	.691	.744
[Treated1casp6DN0pen1 = 1.0]* [timepointdays = 7.0]* [flashintensitymcd = 3000.0]	.553	.596	.642	.691
[Treated1casp6DN0pen1 = 1.0]* [timepointdays = 7.0]* [flashintensitymcd = 10000.0]	.514	.553	.596	.642
[Treated1casp6DN0pen1 = 1.0]* [timepointdays = 7.0]* [flashintensitymcd = 25000.0]	.477	.514	.553	.596
[Treated1casp6DN0pen1 = 1.0]* [timepointdays = 14.0]* [flashintensitymcd = 300.0]	.443	.477	.514	.553
[Treated1casp6DN0pen1 = 1.0]* [timepointdays = 14.0]* [flashintensitymcd = 1000.0]	.412	.443	.477	.514
[Treated1casp6DN0pen1 = 1.0]* [timepointdays = 14.0]* [flashintensitymcd = 3000.0]	.382	.412	.443	.477
[Treated1casp6DN0pen1 = 1.0]* [timepointdays = 14.0]* [flashintensitymcd = 10000.0]	.355	.382	.412	.443
[Treated1casp6DN0pen1 = 1.0]* [timepointdays = 14.0]* [flashintensitymcd = 25000.0]	.330	.355	.382	.412

Working Correlation Matrix[a]

Measurement	Measurement			
	[Treated1casp6DN0pen1 = .0]* [timepointdays = 14.0]* [flashintensitymcd = 10000.0]	[Treated1casp6DN0pen1 = .0]* [timepointdays = 14.0]* [flashintensitymcd = 25000.0]	[Treated1casp6DN0pen1 = 1.0]* [timepointdays = 7.0]* [flashintensitymcd = 300.0]	[Treated1casp6DN0pen1 = 1.0]* [timepointdays = 7.0]* [flashintensitymcd = 1000.0]
[Treated1casp6DN0pen1 = 1.0]* [timepointdays = 7.0]* [flashintensitymcd = 300.0]	.863	.929	1.000	.929
[Treated1casp6DN0pen1 = 1.0]* [timepointdays = 7.0]* [flashintensitymcd = 1000.0]	.801	.863	.929	1.000
[Treated1casp6DN0pen1 = 1.0]* [timepointdays = 7.0]* [flashintensitymcd = 3000.0]	.744	.801	.863	.929
[Treated1casp6DN0pen1 = 1.0]* [timepointdays = 7.0]* [flashintensitymcd = 10000.0]	.691	.744	.801	.863
[Treated1casp6DN0pen1 = 1.0]* [timepointdays = 7.0]* [flashintensitymcd = 25000.0]	.642	.691	.744	.801
[Treated1casp6DN0pen1 = 1.0]* [timepointdays = 14.0]* [flashintensitymcd = 300.0]	.596	.642	.691	.744
[Treated1casp6DN0pen1 = 1.0]* [timepointdays = 14.0]* [flashintensitymcd = 1000.0]	.553	.596	.642	.691
[Treated1casp6DN0pen1 = 1.0]* [timepointdays = 14.0]* [flashintensitymcd = 3000.0]	.514	.553	.596	.642
[Treated1casp6DN0pen1 = 1.0]* [timepointdays = 14.0]* [flashintensitymcd = 10000.0]	.477	.514	.553	.596
[Treated1casp6DN0pen1 = 1.0]* [timepointdays = 14.0]* [flashintensitymcd = 25000.0]	.443	.477	.514	.553

Working Correlation Matrix[a]

Measurement	Measurement			
	[Treated1casp6DN0pen1 = 1.0]* [timepointdays = 7.0]* [flashintensitymcd = 3000.0]	[Treated1casp6DN0pen1 = 1.0]* [timepointdays = 7.0]* [flashintensitymcd = 10000.0]	[Treated1casp6DN0pen1 = 1.0]* [timepointdays = 7.0]* [flashintensitymcd = 25000.0]	[Treated1casp6DN0pen1 = 1.0]* [timepointdays = 14.0]* [flashintensitymcd = 300.0]
[Treated1casp6DN0pen1 = 1.0]* [timepointdays = 7.0]* [flashintensitymcd = 300.0]	.863	.801	.744	.691
[Treated1casp6DN0pen1 = 1.0]* [timepointdays = 7.0]* [flashintensitymcd = 1000.0]	.929	.863	.801	.744
[Treated1casp6DN0pen1 = 1.0]* [timepointdays = 7.0]* [flashintensitymcd = 3000.0]	1.000	.929	.863	.801
[Treated1casp6DN0pen1 = 1.0]* [timepointdays = 7.0]* [flashintensitymcd = 10000.0]	.929	1.000	.929	.863
[Treated1casp6DN0pen1 = 1.0]* [timepointdays = 7.0]* [flashintensitymcd = 25000.0]	.863	.929	1.000	.929
[Treated1casp6DN0pen1 = 1.0]* [timepointdays = 14.0]* [flashintensitymcd = 300.0]	.801	.863	.929	1.000
[Treated1casp6DN0pen1 = 1.0]* [timepointdays = 14.0]* [flashintensitymcd = 1000.0]	.744	.801	.863	.929
[Treated1casp6DN0pen1 = 1.0]* [timepointdays = 14.0]* [flashintensitymcd = 3000.0]	.691	.744	.801	.863
[Treated1casp6DN0pen1 = 1.0]* [timepointdays = 14.0]* [flashintensitymcd = 10000.0]	.642	.691	.744	.801
[Treated1casp6DN0pen1 = 1.0]* [timepointdays = 14.0]* [flashintensitymcd = 25000.0]	.596	.642	.691	.744

Working Correlation Matrix[a]

Measurement	Measurement			
	[Treated1casp6DN0pen1 = 1.0]* [timepointdays = 14.0]* [flashintensitymcd = 1000.0]	[Treated1casp6DN0pen1 = 1.0]* [timepointdays = 14.0]* [flashintensitymcd = 3000.0]	[Treated1casp6DN0pen1 = 1.0]* [timepointdays = 14.0]* [flashintensitymcd = 10000.0]	[Treated1casp6DN0pen1 = 1.0]* [timepointdays = 14.0]* [flashintensitymcd = 25000.0]
[Treated1casp6DN0pen1 = 1.0]* [timepointdays = 7.0]* [flashintensitymcd = 300.0]	.642	.596	.553	.514
[Treated1casp6DN0pen1 = 1.0]* [timepointdays = 7.0]* [flashintensitymcd = 1000.0]	.691	.642	.596	.553
[Treated1casp6DN0pen1 = 1.0]* [timepointdays = 7.0]* [flashintensitymcd = 3000.0]	.744	.691	.642	.596
[Treated1casp6DN0pen1 = 1.0]* [timepointdays = 7.0]* [flashintensitymcd = 10000.0]	.801	.744	.691	.642
[Treated1casp6DN0pen1 = 1.0]* [timepointdays = 7.0]* [flashintensitymcd = 25000.0]	.863	.801	.744	.691
[Treated1casp6DN0pen1 = 1.0]* [timepointdays = 14.0]* [flashintensitymcd = 300.0]	.929	.863	.801	.744
[Treated1casp6DN0pen1 = 1.0]* [timepointdays = 14.0]* [flashintensitymcd = 1000.0]	1.000	.929	.863	.801
[Treated1casp6DN0pen1 = 1.0]* [timepointdays = 14.0]* [flashintensitymcd = 3000.0]	.929	1.000	.929	.863
[Treated1casp6DN0pen1 = 1.0]* [timepointdays = 14.0]* [flashintensitymcd = 10000.0]	.863	.929	1.000	.929
[Treated1casp6DN0pen1 = 1.0]* [timepointdays = 14.0]* [flashintensitymcd = 25000.0]	.801	.863	.929	1.000

Dependent Variable: bwaveamplitudev
Model: (Intercept), timepointdays, flashintensitymcd, Treated1casp6DN0pen1, flashintensitymcd * Treated1casp6DN0pen1

a. The AR(1) working correlation matrix structure is computed assuming the measurements are equally

a. The AR(1) working correlation matrix structure is computed assuming the measurements are equally spaced for all subjects.

Estimated Marginal Means 1: Treated1casp6DN0pen1

Estimates

Treated1casp6DN0pen1	Mean	Std. Error	95% Wald Confidence Interval	
			Lower	Upper
.0	38.227	6.1584	27.876	52.420
1.0	34.776	3.9163	27.888	43.364

Estimated Marginal Means 2: timepointdays* flashintensitymcd* Treated1casp6DN0pen1

Estimates

timepointdays	flashintensitymcd	Treated1casp6DN0pen1	Mean	Std. Error	95% Wald ...
					Lower
7.0	300.0	.0	11.487	2.5444	7.441
		1.0	10.946	1.5712	8.262
	1000.0	.0	27.109	4.5704	19.481
		1.0	25.967	3.6923	19.651
	3000.0	.0	57.313	10.2916	40.309
		1.0	50.596	6.0531	40.020
	10000.0	.0	85.579	15.6533	59.797
		1.0	77.449	8.0206	63.222
	25000.0	.0	104.102	16.4963	76.308
		1.0	88.947	8.2070	74.232
14.0	300.0	.0	8.798	1.8300	5.852
		1.0	8.384	1.0240	6.599
	1000.0	.0	20.763	2.8840	15.814
		1.0	19.888	3.1393	14.596
	3000.0	.0	43.896	6.7799	32.431
		1.0	38.751	5.2367	29.734
	10000.0	.0	65.546	12.1748	45.545
		1.0	59.319	8.3012	45.089
	25000.0	.0	79.732	12.8925	58.076
		1.0	68.125	8.8868	52.755

Estimates

timepointdays	flashintensitymcd	Treated1casp6DN0pen1	95% Wald ... Upper
7.0	300.0	.0	17.731
		1.0	14.502
	1000.0	.0	37.724
		1.0	34.313
	3000.0	.0	81.489
		1.0	63.966
	10000.0	.0	122.479
		1.0	94.878
	25000.0	.0	142.017
		1.0	106.578
14.0	300.0	.0	13.226
		1.0	10.651
	1000.0	.0	27.260
		1.0	27.099
	3000.0	.0	59.415
		1.0	50.503
	10000.0	.0	94.330
		1.0	78.039
	25000.0	.0	109.464
		1.0	87.972

APPENDIX 18

1. The neuroprotective effect of progesterone after high velocity injury

Female rats have better functional outcomes and develop less cerebral oedema after traumatic brain injury than male rats, and this effect is more pronounced in pseudo-pregnant rats, which have high circulating progesterone and low oestrogen [1,2]. In contrast, female gender in humans is associated with a worse outcome after TBI [3]. Nonetheless, the beneficial effects of female gender in animal studies of CNS trauma are attributable to the higher levels of circulating progesterone compared to male rats and, in humans, phase II trials of progesterone after traumatic brain injury have shown promising results [4].

Ocular trauma is common in military and civilian personnel and has a civilian lifetime prevalence of 20%[5,6]. Commotio retinae is a condition characterised by photoreceptor damage after blunt ocular trauma and comprises 15% of military and 0.4% of civilian eye injuries [5,7]. The macula is affected in 73% of military and 31% of civilian cases[5,8] and photoreceptor degeneration permanently reduces vision in 26% of these [8,9]. In animal models of commotio retinae, photoreceptors die by apoptosis and necrosis [10,11]. Thus, regulated apoptotic signalling mediates cell death in a proportion of photoreceptors, implying that antiapoptotic neuroprotective therapies have a potential role in the treatment of commotio retinae. We have recently studies have identified a possible protective effect of female gender after commotio retinae [8], suggesting that progesterone should be considered as a potential neuroprotective therapy after retinal injury.

Results from preclinical studies of progesterone in photoreceptor cell death models are variable. In Sprague-Dawley rats exposed to 2700 lux for 24 hr, progesterone was not neuroprotective when given IP at a dose of 60mg/kg daily in benzyl alcohol whereas, the synthetic progestin Norgestrel was neuroprotective when given IP to both Balb/c mice exposed to 5000 lux for 2 hr and rd10 retinal degeneration mice [12,13]. The efficacy of Norgestrel conflicts with previous work suggesting that metabolites are responsible for the neuroprotective effect [14] and there were more TUNEL-positive cells in the Norgestrel-treated animals 14 days after injury[13], suggesting that apoptosis had been

delayed rather than prevented. Two other pre-clinical studies in phototoxicity models did not show a beneficial effect of progesterone [15,12], and one showed that ovariectomy (which lowers serum progesterone) was neuroprotective [15]. One study using rd1 mice (a retinitis pigmentosa model) showed reduced photoreceptor death with progesterone treatment [16].

There are limited pharmacokinetic data on progesterone in rats, reporting a half-life from ½ hr to 10 hr [17, 18]. Therapeutic dosing range of progesterone in rats has not been reported, though peak plasma progesterone concentrations in pregnant mice range from 45.5 -81.9ng/ml [19,20].

In the current study, we hypothesised that progesterone would reduce photoreceptor death and preserve photoreceptor function after ballistic injury and that continuous progesterone infusion would be the most effective means of delivery. Surprisingly, we demonstrated that low dose continuously administered progesterone increases photoreceptor degeneration after ballistic injury. We also found progesterone pharmacokinetics in the rat at variance with previous reports [17,18].

1.1. Materials and Methods

1.1.1. Animal Care and Procedures

Animal procedures were licensed by the UK Home Office, approved by the University of Birmingham's Biomedical Ethics Review Sub-Committee and conducted in accordance with the ARVO Statement for the Use of Animals in Ophthalmic and Vision Research. Female Lister-hooded rats weighing 170-200g were purchased from Charles River Laboratories (Margate, UK), kept on a 12 hour light-dark cycle with a daytime luminance of 80 lux and fed and watered ad libitum. Surgery and electroretinogram (ERG) recording were performed under inhalation anaesthesia with 2.5% isofluorane in oxygen. Ballistic injury was induced as previously described[10]: a spherical 0.095g spherical plastic pellet was fired using compressed air to directly impact the inferior scleral surface at 20m/s.

1.1.2. Progesterone Treatment

Progesterone was administered in ethyl oleate vehicle, as an 8mg/kg IP loading dose immediately after injury and then by continuous subcutaneous infusion of 100μg/h/kg from an osmotic minipump (Charles River) for the duration of the study. Using data from Gangrade et al. (1992) this would be expected to give a steady state plasma concentration of 36.4ng/ml (infusion rate = steady state concentration x clearance; clearance = 2.75l/kg/hr) or 263ng/ml using data from Petroff et al. (2003; clearance =0.38l/kg/hr)[17,18].

1.1.3. Neuroprotection Experimental Protocol

The right eyes of 16 male Lister-hooded rats (170-200g) were injured by ballistic trauma. Eight rats were treated with progesterone and 8 with ethyl oleate vehicle. ERG were recorded under inhalational anaesthesia at stimulus intensities ranging from -2.5 to +1 log units with respect to standard flash at 7 and 14 days after injury. Animals were killed 14 days after injury and the right eyes processed as previously described (Section 8.7.4.) for measurement of ONL thickness. Blood for serum progesterone enzyme linked immunosorbant assay (ELISA) was taken from the tail vein 2 hours after progesterone injection and from the jugular vein before perfusion fixation, 14 days after injury.

1.1.4. ERG

ERG were recorded (HMsERG – Ocuscience, Kansas City, MO USA) at 7 and 14 days after injury and interpreted using ERGView (Ocuscience). Animals were dark-adapted overnight and prepared for ERG under dim red light (>630nm). Scotopic flash ERG were recorded from -2.5 to +1 log units with respect to standard flash in half log unit steps and photopic flash ERG were recorded with background illumination of 30,000mcd/m2 over the same range. DTL fibre (Unimed Electrode Supplies, Farnham, UK) corneal electrodes with pressure-moulded Aclar (Agar scientific, Stansted, UK) contact lenses were used with needle skin electrodes (Unimed).

1.1.5. Assessment of Photoreceptor Survival

Animals were killed by perfusion fixation with 4% paraformaldehyde in phosphate buffered saline (PBS) and right eyes were removed, cryoprotected in ascending concentrations of sucrose in PBS at 4°C, the anterior segments removed and the retinal cup embedded in OCT and stored at -80°C until required. Sections were cut at 15µm thick using a cryostat (Bright Instruments, Huntingdon, UK) and adhered onto SuperfrostTM (Fisher, UK) coated glass microscope slides. Sections through the optic disc and centre of the impact site and at 600, 1200 and 1800µm to either side of this plane were stained with haematoxyllin and eosin (H&E) and scanned on a MIrax slide scanner (Zeiss, Cambridge, UK) and the ONL manually segmented in Adobe Photoshop by a blinded observer. ONL images were thresholded and average thickness measured as area of above threshold pixels divided by section length using ImageJ (http://rsbweb.nih.gov/ij).

1.1.6.Pharmacokinetics Experimental Protocol

Three rats were given IP injections of 8mg/kg progesterone in ethyl oleate vehicle. Blood samples were taken from the tail veins at 2, 6, 24 and 72 hr after injection.

1.1.7.ELISA

Blood was centrifuged for 5 mins at 10,000 rpm and the serum removed and frozen to -80°c for storage.

Serum progesterone concentration was measured by competitive ELISA according to the manufacturer's instructions. Briefly, 20µl of diluted serum at 1/4 and 1/10 dilutions was used loaded into the wells, 200µl of progesterone-HRP conjugate added to each well and the plate incubated for 1 hour at 37°C before adding 100µl of tetramethylbenzidine/H_2O_2 substrate, incubating for 15 mins and stopping the reaction by adding 100µl 0.15M sulphuric acid. Absorbance was measured at 450nm.

1.1.8.Statistics

All statistical analysis was performed in SPSS 21. ERG and ONL thickness data were analysed using generalised estimating equations (type III sum of squares; autoregressive correlation matrix; gamma distribution with log link) and model fit assessed by plotting residuals and calculating quasi-likelihood information criteria.

1.2. Results

1.2.1. Progesterone Treatment Increased Photoreceptor Degeneration

The ONL thickness in the injured eyes was significantly reduced in animals treated with progesterone compared to the vehicle-treated control animals ($p=0.002$; Figure 1.A-B), an effect that was greater further away from the impact site ($p=0.051$; Figure 1.A-B).

1.2.2. Progesterone Treatment Reduced Retinal Function

ERG data are presented in Figure 2. Combining data from both 7 and 14 days, progesterone reduced a-wave amplitude compared to vehicle-treated controls ($p<0.001$ for flashintensitymcd * TreatedProgesteronevsControl). However, progesterone increased a-wave amplitude at 7 days, whilst reducing it at 14 days after injury ($p=0.001$ for timepointdays * flashintensitymcd * TreatedProgesteronevsControl). These changes in a-wave amplitude caused by progesterone were greater in the uninjured left eyes than the injured right eyes (Figure 2).

1.2.2.1. Progesterone Pharmacokinetics

In the injured animals, serum progesterone concentration 2 hours after 8mg/kg IP injection was 64.2ng/ml and after 14 days of progesterone delivery at 100μg/kg/hr from an osmotic minipump serum progesterone was 6.04ng/ml, from which clearance was calculated as 16.7l/kg/hr (infusion rate = steady state concentration x clearance). The serum progesterone in control animals was 2.1ng/ml.

To verify progesterone pharmacokinetics, 3 rats were given an 8mg/kg IP bolus of progesterone and serum levels measured 2, 6, 24 and 72 hours after injection. The serum progesterone 2 hours after injection was 67.1ng/ml and 6 hours after, 25.9ng/ml (Figure 3). The half-life derived from these measurements is 2.91 hrs. Working back from a 2 hr level of 67.1ng/ml gives an initial concentration of 108ng/ml, from which the volume of distribution was calculated as 74.1l/kg (Initial concentration = dose/volume of distribution). The elimination rate constant, $k_{e,}$ was calculated as 0.238/hr (ln2/half-life) and clearance was calculated as 17.6l/kg/hr (volume of distribution x k_e).

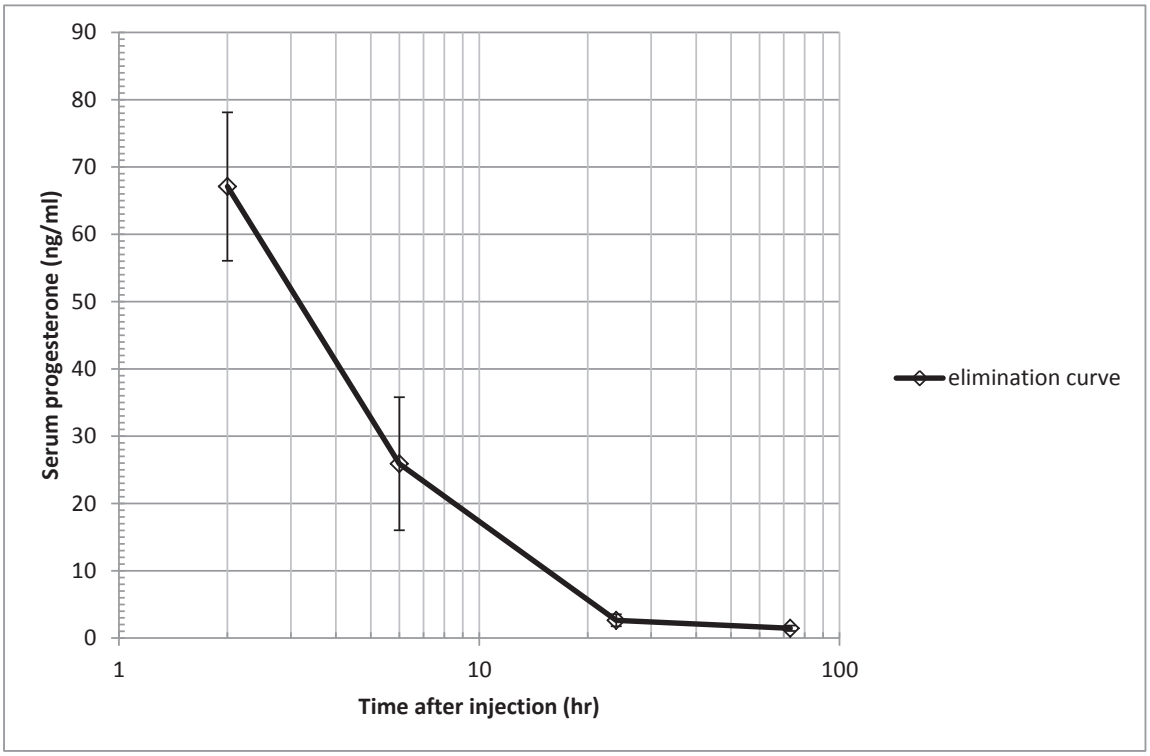

Figure 3. Serum progesterone against time after IP injection.

1.3. Discussion

Progesterone treatment increases photoreceptor degeneration after ballistic injury and reduces photoreceptor function. To our knowledge this is the first report of progesterone treatment increasing cell death.

Progesterone treatment significantly reduced ONL thickness after injury compared to vehicle-treated controls. As 98% of rat photoreceptors are rods and the ONL contains photoreceptor somata only, ONL thickness reflects rod survival [21]. After traumatic brain injury, progesterone treatment reduces oedema and lesion size [22]. It is possible that a reduction in ONL thickness could occur because of reduced oedema. However, the ONL thickness measurement assessed only haematoxylin-stained nuclei, thus excluding any oedema and the ONL is not oedematous 14 days after ballistic injury [10]. Thus, it is likely that the reduction in ONL thickness occurred because treatment with progesterone increased the number of photoreceptors that died after ballistic injury.

With a half-life of 2.9 hr, serum progesterone levels would have peaked at near to 100ng/ml and reached steady-state at 6ng/ml 11.6-14.5 hr after injury, which could be considered an abrupt withdrawal of treatment. After traumatic brain injury, abrupt withdrawal of progesterone treatment increases the expression of cell death markers and worsens outcome compared to tapered withdrawal; however, both treatment regimens are still beneficial compared to placebo [23,22]. Thus, abrupt withdrawal is unlikely to explain the increase in cell death observed in the current study.

Too short a duration of therapeutic plasma levels might explain the observed increase in photoreceptor death. A mechanism for increased cell death could be that brief inhibition of programmed cell death pathways causes cells to undergo less regulated and more inflammatory necrotic cell death, with bystander damage to healthy cells, though this has not been reported to our knowledge.

The a-wave is the first negative deflection on ERG after a light stimulus and is commonly used to assess photoreceptor function. Progesterone treatment significantly reduced ERG a-wave amplitude in both injured and uninjured eyes. An effect of sex steroids on the ERG has been previously reported [24]; however, an effect of progesterone on the uninjured eye makes it difficult to assess the functional effects of treatment with respect to injury. Considering data from both eyes, progesterone reduced a-wave amplitude differently in the injured and uninjured eyes, but the

reduction was greater in the uninjured eyes. An interaction between progesterone treatment and injury is possible, for example injury could cause paracrine changes that prime the retina to decrease a-wave amplitude less in response to progesterone treatment than uninjured retina.

The current studies of the neuroprotective effects of progesterone used a non-standard dosing regimen and found treatment to be detrimental to retinal structure and function. Repeating the study using a previously reported intermittent regimen would clarify whether the detrimental effect is specific to the current dosing regimen [22]. However, a significant detrimental effect after administration of low dose treatment is not encouraging with respect to the translational potential of progesterone in ocular injury.

After a bolus IP injection, progesterone was delivered by continuous subcutaneous infusion. The dose for the bolus injection was derived from previous studies in which 8mg/kg bolus doses were used successfully to treat traumatic brain injury [25]. The rate of infusion of 100μg/kg/hr was derived from data suggesting that, in rats, the clearance of progesterone is 0.38-2.75/hr [17,18], which would have resulted in plasma levels of 36.4-236ng/ml. The clearance in the current study was 17l/kg/hr, considerably higher than has been previously reported [17,18]. On this data (clearance = 17l/kg/hr), an infusion rate of 850μg/kg/hr or 20.4mg/kg/day would be required to maintain plasma progesterone at 50ng/ml, which is higher than has been administered in most studies of the neuroprotective effects of progesterone (which administer intermittent doses of 4-16mg/kg/day) [25]. Were the commonly used intermittent dosing regimen of 0, 6, 24, 48. 72, 96 and 120 hr after injury administered to 200g Lister-hooded rats, plasma progesterone levels would be at baseline from 18-24, 36-48, 59-72, 73-96 and 107-120 hr after injury [25]. Male Sprague-Dawley rats weighing approx. 300g are commonly used for traumatic brain injury studies and – though we do not have data on their pharmacokinetics – it seems unlikely that Sprague-Dawley rats would have radically different pharmacokinetics than the Lister-hooded rats used in the current studies.

Three days of daily dosing progesterone after traumatic brain injury is less effective than 5 at improving functional outcomes and reducing lesion size, suggesting that intermittent therapeutic serum levels of progesterone do not preclude a therapeutic effect [26]. Cutler et al. (2005) found that tapering progesterone dosing over 2 days reduced levels of inflammatory markers, apoptotic markers and behavioural tests for anxiety compared to an abrupt withdrawal after a daily dosing regimen continued for the same length of time, thus either, (1), the beneficial effects of progesterone in the brain do not directly relate to its persistence in the plasma which would contradict the mouse data of Wong et al. (2012) that brain progesterone levels drop below plasma levels approx. 2hr post-dosing [27], or (2), in the tapered dose group the beneficial effect was seen because levels became sub-therapeutic after 5 days whereas in the abrupt withdrawal group, therapeutic levels continued for 7 days and this prolonged dosing was damaging [23]. The latter explanation would also be consistent with our data in which treatment was continued for 14 days.

Progesterone treatment administered as a high dose bolus followed by a low-dose infusion increased rod death 14 days after injury and reduced rod function. Progesterone treatment affects ERG a-wave amplitude independent of the injury condition and this effect confounds ERG as a means of evaluating retinal function after progesterone treatment. Progesterone clearance in 200g male Lister-hooded rats is 17l/kg/hr and the half-life is 2.91 hr. In conclusion, progesterone is not therefore a translatable treatment for ballistic ocular injury, due to the potential for detrimental effects with low dose treatment.

References:

1. Attella MJ, Nattinville A, Stein DG. Hormonal state affects recovery from frontal cortex lesions in adult female rats. Advances.in Experimental.Medicine &.Biology. 1987;48(3):352-67.

2. Roof RL, Duvdevani R, Stein DG. Gender influences outcome of brain injury: progesterone plays a protective role. Advances.in Experimental.Medicine &.Biology. 1993;607(1-2):333-6.

3. Farace E, Alves WM. Do women fare worse: a metaanalysis of gender differences in traumatic brain injury outcome. Advances.in Experimental.Medicine &.Biology. 2000;93(4):539-45.

4. Xiao G, Wei J, Yan W, et al. Improved outcomes from the administration of progesterone for patients with acute severe traumatic brain injury: a randomized controlled trial. Advances.in Experimental.Medicine &.Biology. 2008;12(2):R61 LID-10.1186/cc6887 [doi].

5. Weichel ED, Colyer MH, Ludlow SE, et al. Combat ocular trauma visual outcomes during operations Iraqi and Enduring Freedom. Advances.in Experimental.Medicine &.Biology. 2008;115(12):2235-45.

6. Wong TY, Klein BE, Klein R. The prevalence and 5-year incidence of ocular trauma. The Beaver Dam Eye Study. Advances.in Experimental.Medicine &.Biology. 2000;107(12):2196.

7. Jones NP, Hayward JM, Khaw PT, et al. Function of an ophthalmic "accident and emergency" department: results of a six month survey. Advances.in Experimental.Medicine &.Biology. 1986;292(6514):188-90.

8. Blanch RJ, Good PA, Shah P, et al. Visual outcomes after blunt ocular trauma. http://dx.doi.org/10.1016/j.ophtha.2013.01.009. Advances.in Experimental.Medicine &.Biology. 2013.

9. Souza-Santos F, Lavinsky D, Moraes NS, et al. Spectral-domain optical coherence tomography in patients with commotio retinae. Advances.in Experimental.Medicine &.Biology. 2012;32:711-8.

10. Blanch RJ, Ahmed Z, Sik A, et al. Neuroretinal cell death in a murine model of closed globe injury; pathological and functional characterisation. Advances.in Experimental.Medicine &.Biology. 2012.

11. Sipperley JO, Quigley HA, Gass JD. Traumatic retinopathy in primates: the explanation of commotio retinae. Advances.in Experimental.Medicine &.Biology. 1978;96(12):2267.

12. Kaldi I, Berta A. Progesterone administration fails to protect albino male rats against photostress-induced retinal degeneration. Advances.in Experimental.Medicine &.Biology. 2004;14(4):306-14.

13. Doonan F, O'Driscoll C, Kenna P, Cotter TG. Enhancing survival of photoreceptor cells in vivo using the synthetic progestin Norgestrel. Advances.in Experimental.Medicine &.Biology. 2011;118(5):915-27 LID - 10.1111/j.1.

14. Ciriza I, Carrero P, Frye CA, Garcia-Segura LM. Reduced metabolites mediate neuroprotective effects of progesterone in the adult rat hippocampus. The synthetic progestin medroxyprogesterone acetate (Provera) is not neuroprotective. Advances.in Experimental.Medicine &.Biology. 2006;66(9):916-28.

15. O'Steen WK. Ovarian steroid effects on light-induced retinal photoreceptor damage. Advances.in Experimental.Medicine &.Biology. 1977;25(4):361-9.

16. Sánchez-Vallejo V, Almansa I, López-Pedrajas R, et al. The effect of progesterone on retinitis pigmentosa. Advances.in Experimental.Medicine &.Biology. 2012.

17. Gangrade NK, Boudinot FD, Price JC. Pharmacokinetics of progesterone in ovariectomized rats after single dose intravenous administration. Advances.in Experimental.Medicine &.Biology. 1992;13(9):703-9.

18. Petroff BK, Mizinga KM. Pharmacokinetics of ovarian steroids in Sprague-Dawley rats after acute exposure to 2,3,7,8-tetrachlorodibenzo-p-dioxin (TCDD). Advances.in Experimental.Medicine &.Biology. 2003;3(2):131-41.

19. McCormack JT, Greenwald GS. Progesterone and oestradiol-17beta concentrations in the peripheral plasma during pregnancy in the mouse. Advances.in Experimental.Medicine &.Biology. 1974;62(1):101-7.

20. Virgo BB, Bellward GD. Serum progesterone levels in the pregnant and postpartum laboratory mouse. Advances.in Experimental.Medicine &.Biology. 1974;95(5):1486-90.

21. Blanch RJ, Ahmed Z, Berry M, et al. Animal Models of Retinal Injury. Advances.in Experimental.Medicine &.Biology. 2012;53(6):2913-20.

22. Stein DG. Progesterone exerts neuroprotective effects after brain injury. Advances.in Experimental.Medicine &.Biology. 2008;57(2):386-97.

23. Cutler SM, Pettus EH, Hoffman SW, Stein DG. Tapered progesterone withdrawal enhances behavioral and molecular recovery after traumatic brain injury. Advances.in Experimental.Medicine &.Biology. 2005;195(2):423-9.

24. Brule J, Lavoie MP, Casanova C, et al. Evidence of a possible impact of the menstrual cycle on the reproducibility of scotopic ERGs in women. Advances.in Experimental.Medicine &.Biology. 2007;114(3):125-34.

25. Goss CW, Hoffman SW, Stein DG. Behavioral effects and anatomic correlates after brain injury: a progesterone dose-response study. Advances.in Experimental.Medicine &.Biology. 2003;76(2):231-42.

26. Shear DA, Galani R, Hoffman SW, Stein DG. Progesterone protects against necrotic damage and behavioral abnormalities caused by traumatic brain injury. Advances.in Experimental.Medicine &.Biology. 2002;178(1):59-67.

27. Wong R, Ray D, Kendall DA. Progesterone pharmacokinetics in the mouse: implications for potential stroke therapy. Advances.in Experimental.Medicine &.Biology. 2012;64(11):1614-20 LID - 10.1111/j.2.

APPENDIX 19

```
 GET DATA /TYPE=XLSX
  /FILE='C:\Users\Public\Documents\PhD\lab work\Results\Z\average thickness spreadsheet shee
  /SHEET=name 'Sheet2'
  /CELLRANGE=full
  /READNAMES=on
  /ASSUMEDSTRWIDTH=32767.
EXECUTE.
DATASET NAME DataSet1 WINDOW=FRONT.
* Generalized Estimating Equations.
GENLIN AveragethicknessBCpixels BY Treatment0control1progesterone NORMALISEDSLIDENO (ORDER=A
  /MODEL Treatment0control1progesterone NORMALISEDSLIDENO Treatment0control1progesterone*NOR
 DISTRIBUTION=GAMMA LINK=LOG
  /CRITERIA METHOD=FISHER(1) SCALE=MLE MAXITERATIONS=100 MAXSTEPHALVING=5 PCONVERGE=1E-006(A
  /EMMEANS TABLES=Treatment0control1progesterone*NORMALISEDSLIDENO SCALE=ORIGINAL
  /REPEATED SUBJECT=ANIMALNUMBER*Treatment0control1progesterone WITHINSUBJECT=NORMALISEDSLID
  /MISSING CLASSMISSING=EXCLUDE
  /PRINT CPS DESCRIPTIVES MODELINFO FIT SUMMARY WORKINGCORR
  /SAVE RESID PEARSONRESID.
```

Generalized Linear Models

Notes

Output Created		07-JUN-2013 13:33:03
Comments		
Input	Active Dataset	DataSet1
	Filter	<none>
	Weight	<none>
	Split File	<none>
	N of Rows in Working Data File	439
Missing Value Handling	Definition of Missing	User-defined missing values for factor, subject and within-subject variables are treated as missing.
	Cases Used	Statistics are based on cases with valid data for all variables in the model.
Weight Handling		not applicable

Notes

Syntax		GENLIN AveragethicknessBCpixels BY Treatment0control1progesterone NORMALISEDSLIDENO (ORDER=ASCENDING) /MODEL Treatment0control1progesterone NORMALISEDSLIDENO Treatment0control1progesterone*NORMALISEDSLIDENO INTERCEPT=YES DISTRIBUTION=GAMMA LINK=LOG /CRITERIA METHOD=FISHER(1) SCALE=MLE MAXITERATIONS=100 MAXSTEPHALVING=5 PCONVERGE=1E-006(ABSOLUTE) SINGULAR=1E-012 ANALYSISTYPE=3(WALD) CILEVEL=95 LIKELIHOOD=FULL /EMMEANS TABLES=Treatment0control1progesterone*NORMALISEDSLIDENO SCALE=ORIGINAL /REPEATED SUBJECT=ANIMALNUMBER*Treatment0control1progesterone WITHINSUBJECT=NORMALISEDSLIDENO SORT=YES CORRTYPE=AR(1) ADJUSTCORR=YES COVB=ROBUST MAXITERATIONS=100 PCONVERGE=1e-006(ABSOLUTE) UPDATECORR=1 /MISSING CLASSMISSING=EXCLUDE /PRINT CPS DESCRIPTIVES MODELINFO FIT SUMMARY ...
Resources	Processor Time	00:00:00.20
	Elapsed Time	00:00:00.19
Variables Created or Modified	Raw Residual	Residual
	Pearson Residual	PearsonResidual

[DataSet1]

Model Information

Dependent Variable		AveragethicknessBCpixels
Probability Distribution		Gamma
Link Function		Log
Subject Effect	1	ANIMALNUMBER
	2	Treatment0control1progesterone
Within-Subject Effect	1	NORMALISEDSLIDENO
Working Correlation Matrix Structure		AR(1)

Case Processing Summary

	N	Percent
Included	111	25.3%
Excluded	328	74.7%
Total	439	100.0%

Correlated Data Summary

Number of Levels	Subject Effect	ANIMALNUMBER	16
		Treatment0control1progesterone	2
	Within-Subject Effect	NORMALISEDSLIDENO	7
Number of Subjects			16
Number of Measurements per Subject	Minimum		6
	Maximum		7
Correlation Matrix Dimension			7

Categorical Variable Information

			N	Percent
Factor	Treatment0control1progesterone	.0	55	49.5%
		1.0	56	50.5%
		Total	111	100.0%
	NORMALISEDSLIDENO	1.0	16	14.4%
		2.0	16	14.4%
		3.0	16	14.4%
		4.0	16	14.4%
		5.0	16	14.4%
		6.0	16	14.4%
		7.0	15	13.5%
		Total	111	100.0%

Continuous Variable Information

		N	Minimum	Maximum
Dependent Variable	AveragethicknessBCpixels	111	12.29820825	74.77330651

Continuous Variable Information

		Mean	Std. Deviation
Dependent Variable	AveragethicknessBCpixels	33.03051119	14.23112397

Goodness of Fit[a]

	Value
Quasi Likelihood under Independence Model Criterion (QIC)[b]	34.512
Corrected Quasi Likelihood under Independence Model Criterion (QICC)[b]	34.724

Dependent Variable: AveragethicknessBCpixels
Model: (Intercept), Treatment0control1progesterone, NORMALISEDSLIDENO, Treatment0control1progesterone * NORMALISEDSLIDENO

a. Information criteria are in small-is-better form.

b. Computed using the full log quasi-likelihood function.

Tests of Model Effects

Source	Type III		
	Wald Chi-Square	df	Sig.
(Intercept)	7620.857	1	.000
Treatment0control1progesterone	9.838	1	.002
NORMALISEDSLIDENO	256.968	6	.000
Treatment0control1progesterone * NORMALISEDSLIDENO	12.526	6	.051

Dependent Variable: AveragethicknessBCpixels
Model: (Intercept), Treatment0control1progesterone, NORMALISEDSLIDENO, Treatment0control1progesterone * NORMALISEDSLIDENO

Working Correlation Matrix[a]

Measurement	Measurement			
	[NORMALISEDSLIDENO = 1.0]	[NORMALISEDSLIDENO = 2.0]	[NORMALISEDSLIDENO = 3.0]	[NORMALISEDSLIDENO = 4.0]
[NORMALISEDSLIDENO = 1.0]	1.000	.606	.367	.222
[NORMALISEDSLIDENO = 2.0]	.606	1.000	.606	.367
[NORMALISEDSLIDENO = 3.0]	.367	.606	1.000	.606
[NORMALISEDSLIDENO = 4.0]	.222	.367	.606	1.000
[NORMALISEDSLIDENO = 5.0]	.134	.222	.367	.606
[NORMALISEDSLIDENO = 6.0]	.081	.134	.222	.367
[NORMALISEDSLIDENO = 7.0]	.049	.081	.134	.222

Working Correlation Matrix[a]

Measurement	Measurement		
	[NORMALISEDSLIDENO = 5.0]	[NORMALISEDSLIDENO = 6.0]	[NORMALISEDSLIDENO = 7.0]
[NORMALISEDSLIDENO = 1.0]	.134	.081	.049
[NORMALISEDSLIDENO = 2.0]	.222	.134	.081
[NORMALISEDSLIDENO = 3.0]	.367	.222	.134
[NORMALISEDSLIDENO = 4.0]	.606	.367	.222
[NORMALISEDSLIDENO = 5.0]	1.000	.606	.367
[NORMALISEDSLIDENO = 6.0]	.606	1.000	.606
[NORMALISEDSLIDENO = 7.0]	.367	.606	1.000

Dependent Variable: AveragethicknessBCpixels
Model: (Intercept), Treatment0control1progesterone, NORMALISEDSLIDENO, Treatment0control1progesterone * NORMALISEDSLIDENO

a. The AR(1) working correlation matrix structure is computed assuming the measurements are equally spaced for all subjects.

Estimated Marginal Means: Treatment0control1progesterone* NORMALISEDSLIDENO

Estimates

Treatment0control1progesterone	NORMALISEDSLIDENO	Mean	Std. Error
.0	1.0	60.07650718	4.383263739
	2.0	43.11638104	3.730768509
	3.0	32.05467463	3.084917918
	4.0	24.28038784	2.691763282
	5.0	27.80060506	2.895738289
	6.0	32.38464861	3.800737267
	7.0	38.38837737	4.792423572
1.0	1.0	51.09394954	2.225512732
	2.0	36.76008455	2.768839079
	3.0	26.31099924	1.600848052
	4.0	21.65108026	1.253842762
	5.0	20.21749075	1.002441065
	6.0	20.55869538	1.457280259
	7.0	27.72464911	2.686536112

Estimates

Treatment0control1progesterone	NORMALISEDSLIDENO	95% Wald Confidence Interval	
		Lower	Upper
.0	1.0	52.07147164	69.31217040
	2.0	36.39063609	51.08518326
	3.0	26.54436698	38.70885927
	4.0	19.53844660	30.17318857
	5.0	22.66690689	34.09700519
	6.0	25.73002494	40.76037501
	7.0	30.05628800	49.03025671
1.0	1.0	46.91302774	55.64747800
	2.0	31.71483029	42.60794725
	3.0	23.35325546	29.64334810
	4.0	19.32793071	24.25346424
	5.0	18.34519127	22.28087603
	6.0	17.89200772	23.62283554
	7.0	22.92894582	33.52339765

```
GET
  FILE='C:\Users\Public\Documents\PhD\ERG\Results\Z-CEM1376-7\progesterone scotopic ERG data
DATASET NAME DataSet2 WINDOW=FRONT.
* Generalized Estimating Equations.
GENLIN awaveamplitudev BY timepointdays flashintensitymcd Treated1progesterone0vehicle EyeO
  /MODEL timepointdays flashintensitymcd Treated1progesterone0vehicle EyeOD1OS2 timepointday
    Treated1progesterone0vehicle*EyeOD1OS2 timepointdays*flashintensitymcd*Treated1progester
    timepointdays*flashintensitymcd*Treated1progesterone0vehicle*EyeOD1OS2 INTERCEPT=YES
 DISTRIBUTION=GAMMA LINK=LOG
```

```
/CRITERIA METHOD=FISHER(1) SCALE=MLE MAXITERATIONS=100 MAXSTEPHALVING=5 PCONVERGE=1E-006(A
/EMMEANS TABLES=timepointdays*flashintensitymcd*Treated1progesterone0vehicle*EyeOD1OS2 SCA
/REPEATED SUBJECT=animal WITHINSUBJECT=Treated1progesterone0vehicle*EyeOD1OS2*timepointday
/MISSING CLASSMISSING=EXCLUDE
/PRINT CPS DESCRIPTIVES MODELINFO FIT SUMMARY WORKINGCORR
/SAVE RESID PEARSONRESID.
```

Generalized Linear Models

Notes

Output Created		07-JUN-2013 16:17:50
Comments		
Input	Data	C:\Users\Public\Documents\PhD\ERG\Results\Z-CEM1376-7\progesterone scotopic ERG data.sav
	Active Dataset	DataSet2
	Filter	<none>
	Weight	<none>
	Split File	<none>
	N of Rows in Working Data File	512
Missing Value Handling	Definition of Missing	User-defined missing values for factor, subject and within-subject variables are treated as missing.
	Cases Used	Statistics are based on cases with valid data for all variables in the model.
Weight Handling		not applicable

Notes

Syntax	GENLIN awaveamplitudev BY timepointdays flashintensitymcd Treated1progesterone0vehicle EyeOD1OS2 (ORDER=ASCENDING) /MODEL timepointdays flashintensitymcd Treated1progesterone0vehicle EyeOD1OS2 timepointdays*flashintensitymcd timepointdays*Treated1progesterone0vehicle timepointdays*EyeOD1OS2 flashintensitymcd*Treated1progesterone0vehicle flashintensitymcd*EyeOD1OS2 Treated1progesterone0vehicle*EyeOD1OS2 timepointdays*flashintensitymcd*Treated1progesterone0vehicle timepointdays*flashintensitymcd*EyeOD1OS2 timepointdays*Treated1progesterone0vehicle*EyeOD1OS2 flashintensitymcd*Treated1progesterone0vehicle*EyeOD1OS2 timepointdays*flashintensitymcd*Treated1progesterone0vehicle*EyeOD1OS2 INTERCEPT=YES DISTRIBUTION=GAMMA LINK=LOG /CRITERIA METHOD=FISHER(1) SCALE=MLE MAXITERATIONS=100 MAXSTEPHALVING=5 PCONVERGE=1E-006(ABSOLUTE) SINGULAR=1E-012 ANALYSISTYPE=3(WALD) CILEVEL=95 LIKELIHOOD=FULL /EMMEANS TABLES=timepointdays*flashintensitymcd*Treated1progesterone0vehicle*EyeOD1OS2 SCALE=ORIGINAL /REPEATED SUBJECT=animal WITHINSUBJECT=Treated1progesterone0vehicle*EyeOD1OS2*timepointdays*flashintensitymcd SORT=YES CORRTYPE=AR(1) ADJUSTCORR=YES COVB=ROBUST MAXITERATIONS=100 PCONVERGE=1e-006(ABSOLUTE) UPDATECORR=1 /MISSING CLASSMISSING=EXCLUDE /PRINT CPS DESCRIPTIVES MODELINFO FIT SUMMARY WORKINGCORR...

Notes

Resources	Processor Time	00:00:03.81
	Elapsed Time	00:00:03.80
Variables Created or Modified	Raw Residual	Residual
	Pearson Residual	PearsonResidual

[DataSet2] C:\Users\Public\Documents\PhD\ERG\Results\Z-CEM1376-7\progesterone scotopic ERG data.sav

Model Information

Dependent Variable		awaveamplitudev
Probability Distribution		Gamma
Link Function		Log
Subject Effect	1	animal
Within-Subject Effect	1	Treated1progesterone0vehicle
	2	EyeOD1OS2
	3	timepointdays
	4	flashintensitymcd
Working Correlation Matrix Structure		AR(1)

Case Processing Summary

	N	Percent
Included	496	96.9%
Excluded	16	3.1%
Total	512	100.0%

Correlated Data Summary

Number of Levels	Subject Effect	animal	16
	Within-Subject Effect	Treated1progesterone0vehicle	2
		EyeOD1OS2	2
		timepointdays	2
		flashintensitymcd	8
Number of Subjects			16
Number of Measurements per Subject	Minimum		16
	Maximum		32
Correlation Matrix Dimension			64

Categorical Variable Information

			N	Percent
Factor	timepointdays	7	256	51.6%
		14	240	48.4%
		Total	496	100.0%
	flashintensitymcd	10	62	12.5%
		30	62	12.5%
		100	62	12.5%
		300	62	12.5%
		1000	62	12.5%
		3000	62	12.5%
		10000	62	12.5%
		25000	62	12.5%
		Total	496	100.0%
	Treated1progesterone0vehicle	0	256	51.6%
		1	240	48.4%
		Total	496	100.0%
	EyeOD1OS2	1	248	50.0%
		2	248	50.0%
		Total	496	100.0%

Continuous Variable Information

		N	Minimum	Maximum	Mean
Dependent Variable	awaveamplitudev	496	0	382	89.58

Continuous Variable Information

		Std. Deviation
Dependent Variable	awaveamplitudev	85.630

Goodness of Fit[a]

	Value
Quasi Likelihood under Independence Model Criterion (QIC)[b]	275.800
Corrected Quasi Likelihood under Independence Model Criterion (QICC)[b]	304.230

Dependent Variable: awaveamplitudev
Model: (Intercept), timepointdays, flashintensitymcd, Treated1progesterone0vehicle, EyeOD1OS2, timepointdays * flashintensitymcd, timepointdays * Treated1progesterone0vehicle, timepointdays * EyeOD1OS2, flashintensitymcd * Treated1progesterone0vehicle, flashintensitymcd * EyeOD1OS2, Treated1progesterone0vehicle * EyeOD1OS2, timepointdays * flashintensitymcd * Treated1progesterone0vehicle, timepointdays * flashintensitymcd * EyeOD1OS2, timepointdays * Treated1progesterone0vehicle * EyeOD1OS2, flashintensitymcd * Treated1progesterone0vehicle * EyeOD1OS2, timepointdays * flashintensitymcd * Treated1progesterone0vehicle * EyeOD1OS2

a. Information criteria are in small-is-better form.

b. Computed using the full log quasi-likelihood function.

Tests of Model Effects

Source	Type III		
	Wald Chi-Square	df	Sig.
(Intercept)	8914.011	1	.000
timepointdays	.517	1	.472
flashintensitymcd	13543.551	7	.000
Treated1progesterone0vehicle	.000	1	.998
EyeOD1OS2	12.032	1	.001
timepointdays * flashintensitymcd	7.459	7	.383
timepointdays * Treated1progesterone0vehicle	3.006	1	.083
timepointdays * EyeOD1OS2	.006	1	.936
flashintensitymcd * Treated1progesterone0vehicle	29.230	7	.000
flashintensitymcd * EyeOD1OS2	25.888	7	.001
Treated1progesterone0vehicle * EyeOD1OS2	.512	1	.474
timepointdays * flashintensitymcd * Treated1progesterone0vehicle	24.007	7	.001
timepointdays * flashintensitymcd * EyeOD1OS2	7.746	7	.356
timepointdays * Treated1progesterone0vehicle * EyeOD1OS2	.000	1	.986
flashintensitymcd * Treated1progesterone0vehicle * EyeOD1OS2	16.844	7	.018
timepointdays * flashintensitymcd * Treated1progesterone0vehicle * EyeOD1OS2	22.618	7	.002

Dependent Variable: awaveamplitudev
Model: (Intercept), timepointdays, flashintensitymcd, Treated1progesterone0vehicle, EyeOD1OS2, timepointdays * flashintensitymcd, timepointdays * Treated1progesterone0vehicle, timepointdays * EyeOD1OS2, flashintensitymcd * Treated1progesterone0vehicle, flashintensitymcd * EyeOD1OS2, Treated1progesterone0vehicle * EyeOD1OS2, timepointdays * flashintensitymcd * Treated1progesterone0vehicle, timepointdays * flashintensitymcd * EyeOD1OS2, timepointdays * Treated1progesterone0vehicle * EyeOD1OS2, flashintensitymcd * Treated1progesterone0vehicle * EyeOD1OS2, timepointdays * flashintensitymcd * Treated1progesterone0vehicle * EyeOD1OS2

Estimated Marginal Means: timepointdays* flashintensitymcd* Treated1progesterone0vehicle* EyeOD1OS2

Estimates

timepointdays	flashintensitymcd	Treated1progesterone0vehicle	EyeOD1OS2	Mean	Std. Error
7	10	0	1	1.75	.469
			2	6.14	2.498
		1	1	4.05	.911
			2	6.36	.879
	30	0	1	7.88	.920
			2	12.30	3.065
		1	1	9.64	2.058
			2	11.90	2.651
	100	0	1	18.35	2.856
			2	32.19	7.041
		1	1	26.34	4.458
			2	34.38	4.929
	300	0	1	49.39	5.643
			2	62.88	10.654
		1	1	63.02	11.042
			2	83.70	11.756
	1000	0	1	90.46	8.712
			2	106.04	17.682
		1	1	107.49	17.092
			2	140.71	17.462
	3000	0	1	115.50	11.202
			2	143.72	23.410
		1	1	142.30	19.537
			2	181.01	22.087
	10000	0	1	139.50	12.077
			2	187.24	28.090
		1	1	168.93	24.919
			2	220.61	23.182

Estimates

timepointdays	flashintensitymcd	Treated1progesterone0vehicle	EyeOD1OS2	95% Wald ... Lower
7	10	0	1	1.03
			2	2.76
		1	1	2.61
			2	4.85
	30	0	1	6.26
			2	7.55
		1	1	6.34
			2	7.69
	100	0	1	13.53
			2	20.96
		1	1	18.90
			2	25.95
	300	0	1	39.48
			2	45.11
		1	1	44.71
			2	63.56
	1000	0	1	74.90
			2	76.47
		1	1	78.71
			2	110.33
	3000	0	1	95.51
			2	104.45
		1	1	108.73
			2	142.51
	10000	0	1	117.73
			2	139.54
		1	1	126.51
			2	179.55

Estimates

timepointdays	flashintensitymcd	Treated1progesterone0vehicle	EyeOD1OS2	95% Wald ... Upper
7	10	0	1	2.96
			2	13.63
		1	1	6.29
			2	8.34
	30	0	1	9.90
			2	20.05
		1	1	14.65
			2	18.42
	100	0	1	24.89
			2	49.42
		1	1	36.70
			2	45.53
	300	0	1	61.79
			2	87.64
		1	1	88.85
			2	110.22
	1000	0	1	109.26
			2	147.03
		1	1	146.79
			2	179.46
	3000	0	1	139.68
			2	197.78
		1	1	186.24
			2	229.92
	10000	0	1	165.30
			2	251.24
		1	1	225.56
			2	271.07

Estimates

timepointdays	flashintensitymcd	Treated1progesterone0vehicle	EyeOD1OS2	Mean	Std. Error
	25000	0	1	160.03	11.481
			2	208.15	28.875
		1	1	189.61	28.086
			2	249.68	27.645
14	10	0	1	3.26	1.021
			2	5.46	1.226
		1	1	2.97	.498
			2	6.04	1.450
	30	0	1	6.26	1.476
			2	11.85	1.931
		1	1	7.44	1.154
			2	11.31	3.537
	100	0	1	21.19	5.327
			2	36.36	5.351
		1	1	19.07	3.811
			2	20.52	3.646
	300	0	1	56.06	12.832
			2	89.21	10.151
		1	1	45.09	9.821
			2	58.78	11.084
	1000	0	1	94.95	21.329
			2	145.16	15.341
		1	1	78.75	16.822
			2	90.75	17.462
	3000	0	1	125.23	27.224
			2	180.31	18.020
		1	1	102.61	20.415
			2	122.42	20.602
	10000	0	1	151.58	31.987
			2	218.06	22.756
		1	1	112.48	20.592
			2	156.79	19.998
	25000	0	1	173.31	33.635
			2	239.18	23.546
		1	1	135.43	23.851
			2	177.62	21.151

Estimates

timepointdays	flashintensitymcd	Treated1progesterone0vehicle	EyeOD1OS2	95% Wald ... Lower
	25000	0	1	139.03
			2	158.60
		1	1	141.84
			2	200.97
14	10	0	1	1.77
			2	3.52
		1	1	2.14
			2	3.77
	30	0	1	3.95
			2	8.61
		1	1	5.49
			2	6.13
	100	0	1	12.94
			2	27.25
		1	1	12.89
			2	14.48
	300	0	1	35.80
			2	71.38
		1	1	29.42
			2	40.62
	1000	0	1	61.14
			2	118.01
		1	1	51.81
			2	62.24
	3000	0	1	81.78
			2	148.24
		1	1	69.47
			2	88.02
	10000	0	1	100.23
			2	177.73
		1	1	78.57
			2	122.11
	25000	0	1	118.48
			2	197.20
		1	1	95.90
			2	140.65

Estimates

timepointdays	flashintensitymcd	Treated1progesterone0vehicle	EyeOD1OS2	95% Wald ... Upper
	25000	0	1	184.19
			2	273.19
		1	1	253.48
			2	310.19
14	10	0	1	6.03
			2	8.48
		1	1	4.13
			2	9.67
	30	0	1	9.94
			2	16.31
		1	1	10.08
			2	20.88
	100	0	1	34.68
			2	48.52
		1	1	28.21
			2	29.06
	300	0	1	87.80
			2	111.50
		1	1	69.10
			2	85.06
	1000	0	1	147.47
			2	178.57
		1	1	119.70
			2	132.32
	3000	0	1	191.75
			2	219.33
		1	1	151.54
			2	170.25
	10000	0	1	229.22
			2	267.55
		1	1	161.03
			2	201.32
	25000	0	1	253.53
			2	290.08
		1	1	191.26
			2	224.31

```
EXAMINE VARIABLES=Residual PearsonResidual
 /PLOT BOXPLOT STEMLEAF NPPLOT
 /COMPARE GROUPS
 /STATISTICS DESCRIPTIVES
 /CINTERVAL 95
```

```
  /MISSING LISTWISE
  /NOTOTAL.
```

Explore

Notes

Output Created		07-JUN-2013 16:19:26
Comments		
Input	Data	C:\Users\Public\Documents\PhD\ERG\Results\Z-CEM1376-7\progesterone scotopic ERG data.sav
	Active Dataset	DataSet2
	Filter	<none>
	Weight	<none>
	Split File	<none>
	N of Rows in Working Data File	512
Missing Value Handling	Definition of Missing	User-defined missing values for dependent variables are treated as missing.
	Cases Used	Statistics are based on cases with no missing values for any dependent variable or factor used.
Syntax		EXAMINE VARIABLES=Residual PearsonResidual /PLOT BOXPLOT STEMLEAF NPPLOT /COMPARE GROUPS /STATISTICS DESCRIPTIVES /CINTERVAL 95 /MISSING LISTWISE /NOTOTAL.
Resources	Processor Time	00:00:02.50
	Elapsed Time	00:00:02.24

```
[DataSet2] C:\Users\Public\Documents\PhD\ERG\Results\Z-CEM1376-7\progesterone scotopic ERG data.sav
```

Case Processing Summary

	Cases					
	Valid		Missing		Total	
	N	Percent	N	Percent	N	Percent
Raw Residual	496	96.9%	16	3.1%	512	100.0%
Pearson Residual	496	96.9%	16	3.1%	512	100.0%

Descriptives

			Statistic	Std. Error
Raw Residual	Mean		.17798	2.018593
	95% Confidence Interval for Mean	Lower Bound	-3.78809	
		Upper Bound	4.14404	
	5% Trimmed Mean		-.22467	
	Median		-.11241	
	Variance		2021.060	
	Std. Deviation		44.956205	
	Minimum		-149.350	
	Maximum		162.588	
	Range		311.937	
	Interquartile Range		35.302	
	Skewness		.114	.110
	Kurtosis		1.540	.219
Pearson Residual	Mean		.00318	.022900
	95% Confidence Interval for Mean	Lower Bound	-.04181	
		Upper Bound	.04817	
	5% Trimmed Mean		-.01134	
	Median		-.01118	
	Variance		.260	
	Std. Deviation		.510000	
	Minimum		-.981	
	Maximum		2.503	
	Range		3.484	
	Interquartile Range		.736	
	Skewness		.522	.110
	Kurtosis		.570	.219

Tests of Normality

	Kolmogorov-Smirnov[a]			Shapiro-Wilk		
	Statistic	df	Sig.	Statistic	df	Sig.
Raw Residual	.115	496	.000	.957	496	.000
Pearson Residual	.069	496	.000	.979	496	.000

a. Lilliefors Significance Correction

Raw Residual

```
Raw Residual Stem-and-Leaf Plot

 Frequency    Stem &  Leaf

    30.00 Extremes    (=<-71)
    12.00       -6 .  245&&&
    15.00       -5 .  02479&
```

```
   28.00       -4 .  002333356779&
   18.00       -3 .  012357&
   14.00       -2 .  13458&
   35.00       -1 .  000111255666889&
   98.00       -0 .  00000011111111122222222233333344455556777888899
   96.00        0 .  000000001111111122222333333444455566677889999999
   36.00        1 .  01112245557778 89&
   23.00        2 .  00134589&
   14.00        3 .  0257&
   19.00        4 .  167778&&
   16.00        5 .  34567&
    8.00        6 .  26&
   34.00 Extremes    (>=71)

Stem width:    10.000
Each leaf:       2 case(s)


& denotes fractional leaves.
```

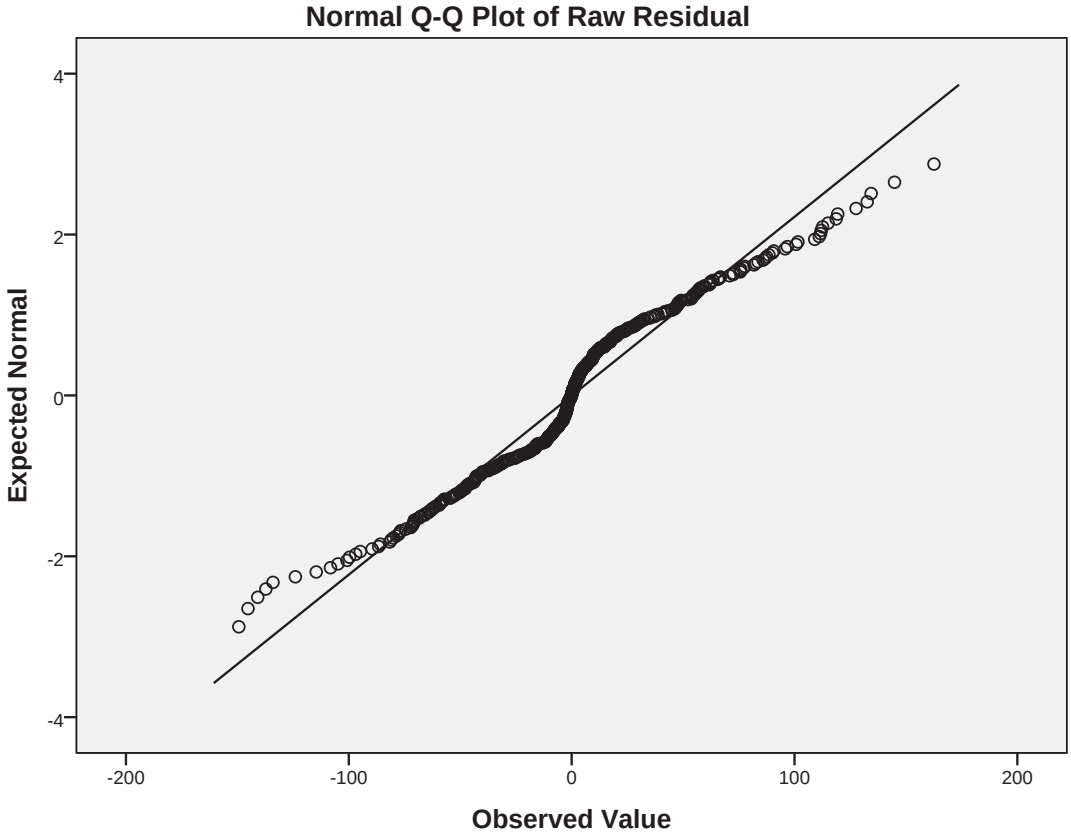

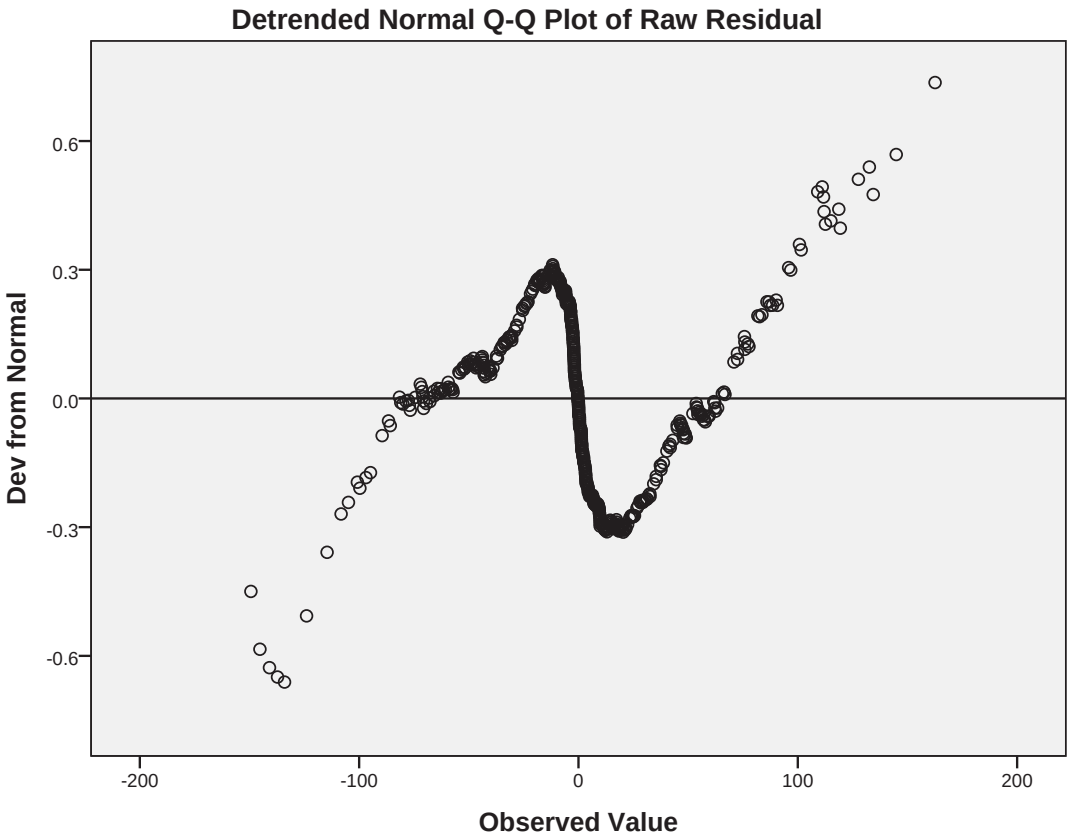
Detrended Normal Q-Q Plot of Raw Residual
Dev from Normal
0.6
0.3
0.0
-0.3
-0.6
-200
-100
0
100
200
Observed Value

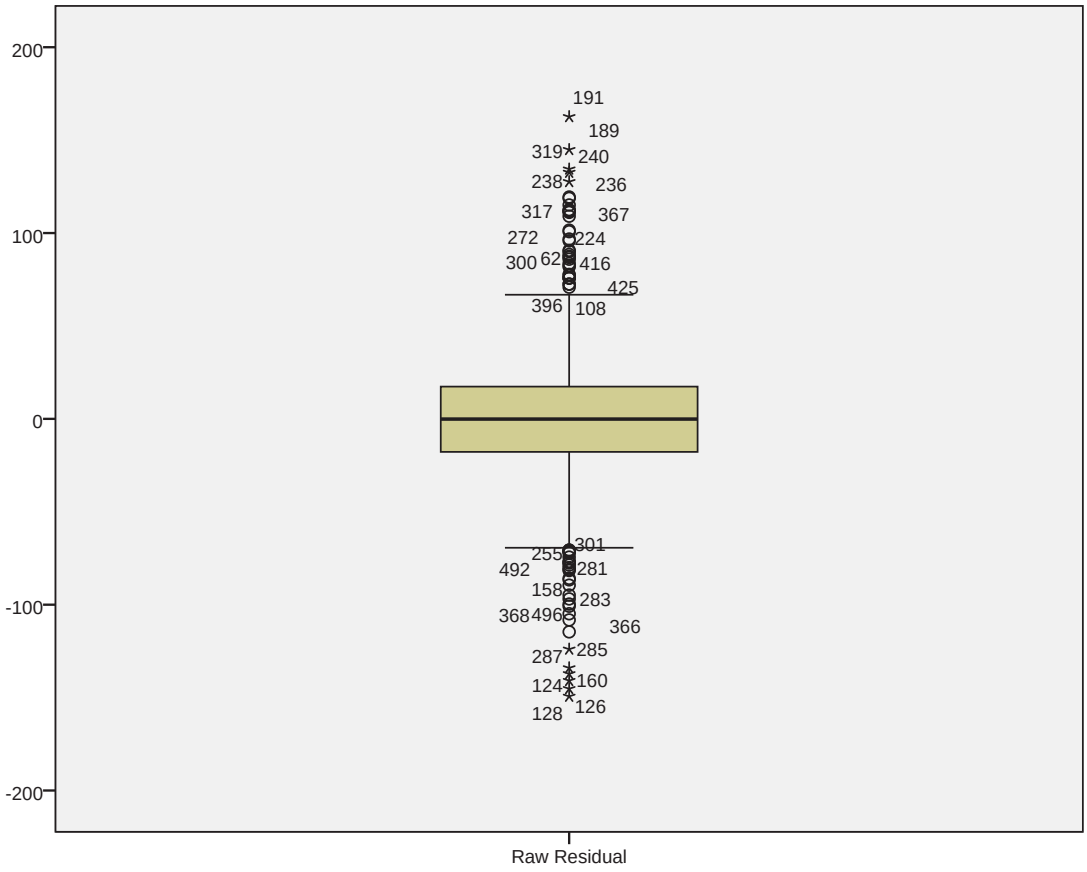

Pearson Residual

```
Pearson Residual Stem-and-Leaf Plot

 Frequency    Stem &  Leaf

    21.00       -0 .  88888888888999999999
    32.00       -0 .  66666666666666677777777777777777
    70.00       -0 .  44444444444444444444444444444444444444444444455555
555555555555555555
    68.00       -0 .  22222222222222222222233333333333333333333333333333
3333333333333333
    59.00       -0 .  00000000000000000000000000000000011111111111111111
1111111
    77.00        0 .  00000000000000000000000000000000000000000000000000001
11111111111111111111111111
    64.00        0 .  22222222222222222222222222233333333333333333333333333
333333333333
    47.00        0 .  44444444444444444444445555555555555555555555555
    22.00        0 .  6666666667777777777777
    23.00        0 .  88888888888888888999999
```

```
    5.00        1 .  00111
    5.00        1 .  22233
    1.00        1 .  4
    2.00 Extremes    (>=1.5)

Stem width:     1.000
Each leaf:       1 case(s)
```

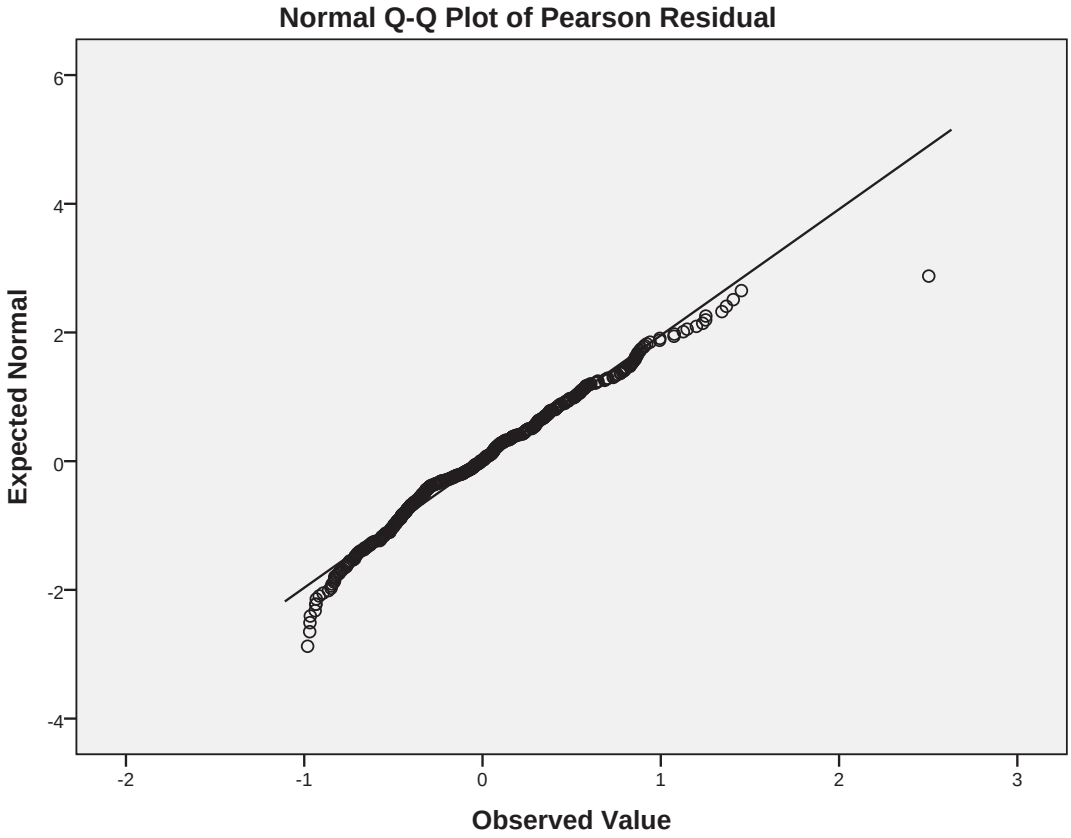

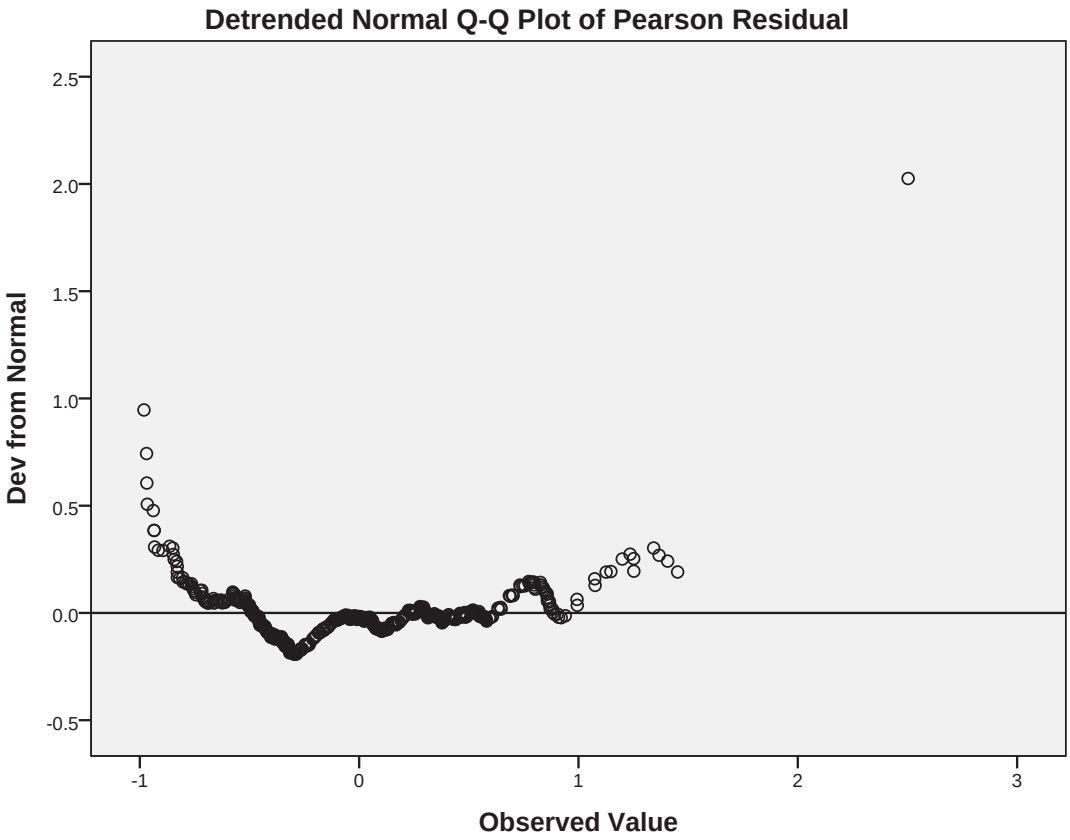
Detrended Normal Q-Q Plot of Pearson Residual
Dev from Normal
2.5
2.0
1.5
1.0
0.5
0.0
-0.5
-1
0
1
2
3
Observed Value

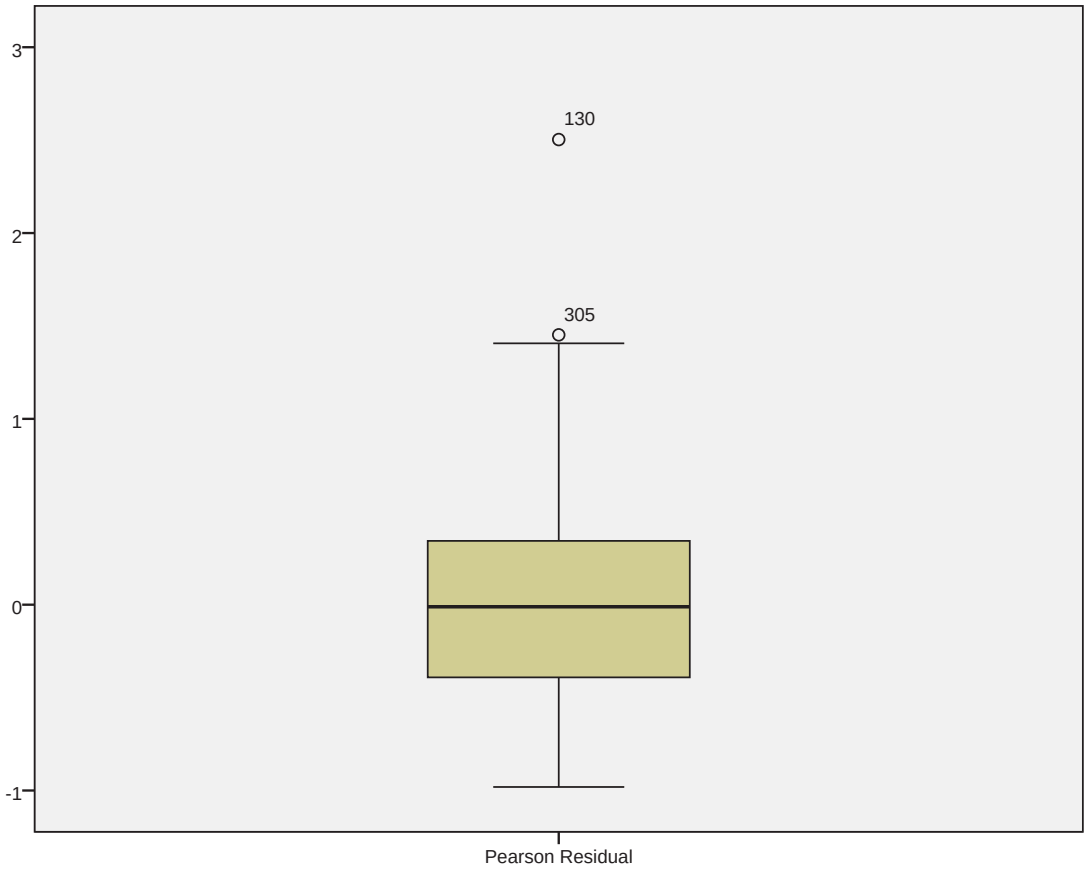


```
 * Generalized Estimating Equations.
GENLIN awaveamplitudev BY timepointdays flashintensitymcd Treated1progesterone0vehicle EyeO
  /MODEL timepointdays flashintensitymcd Treated1progesterone0vehicle EyeOD1OS2 timepointday
    Treated1progesterone0vehicle*EyeOD1OS2 timepointdays*flashintensitymcd*Treated1progester
    timepointdays*flashintensitymcd*Treated1progesterone0vehicle*EyeOD1OS2 INTERCEPT=YES
 DISTRIBUTION=GAMMA LINK=LOG
  /CRITERIA METHOD=FISHER(1) SCALE=MLE MAXITERATIONS=100 MAXSTEPHALVING=5 PCONVERGE=1E-006(A
  /EMMEANS TABLES=flashintensitymcd*Treated1progesterone0vehicle SCALE=ORIGINAL
  /REPEATED SUBJECT=animal WITHINSUBJECT=Treated1progesterone0vehicle*EyeOD1OS2*timepointday
  /MISSING CLASSMISSING=EXCLUDE
  /PRINT CPS DESCRIPTIVES MODELINFO FIT SUMMARY.
```

Estimated Marginal Means 1: flashintensitymcd* Treated1progester one0vehicle

Estimates

flashintensitymcd	Treated1progesterone0vehicle	Mean	Std. Error	95% Wald Confidence Interval	
				Lower	Upper
10	0	3.72	.476	2.90	4.78
	1	4.64	.351	4.00	5.38
30	0	9.21	.763	7.83	10.83
	1	9.91	.757	8.53	11.51
100	0	25.97	2.180	22.03	30.62
	1	24.39	1.504	21.62	27.53
300	0	62.78	4.542	54.48	72.34
	1	61.15	4.045	53.71	69.61
1000	0	107.23	7.374	93.71	122.70
	1	101.96	5.599	91.56	113.55
3000	0	139.14	9.740	121.30	159.60
	1	134.12	7.204	120.72	149.01
10000	0	171.41	11.560	150.19	195.64
	1	160.11	7.056	146.86	174.56
25000	0	192.76	11.346	171.76	216.34
	1	183.70	7.737	169.15	199.51

Estimated Marginal Means 2: flashintensitymcd* EyeOD1OS2

Estimates

flashintensitymcd	EyeOD1OS2	Mean	Std. Error	95% Wald Confidence Interval	
				Lower	Upper
10	1	2.88	.416	2.17	3.82
	2	5.99	.673	4.81	7.47
30	1	7.71	.664	6.51	9.13
	2	11.84	1.414	9.36	14.96
100	1	21.02	1.575	18.15	24.35
	2	30.14	2.288	25.98	34.98
300	1	52.96	3.736	46.12	60.81
	2	72.48	4.987	63.34	82.94
1000	1	92.34	5.871	81.52	104.59
	2	118.40	7.990	103.74	135.15
3000	1	120.55	7.506	106.70	136.20
	2	154.80	9.543	137.18	174.68
10000	1	141.58	8.733	125.45	159.77
	2	193.86	11.019	173.42	216.70
25000	1	163.36	9.303	146.11	182.65
	2	216.76	10.417	197.28	238.17

Estimated Marginal Means 3: Treated1progesterone0vehicle* EyeO D1OS2

Estimates

Treated1progesterone0vehicle	EyeOD1OS2	Mean	Std. Error	95% Wald Confidence Interval	
				Lower	Upper
0	1	38.37	4.176	31.00	47.49
	2	59.70	6.920	47.56	74.92
1	1	41.39	3.403	35.23	48.63
	2	55.36	3.370	49.14	62.38

Estimated Marginal Means 4: timepointdays* flashintensitymcd* Treated1progesterone0vehicle

Estimates

timepointdays	flashintensitymcd	Treated1progesterone0vehicle	Mean	Std. Error	95% Wald ...
					Lower
7	10	0	3.28	.607	2.28
		1	5.08	.799	3.73
	30	0	9.84	1.301	7.60
		1	10.71	1.389	8.31
	100	0	24.30	2.834	19.34
		1	30.09	3.275	24.31
	300	0	55.72	6.413	44.47
		1	72.63	8.578	57.62
	1000	0	97.94	10.551	79.30
		1	122.98	12.516	100.74
	3000	0	128.84	14.404	103.49
		1	160.49	15.713	132.47
	10000	0	161.62	16.376	132.51
		1	193.05	19.349	158.62
	25000	0	182.51	15.084	155.21
		1	217.58	22.313	177.96
14	10	0	4.22	.819	2.89
		1	4.24	.434	3.47
	30	0	8.61	.861	7.08
		1	9.17	1.525	6.62
	100	0	27.76	2.974	22.50
		1	19.78	2.962	14.75
	300	0	70.72	6.531	59.01
		1	51.48	8.866	36.73
	1000	0	117.40	11.084	97.57
		1	84.54	13.421	61.93
	3000	0	150.27	13.828	125.47
		1	112.08	16.415	84.11
	10000	0	181.80	16.505	152.17
		1	132.80	15.885	105.05

Estimates

timepointdays	flashintensitymcd	Treated1progesterone0vehicle	95% Wald ... Upper
7	10	0	4.71
		1	6.91
	30	0	12.75
		1	13.81
	100	0	30.54
		1	37.24
	300	0	69.82
		1	91.55
	1000	0	120.96
		1	150.13
	3000	0	160.40
		1	194.44
	10000	0	197.12
		1	234.95
	25000	0	214.60
		1	266.02
14	10	0	6.18
		1	5.18
	30	0	10.48
		1	12.71
	100	0	34.24
		1	26.53
	300	0	84.75
		1	72.15
	1000	0	141.27
		1	115.39
	3000	0	179.97
		1	149.34
	10000	0	217.21
		1	167.89

Estimates

timepointdays	flashintensitymcd	Treated1progesterone0vehicle	Mean	Std. Error	95% Wald ... Lower
	25000	0	203.60	17.092	172.71
		1	155.10	18.924	122.11

Estimates

timepointdays	flashintensitymcd	Treated1progesterone0vehicle	95% Wald ... Upper
	25000	0	240.01
		1	197.00

Estimated Marginal Means 5: timepointdays* flashintensitymcd* EyeOD1OS2

Estimates

timepointdays	flashintensitymcd	EyeOD1OS2	Mean	Std. Error	95% Wald ... Lower
7	10	1	2.66	.466	1.89
		2	6.25	1.343	4.10
	30	1	8.71	1.060	6.86
		2	12.10	2.022	8.72
	100	1	21.98	2.527	17.55
		2	33.26	4.350	25.74
	300	1	55.79	5.835	45.45
		2	72.54	7.983	58.47
	1000	1	98.61	9.166	82.19
		2	122.15	12.695	99.64
	3000	1	128.20	10.775	108.73
		2	161.29	16.413	132.13
	10000	1	153.51	13.128	129.82
		2	203.24	18.613	169.85
	25000	1	174.19	14.334	148.25
		2	227.97	20.232	191.57
14	10	1	3.12	.553	2.20
		2	5.74	.944	4.16
	30	1	6.82	.963	5.18
		2	11.58	2.041	8.20
	100	1	20.10	3.228	14.67
		2	27.31	3.151	21.79
	300	1	50.28	7.943	36.89
		2	72.41	7.974	58.36
	1000	1	86.47	13.402	63.82
		2	114.77	12.598	92.56
	3000	1	113.35	16.703	84.92
		2	148.57	14.540	122.64
	10000	1	130.57	18.239	99.30
		2	184.91	15.236	157.33
	25000	1	153.20	20.075	118.50
		2	206.11	15.923	177.15

Estimates

timepointdays	flashintensitymcd	EyeOD1OS2	95% Wald ... Upper
7	10	1	3.75
		2	9.52
	30	1	11.06
		2	16.79
	100	1	27.54
		2	42.98
	300	1	68.48
		2	90.01
	1000	1	118.31
		2	149.75
	3000	1	151.16
		2	196.90
	10000	1	181.52
		2	243.20
	25000	1	204.68
		2	271.28
14	10	1	4.41
		2	7.93
	30	1	9.00
		2	16.36
	100	1	27.53
		2	34.24
	300	1	68.52
		2	89.86
	1000	1	117.17
		2	142.32
	3000	1	151.31
		2	179.99
	10000	1	171.69
		2	217.32
	25000	1	198.06
		2	239.81

Estimated Marginal Means 6: timepointdays* Treated1progesterone 0vehicle* EyeOD1OS2

Estimates

timepointdays	Treated1progesterone0vehicle	EyeOD1OS2	Mean	Std. Error	95% Wald ... Lower
7	0	1	36.14	3.035	30.66
		2	55.56	9.409	39.86
	1	1	48.72	7.860	35.51
		2	64.66	7.577	51.39
14	0	1	40.73	9.434	25.87
		2	64.15	7.604	50.85
	1	1	35.17	5.623	25.71
		2	47.40	8.423	33.46

Estimates

timepointdays	Treated1progesterone0vehicle	EyeOD1OS2	95% Wald ... Upper
7	0	1	42.61
		2	77.43
	1	1	66.84
		2	81.36
14	0	1	64.14
		2	80.92
	1	1	48.11
		2	67.15

Estimated Marginal Means 7: flashintensitymcd* Treated1progesterone0vehicle* EyeOD1OS2

Estimates

flashintensitymcd	Treated1progesterone0vehicle	EyeOD1OS2	Mean	Std. Error	95% Wald ... Lower
10	0	1	2.39	.596	1.47
		2	5.79	1.110	3.98
	1	1	3.47	.504	2.61
		2	6.20	.725	4.93
30	0	1	7.02	.816	5.59
		2	12.07	2.260	8.36
	1	1	8.47	1.075	6.60
		2	11.60	1.723	8.67
100	0	1	19.72	1.977	16.20
		2	34.21	4.645	26.22
	1	1	22.41	2.495	18.02
		2	26.56	1.803	23.25
300	0	1	52.62	4.951	43.76
		2	74.89	8.859	59.40
	1	1	53.31	5.603	43.38
		2	70.14	4.932	61.11
1000	0	1	92.68	8.447	77.52
		2	124.07	14.319	98.95
	1	1	92.00	8.157	77.33
		2	113.00	7.907	98.52
3000	0	1	120.26	10.966	100.58
		2	160.98	17.437	130.19
	1	1	120.84	10.249	102.33
		2	148.86	8.767	132.63
10000	0	1	145.41	12.966	122.10
		2	202.06	21.889	163.41
	1	1	137.84	11.753	116.63
		2	185.99	6.410	173.84
25000	0	1	166.54	14.025	141.20
		2	223.12	19.964	187.23
	1	1	160.25	12.289	137.88
		2	210.59	7.390	196.59

Estimates

flashintensitymcd	Treated1progesterone0vehicle	EyeOD1OS2	95% Wald ... Upper
10	0	1	3.90
		2	8.43
	1	1	4.61
		2	7.80
30	0	1	8.82
		2	17.43
	1	1	10.86
		2	15.52
100	0	1	24.00
		2	44.64
	1	1	27.87
		2	30.34
300	0	1	63.27
		2	94.43
	1	1	65.50
		2	80.51
1000	0	1	110.80
		2	155.56
	1	1	109.46
		2	129.61
3000	0	1	143.80
		2	199.06
	1	1	142.69
		2	167.07
10000	0	1	173.18
		2	249.86
	1	1	162.91
		2	198.98
25000	0	1	196.42
		2	265.89
	1	1	186.24
		2	225.58

Estimated Marginal Means 8: timepointdays* flashintensitymcd* Treated1progesterone0vehicle* EyeOD1OS2

Estimates

timepointdays	flashintensitymcd	Treated1progesterone0vehicle	EyeOD1OS2	Mean	Std. Error
7	10	0	1	1.75	.469
			2	6.14	2.498
		1	1	4.05	.911
			2	6.36	.879
	30	0	1	7.88	.920
			2	12.30	3.065
		1	1	9.64	2.058
			2	11.90	2.651
	100	0	1	18.35	2.856
			2	32.19	7.041
		1	1	26.34	4.458
			2	34.38	4.929
	300	0	1	49.39	5.643
			2	62.88	10.654
		1	1	63.02	11.042
			2	83.70	11.756
	1000	0	1	90.46	8.712
			2	106.04	17.682
		1	1	107.49	17.092
			2	140.71	17.462
	3000	0	1	115.50	11.202
			2	143.72	23.410
		1	1	142.30	19.537
			2	181.01	22.087
	10000	0	1	139.50	12.077
			2	187.24	28.090
		1	1	168.93	24.919
			2	220.61	23.182
	25000	0	1	160.03	11.481
			2	208.15	28.875
		1	1	189.61	28.086
			2	249.68	27.645
14	10	0	1	3.26	1.021
			2	5.46	1.226
		1	1	2.97	.498
			2	6.04	1.450
	30	0	1	6.26	1.476
			2	11.85	1.931
		1	1	7.44	1.154
			2	11.31	3.537
	100	0	1	21.19	5.327
			2	36.36	5.351

Estimates

timepointdays	flashintensitymcd	Treated1progesterone0vehicle	EyeOD1OS2	95% Wald ... Lower
7	10	0	1	1.03
			2	2.76
		1	1	2.61
			2	4.85
	30	0	1	6.26
			2	7.55
		1	1	6.34
			2	7.69
	100	0	1	13.53
			2	20.96
		1	1	18.90
			2	25.95
	300	0	1	39.48
			2	45.11
		1	1	44.71
			2	63.56
	1000	0	1	74.90
			2	76.47
		1	1	78.71
			2	110.33
	3000	0	1	95.51
			2	104.45
		1	1	108.73
			2	142.51
	10000	0	1	117.73
			2	139.54
		1	1	126.51
			2	179.55
	25000	0	1	139.03
			2	158.60
		1	1	141.84
			2	200.97
14	10	0	1	1.77
			2	3.52
		1	1	2.14
			2	3.77
	30	0	1	3.95
			2	8.61
		1	1	5.49
			2	6.13
	100	0	1	12.94
			2	27.25

Estimates

timepointdays	flashintensitymcd	Treated1progesterone0vehicle	EyeOD1OS2	95% Wald ... Upper
7	10	0	1	2.96
			2	13.63
		1	1	6.29
			2	8.34
	30	0	1	9.90
			2	20.05
		1	1	14.65
			2	18.42
	100	0	1	24.89
			2	49.42
		1	1	36.70
			2	45.53
	300	0	1	61.79
			2	87.64
		1	1	88.85
			2	110.22
	1000	0	1	109.26
			2	147.03
		1	1	146.79
			2	179.46
	3000	0	1	139.68
			2	197.78
		1	1	186.24
			2	229.92
	10000	0	1	165.30
			2	251.24
		1	1	225.56
			2	271.07
	25000	0	1	184.19
			2	273.19
		1	1	253.48
			2	310.19
14	10	0	1	6.03
			2	8.48
		1	1	4.13
			2	9.67
	30	0	1	9.94
			2	16.31
		1	1	10.08
			2	20.88
	100	0	1	34.68
			2	48.52

Estimates

timepointdays	flashintensitymcd	Treated1progesterone0vehicle	EyeOD1OS2	Mean	Std. Error
		1	1	19.07	3.811
			2	20.52	3.646
	300	0	1	56.06	12.832
			2	89.21	10.151
		1	1	45.09	9.821
			2	58.78	11.084
	1000	0	1	94.95	21.329
			2	145.16	15.341
		1	1	78.75	16.822
			2	90.75	17.462
	3000	0	1	125.23	27.224
			2	180.31	18.020
		1	1	102.61	20.415
			2	122.42	20.602
	10000	0	1	151.58	31.987
			2	218.06	22.756
		1	1	112.48	20.592
			2	156.79	19.998
	25000	0	1	173.31	33.635
			2	239.18	23.546
		1	1	135.43	23.851
			2	177.62	21.151

Estimates

timepointdays	flashintensitymcd	Treated1progesterone0vehicle	EyeOD1OS2	95% Wald ... Lower
		1	1	12.89
			2	14.48
	300	0	1	35.80
			2	71.38
		1	1	29.42
			2	40.62
	1000	0	1	61.14
			2	118.01
		1	1	51.81
			2	62.24
	3000	0	1	81.78
			2	148.24
		1	1	69.47
			2	88.02
	10000	0	1	100.23
			2	177.73
		1	1	78.57
			2	122.11
	25000	0	1	118.48
			2	197.20
		1	1	95.90
			2	140.65

Estimates

timepointdays	flashintensitymcd	Treated1progesterone0vehicle	EveOD1OS2	95% Wald ... Upper
		1	1	28.21
			2	29.06
	300	0	1	87.80
			2	111.50
		1	1	69.10
			2	85.06
	1000	0	1	147.47
			2	178.57
		1	1	119.70
			2	132.32
	3000	0	1	191.75
			2	219.33
		1	1	151.54
			2	170.25
	10000	0	1	229.22
			2	267.55
		1	1	161.03
			2	201.32
	25000	0	1	253.53
			2	290.08
		1	1	191.26
			2	224.31